

# Oil & Natural Gas Technology

DOE Award No.: DE-FG26-08NT05679

## Final Report

October 2008 - March 2012

### Bridging the Gap between Chemical Flooding and Independent Oil Producers

Submitted by:  
University of Kansas Center for Research, Inc.  
2385 Irving Hill Rd  
Lawrence, KS 66045-7563

Stan McCool, Tony Walton, Paul Willhite, Mark Ballard  
Miguel Rondon, Kaixu Song, Zhijun Liu, Shahab Ahmed, Peter Senior

Prepared for:  
United States Department of Energy  
National Energy Technology Laboratory

August, 2012



Office of Fossil Energy

**Disclaimer**

This report was prepared as an account of work sponsored by an agency of the United States Government. Neither the United States Government nor any agency thereof, nor any of their employees, makes any warranty, express or implied, or assumes any legal liability or responsibility for the accuracy, completeness, or usefulness of any information, apparatus, product, or process disclosed, or represents that its use would not infringe privately owned rights. Reference herein to any specific commercial product, process, or service by trade name, trademark, manufacturer, or otherwise does not necessarily constitute or imply its endorsement, recommendation, or favoring by the United States Government or any agency thereof. The views and opinions of authors expressed herein do not necessarily state or reflect those of the United States Government or any agency thereof.

## **Abstract**

Ten Kanas oil reservoirs/leases were studied through geological and engineering analysis to assess the potential performance of chemical flooding to recover oil. Reservoirs/leases that have been efficiently waterflooded have the highest performance potential for chemical flooding. Laboratory work to identify efficient chemical systems and to test the oil recovery performance of the systems was the major effort of the project. Efficient chemical systems were identified for crude oils from nine of the reservoirs/leases. Oil recovery performance of the identified chemical systems in Berea sandstone rocks showed 90<sup>+</sup> % recoveries of waterflood residual oil for seven crude oils. Oil recoveries increased with the amount of chemical injected. Recoveries were less in Indiana limestone cores. One formulation recovered 80% of the tertiary oil in the limestone rock. Geological studies for nine of the oil reservoirs are presented. Pleasant Prairie, Trembley, Vinland and Stewart Oilfields in Kansas were the most favorable of the studied reservoirs for a pilot chemical flood from geological considerations. Computer simulations of the performance of a laboratory coreflood were used to predict a field application of chemical flooding for the Trembley Oilfield. Estimates of field applications indicated chemical flooding is an economically viable technology for oil recovery.

## Table of Contents

	<u>page</u>
Abstract.....	i
List of Figures.....	iv
List of Tables .....	xvi
Executive Summary .....	xix
Chapter 1 - Identification and Selection of Oil Reservoirs for Study.....	1-1
Geological Prospects for Chemical Flooding in Kansas.....	1-1
Databases of Kansas Oilfields and Reservoirs.....	1-4
Identification of Chemical Flooding Prospect through Interviews with Oil Producers.....	1-4
Criteria for Selection of Leases.....	1-5
Leases Selected for Laboratory Studies.....	1-8
Sample and Data Collection.....	1-10
Geological Investigations of Reservoirs .....	1-10
Chapter 2 - Formulation and Performance of Chemical Systems.....	2-1
Experimental Procedures and Materials and Analysis Methods.....	2-2
Results .....	2-10
Total Acid Numbers.....	2-10
Phase Behavior Studies.....	2-10
Corefloods.....	2-13
Chapter 3 – Selection and Performance of Chemical Systems for Trembley Oilfield.....	3-1
Phase Behavior Results.....	3-1
Coreflood Results.....	3-37

Chapter 4 - Reservoir Studies .....	4-1
Summary of the Geological Evaluation of Selected Reservoirs for Chemical Flooding ...	4-1
Simulation of Chemical Flooding.....	4-14
Laboratory Coreflood Simulations .....	4-15
Trembley Oilfield Simulations .....	4-17
Economics of Field Applications of Chemical Floods .....	4-22
Economic Estimates by Material Balances.....	4-22
Economic Analysis using Simulation Results .....	4-27
Chapter 5 - Technology Transfer.....	5-1
Chapter 6 – Summary and Relevancy of Results.....	6-1
References .....	7-1
Appendix - Geological Studies on Selected Reservoirs	
Beaver Creek Field, Rawlins County, KS .....	A-1
Celia South Waterflood Unit, Rawlins County, Kansas .....	A-19
Missouri Flats Waterflood Unit, Gove County, Kansas .....	A-55
Pleasant Prairie Oilfield, Haskell and Finney Counties, Kansas .....	A-78
Trembley Oilfield, Reno County, Kansas.....	A-96
Woodhead Unit, Vinland Oilfield, Douglas County, Kansas .....	A-121
Muddy Creek Southwest Unit, Butler County, Kansas .....	A-157
Stewart Oilfield, Finney County, Kansas .....	A-178

## List of Figures

<b><u>Fig. No.</u></b>	<b><u>Title</u></b>	<b><u>Page No.</u></b>
1.1	Oil production in Kansas by stratigraphic unit. (Kansas Geological Survey).	1-2
1.2	Location of oilfields containing the selected leases.	1-8
2.1	A schematic of the core with pressure measurement setup.	2-7
2.2	Oil recovery as a function of the amount of chemical injected.	2-24
2.3	Phase behavior and solubilization parameters for the chemical formulation used in Core 30 (limestone).	2-26
2.4	Photographs of the effluent vials from chemical flooding in Core 30.	2-27
2.5	Oil cut and tertiary oil recovery for chemical flood in Core 30.	2-28
2.6	On top: Overall and sections differential pressure during chemical flooding of Core 30. At the bottom: Zoom for the first 0.1 pore volume injected.	2-29
3.1	Low solubilization of oil and water and gels from tube 8 to 11 observed for Series A25, a ratio 3:1 of Petrostep S1 to Petrostep S2 at 1 wt% total surfactant concentration and 1.5 wt% SBA with Trembley crude oil @ 46.1 °C after equilibrating for 63 days. Salinity varied from 2.0 wt% to 5.0 wt% NaCl at 0.30 wt% increments, left to right.	3-6
3.2	Effect of varying Petrostep S1 to Petrostep S2 ratio and total surfactant concentration on optimum salinity with various SBA concentrations without alkali. Oil is Trembley crude oil @ 46.1 °C.	3-6
3.3	Comparison of time required (equilibration time) for optimum solubilization ratio to attain a stable value with and without alkali for the same formulation, 0.625 wt% Petrostep S1 0.375 wt% Petrostep S2, 2 wt% SBA. Oil is Trembley crude oil @ 46.1 °C.	3-9
3.4	Formulation 27-4 containing 0.625 wt% Petrostep S1 0.375 wt% Petrostep S2, 2 wt% SBA with 0.05 wt% NaOH. The microemulsion phase is shown at 3 days. The middle phase microemulsion at 4.6 wt% and 4.7 wt% salinity are near the optimum. With alkali, microemulsion phase equilibrated in 3 days and showed sharp interfaces. Oil is Trembley crude oil @ 46.1 °C.	3-9

<b>Fig. No.</b>	<b>Title</b>	<b>Page No.</b>
3.5	Formulation 25-16 containing 0.75 wt% Petrostep S1 0.25 wt% Petrostep S2, 2 wt% SBA with 0.25 wt% NaOH. The microemulsion phase was creamy and viscous compared to formulations containing smaller proportion of S1. Oil is Trembley crude oil @ 46.1 °C.	3-14
3.6	Phase behavior results at 7 days for formulation 40-3 (X-1) containing 0.625 wt% Petrostep S1 0.375 wt% Petrostep S2, 2 wt% SBA with 1 wt% Na <sub>2</sub> CO <sub>3</sub> . WOR =1.5. Oil is Trembley crude oil @ 46.1 °C.	3-15
3.7	Solubilization parameters for formulation 40-3 (X-1) containing 0.625 wt% Petrostep S1 0.375 wt% Petrostep S2, 2 wt% SBA with 1 wt% Na <sub>2</sub> CO <sub>3</sub> . WOR =1.5. Oil is Trembley crude oil @ 46.1 °C.	3-15
3.8	Phase behavior results at 6 days for formulation 40-9 (X-2) containing 0.31 wt% Petrostep S1 0.19 wt% Petrostep S2, 1.25 wt% SBA with 1 wt% Na <sub>2</sub> CO <sub>3</sub> . WOR =1.5. Oil is Trembley crude oil @ 46.1 °C.	3-16
3.9	Solubilization parameters for formulation 40-9 (X-2) containing 0.31 wt% Petrostep S1 0.19 wt% Petrostep S2, 1.25 wt% SBA with 1 wt% Na <sub>2</sub> CO <sub>3</sub> . WOR =1.5. Oil is Trembley crude oil @ 46.1 °C.	3-16
3.10	Phase behavior results at 3 days for formulation 40-18 (X-3) containing 0.31 wt% Petrostep S1 0.19 wt% Petrostep S2, 1.375 wt% DGBE with 1 wt% Na <sub>2</sub> CO <sub>3</sub> . WOR =1.5. Oil is Trembley crude oil @ 46.1 °C.	3-17
3.11	Solubilization parameters for formulation 40-18 (X-3) containing 0.31 wt% Petrostep S1 0.19 wt% Petrostep S2, 1.375 wt% DGBE with 1 wt% Na <sub>2</sub> CO <sub>3</sub> . WOR =1.5. Oil is Trembley crude oil @ 46.1 °C.	3-17
3.12	Photo of a salinity scan for a formulation X-4 containing 0.625 wt% Alfoterra® 123-8s, 0.375 wt% Petrostep® S-2, 0.75 wt% IBA and 0.05 wt% NaOH with Trembley crude oil @ 46.1 °C after equilibrating for 22 days.	3-23
3.13	Solubilization Parameters plot for formulation (A3) containing 0.625 wt% Alfoterra® 123-8s, 0.375 wt% Petrostep® S-2, 0.75 wt% IBA and 0.05 wt% NaOH with Trembley crude oil @ 46.1 °C after equilibrating for 22 days.	3-24
3.14	Determination of equilibration time for formulation X-4 containing 0.625 wt% Alfoterra® 123-8s, 0.375 wt% Petrostep® S-2, 0.75 wt% IBA and 0.05 wt% NaOH with Trembley crude oil @ 46.1 °C.	3-24

<b><u>Fig. No.</u></b>	<b><u>Title</u></b>	<b><u>Page No.</u></b>
3.15	A picture of spinning drop in action during IFT measurement between aqueous and microemulsion phase from the same pipet. The formulation contained 0.62% Petrostep S1, 0.38% Petrostep S2, 2% SBA, 0.5 wt% NaOH and Trembley crude oil with WOR=1 at 4 % salinity and 46.1 C.	3-32
3.16	Microemulsion viscosity for formulation X-1 and X-4. Viscosities were measured at a constant shear rate of 75 sec <sup>-1</sup> .	3-32
3.17	Optimum salinity and solubilization ratios for 1 wt% surfactant formulation X-1 versus different oil percent in pipettes for Trembley. The blue arrow, which represents a hypothetical surfactant slug salinity, shows the effect of oil concentration change on microemulsion phase behavior in the surfactant slug as an ASP flood progresses.	3-34
3.18	Optimum equivalent salinity and phase transition boundaries for surfactant concentration range 0 wt% to 1 wt% for Formulation X-1 are plotted. The curves were interpolated and extrapolated to cover the entire range. The dilution of surfactant at the back of surfactant bank and corresponding equivalent salinity (NaCl + Na <sub>2</sub> CO <sub>3</sub> ) change is shown by the dotted blue arrow.	3-34
3.19	Dispersion characterization of Core #2 for core flood T-1.	3-40
3.20	Oil flood differential pressures for Core #2 for core flood T-1.	3-42
3.21	Waterflood differential pressures for Core #2 for core flood T-1.	3-42
3.22	Viscosities of surfactant and polymer slug for core flood T-1 (Core #2).	3-43
3.23	Oil cut and oil recovery for core flood T-1 (Core #2).	3-43
3.24	Photo of effluent vials from ASP T-1 (core #2) with formulation X-1 @ 46.1°C after equilibrating for 7 days.	3-45
3.25	Viscosity, salinity and pH of aqueous phase in effluent vials from ASP T-2. Viscosity was measured at 46.1 °C with variable shear rates ranging between 37.5 – 75 s <sup>-1</sup> on Brookfield rheometer.	3-46
3.26	Overall core and section pressures during ASP T-1.	3-46
3.27	Dimensionless distance versus dimension less time plot for ASP T-1 allows identification of fluid regions and validation that dimensionless velocities are constant.	3-47



<b><u>Fig. No.</u></b>	<b><u>Title</u></b>	<b><u>Page No.</u></b>
3.28	Section 1 pressure during ASP T-1 with identification of fluid regions using dimensionless velocities and pressure analysis.	3-47
3.29	Section 2 pressure during ASP T-1 with identification of fluid regions using dimensionless velocities and pressure analysis.	3-48
3.30	Section 3 pressure during ASP T-1 with identification of fluid regions using dimensionless velocities and pressure analysis.	3-48
3.31	Section 4 pressure during ASP T-1 with identification of fluid regions using dimensionless velocities and pressure analysis.	3-49
3.32	Section 5 pressure during ASP T-1 with identification of fluid regions using dimensionless velocities and pressure analysis.	3-49
3.33	Section 6 pressure during ASP T-1 with identification of fluid regions using dimensionless velocities and pressure analysis.	3-50
3.34	Dispersion characterization of Core #4 for core flood T-2.	3-53
3.34	Oil flood differential pressures for Core #4 for core flood T-2.	3-54
3.36	Waterflood differential pressures for Core #4 for core flood T-2.	3-54
3.37	Oil cut and oil recovery for core flood T-2 (Core #4).	3-56
3.38	Aqueous phase viscosity of effluent of core flood T-2 (Core #4) measured at $T_{res}$ . Aqueous phase viscosity was badly affected by polymer degradation.	3-56
3.39	Overall pressure during ASP flood T-2 (Core #4). Polymer drive degradation caused the pressure to drop after 0.3 PV.	3-57
3.40	Dispersion characterization of Core #23 for core flood T-3.	3-59
3.41	Oil flood differential pressures for Core #23 for core flood T-3. Temperature controller was accidentally switched that caused the pressures to rise after 0.5 pore volumes had been injected.	3-59
3.42	Waterflood differential pressures for Core #23 for core flood T-3.	3-60
3.43	Viscosities of surfactant and polymer slug vs shear rate for Core #23 for ASP flood T-3 at 46.1 °C.	3-60
3.44	Oil cut and oil recovery for core flood T-3 (Core #23).	3-61

<b><u>Fig. No.</u></b>	<b><u>Title</u></b>	<b><u>Page No.</u></b>
3.45:	Photo of effluent vials from ASP T-3 (core #23) with formulation X-1 @ 46.1 °C after equilibrating for 3 days.	3-63
3.46	Viscosity, salinity and pH of aqueous phase in effluent vials from ASP T-3. Viscosity was measured at 46.1°C with variable shear rates ranging between 37.5 – 75 s <sup>-1</sup> on Brookfield rheometer.	3-64
3.47	Overall core and section pressures during ASP T-3.	3-64
3.48	Section 1 pressure during ASP T-3 with identification of fluid regions using dimensionless velocities and pressure analysis.	3-66
3.49	Section 2 pressure during ASP T-3 with identification of fluid regions using dimensionless velocities and pressure analysis.	3-66
3.50	Section 3 pressure during ASP T-3 with identification of fluid regions using dimensionless velocities and pressure analysis.	3-67
3.51	Section 4 pressure during ASP T-3 with identification of fluid regions using dimensionless velocities and pressure analysis.	3-67
3.52	Section 5 pressure during ASP T-3 with identification of fluid regions using dimensionless velocities and pressure analysis.	3-68
3.53	Section 6 pressure during ASP T-3 with identification of fluid regions using dimensionless velocities and pressure analysis.	3-68
3.54	Dimensionless distance versus dimension less time plot for ASP T-3.	3-69
3.55	Dispersion characterization of Core #37 for core flood T-8.	3-69
3.56	Oil flood differential pressures for Core #37 for core flood T-8. Only pressures after the leak had been fixed are plotted. This data was used for end point relative permeabilities.	3-70
3.57	Waterflood differential pressures for Core #37 for core flood T-3. Pressures shown are after the leak was fixed. The data was used for estimating end point relative permeabilities.	3-70
3.58	Optimum equivalent salinity and phase transition boundaries for 1 wt% surfactant formulation X-1 for ASP T-8 (Core 39) versus different oil percent in pipettes for Trembley. Equivalent salinity of surfactant slug (NaCl + Na <sub>2</sub> CO <sub>3</sub> ) and formation brine are indicated by the blue arrow and orange line, respectively.	3-72

<b><u>Fig. No.</u></b>	<b><u>Title</u></b>	<b><u>Page No.</u></b>
3.59	Viscosities of surfactant and polymer slug for core flood T-8 (Core #37)	3-72
3.60	Optimum equivalent salinity and phase transition boundaries for surfactant concentration range 0 wt% to 1 wt% for Formulation X-1 are plotted. The curves were interpolated and extrapolated to cover the entire range. The dilution of surfactant at the back of surfactant bank and corresponding equivalent salinity (NaCl + Na <sub>2</sub> CO <sub>3</sub> ) change is shown by the dotted blue arrow. A polymer salinity of 4.5 wt% for ASP-T-8 would ensure a slow transition to Type I microemulsion.	3-73
3.61	Oil cut and oil recovery for ASP flood T-8 (Core #37) is compared with ASP T-3 (Core #23).	3-73
3.62	Photo of effluent vials from ASP T-8 (core #37) with formulation X-1 @ 46.1 °C after equilibrating for 3 days.	3-74
3.63	Viscosity and salinity of aqueous phase in effluent vials from ASP T-8. Viscosity was measured at 46.1 °C with variable shear rates ranging between 37.5 – 75 s <sup>-1</sup> on Brookfield rheometer.	3-76
3.64	Overall core and section pressures during ASP T-8.	3-77
3.65	Dimensionless distance versus dimensionless time plot for ASP T-8.	3-77
3.66	Section 1 pressure during ASP T-8 with identification of fluid regions using dimensionless velocities and pressure analysis.	3-78
3.67	Section 2 pressure during ASP T-8 with identification of fluid regions using dimensionless velocities and pressure analysis.	3-78
3.68	Section 3 pressure during ASP T-8 with identification of fluid regions using dimensionless velocities and pressure analysis.	3-79
3.69	Section 4 pressure during ASP T-8 with identification of fluid regions using dimensionless velocities and pressure analysis.	3-79
3.70	Section 5 pressure during ASP T-8 with identification of fluid regions using dimensionless velocities and pressure analysis.	3-80
3.71	Section 6 pressure during ASP T-8 with identification of fluid regions using dimensionless velocities and pressure analysis.	3-80
3.72	Dispersion characterization of Core #39 for core flood T-9.	3-83

<b>Fig. No.</b>	<b>Title</b>	<b>Page No.</b>
3.73	Oil saturation change in the core during oil flood on core #39.	3-83
3.74	Oil flood differential pressures for Core #39 for core flood T-9.	3-84
3.75	Waterflood differential pressures for Core #39 for core flood T-9.	3-84
3.76	Oil saturation change in the core during waterflood on core #39.	3-85
3.77	Optimum equivalent salinity and phase transition boundaries for 1 wt% surfactant formulation X-1 for ASP T-9 (Core 39) versus different oil percent in pipettes for Trembley. Equivalent salinity of surfactant slug (NaCl + Na <sub>2</sub> CO <sub>3</sub> ) is indicated by the blue arrow.	3-87
3.78	Optimum equivalent salinity and phase transition boundaries for surfactant concentration range 0 wt% to 1 wt% for Formulation X-1 are plotted. The curves were interpolated and extrapolated to cover the entire range. A polymer salinity of 4.1 wt% was used for ASP-T-9. The dilution of surfactant at the back of surfactant bank and corresponding equivalent salinity (NaCl + Na <sub>2</sub> CO <sub>3</sub> ) change is shown by the dotted blue arrow.	3-88
3.79	Oil cut and oil recovery for ASP flood T-8 (Core #37) is compared with ASP T-3 (Core #23).	3-89
3.80	Photo of effluent vials from ASP T-9 (core #39) with formulation X-1 @ 46.1 °C after equilibrating for 3 days.	3-90
3.81	Viscosity and salinity of aqueous phase in effluent vials from ASP T-9. Viscosity was measured at 46.1 °C. Shear rates ranged between 37.5–75 s <sup>-1</sup> on Brookfield rheometer.	3-91
3.82	pH of aqueous phase in effluent vials from ASP T-9.	3-93
3.83	Comparison of ASP T-8 (Core 37) and ASP T-9 (Core 39) effluent salinities.	3-93
3.84	Comparison of ASP T-8 (Core 37) and ASP T-9 (Core 39) effluent viscosities at Tres. Shear rates ranged between 37.5 – 75 s <sup>-1</sup> on Brookfield rheometer.	3-94
3.85	Comparison of ASP T-8 (Core 37) and ASP T-9 (Core 39) effluent pH.	3-94
3.86	Overall core and section pressures during ASP T-9.	3-96
3.87	Dimensionless distance versus dimension less time plot for ASP T-9.	3-96

<b><u>Fig. No.</u></b>	<b><u>Title</u></b>	<b><u>Page No.</u></b>
3.88	Section 1 pressure during ASP T-9 with identification of fluid regions using dimensionless velocities and pressure analysis.	3-97
3.89	Section 2 pressure during ASP T-9 with identification of fluid regions using dimensionless velocities and pressure analysis.	3-97
3.90	Section 3 pressure during ASP T-9 with identification of fluid regions using dimensionless velocities and pressure analysis.	3-98
3.91	Section 4 pressure during ASP T-9 with identification of fluid regions using dimensionless velocities and pressure analysis.	3-98
3.92	Section 5 pressure during ASP T-9 with identification of fluid regions using dimensionless velocities and pressure analysis.	3-99
3.93	Section 6 pressure during ASP T-9 with identification of fluid regions using dimensionless velocities and pressure analysis.	3-99
3.94	Dispersion characterization of Core #26 for core flood T-4.	3-100
3.95	Oil flood differential pressures for Core #26 for core flood T-4.	3-102
3.96	Waterflood differential pressures for Core #26 for core flood T-4.	3-102
3.97	Viscosities of surfactant and polymer slug for core #26 (T-4) at 46.1°C.	3-103
3.98	Oil cut and oil recovery for ASP flood T-4 (Core #26).	3-103
3.99	Photo of effluent vials from ASP T-4 (core #26) with formulation X-2 @ 46.1 °C after equilibrating for 3 days.	3-104
3.100	Viscosity, salinity and pH of aqueous phase in effluent vials from ASP T-4 (Core #26). Viscosity was measured at 37.5 s <sup>-1</sup> and 46.1 °C.	3-105
3.101	Overall core and section pressures during ASP T-4 (Core #26).	3-107
3.102	Dispersion characterization of Core #27 for core flood T-5.	3-109
3.103	Oil flood differential pressures for Core #27 for core flood T-5.	3-109
3.104	Oil saturation change in the core during oil flood on core #27.	3-110
3.105	Waterflood differential pressures for Core #27 for core flood T-5.	3-110

<b><u>Fig. No.</u></b>	<b><u>Title</u></b>	<b><u>Page No.</u></b>
3.106	Oil saturation change in the core during waterflood on core #27.	3-111
3.107	Optimum salinity and Type III microemulsion phase boundaries for Formulation X-3 (0.5 wt% total surfactant concentration) at oil concentration range of 50% to 10%. A salinity of 6 wt% TDS was selected because it gave Type III microemulsion at all oil concentrations. APSL for this system was 7.4 wt% TDS (6.4 wt% NaCl + 1.0 wt% Na <sub>2</sub> CO <sub>3</sub> ).	3-111
3.108	Optimum equivalent salinity and phase transition boundaries for surfactant concentration range 0 wt% to 0.5 wt% for Formulation X-3 are plotted. The curves were interpolated and extrapolated to cover the entire range. A minimum polymer salinity of 4.9 wt% would be necessary to cause a transition to Type I microemulsion phase. The dilution of surfactant at the back of surfactant bank and corresponding equivalent salinity (NaCl + Na <sub>2</sub> CO <sub>3</sub> ) change is shown by the dotted blue arrow.	3-112
3.109	Viscosities of surfactant and polymer slug for core #27 (T-5) at 46.1°C.	3-112
3.110	Oil cut and oil recovery for ASP flood T-5 (Core #27).	3-114
3.111	Photo of effluent vials from ASP T-5 (core #27) with formulation X-3 @ 46.1°C after equilibrating for 3 days.	3-115
3.112	Viscosity, salinity and pH of aqueous phase in effluent vials from ASP T-5 (Core #27). Viscosity was measured at 37.5 s <sup>-1</sup> and 46.1°C.	3-116
3.113	Overall core and section pressures during ASP T-5 (Core #27).	3-116
3.114	Dispersion characterization of Core #31 for core flood T-6.	3-118
3.115	Oil flood differential pressures for Core #31 for core flood T-6.	3-118
3.116	Oil saturation change in the core during oil flood on core #31.	3-119
3.117	Waterflood differential pressures for Core #31 for core flood T-6.	3-119
3.118	Oil saturation change in the core during waterflood on core #31.	3-120
3.119	Viscosities of surfactant and polymer slug for core #31 (T-6) at 46.1°C.	3-120
3.120	Oil cut and oil recovery for ASP flood T-6 (Core #31).	3-122

<b><u>Fig. No.</u></b>	<b><u>Title</u></b>	<b><u>Page No.</u></b>
3.121	Sliced view of Core 31 sections after ASP flood. Section numbers given in top left corner. The face shown is the downstream side of section. Oil is trapped at the bottom part of the sections.	3-123
3.122	Photo of effluent vials from ASP T-6 (core #31) with 0.6 PV Formulation X-3 @ 46.1 °C after equilibrating for 3 days.	3-125
3.123	Viscosity, salinity and pH of aqueous phase in effluent vials from ASP T-5 (Core #27). Viscosity was measured at 37.5 s-1 and 46.1°C.	3-126
3.124	Overall core and section pressures during ASP T-6 (Core #31).	3-126
3.125	Dispersion characterization of Core #32 for core flood T-7.	3-128
3.126	Oil flood differential pressures for Core #32 for core flood T-7.	3-128
3.127	Oil saturation change in the core during oil flood on core #32.	3-129
3.128	Core #32 section 6 at the end of oil flood.	3-129
3.129	Waterflood differential pressures for Core #32 for core flood T-7.	3-130
3.130	Oil saturation change in the core during waterflood on core #32.	3-130
3.131	Core #32 section 6 at the end of waterflood.	3-131
3.132	Viscosities of surfactant and polymer slug for core #32 (T-7) at 46.1°C.	3-133
3.133	Oil cut and oil recovery for ASP flood T-7 (Core #32).	3-133
3.134	Sliced view of Core 32 sections after ASP flood. Section numbers given in top left corner. The face shown is the downstream side of section. Oil is trapped at the bottom left part of the sections.	3-134
3.135	Photo of effluent vials from ASP T-7 (core #32) with formulation X-3 @ 46.1°C after equilibrating for 3 days.	3-135
3.136	Viscosity, salinity and pH of aqueous phase in effluent vials from ASP T-7 (Core #32). Viscosity was measured at 37.5 s-1 and 46.1°C.	3-137
3.137	Overall core and section pressures during ASP T-7 (Core #32).	3-137
3.138	Dimensionless distance versus dimension less time plot for ASP T-7 (Core#32).	3-138

<b><u>Fig. No.</u></b>	<b><u>Title</u></b>	<b><u>Page No.</u></b>
3.139	Section 1 pressure during ASP T-7 (core#32) with identification of fluid regions using dimensionless velocities and pressure analysis.	3-138
3.140	Section 2 pressure during ASP T-7 (core#32) with identification of fluid regions using dimensionless velocities and pressure analysis.	3-139
3.141	Section 3 pressure during ASP T-7 (core#32) with identification of fluid regions using dimensionless velocities and pressure analysis.	3-139
3.142	Section 4 pressure during ASP T-7 (core#32) with identification of fluid regions using dimensionless velocities and pressure analysis.	3-140
3.143	Section 5 pressure during ASP T-7 (core#32) with identification of fluid regions using dimensionless velocities and pressure analysis.	3-140
3.144	Section 6 pressure during ASP T-7 (core#32) with identification of fluid regions using dimensionless velocities and pressure analysis.	3-141
4.1	Comparison of simulated and experimental oil production of coreflood.	4-16
4.2	Reservoir thickness of the Trembley Oilfield.	4-18
4.3	Porosity of the Trembley Oilfield.	4-18
4.4	Initial oil saturation of the Trembley Oilfield.	4-19
4.5	Comparison of simulated and actual oil production during primary and secondary operations of the Trembley Oilfield.	4-20
4.6	Oil production of the simulated chemical flood of the Trembley Oilfield. Simulated and actual oil production during primary and secondary operations are shown for comparison.	4-21
4.7	Oil saturation of the Trembley Oilfield after simulated chemical flood.	4-21
4.8	Intro worksheet of the Surfactant Flooding Economics spreadsheet.	4-26
4.9	Capital Expenses worksheet of the Surfactant Flooding Economics spreadsheet.	4-27
4.10	Operating Costs worksheet of the Surfactant Flooding Economics spreadsheet.	4-28



<b><u>Fig. No.</u></b>	<b><u>Title</u></b>	<b><u>Page No.</u></b>
4.11	Prod and Inj worksheet of the Surfactant Flooding Economics spreadsheet. Project life of table is truncated.	4-28
4.12	Economics worksheet of the Surfactant Flooding Economics spreadsheet.	4-29

## List of Tables

<b><u>Tab. No.</u></b>	<b><u>Title</u></b>	<b><u>Page No.</u></b>
1.1	Stratigraphic chart of oil producing formations in Kansas. Commonly waterflooded formations in central and western Kansas are highlighted in red print.	1-3
1.2	Information listed in the database of Kansas oilfields.	1-4
1.3	Oil Producers contacted/interviewed for discussions of chemical flooding opportunities.	1-6
1.4	Leases selected for laboratory studies.	1-9
2.1	List of chemicals that were evaluated in phase behavior studies.	2-4
2.2	Acid numbers of crude oils of the leases.	2-10
2.3	Efficient chemical formulations for nine crude oils.	2-12
2.4	Core properties and results of oil and waterfloods.	2-14
2.5	Parameters and results of chemical floods in laboratory cores.	2-20
2.6	Highest oil recovery achieved for each crude oil.	2-24
2.7	Summary of chemical floods with Warhman crude oil in Indiana Limestone.	2-25
2.8	Chemical formulation for tertiary recovery of Warhman crude oil in limestone.	2-25
2.9	Chemical flood injection plan used for Core 30.	2-26
2.10	Results of chemical flood in Core 30 and comparison with previous corefloods.	2-28
3.1	Screening of Petrostep® S-1 and Petrostep® S-2 with Trembley crude oil without alkali. Total surfactant is 2 wt%.	3-3
3.2	Screening of Petrostep® S-1 and Petrostep® S-2 with Trembley crude oil without alkali. Total surfactant is 1 wt%.	3-4
3.3	Screening of Petrostep® S-1 and Petrostep® S-2 with Trembley crude oil without alkali. Total surfactant is 0.5 wt%.	3-5

<b><u>Tab. No.</u></b>	<b><u>Title</u></b>	<b><u>Page No.</u></b>
3.4	Screening of Petrostep® S-1 and Petrostep® S-2 with Trembley crude oil with alkali. Total surfactant is 1 wt%. Surfactant ratio S-1:S-2 was kept constant at 5:3. Oil is Trembley and temperature was maintained at 46.1 °C.	3-8
3.5	Optimization of Petrostep® S-1 and Petrostep® S-2 with Trembley crude oil with alkali. Total surfactant is 1 wt%. Surfactant ratio, co-solvent concentration and type were varied. Oil is Trembley and temperature was maintained at 46.1 °C.	3-11
3.6	Optimization of Petrostep® S-1 and Petrostep® S-2 with Trembley crude oil with alkali. Total surfactant was 0.5 wt%. Surfactant ratio, co-solvent concentration and type were varied. Oil is Trembley and temperature was maintained at 46.1 °C.	3-12
3.7	Optimized formulation from Petrostep® S-1 and Petrostep® S-2 screening with Trembley crude oil. Temperature was maintained at 46.1 °C.	3-13
3.8	Screening of Alfoterra 123-8s, Petrostep S-8B, Petrostep S-8C surfactants and Petrostep® S-2, Petrostep C-1, Petrostep C-5 co-surfactant with Trembley crude oil. Oil is Trembley and temperature was maintained at 46.1°C.	3-19
3.9	Optimized formulation from Alfoterra 123-8s, Petrostep S-8B, Petrostep S-8C surfactants and Petrostep® S-2, Petrostep C-1, Petrostep C-5 co-surfactant screening with Trembley crude oil. Temperature was maintained at 46.1 °C.	3-21
3.10	Screening of Petrostep S13-D, Petrostep S-2 and TDA-12-EO with Trembley crude oil. Temperature was maintained at 46.1 °C and WOR was either 1 or 1.5.	3-22
3.11	Effect of surfactant concentration on the amount of co-solvent to give non-viscous middle phase. Selected results from Petrostep S-1 and S-2 screening with Trembley crude oil. Temperature was maintained at 46.1 °C.	3-26
3.12	Relationship between surfactant to co-surfactant ratio and phase behavior. Temperature was maintained at 46.1 °C.	3-27
3.13	Relationship between co-solvent concentration and phase behavior. Temperature was maintained at 46.1 °C.	3-28
3.14	Formulation X-1 and another formulation with and without polymer and the associated phase behavior results.	3-30

<b><u>Tab. No.</u></b>	<b><u>Title</u></b>	<b><u>Page No.</u></b>
3.15	The five optimized formulations from phase behavior studies and their phase behavior results. Only Formulations X-1, X-2 and X-3 passed all screening criteria and therefore were selected for core flood demonstration.	3-35
3.16	Summary of Trembley core floods' core dimensions and permeabilities.	3-38
3.17	Summary of Trembley core floods' important parameters and results. The floods were performed at reservoir temperature (Tres) 46.1 °C.	3-39
3.18	Summary of oil bank and surfactant bank mobilities for all ASP floods. T-2 was not analyzed due to polymer drive degradation.	3-52
3.19	Composition of Trembley field brine sample.	3-82
3.20	Synthetic formation brine composition used for brine flood of core #39 (T-9). Brine was formulated to mimic concentrations of actual field brine sample but salts of Barium, Iron, Bicarbonate, Carbonate and Sulfate had to be eliminated to avoid precipitate formation.	3-82
4.1	List of selected properties, their location, and current operators	4-4
4.2	Stratigraphy, Traps, and waterfloods on selected properties	4-5
4.3	Coreflood parameters for simulation runs.	4-15
4.4	Fluid saturations and relative permeabilities of the coreflood that were used for history-matching simulations.	4-15
4.5	Relative permeability parameters for the coreflood simulations.	4-17
4.6	Parameters for the relative permeability correlation for the Trembley Oilfield.	4-19
4.7	Economic estimates of field application of chemical flooding.	4-23
4.8	Unit chemical costs for economic evaluations.	4-22
4.9	Economic estimates of pilot application of chemical flooding.	4-24

## Executive Summary

Chemical flooding using surfactants, polymers and alkali has the potential to significantly increase oil production from reservoirs that would otherwise be abandoned after primary and secondary production operations. The purpose of this investigation was to introduce chemical flooding and to promote field testing to independent oil producers in Kansas and beyond. This purpose was achieved by providing preliminary designs of chemical floods for selected applications through formulation of reservoir-specific chemical systems and by providing estimated economics of field applications.

Ten Kansas oil reservoirs/leases were selected for study by assessing the potential performance of chemical flooding through geological and engineering characteristics. The reservoirs/leases surveyed represented about 45% of past Kansas oil production. Reservoirs/leases that have been efficiently waterflooded have the highest performance potential for chemical flooding.

Laboratory work to identify efficient chemical systems and to test the oil recovery performance of the systems was the major effort of the project. Efficient chemical systems were identified for crude oils from nine of the reservoirs/leases through phase behavior studies where the behavior of various aqueous surfactant/polymer systems is observed before and after they are mixed with a crude oil. Efficient chemical systems met a set of formalized criteria. Most of the Kansas crude oils responded favorably to chemical systems that contained two surfactants: an alcohol propoxy sulfate and an internal olefin sulfonate. This system also required relatively high concentrations of alcohol solvents. The performance of the chemical systems in phase behavior studies was enhanced with the addition of sodium carbonate (alkali). All of the crude oils had low acid numbers, negating the use of alkali in the chemical system for soap production.

Oil recovery performance of the identified chemical systems was tested in coreflood experiments using quarried Berea sandstone and Indiana limestone rocks. Performance was measured as the percentage of oil recovered from cores initially at a waterflooded residual saturation. Chemical formulations recovered 90% or more of the residual oil for seven crude oils in Berea sandstone cores. Oil recoveries increased with the amount of chemical injected for floods conducted in Berea sandstone cores.

Chemical floods were conducted with formulations for the Wahrman crude oil in Indiana limestone cores. Oil recoveries were 50% or less in the Indiana limestone cores for the same chemical formulation that had 90<sup>+</sup> % recoveries in Berea sandstone cores. An alternate system containing an alcohol propoxy sulfate and an ethoxylated alcohol without alcohol co-solvent recovered 80% of the Wahrman crude from a limestone core. Tracer experiments showed

significantly larger mixing zones in the limestone cores. Dilution of the chemical slug due to greater mixing in the limestone rocks contributed to the lower oil recoveries.

Geological evaluations were used in the selection of the ten reservoirs/leases for study. Geological studies for nine of the oil reservoirs were prepared and the Pleasant Prairie, Trembley, Vinland and Stewart Oilfields were the most advantageous for a pilot chemical flood from geological considerations.

Simulation software was used to model the performance of a laboratory coreflood and predict the performance of a field application of chemical flooding for the Trembley Oilfield. Economics estimates of field applications indicated chemical flooding is a viable technology for oil recovery.

# Chapter 1

## Identification and Selection of Oil Reservoirs for Study

An initial objective of this work was the selection of approximately ten oil leases in Kansas for which laboratory studies will be conducted on the crude oils from those leases in the effort to design efficient chemical formulations for flooding applications. Two approaches were used to identify and evaluate potential leases/reservoirs. The first was a broad approach where a database of pertinent information on Kansas oilfields was assembled from available public information. Geological and engineering analysis of the database would then provide a resource base for chemical flooding and target specific reservoirs for study. The second approach was to consult with technical employees of companies producing the largest amounts of oil in Kansas to determine specific leases that would be candidates for chemical flooding. Personal contacts with personnel from the oil producers proved the best approach. Sufficient information was lacking in public data for analysis. The selection processes are described.

It became evident through our work that successful waterfloods are the best indicator of favorable characteristics of a reservoir/lease for application of chemical flooding, both as a general criterion for specific rock formations and for specific leases. Rationale for focusing on waterfloods and additional criteria for selection of leases are presented.

### Geological Prospects for Chemical Flooding in Kansas

Geological characteristics and oil production mechanisms were used to classify and select producing horizons that are favorable to chemical flooding. Engineers and geologists from several of the largest independent oil producers confirmed the production mechanisms and classifications.

Oil is produced in Kansas from rocks ranging from Proterozoic to Permian in age (**Figure 1.1**). The stratigraphic intervals shown in **Figure 1.1** may include many different units, some of which are fundamentally different reservoir types. **Table 1.1** indicates many subdivisions of the stratigraphic systems, stages, and groups that are productive and highlights the intervals that are responsive to waterflood applications.

Each productive horizon has one or more characteristic types of traps and drive mechanisms. For example, both limestone and dolomite of the Arbuckle Group, the most prolific unit, and chert or chert breccia of the Mississippian Osagean Stage, produce from high points on an overlying unconformity surface. Some such high points are faulted blocks, while others are residual highs on karsted unconformity surfaces. Strong water drive provides energy for production in most Arbuckle Group fields, whereas Mississippian reservoirs have weaker water drives. Both the Arbuckle and Osagean are generally not good candidates for flooding processes.

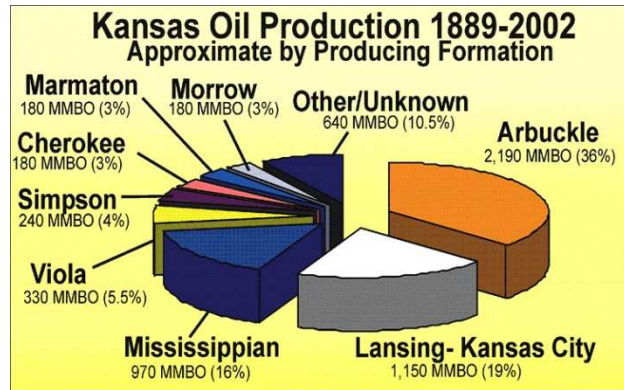


**Figure 1.1** - Oil production in Kansas by stratigraphic unit. (Kansas Geological Survey).

To the extent that the most likely targets for successful chemical floods are oilfields that waterflood well, a few characteristic combinations of lithology, trap and drive are most promising among those in Kansas. Among the sandstone producing units in Kansas, good waterfloods are common in Chesteran (Mississippian) and in Morrowan and Cherokee and other Pennsylvanian sandstones. However, productive Permian sandstone may also be a candidate; the 650 ft. sandstone in the El Dorado Field has been flooded (Van Horn, 1983). Cherokee reservoirs are concentrated in southeastern Kansas, east of the Nemaha uplift. Most of the oil production comes from elongate sandstone bodies that probably fill valleys. Other pre-Marmaton, post-Atokan Pennsylvanian reservoirs on the margins of the Central Kansas Uplift are either assigned to the Cherokee Group or the informal Pennsylvanian basal conglomerate. Recently, development has occurred in channel-like sandstones of Cherokee age rocks in Ness County, first pointed out by Walters et al. (1979). The Pennsylvanian basal conglomerate is a discontinuous sheet of residual breccia, sandstone, and clay that thickens and thins over underlying irregularities in karsted Mississippian rocks. Beach and shallow marine sandstones of the Simpson Group (Ordovician) waterflood well, at least in the Tobias Field, but other lower Paleozoic units, limestone or dolomite for the most part (Viola, Hunton) do not.

Many grainstone reservoirs in the Lansing and Kansas City groups (Missourian, referred to as LKC), the Fort Scott Limestone and other Marmaton Group reservoirs (Desmoinesian), and the Topeka Limestone (Virgilian) have also waterflooded well. Oolitic grainstone is a common reservoir type in Lansing and Kansas City group reservoirs. Some such reservoirs are bending-fold anticlinal traps over faulted basement highs, perhaps with preferential development of oolites on the highs. Others are isolated oolite or other grainstone bodies.



**Table 1.1** - Stratigraphic chart of oil producing formations in Kansas. Commonly waterflooded formations in central and western Kansas are highlighted in red print.

Era	System	Stage	Group	Producing Rock Units	
Mesozic	Cretaceous		Colorado	Niabrara	
Paleozoic	Permian	Guadalupian			
		Leonardian	Nippewalla		
			Sumner	Red Cave	
		Wolfcampian	Chase	Herington, Krider, Winfield, Towanda, Fort Riley	
			Council Grove	Neva, Cottonwood	
		Virgilian	Admire	Indian Cave	
			Wabaunsee	Langdon, Tarkio, Willard, White Cloud, Howard, Severy	
			Shawnee	Topeka, Elgin, Hoover, Toronto	
		Pennsylvanian	Missourian	Douglas	Ireland, Stalnaker
	<i>Lansing</i>				
	<i>Kansas City</i>			Layton, Perry Gas	
			Pleasanton	Cleveland, Knobtown, Hepler	
			<i>Marmaton</i>	New Albany, Wayside, Bandera, Weiser, Pawnee, Peru, Fort Scott, Oswego	
			<i>Cherokee</i>	Mulky Coal, <i>Prue</i> , Bevier Coal, <i>Squirrel</i> , <i>Cattleman</i> , <i>Bartlesville</i> , Weir-Pittsburg, <i>McLouth</i> , Riverton Coal, <i>Burgess</i>	
			Atokan		
	Morrowan		<i>Morrow</i>		
	Mississippian				<i>Basal Pennsylvanian Conglomerate</i> , Gorham
			Chesteran	<i>Chester</i>	
		Meramecian		Saint Genevieve, Saint Louis, Spergen, Warsaw	
		Osagian			
	Devonian	Kinderhookian			
				Misener	
	Silurian		Hunton		
Ordovician				Maquoketa	
				Viola	
		<i>Simpson</i>			
Cambrian		Arbuckle			
				Reagan	
				Granite Wash	

## **Databases of Kansas Oilfields and Reservoirs**

Databases of Kansas oil fields and oil reservoirs were assembled with the purpose to select reservoirs and individual oil leases using the producing horizons that were identified above to be favorable for chemical flooding. Databases were assembled in Excel spreadsheets from a database derived from public data and maintained by the Kansas Geological Survey (KGS). KGS's database can be queried by the public at <http://www.kgs.ku.edu>. KGS obtains field names, counties in which the field is located and producing zones from public records that the Kansas Corporation Commission requires when wells are initially drilled. Production data are obtained from public records from the Kansas Department of Revenue where production is given by lease.

The information was cross referenced by location for 6,536 Kansas oilfields with the information listed in **Table 1.2**. Several issues made the development of a representative database of Kansas oil reservoirs from public data impractical for our purpose. The number of producing zones (reservoirs) for each oilfield ranged from one to ten. Producing zones were identified when the well was initially completed and subsequent completions in other zones are not usually known. Oilfields with the largest oil production commonly had many oil producing zones (reservoirs). Oil production from an oilfield could not be reliably allocated to individual reservoirs with the public data. This was the primary issue that prevented the establishment of a resource base for chemical flooding. It was concluded that types of information derived from the public records was not sufficient to identify reservoirs and leases for chemical flooding applications.

**Table 1.2** – Information listed in the database of Kansas oilfields.

---

Field name  
Producing zones (up to 9 zones)  
Discovery date  
Total cumulative oil production (bbls)  
Total cumulative gas production (mcf)  
Area (acres)  
Total number of wells  
2008 oil production (bbls)  
Number of oil wells in 2008  
2008 gas production (mcf)  
Number of gas wells in 2008  
Location by county (up to 19)

---

## **Identification of Chemical Flooding Prospect through Interviews with Oil Producers**

The Top 30 oil producers in Kansas were contacted to discuss chemical flooding applications for their leases. The Top 30 producers were determined using 2008 data obtained from the Kansas Geological Survey. Only one company of the Top 30 did not respond to our repeated attempts to contact. Production by the Top 30 was concentrated in central and western Kansas and production in eastern Kansas was not represented. Eastern Kansas oil production is characterized by shallow depths and oils with lower API gravities than in central and western Kansas which brings different opportunities for chemical flooding applications. We identified the Top 10 oil producers in eastern Kansas and contacted them as well as other producers that responded to our

calls for participation. A listing of the oil companies that were contacted is given in **Table 1.3**. The 47 companies that were contacted represented more than 45 % of the oil produced in Kansas. It is noted that more than 5,500 companies produced oil in Kansas in 2008.

Initial contacts were conducted by telephone and followed by email to (1) describe and explain the chemical flooding process, (2) determine and confirm general chemical flooding prospects in Kansas from the company's waterflooding applications (3) inform company personnel about possible positive benefits from participating in this design project, and (4) identify their best performing waterfloods as prospects for our design work. Follow up meetings with many of the companies, both in-person and by phone, were conducted to assess their data on their prospective leases as well as determine their interest and their ability to support a chemical flood application. Criteria for the selection of leases are given in the following section.

Cooperation and support of independent oil producers is a key component of this project. The process to contact and interview oil producers was time intensive but worth the effort in terms of identifying prospects for chemical flooding as well as educating independent oil producers and generating interest in this project and chemical flooding applications. The personnel contacted represent a significant portion of the oil produced in Kansas.

### **Criteria for Selection of Leases**

The performance of a chemical flood is a function of the microscopic efficiency of the chemical system to mobilize and displace contacted oil and the macroscopic efficiency of the chemical slug to contact the reservoir volume. Formulation of the chemical system for microscopic efficiency is addressed in chapter on chemical formulations. Assuming that efficient chemical systems can be formulated, reservoirs with efficient sweep are the best candidates for chemical flooding so that the integrity of the chemical slug as it flows through the reservoir can be maintained.

It became evident during our initial interviews with oil producers that a successful waterflooding application was the best indicator of favorable characteristics for chemical flooding, both as a general criterion for specific rock formations and for a particular lease. Waterfloods were targeted because an oil operator has previously made the assessment that the reservoir would respond favorably to a flooding process and reservoir information is more abundant in waterflooded leases/units. A waterflood that has a high and sustained oil-recovery response indicates favorable fluid flow characteristics that are required for high performance of the slug-type process of chemical flooding.

Technical personnel from the oil companies were asked to survey their company's waterflooded properties and present what they determined were their best-performing leases/units. In these interviews, which were typically in person, we assessed the performance of the waterfloods and

**Table 1.3** –Oil Producers contacted/interviewed for discussions of chemical flooding opportunities.

Kansas Rank	Name	2008 KS oil production (bbls)	City	State	% of KS production
1	Murfin Drilling Company	1,067,615	Wichita	KS	3.62
2	Vess Oil Corporation	1,020,954	Wichita	KS	3.47
3	Berexco	1,002,979	Wichita	KS	3.41
4	EOG Resources	814,645	Oklahoma City	OK	2.77
5	American Warrior	702,850	Garden City	KS	2.39
6	Anadarko Petroleum Corporation	586,161	Houston	TX	1.99
7	OXY USA	580,231	Houston	TX	1.97
8	Hartman Oil Company	383,870	Garden City	KS	1.30
9	McCoy Petroleum Corporation	378,387	Wichita	KS	1.28
10	Ritchie Exploration	373,282	Wichita	KS	1.27
11	John O. Farmer	362,605	Russell	KS	1.23
12	Mull Drilling Company	334,238	Wichita	KS	1.13
13	Lario Oil & Gas Company	323,614	Wichita	KS	1.10
14	Merit Energy Company	318,999	Dallas	TX	1.08
15	Woolsey Operating Company	317,614	Wichita	KS	1.08
16	Presco Western	301,961	Boulder	CO	1.03
17	T-N-T Engineering	298,368	Wichita Falls	TX	1.01
18	Mai Oil Operations	294,190	Dallas	TX	1.00
19	Herman L. Loeb	286,317	Lawrenceville	IL	0.97
20	Cimarex Energy Company	261,136	Tulsa	OK	0.89
21	Carmen Schmitt	257,725	Great Bend	KS	0.88
22	Abercrombie Energy	252,239	Wichita	KS	0.86
23	Elysium Energy	251,869	Denver	CO	0.86
24	PetroSantander (USA)	239,486	Houston	TX	0.81
25	Falcon Exploration	237,963	Wichita	KS	0.81
26	L.D. Drilling	227,863	Great Bend	KS	0.77
27	Palomino Petroleum	222,512	Newton	KS	0.76
28	Larson Operating Company	214,895	Olmitz	KS	0.73
29	Oil Producers Inc. of Kansas	211,341	Wichita	KS	0.72
30	Pintail Petroleum, Ltd.	204,604	Wichita	KS	0.69
31	Trans Pacific Oil Corporation	199,759	Wichita	KS	0.68

\*\*Continued on next page.

**Table 1.3** –Oil Producers contacted/interviewed for discussions of chemical flooding opportunities. (continued).

Kansas Rank	Eastern Kansas Rank	Name	2008 KS oil production (bbls)	City	State	% of KS production
66	1	Haas Petroleum	100,107	Kansas City	MO	0.34
70	2	Laymon Oil II	93,284	Neosho Falls	KS	0.32
75	3	D. E. Exploration	81,956	Wellsville	KS	0.28
89	4	Colt Energy	68,389	Fairway	KS	0.23
48	5	Stelbar Oil Corporation	147,584	Wichita	KS	0.50
165	6	Trimble & Maclaskey Oil	31,801	Gridley	KS	0.11
108	7	M.A.E. Resources	49,848	Parker	KS	0.17
110	8	Viva International	49,084	Lenexa	KS	0.17
135	9	Enerjex Kansas	39,205	Overland Park	KS	0.13
101	10	Piqua Petro	55,328	Piqua	KS	0.19
142	11	R J Enterprises	37,236	Garnett	KS	0.13
172	12	Town Oil Company	30,306	Paola	KS	0.10
183	13	Thomas Well Service	28,385	Mclouth	KS	0.10
193	14	KLM Exploration Co.	25,631	Mclouth	KS	0.09
204	15	Ensminger Oil	24,421	Moran	KS	0.08
208	16	Verde Oil Company	23,638	Savonburg	KS	0.08
Total % KS oil production represented						<b>45.55</b>

the state of the wells and surface equipment and determined the types of data they had available. In addition, we judged their interest and the capability of the oil company to engage in a relatively expensive chemical flooding project. This process allowed for the survey of a significant number of leases/units in Kansas and to narrow the selection to leases/units that have favorable characteristics for chemical flooding.

All of the selected leases/units met the following criteria:

- The waterflood showed a substantial, sustained oil recovery response.
- The condition of the wells and surface equipment were satisfactory. There were no or a limited number of plugged wells.
- The timing for a chemical flood in the year 2012 or so was appropriate.
- The oil company expressed considerable interest and was judged capable of participating in a chemical flooding application.

An objective of this project is to provide public information about the design of chemical floods to independent oil operators and this influenced the lease selections. A range of reservoir types with both sandstones and carbonate rocks was preferred. Three different sandstone beds and four different carbonate units are represented in central and western Kansas. The reservoirs in eastern Kansas are two different sandstone layers in the Cherokee Group.

Assessment of a demonstration project for chemical flood is improved if the flood is contained within the specified pattern area. An effective way to satisfy this criterion is to use leases where containment is indicated. Several small reservoirs were identified where the fluid containment was strongly indicated. These reservoirs appear to be representative of the larger resource of the same producing formation and are prime candidates for a demonstration project. Leases in larger reservoirs were also selected if there was reservoir information, usually based on injection and production data, that a chemical flood could be contained in the lease.

Two additional sandstone reservoirs were selected in eastern Kansas. Many of the reservoirs in eastern Kansas were heavily fractured at discovery to accelerate primary production rates. Also, many of the reservoirs are waterflooded but the waterflood performance is often poor in part due to the fracturing practices at discovery. The eastern Kansas leases were selected for economic considerations due to the shallow depths and much lower development and operating costs as compared to the rest of the state.

### Leases Selected for Laboratory Studies

Ten leases were selected for investigating the application of chemical flooding in Kansas. General information about the ten leases and the oil company operating the lease are given in **Table 1.4**. Locations of the oilfields containing the leases are shown in **Figure 1.2**. The leases are presently under waterflood and represent most of the oil-producing horizons in Kansas that we have identified as targets for chemical flooding applications (see **Table 1.1**).

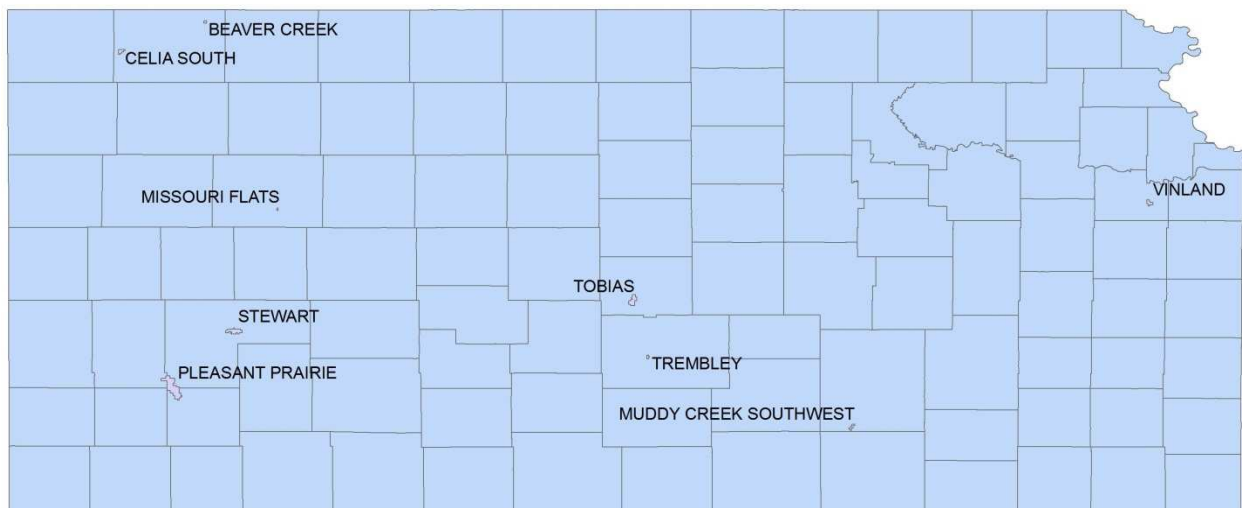


**Figure 1.2** - Location of oilfields containing the selected leases.

**Table 1.4 - Leases selected for laboratory studies.**

Lease/Unit	Trembley	Wahrman	Missouri Flats	Tobias	Celia South	Chester Waterflood	Pleasant Prairie – Chester Unit	Stewart	Woodhead	Muddy Creek SW
Operator	Berexco	Vess	Merit	Berexco	Murfin	Cimerex	Oxy	PetroSantander	Colt	Stelbar
County	Reno	Rawlins	Gove	Rice	Rawlins	Haskell	Haskell	Finney	Douglas	Butler
Field name	Trembley	Beaver Creek	Missouri Flats	Tobias	Celia South	Pleasant Prairie	Pleasant Prairie	Stewart	Vinland	Muddy Creek SW
Res. temp (°F)	110 - 115	110 - 118	118	105	138		120	108 - 120		105
Oil gravity (API)	37.3 - 35.8	33	38	35	27.5		35.7	27	27.9	38
Producing wells	4	2	7	5	19		6		14	5
Injection wells	3	1	4	5	8		4		8	2
TA wells	0	0	1	2	4		0		18 + 23	0
Net area (acre)		30	1260		1440			1550	160	160
Avg thickness (ft)	5		47	12	5		29.3	18.5	5	20
Zone	LKC “J” - Hertha	LKC “J”	Lansing & Marmaton	Simpson Sand	Cherokee Lime	Chester Sand	Chester Sand	Morrow	Cherokee Squirrel	Cherokee Bartlesville
Rock type	Limestone	Limestone	Limestone	Sandstone	Limestone	Sandstone	Sandstone	Sandstone	Sandstone	Sandstone
Comments	6' to 10' local porous zone in Hertha (LKC “J”) Limestone	Thin (4') porous zone at top of LKC "J" zone or Hertha Limestone . Geologist's log implies grainstone or packstone.	Few logs have been scanned. Available materials suggest production from several different LKC layers.	Multiple producing horizons. Only interested in Simpson waterflood. No new wells since 1985.	Thin zone: few feet. Cherokee limestone wells IP at 100 bopd. Also produces from LKC B zone. No new wells since 1983.	Long, narrow field, apparently a fluvial sandstone filling an incised valley. 70' thick, but only partially saturated. Cimerex Chester waterflood is continuous with Oxy's Pleasant Prairie Chester Unit.	The reservoir fills a valley eroded into underlying limestones. Rock appears to have fluvial characteristics. May actually be Atokan rather than Morrowan.	Shallow field, 600 to 700'. Logs are mostly gamma-unscaled neutron; few quantitative logs. Very dense well spacing.	Bartlesville sandstone is at about 2850', consists of a number of stringers, generally fining upward. May be incised-valley fill sandstone like other Bartlesville reservoirs.	

### **Sample and Data Collection**

Oil samples were collected from the leases. Most of the leases had chemical treatment programs that often included corrosion inhibitors in the production well and emulsion breakers for the flow lines and separation facilities. General procedures were developed and specific arrangements were made with office and field personnel of the production companies to collect crude oil samples that contained no or the minimal amounts of treatment chemicals. This was done in order to reduce or eliminate any effect the treatment chemicals might have on the laboratory testing.

Oil collection procedures varied according to each situation. Generally, the oil collection procedures were to suspend chemical treatment of the well for one or two applications and then collect the sample at the wellhead just before the subsequent treatment. Water was separated from the oil using barrel-testing equipment at the wellhead if equipped or using 5-gallon buckets and siphoning the oil into collection jugs.

Technical data for each lease were collected for use during the design process. The laboratory study to formulate chemical systems requires several critical data for each lease, which include the reservoir temperature, salinity and hardness of the injected water and mineralogy of the reservoir rock. These data are usually not readily known by the operators and efforts by the operators to determine these data were conducted by reviewing reports and obtaining analyses of injected brines.

### **Geological Investigations of Reservoirs**

The objectives of the geological study are 1) to identify specific producing horizons, their continuity and their suitability for chemical flood, 2) to use studies of cores to improve the understanding of the particular reservoirs, and 3) to gather the petrophysical data necessary for future modeling studies. Basic geological mapping of reservoirs, using log information in Petra, a subsurface geological information system, provided information on continuity.

Sedimentological studies of cores will provide information on vertical continuity of reservoirs, depositional environments, and obvious diagenetic features that may be relevant. Core permeability-core porosity relationships formed the basis for log porosity-permeability estimators, which allowed mapping of porosity and permeability, to accompany log-based petrophysical studies of initial fluid saturation in the reservoirs. Mineralogical studies of cores were used to predict interaction with any injected chemicals. Field cores were unavailable for all the leases except for the Stewart Field.

A summary of the geological studies are presented in Chapter 4. Reports on individual oilfields are presented in the Appendices.



## **Chapter 2**

### **Formulation and Performance of Chemical Systems**

A laboratory study to formulate chemical systems and to test the performance of the systems in flow experiments through rock material is the major component of this investigation and the subject of this and the following chapter. Results from this study are used to demonstrate the potential of chemical flooding to independent oil producers with the expressed purpose to generate commitment from producers to engage in a field demonstration of chemical flooding technology.

This chapter presents the experimental procedures, analysis methods and a summary of the results for all the selected leases/fields. In-depth studies were conducted with the crude oils from the Trembley Oilfield and the Wahrman Lease. Detailed experimental results are presented in Chapter 3 for the Trembley crude. Additional information on the study for Trembley oil [Methodology for Designing and Evaluating Chemical Systems for Improved Oil Recovery, Muhammad Shahab Ahmed, MS thesis, University of Kansas, Lawrence, KS 2012] and details of a study on the Wahrman oil [Experimental Evaluation of Surfactant Application to Improve Oil Recovery, Zhijun Liu, MS thesis, University of Kansas, Lawrence, KS, 2011] are publicly available through the libraries at the University of Kansas. Experience from these two studies was used to more quickly target chemical formulations for the other crude oils.

Chemical systems are prepared, mixed with the crude oil and observed for many days in a procedure known as phase behavior studies. Approximately 16 thousand chemical formulations were prepared for phase behavior studies. Many of these formulations were unremarkable except for possible clues to adjustment of composition for subsequent formulations. Formulations displaying favorable phase-behavior characteristics are reported.

Chemical systems that form middle-phase microemulsions with appropriate characteristics are sought during the phase behavior studies. These characteristics include: (1) the microemulsion, type III, phase that coalesce and equilibrate in less than seven days, (2) values of the equilibrium solubilization parameters for both oil and brine are greater than ten, (3) the absence of viscous phases and macroemulsions, and (4) the aqueous surfactant mixture selected for injection must be a one-phase, clear homogeneous mixture at both room temperature (simulated surface mixing facilities) and at reservoir temperature. Formulations exhibiting these criteria have been shown to correlate with efficient recovery of crude oil from rock material.

Corefloods are conducted to test the performance of chemical systems identified in the phase behavior studies. Cores are prepared at residual oil saturation by a waterflood. A chemical slug is injected and followed by the injection of a polymer drive to displace the chemical slug through the rock. The principal measure of performance is the percentage of residual oil that is recovered. Formulations that recover about 90% or better are considered efficient chemical systems.

## Experimental Procedures and Materials and Analysis Methods

**Acid numbers of the crude oils.** Alkali is a potential component of chemical formulations depending on conditions. Alkali can reduce surfactant retention in carbonate-containing rocks and can react with acidic crude oils to produce surface-active soaps which can reduce surfactant loading of the system. The acid number of a crude oil can be used to assess the responsiveness of the oil to soap production. A non-aqueous phase titration method detailed by Fan and Buckley and laboratory kit manufactured by Dexsil were used to determine the total acid number of the crude oils.

**Phase behavior studies.** Phase behavior studies are conducted by selecting a chemical system (surfactants and co-solvents) and preparing a series of solutions of the chemical system where only one formulation parameter or concentration is varied. Most often the series is prepared over a salinity range, i.e., a salinity scan. The solutions are contained in ten milliliter disposable pipettes with sealed bottoms and with markings to determine liquid phase volumes. Two series, or salinity scans, are prepared, one with and one without the crude oil being tested. The aqueous phase stability limit, APSL, is determined with the series without oil. The series with crude oil is used to determine optimum salinity, solubilization ratios and the appearance of viscous phases and gels are determined with the oil. The pipettes are sealed, shaken and then allowed to equilibrate in an oven at reservoir temperature. The tubes are visually inspected periodically to measure phase volumes and then tipped to determine fluidity of the phases. Pictures of the pipettes were taken periodically, two or three times in first seven days, to preserve an image of the microemulsion. The images were utilized to measure solubilization ratios from the interface levels. Additionally, the microemulsion phase was also visually observed for viscosity and macroemulsions. Pipettes at and near optimum salinity were the focus of the visual observations.

Optimum salinity and solubilization ratio were determined by plotting oil and water solubilization ratios as a function of salinity (Green and Willhite 1998) for the salinity scans of interest. Solubilization ratios of water,  $P_w$ , and oil,  $P_o$ , are defined as the ratio of the volume of the respective phase solubilized in the microemulsion phase to the volume of surfactant present in the microemulsion phase.

$$P_w = V_w / V_s = \frac{\text{volume of water in microemulsion phase}}{\text{volume of surfactant in microemulsion phase}} \dots\dots\dots (3.2)$$

$$P_o = V_o / V_s = \frac{\text{volume of oil in microemulsion phase}}{\text{volume of surfactant in microemulsion phase}} \dots\dots\dots (3.3)$$

All the surfactant was assumed to be in the microemulsion phase and the assumed density of the surfactant was 1.0 g/mL. In the Type III systems,  $P_w$  decrease while  $P_o$  increase with salinity. At the salinity where both become equal, that salinity is termed optimum salinity. Alkalis, NaOH and  $\text{Na}_2\text{CO}_3$  also contributed electrolytes to the formulation but the optimum salinity were generally reported exclusive of their contribution. Where the optimum salinity had to be reported as the sum of both NaCl and alkalis, the term equivalent salinity was used. Equivalent salinity was calculated as the sum of weight percent of the NaCl and the alkali.

The value where  $P_o$  and  $P_w$  are equal is defined as the optimum solubilization ratio. An optimum solubilization ratio of higher than 10 mL/mL corresponds to an ultra low IFT between the microemulsion and the oil and aqueous phase. IFT at the optimum salinity can be estimated from the solubilization ratios with the simplified Chun Huh correlation as follows:

$$\gamma = \frac{0.3}{(\sigma^*)^2} \dots\dots\dots (3.4)$$

$\gamma$  = interfacial tension  
 $\sigma^*$  = optimum solubilization ratio

Example:

at  $\sigma^* = 10$ ,

$$\gamma = \frac{0.3}{(10)^2} = 3 \times 10^{-3}$$

After mixing the surfactant formulation and oil, the fluids in the pipettes were scanned in subsequent days for presence of any *macroemulsions*, gels or other viscous phases, particularly at the optimum tube. Also, a quick evaluation of the viscosity of the type III microemulsion phase was performed by tilting and twisting the pipette, and noting the fluidity and dispersion behavior of aqueous and microemulsion phase interface. If gels or viscous microemulsion were observed, the surfactant slug was not feasible as it could potentially get trapped and cause large pressure drop in core flood.

Equilibration time, another parameter sought in the lab screening, was obtained from observing the time taken by the optimum pipettes to reach stable solubilization ratios of both water and oil. Slow equilibration time indicated a viscous microemulsion or an unstable microemulsion. Solubilization ratios may continue to drop significantly over a long time, therefore, it was necessary to keep a track of solubilization ratios with time until no change occurred to determine the equilibrium solubilization ratio.

The formulation must remain clear single phase solution at the optimum salinity at reservoir temperature after polymer has been added to it. This is to ensure the transport of surfactant through the formation. Aqueous phase stability limit (APSL) is defined as that salinity (NaCl only) at which the formulation becomes unstable either by precipitation or phase separation. For formulations that look promising, their aqueous phase stability limit (APSL) was determined. Pipettes were prepared similar to a salinity scan but without oil. A salinity gradient of 0.2-0.3wt% NaCl was used for a range of salinity encompassing the salinities below and above the optimum. The pipettes were sealed and put in the oven at reservoir temperature. The aqueous phase appearance was observed over the next 3 days to check for haziness or separation of phases.

The characteristics sought for a chemical flood formulation are:

- (1) the microemulsion, type III, phase must coalesce and equilibrate in less than seven days,
- (2) values of the equilibrium solubilization parameters for both oil and brine are greater than ten,
- (3) the absence of viscous phases and macroemulsions, and

(4) the aqueous surfactant mixture selected for injection must be a one-phase clear homogeneous mixture at both room temperature and at reservoir temperature.

Chemical formulations were prepared with surfactants, solvents, alkali and polymers in an aqueous brine solution. Surfactants, solvents and polymers tested are listed in **Table 2.1**. Alkali tested were sodium hydroxide and sodium carbonate. The alkali and other salts used to prepare brine solutions were obtained from Fisher Scientific with a USP/FCC reagent grade.

**Table 2.1** - List of chemicals that were evaluated in phase behavior studies.

<b>Trade Name(Acronym)</b>	<b>Common Chemical Name</b>	<b>Supplier</b>
<b><u>SURFACTANTS</u></b>		
Petrostep® S-1 (S1)	Alcohol Propoxy Sulfate	Stepan (via TIORCO)
Petrostep® S-2 (S2)	Internal Olefin Sulfonate	Stepan (via TIORCO)
Petrostep® S-3 (S3)	Internal Olefin Sulfonate	Stepan (via TIORCO)
Petrostep® S-8B (S8B)	Alcohol Propoxy Sulfate	Stepan (via TIORCO)
Petrostep® S-8C (S8C)	Alcohol Propoxy Sulfate	Stepan (via TIORCO)
Petrostep® S-13D (S13D)	Alcohol Propoxy Sulfate	Stepan (via TIORCO)
Petrostep C-1 (C1)	Alpha Olefin Sulfonate	Stepan (via TIORCO)
Petrostep C-5 (C5)	Alpha Olefin Sulfonate	Stepan (via TIORCO)
Alfoterra® 123-8S (A123-8S)	Alcohol Propoxy Sulfate	Sasol
Novel® TDA-3EO (TDA3)	Ethoxylated Alcohol	Sasol
Novel® TDA-6EO (TDA6)	Ethoxylated Alcohol	Sasol
Novel® TDA-9EO (TDA9)	Ethoxylated Alcohol	Sasol
Novel® TDA-12EO (TDA12)	Ethoxylated Alcohol	Sasol
Novel® TDA-30EO (TDA30)	Ethoxylated Alcohol	Sasol
<b><u>SOLVENTS</u></b>		
(SBA)	Sec butyl alcohol or 2-butanol	Fisher Scientific
(EGBE)	Ethylene glycol butyl ether	Sigma-Aldrich
(DGBE)	Diethylene glycol butyl ether	Sigma-Aldrich
(BD)	1,3 butanediol	Fisher Scientific
<b><u>POLYMERS</u></b>		
Flopaam 3330S (F3330)	Polyacrylamide (8 million Dalton, 30% hydrolysis)	SNF
Flopaam 3350S (F3350)	Polyacrylamide (12 million Dalton, 30% hydrolysis)	SNF
Flopaam 3530S (F3530)	Polyacrylamide (16 million Dalton, 30% hydrolysis)	SNF

**Corefloods.** Chemical formulations selected from phase behavior studies are then tested in flow experiments by determining the performance of the system to mobilize and displace residual oil in porous media. Field cores were not available from the 9 leases/fields that were tested. Corefloods were conducted in quarried rocks prepared from Berea sandstone and Indiana Limestone.

One-foot long and approx. 2-inch diameter cores were used for core floods. The cores were vacuumed with a brush attachment to clean the surface of any loose dirt. Next, end caps were glued with quick curing epoxy, Cytec K-20. The cores were then centered into an acrylic sleeve and the annulus was filled with an epoxy comprising Epon Resin 828 and Versamid 125 Hardner in the ratio 2:1. The epoxy was cured for 2 days, at least, before the holes were drilled to attach pressure ports. For securing pressure port tubing in the holes, several epoxies were tried; Cytec K-20 epoxy, Loctite Epoxy Marine and Superglue waterproof epoxy. All performed very well with Nickel tubing. Cytec K-20 was used with FEP 1/8 inch tubings in the pressure ports for most core floods while few later floods used nickel tubing with the other epoxies. Swagelok fittings and valves are used for connecting tubings.

Crude oil was filtered prior to injecting in the core to avoid any particulate matter in the crude oil blocking the pores. The filtration was performed by pumping the crude oil at reservoir temperature, 46.1 °C, through two 47 mm diameter membranes, a 1-micron Teflon membrane and a 1.6 micron laminated fiber glass fiber membrane. Pressure across the filter was monitored to ensure there was no break in the filter paper.

All the brines that are pumped into cores were filtered with either a 0.2 or 0.45 micron filter to filter out particulate matter and to degas. A vacuum filter flask accomplished the filtration quickly.

Quizix QX® positive displacement pump with two cylinders in tandem was used for brine pumping. During the brine and waterflood the brines were directly pumped from the pump into the core except for the synthetic formation case. For tracer, synthetic brine, oil, surfactant and polymer drive, transfer cylinders were used.

Water bath was used to maintain reservoir temperature for both horizontal and vertical core floods. They provided a fast and better temperature control as well as easier workability compared to convection oven. A Fisher Scientific Isotemp Immersion Circulator model 730 was used for controlling the temperature bath uniformly.

Varian ProStar model 350 RI Detector was used in the tracer tests on Berea sandstone core. Two brines that differed by 0.2 wt% NaCl were used as resident brine and tracer. The data from the detector was acquired with a LabView data acquisition program installed on the core flood station computers.

Chromaflex® glass transfer cylinders from Kontes Glass Co. were used to store tracer brine, synthetic formation brine, surfactant slug and polymer drive. A sliding piston separated the displacing and displaced fluids in the transfer cylinder. The pressure limit on these cylinders was

100 psi. An in house transfer cylinder was used for oil pumping. In all the cases, either brine or water was used for displacing the fluids.

To acquire pressure data from core floods, Validyne transducers model DP15-46 with diaphragms of a maximum range of 10 psi for short sections and 100 psi for the overall core pressures were used. These transducers are accurate to within a value of 0.25% of full scale. Their calibration must be checked and performed from time to time to ensure their accuracy.

ISCO Retriever IV fraction collector was used to automatically collect effluent samples from chemical flood at 30 minutes intervals. A 4.5 mL sample was collected in each 8mL vials. The number of samples and volume was just right for analysis of the aqueous phase and a good resolution of the oil cut against pore volume injected.

A handheld pH meter from Horiba model B-213 was used to measure the pH for the surfactant slug and polymer drive. Additionally, the pH meter was also used for determining pH of core flood effluent, which enables us to ascertain the transport of alkali to the end of the core.

A YSI 3200 conductivity instrument with an YSI 3252 model conductivity cell was used to measure conductivity of the waterflood brine, surfactant slug and polymer drive and finally the effluent. The cell used only 1mL of sample. Conductivity provides a measure of electrolyte concentration in the aqueous phase. A correlation between conductivity and NaCl concentration was used to determine the salinity of the samples from their conductivity. The measurement allows interpretation of the mixing behavior during the chemical flood and improving the salinity gradient design as necessary by adjusting salinity in surfactant slug and polymer drive.

The core flood procedure involved meticulous observations and measurements at all steps. From the first saturation of the core with brine to the end of chemical flood, pressure data and fluid saturations data were collected and measurements made to determine the core permeabilities, saturations, fluid mobilities and surfactant transport. The various stages in core flood experiments are described. First stage of the core flooding procedure was saturating the core with brine whose salinity was equal or close to the waterflood brine salinity. To ensure that no air was left trapped in the core, it was first flushed with CO<sub>2</sub> and then vacuumed. After saturation under vacuum, approximately 200mL of the brine was run through at back pressure of 45-55 psi to dissolve any trapped air bubbles in the rock pores. To ensure an air free core, the core was pressurized with fluid to approximately 60 psi and then shut in. After few second, outlet valve is open to let the pressurized fluid out. If the fluid volume expelled was less than 1mL, the core was deemed free of air. Otherwise more brine was flowed through with back pressure. The weight of empty core (vacuumed) and saturated core was measured to determine the volume of liquid in the core, or the pore volume.

A tracer was displaced through the core at 100% brine saturation. Generally, brine that has 0.2wt% higher salt concentration as the brine used for saturation is used as the tracer. A second run of tracer was performed with the original brine, and restored the core salinity back to starting salinity. The outlet fluid of the core was routed through the RI detector that continuously measured and sent the refractive index to the data acquisition. The temperature of the RI detector was controlled to just above the room temperature, typically at 30°C. The Quizix QX model

pump delivered and measured the volume of the injected brine accurately. The tracer was plotted against the volume of brine injected. Tracer was used to analyze the dispersion characteristic of the core. Only the cores that showed the typical longitudinal dispersion behavior were selected for further floods. Tracer was also used to verify the pore volume calculated with the gravimetric method.

Purpose of brine flood was to measure the permeability of the rock,  $k_{brine}$ , and to saturate the core with formation brine.  $K_{brine}$  was determined at 100% brine saturation. Viscosity of the brine used was measured at reservoir temperature. The core had five equally spaced pressure taps along its length. These were connected to transducers at this point and gave pressure detail at finer resolution in addition to the overall pressure. A schematic of the core and pressure transducer setup for floods is given in **Figure 2.1**. A 100 psi range transducers was used to measure the overall pressure while 10 psi range transducers were used to measure pressure in each of the six sections. The six sections were named 1 to 6 in an order from the inlet to outlet. A water bath was used to contain the core in horizontal orientation and keep it at reservoir temperature. Vertical orientation was also used for some floods. Measurements were begun only after the old brine had been fully displaced out of the core and the core had reached the reservoir temperature. Flow rates in the range of 2-6 mL/min were used to calculate permeability. The pressures across each section and the whole core were measured and used to calculate the permeability of each section.

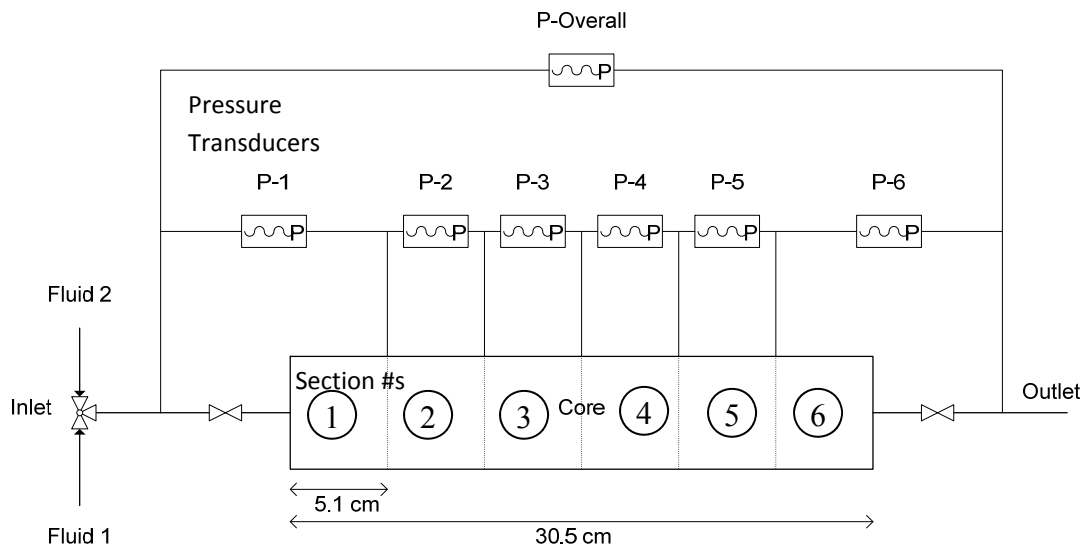


**Figure 2.1** - A schematic of the core with pressure measurement setup.

The purpose of the oil flood was to saturate the core with the oil to be tested. Oil was contained in a transfer cylinder and was displaced by brine or water being pumped into the cylinder by Quizix pump. A flow rate of 2.5-4.0 mL was used for oil flood, depending on rock permeability and utilizing the maximum range of section transducers. Pressures between 6 and 10 psi were achieved per section. Oil was pushed through a heating coil of stainless steel submerged in the same water bath as the core to bring it to reservoir temperature prior to its ingress into the core. A 100 mL burette was used to collect the brine displaced from the core. Brine collected at the

end of the oil flood represented the pore volume in the core occupied by oil. The ratio of brine volume to total pore volume of core gave the oil saturation. During the oil flood, the pressure across the sections and the whole core were monitored. When the pressures had reached steady state for all the sections and overall, the flood was stopped. Typically 4 to 5 PV oil were injected before steady state was reached. The relative permeability of oil at the end of oil flood was calculated from the pressure data, flow rate and absolute permeability measured in the brine flood.

A waterflood was carried out on the core after oil flood. Brine used could be the same as that used for brine flood or the intended formation brine, if it was synthetic formation brine. The flow rate used was 0.3 mL/min which equates to a displacement rate of 4 ft/day for the 2 inch diameter sandstone cores used. The flood was carried out at reservoir temperature. The oil displaced from the core was collected and measured in a 50 mL burette, and was used to estimate the remaining oil saturation in the core. Brine was injected into the core until the WOR in the effluent was greater than 100. Typically, this was achieved after 0.5 PV injected in sandstone cores. Pressure measurements during the floods were interpreted to monitor the movement of the oil/water interface of the oil bank. The pressure values at the end of the flood were used to calculate end point relative permeabilities to water. Oil saturation was determined by material balance.

Base permeability for relative permeability calculations was the permeability to brine at  $S_w=1.0$ . In some sandstone cores, tracer was run after the waterflood to reevaluate the dispersion characteristic of the core after it had been saturated with oil.

The most important considerations of the chemical flood were the injected surfactant slug and polymer drive design. The design considerations included salinity and viscosity of the slugs, and the slug size. Phase behavior results were used to select the optimum salinity for the slugs.

An optimized surfactant slug requires maintaining Type III conditions in the displacement region and a transition to Type I system via lower salinity at the back of the displacement region. For this purpose, the surfactant slug salinity was chosen to be at the optimum at the WOR ( $S_w/S_{orw}$ ) the surfactant would encounter when injected into the core. The salinity of polymer drive was chosen so as to induce a moderate Type III to Type I transition.

The viscosities of the surfactant slug must be sufficient to give favorable mobility control, i.e. mobility ratio of oil bank to surfactant slug of greater than 1. The required viscosity was first approximated from the end point relative permeability data from the oil and waterfloods. A starting approximation for the chemical slug viscosity was that it should be 2 to 5 times the inverse of total relative mobility ( $\lambda_{rel}$ ), defined as:

$$\mu_{app} = (\lambda_{rel})^{-1} = \left( \frac{k_{ro}^o}{\mu_o} + \frac{k_{rw}^o}{\mu_w} \right)^{-1} \dots\dots\dots (3.13)$$

Once a chemical flood had been conducted on the core, the mobilities of oil bank and surfactant slug were obtained from the pressure data of the individual sections. This information was used



to select the appropriate viscosity for the surfactant slug for next core floods. Surfactant slug size depends on the chemical slug efficiency. A 0.3 PV slug was the starting slug size, which was increased to 0.6 PV if the recovery was low with the smaller slug.

Each chemical flood was carried out at a frontal advance rate of 2 ft/day at reservoir temperature. At this flow rate, the maximum pressures during a good chemical flood ranged between 3 to 8 psi/ft depending on the rock permeability and viscosity of the slugs. The rules of thumb from field experience to simulate real conditions are to target a displacement rate of 1ft/day or a pressure drop of 1 psi/ft. However, it is believed that the oil displacement mechanism was not affected by exceeding the conventional values, and therefore, no need to lower the flow rate of the chemical flood. The core setup was the same as that used for brine flood. Both horizontal and vertical orientations were used in a water bath at reservoir temperature. The surfactant slug and polymer drive were placed in separate transfer cylinder and were pushed by either water or brine drive via piston. The Quizix pump was used to accurately deliver the flow rate. Surfactant slug was followed by polymer drive of 1.5 to 2 PV. Effluents were collected in 8 mL vials on a fraction collector. 4.5 mL was collected in each vial, which took 30 minutes at the flow rate used. Generally, the flood was stopped when the effluent became clear or the oil cut was less than 1%.

Effluents of the chemical flood were visually observed and also captured in pictures at room temperature and at reservoir temperature. Initially, the effluent produced in chemical flood was the formation brine until the oil bank broke through. The oil bank was followed by microemulsion systems and lastly by the clear polymer drive. Oil cut and oil volume were measured in each vial by measuring the height of the oil column in the vial and correlating it to respective volume. The type III microemulsion phase was treated as containing equal portions of oil and aqueous phase in volume calculations. The oil recovery is then given by:

$$\% \text{ Recovery} = \frac{\sum_{i=1}^n V_{o,i}}{S_{or} V_p} \times 100\% \dots\dots\dots (3.14)$$

- % Recovery = percent residual oil recovered
- $V_{o,i}$  = volume of oil in vial i
- $S_{ro}$  = residual oil saturation
- $V_p$  = pore volume

The aqueous phase was extracted from the vials at reservoir temperature and its viscosity, salinity and pH were measured. These measurements help understand the chemical and physical changes to the displacing and displaced fluids as a result of dispersive mixing in the core. Viscosity was measured at reservoir temperature and the other measurements on the effluent fractions were made at room conditions.

The Brookfield DV-I+ was used to measure the viscosity as only a 0.5 mL sample was needed. The lowest possible shear rate that gave accurate measurement was used for measuring the viscosity. This measurement was mostly for qualitative analysis and gave us some idea of the polymer concentration in effluent. The salinity was determined by measuring conductivity of the aqueous phase. A correlation of conductivity versus NaCl concentration was used to back calculate the salinity of the effluent sample in terms of NaCl concentration equivalents. The

salinity determination was useful for evaluating the salinity gradient design and improving them. Finally, pH was measured with Horiba portable pH meter. This measurement was also qualitative and gives an idea about the transport and consumption of alkali during the chemical flood.

## RESULTS

### Total Acid Numbers

Total acid numbers (TAN) were measured for the nine crude oils and the results are given in **Table 2.2** for two measurement techniques. Values of the total acid numbers are low and indicate the use of alkali in the chemical formulations for the purpose of producing soap is not warranted. Crude oils with acid numbers of greater than 0.5 mg KOH/g oil are considered for alkali use for soap production. The difference in values between the two methods is not significant considering the low sensitivity of the measurements at the low TAN values.

**Table 2.2** – Acid numbers of crude oils of the leases.

Lease/Unit name	Acid number (mg KOH/g of oil)	
	Non-aqueous titration	Titra-Lube TAN Kit
Trembley	0.08	0.28
Wahrman-Beaver Creek	0.11	0.19
Missouri Flats	0.09	0.23
Tobias	0.07	0.18
Celia South	0.07	0.16
Chester Waterflood	0.03	0.20
Pleasant Prairie Chester Unit	0.03	0.16
Stewart	0.21	0.17
Muddy Creek SW	0.02	0.12
Woodhead-Vinland	-	0.24

### Phase Behavior Studies

Phase behavior studies identified chemical formulations that met the criteria for efficient performance for eight of the ten crude oils. One formulation for each crude oil is given in **Table 2.3**. During the studies, formulations were prepared and tested where small changes in the concentration of one component and frequently several formulations met the criteria. The listed formulation in **Table 2.3** was deemed the best formulation in that it usually had the highest optimum solubilization ratio with a sufficient difference between the optimum salinity and the aqueous stability values. Performance of the listed formulations was tested in coreflooding experiments. The formulation for the Vinland crude oil did not meet the aqueous stability

criterion in that the chemical system was hazy and not a true solution. No formulations were identified that meet the criteria for the Stewart Field crude oil.

Surfactants in the formulations listed in Table 2.3 are a combination of an alcohol propoxy sulfate (APS) and an internal olefin sulfonate (IOS). Petrostep S1 and Petrostep S13D are APSs and Petrostep S2 is an IOS. The APS-IOS surfactant combination has been identified as a preferred system in other studies as well [Levitt et al., 2006; Flaaten et al., 2008]. The APS is the primary surfactant that reduces the IFT. The IOS is sometimes referred to as a co-surfactant that is thought to reduce ordering of the primary surfactant and the formation of highly viscous liquid crystals. The two hydrocarbon chains connected to the sulfonate group in the IOS are thought to produce the desired behavior. The favorable results of the APS-IOS system for eight of the ten crude oils indicate the widespread application of this system to crude oils from low temperature reservoirs. Sulfate-containing surfactants are susceptible to degradation at temperatures above 80 to 90 °C.

**Table 2.3** –Efficient chemical formulations for nine crude oils.

Lease name/ Crude oil	Chemical slug formulation	Temp. (°C)	Optimum solubilization ratio (mL/mL)	Optimal salinity (wt% NaCl)	Aqueous stability (wt% NaCl)
<b>Trembley</b>	0.62% Petrostep® S1 0.38% Petrostep® S2 2% SBA 1% Na <sub>2</sub> CO <sub>3</sub> 2200ppm SNF 3330S	46.1	14	4.14	4.80
<b>Wahrman- Beaver Creek</b>	0.36% Petrostep® S1 0.14% Petrostep® S2 1.75% DGBE 1% Na <sub>2</sub> CO <sub>3</sub> 1800ppm SNF 3530S	43.3	12	5.6	5.85
<b>Muddy Creek SW</b>	0.67% Petrostep® S13D 0.33% Petrostep® S2 1.5% SBA 2000ppm SNF 3330S	40.6	16	4.0	4.65
<b>Tobias</b>	0.75% Petrostep® S13D 0.25% Petrostep® S2 1.5% EGBE 1% Na <sub>2</sub> CO <sub>3</sub> 2000ppm SNF 3330S	40.6	22	2.63	3.5
<b>Missouri Flats</b>	0.42% Petrostep® S13D 0.083% Petrostep® S2 1.75% DGBE 1% Na <sub>2</sub> CO <sub>3</sub> 2500ppm SNF 3330S	47.8	16	4.12	4.25
<b>Chester Unit - Pleasant Prairie</b>	0.42% Petrostep® S13D 0.083% Petrostep® S2 1.75% DGBE 1% Na <sub>2</sub> CO <sub>3</sub> 2200ppm SNF 3330S	48.9	13	4.12	-
<b>Chester Waterflood - Pleasant Prairie</b>	0.42% Petrostep® S13D 0.083% Petrostep® S2 1.75% DGBE 1% Na <sub>2</sub> CO <sub>3</sub> 2200ppm SNF 3330S	48.9	12	3.02	4.3
<b>Celia South</b>	0.42% Petrostep® S13D 0.083% Petrostep® S2 1.75% DGBE 1% Na <sub>2</sub> CO <sub>3</sub> 3500ppm SNF 3330S	58.9	10.4	3.51	3.85
<b>Vinland – Woodhead</b>	0.45% Petrostep® S13D 0.68% Petrostep® S2 0.13% TDA6* 0.1% SNF 3530S	29	12	field brine	Hazy

The formulations in Table 2.3 contained solvents, either sec butyl alcohol (SBA), ethylene glycol butyl ether (EGBE) or Diethylene glycol butyl ether (DGBE). Solvents are used to keep the

surfactants dissolved in aqueous solution. Increased solvent concentration increases the aqueous stability and to a lesser extent the optimal salinity. Relative high concentrations of solvent were required to increase the aqueous stability value to value higher than the optimal salinity value. However, increased solvent concentration reduces the solubilization parameters. The solvent concentrations were judged to be high and reduction in solvent concentration is a target for additional optimization of the formulations.

Seven of the formulations contained sodium carbonate, an alkali component. Sodium hydroxide was also tested as an alkali component but sodium carbonate was selected for most of the formulations since similar results were obtained as for the hydroxide and due to reported field scaling issues with the use of hydroxide. Alkali was not used to produce soaps since the crude oils have low acid numbers and are not reactive. Alkali was used for the crude oils from carbonate formations in that surfactant adsorption in carbonates is reduced when the pH of the surfactant fluid is above 9.5. We found that alkali also improved the phase behavior characteristics in that formulations with alkali were more fluid and less likely to produce viscous phases. Being relative inexpensive, alkali was also used in formulations for the sandstone reservoirs. Formulations and corefloods for Muddy Creek SW were prepared with and without alkali.

The influence of adjusting the concentration of different components on the phase behavior parameters is detailed in Chapter 3 for the Trembley oil and in a Master's thesis by Liu [2011].

### **Corefloods**

Corefloods were conducted to measure the oil recovery performance of formulations identified in phase behavior studies. Performance is determined by the percentage of waterflood residual oil the chemical flood recovered. Core properties and the results of the oil floods and waterfloods conducted prior to the chemical flood are presented in **Table 2.4**. Twenty –seven floods were conducted in Berea sandstone and six floods were conducted in Indiana limestone with the Wahrman crude oil. Core #42 was prepared from crushing the limestone rock and preparing a sandpack.

**Table 2. 4 – Core properties and results of oil and waterfloods.**

Core number	Trembley								
	#2	#4	#23	#26	#27	#31	#32	#37	#39
Run #	TR1	TR2	TR3	TR4	TR5	TR6	TR7	TR8	TR9
<b>CORE PROPERTIES</b>									
Rock	Berea	Berea	Berea	Berea	Berea	Berea	Berea	Berea	Berea
Injection shape	round	round	round	round	round	round	round	round	round
Diameter (cm)	5.08	5.08	5	5	5	5	5	5	5
Area (cm <sup>2</sup> )	20.3	20.3	19.6	19.6	19.6	20.3	20.3	20.3	20.3
Length (cm)	27.5	30.5	31.0	32.0	30.5	30.3	30.3	30.3	30.3
Core Vol. (mL)	558	618	609	628	599	615	615	615	615
Pore Vol. (mL)	92	109	109	110	107	116	110	110	111
Porosity	0.16	0.18	0.18	0.17	0.18	0.19	0.18	0.18	0.18
Permeability (mD)	430	645	182	150	141	195	120	225	235
<b>OIL FLOOD</b>									
Flowrate (mL/min)	1	10	2.5	2.5	2.5	2.75	2	3.5	3.5
Swi	0.40	0.34	0.34	0.36	0.37	0.36	0.36	0.34	0.35
del P @Swi (psi)	3.2	27.2	22.5	28.1	30.0	22.0	28.0	25.0	29.0
Ko@Swi (mD)	422	550	174	144	129	186	106	208	179
Kro@Swi	0.98	0.85	0.96	0.96	0.91	0.95	0.88	0.92	0.80
Oil mobility at Swi (md/cp)	104.0	135.5	43.0	35.5	31.7	45.7	26.1	51.2	44.1
<b>WATER FLOOD- Flowrate = 0.3mL/min</b>									
Water visc (cp)	0.64	0.64	0.64	0.64	0.64	0.64	0.64	0.64	0.64
Salinity	5.15% NaCl	5.15% NaCl	5.15% NaCl	5.0% NaCl	5.0% NaCl	5.0% NaCl	6.5% NaCl	6.5% NaCl	SFB
Sor	0.361	0.377	0.413	0.389	0.367	0.386	0.401	0.378	0.368
Waterflood rec, (%)	40.3	43.1	37.3	39.1	42.0	40.0	36.0	42.4	43.8
del P @Sor (psi)	1.06	1.82	9.00	11.10	11.50	7.75	14.50	6.30	7.30
Kw@Sor (md)	60.2	38.9	8.3	6.9	6.4	9.1	4.8	11.1	9.6
Water Mob. at Sor (md/cp)	94.1	60.8	12.9	10.8	9.9	14.2	7.6	17.4	15.0
Krw@Sor	0.053	0.060	0.045	0.046	0.045	0.046	0.040	0.093	0.043
Oil/Water Mobility	1.1	2.2	3.3	3.3	3.2	3.2	3.5	2.9	2.9
Water arrival (PV)	0.62	0.325			0.230	0.260	0.225	0.225	1.225
Krw / Sw@Sor	0.03	0.04	0.03	0.03	0.03	0.03	0.02	0.06	0.03

**Table 2. 4 (continued)** – Core properties and results of oil and waterfloods.

Lease/Unit	Wahrman							
	#5	#8	#12	#14	#17	#22	#28	#29
Core number	WM1	WM2	WM3	WM4	WM5	WM6	WM7	WM8
<b>CORE PROPERTIES</b>								
Rock	Berea	Berea	Berea	Berea	Berea	Berea	-- Lime-stone --	
Injection shape	round	round	round	round	round	round	round	round
Diameter (cm)	5.08	4.9	4.9	4.9	4.9	4.9	5.1	5
Area (cm <sup>2</sup> )	20.3	18.9	18.9	18.9	18.9	18.9	20.4	19.6
Length (cm)	27.9	30.5	30.5	30.5	30.5	30.3	30.3	30.3
Core Vol. (mL)	566	575	575	575	575	571	619	595
Pore Vol. (mL)	99	100.2	98	96.4	96.4	105.1	107	104.7
Porosity	0.175	0.174	0.170	0.168	0.168	0.184	0.173	0.176
Permeability (mD)	230	179	190	191	186	190	374	189
<b>OIL FLOOD</b>								
Flowrate (mL/min)	2.97	1.5	2	2	2	2	2	2
Swi	0.316	0.34	0.337	0.348	0.336	0.349	0.474	0.467
del P @Swi (psi)	36.0	28.5	35.5	35.5	32.0	32.5	22.0	35.5
Ko@Swi (mD)	230	172	184.2	184.2	204.3	199.9	272.5	175.7
Kro@Swi	1.00	0.96	0.97	0.96	1.10	1.05	0.73	0.93
Oil mobility at Swi (md/cp)	27.9	20.9	22.3	22.3	24.8	24.2	33.0	21.3
<b>WATER FLOOD- Flowrate = 0.3mL/min</b>								
Water visc (cp)	0.64	0.64	0.64	0.64	0.65	0.76	0.73	0.60
Salinity	5.5% NaCl 1% Na <sub>2</sub> CO <sub>3</sub>	6.55% NaCl	6.55% NaCl	6.55% NaCl	5.12% NaCl	SFB 12%TDS	SFB 12%TDS	6.5% NaCl
Sor	0.302	0.393	0.414	0.404	0.423	0.440	0.336	0.276
Waterflood rec, (%)	55.8	40.5	37.6	38.0	36.3	32.5	36.2	48.2
del P @Sor (psi)	3.90	10.60	12.30	11.80	11.50	12.50	3.70	8.35
Kw@Sor (md)	16.63	7.18	6.19	6.45	6.72	7.21	21.51	8.15
Water Mob. at Sor (md/cp)	26.0	11.2	9.7	10.1	10.3	9.4	29.5	13.6
Krw@Sor	0.072	0.040	0.033	0.034	0.036	0.038	0.058	0.043
Oil/Water Mobility	1.1	1.9	2.3	2.2	2.4	2.6	1.1	1.6
Water arrival (PV)	0.38	0.27	0.25	0.23			0.12	0.26
Krw / Sw@Sor	0.05	0.02	0.019	0.020	0.021	0.021	0.038	0.031

**Table 2. 4 (continued)** – Core properties and results of oil and waterfloods.

Lease/Unit	----- Wahrman -----				MuddyCreek		Tobias	MO Flats
Core number	#42	#47	#48	#30	#6	#43	#7	#15
Run #	WM9	WM10	WM11	WM12	MC1	MC2	TB1	MF1
<b>CORE PROPERTIES</b>								
Rock	crushed LS	----- Limestone -----			Berea	Berea	Berea	Berea
Injection shape	round	Round	round	round	round	round	round	round
Diameter (cm)	5.08	5.08	3.81	5.1	5.08	5.0	5.08	4.9
Area (cm <sup>2</sup> )	20.3	20.3	11.4	20.4	20.3	19.6	20.3	18.9
Length (cm)	30.3	30.3	30.3	30.5	27.7	30.3	28.8	30.5
Core Vol. (mL)	614	614	345	623	561	595	584	575
Pore Vol. (mL)	108.9	95.3	140	110	101.3	117.1	101.7	105.2
Porosity	0.177	0.155	0.405	0.177	0.180	0.197	0.174	0.183
Permeability (mD)	286	257	908	200	282	226	265	141
<b>OIL FLOOD</b>								
Flowrate (mL/min)	1	1.5	5	3	5	5	4.36	2.5
Swi	0.370	0.410	0.336	0.491	0.37	0.354	0.356	0.37
del P @Swi (psi)	34.6	22.9	19.5	39.3	22.7	32.5	28.0	36.0
Ko@Swi (mD)	87.3	197.9	1377.4	230.4	282	210	260	140.3
Kro@Swi	0.31	0.77	1.52	1.15	1.00	0.93	0.98	1.00
Oil mobility at Swi (md/cp)	10.6	24.0	167.0	27.9	73.6	58.2	54.2	27.5
<b>WATER FLOOD- Flowrate = 0.3mL/min</b>								
Water visc (cp)	0.70	0.70	0.70	0.76	0.67	0.70	0.67	0.62
Salinity	2.0% NaCl	8.5% NaCl	6.25% NaCl	SFB 12%TDS	4.1% NaCl	4.02% NaCl	3.49% NaCl	4.27% NaCl
Sor	0.434	0.337	0.278	0.316	0.355	0.341	0.377	0.409
Waterflood rec, (%)	31.1	42.8	58.2	37.9	43.7	47.2	41.5	35.1
del P @Sor (psi)	9.48	10.60	2.55	6.60	4.26	4.84	4.55	15.10
Kw@Sor (md)	8.12	7.26	178.74	12.64	15.84	16.40	15.40	4.88
Water Mob. at Sor (md/cp)	11.6	10.4	255.3	16.6	23.6	23.4	23.0	7.9
Krw@Sor	0.028	0.028	0.197	0.063	0.056	0.073	0.058	0.035
Oil/Water Mobility	0.9	2.3	0.7	1.7	3.1	2.5	2.4	3.5
Water arrival (PV)	0.20			0.06	0.27	0.21	0.26	0.22
Krw / Sw@Sor	0.016	0.019	0.142	0.043	0.04	0.05	0.04	0.02



**Table 2. 4 (continued)** – Core properties and results of oil and waterfloods.

Lease/Unit	Chester		Chester Unit		----- Woodhead- Vinland -----			
	Celia	WF	#16	#18	#38	#44	#45	#33
Core number	#19	#25	#16	#18	#38	#44	#45	#33
Run #	CS1	CWF1	PP1	PP2	VN1	VN2	VN3	VN4
<b>CORE PROPERTIES</b>								
Rock	Berea	Berea	Berea	Berea	Berea	Berea	Berea	Berea
Injection shape	round	Round	round	square	round	round	round	round
Diameter (cm)	5	4.9	4.9	5.08	5	5	5.05	5.1
Area (cm <sup>2</sup> )	19.6	18.9	18.9	25.8	20.5	19.6	20.0	20.4
Length (cm)	30.3	30.5	30.5	30.5	30.5	30.5	29.5	30.5
Core Vol. (mL)	595	576	575	787	625	599	591	623
Pore Vol. (mL)	112.8	105.9	99	145.5	116.5	119	111	109.5
Porosity	0.190	0.184	0.172	0.185	0.186	0.199	0.188	0.176
Permeability (mD)	136	143.5	210	152	166.5	204	202	177
<b>OIL FLOOD</b>								
Flowrate (mL/min)	1	1.75	2.25	2.5	0.5	0.3	0.3	0.4
Swi	0.322	0.374	0.33	0.337	0.312	0.328	0.306	0.342
del P @Swi (psi)	25.2	34.6	28.5	33.8	40.0	20.9	21.0	31.7
Ko@Swi (mD)	135.2	162.0	225.2	156.3	191.4	229.4	216.5	193.9
Kro@Swi	0.99	1.13	1.07	1.03	1.15	1.12	1.07	1.10
Oil mobility at Swi (md/cp)	15.0	20.0	31.3	21.4	4.6	5.5	5.2	4.6
<b>WATER FLOOD- Flowrate = 0.3mL/min</b>								
Water visc (cp)	0.51	0.61	0.60	0.61	0.93	0.93	0.93	0.93
Salinity	5.08% NaCl	5.08% NaCl	5.12% NaCl	4.43% NaCl	6.25% NaCl	3.25	2.3	2.3
Sor	0.419	0.384	0.434	0.463	0.440	0.408	0.441	0.418
Waterflood rec, (%)	38.2	38.6	35.0	30.2	36.0	39.4	36.5	36.4
del P @Sor (psi)	3.60	15.20	9.80	7.30	22.20	13.00	13.75	16.80
Kw@Sor (md)	5.36	4.76	7.28	7.26	4.56	8.12	7.28	6.04
Water Mob. at Sor (md/cp)	10.5	7.8	12.1	11.9	4.9	8.8	7.9	6.5
Krw@Sor	0.039	0.033	0.035	0.048	0.027	0.040	0.036	0.034
Oil/Water Mobility	1.4	2.6	2.6	1.8	0.9	0.6	0.7	0.7
Water arrival (PV)		0.23	0.195	0.225	0.280			
Krw / Sw@Sor	0.02	0.02	0.02	0.03	0.015	0.024	0.020	0.020

Core properties were reasonably consistent for quarried rock cores. Permeabilities of the Berea sandstone cores mostly ranged between 150 and 250 md. Berea cores #2 and #4 were from earlier purchases and had higher permeabilities. Permeabilities of the Indiana limestone cores were more variable. Initial tracer curves at 100% brine saturations showed significantly larger mixing zones developed during flow through the limestone cores than in the sandstone cores.

Oil floods were conducted at high flow rates, within pressure constraints, to achieve initial oil saturations. Waterfloods were conducted at 0.3 mL/min which corresponded to approximately 2 ft/day frontal advance rates. Relative endpoint permeabilities to oil and water indicate water wettability for both Berea and Indiana cores, with the Berea being more consistently water wet.

Parameters and results of the chemical floods are given in **Table 2.5**. Recoveries of tertiary oil ranged from 21 to 99%. Recoveries were higher in the Berea sandstone cores with 22 of the 27 runs recovering 70% or greater of the waterflood residual oil. Oil recovery was greater than 70% in only one of the six experiments conducted in the Indiana limestone. The limestone corefloods are described separately.

An arbitrary benchmark for oil recovery from the chemical flood corefloods was set at 90% or greater. **Table 2.6** presents the highest recoveries achieved for each crude oil. The benchmark recovery value was achieved for seven of the nine crude oils tested. The high oil recoveries were indicative of suitable procedures and sufficient criteria for the phase behavior studies to identify efficient chemical systems.

Nine corefloods conducted with Trembley crude oil are these runs are described in detailed in Chapter 3. Detailed description of the twelve corefloods conducted with the Wahrman-Beaver Creek oil are given by Liu [20110]. Four corefloods were conducted with the Woodhead-Vinland crude oil. These runs used chemical formulations in which the phase behavior criteria were not attained. The highest oil recovery was 82%, again indicating the utility of the phase behavior criteria for identifying formulations.

Two corefloods were conducted with Muddy Creek crude oil using the similar chemical formulations. Both formulations met the phase behavior criteria but one formulation contained alkali (1.0% sodium carbonate) and the other did not. The system containing alkali recovered 99% of the tertiary oil while the system without alkali recovered 77%. These runs imply that alkali might play an important role in high recovery systems. All the corefloods that recovered 90% or greater of the tertiary crude oil in this study contained 1.0% alkali.

Attempts were made to correlate results and parameters from all the corefloods. The one relationship that correlated well was oil recovery as a function of the amount of chemical injected. This is shown in **Figure 2.2** where tertiary oil recovery is plotted versus the amount of chemical injected in the chemical slug. The amount of chemical was assessed by multiplying the chemical slug size in terms of % of pore volume by the total weight percent of surfactant, alcohol and polymer in the chemical slug. Alkali is a relatively inexpensive component and not considered. The results in the figure for the Berea sandstone runs shows oil recovery increases with the amount of chemical injected. Little improvement in recovery is seen in the Berea

sandstone cores with increases in the amount of chemical injected above a value of about 1.0. Oil recoveries in limestone cores were generally poor and no correlation was indicated.

***Chemical floods in limestone.*** The largest portion of the laboratory work including the coreflooding was conducted with crude oils from Trembley and Wahrman-Beaver Creek, both of which produce from limestone formations. Chemical formulations for the Wahrman oil were selected for testing in limestone. Six chemical floods were conducted in quarried Indiana limestone since field cores from the selected leases were not available. Chemical formulations that recovered greater than 90% of the oil from Berea sandstone cores only recovered between 27 and 50% in the limestone cores [Cores #28, #29, #47 and #48]. Several possibilities for the reduced performance in limestone were investigated. The greater dispersive mixing in the limestone was addressed by injecting the chemical slug continuously in order to reduce the effects of mixing in Core #42. In addition, a core was crushed, sieved and a sandpack prepared to have a medium with much less dispersive mixing. A 0.6 PV chemical slug followed by a polymer drive were injected through the sandpack in the Core #48 flow experiment. The possibility of insufficient mobility control during chemical flooding was addressed by conducting a flood with increased polymer concentration in Core #47. A summary of the chemical floods in the limestone media for the Wahrman crude oil and the Petrostep S1 and S2 formulation are given in **Table 2.7**. Greater oil recoveries were measured for the process modifications but the values were not at the 90% recovery level measured for the same chemical formulation in the Berea sandstone cores.

Another possible cause of the reduced performance in limestone is increased surfactant adsorption. We tested several wet chemistry methods (ion specific electrodes, two-phase and one phase titrations) and liquid chromatography (LC) with a UV/Vis detector to determine surfactant concentrations in effluents from flow experiments. None of the methods provided the accuracy

**Table 2.5** – Parameters and results of chemical floods in laboratory cores.

Lease/Unit	Trembley								
Core number	#2	#4	#23	#26	#27	#31	#32	#37	#39
Run #	TR1	TR2	TR3	TR4	TR5	TR6	TR7	TR8	TR9
<b>Chemical Flood Parameters</b>									
Surfactant 1	0.62% S1	0.62% S1	0.62% S1	0.31% S1	0.31% S1	0.31% S1	0.62% S1	0.62% S1	0.62% S1
Surfactant 2	0.38% S2	0.38% S2	0.38% S2	0.19% S2	0.19% S2	0.19% S2	0.38% S2	0.38% S2	0.38% S2
Surfactant 3									
Alcohol	2% SBA	2% SBA	2% SBA	1.25% SBA	1.38% DGBE	1.38% DGBE	1.38% DGBE	2% SBA	2% SBA
Na2CO3 (%)	1.0	1.0	1.0	1.0	1.0	1.0	1.0	1.0	1.0
Polymer	0.20% F3330s	0.20% F3330s	0.22% F3330s	0.22% F3330s	0.22% F3330s	0.20% F3330s	0.23% F3330s	0.22% F3330s	0.22% F3330s
NaCl (%)	4.15	4.14	4.25	4.25	5	5	5.05	4.4	4.4
Slug vol. (PV)	0.3	0.3	0.3	0.3	0.3	0.6	0.6	0.3	0.3
Tot. Conc (%)	3.2	3.2	3.225	1.975	1.975	2.1	2.11	3.22	3.22
Flowrate (mL/min)	0.15	0.15	0.15	0.15	0.15	0.15	0.15	0.15	0.15
Velocity (ft/day)	2.13	1.98	2.01	2.07	2.01	1.86	1.97	1.97	1.96
Solub Ratio	14	14				12.5			
Low S.R. Visc (cp)	15	12	21	19		15.7	17.5	21	
<b>Polymer Drive</b>									
Poly. conc. (%)	0.25	0.25	0.25	0.23	0.23	0.23	0.24	0.25	0.25
NaCl (%)	2.94	2.94	2.94	3.33	4.90	4.30	4.30	4.10	4.10
Low S.R. visc (cp)			27	21		18.1	21	21	
<b>Chemical Flood Results</b>									
Oil arrival (PV)	0.19	0.245	0.15	0.2	0.18	0.18	0.15	0.15	0.15
Max Oil cut (%)	50	51	56.5	40	47	46	46	44	44
<b>Mobility (md/cp)</b>									
Oil bank	75	49	10.3	8.6	7.9	11.3	6.1	13.9	12
Chem. slug	59	132	4.2	3.0	2.9	6.4	3.9	5.8	5.8
Poly. drive	1.3	1.3	3.5	12.7	13.7	14.8	7.5	7.5	7.5
<b>Tertiary oil rec. (%)</b>	<b>90</b>	<b>72</b>	<b>87</b>	<b>59</b>	<b>62</b>	<b>75</b>	<b>82</b>	<b>91</b>	<b>86</b>
Chem use (lb/bbl oil)	10.3	12.4	9.4	9.0	9.1	15.3	13.5	9.8	10.7

**Table 2.5 (continued)** – Parameters and results of chemical floods in laboratory cores.

Lease/Unit	Wahrman							
	#5	#8	#12	#14	#17	#22	#28	#29
Core number								
Run #	WM1	WM2	WM3	WM4	WM5	WM6	WM7	WM8
<b>Chemical Flood Parameters</b>								
Surfactant 1	0.36% S1	0.36% S1	0.36% S1	0.36% S1	0.36% S1	0.36% S1	0.36% S3	0.36% S4
Surfactant 2	0.14% S2	0.14% S2	0.14% S2	0.14% S2	0.14% S2	0.14% S2	0.14% S4	0.14% S5
Surfactant 3								
Alcohol	1.75% DGBE	1.75% DGBE	1.75% DGBE	1.75% DGBE	1.75% DGBE	1.75% DGBE	1.75% DGBE	1.75% DGBE
Na2CO3 (%)	1.0	1.0	1.0	1.0	1.0	1.0	1.0	1.0
Polymer	0.23% F3350s	0.3% F3350s	0.3% F3350s	0.18% F3530s	0.18% F3530s	0.18% F3530s	0.18% F3530s	0.18% F3530s
NaCl (%)	5.55	5.65	5.65	5.65	5.65	5.65	5.65	5.65
Slug vol. (PV)	0.3	0.6	0.3	0.6	0.6	0.6	0.6	0.6
Tot. Conc (%)	2.48	2.55	2.55	2.43	2.43	2.43	2.43	2.43
Flowrate (mL/min)	0.15	0.15	0.15	0.15	0.15	0.15	0.15	0.15
Velocity (ft/day)	2.00	2.16	2.20	2.24	2.24	2.04	2.01	2.05
Solub Ratio	11.2	11.2	11.2	11.2	12	12	12	12
Low S.R. Visc (cp)	29	60	60	16	16	19.5	19.5	23
<u>Polymer Drive</u>								
Poly. conc. (%)	0.30	0.30	0.30	0.30	0.18	0.18	0.18	0.18
NaCl (%)	4.60	4.60	4.60	4.60	4.60	4.60	4.60	4.60
Low S.R. visc (cp)		60	60	60	16	27	27	35
<b>Chemical Flood Results</b>								
Oil arrival (PV)	0.38	0.21	0.16	0.19	0.15	0.13	0.17	0.31
Max Oil cut (%)	38.6	55	57	59	50	50	26	15
<u>Mobility (md/cp)</u>								
Oil bank	20.8	9.0	7.7	8.1	8.3	7.6	23.6	10.9
Chemical slug	6.5	4.2	2.2	6.2	8.6		24.8	2.5
Polymer drive	4.80	11.40	18.00	6.00	4.94		4.32	10.50
<b>Tertiary oil recovery (%)</b>	<b>70</b>	<b>97</b>	<b>88</b>	<b>99</b>	<b>95</b>	<b>98</b>	<b>39</b>	<b>27</b>
Chem use (lb/bbl oil)	12.3	14.1	7.4	12.8	12.7	11.9	39.0	68.5

**Table 2.5 (continued)** – Parameters and results of chemical floods in laboratory cores.

Lease/Unit	----- Wahrman -----				-- MuddyCreek --		Tobias	MO Flats
Core number	#42	#47	#48	#30	#6	#43	#7	#15
Run #	WM9	WM10	WM11	WM12	MC1	MC2	TB1	MF1
<b>Chemical Flood Parameters</b>								
Surfactant 1	0.36% S1	0.36% S1	0.36% S1	0.66% TDA12	0.67% S13D	0.67% S13D	0.75% S13D	0.417% S1
Surfactant 2	0.14% S2	0.14% S2	0.14% S2	0.39% S1	0.33% S2	0.33% S2	0.25% S2	0.083% S2
Surfactant 3								
Alcohol	1.75% DGBE	1.75% DGBE	1.75% DGBE		1.5% SBA	1.5% SBA	1.5% EGBE	1.75% DGBE
Na2CO3 (%)	1.0	1.0	1.0		1.0		1.0	1.0
Polymer	0.18% F3530s	0.3% F3530s	0.18% F3530s	0.15% F3530s	0.3% F3330s	0.2% F3330s	0.3% F3330s	0.25% F3330s
NaCl (%)	5.65	5.65	5.65	SFB	3.11	4.02	2.49	4.12
Slug vol. (PV)	2	0.6	0.6	0.6	0.6	0.3	0.6	0.6
Tot. Conc (%)	2.43	2.43	2.43	1.2	2.8	2.7	2.8	2.5
Flowrate (mL/min)	0.15	0.15	0.3	0.15	0.15	0.15	0.15	0.15
Velocity (ft/day)	1.97	2.25	3.07	1.96	1.94	1.83	2.01	2.05
Solub Ratio	12	12	12		15	16	12	12
Low S.R. Visc (cp)								
<u>Polymer Drive</u>								
Poly. conc. (%)		0.18	0.21	0.15	0.30	0.30	0.30	0.28
NaCl (%)		4.60	4.60	11.50	2.17	3.20	2.44	3.58
Low S.R. visc (cp)								31
<b>Chemical Flood Results</b>								
Oil arrival (PV)	0.06	0.24	0.52	0.04	0.17	0.31	0.17	0.15
Max Oil cut (%)	28	34	35.5	31	55	48	49	56
<u>Mobility (md/cp)</u>								
Oil bank			204	12	19	19	18	6.3
Chemical slug	5.3		36.9	15.7	5.5	5.5	8.7	3.7
Polymer drive			3.0	1.9	7.5	7.5	6.0	12.9
<b>Tertiary oil recovery (%)</b>	<b>60</b>	<b>50</b>	<b>47</b>	<b>80</b>	<b>99</b>	<b>77</b>	<b>98</b>	<b>91</b>
Chem use (lb chem/bbl oil)	65.3	30.3	39.1	10.0	16.8	10.8	15.9	14.1

**Table 2.5 (continued)** – Parameters and results of chemical floods in laboratory cores.

Lease/Unit	Celia	Chester WF	Chester Unit		----- Woodhead- Vinland ----			
Core number	#19	#25	#16	#18	#38	#44	#45	#33
Run #	CS1	CWF1	PP1	PP2	VN1	VN2	VN3	VN4
<b>Chemical Flood Parameters</b>								
Surfactant 1	0.417% S1	0.417% S1	0.417% S1	0.07% S13D	0.15% S13D	0.33% S13D	0.45% S13D	0.4% S13D
Surfactant 2	0.083% S2	0.083% S2	0.083% S2	0.07% S2	0.1% S2	0.11% TDA6	0.13% TDA6	0.25% TDA6
Surfactant 3				0.36% S3	0.25% S3	0.55% S3	0.68% S3	0.6% S3
Alcohol	1.75% DGBE	1.75% DGBE	1.75% DGBE	0.25% BD	0.25% BD	0	0	0
Na2CO3 (%)	1.0	1.0	1.0	1.0	1.0	0	0	0
Polymer	0.35% F3330s	0.22% F3330s	0.25% F3330s	0.2% F3330s	0.2% F3330s	0.1% F3530s	0.1% F3530s	0.1% F3530s
NaCl (%)	3.51	4.02	4.12	3.43	5.25	3.3	SFB	SFB
Slug vol. (PV)	0.6	0.6	0.6	0.6	0.3	0.30	0.45	0.45
Tot. Conc (%)	2.6	2.47	2.5	0.95	0.95	1.1	1.35	1.35
Flowrate (mL/min)	0.1	0.15	0.1	0.15	0.15	0.15	0.15	0.15
Velocity (ft/day)	1.27	2.04	1.45	1.48	1.85	1.82	1.88	1.97
Solub Ratio	10.4	12	13	12	12	10	12	15
Low S.R. Visc (cp)	20		19.7		25.0	25.0	25.0	
<u>Polymer Drive</u>								
Poly. conc. (%)	0.25	0.25	0.28	0.20	0.20	0.10	0.11	0.10
NaCl (%)	3.16	3.56	3.58	3.10	6.25	2.75	1.76	1.76
Low SR visc (cp)	25		30				25	
<b>Chemical Flood Results</b>								
Oil arrival (PV)	0.19	0.15	0.15	0.16	0.24	0.22	0.22	0.22
Max Oil cut (%)	48	48	60	30	24	50	55	40
<u>Mobility (md/cp)</u>								
Oil bank	8.4	6.2	9.7	9.5	3.9	7.0	6.3	5.2
Chemical slug	4.7	4.8	7.1	2.2	0.4	1.3	7.2	1.6
Polymer drive	4.8	12.0	5.7	12.0	48.0	12.0	7.5	18.0
<b>Tertiary oil recovery (%)</b>	<b>72</b>	<b>98</b>	<b>98</b>	<b>54</b>	<b>21</b>	<b>46</b>	<b>82</b>	<b>70</b>
Chem use(lb chem/bbl oil)	18.1	13.8	12.3	8.0	10.8	6.2	5.9	7.3

**Table 2.6** – Highest oil recovery achieved for each crude oil.

Field/Lease	Number of chemical flood tests	Rock	Highest Oil Recovery (% tertiary)
Trembley	9	Berea SS	91
Wahrman	6	Berea SS	98
	6	Indiana LS	79
Pleasant Prairie	2	Berea SS	95
Muddy Creek	2	Berea SS	97
Missouri Flats	1	Berea SS	93
Tobias	1	Berea SS	97
Chester WF	1	Berea SS	94
Celia South	1	Berea SS	72
Woodhead	4	Berea SS	82

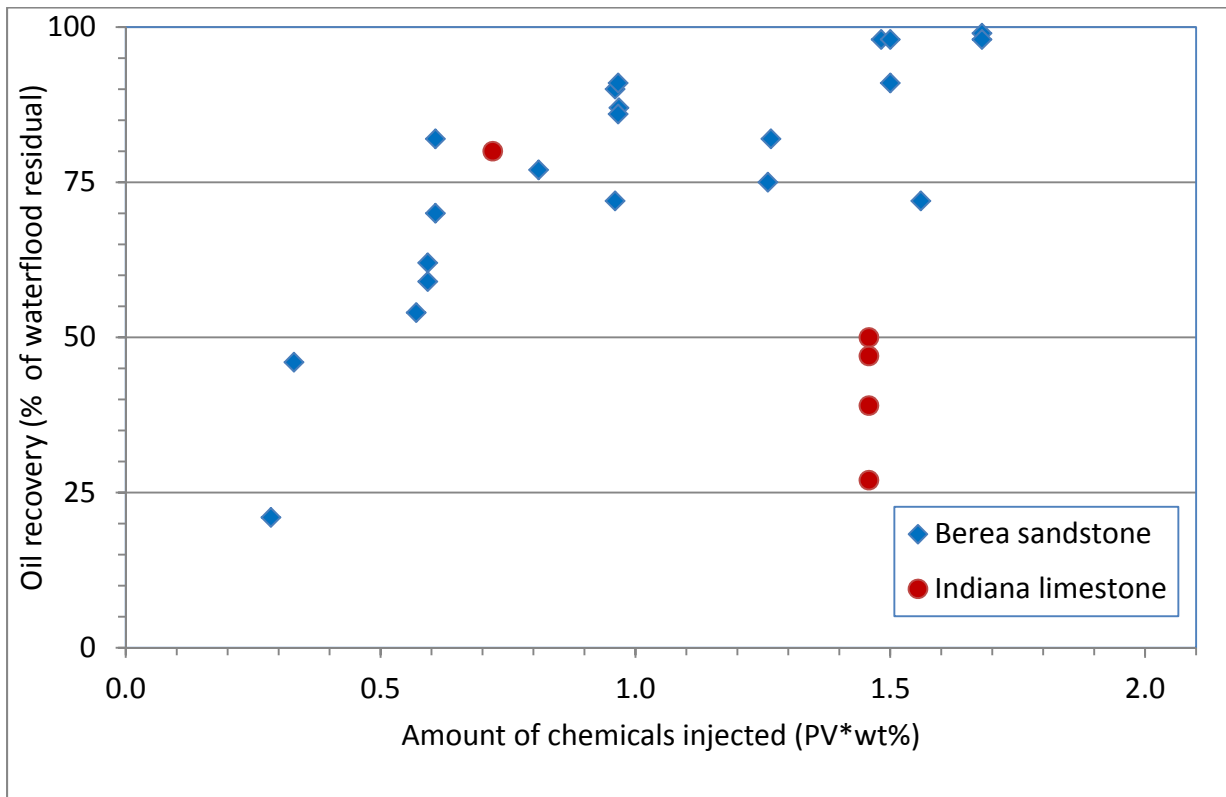


**Figure 2.2** – Oil recovery as a function of the amount of chemical injected.



required for surfactant concentrations in core effluent samples to perform an accurate surfactant mass balance for the flow experiments. An LC method using an evaporative light scattering detector (ELSD) was developed at the University of Texas Chemical Enhanced Oil Recovery (UT-CEOR) project for this type of analysis. This method was attempted but was not operational before the end of this research project.

**Table 2.7** - Summary of chemical floods with Warhman crude oil in Indiana Limestone.

Core#	Formulation/Plan modification	Oil recovery (%)	Results / comments
Core 28	First limestone run; 0.6PV slug, SFB resident in core.	39	Mixing/dispersion was thought to be the reason of low oil recovery.
Core 29	NaCl brine was at optimum salinity in core; 0.6PV slug.	27	Resident brine did not cause low oil recovery.
Core42	Continuous chemical slug injection, NaCl brine.	60	Mixing (dispersion) or adsorption does not appear to be the problem.
Core47	0.6PV slug; Increased polymer concentration.	50	Decreasing mobility ratio provided some improvement.
Core48	0.6PV slug. Sandpack prepared with crushed limestone; Much lower dispersive mixing.	55	Mixing/dispersion does not appear to be the problem.

Work was conducted to formulate an alternate chemical system for the Warhman crude oil using synthetic formation brine and alternate surfactants. Phase behavior studies were conducted using different anionic/nonionic surfactant blends without alcohol or alkali and using synthetic formation brine as the vehicle. **Table 2.8** shows the composition and characteristics of the selected chemical formulation. This formulation does not meet the aqueous phase stability criterion at reservoir temperature and it has a relatively low viscosity (6 cp). A photograph of the phase behavior tubes and a plot of the solubilization parameters as a function of water-oil ratio (WOR) is presented in **Figure 2.3** for the selected formulation.

**Table 2.8** - Chemical formulation for tertiary recovery of Warhman crude oil in limestone.

OIL	Temp (°C)	Surfactant	Alcohol	Alkali	Polym	Aqueous phase Appearance	Salt	Solub Ratio	Age (days)
Warhman (Beaver Creek)	43	NovelTDA12 PetrostepS1 5:3 1.05%	No	No	1500 ppm Flopaam 3530s	Transparent @ room T Separates after 1day at 43C	SFB ~12% TDS	11.0 @ WOR= 3.5	7

Core #30 is an Indiana limestone rock sample having 2 in. diameter x1 ft long and a pore volume of 108.5 mL determined by the gravimetric method and the integration of the tracer curve. The core has 0.176 porosity and 200 mD overall permeability and section permeabilities ranging from 126 to 246 mD. Tracer breakthrough was after 50 ml injected representing 45.5% of the

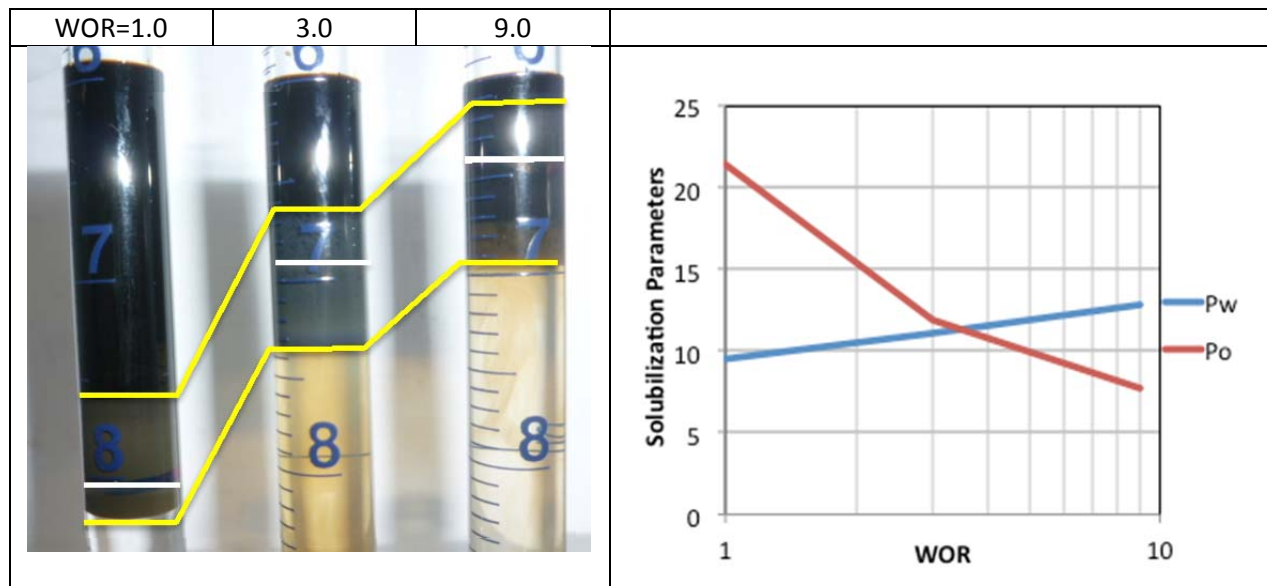


**Figure 2.3** - Phase behavior and solubilization parameters for the chemical formulation used in Core 30 (limestone).

pore volume, which is relatively early and consistent with relatively high dispersivity observed for the Indiana limestone cores. 99% of the tracer concentration is detected at the production port after 160 ml or after 1.48 pore volumes injected. Oil flood and waterflood data are given in Table 2.4.

The injection plan for the chemical flood is presented in **Table 2.9**. Chemical flooding was conducted at 0.15 ml/min (2.15 ft/day) flow rate by injecting 0.6 PV of the chemical formulation followed by the polymer drive until low oil cut was observed in the effluent.

**Figure 2.4** presents photographs of the effluent vials after 3 days of equilibration at reservoir temperature. Oil and surfactant breakthrough occurred early. Although this is considered negative, the oil recovery was higher than in previous comparable core floods. Middle phase microemulsions were observed in most of the effluent vials, indicating that optimum conditions were obtained for most of the flood. Oil recovery performance of the chemical flood is presented in **Figure 2.5**. **Table 2.10** shows parameters extracted from chemical flooding results and the comparison with previous runs in Indiana limestone cores.

**Table 2.9** - Chemical flood injection plan used for Core 30.

	Surfactant 1	Surfactant 2	Alcohol	Alkali	Polymer	Salt
	<b>Petrostep S1</b>	<b>Novel TDA-12</b>			<b>Flopaam 3530s</b>	<b>Synthetic formation Brine</b>
Surfactant Slug <b>0.6 PV</b>	<b>0.39%</b>	<b>0.66%</b>	<b>No</b>	<b>No</b>	<b>1500ppm</b>	<b>about 12.5%TDS</b>
<b>Polymer Drive</b>					<b>1500ppm</b>	<b>80% Synthetic formation brine + 20% water</b>

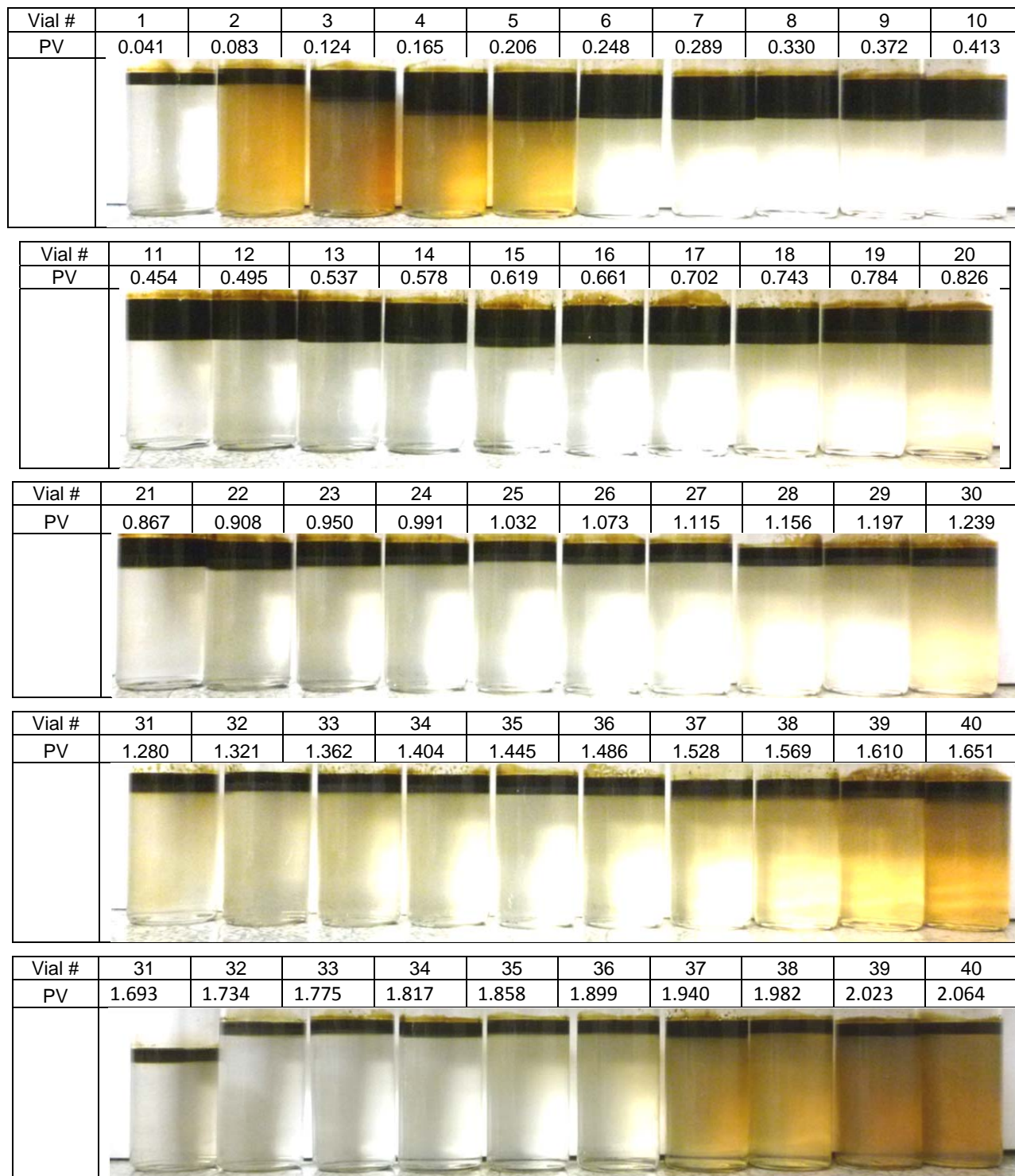


**Figure 2.4 - Photographs of the effluent vials from chemical flooding in Core 30.**

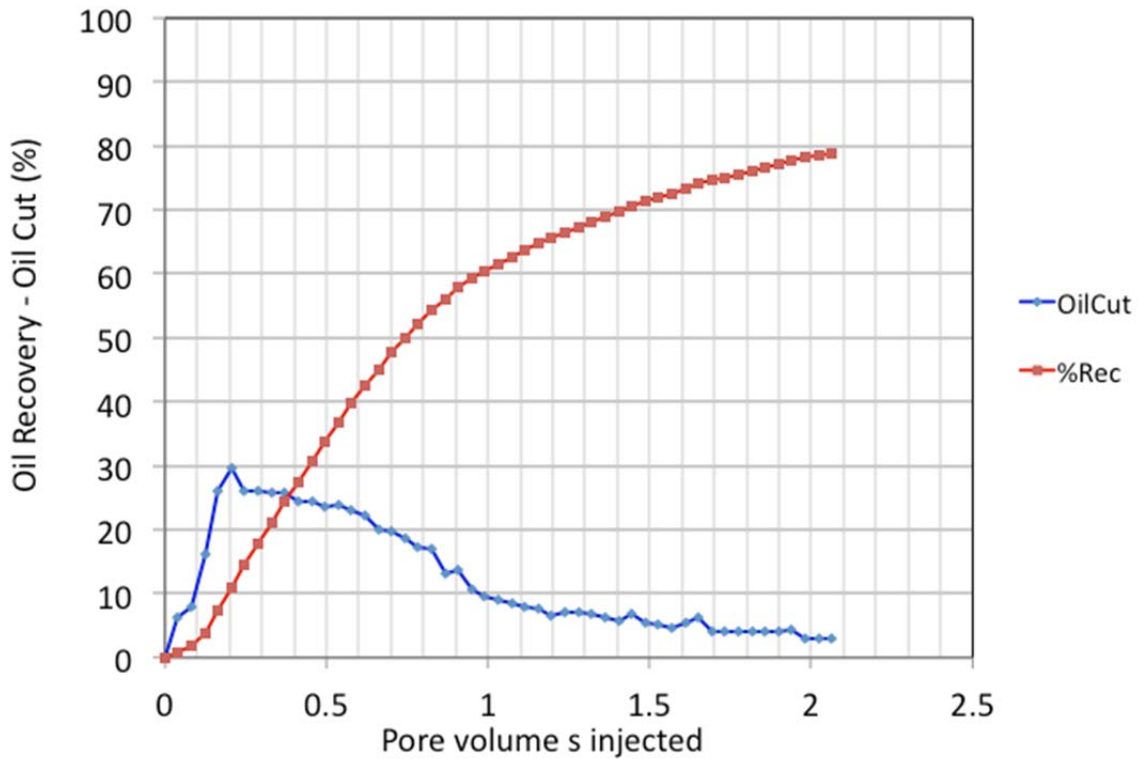


**Figure 2.5** - Oil cut and tertiary oil recovery for chemical flood in Core 30.

**Table 2.10** - Results of chemical flood in Core 30 and comparison with previous corefloods.

	Oil Bank BT (PVI)	Max Oil Cut %	Max DeltaP (psi)	Surf-BT (PVI)	%TertRec @Surf-BT	% TOR	Sor	Chem Usage (lb of chemicals/bbl of oil produced)
Core 28	0.17	26	2.2	0.6	33	39	0.20	39.0
Core 29	0.31	25	23	0.3	17	27	0.20	68.5
Core 30	0.025	30	3.8	0.04	2	79	0.08	10.1

**Figure 2.6** shows the overall and sections differential pressure during chemical flooding of Core #30. The oil bank differential pressure is about 0.8 psi/section. The differential pressure of the surfactant solution flowing at near 100% saturation is about 0.3 psi/section which is lower than the 0.8 psi/section for the oil bank meaning. Apparent viscosity of the surfactant slug is about 6.5 cp. The early surfactant breakthrough was in part due to the lack of mobility control.

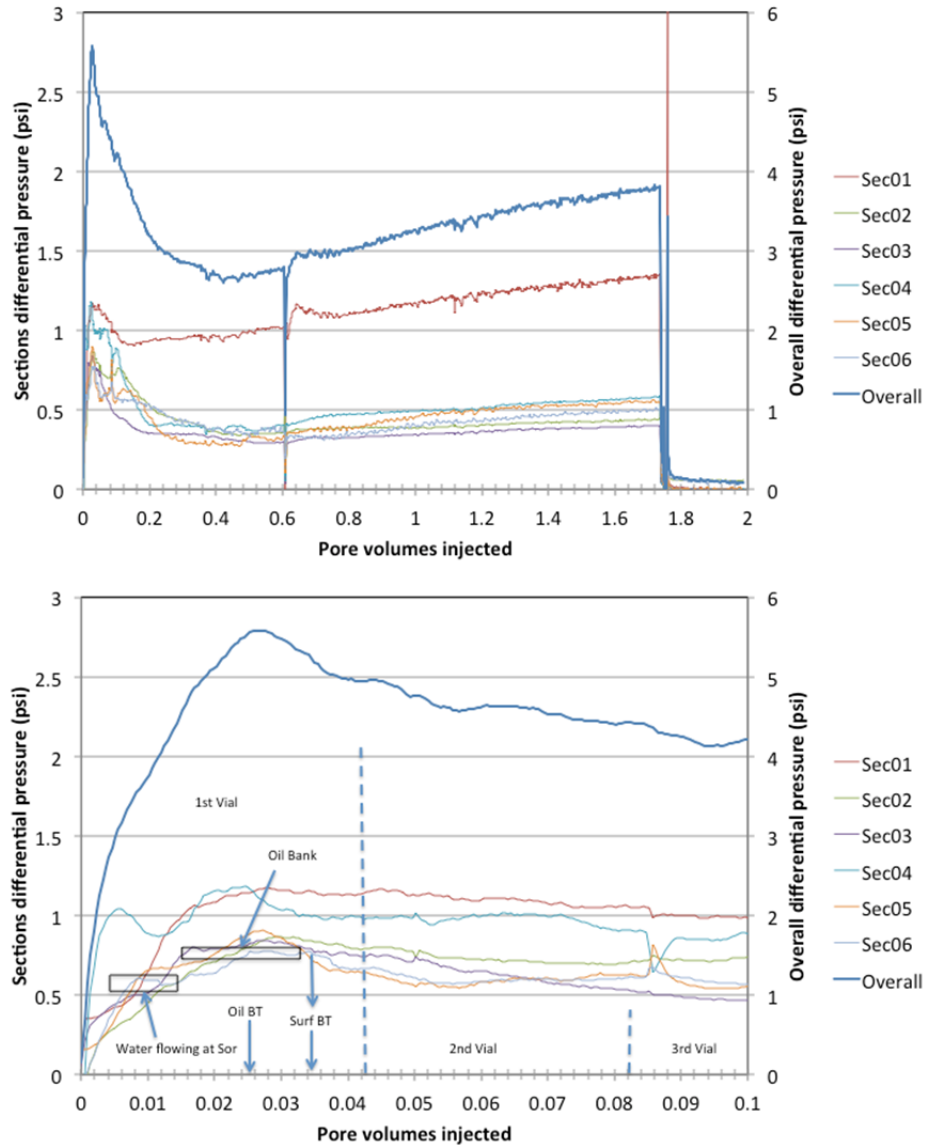


**Figure 2.6** - On top: Overall and sections differential pressure during chemical flooding of Core 30. At the bottom: Zoom for the first 0.1 pore volume injected.

In terms of tertiary oil recovery and chemical usage (lbm of surfactant/bbl of oil), the new formulation used in Core #30 outperformed the other floods in the limestone rock. This formulation also did not contain alcohol or alkali and no additional salt to the formation brine composition. Additional polymer to improve mobility control is likely to improve the performance even more.

## Chapter 3

### Selection and Performance of Chemical Systems for the Trembley Oilfield

This chapter presents the results of phase behavior studies and core floods for the Trembley crude oil. Phase behavior studies were conducted to select and optimize chemical formulations and core floods were conducted to test the performance of the formulations. Even though the phase behavior studies and core floods are dealt with separately, there is a connection between phase behavior studies and core flooding results. Without the results of core flood, success of a chemical formulation could not be validated, while the insight gained from each chemical flood further allowed us to relate the performances of the floods to the phase behavior observations and results.

#### PHASE BEHAVIOR RESULTS

The purpose of phase behavior studies was to develop chemical formulations that would efficiently mobilize residual oil recovery from Berea sandstone cores for Trembley crude oil at reservoir temperature. Trembley Crude Oil had a low viscosity of 4.08 cp at 46.1 °C, reservoir temperature ( $T_{res}$ ). The oil had a low acid content of 0.08 mg KOH/g. Reservoir salinity from field samples showed total dissolved solids up to 154,677 mg/L. NaCl was used as the electrolyte for the studies.

The process for developing formulation involved mixing carefully chosen combinations of chemical components with the crude oil in glass pipettes and assessing the solubilization ratio, equilibration time, and viscosity both qualitatively and quantitatively at  $T_{res}$ . The criteria that must be met for a formulation to have good prospects of mobilizing residual oil are as follows:

- i. On mixing with oil, the formulation should give a middle-phase microemulsion which is free of gels, macroemulsion and other viscous phases.
- ii. The microemulsion formed must equilibrate in less than 7 days and preferably within 3 days at optimum salinity.
- iii. The optimum solubilization ratio for the equilibrated microemulsion phase must be at least 10 mL/mL.
- iv. The surfactant formulation with addition of polymer in aqueous phase must remain clear and single phase at reservoir temperature at the optimum salinity i.e. the aqueous phase stability limit (APSL) must be higher than optimum salinity.

Each sub section details how each component of the chemical formulation was selected and their concentrations optimized leading to the final recipes for the formulations. In general, the methodology followed was to vary the concentrations of only the component of interest while keeping the remaining components constant and study the effects on the microemulsion behavior.

**Surfactant and Co-Surfactant Screening and Formulation** Various surfactant and co-surfactants were tried in the screening process in pairs. Surfactants and co-surfactants were identified as such by the information provided by vendors, literature review and inference from chemistry. Alfoterra® 123-8S, Petrostep® S-1, Petrostep® S-8B, Petrostep® S-8C,

Petrostep® S-13C, and Petrostep® S-13D were treated as surfactant as they are all alcohol propoxy sulfates (APS), containing hydrocarbon chain of various lengths and various levels of propoxylation. These molecules are tailored to provide high solubilization of oil, good solubility in brine and tolerance to salts, and are good for low temperature application. On the other hand, Petrostep® S-2, Petrostep C-1, Petrostep C-5 were treated as co-surfactants. These are sulfonates that do not have propoxylene oxide groups and are less effective in solubilizing oil compared to APS.

All surfactant screening experiments used two surfactants simultaneously, a primary surfactant and a co-surfactant. The pairs of surfactant and co-surfactant explored and screened in the research and their results are presented in the following sections.

***Petrostep® S-1 and Petrostep® S-2*** Screening without alkali. The pair of Petrostep® S-1, surfactant, and Petrostep® S-2, co-surfactant, had been previously reported to work well for a variety of crude oils, especially for low reservoir temperature application i.e. less than 60 °C (Levitt, Jackson et al. 2006; Barnes, Smit et al. 2008; Flaaten, Nguyen et al. 2008). The pair was selected for screening with Trembley crude. Petrostep® S-1 is a C<sub>16-17</sub> alcohol propoxy sulfate with 7 PO groups. It was one of the longer hydrocarbon chain surfactants available and therefore was expected to give more efficient solubilization of oil. Petrostep® S-2 is an internal olefin sulfonate (IOS) containing 15-18 carbons in its hydrocarbon skeletal. It has a highly branched structure that makes it a good co-surfactant. Total concentration of the surfactants as well as the ratio of the two surfactants at each concentration was varied. S-1 being the primary surfactant was most often the bigger proportion of the mix. Other components in the surfactant solution were sec-butanol as co-solvent. Initially, no alkali was added to the formulations. The results of the screening are tabulated in **Table 3.1, 3.2 and 3.3**, each table summarizes results for 2wt%, 1wt% and 0.5 wt% concentration of total surfactant, respectively. Surfactant ratios of 1:1 and 5:3 achieved the highest solubilization ratios at all three concentrations. At all three concentrations and all surfactant ratios, equilibration of phases took longer than 7 days and therefore did not meet the less than 7 day equilibration criterion. At 7:1 and 3:1 ratios of S-1:S-2, viscous phase and gels were observed in the pipettes, which hindered equilibration, and microemulsion phase could not be distinguished from viscous phases, for example see **Figure 3.1**. At 0.5 wt% total surfactant concentration, these ratios showed very low solubilization of oil.

A key observation was that optimum salinity was affected by the surfactant ratio. Higher S-1 concentration gave lower optimal salinity as depicted in **Figure 3.2**. This is explained by the fact that surfactant S-1 is more hydrophobic than S-2. No clear trend was observed in optimal salinity versus change in alcohol concentration. Though, alcohol should help with faster equilibration of phases, but in this case, the effect could not be validated with equilibration taking extremely long time in all formulations.

**Table 3.1:** Screening of Petrostep® S-1 and Petrostep® S-2 with Trembley crude oil without alkali. Total surfactant is 2 wt%.

Series #	Total Surfactant (wt%)	Surfactant 1	Surfactant 2	Ratio surf : co-surf	Co-Solvent SBA (wt%)	Optimal Solubilization Ratio, $\sigma^*$ (mL/mL)	Time at Last Readings (days)	Optimal Salinity, S* (wt% NaCl)	Remarks
		Petrostep S1 (wt%)	Petrostep S2 (wt%)						
A1	2	1	1	1:1	1	17	118	6.50	Equilibration > 7 days
A2		1.25	0.75	5:3	1	11	118	5.40	Equilibration > 7 days
A8		1.25	0.75	5:3	2	11.5	118	5.00	Equilibration > 7 days
A3		1.5	0.5	3:1	1	Viscous gels			
A7		1.5	0.5	3:1	1.5	5	118	3.8	Not enough solubilization
A4		1.75	0.25	7:1	1	Viscous gels			



**Table 3.2:** Screening of Petrostep® S-1 and Petrostep® S-2 with Trembley crude oil without alkali. Total surfactant is 1 wt%.

Series #	Total Surfactant (wt%)	Surfactant 1	Surfactant 2	Ratio surf : co-surf	Co-Solvent SBA (wt%)	Optimal Solubilization Ratio, $\sigma^*$ (mL/mL)	Time at Last Readings (days)	Optimal Salinity, $S^*$ (wt% NaCl)	Remarks
		Petrostep S1 (wt%)	Petrostep S2 (wt%)						
A40		0.375	0.625	3:5	2	9	44	8.10	Equilibration > 7 days. $\sigma^*$ is too low
A10		0.5	0.5	1:1	0.5	18	83	6.35	Equilibration > 7 days
A22		0.5	0.5	1:1	1.5	11	63	6.3	Equilibration > 7 days. $\sigma^*$ is ok.
A35		0.5	0.5	1:1	3	7	49	6.3	$\sigma^*$ is too low
A11		0.625	0.375	5:3	1	11	83	4.75	Equilibration > 7 days
A23		0.625	0.375	5:3	1	16	63	4.6	Equilibration > 7 days
A32	1	0.625	0.375	5:3	1	10	56	4.81	Equilibration > 7 days
A12		0.625	0.375	5:3	1.5	No Solubilization or gels present			Abandon
A24		0.625	0.375	5:3	2	12	63	4.7	Equilibration > 7 days. $\sigma^*$ is ok.
A33		0.625	0.375	5:3	2	7.5	56	4.8	Equilibration > 7 days. $\sigma^*$ is too low
A36		0.625	0.375	5:3	2	9	49	4.66	Equilibration > 7 days. $\sigma^*$ is too low
A34		0.625	0.375	5:3	3	7.5	49	4.7	Equilibration > 7 days. $\sigma^*$ is too low
A25		0.75	0.25	3:1	1.5	No Solubilization or gels present			

**Table 3.3:** Screening of Petrostep® S-1 and Petrostep® S-2 with Trembley crude oil without alkali. Total surfactant is 0.5 wt%.

Series #	Total Surfactant (wt%)	Surfactant 1	Surfactant 2	Ratio surf : co-surf	Co-Solvent	Optimal Solubilization Ratio, $\sigma^*$ (mL/mL)	Time at Last Readings (days)	Optimal Salinity, S* (wt% NaCl)	Remarks
		Petrostep S1 (wt%)	Petrostep S2 (wt%)		SBA (wt%)				
A41	0.5	0.19	0.31	3:5	0.5	11	45	6.6	Equilibration > 7 days
A15		0.25	0.25	1:1	0.125	10	97	5	Equilibration > 7 days
A28		0.25	0.25	1:1	0.125	21	63	4.78	Equilibration > 7 days
A14		0.25	0.25	1:1	0.25	16.5	82	4.5	Equilibration > 7 days
A27		0.25	0.25	1:1	0.25	18	63	4.72	Equilibration > 7 days
A31		0.25	0.25	1:1	0.375	12.0	56	4.78	Equilibration > 7 days
A13		0.25	0.25	1:1	0.5	15	82	5	Equilibration > 7 days
A26		0.25	0.25	1:1	0.5	15	63	4.77	Equilibration > 7 days
A37		0.25	0.25	1:1	0.5	11.5	49	4.67	Equilibration > 7 days
A19		0.31	0.19	5:3	0.125	No Solubilization	Equilibration > 7 days		
A18		0.31	0.19	5:3	0.25	14	82	3	Equilibration > 7 days
A29		0.31	0.19	5:3	0.375	No Solubilization or gels present	Abandon		
A17		0.31	0.19	5:3	0.5	No Solubilization	Abandon		
A16		0.31	0.19	5:3	0.75	No Solubilization	Abandon		
A20	0.375	0.125	3:1	0.5	No Solubilization	Abandon			
A21	0.375	0.125	3:1	1	No Solubilization	Abandon			



**Figure 3.1:** Low solubilization of oil and water and gels from tube 8 to 11 observed for Series A25, a ratio 3:1 of Petrostep S1 to Petrostep S2 at 1 wt% total surfactant concentration and 1.5 wt% SBA with Trembley crude oil @ 46.1 °C after equilibrating for 63 days. Salinity varied from 2.0 wt% to 5.0 wt% NaCl at 0.30 wt% increments, left to right.

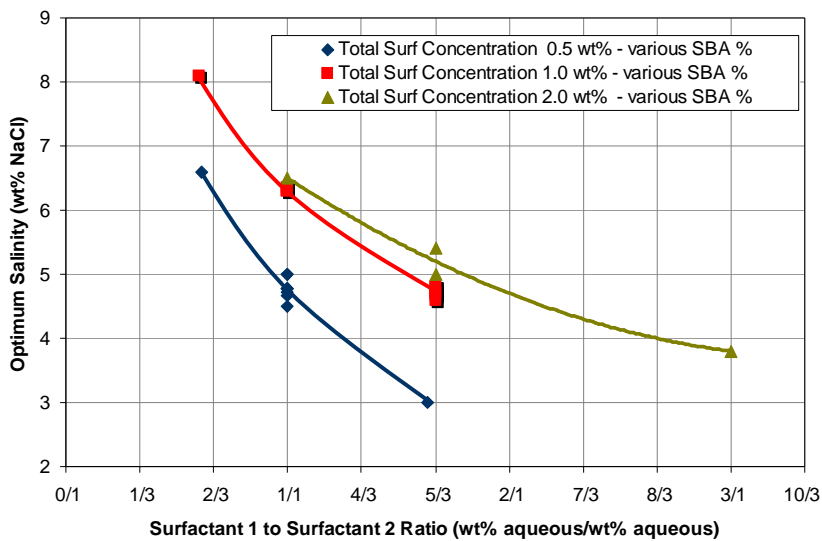


**Figure 3.2:** Effect of varying Petrostep S1 to Petrostep S2 ratio and total surfactant concentration on optimum salinity with various SBA concentrations without alkali. Oil is Trembley crude oil @ 46.1 °C.

*Screening with Alkali.* The pair of S-1 and S-2 without alkali failed to give a fast equilibration. Next, alkali, NaOH and Na<sub>2</sub>CO<sub>3</sub>, were added to the formulation. Alkali was expected to quicken equilibration time. The results of S-1 and S-2 formulation screening with Trembley crude oil at 46.1 °C with alkali are presented in **Table 3.4**. Concentrations of both alkalis were varied between zero to 1 wt%. Surfactant and co-surfactant concentrations and ratios as well as co-solvent concentrations were held constant for this experiment. The results prove that equilibration time was dramatically reduced with as little as 0.02 wt% NaOH or 0.2 wt% Na<sub>2</sub>CO<sub>3</sub> as in series 27-10 and 27-8 in Table 3.. The difference in equilibration rate with and without can be observed in **Figure 3.**, which compares the optimum solubilization ratio of similar formulations with and without alkali. In series A36, the microemulsion phase continued to shrink over time and the final value of optimum solubilization ratio was only 9. On the other hand, the optimum solubilization ratio of series 27-4 became stable after 3 days indicating that the microemulsion phase equilibrated much quicker.

With alkali, the optimum solubilization ratio exceeded the minimum criterion of 10 mL/mL. The microemulsion phase also looked free of gels and macroemulsion after stabilization, and had sharper interfaces with alkali, especially near optimum salinity. **Figure 3.** shows series 27-4 pipettes at 3<sup>rd</sup> day of equilibration. The microemulsion phases coalesced in 3 days and the microemulsion middle phase was free of viscous phases or gels at optimum salinity of 4.65 wt% NaCl.

Alkali offered a breakthrough in equilibration time reduction to enable meet the less than 7 day criterion. In addition, the microemulsion showed improved solubilization ratios and low viscosity microemulsions. Alkali became an essential component in the formulations for S-1 and S-2.

*Optimized Formulation.* To select the best combination of chemicals that achieve the criteria for phase behavior screening, the effect of total surfactant concentrations, surfactant to co-surfactant ratio, co-solvent and alkali concentration were studied. Decision about the best performing combination was rationalized by comparing the results of the systematically ran salinity scans.

During the screening of this pair of surfactants without alkali, an increasing trend in equilibration time had been observed with an increase in total surfactant concentration. Also, to minimize surfactant adsorption in core, lower concentrations are desired. Therefore, only 1 wt% and 0.5 wt% surfactant concentrations were considered for

**Table 3.4:** Screening of Petrostep® S-1 and Petrostep® S-2 with Trembley crude oil with alkali. Total surfactant is 1 wt%. Surfactant ratio S-1:S-2 was kept constant at 5:3. Oil is Trembley and temperature was maintained at 46.1 °C.

Series	Surfactant		Co-Solvent		Ratio	Alkali		Solubilization ratio (mL/mL)	Time to equilibrate (days)	Optimal salinity (wt% NaCl)
	Petrostep S-1 (wt%)	Petrostep S2 (wt%)	Sec-Butyl Alcohol (SBA) (wt%)	Alcohol (wt%)		Name	(wt%)			
#A-36	0.625	0.375	2	2	5:3	None	0.00	7.5	>50	4.65
#27-10	0.625	0.375	2	2	5:3	NaOH	0.02	15.0	7	5.00*
#27-4	0.625	0.375	2	2	5:3	NaOH	0.05	15.0	3	4.60
#27-5	0.625	0.375	2	2	5:3	NaOH	0.2	14.6	3	4.35
#27-6	0.625	0.375	2	2	5:3	NaOH	1	14.8	3	3.10
#27-7	0.625	0.375	2	2	5:3	Na <sub>2</sub> CO <sub>3</sub>	0.05	slow to equilibrate	>6	5.00
#27-8	0.625	0.375	2	2	5:3	Na <sub>2</sub> CO <sub>3</sub>	0.2	16.0	6	4.80
#27-9	0.625	0.375	2	2	5:3	Na <sub>2</sub> CO <sub>3</sub>	1	14.0	6	4.20

\* Higher than expected, could be due to experimental error

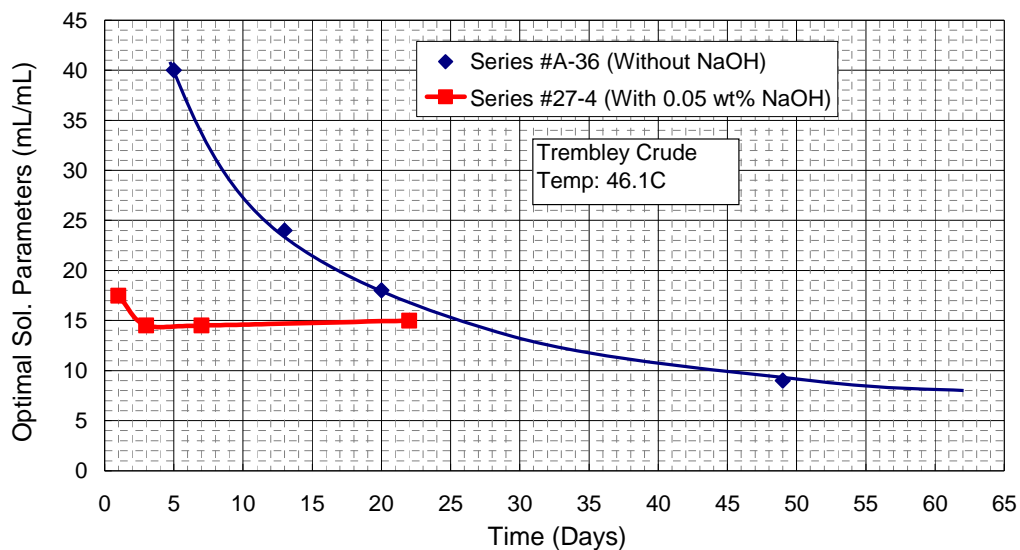


**Figure 3.3:** Comparison of time required (equilibration time) for optimum solubilization ratio to attain a stable value with and without alkali for the same formulation, 0.625 wt% Petrostep S1 0.375 wt% Petrostep S2, 2 wt% SBA. Oil is Trembley crude oil @ 46.1 °C.

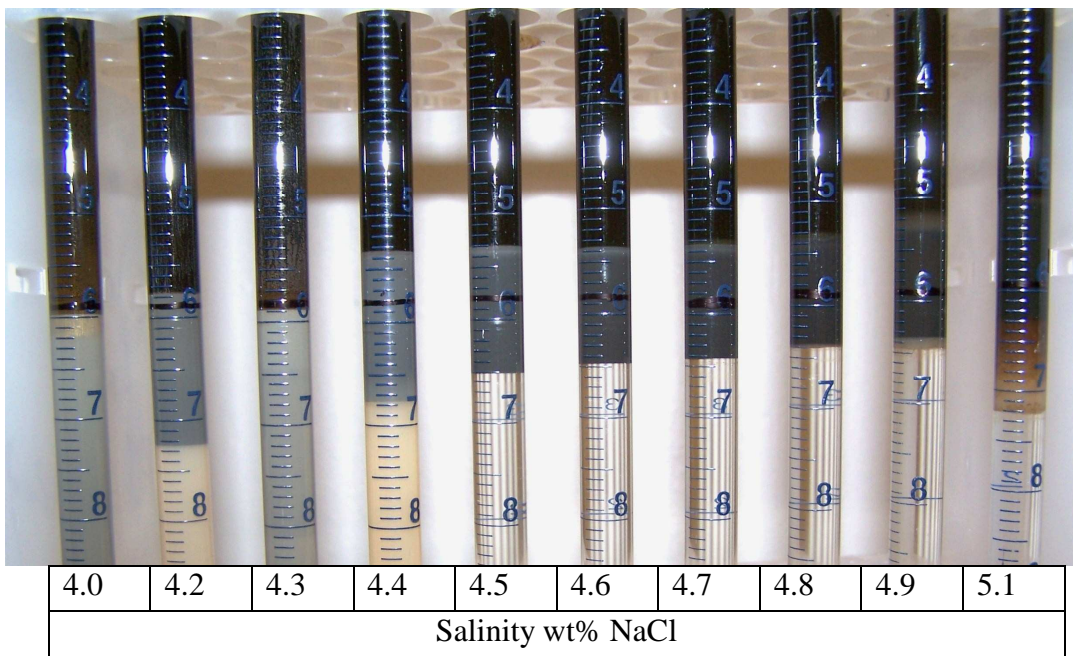


**Figure 3.4:** Formulation 27-4 containing 0.625 wt% Petrostep S1 0.375 wt% Petrostep S2, 2 wt% SBA with 0.05 wt% NaOH. The microemulsion phase is shown at 3 days. The middle phase microemulsion at 4.6 wt% and 4.7 wt% salinity are near the optimum. With alkali, microemulsion phase equilibrated in 3 days and showed sharp interfaces. Oil is Trembley crude oil @ 46.1 °C.

further optimization. The runs performed to optimize the formulation are tabulated in **Table 3.5** and **Table 3.6**.

For 1 wt% formulations, 3:1 surfactant to co-surfactant ratio gave a viscous phase and equilibrated slowly (**Figure 3.5**). Both 5:3 and 1:1 equilibrated within 7 days, however, 1:1 required the least amount of co-solvent. Though, some viscous phases were observed at 1:1 ratio near the optimum salinity, none were observed for 5:3 ratio. Therefore 5:3 surfactant to co-surfactant ratio was the best choice for S-1:S-2 formulation. The minimum co-solvent concentration required at 5:3 ratio for fluid microemulsion middle phase was 2 wt% SBA or 1.5% DGBE. 1 wt% Na<sub>2</sub>CO<sub>3</sub> was the standard amount of alkali used in most formulations. Optimum solubilization ratios were greater than 10 in all 1 wt% formulations.

For 0.5 wt% surfactant formulations, only two surfactant to co-surfactant ratios were tried, 1:1 and 5:3. 5:3 ratio showed good results in this case as well. Minimum co-solvent requirement for non-viscous microemulsion middle phase was 1.25-1.5wt% SBA or 1.375wt% DGBE. 1wt% Na<sub>2</sub>CO<sub>3</sub> was standard. These formulations also contained polymer, Flopaam 3330S, which had a minimal effect on phase behavior in this case. Optimum solubilization parameters were greater than 10 in all 0.5wt% formulations.

The formulations identified having good microemulsion behavior from behavior screening for Petrostep S1 and Petrostep S2 are given in **Table 3.7**. Formulation 40-3, code name X-1, contained formulations with a total of 1 wt% surfactant at 5:3 ratio. It had an optimum solubilization parameter of 13 mL/mL and equilibrated in 3 days. The optimum pipettes were free of viscous phases (**Figure 3.6**). Solubilization parameters for this formulation are plotted in **Figure 3.7**. A 0.5 wt% formulation, 40-9, was also selected to move forward from the screening for potential core flood validation. This was code named X-2. The solubilization parameters for X-2 were 12 mL/mL and samples equilibrated in 3 days. The phase behavior for X-2 is shown in **Figure 3.8** and associated solubilization parameters are plotted in **Figure 3.9**. The microemulsion phase looked lighter color and viscous compared to Formulation X-1. The third and final formulation selected from screening was 40-18 and code named X-3. This formulation was similar to X-2 except it used DGBE as co-solvent. Visually, DGBE showed lower viscosity than SBA. The middle phases looked cleaner and less viscous and solubilization parameters were slightly higher at 14 mL/mL. Equilibration was within 3 days. Phase behavior for X-3 appears in **Figure 3.10** and associated solubilization parameters are plotted in **Figure 3.11**.

The phase behavior and aqueous stability limit of two formulations, X-1 and X-3, were examined with polymer and are reported in **Table 3.7**. Flopaam 3330S (2200 ppm (0.22 wt%)) was added to the solutions. Both formulations X-1 and X-3 gave APSL higher than the optimum salinity. The margins between optimum salinity and APSL were 0.4 and 1.6 wt% respectively. DGBE seemed to enhance APSL and thus the higher margin with it for formulation X-3. APSL was not determined for X-2. However, as it was similar to X-1 in make up but half the surfactant concentration, aqueous stability was assumed to be at least the same or better. As was noted earlier, lower surfactant concentration lowers S\*, which would support the assumption.

**Table 3.5:** Optimization of Petrostep® S-1 and Petrostep® S-2 with Trembley crude oil with alkali. Total surfactant is 1 wt%. Surfactant ratio, co-solvent concentration and type were varied. Oil is Trembley and temperature was maintained at 46.1 °C.

Series #	Surfactant		Co-Solvent wt%	Co-Solvent		surf : co-surf		alkali		WOR	Optimal Salinity, S* wt% NaCl	Optimal Solubilization Ratio, $\sigma^*$ (mL/mL)	Eq. Time at reading (days)	Microemulsion Comments
	Petrostep S1	Petrostep S2		Type	Ratio	NaOH (wt%)	Na <sub>2</sub> CO <sub>3</sub> (wt%)							
#25-18	0.5	0.5	2	SBA	1:1	0.25		1	5.8	10.4	10	Fluid middle phase/equilibrated/Low Solubilization		
#40-1	0.5	0.5	1.5	SBA	1:1		1	1.5	5.81	12.02	3	Interface has viscous phase		
#40-2	0.5	0.5	1	SBA	1:1		1	1.5	6.05	15.48	3	Interface has viscous phase		
#25-16	0.75	0.25	2	SBA	3:1	0.25		1	3.06	19	12	Creamy viscous non-fluid middle phase/ <b>not equilibrated</b>		
#40-3	0.625	0.375	2	SBA	5:3		1	1.5	4.15	12.88	3	Middle phase at optimum free of viscous phase		
#25-17	0.625	0.375	2	SBA	5:3	0.25		1	4.25	13.8	5	Fluid middle phase/equilibrated/Good Solubilization ratio		
#40-28	0.625	0.375	2	DGBE	5:3		1	1.5	5.4	10	2	Fluid middle phase, low solubilization ratio		
#40-33	0.625	0.375	1.5	DGBE	5:3		1	1.5	5.3	13	1	Fluid middle phase, good solubilization ratio		
#40-31	0.625	0.375	1.25	DGBE	5:3		1	1.5	5.25	15	2*	slightly viscous and slow to equilibrate		



**Table 3.6:** Optimization of Petrostep® S-1 and Petrostep® S-2 with Trembley crude oil with alkali. Total surfactant was 0.5 wt%. Surfactant ratio, co-solvent concentration and type were varied. Oil is Trembley and temperature was maintained at 46.1 °C.

Series #	Surfactant	Co-Surfactant	Polymer	Co-Solvent		surf : co-surf		alkali	WOR	Optimal Salinity, S* wt% NaCl	Optimal Solubilization Ratio, $\sigma^*$ (mL/mL)	Eq. Time at reading (days)	Microemulsion
				wt%	Type	Ratio	Na <sub>2</sub> CO <sub>3</sub> (wt%)						
#40-10	0.31	0.19	2250	1.5	SBA	5:3	1	1.5	3.84	10.3	3	Fluid middle phase at optimum salinity, solubilization low	
#40-9	0.31	0.19	2250	1.25	SBA	5:3	1	1.5	3.95	12.3	3	Fluid middle phase, may need mc alcohol, low solubilization	
#40-8	0.31	0.19	2000	1	SBA	5:3	1	1.5	3.94	12.6	6	Middle phase viscous, low solubilization	
#40-12	0.31	0.19	2250	0.75	SBA	5:3	1	1.5	-	-	2	Middle phase viscous, low solubilization	
#40-15	0.31	0.19	2250	1.50	DGBE	5:3	1	1.5	4.61	11.0	4	Fluid middle phase at optimum salinity, solubilization low	
#40-18	0.31	0.19	2250	1.375	DGBE	5:3	1	1.0	4.65	14	2	Fluid middle phase at optimum salinity, solubilization okay	
#40-21	0.31	0.19	2250	1.25	DGBE	5:3	1	1.5	4.48	13.9	2	More co solvent needed for less viscous middle phase	

**Table 3.7:** Optimized formulation from Petrostep® S-1 and Petrostep® S-2 screening with Trembley crude oil. Temperature was maintained at 46.1 °C.

Series #	Co-Surfactant		Co-Solvent		surf: Alkali		WOR	Optimal Salinity, S*, wt% NaCl		Optimal Solubilization Ratio, $\sigma^*$ (mL/mL)	Eq. Time at reading (days)	Formulation Code	
	Petrostep S1	Petrostep S2	wt%	Type	Ratio	Na <sub>2</sub> CO <sub>3</sub> (wt%)		without polymer	with polymer				
#40-3	0.625	0.375	2	SBA	5:3	1	1.5	4.15	4.30	4.7	12.88	3	X-1
#40-9	0.31	0.19	1.25	SBA	5:3	1	1.5	3.95	3.95	NA	12.3	3	X-2
#40-18	0.31	0.19	1.375	DGBE	5:3	1	1.0	4.65	4.8	6.4	14	2	X-3

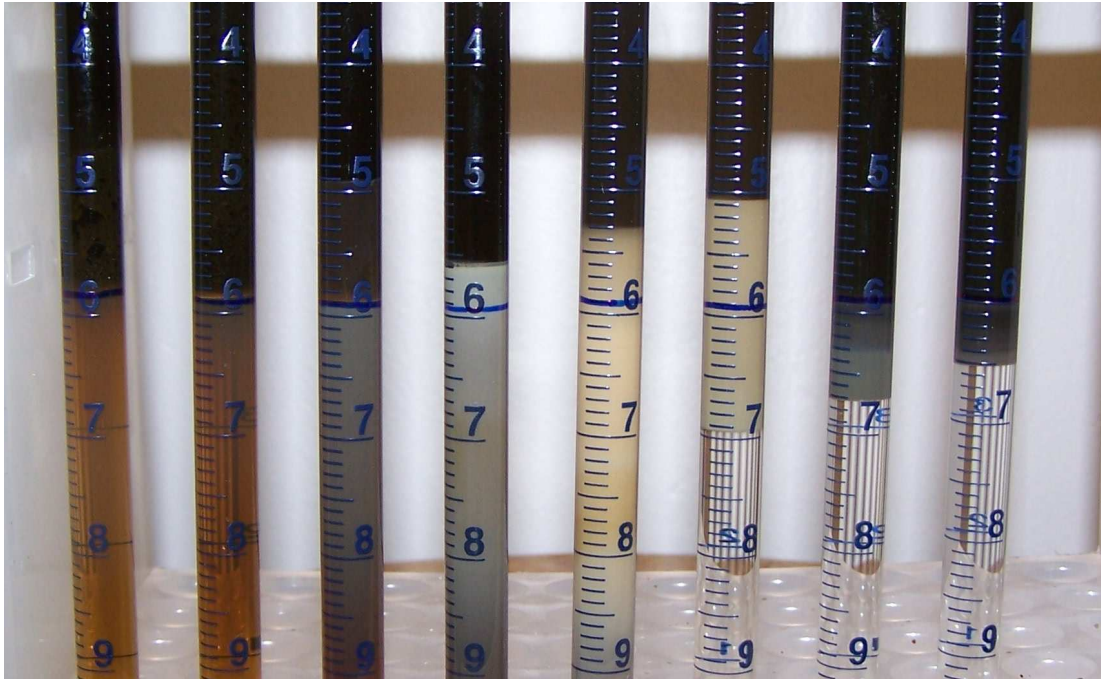


**Figure 3.5:** Formulation 25-16 containing 0.75 wt% Petrostep S1 0.25 wt% Petrostep S2, 2 wt% SBA with 0.25 wt% NaOH. The microemulsion phase was creamy and viscous compared to formulations containing smaller proportion of S1. Oil is Trembley crude oil @ 46.1 °C.

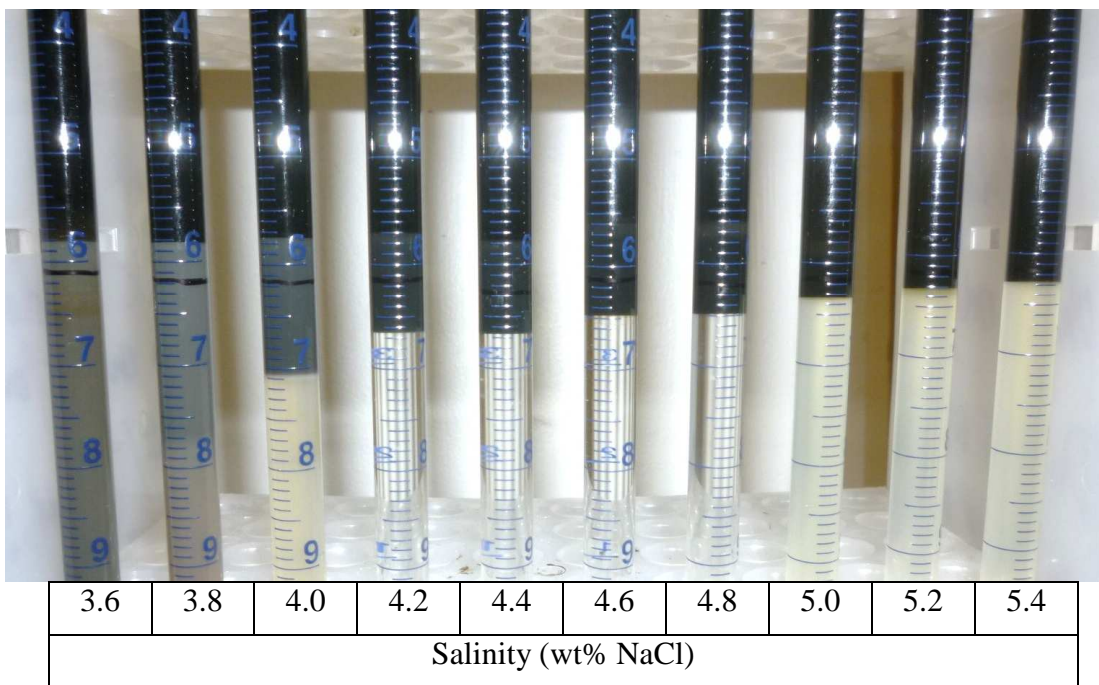


**Figure 3.6:** Phase behavior results at 7 days for formulation 40-3 (X-1) containing 0.625 wt% Petrostep S1 0.375 wt% Petrostep S2, 2 wt% SBA with 1 wt%  $\text{Na}_2\text{CO}_3$ . WOR =1.5. Oil is Trembley crude oil @ 46.1 °C.

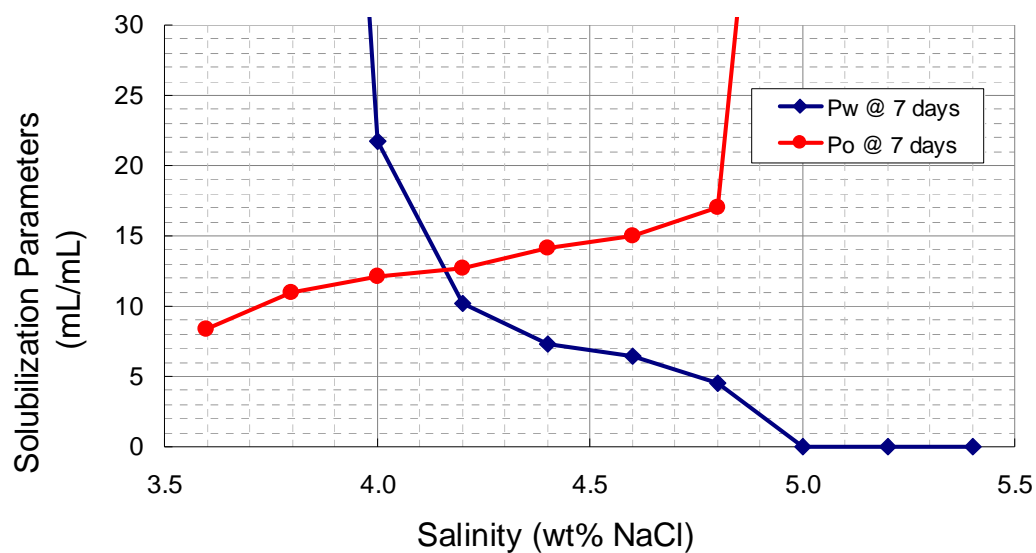


**Figure 3.7:** Solubilization parameters for formulation 40-3 (X-1) containing 0.625 wt% Petrostep S1 0.375 wt% Petrostep S2, 2 wt% SBA with 1 wt%  $\text{Na}_2\text{CO}_3$ . WOR =1.5. Oil is Trembley crude oil @ 46.1 °C.

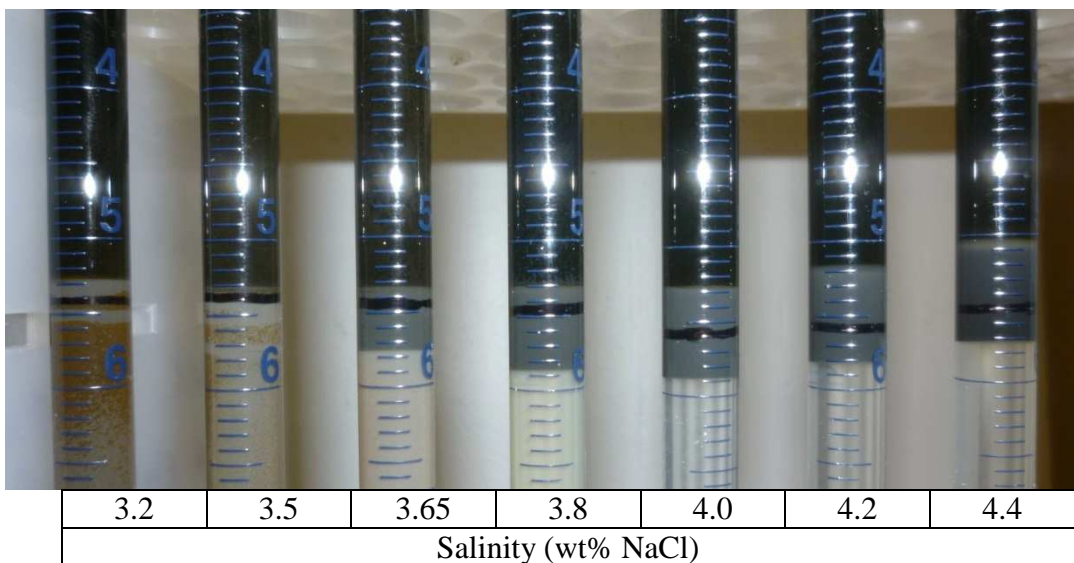


**Figure 3.8:** Phase behavior results at 6 days for formulation 40-9 (X-2) containing 0.31 wt% Petrostep S1 0.19 wt% Petrostep S2, 1.25 wt% SBA with 1 wt%  $\text{Na}_2\text{CO}_3$ . WOR =1.5. Oil is Trembley crude oil @ 46.1 °C.

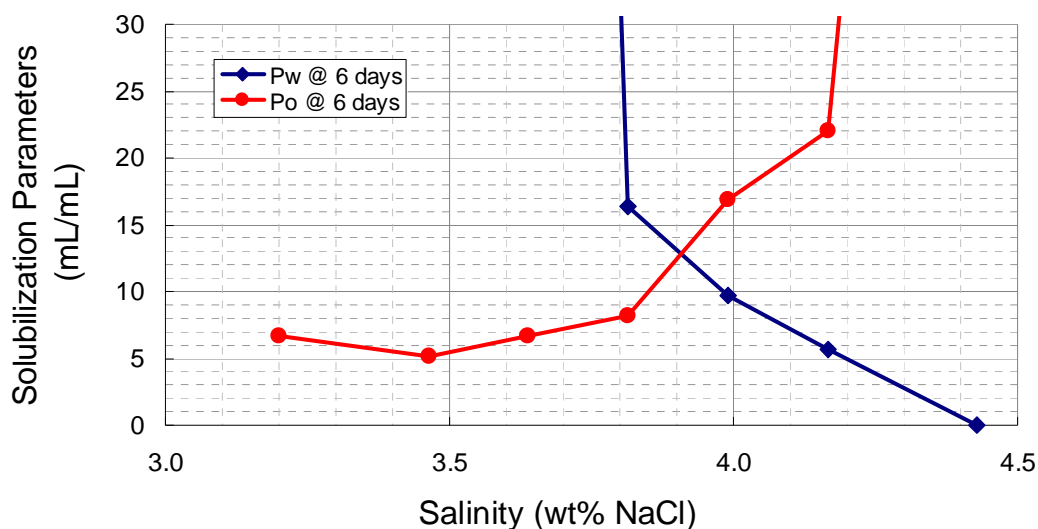


**Figure 3.9:** Solubilization parameters for formulation 40-9 (X-2) containing 0.31 wt% Petrostep S1 0.19 wt% Petrostep S2, 1.25 wt% SBA with 1 wt%  $\text{Na}_2\text{CO}_3$ . WOR =1.5. Oil is Trembley crude oil @ 46.1 °C.

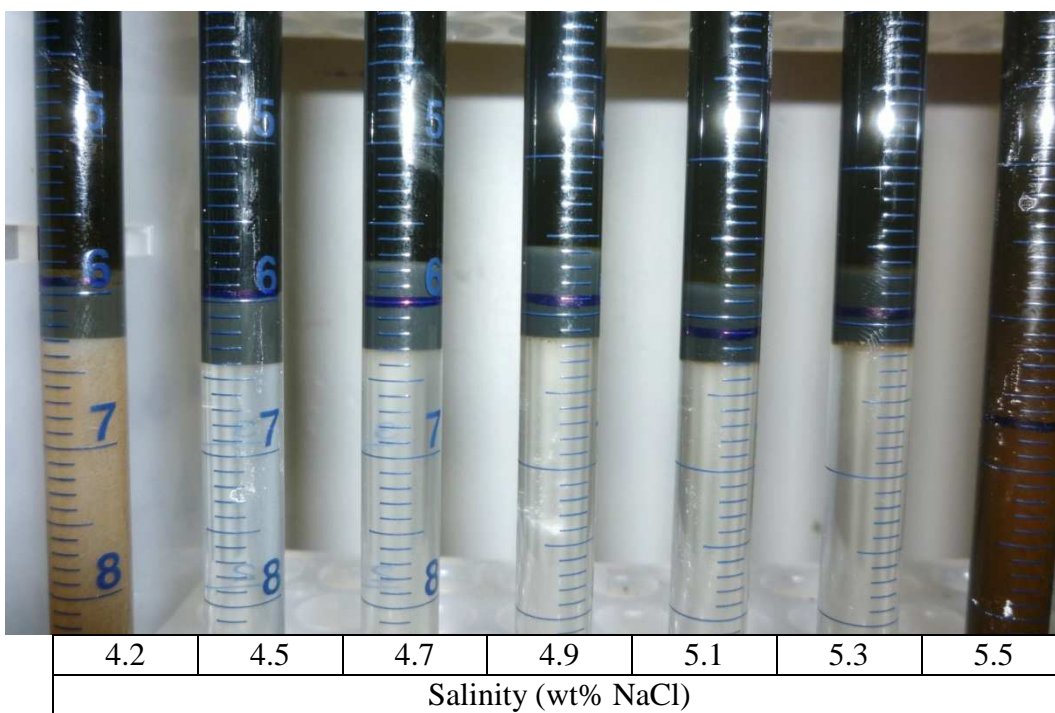


**Figure 3.10:** Phase behavior results at 3 days for formulation 40-18 (X-3) containing 0.31 wt% Petrostep S1 0.19 wt% Petrostep S2, 1.375 wt% DGBE with 1 wt%  $\text{Na}_2\text{CO}_3$ . WOR =1.5. Oil is Trembley crude oil @ 46.1 °C.

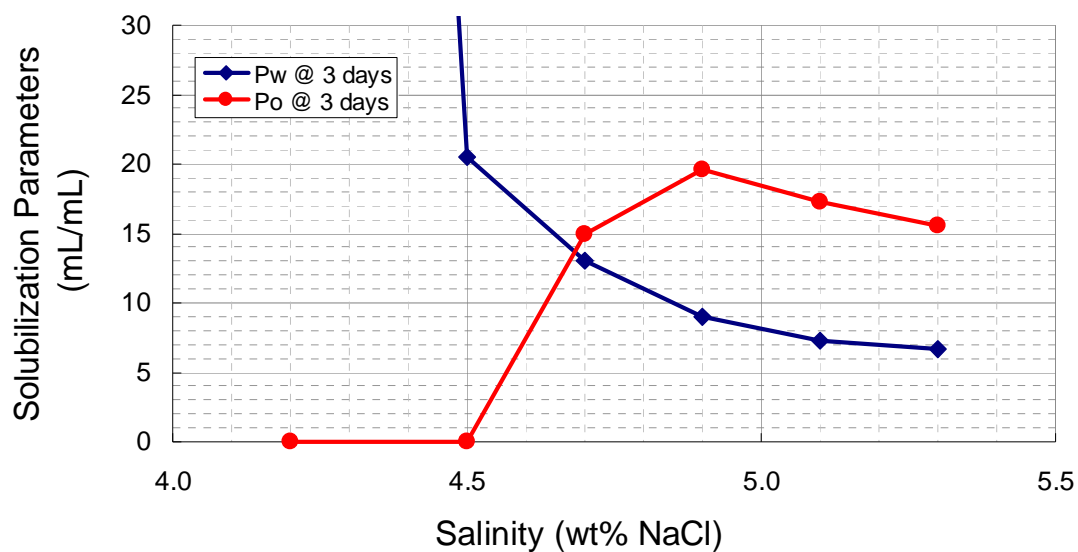


**Figure 3.11:** Solubilization parameters for formulation 40-18 (X-3) containing 0.31 wt% Petrostep S1 0.19 wt% Petrostep S2, 1.375 wt% DGBE with 1 wt%  $\text{Na}_2\text{CO}_3$ . WOR =1.5. Oil is Trembley crude oil @ 46.1 °C.

Optimized formulations X-1 and X-3 met all the criteria of phase behavior screening and therefore were selected as candidates for core flood testing along with. X-2 was also selected for coreflood on the assumption that it should pass the APSL.

***Alfoterra 123-8s, Petrostep S-8B, Petrostep S-8C with Petrostep® S-2, Petrostep C-1, Petrostep C-5*** This screening experiment was performed to study the phase behavior of shorter carbon chain primary surfactants and to trials linear alpha olefin sulfonate (LAOS) as co-surfactant. Alfoterra 123-8s ( $C_{12-13}-(PO)_8-SO_4^-$ ) and Petrostep S-8B ( $TDA-(PO)_7-SO_4^-$ ) and Petrostep S-8C ( $TDA-(PO)_9-SO_4^-$ ) were used as main surfactant, and Petrostep S-2 ( $C_{15-18} IOS$ ), Petrostep C-1 (LAOS) and Petrostep C-5 (LAOS) as co-surfactants. All the primary surfactants contained  $C_{12-13}$  hydrocarbon chain and therefore were shorter molecules compared to Petrostep S-1, which was  $C_{16-17}$ , used in experiment series #A, #25, #27 and #40. C-1 and C-5 were different than S-2 as their molecules were linear, whereas, S-2 was an internal olefin sulfonate (IOS) that had a highly branched molecule.

In the screening experiment, based on positive experience from adding alkali, NaOH (1 drop) was added to all the tubes and IBA & SBA were used as co-solvents. IBA and SBA could be used interchangeable because of their similar partitioning capability. Compositions and results of the screening experiments are presented in **Table 3.8**. Alfoterra 123-8s ( $C_{12-13}-(PO)_8-SO_4^-$ ) was tested with all three co-surfactants, S-2, C-1 and C-5, but Petrostep S-8B and S-8C were only tested with Petrostep S-2 as the co-surfactant.

Experiments with Alfoterra 123-8s ( $C_{12-13}-(PO)_8-SO_4^-$ ) and S-2, C-1 and C-5 showed that for all ratios for the main surfactant to co-surfactant, 3:1, 2:1 and 5:3, only S-2 and C-5 gave fluid middle phase. C-1 gave viscous middle phase. Optimum solubilization ratios ranged between 9-12.5 mL/mL though solubilizations were higher when S-2 was used as co-surfactant, for instance compare #28-6 to #28-8.

Surfactants S-8B and S-8C were paired with co-surfactant S-2 and in general gave fluid middle phase microemulsion and quick equilibration for all ratios but their optimum solubilization ratios were not as high as for Alfoterra 123-8S. For instance, compare #28-6 to #28-9 and #28-10.

From the screening results, Alfoterra 123-8S and Petrostep S-2 had the most consistent performs in terms of optimum solubilization ratios of higher than 10 mL/mL, equilibration time of under 5 days and non-viscous microemulsion middle phase.

*Optimized Formulation.* Surfactants Sasol Alfoterra 123-8s and Petrostep S-8C gave higher optimum solubilization ratios than S-8B and also formed fluid middle phases at all three surfactant to co-surfactant ratios except when the co-surfactant was C-1. Both these surfactants contained 9 PO groups, whereas S-8B contained only 7 PO groups. It must be noted that the carbon chain length was similar for all three primary surfactants. Therefore, the additional PO groups were responsible for the relatively higher optimum solubilization ratios

**Table 3.8:** Screening of Alfoterra 123-8s, Petrostep S-8B, Petrostep S-8C surfactants and Petrostep® S-2, Petrostep C-1, Petrostep C-5 co-surfactant with Trembley crude oil. Oil is Trembley and temperature was maintained at 46.1 °C.

Series #	Surf 1	Surf 2	Surf 3	Co-Surf 1	Co-Surf 2	Co-Surf 3	Co-Solvent	Ratio	Alkali	Approximate Solubilization Ratio, $\sigma^*$ (mL/mL)	Recording time (days)	Optimal Salinity, S* (wt% NaCl)	Comments
	Sasol 123-8s (wt%)	Petrostep S-8B (wt%)	Petrostep S-8C (wt%)	Petrostep S2 (wt%)	Petrostep C1 (wt%)	Petrostep C5 (wt%)	IBA/SBA (wt%)	surf : co-surf	NaOH (wt%)				
#28-1	0.75			0.25			1.5 (IBA)	3:1	0.25	~12.5	5	~3.2	Quite Fluid Interfaces
#28-2	0.75				0.25		1.5 (IBA)	3:1	0.25	~13	5	~4.6	Moderately Fluid Interfaces
#28-3	0.75					0.25	1.5 (IBA)	3:1	0.25	~12	5	~5.55	Quite Fluid Interfaces
#28-4		0.75		0.25			1.5 (IBA)	3:1	0.25	~12	5	~3.85	Most Fluid middle phases
#28-5			0.75	0.25			1.5 (IBA)	3:1	0.25	~12.5	5	~3.1	Most Fluid middle phases
#28-11	0.67			0.33			1 (SBA)	2:1	0.25	~12	2	~4.5	Fluid/Slightly viscous just above optimum
#28-12	0.67				0.33		1 (SBA)	2:1	0.25	na	2	na	Optimum not reached/Middle not fluid
#28-13	0.67					0.33	1 (SBA)	2:1	0.25	na	2	na	Optimum not reached
#28-14		0.67		0.33			1 (SBA)	2:1	0.25	~10	2	~5.2	Not quite fluid
#28-15			0.67	0.33			1 (SBA)	2:1	0.25	~11	2	~4.6	Quite Fluid
#28-6	0.63			0.375			0.75 (IBA)	5:3	0.25	~12	4	~4.6	Very Fluid Middle Phase
#28-7	0.63				0.375		0.75 (IBA)	5:3	0.25	na	3	na	Viscous & Creamy Middle
#28-8	0.63					0.375	0.75 (IBA)	5:3	0.25	~9	3	~9.5	Fluid Middle/Low Oil Sol.
#28-9		0.625		0.375			0.75 (IBA)	5:3	0.25	~7	3	~5.2	Fluid Middle/Low Oil Sol.
#28-10			0.625	0.375			0.75 (IBA)	5:3	0.25	~11	3	~4.7	Quite Fluid/Slight Creaminess



compared to S-8B. Petrostep S-2 outperformed the other two co-surfactants in terms of higher optimum solubilization ratios and quality of middle phase i.e. avoiding viscous phases. It was observed that as co-surfactant proportion was increased less co-solvent was required. Therefore a ratio of 5:3 was chosen as the optimum ratio in this case.

The advantages observed of using these shorter chain surfactants compared to the longer chain (Petrostep S-1) were that these required relatively less amount of co-solvent, showed quicker equilibration, and showed better fluidity in the middle phase. The optimized formulation proposed after the screening result is given in **Table 3.9** and was named X-4. The formulation pipettes are pictured in **Figure 3.12** and the associated solubility parameters are plotted in **Figure 3.13**. It can be observed that the formulation showed good phase behavior and was free of viscous phase. Optimum solubilization parameters were close to 15 mL/mL and the equilibration was fast, within 3 days, as shown in **Figure 3.14**.

APSL of the formulation is given in **Table 3.9**. APSL was 4.5 wt% whereas the optimum salinity of the formulation was 5 wt% NaCl. The formulation failed to meet APSL requirement. The formulation was not considered for further optimization nor core flood validation.

**Petrostep® S-13 D, Petrostep® S-2 and Novel® TDA-12EO.** In a new screening series an ethoxylate was tried as the co-solvent. Ethoxylates are non-ionic surfactants. Primary surfactant was Petrostep S-13D, which is a C<sub>13</sub> APS with 13 PO groups. Co-surfactant was S-2, and Novel TDA-12EO was used as the co-solvent. The screening results are presented in **Table 3.10**. During screening experiments, total surfactant concentration was varied between 0.5 wt% to 1.0wt%. TDA-12 EO concentration was varied between 0.25wt% to 2wt%. Though equilibration times were not documented, the pipettes showed fast equilibration for most combinations, and in some cases less than a day. Surfactant:co-surfactant ratio was varied between 1.7 and 1.0. As the surf:co-surf ratio got smaller, less ethoxylate was required to keep viscous phases away and equilibration got quicker. For instance, #36-55, which had equal parts surfactant and co-surfactant, 0.25wt% each produced very good phase behavior and with equilibration time on the order of hours only. The amount of ethoxylate was much less in comparison to the amount of alcohol that would be required to eliminate viscous phases. Secondly, since ethoxylate had surfactant properties, it did not compromise solubilization parameters like the alcohol. #36-55 was also the optimized formulation from this screening, showing very good phase behavior with optimum solubilization parameters higher than 10. It was code named X-5. However, aqueous phase stability being very close to the optimum salinity was a concern for this system. Due to APSL being same as optimum salinity, the formulation was not a candidate for core floods.

### **Phase Behavior Relationships**

During the surfactant screening phase, relationship between the chemical constituents of formulation and the phase behavior results were observed and understood. These relationships and trends were essential for optimization of formulations in a systematic and rational way. The important relationships established for each constituent are discussed here.

**Table 3.9:** Optimized formulation from Alfoterra 123-8s, Petrostep S-8B, Petrostep S-8C surfactants and Petrostep® S-2, Petrostep C-1, Petrostep C-5 co-surfactant screening with Trembley crude oil. Temperature was maintained at 46.1 °C.

Series #	Surf 1	Co-Surf 1	Co-Solvent	Ratio	Alkali	Approximate Solubilization Ratio, $\sigma^*$ (mL/mL)	Recording time (days)	Optimal Salinity, S* (wt% NaCl)	APSL (wt% NaCl)	Comments
	Sasol 123-8s (wt%)	Petrostep S2 (wt%)	IBA/SBA (wt%)	surf : co-surf	NaOH (wt%)					
X-4	0.63	0.375	0.75 (IBA)	5:3	0.05	15	3	5.0	4.5	Actual results

**Table 3.10:** Screening of Petrostep S13-D, Petrostep S-2 and TDA-12-EO with Trembley crude oil. Temperature was maintained at 46.1 °C and WOR was either 1 or 1.5.

Series #	Surf Petrostep S13D (wt%)	Co-Surf Petrostep S2 (wt%)	Ethoxylate TDA-12-EO (wt%)	Alkali Na <sub>2</sub> CO <sub>3</sub> (wt%)	Ratio Surf : Co-Surf	Ratio Surf : TDA	Optimal Salinity, S* wt% NaCl	Optimal Solubilization Ratio, σ* (mL/mL)	Eq. Time (days)	Aqueous Stability (wt% NaCl)	Comments
#36-7	0.63	0.38	1.00	0.5	1.7	0.6	>9	-	-	-	viscous phase in tube 6
#36-8	0.63	0.38	2.00	0.5	1.7	0.3	>9	-	-	-	Optimum not reached
#36-21	0.63	0.38	0.50	0.5	1.7	1.3	5.5	>10	-	-	slightly viscous, more alcohol needed
#36-22	0.31	0.19	0.25	0.5	1.7	1.3	5.0	>10	-	-	viscous
#36-24	0.50	0.50	0.50	0.5	1.0	1.0	7.5	>10	<3	6.5	non viscous, free flowing
#36-25	0.50	0.50	0.25	0.5	1.0	2.0	6.5	>10	-	-	slightly viscous
#36-38	0.38	0.38	0.25	0.5	1.0	1.5	6.75	>10	-	7	ok
#36-39	0.40	0.40	0.20	0.5	1.0	2.0	7.75	>10	-	6.7	slightly viscous
#36-44	0.40	0.30	0.30	0.5	1.3	1.3	6.05	>10	-	-	Viscous
#36-47	0.40	0.28	0.82	0.5	1.4	0.5	7.25	-	-	7.2	-
#36-49	0.36	0.27	0.36	0.5	1.3	1.0	6.5	>10	-	-	Contains viscous phase
#36-50	0.33	0.25	0.42	0.5	1.3	0.8	7	-	-	-	Contains viscous phase
#36-54	0.25	0.25	0.25	1.0	1.0	1.0	6.75	>10	<3	6.75	Good phase behavior
#36-55	0.25	0.25	0.25	0.5	1.0	1.0	7.3	>10	<3	7.3	Good phase behavior

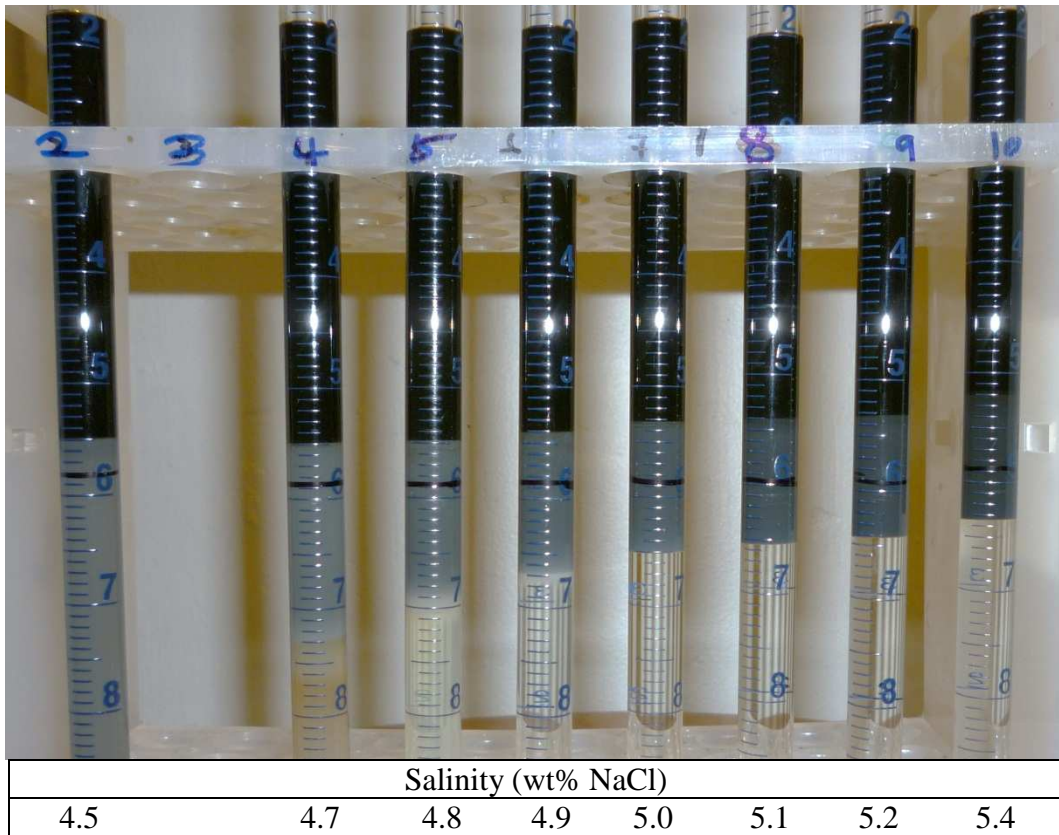


**Figure 3.12** Photo of a salinity scan for a formulation X-4 containing 0.625 wt% Alfoterra® 123-8s, 0.375 wt% Petrostep® S-2, 0.75 wt% IBA and 0.05 wt% NaOH with Trembley crude oil @ 46.1 °C after equilibrating for 22 days.

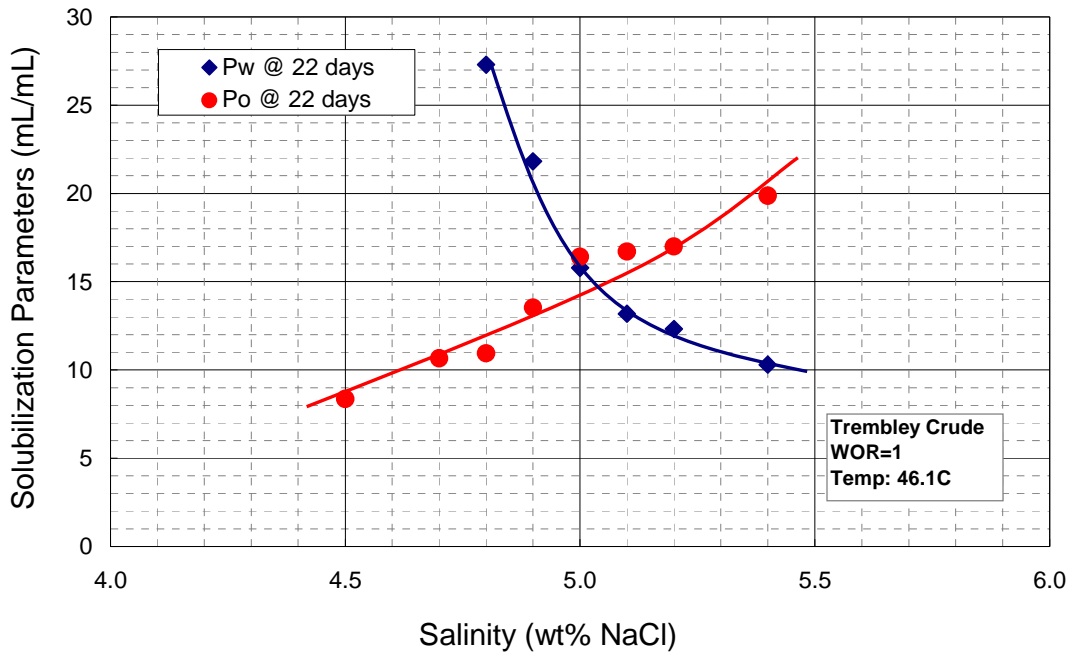


**Figure 3.13:** Solubilization Parameters plot for formulation (A3) containing 0.625 wt% Alfoterra® 123-8s, 0.375 wt% Petrostep® S-2, 0.75 wt% IBA and 0.05 wt% NaOH with Trembley crude oil @ 46.1 °C after equilibrating for 22 days.

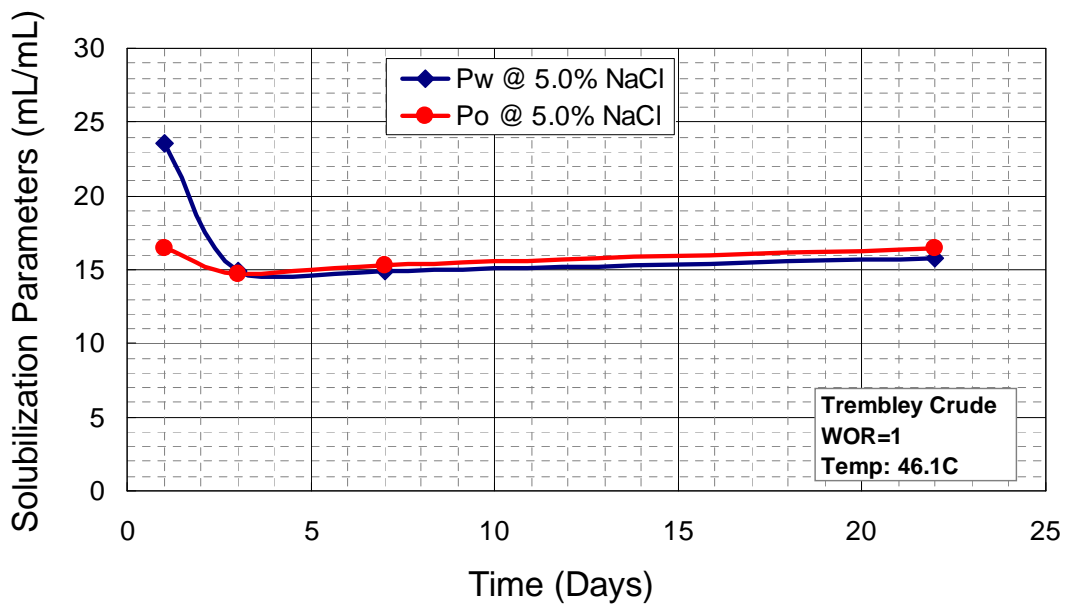


**Figure 3.14:** Determination of equilibration time for formulation X-4 containing 0.625 wt% Alfoterra® 123-8s, 0.375 wt% Petrostep® S-2, 0.75 wt% IBA and 0.05 wt% NaOH with Trembley crude oil @ 46.1 °C.

### ***Effect of Surfactant Concentration***

Effects of total surfactant concentration were studied using formulations containing Petrostep S-1 and S-2 and SBA as co-solvent. The first effect observed was on the optimum salinity of the formulations and is captured in **Figure 3.2**. A shift in optimum salinity was seen towards lower values as total surfactant concentration was reduced at all surfactant to co-surfactant ratios studied. The same effect was observed when DGBE was used as the co-solvent and alkali was added to the formulations (**Table 3.11**). Another observation for varying surfactant concentration was in the co-solvent requirement to give non-viscous microemulsion middle phase. Table 3. presents similar formulation except total surfactant and co-solvent concentrations were varied. To give non-viscous microemulsion middle phase, at 0.5 wt% surfactant concentration, a higher alcohol ratio relative to surfactant was necessary compared to 1 wt% total surfactant for same formulation. For #40-33, which is 1 wt% total surfactant, 1.5 wt% co-solvent was needed, but #40-13, which is 0.5 wt% total surfactant, was viscous even with 1.25 wt% co-solvent. This shows that the proportion of co-solvent needed for non-viscous middle phase increases as surfactant concentration is reduced. Consequently, reducing surfactant concentration may require a higher proportion of co-solvent which would in turn reduce the optimum solubilization ratios.

### ***Effect of Co-surfactant***

**Table 3.12** presents selected screening results that summarize the effect of varying surfactant to co-surfactant ratio. Alcohol concentration was the same in all series. #25-16 had a viscous middle phase and did not equilibrate to form a fluid type III microemulsion. However, the higher proportion of co-surfactant in subsequent series, #25-17 and #25-18, gave fluid type III microemulsions. These results indicate that the co-surfactant reduced the viscosity of the microemulsion phase and promoted coalescence to a stable microemulsion that would otherwise require additional alcohol co-solvents. This improvement may be attributed to the disorder created by different molecular structures of the surfactant and co-surfactant at the water and oil interface disallowing them to pack closely to form viscous phases (Hirasaki, Miller et al. 2008).

Secondly, we observe in **Table 3.12** that the optimum salinity increased as the proportion of co-surfactant was increased, indicating relative higher hydrophilic-lipophilic balance (HLB) of co-surfactant. The other significant impact of using co-surfactant was on requirement for alcohol. Both #28-1 and #28-6 had 1 wt% total surfactant and had similar solubilization ratios and equilibration times, but #28-1 required half the amount of alcohol as #28-6 due to higher proportion of co-surfactant. This was a significant reduction in alcohol in view of scale of field application volume requirements.

### ***Effect of Co-solvent Concentration***

In screening with Trembley crude oil, one formulation was analyzed for co-solvent effect. This formulation contained 0.625 wt% Petrostep S-1 surfactant, 0.375 wt% Petrostep S-2 as co-surfactant and DGBE as the co-solvent. Results are presented in **Table 3.13**. Alcohol concentration was varied keeping other constituents of the formulation constant. A reduction in optimum solubilization ratio from 15 to 10 mL/mL was observed as co-solvent concentration was increased from 1.25 wt% aqueous to 2.0 wt% while the middle phase

**Table 3.11:** Effect of surfactant concentration on the amount of co-solvent to give non-viscous middle phase. Selected results from Petrostep S-1 and S-2 screening with Trembley crude oil. Temperature was maintained at 46.1 °C.

Series #	Surf	Petrostep S1	Co-Surf	Petrostep S2	Polymer	Co-Solvent		Ratio	Alkali	WOR	Optimum		Time	Remarks
						wt%	Co-solvent type				Surf : co-surf	Na <sub>2</sub> CO <sub>3</sub> (wt%)		
#40-13	0.31	0.19	0	1.25	DGBE	5:3	1	1.5	4.65	-	-	-	More co solvent needed for less viscous middle phase	
#40-14	0.31	0.19	0	1.5	DGBE	5:3	1	1.5	4.65	-	-	-	Fluid ME, low Solubilization ratio	
#40-28	0.625	0.375	0	2	DGBE	5:3	1	1.5	5.4	10	2	2	Fluid ME, low solubilization ratio	
#40-31	0.625	0.375	0	1.25	DGBE	5:3	1	1.5	5.25	>15	2*	2*	Slightly viscous and slow to equilibrate	
#40-33	0.625	0.375	0	1.5	DGBE	5:3	1	1.5	5.3	13	1	1	Fluid ME, good solubilization ratio	

**Table 3.12:** Relationship between surfactant to co-surfactant ratio and phase behavior. Temperature was maintained at 46.1 °C.

Series #	Surfactant		Co-Surfactant	Co-Solvent		surf : co-surf Ratio	alkali NaOH (wt%)	WOR	Optimal Salinity, S* wt% NaCl	Optimal Solubilization Ratio, $\sigma^*$ (mL/mL)	Eq. Time at reading (days)	Microemulsion	
	Petrostep S1 (wt%)	Sasol 123-8s (wt%)		wt%	Type							Comments	
#25-16	0.75		0.25	2	SBA	3:1	0.25	1	3.06	19	12	Creamy viscous non-fluid middle phase/ <b>not equilibrated</b>	
#25-17	0.625		0.375	2	SBA	5:3	0.25	1	4.25	13.8	5	Fluid middle phase/equilibrated/Good Solubilization ratio	
#25-18	0.5		0.5	2	SBA	1:1	0.25	1	5.8	10.4	10	Fluid middle phase/equilibrated/Low Solubilization	
#28-1		0.75	0.25	1.5	IBA	3:1	0.25	1	~3.2	~12.5	5	Quite Fluid Interfaces	
#28-6		0.625	0.375	0.75	IBA	5:3	0.25	1	~4.6	~12	4	Very Fluid Middle Phase	



**Table 3.13:** Relationship between co-solvent concentration and phase behavior. Temperature was maintained at 46.1 °C.

Series #	Surfactant	Petrostep S1	Co-Surfactant	Co-Solvent		surf : co-surf Ratio	alkali		WOR	Optimal Salinity, S* wt% NaCl	Optimal Solubilization Ratio, $\sigma^*$ (mL/mL)	Eq. Time at reading (days)	Microemulsion
				wt%	Type		NaOH (wt%)	Na <sub>2</sub> CO <sub>3</sub> (wt%)					
#40-28		0.625	0.375	2	DGBE	5:3		1	1.5	5.4	10	2	Fluid middle phase, low solubilization ratio
#40-33		0.625	0.375	1.5	DGBE	5:3		1	1.5	5.3	13	1	Fluid middle phase, good solubilization ratio
#40-31		0.625	0.375	1.25	DGBE	5:3		1	1.5	5.25	15	2*	slightly viscous and slow to equilibrate

microemulsion appeared less viscous. In this case, a minimum concentration of 1.5 wt% DGBE was necessary to obtain non-viscous microemulsion and that still achieved optimum solubilization of higher than 10 mL/mL. A slight increase in optimum salinity was observed with increase in co-solvent concentration due to the high HLB of DGBE. SBA and IBA were noted to have minimal effect on optimum salinity. All these results are in agreement with the theory on the effects of alcohol.

#### ***Effect of Alkali Concentration***

The formulation containing Petrostep S-1 and Petrostep S-2 with SBA as the co-solvent was studied with and without alkali. Equilibration time was a problem for this formulation until an alkali was added. Not even high concentrations of alcohol reduced the equilibration time without alkali as observed in the behavior of series #A36 in **Table 3.4**. Results in the table show that an addition of up to 0.05 wt% NaOH or 0.2 wt% Na<sub>2</sub>CO<sub>3</sub> to this formulation gave almost double optimum solubilization ratio and dramatically reduced equilibration time. The microemulsion phase was more fluid with alkali. Although more Na<sub>2</sub>CO<sub>3</sub> by mass compared to NaOH was required to produce the desired alkali effect, Na<sub>2</sub>CO<sub>3</sub> was preferred due to its much lower cost and much better performance at lowering surfactant adsorption compared to NaOH (Hirasaki, Miller et al. 2008).

Alkali contributes to electrolytes in the system. Therefore, amount of NaCl, the primary electrolyte, required to obtain optimum salinity is reduced when alkali is also added to the formulation. This is seen in **Table 3.4**. The optimum salinity of the formulation without alkali was 4.65 wt% NaCl. As concentrations of NaOH and Na<sub>2</sub>CO<sub>3</sub> were increased, NaCl concentration for optimum salinity was decreased. For the phase behavior studies results, the optimum salinity was not corrected and reported in terms of nominal concentration of NaCl concentration in the formulations. NaOH showed a much greater effect on optimum salinity compared to Na<sub>2</sub>CO<sub>3</sub> on wt% equivalence. 1 wt% NaOH reduced the optimum salinity by 1.5 wt% NaCl, whereas, the same amount of Na<sub>2</sub>CO<sub>3</sub> dropped the optimum salinity by 0.8 wt% NaCl. Molecular weights (MW) of NaOH, NaCl and Na<sub>2</sub>CO<sub>3</sub> are 39.9, 58.4 and 105.9 respectively. NaOH and NaCl ionize into two and Na<sub>2</sub>CO<sub>3</sub> into 3 ions. Ions/MW ratio of the three simplifies to 1.46 (NaOH):1.00 (NaCl):0.83 (Na<sub>2</sub>CO<sub>3</sub>). The ratio represents the relative number of moieties released for the same weight of the three electrolytes. The effect of alkali on optimum salinity in terms of NaCl was directly proportional to the ratio.

#### ***Effect of Polymer on Phase Behavior***

**Table 3.14** presents the phase behavior results of two formulations with and without polymer. Both formulations had similar surfactant, alkali and polymer concentrations but used different alcohols, SBA and DGBE. One formulation is the core flood candidate, Formulations X-1. Formulation X-1 showed a small reduction in APSL from 5.0 wt% NaCl to 4.7 wt% NaCl when 2200ppm Flopaam 3330S polymer was added. It still remained higher than the optimum salinity, which was 4.3 wt% NaCl at WOR of 1.5. Optimum solubilization ratios were altered from 12.9 to 13.5 mL/mL, which may not necessarily have been caused by the polymer. More important result was that polymer did not reduce the optimum solubilization ratio for Formulation X-1.

**Table 3.14:** Formulation X-1 and another formulation with and without polymer and the associated phase behavior results.

#	Series Surfactant		Co-Solvent		Ratio		Alkali		Polymer Flopaam 3330S (wt%)	WOR	Optimum Salinity (wt% NaCl)	APSL at $T_{res}$ , 46.1 C (wt% NaCl)	Optimum Sol. Ratio (mL/mL)	Equil. Time (Days)	Formulation code
	Petrostep S1	Petrostep S2	wt%	type	surf : co-surf	wt%	Type								
40-55	0.625	0.375	2	SBA	5:3	1	Na <sub>2</sub> CO <sub>3</sub>	0	1.5	4.4	5	12.9	3	X-1	
40-57	0.625	0.375	2	SBA	5:3	1	Na <sub>2</sub> CO <sub>3</sub>	0.22	1.5	4.3	4.7	13.5	3	X-1	
40-54	0.625	0.375	1.5	DGBE	5:3	1	Na <sub>2</sub> CO <sub>3</sub>	0		5.2	5.8	13	2		
40-62	0.625	0.375	1.5	DGBE	5:3	1	Na <sub>2</sub> CO <sub>3</sub>	0.22	1.5	5.2	6.6	14	3		

The other formulation that used DGBE instead of SBA, showed an increase in APSL. This was not caused by polymer addition but actually was due to the aging of the surfactant bulk solutions. Aged surfactant bulk solutions showed lower APSL and lower optimum solubilization ratios, which was verified in unreported experiments. APSL was still greater than the optimum salinity of the formulation with and without polymer. For this formulation as well, polymer did not cause a reduction in optimum solubilization ratio.

The results showed that polymer has a minimal effect on APSL and optimum solubilization ratios. The evidence was not sufficient to conclude if polymer caused a reduction in APSL.

### **Measurement of Microemulsion Phase Properties**

During the phase behavior screening experiments, inference about the potential success of a formulation were primarily based on the visual and qualitative assessments of the microemulsion phase. These qualitative assessments were in effect the indicators of the important physical properties of the microemulsion phases, which were its viscosity, and interfacial tension (IFT) with the oil and water phase. In order to validate the results of visual assessment, the IFT and viscosities of the good performing formulations were measured.

#### ***Interfacial Tension (IFT)***

IFT measurement between aqueous and microemulsion phase was performed for a formulation containing 0.62% Petrostep S1, 0.38% Petrostep S2, 2% SBA, 0.5 wt% NaOH, 4 wt% NaCl and Trembley crude oil with WOR=1. The solubilization of water and oil were 13.5 mL/mL and 21 mL/mL respectively for this sample. The IFT value measured using spinning drop tensiometer was 0.0006 dynes/cm, which was ultra low and satisfied the assumption that a solubilization ratio of above 10 mL/mL correlates to ultra low IFT. A picture of the spinning drop for this measurement is given in **Figure 3.15**. Correlating solubilization parameters with IFT was not undertaken as it was time consuming and out of scope for this study.

#### ***Viscosity Measurement***

Viscosities of microemulsion phase of two optimized formulations X-1 and X-4 were measured in the range of salinities encompassing type I, type III and type II microemulsion. The viscosities versus the salinity for the two formulations are plotted in **Figure 3.16**. Polymer was not added to these formulations. Viscosities of both formulations showed two peaks, one at the type I to type III microemulsion phase transition salinity and the other at the type III to type II transition. In both cases, a local minimum viscosity was reached between the two peaks, and this salinity coincided with the optimum salinity of the two formulations. This behavior was similar to that observed by Bennet et al for microemulsion systems (Bennett, Macosko et al. 1981).

The highest viscosity for the microemulsion phase was ~ 11cp for the formulation X-4 and ~9 for X-1. Viscosity at the optimum salinity was ~8 cp, which was twice as much as Trembley crude oil viscosity. The viscosity value did not pose a concern and corroborated the visual assessment made earlier, that of it being non-viscous.

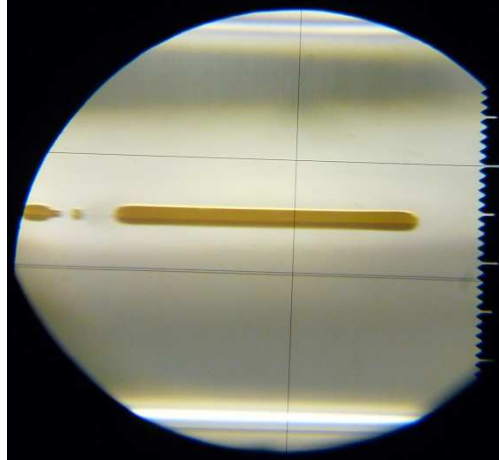


**Figure 3.15:** A picture of spinning drop in action during IFT measurement between aqueous and microemulsion phase from the same pipet. The formulation contained 0.62% Petrostep S1, 0.38% Petrostep S2, 2% SBA, 0.5 wt% NaOH and Trembley crude oil with WOR=1 at 4 % salinity and 46.1 C.

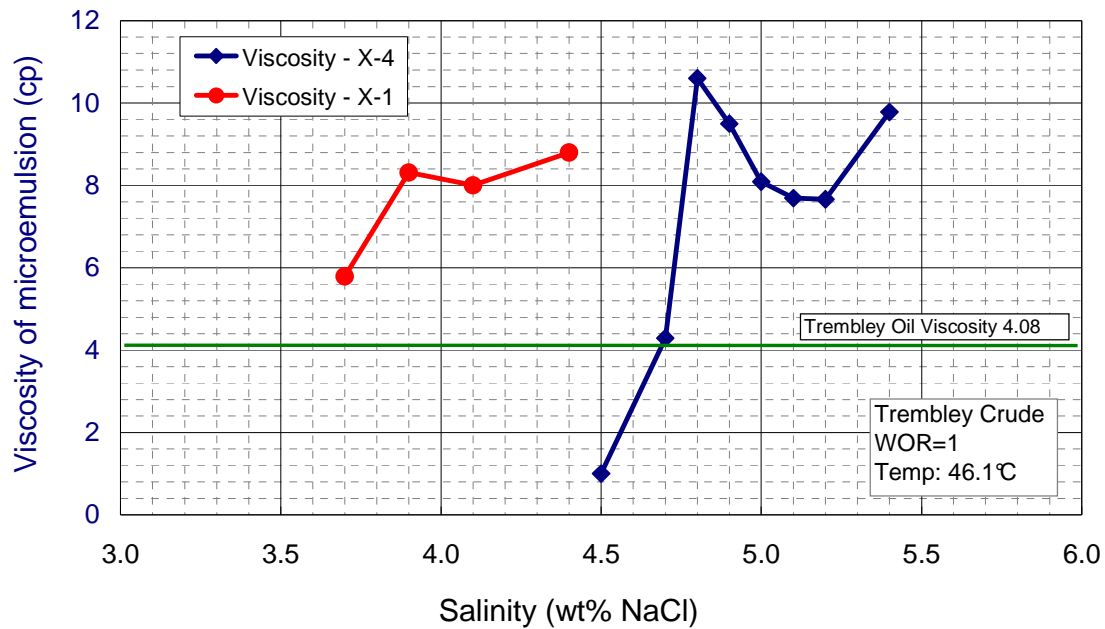


**Figure 3.16:** Microemulsion viscosity for formulation X-1 and X-4. Viscosities were measured at a constant shear rate of  $75 \text{ sec}^{-1}$ .

### Salinity Requirement for Surfactant and Polymer Drive

Understanding the phase behavior relationships between optimum salinity, WOR and surfactant concentration was key to an optimized surfactant and polymer slugs for core flooding. The optimum salinity and the microemulsion phase transition boundaries of 1 wt% surfactant Formulation X-1 for Trembley changed with water to oil ratio (WOR) as illustrated in **Figure 3.17**. The y-axis of the figure is in terms of total dissolved solid and  $\text{Na}_2\text{CO}_3$  was treated as being equivalent to NaCl on weight basis. Optimum and phase transition salinities were higher for lower oil concentrations. Typically, sandstone cores have waterflood residual oil saturation around 40%. This would be the initial oil concentration that the surfactant slug would meet during a surfactant flood. As the flood would proceed, the oil saturation in contact with the slug would become lower. The salinity of surfactant slug therefore must be chosen such that the slug would remain near the optimum conditions for the whole range of oil concentrations. For the case in Figure 3., an equivalent salinity of 5.6 wt% (4.6wt% NaCl + 1wt%  $\text{Na}_2\text{CO}_3$ ) would be a good choice. The blue dotted arrow shows the microemulsion phase changes if this salinity were to be selected. In this case, the three phase window was wide and the microemulsion phase formed in the entire range of 0% to 40% oil concentration would be Winsor Type III. The microemulsion phase change would be from slightly over optimum to under optimum.

Salinity of the polymer drive should be such so as to induce a moderate Type III to Type I microemulsion transition in the core. This would reduce trapping of surfactant and mobilized oil. Correct salinity selection of the slug and the polymer drive are more important for a shorter slug. To determine polymer salinity, investigating how the Type III to Type I microemulsion transition salinity requirement changed with surfactant concentration for Formulation X-1 was helpful (**Figure 3.18**). The y-axis of the figure is in terms of total dissolved solid and  $\text{Na}_2\text{CO}_3$  was treated as being equivalent to NaCl on weight basis. The figure shows that at lower surfactant concentration, the optimum salinity and the phase transition salinities are lower. If the salinity of the polymer slug was matched with the surfactant slug, the conditions in the ASP flood would not transition to Type I. The equivalent salinity in polymer drive must be therefore lowered so that when the surfactant concentration becomes zero, the transition to type I must have occurred. In this case, a polymer equivalent salinity of 4.5 wt% (NaCl only) would ensure that the ASP flood ended in Type I system as the surfactant slug was diluted by the polymer drive at the back of the surfactant slug. The dilution path of the surfactant as it gets dispersed with polymer drive at the back end is depicted in the figure by blue dotted arrow. According to the dilution path, the microemulsion phase would become Type I when the surfactant concentration goes below 0.6 wt%.

### SUMMARY OF PHASE BEHAVIOR STUDIES RESULTS

Five optimized formulations, X-1 to X-5, that comprised three unique surfactant and co surfactant combinations were formulated from phase behavior studies. The five formulations are presented in **Table 3.15**. The three pairs of surfactant and co-surfactant used were Petrostep S1 and Petrostep S2 (Formulations X-1, X-2 and X-3), Alfoterra 123-8s and Petrostep S2 (formulation X-4), and Petrostep S-13D and Petrostep S-2 with Novel TDA-12EO as the only co-solvent (formulation X-5). All formulations showed optimum solubilization ratios greater than 10 mL/mL and low viscosity microemulsions, and

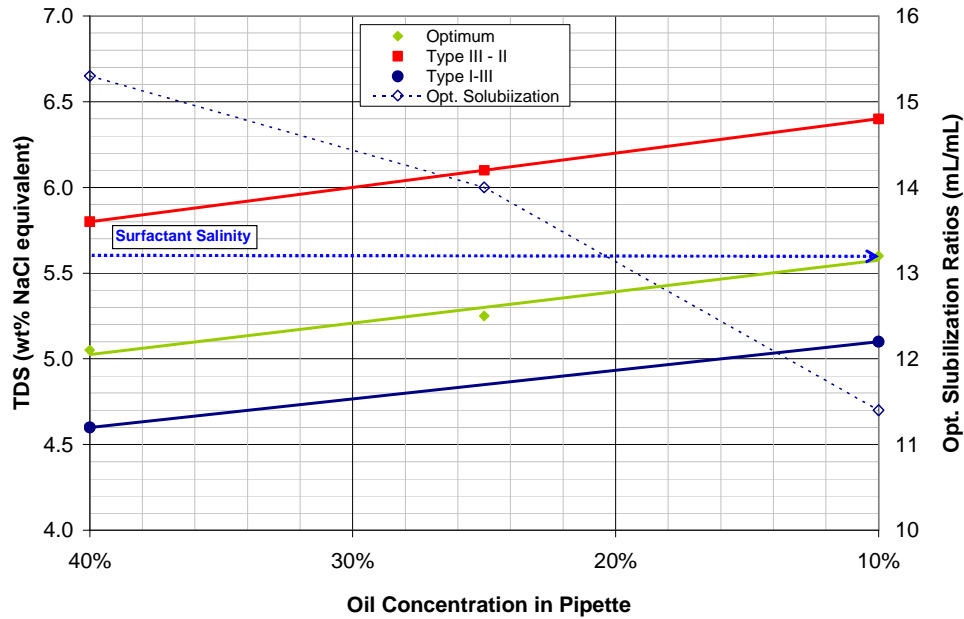


**Figure 3.17:** Optimum salinity and solubilization ratios for 1 wt% surfactant formulation X-1 versus different oil percent in pipettes for Trembley. The blue arrow, which represents a hypothetical surfactant slug salinity, shows the effect of oil concentration change on microemulsion phase behavior in the surfactant slug as an ASP flood progresses.

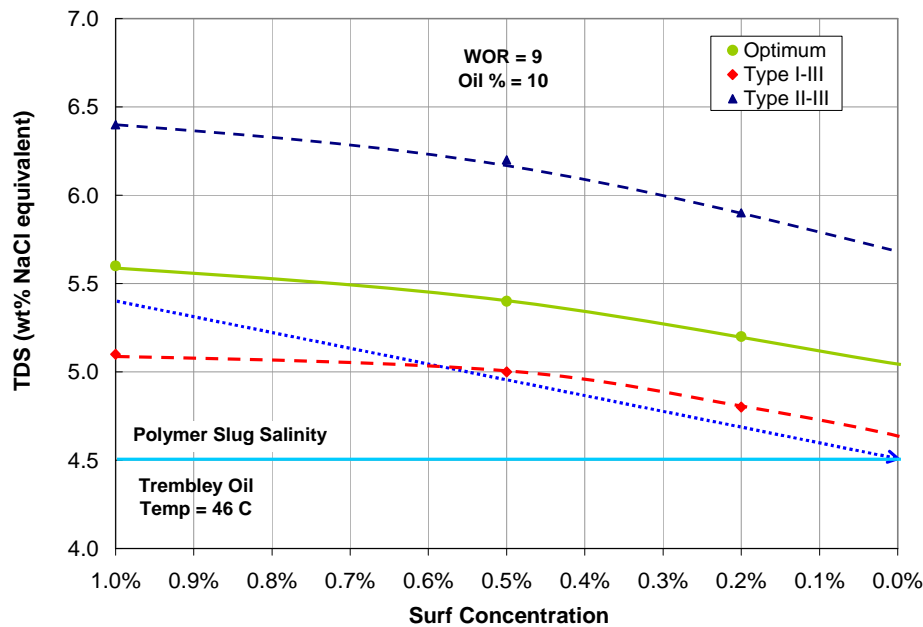


**Figure 3.18:** Optimum equivalent salinity and phase transition boundaries for surfactant concentration range 0 wt% to 1 wt% for Formulation X-1 are plotted. The curves were interpolated and extrapolated to cover the entire range. The dilution of surfactant at the back of surfactant bank and corresponding equivalent salinity (NaCl + Na<sub>2</sub>CO<sub>3</sub>) change is shown by the dotted blue arrow.

**Table 3.15:** The five optimized formulations from phase behavior studies and their phase behavior results. Only Formulations X-1, X-2 and X-3 passed all screening criteria and therefore were selected for core flood demonstration.

Series #	Surfactant		Co-Surf		Co-Solvent		Ratio		Alkali		Polymer		Optimum Salinity (wt% NaCl)	APSL at $T_{res}$ , 46.1 C (wt% NaCl)	Optimum Sol. Ratio (mL/mL)	Equil. Time (Days)	Formulation code
	Petrostep S1	Alfoterra 123-8S	Petrostep S2	wt%	type	surf : co-surf	wt%	Type	Flopaam 3330S (wt%)	WOR							
40-57	0.625		0.375	2	SBA	5:3	1	Na <sub>2</sub> CO <sub>3</sub>	0.22	1.5	4.3	4.7	13.5	3	X-1		
40-9	0.313		0.188	1.25	SBA	5:3	1	Na <sub>2</sub> CO <sub>3</sub>	0.22	1.5	4.0	-	12.3	3	X-2		
40-18	0.313		0.188	1.375	DGBE	5:3	1	Na <sub>2</sub> CO <sub>3</sub>	0.23	1.5	4.65	6.4	14	2	X-3		
-		0.625	0.375	0.75	IBA	5:3	0.05	NaOH	0	1	5.0	4.5	15	3	X-4		
36-55	0.25		0.25	0.25	Novel TDA-12-EO	1:1	1	Na <sub>2</sub> CO <sub>3</sub>	0	1	6.75	6.75	13	3	X-5		



equilibrated in less than 7 days. However, only three formulations, X-1, X-2 and X-3, containing Petrostep S-1 and Petrostep S-2 surfactants gave aqueous phase stability limit (APSL) higher than the optimum salinity. In conclusion, only Formulations X-1, X-2 and X-3 successfully passed all four criteria of phase behavior screening with the assumption that APSL was higher than optimum salinity for X-2. The formulations were selected as candidates for core flood evaluation.

## CORE FLOOD RESULTS

Core floods were performed to determine oil recovery of the optimized formulations. These floods were also essential to validate the theory of the fluid displacement mechanism and to optimize the surfactant and polymer slug injection design, which includes surfactant and polymer slug sizes, salinity and polymer concentrations. Core floods for Trembley crude oil were performed in Berea sandstone cores. A total of nine core floods were performed, named T-1 to T-9. The associated core numbers are given in **Table 3.16** along with the dimensions and permeability of the cores. Important parameters related to core floods and the results of the floods are summarized in **Table 3.17**.

Alkaline surfactant polymer (ASP) floods T-1, T-2, T-3, T-8 and T-9 were performed with 1wt% formulation, X-1. Flood T-4 was performed with formulation X-2, and floods T-5, T-6 and T-7 were performed with formulation X-3. Flood T-9 was the only flood in which the core was saturated with synthetic formation brine (SFB).

### Core Floods with Formulation X-1

Surfactant slug designed after formulation X-1 contained 0.625wt% Petrostep S-1, 0.375 wt% Petrostep S-2, 2 wt% SBA, 1 wt% Na<sub>2</sub>CO<sub>3</sub>. NaCl concentrations at the end of waterflood and ranged between 4.1 wt% NaCl (41000 ppm) and 4.4 wt% NaCl (46000 ppm) not counting alkali. For floods T-1, T-2 and T-3 optimum salinity for surfactant slug was chosen for WOR of 1.5, which equaled 4.10-4.15 wt% NaCl. For T-8 and T-9, the optimum salinity was chosen at WOR of 3, which equaled 4.4-4.6 wt% NaCl. SNF 3330 polymer was used for all floods and the concentration for surfactant slug ranged between 2000ppm and 2450ppm. The exact values for each core flood are tabulated in **Table 3.17**.

The polymer slug for the floods using this formulation contained NaCl ranging between 2.94 wt% NaCl (29400ppm) and 4.4 wt% NaCl (45000ppm). Salinities were varied in core floods for this formulation to improve the recovery results. Polymer concentrations in the polymer drive ranged between 2000 ppm and 2450 ppm.

### Core Flood T-1 (Core #2)

T-1 was the first chemical flood performed for Trembley crude oil. The objective of the core flood was to understand the displacement mechanisms, the effectiveness of surfactant slug and gain insights into mobility control from pressures in order to further optimize the surfactant and polymer slug size and composition for better recovery. Chemical flood was performed at reservoir temperature, 46.1 °C but the core was saturated with 4.2 wt% NaCl, which was less than the equivalent salinity of surfactant slug (4.13wt% NaCl + 1.0 wt% Na<sub>2</sub>CO<sub>3</sub>). The objective was to keep the formation equivalent salinity equal to the surfactant effective salinity. However, that objective was not met.

### Core Characterization

Core #2, sandstone, was set up for flooding in horizontal orientation. First its dispersion was characterized (**Figure 3.19**) and found to have a typical profile for sandstones. Pore volume was determined from tracer curve integration and gravimetric method, and determined to be 93 mL. Porosity was estimated to be 0.167. Permeabilities of the core and sections were

**Table 3.16:** Summary of Trembley core floods' core dimensions and permeabilities.

ASP #	T-1		T-2		T-3		T-4		T-5		T-6		T-7		T-8		T-9		
	Core #	2	length (cm)	k <sub>br</sub> (md)	length (cm)	k <sub>br</sub> (md)	length (cm)	k <sub>br</sub> (md)	length (cm)	k <sub>br</sub> (md)	length (cm)	k <sub>br</sub> (md)	length (cm)	k <sub>br</sub> (md)	length (cm)	k <sub>br</sub> (md)	length (cm)	k <sub>br</sub> (md)	length (cm)
Overall		27.53	645	30.5	184	31	30.2	141	30.4	195	30.4	118	30.5	225	30.5	232	30.5	232	30.5
Section 1		2.13	640	4.8	145	4.95	4.90	153	4.95	167	5	87	5.1	215	5.1	199	5.1	199	5.1
Section 2		5.08	685	5.10	218	5.15	5.10	156	5.2	246	5.2	123	5.1	223	5.1	225	5.1	225	5.1
Section 3		5.08	634	5.10	200	5.25	5.10	144	5.1	194	5.1	112	5.1	237	5.1	241	5.1	241	5.1
Section 4		5.08	625	5.10	199	5.25	5.25	163	5.1	205	5.1	109	5.1	232	5.1	263	5.1	263	5.1
Section 5		5.08	666	5.25	192	5.2	5.150	124	5.1	180	5.1	122	5.1	212	5.1	253	5.1	253	5.1
Section 6		5.08	619	4.85	182	5.2	4.7	128	4.9	187	4.9	218	5.0	250	5	235	5.0	235	5.0

**Table 3.17:** Summary of Trembley core floods' important parameters and results. The floods were performed at reservoir temperature ( $T_{res}$ ) 46.1 °C.

ASP #	T-1	T-2	T-3	T-4	T-5	T-6	T-7	T-8	T-9
Core #	2	4	23	26	27	31	32	37	39
Formulation	X-1	X-1	X-1	X-2	X-3	X-3	X-3	X-1	X-1
Rock	Sandstone								
$k_{br}$ (md)	430	645	184	151	141	195	120	225	232
$k_{ro}$	1.11	0.87	0.90	0.82	0.85	0.91	0.85	0.75	0.74
$k_{rw}$	0.053	0.064	0.045	0.044	0.047	0.050	0.042	0.054	0.043
$S_{oi}$	0.605	0.662	0.659	0.639	0.633	0.643	0.626	-	0.654
$S_{or}$	0.361	0.377	0.413	0.389	0.384	0.386	0.401	0.383	0.367
Formation Brine	4.2% NaCl	5.0% NaCl	5.2% NaCl	5.0% NaCl	6.5% NaCl	6.1% NaCl	6.5% NaCl	5.5% NaCl	SFB
	Surfactant Slug								
$C_{surf}$ (wt%)	0.625	0.625	0.625	0.31	0.31	0.31	0.31	0.625	0.625
$C_{cosurf}$ (wt%)	0.375	0.375	0.375	0.19	0.19	0.19	0.19	0.375	0.375
$C_{atchd}$ (wt%)	2% SBA	2% SBA	2% SBA	1.25% SBA	1.375% DGBE	1.375% DGBE	1.375% DGBE	2% SBA	2% SBA
$C_{polymer}$ (ppm SNF 3330S)	2000	2000	2250	2250	2250	2000	2200	2200	2450
Salinity (ppm)	41300 NaCl 10000 Na <sub>2</sub> CO <sub>3</sub>	41500 NaCl 10000 Na <sub>2</sub> CO <sub>3</sub>	42500 NaCl 10000 Na <sub>2</sub> CO <sub>3</sub>	42500 NaCl 10000 Na <sub>2</sub> CO <sub>3</sub>	50000 NaCl 10000 Na <sub>2</sub> CO <sub>3</sub>	50000 NaCl 10000 Na <sub>2</sub> CO <sub>3</sub>	50500 NaCl 10000 Na <sub>2</sub> CO <sub>3</sub>	48000 NaCl 10000 Na <sub>2</sub> CO <sub>3</sub>	44000 NaCl 10000 Na <sub>2</sub> CO <sub>3</sub>
PV Injected	0.3	0.3	0.3	0.3	0.3	0.6	0.6	0.3	0.3
$\mu_{slug}$ (cp)	11 @ 45 s <sup>-1</sup>	9.4 @ 45 s <sup>-1</sup>	21 @ 1 s <sup>-1</sup>	19 @ 1 s <sup>-1</sup>	18 @ 1 s <sup>-1</sup>	16 @ 1 s <sup>-1</sup>	18 @ 1 s <sup>-1</sup>	21 @ 1 s <sup>-1</sup>	14 @ 38 s <sup>-1</sup>
	Polymer Drive								
$C_{polymer}$ (ppm SNF 3330S)	2500	2500	2500	2250	2250	2250	2350	2450	2450
Salinity (ppm)	29400 NaCl 12.8 @ 45 s <sup>-1</sup>	29400 NaCl 12.5 @ 45 s <sup>-1</sup>	29400 NaCl 27 @ 1 s <sup>-1</sup>	33300 NaCl 21 @ 1 s <sup>-1</sup>	49000 NaCl 25 @ 1 s <sup>-1</sup>	43000 NaCl 18 @ 1 s <sup>-1</sup>	43000 NaCl 20 @ 1 s <sup>-1</sup>	45000 NaCl 21 @ 1 s <sup>-1</sup>	41000 NaCl 14 @ 38 s <sup>-1</sup>
$\mu_{drive}$ (cp)	Results								
$S_{oic}$	0.04	0.11	0.05	0.16	0.15	0.10	0.07	0.04	0.05
% Recovery	90	72	88	60	62	75	82	91	86
% Rec. in Oil Bank	62	62	70	50	56	57	60	71	73
Oil Bank Arrival (PV)	0.2	0.25	0.15	0.21	0.18	0.18	0.15	0.19	0.24
Surfactant Breakthrough (PV)	0.67	0.73	0.74	0.74	0.71	0.69	0.74	0.78	0.95
Flood Date	2/8/2010	5/9/2010	2/16/2011	3/11/2011	3/31/2011	4/16/2011	5/7/2011	6/29/2011	8/5/2011

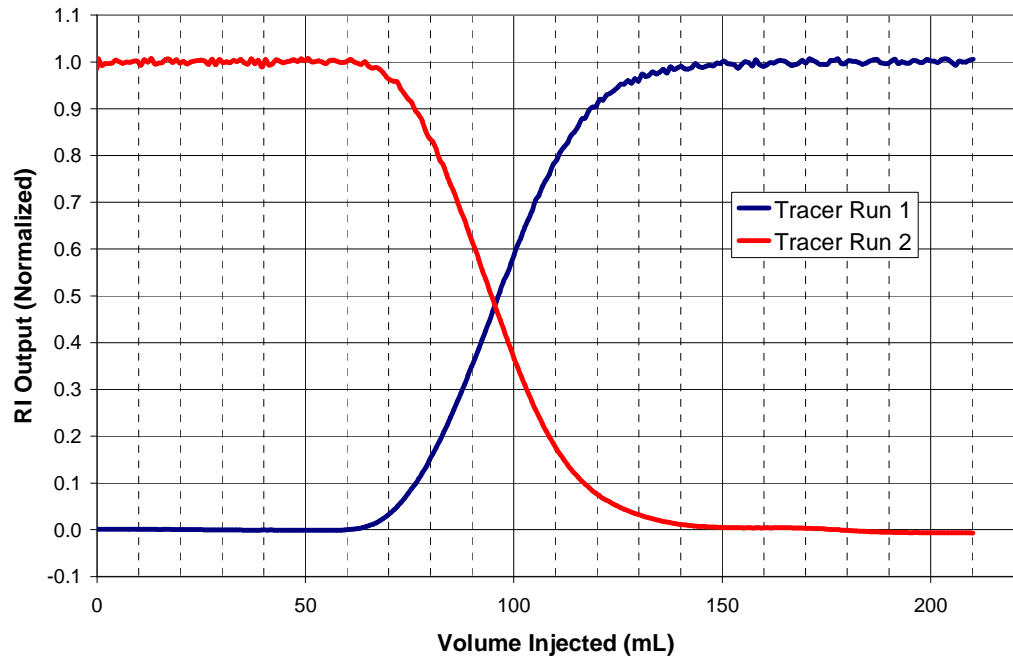


**Figure 3.19:** Dispersion characterization of Core #2 for core flood T-1.

determined next and are tabulated in **Table 3.16**. Overall permeability of the core was 430 md. Core showed an increasing trend in permeability from Section 1 to Section 6, which appeared to be due to the nature of the core.

#### *Brine Flood/Oil Flood/Waterflood*

Brine flood was carried out with 4.2 wt% NaCl. Brine flood salinity was meant to be same as the surfactant slug equivalent salinity, which was (4.13wt% NaCl + 1.0 wt% Na<sub>2</sub>CO<sub>3</sub>), however, the brine that got injected was actually less than that. Oil flood was carried out at 46.1 °C at 14 ft/day (1mL/min) and effluent was collected. Oil saturation obtained at the end of oil flood ( $S_{oi}$ ) was 0.605. Relative permeability ( $k_{ro}^o$ ) to oil at residual water saturation ( $S_{wr}$ ) was 1.11. Pressures were recorded during oil flood (**Figure 3.20**) and once the pressures became stable and oil cut became lower than 1 %, oil flood was stopped. Pressures during oil flood were severely affected by the capillary effects.

Oil flood was followed by waterflood at 2 ft/day (with 4.2 wt% NaCl brine. End point permeability to water at residual oil saturation ( $S_{or}$ ) was determined from overall pressure of the core when the pressures had stabilized (**Figure 3.21**). Final oil saturation ( $S_{orw}$ ) was determined to be 0.36. Brine, oil and waterfloods were run at 46.1 °C, the reservoir temperature.

#### *Surfactant and Polymer Slug*

Surfactant slug had the same composition as the optimized formulation X-1 except that polymer was added to raise viscosity. The final composition of the formulation was 0.625 wt% Petrostep S-1, 0.375 wt% Petrostep S-2, 2 wt% SBA, 1 wt% Na<sub>2</sub>CO<sub>3</sub>, 4.13 wt% NaCl and 2000 ppm Flopaam SNF 3330S. The viscosity of the surfactant slug was 11 cp measured at 45 s<sup>-1</sup> with Brookfield DV-I+ after adding 2000 ppm Flopaam SNF 3330S. This was three times as much as the apparent viscosity (3cp) calculated from the water and oil flood end point relative permeabilities. Equivalent salinity of the slug was 4.13 wt% NaCl and 1 wt% Na<sub>2</sub>CO<sub>3</sub>. The slug was checked with oil before injection and was found to be at optimum at WOR=1.5 and at  $T_{res}$ . WOR=1.5 equates to 40% oil saturation in the core whereas the  $S_{orw}$ =36%. The intent was to use a WOR close to  $S_{orw}$  to determine the optimum salinity for surfactant slug.

Polymer slug salinity was 2.94% NaCl. This was determined by taking 57% of the surfactant slug salinity (NaCl and Na<sub>2</sub>CO<sub>3</sub>) Polymer concentration was 2500 ppm that gave the slug a slightly higher viscosity than surfactant slug, 12.8cp at 45 s<sup>-1</sup>. Comparison of viscosities of the two slugs is given in **Figure 3.22**.

#### *Chemical Flood & Oil Recovery*

Core #2 was flooded at 0.15 mL/min (2.1 ft/day) with 0.3 pore volume (PV) of surfactant slug and followed by 1.7 PV polymer drive. Oil recovery was calculated from the oil displaced during the flood that was collected in vials. Oil bank arrived at 0.2 PV and surfactant breakthrough occurred at 0.67 PV. Oil cut dropped below 1% after 90% residual oil recovery. Oil cut and cumulative oil recovery are plotted in **Figure 3.23**. With 90% recovery, the flood should be termed successful and 0.3 PV surfactant slug proved sufficient for this formulation.

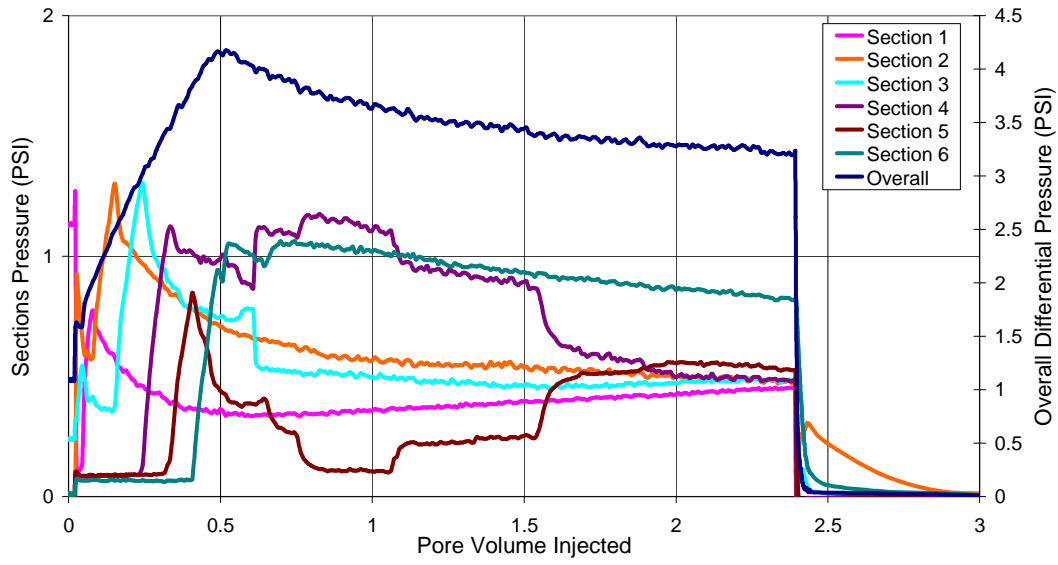


**Figure 3.20:** Oil flood differential pressures for Core #2 for core flood T-1.

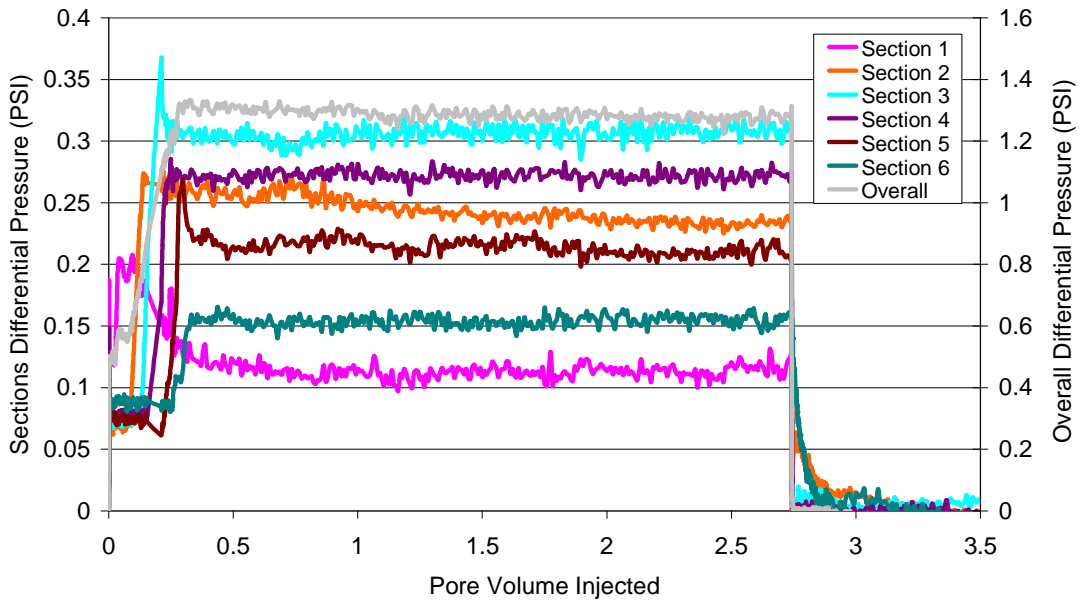


**Figure 3.21:** Waterflood differential pressures for Core #2 for core flood T-1.

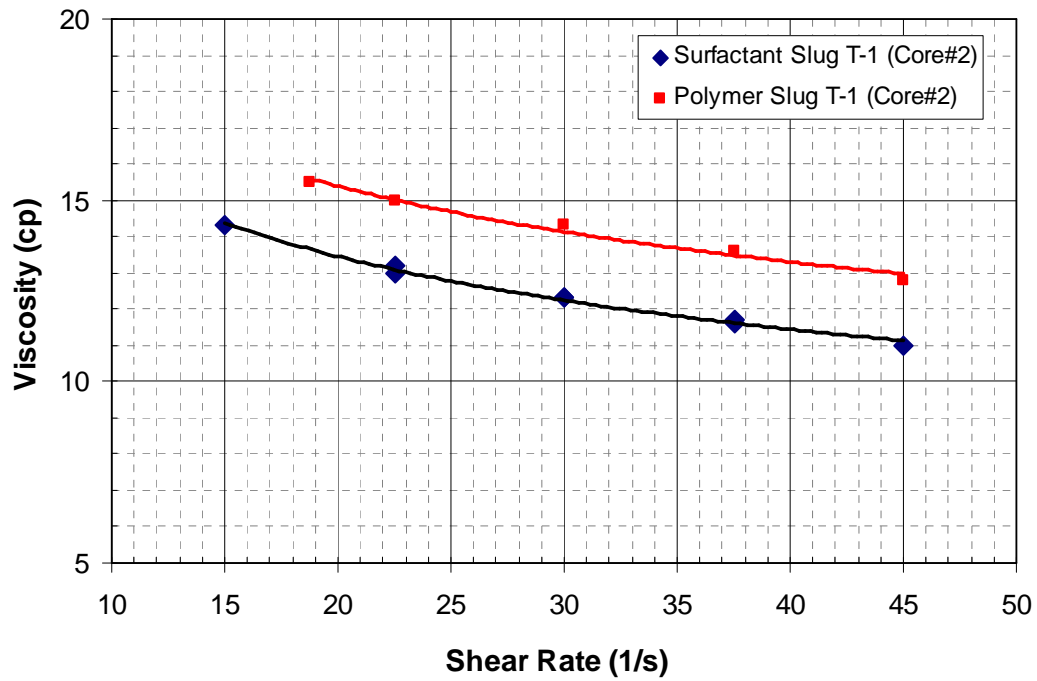


Figure 3.22: Viscosities of surfactant and polymer slug for core flood T-1 (Core #2).

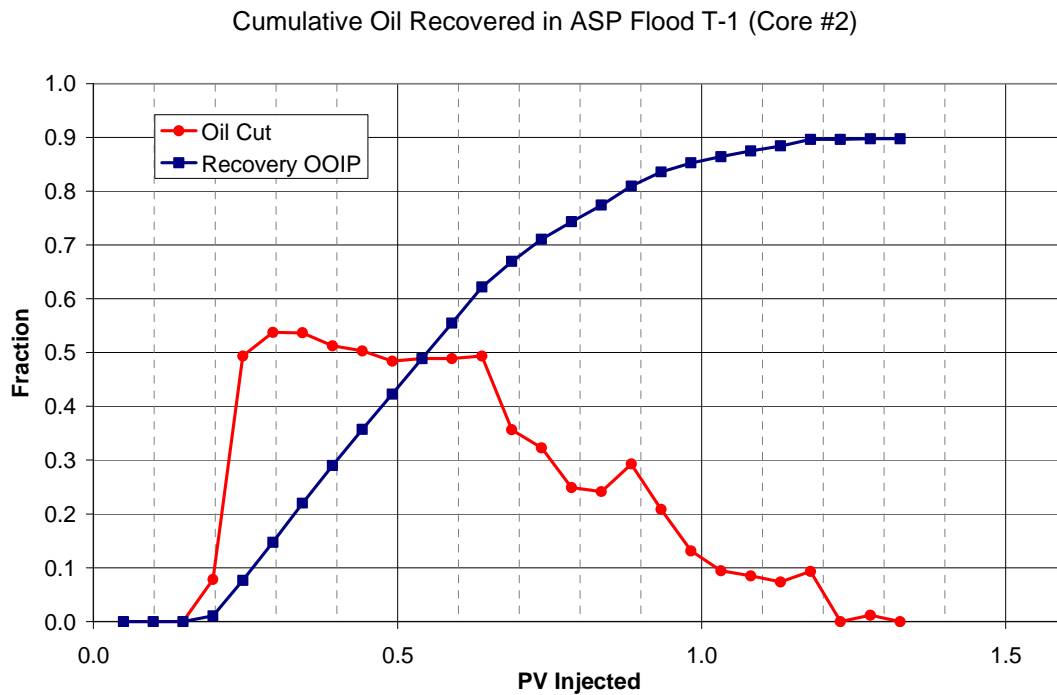


Figure 3.23: Oil cut and oil recovery for core flood T-1 (Core #2).



### *Effluent Analysis*

Effluent samples were equilibrated for 1 week at reservoir temperature and then evaluated. They are shown in **Figure 3.24**. The effluent samples contained oil water and microemulsion phases. Type of microemulsion present in the effluent vials was determined by visual observation after equilibration of samples at  $T_{res}$  for 7 days. Vials 15-33 (0.74-1.62 PV) contained microemulsion; vials 19-23 contained Winsor type III microemulsion while vials 24-33 were Winsor type I. No type II microemulsion was observed. This showed that the formation brine salinity wasn't high enough to reach type II microemulsion.

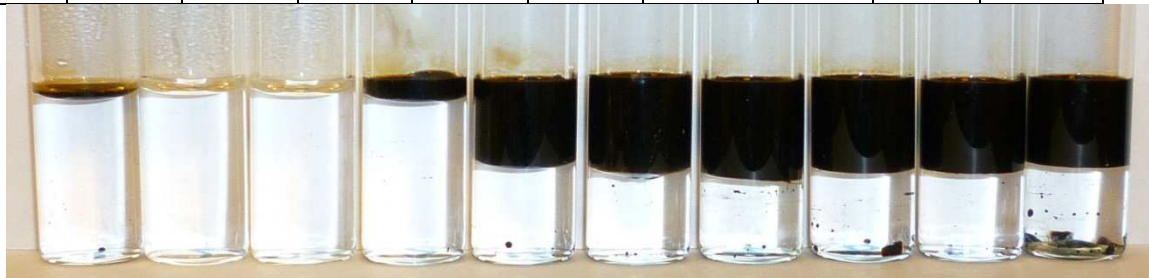
Viscosity, salinity and pH of aqueous phase of the effluent samples were measured and are presented in **Figure 3.25**. Fluid phases produced versus volume injected are indicated in the graph. Microemulsion types on the graph were determined from visual inspection of vials. Measurements show that mixing with core brine and adsorption resulted in dilution of the slug front and therefore a gradual rise in the measured properties is observed after surfactant breakthrough at approximately 0.7 PV. The mixing was attributed to the natural dispersion in the core. The mixing of surfactant slug with core brine that contained lower salinity than the slug caused the slug salinity to be under optimum. Thus when surfactant broke through, Type I microemulsion emerged first consistent with the dilution path on **Figure 3.18**. As salinity rose as indicated in the figure, Type I transitioned to Type III. On the back end of surfactant slug, the salinity started to drop due to mixing with lower salinity polymer drive which induced a transition to Type I again. A 0.2PV type III microemulsion region still made it to the end, which resulted in good oil recovery. Type III region could be further elongated if the salinity gradient between surfactant and polymer slug was not as big, which could further improve the oil recovery.

### *Pressure Analysis*

Pressures measured across the core and each section are plotted in **Figure 3.26** to **Figure 3.33**. Section one showed relatively higher pressure drop than other sections. This could have been caused by plugging of pores due to polymer. Pressures of each section were further analyzed. From observations of pressure and core effluent samples, oil, surfactant and polymer arrival at the end of core were determined. Oil and surfactant arrival at the end of core were easily determined but polymer drive arrival could not be determined accurately due to the dispersion and mixing of polymer drive with surfactant. The transition was not sharp such as in case of oil bank arrival and surfactant breakthrough. Pressure of section 6 was used to determine polymer arrival, and the saddle point at approximately 1.15 PV was considered as the polymer arrival (**Figure 3.33**). Arrival data and assumption that the dimensionless velocity of each bank was constant were used to interpolate arrival and exit of each fluid phase region in each section (**Figure 3.27**). These instances are marked on each individual section's pressure charts in **Figure 3.28** to **Figure 3.33**. The assumption of constant dimensionless velocity is validated as common features are seen on each section's individual pressure plot that coincide with the markings. Pressures of the sections were affected by capillary pressure effects and therefore interpretation of phase pressures and mobilities were difficult

To find out whether the polymer in the surfactant was sufficient to give good mobility control, mobilities of the oil bank and surfactant bank were estimated using the pressure data. Mobility

Vial #	1	2	3	4	5	6	7	8	9	10
PV Injected	0.05	0.10	0.15	0.20	0.25	0.29	0.34	0.39	0.44	0.49



Vial #	11	12	13	14	15	16	17	18	19	20
PV Injected	0.54	0.59	0.64	0.69	0.74	0.79	0.84	0.88	0.93	0.98



Vial #	21	22	23	24	25	26	27	28	29	30
PV Injected	1.03	1.08	1.13	1.18	1.23	1.28	1.33	1.38	1.42	1.47



Vial #	31	32	33	34	35	36	37	38	39	40
PV Injected	1.52	1.57	1.62	1.67	1.72	1.77	1.82	1.87	1.92	1.97

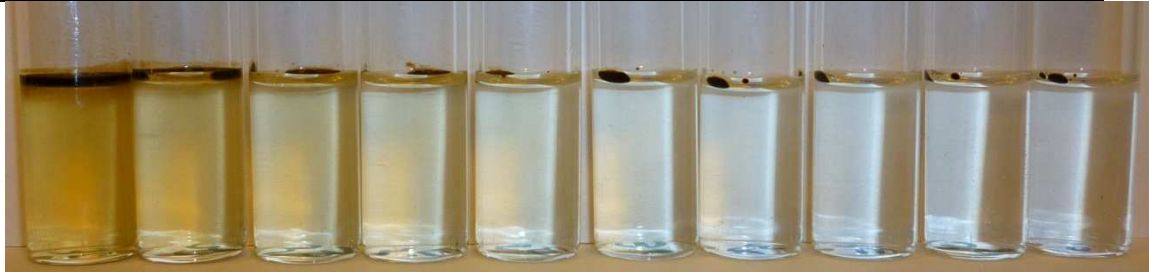


**Figure 3.24:** Photo of effluent vials from ASP T-1 (core #2) with formulation X-1 @ 46.1 °C after equilibrating for 7 days.

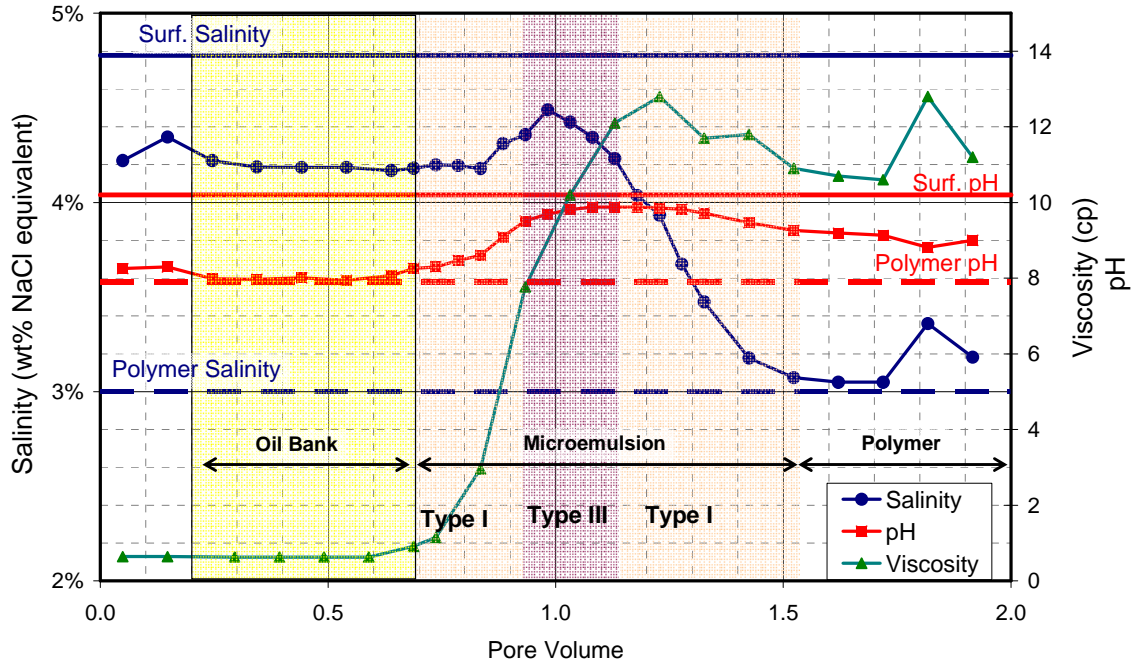


**Figure 3.25:** Viscosity, salinity and pH of aqueous phase in effluent vials from ASP T-2. Viscosity was measured at 46.1 °C with variable shear rates ranging between 37.5 – 75 s<sup>-1</sup> on Brookfield rheometer.

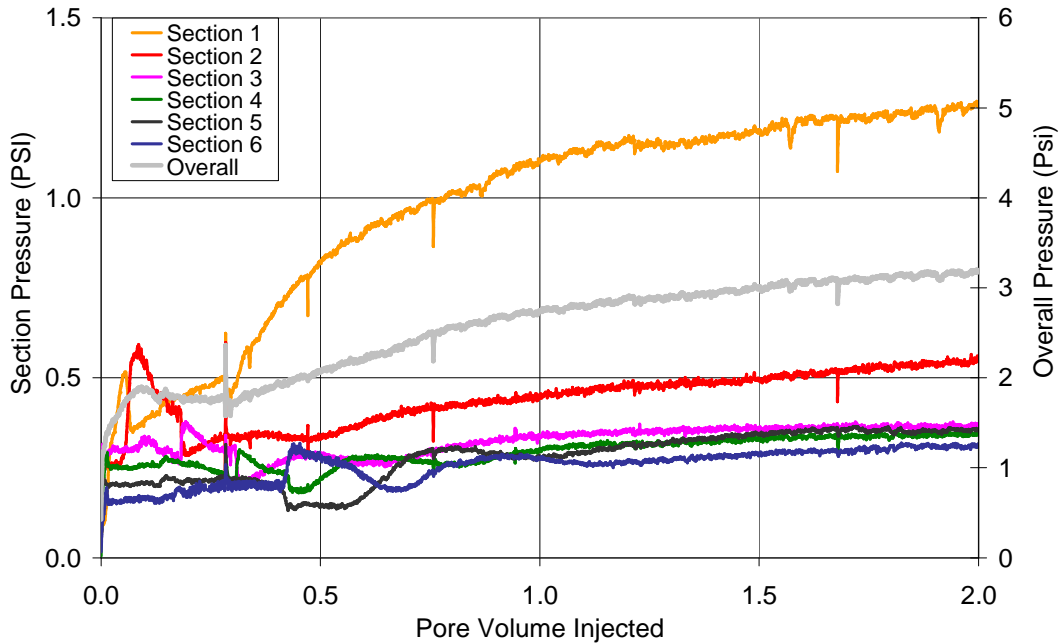


**Figure 3.26:** Overall core and section pressures during ASP T-1.

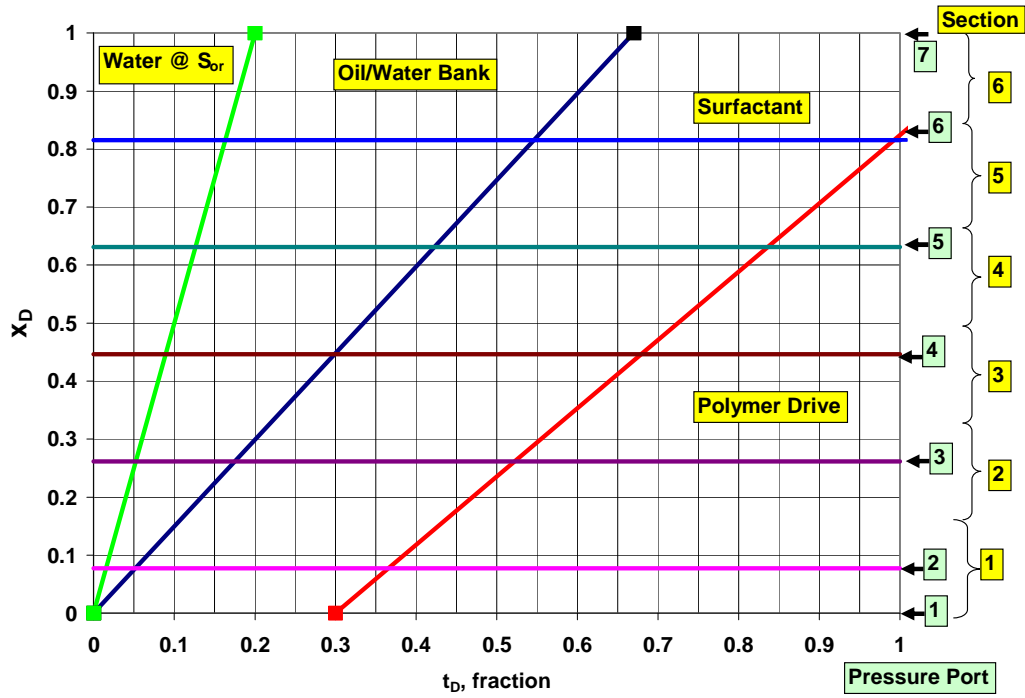


**Figure 3.27:** Dimensionless distance versus dimensionless time plot for ASP T-1 allows identification of fluid regions and validation that dimensionless velocities are constant.

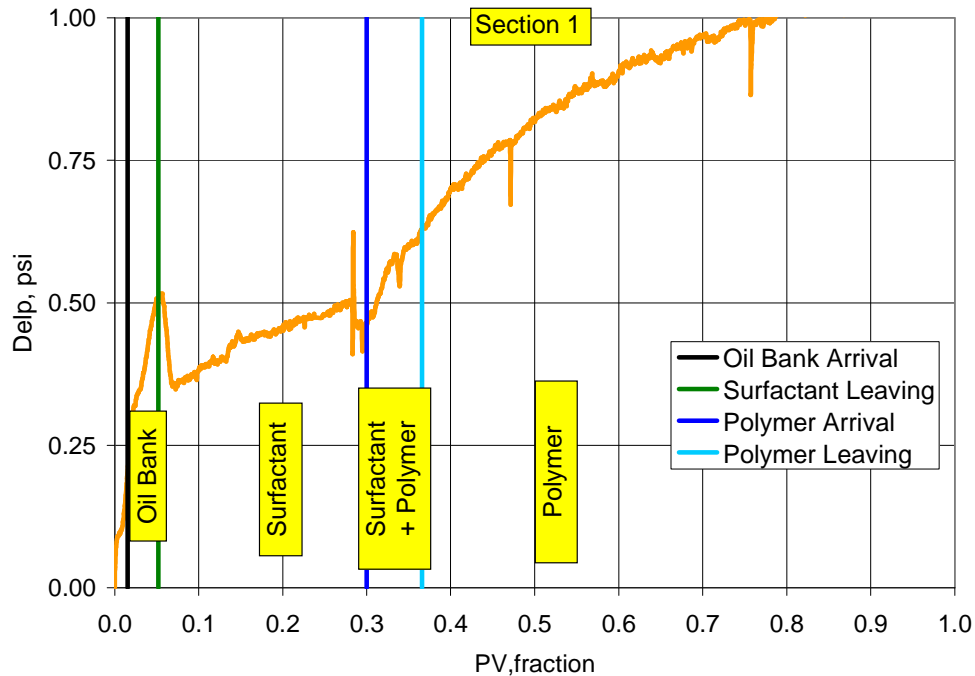


**Figure 3.28:** Section 1 pressure during ASP T-1 with identification of fluid regions using dimensionless velocities and pressure analysis.

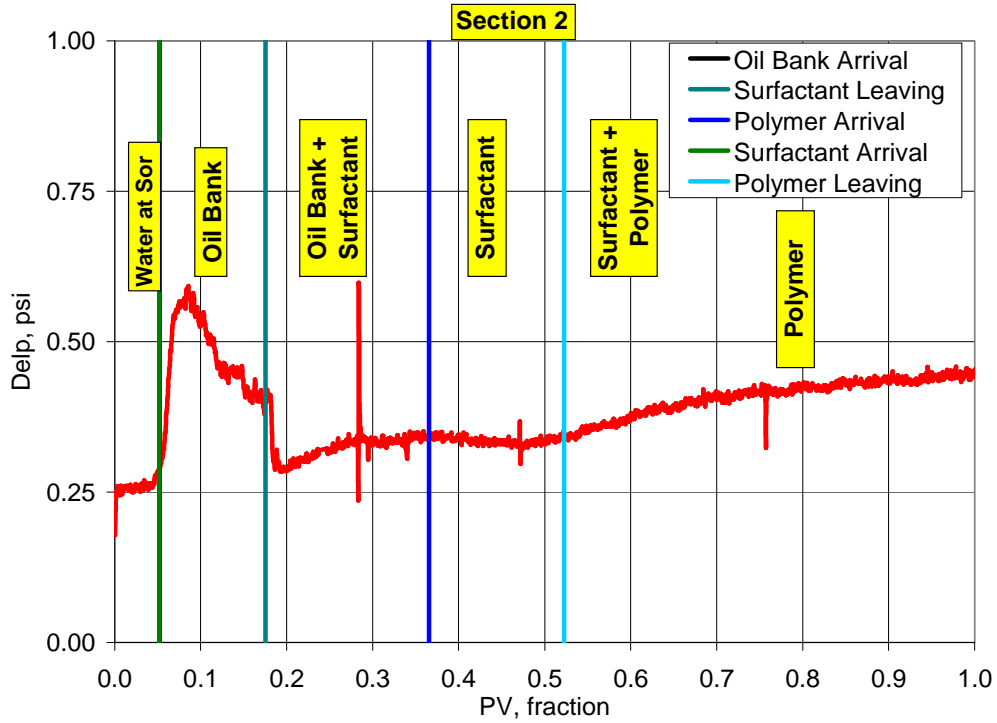


**Figure 3.29:** Section 2 pressure during ASP T-1 with identification of fluid regions using dimensionless velocities and pressure analysis.

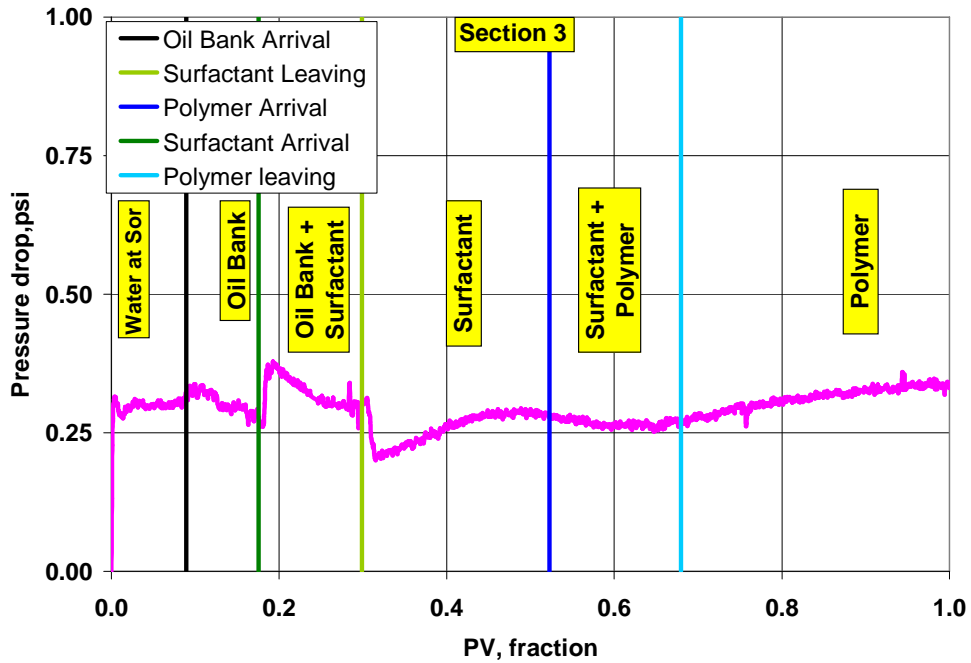


**Figure 3.30:** Section 3 pressure during ASP T-1 with identification of fluid regions using dimensionless velocities and pressure analysis.

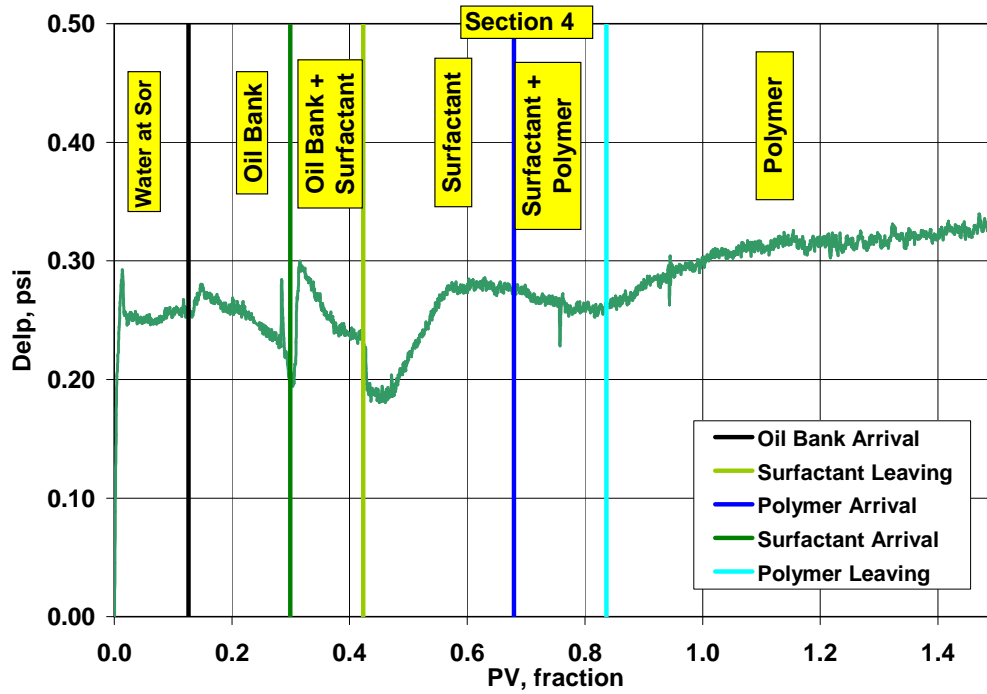


**Figure 3.31:** Section 4 pressure during ASP T-1 with identification of fluid regions using dimensionless velocities and pressure analysis.

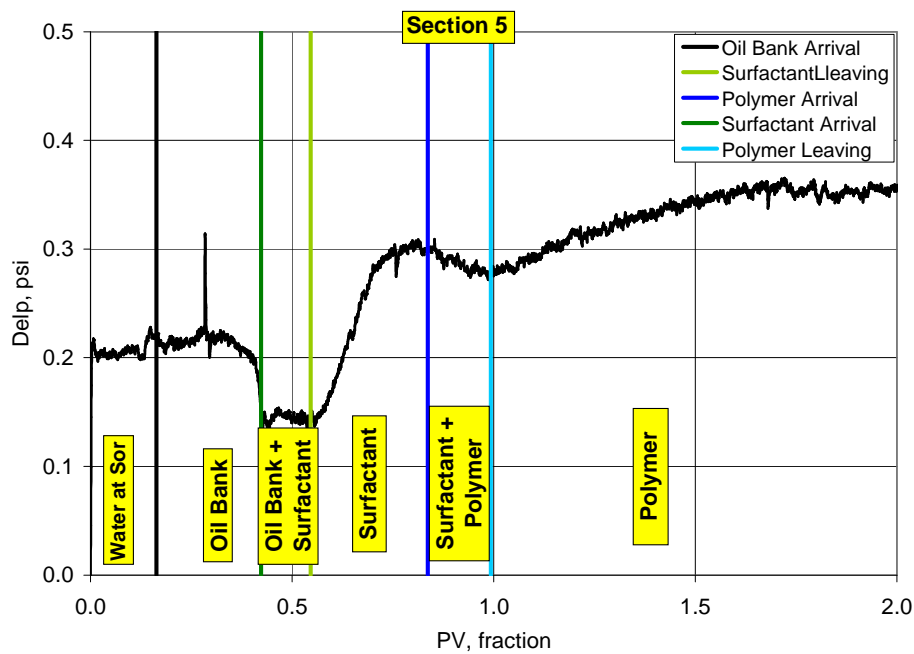


**Figure 3.32:** Section 5 pressure during ASP T-1 with identification of fluid regions using dimensionless velocities and pressure analysis.

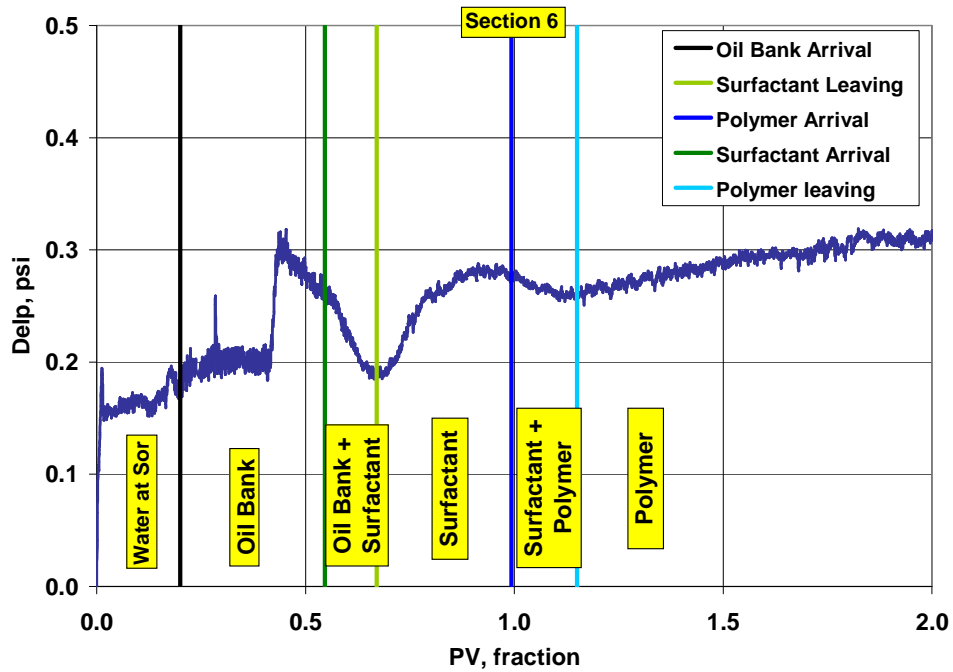


**Figure 3.33:** Section 6 pressure during ASP T-1 with identification of fluid regions using dimensionless velocities and pressure analysis.

of oil bank could only be ascertained for last three sections which saw oil bank for the entire length, or at least most part of it. Mobility for oil was estimated at the pore volume at which surfactant arrived and mobility of surfactant slug was ascertained at the pore volume at which polymer arrived in a particular section. The estimations are tabulated in **Table 3.18**. For ASP T-1 (core #2), mobility of surfactant slug was lower than the oil bank in the last three sections, indicating good mobility control. Therefore polymer in surfactant slug proved sufficient.

#### ***Core Flood T-2 (Core #4)***

Core flood T-2 (core#4) was a repeat of T-1(core#2) but with the correct formation brine. During T-1, the formation brine injected was under optimum but the objective was to match or be slightly higher than the surfactant slug equivalent salinity. For T-2, correct formation brine, which was slight above the optimum salinity of the formulation, was prepared and used. All the floods were performed at 46.1 °C,  $T_{res}$ . Unexpected polymer degradation occurred during the chemical flood for this core. The polymer degradation was traced to the use of brass fittings and copper tube coil as a heat exchanger for injected fluids. Chemical flood oil recovery was low due to loss of mobility control.

#### ***Core Characterization***

Core #4, sandstone, was set up for flooding in horizontal orientation. Its diameter was 5.08 cm. The length and permeabilities of each section and overall are given in **Table 3.16**. Its dispersion was found to be comparatively lower than typically seen for sandstone cores (**Figure 3.34**). Pore volume was determined from tracer curve integration and gravimetric method, and was 109 mL. Porosity was estimated to be 0.176. Overall permeability of the core was 645 md, which was comparatively higher than the sandstone cores used in this research.

#### ***Brine Flood/Oil Flood/Waterflood***

Brine flood was carried out with 5 wt% NaCl brine and the temperature was 46.1 °C. Salinity of brine was higher than the optimum salinity of surfactant slug. Oil flood for core #4 was run at 132 ft/day (10 mL/min) and at 46.1 C. A copper heating coil of volume 1.5 mL was used upstream to inlet to heat the oil to reservoir temperature. Mass of brine displaced from the core was determined accurately by subtracting the mass of brine in the tubing. Then density of brine at reservoir temperature was used to relate the mass to volume of brine displaced by oil from the core.  $S_{oi}$  of 0.662 and  $k_{ro}^o$  of 0.865 was achieved at the end of oil flood. A little more than 3 pore volumes of oil were injected. Pressures during oil flood are plotted in **Figure 3.35**.

Waterflood of core #4 was performed at 46.1 C at a flow rate of 0.3mL/min. Oil volume displaced by the waterflood was accurately determined by measuring the mass of oil displaced and subtracting the volume of oil initially in the tubing. To get clean end point pressure data, the pressure ports were flushed at the same flow rate as the waterflood and then pressures were acquired again at the same flow rate. Pressures during water food are plotted in **Figure 3.36**.  $S_{orw}$  was 0.38 and  $k_{rw}^o$  was 0.064 at end of waterflood.

#### ***Surfactant and Polymer Slug***

Both surfactant and polymer slugs had same composition as the slugs used in T-1 since the purpose of this experiment was to repeat the flood. Surfactant slug contained 0.625 wt%



**Table 3.18:** Summary of oil bank and surfactant bank mobilities for all ASP floods. T-2 was not analyzed due to polymer drive degradation.

ASP #	T-1				T-3				T-4				T-5			
	2				23				26				27			
Core #	$\lambda_{t,Oil\ Bank}$ (mD/cp)	@ PV	$\lambda_{t, Surfactant}$ (mD/cp)	@ PV	$\lambda_{t,Oil\ Bank}$ (mD/cp)	@ PV	$\lambda_{t, Surfactant}$ (mD/cp)	@ PV	$\lambda_{t,Oil\ Bank}$ (mD/cp)	@ PV	$\lambda_{t, Surfactant}$ (mD/cp)	@ PV	$\lambda_{t,Oil\ Bank}$ (mD/cp)	@ PV	$\lambda_{t, Surfactant}$ (mD/cp)	@ PV
Section 1	N/A	N/A	8.2	0.30	N/A	N/A	6.1	0.30	N/A	N/A	5.84	0.30	N/A	N/A	6.27	0.30
Section 2	N/A	N/A	27.2	0.37	N/A	N/A	11.3	0.46	N/A	N/A	3.76	0.50	N/A	N/A	5.10	0.50
Section 3	N/A	N/A	32.6	0.52	N/A	N/A	7.2	0.63	N/A	N/A	3.08	0.70	N/A	N/A	4.72	0.70
Section 4	46.0	0.30	33.5	0.68	20.7	0.48	12.7	0.80	4.66	0.37	2.66	0.65	5.58	0.37	4.25	0.65
Section 5	58.4	0.42	30.8	0.84	14.5	0.61	8.4	0.96	4.68	0.50	2.52	0.77	4.90	0.50	2.92	0.77
Section 6	34.6	0.55	33.3	1.00	10	0.74	7.4	1.13	5.57	0.62	2.96	0.89	6.07	0.62	2.46	0.89
ASP #	T-6				T-7				T-8				T-9			
Core #	31				32				37				39			
Core #	$\lambda_{t,Oil\ Bank}$ (mD/cp)	@ PV	$\lambda_{t, Surfactant}$ (mD/cp)	@ PV	$\lambda_{t,Oil\ Bank}$ (mD/cp)	@ PV	$\lambda_{t, Surfactant}$ (mD/cp)	@ PV	$\lambda_{t,Oil\ Bank}$ (mD/cp)	@ PV	$\lambda_{t, Surfactant}$ (mD/cp)	@ PV	$\lambda_{t,Oil\ Bank}$ (mD/cp)	@ PV	$\lambda_{t, Surfactant}$ (mD/cp)	@ PV
Section 1	N/A	N/A	N/A	N/A	N/A	N/A	3.96	0.30	N/A	N/A	7.8	0.30	N/A	N/A	6.28	0.30
Section 2	N/A	N/A	N/A	N/A	N/A	N/A	4.87	0.50	N/A	N/A	10.8	0.48	N/A	N/A	6.90	0.50
Section 3	N/A	N/A	N/A	N/A	N/A	N/A	4.43	0.70	N/A	N/A	12.3	0.65	N/A	N/A	7.32	0.70
Section 4	N/A	N/A	N/A	N/A	5.36	0.37	4.55	1.07	13.2	0.39	12.6	0.83	13.59	0.64	7.15	0.90
Section 5	N/A	N/A	N/A	N/A	9.63	0.49	5.06	1.22	13.8	0.52	11.1	1.00	11.53	0.79	7.28	1.10
Section 6	N/A	N/A	N/A	N/A	9.72	0.62	7.05	1.38	11.2	0.65	8.8	1.18	14.25	0.95	6.74	1.30

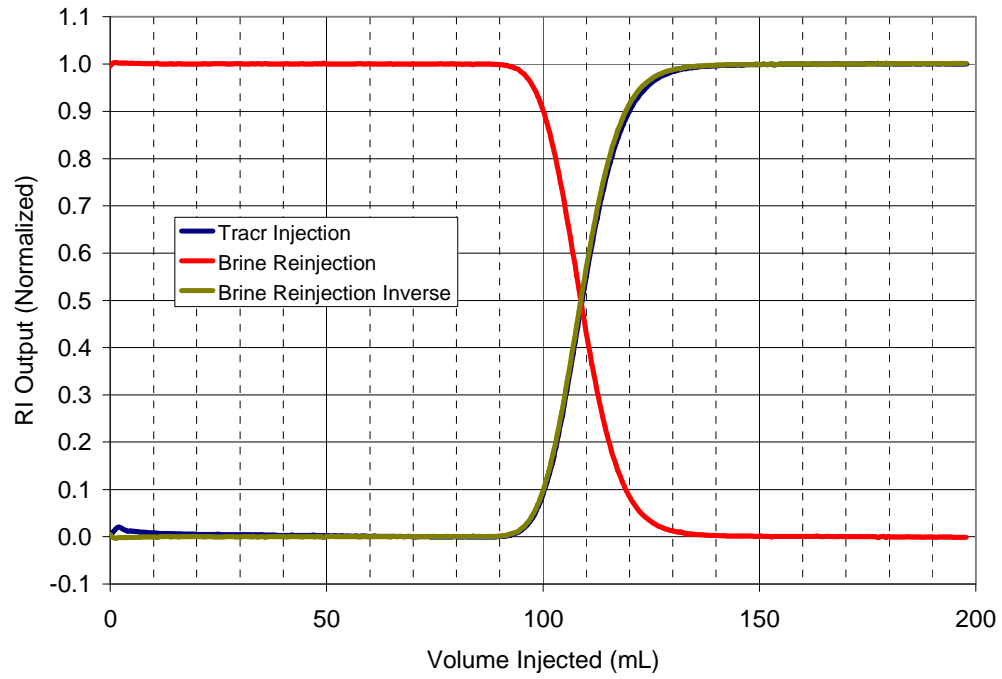


**Figure 3.34:** Dispersion characterization of Core #4 for core flood T-2.

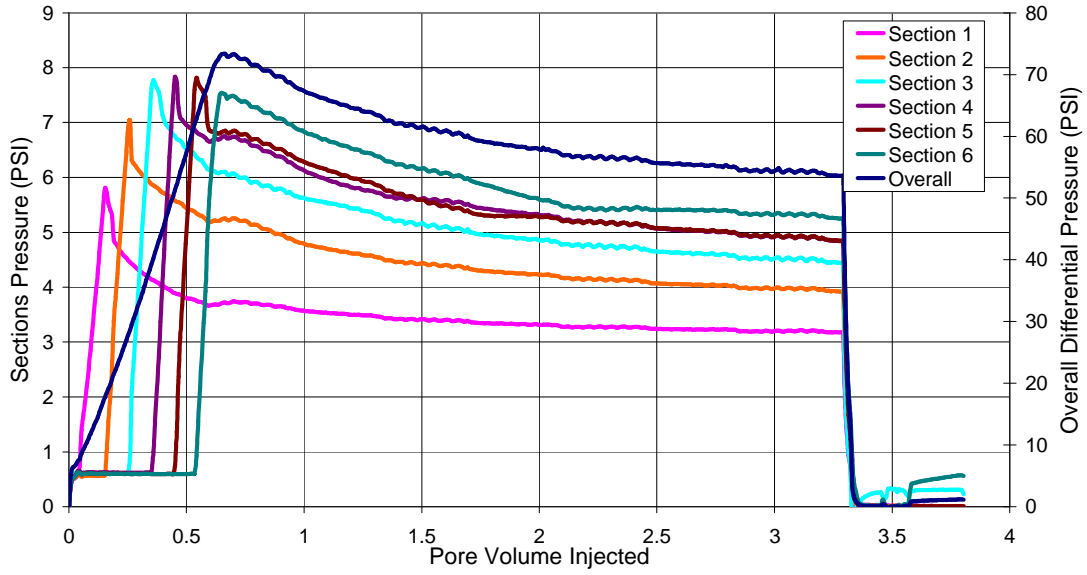


**Figure 3.34:** Oil flood differential pressures for Core #4 for core flood T-2.

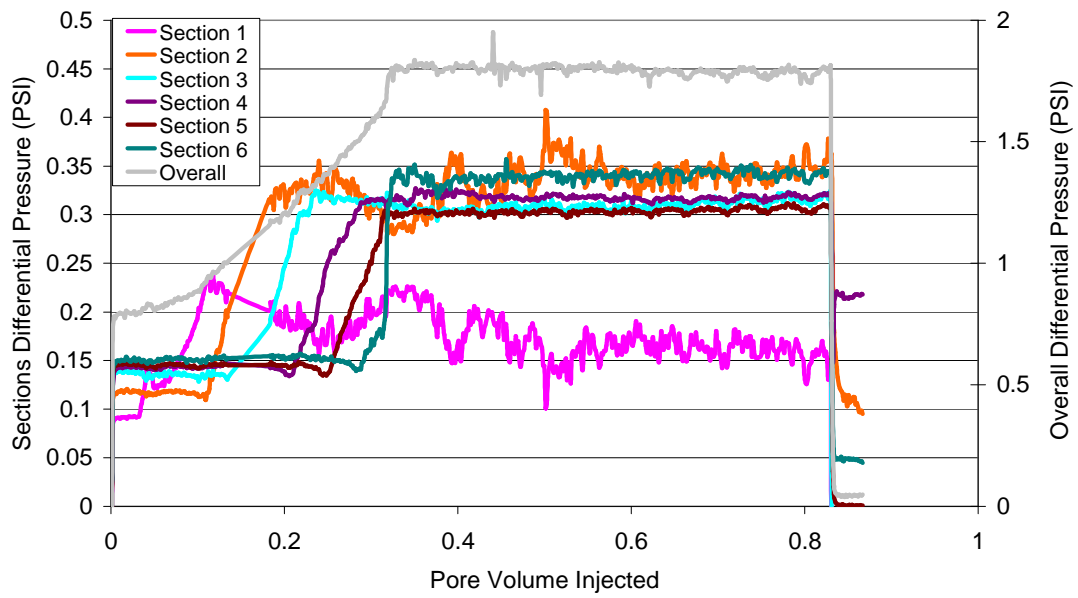


**Figure 3.36:** Waterflood differential pressures for Core #4 for core flood T-2.

Petrostep S-1, 0.375 wt% Petrostep S-2, 2 wt% SBA, 1 wt% Na<sub>2</sub>CO<sub>3</sub>, 4.15 wt% NaCl and 2000 ppm Flopaam SNF 3330S. The viscosity of the surfactant slug was 9.4 cp measured at 45 s<sup>-1</sup> with Brookfield DV-I+ after adding. This was thrice as much as the apparent viscosity calculated (3.2 cp) calculated from the water and oil flood end point relative permeabilities. The slug was checked with oil before injection and was found to be at optimum at WOR=1.5 and at T<sub>Res</sub>.

Polymer slug salinity was 2.94% NaCl, 57% of surfactant slug equivalent salinity. Polymer concentration was 2500 ppm that gave the slug a slightly higher viscosity than surfactant slug, 12.5cp at 45 s<sup>-1</sup>.

#### *Chemical Flood & Oil Recovery*

Core #4 was flooded at 0.15 mL/min (2.1 ft/day) with 0.3 pore volume (PV) of surfactant slug and followed by 1.7 PV polymer drive. Oil bank arrived at 0.25 PV and surfactant breakthrough occurred at 0.73 PV. Oil cut dropped below 1% after 65% residual oil recovery. Oil cut and cumulative oil recovery is plotted in **Figure 3.37**. The recovery was low because the polymer drive degraded.

#### *Effluent Analysis*

Viscosity of the effluent samples was analyzed (**Figure 3.38**). Viscosity of the effluent samples shows that polymer degraded during injection and therefore the viscosity of effluent samples was extremely low. Due to viscosity loss, mobility control was lost which resulted in channeling and inefficient sweep that reduced recovery. The reason for polymer degradation was found to be the copper heating coil used upstream of core inlet for bringing injected solutions to reservoir temperature quickly. A test was done that verified that on contact with copper tubing the polymer experienced fast degradation. Test also showed that sodium carbonate adds resistance to degradation from contact with copper coil.

#### *Pressure Analysis*

Overall pressure for the chemical flood showed a continuous drop once polymer drive entered the core (**Figure 3.39**). The pressure profile indicates that mobility control was lost once polymer drive entered the core, which resulted in lower than expected oil recovery. Surfactant slug did not degrade because of presence of alkali, Na<sub>2</sub>CO<sub>3</sub>.

Detailed pressure analysis of individual sections was not performed as the ASP flood would need to be repeated on another core.

#### **Core Flood T-3 (Core #23)**

Core flood T-3 (core#23) was a repeat of T-1(core#2) in all aspects except that formation brine salinity was raised to 5.2 wt% NaCl, which is the equivalent salinity of the surfactant slug (NaCl + Na<sub>2</sub>CO<sub>3</sub>). This was the second attempt to repeat core flood with Formulation X-1. First repetition, T-2 (core#4) was met with failure due to polymer degradation. This core flood was completed successfully.

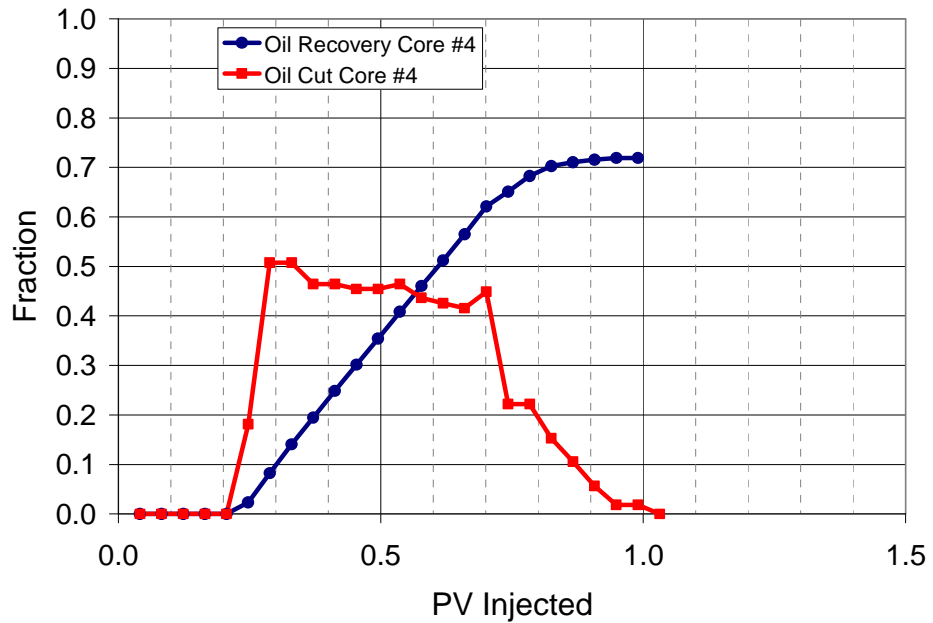


**Figure 3.37:** Oil cut and oil recovery for core flood T-2 (Core #4).

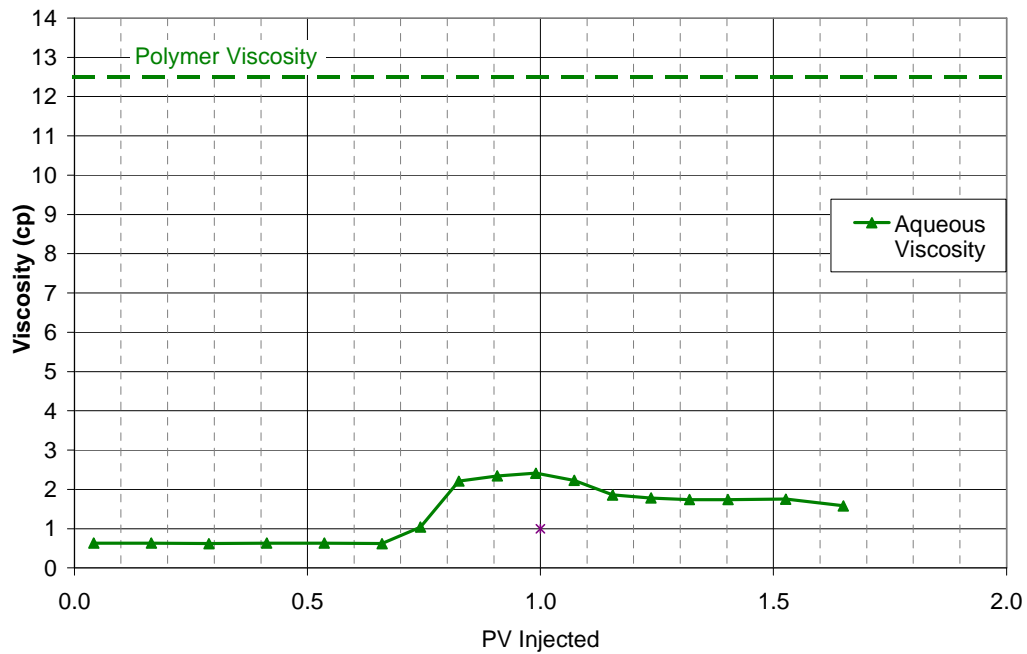


**Figure 3.38:** Aqueous phase viscosity of effluent of core flood T-2 (Core #4) measured at  $T_{res}$ . Aqueous phase viscosity was badly affected by polymer degradation.

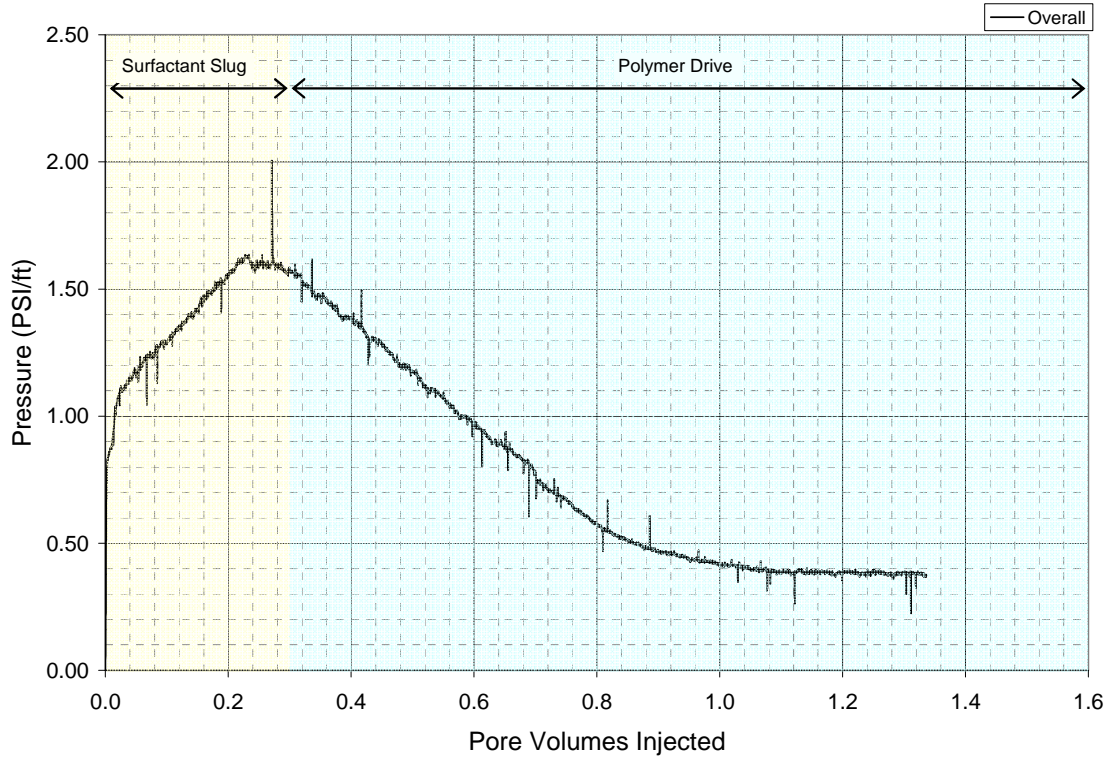


**Figure 3.39:** Overall pressure during ASP flood T-2 (Core #4). Polymer drive degradation caused the pressure to drop after 0.3 PV.

### *Core Characterization*

Core #23, sandstone, was set up for flooding in horizontal orientation. Its diameter was 5.08 cm. The length and permeabilities of each section and overall are given in Table 3.16. Its dispersion was measured (**Figure 3.40**). The dispersion profile showed a longer tail. Pore volume was determined from tracer curve integration and gravimetric method, and was 109 mL. Overall permeability of the core was 184 md which was two to three times lower than Core #2 and Core #4.

### *Brine Flood/Oil Flood/Waterflood*

Brine flood was carried out with 5.2 wt% NaCl brine and the temperature was 46.1 degree °C. Salinity of brine was equivalent to the optimum salinity of surfactant slug (NaCl + Na<sub>2</sub>CO<sub>3</sub>). Oil flood for core #23 was run at 33 ft/day (2.5 mL/min) and at 46.1 C. A stainless steel heating coil of volume 1.5 mL was used upstream to inlet to heat the oil to reservoir temperature. S<sub>oi</sub> was 0.659 and kro<sup>o</sup> of 0.90 was achieved at the end of oil flood. 4.3 pore volume of oil was injected. Pressures during oil flood are plotted in **Figure 3.41**. Pressures show an abnormal trend because the temperature controller was accidentally switched off between 0.5 PV and 2.75 PV. This caused the pressures to rise.

Waterflood of core #23 was performed at 46.1°C at a flow rate of 0.3 mL/min. pressures were measured during the flood (**Figure 3.42**). To get clean end point pressure data, the pressure ports were flushed at the same flow rate as the waterflood and then pressures were acquired again at the same flow rate. S<sub>orw</sub> was 0.413 and krw<sup>o</sup> was 0.045 at end of waterflood.

### *Surfactant and Polymer Slug*

Both surfactant and polymer slugs had same composition as the slugs used in T-1 and T-2 since the purpose of this experiment was to repeat the flood T-1. Only, NaCl and polymer concentration were slightly higher in the surfactant slug.

Surfactant slug contained 0.625 wt% Petrostep S-1, 0.375 wt% Petrostep S-2, 2 wt% SBA, 1 wt% Na<sub>2</sub>CO<sub>3</sub>, 4.25 wt% NaCl and 2250 ppm Flopaam SNF 3330S. The viscosity of the surfactant slug was 21 cp measured at 1 s<sup>-1</sup> with Bohlin rheometer. This was sufficiently above the apparent viscosity (3.4cp) calculated from the water and oil flood end point relative permeabilities.

Polymer slug salinity was 2.94% NaCl, 55% of surfactant slug, only. Polymer concentration was 2500 ppm that gave the slug a slightly higher viscosity than surfactant slug, 27 cp @ 1 s<sup>-1</sup>. Viscosity of the two slugs vs the shear rate are compared in **Figure 3.43**.

### *Chemical Flood & Oil Recovery*

Core #23 was flooded at 0.15mL/min (2.1 ft/day) with 0.3 pore volume (PV) of surfactant slug and followed by 1.7 PV polymer drive. Oil bank arrived at 0.15 PV and surfactant breakthrough occurred at 0.74 PV. Oil cut dropped below 1% after 88% residual oil recovery (**Figure 3.44**). Recovery of the flood was good and very close to ASP T-1. A maximum oil cut of 0.55 was observed at 0.25 PV, which was the early part of the oil bank. Oil cut dropped gradually from 0.74PV to 1.00 PV.

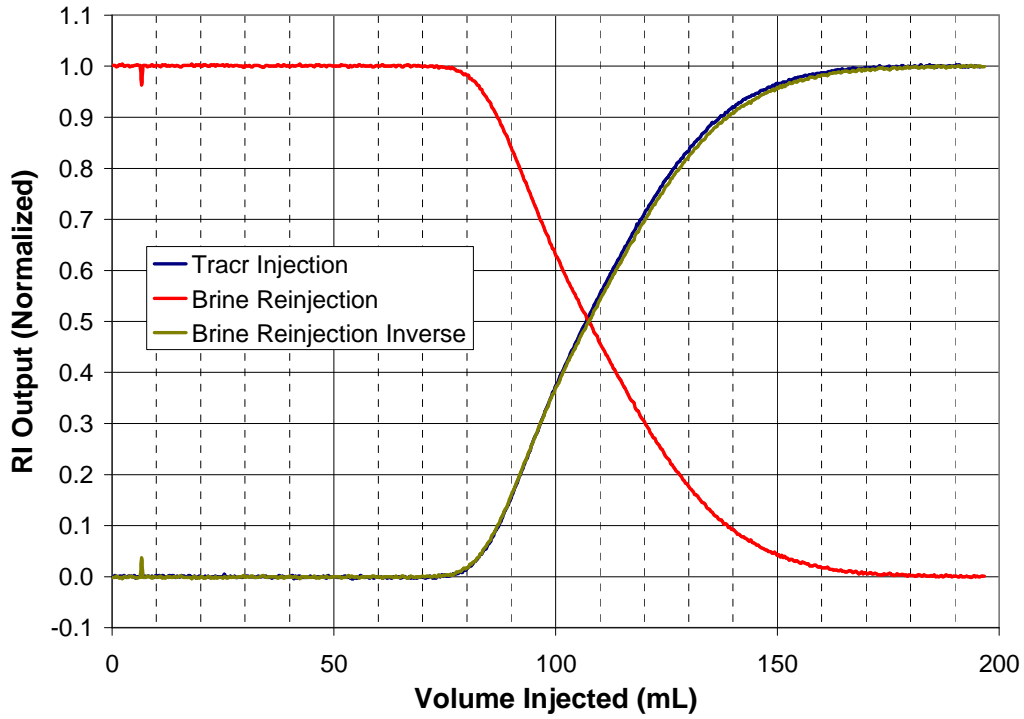


**Figure 3.40:** Dispersion characterization of Core #23 for core flood T-3.

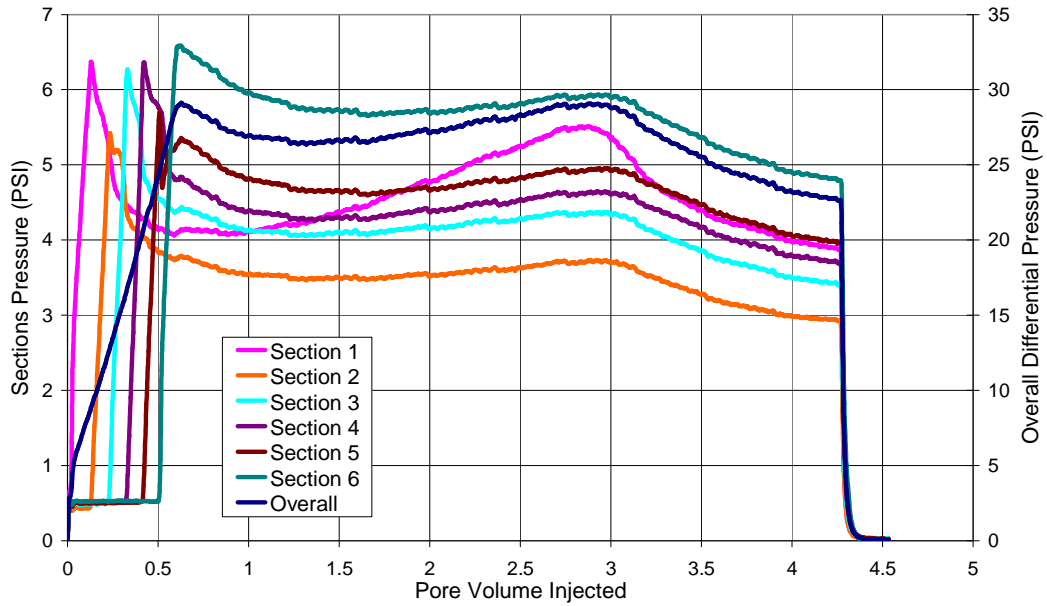


**Figure 3.41:** Oil flood differential pressures for Core #23 for core flood T-3. Temperature controller was accidentally switched that caused the pressures to rise after 0.5 pore volumes had been injected.



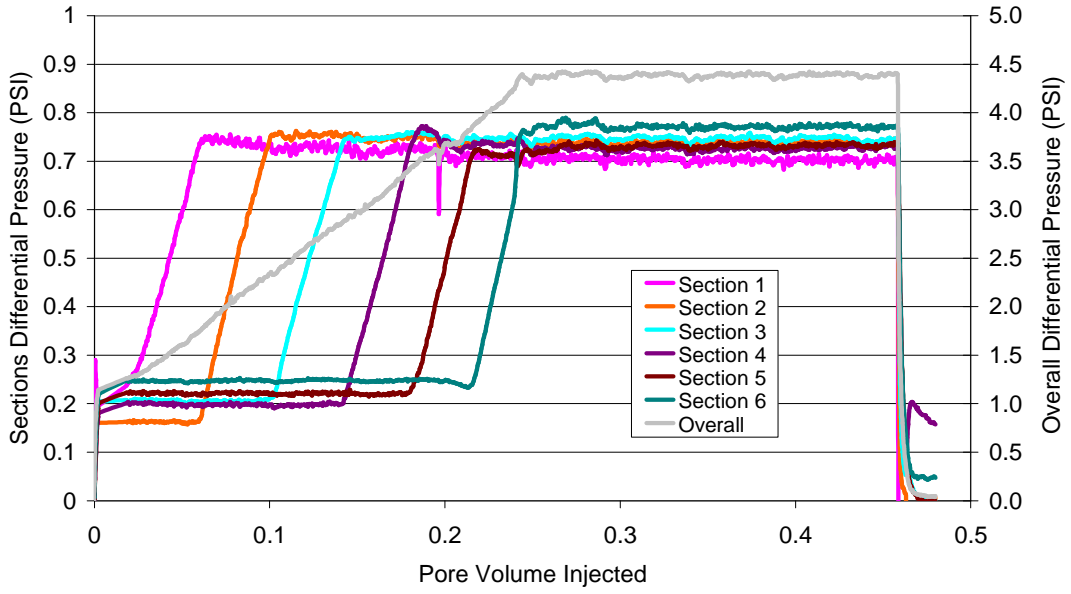


**Figure 3.42:** Waterflood differential pressures for Core #23 for core flood T-3.

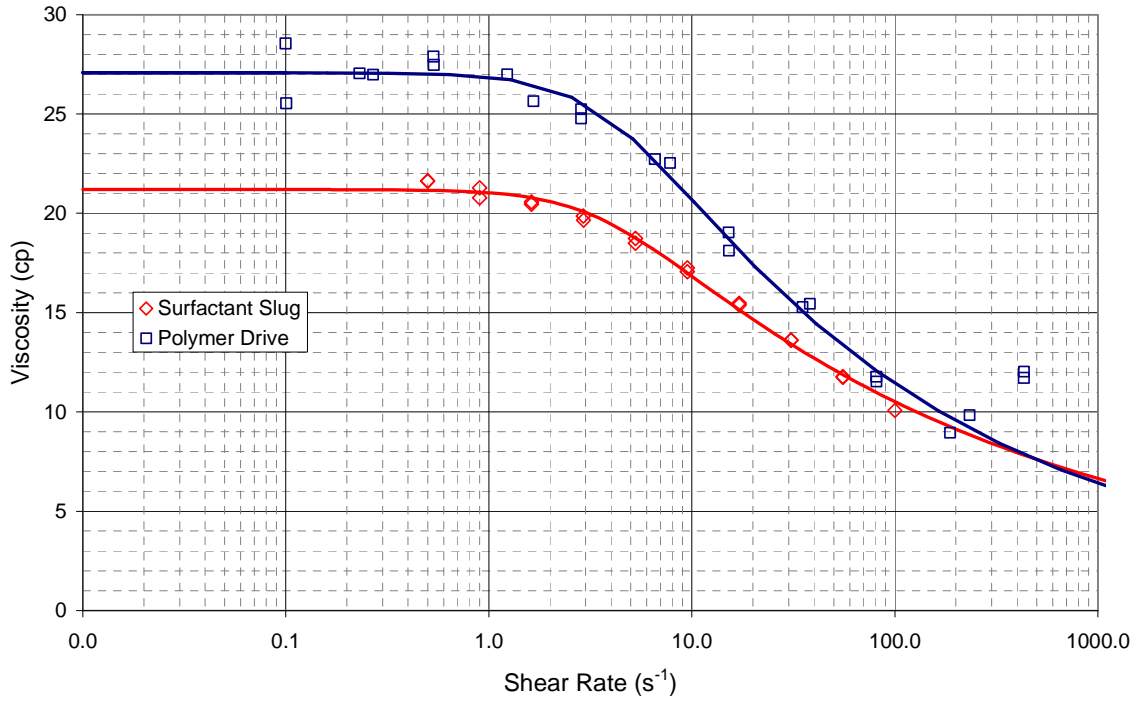


**Figure 3.43:** Viscosities of surfactant and polymer slug vs shear rate for Core #23 for ASP flood T-3 at 46.1 °C.

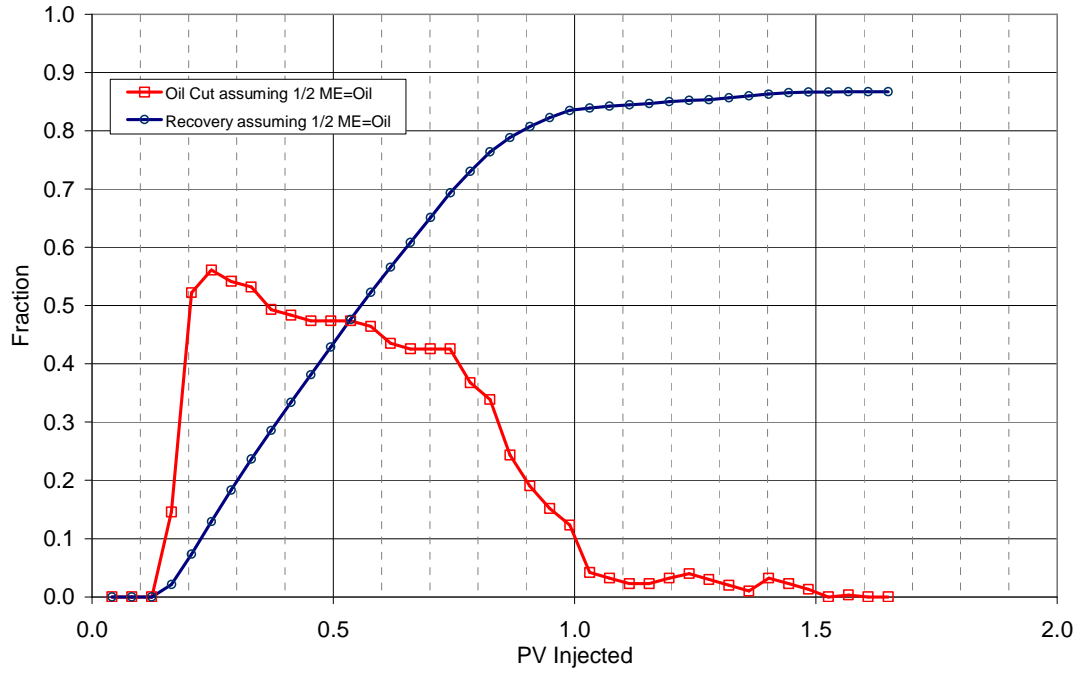


**Figure 3.44:** Oil cut and oil recovery for core flood T-3 (Core #23).

### *Effluent Analysis*

Effluent samples were equilibrated for 3 days at reservoir temperature and then evaluated. They are shown in **Figure 3.45**. Vials 4-19 contained oil and water indicating the oil bank was being produced. Vials 20-21 possibly contained Type II microemulsion phase. The interface of oil and water was flat and color of oil phase had slight brownish tinge, which was similar seen in Type II pipettes in phase behavior experiments. Vial 21 shows a tan phase at the bottom of oil phase which appears to be an emulsion phase, also seen in phase behavior studies in Type II microemulsions. Vials 22-24 contained type III microemulsion and vials 25 onwards were type I microemulsion. Type II→Type III→Type I transition was achieved with the salinity design used. This transition was not intentional but is desired.

Viscosity, salinity and pH of aqueous phase of the effluent samples were measured and are presented in **Figure 3.46**. Microemulsion phase types indicated on the graph were determined from visual inspection of vials. Tracer curve for the core is also plotted in the graph.

Salinity measurements show that from 0.0 to 0.82 PV, the salinity was above the salinity of the surfactant slug. The salinity measurement apparatus indicated lower salinity than the actual salinities of the brine and the slug. The measurements indicated approximately 4.9 wt% NaCl equivalent for formation brine (5.2 wt% NaCl actual) and 4.26 wt% for surfactant slug (4.25 wt% NaCl + 1 wt% Na<sub>2</sub>CO<sub>3</sub> actual). In relative terms, the salinity in the aqueous phase at surfactant breakthrough (0.74 PV) was above the optimum salinity of the formulation. Due to dispersion in the core, the transition to surfactant slug and polymer drive salinity took place gradually. Type III region was approximately 0.15 PV long by the time it reached the end of core. Type III region could be elongated if salinity gradient were smaller.

Viscosity of the aqueous phase increased after oil breakthrough and follows very similar trend to the tracer curve, indicating that intrinsic dispersion of the core also plays a role in viscosity as well as salinity transitions. Sharp rise in viscosity behind the oil bank indicates that the polymer did not get degraded and good mobility control was likely.

pH was measured to analyze the transport of alkali. pH only got to a maximum value of 10 at the end of the core, whereas surfactant slug measured at 10.8. This shows that alkali was consumed in the core and didn't reach the injected concentration. According to literature, a pH of 9 is sufficient to reduce surfactant adsorption in limestones. Though, it should be noted that alkali was already in excess in the formulation. Alkali consumption in limestone may show a completely different behavior.

### *Pressure Analysis*

Pressures measured across the core and each section are plotted in **Figure 3.47**. Sections 5 and 6 seem to have got affected by capillary pressure effects but other sections did not show the effect. After the oil bank had passed through each section, these section pressure drop slowly reached a plateau. Sections 5 and 6 were still not at the plateau at the end of the core flood at 1.8 PV injected. Plateau of the pressure drop indicates that the relative permeability of the sections stabilized as the saturations stopped changing towards the end of flood and

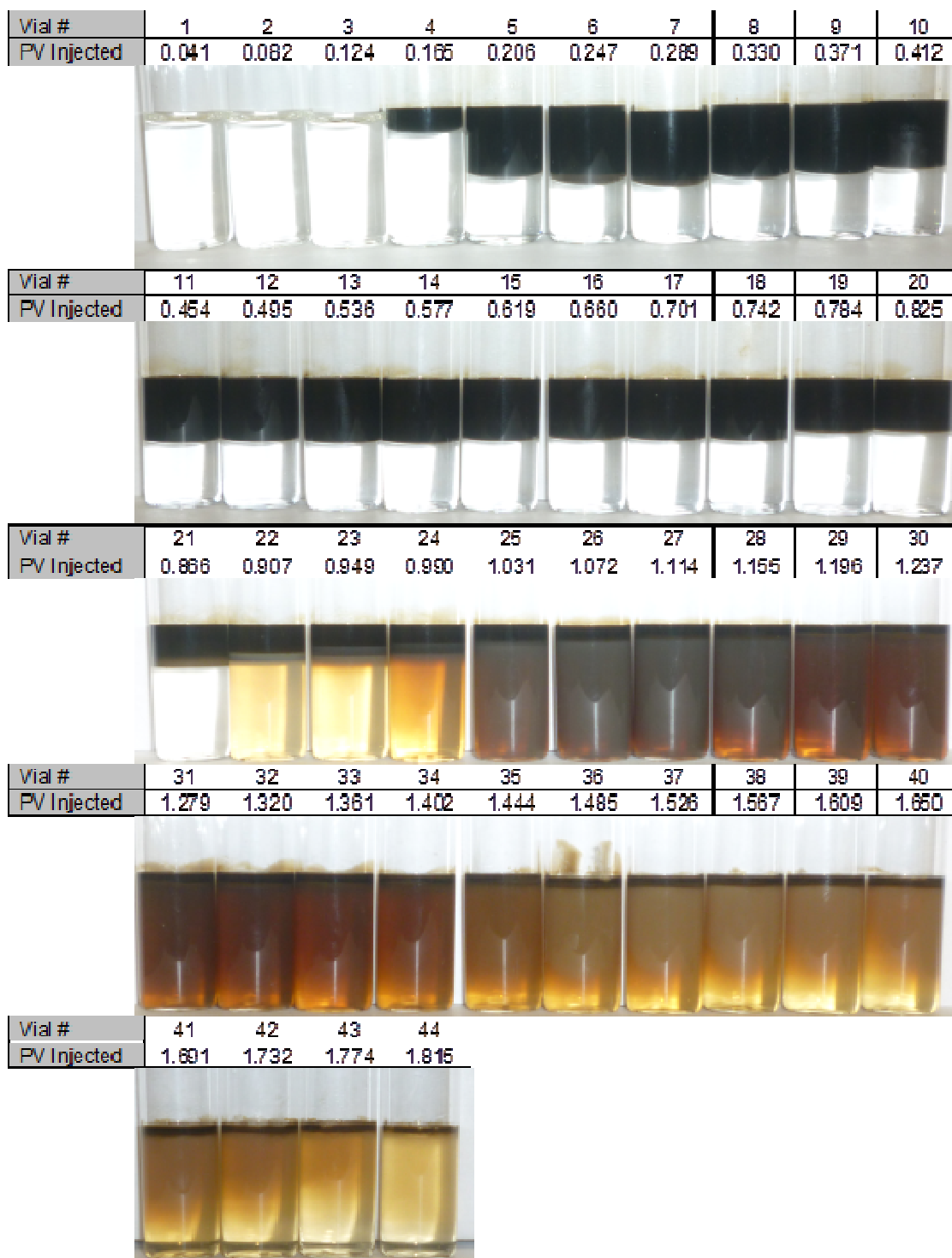


**Figure 3.45:** Photo of effluent vials from ASP T-3 (core #23) with formulation X-1 @ 46.1 °C after equilibrating for 3 days.

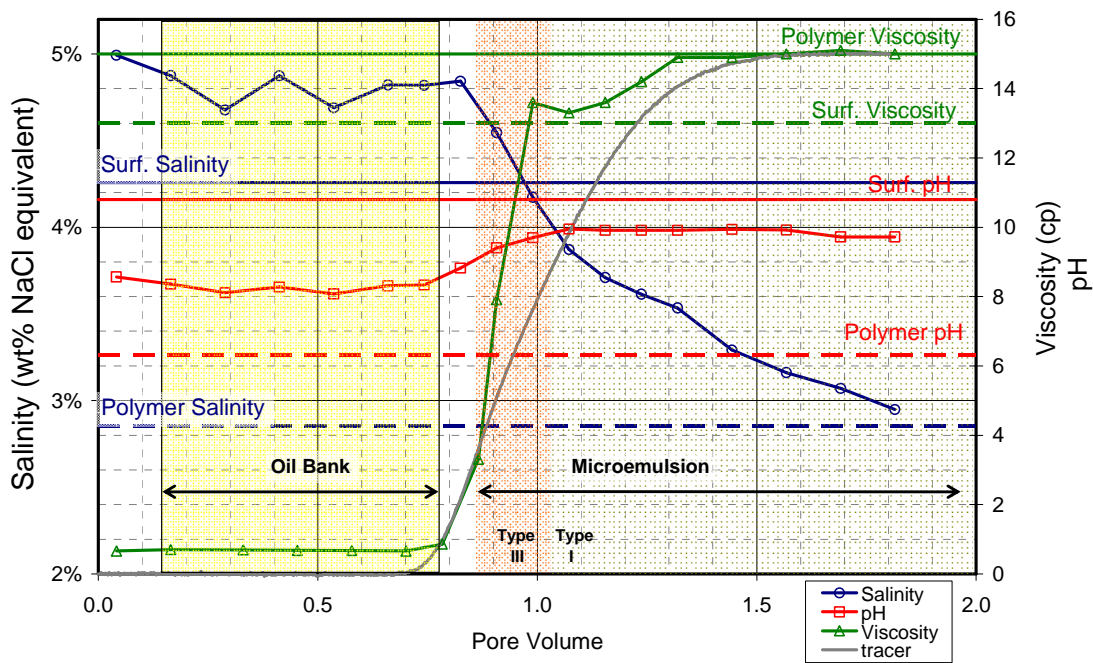


**Figure 3.46:** Viscosity, salinity and pH of aqueous phase in effluent vials from ASP T-3. Viscosity was measured at 46.1 °C with variable shear rates ranging between 37.5 – 75 s<sup>-1</sup> on Brookfield rheometer.

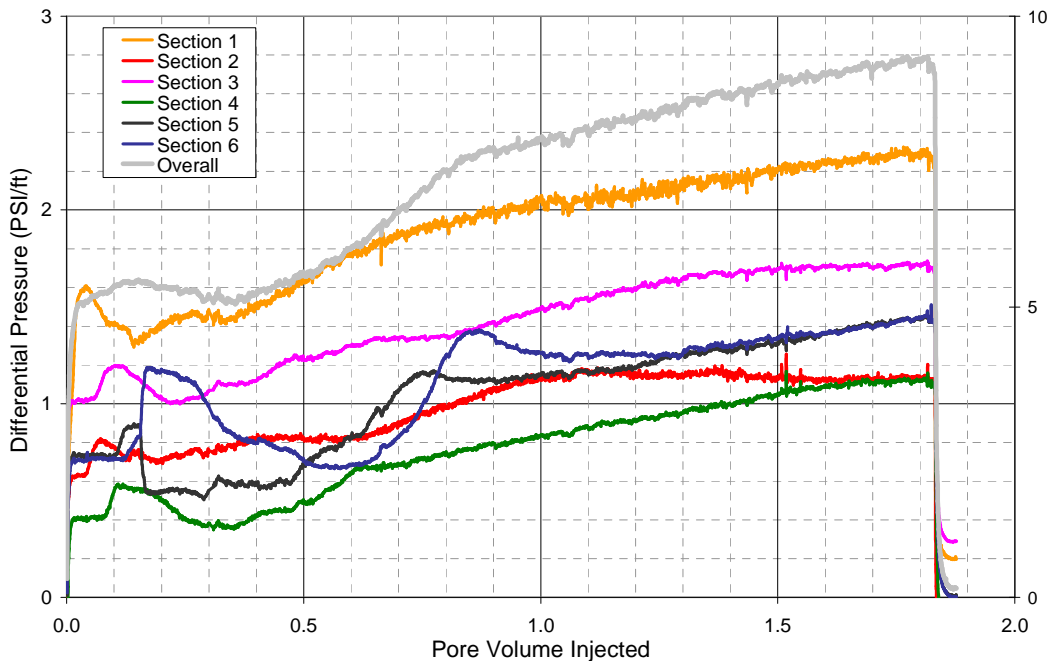


**Figure 3.47:** Overall core and section pressures during ASP T-3.

polymer drive became the only mobile phase. Section 1 seemed to have a high resistance, indicated by relatively higher pressure exhibited in the section, possibly due to low permeability causing polymer retention. Pressures of individual sections were analyzed to determine mobilities of oil bank and surfactant bank (**Figure 3.48** to **Figure 3.53**). Mobility of oil bank could only be ascertained for last three sections which saw oil bank for the entire length, or at least most part of it. Mobility for oil was estimated at the pore volume at which surfactant arrived and mobility of surfactant slug was ascertained at the pore volume at which polymer arrived in a particular section. The estimations are tabulated in **Table 3.18** and plotted in **Figure 3.54**. For ASP T-3 (core #23), mobility of surfactant slug was lower than the oil bank in the last three sections, indicating good mobility control. Therefore polymer in surfactant slug proved sufficient.

#### ***Core Flood T-8 (Core #37)***

Core flood T-8 (core#37) was performed to test Formulation X-1. For this core, salinity design was varied taking into account the observations made in ASP Floods T-1 and T-3. In previous ASP floods of this formulation, a 0.15-0.20 PV type III microemulsion region had been obtained at the end of core. It was postulated that using a less aggressive salinity gradient between surfactant slug and polymer drive could elongate the type III region reaching at the end of the core, which could improve oil recovery. Relationship between optimal salinity of the formulation at WOR range of 1 to 9 and the effect of dilution of formulation with polymer drive were studied in phase behavior experiments to select salinity of the surfactant slug and polymer drive. These experiments' results and salinity selection rationale is presented in the surfactant and polymer slug description.

Core #37, sandstone, was set up for flooding in vertical orientation. Its diameter was 5.08 cm. The length and permeabilities of each section and overall are given in **Table 3.16**. Its dispersion was measured (**Figure 3.55**). Pore volume was determined from tracer curve integration and gravimetric method, and was 113 mL. Overall permeability of the core was 225 md. The core developed leaks in ports 3 and 5 during oil flood. The flood had to be stopped to fix the leaks. Epoxy was poured over the leaks to stop the leak and resume the oil flood. During waterflood, the ports leaked again. This time, FEP tubing was replaced with stainless steel tubing. Leaks did not occur again during the waterflood or chemical flood.

#### ***Brine Flood/Oil Flood/Waterflood***

Brine flood was carried out with 5.5 wt% NaCl brine and the temperature was 46.1 °C. Salinity of brine was kept equal to the surfactant slug surfactant slug (4.6 wt% NaCl + 1 wt% Na<sub>2</sub>CO<sub>3</sub>). Oil flood was run at 33 ft/day (2.5mL/min) and at 46.1 C. S<sub>oi</sub> could not be determined from the brine displaced as it was possible that some brine leaked out. k<sub>ro</sub><sup>o</sup> was measured to be 0.75. Approximately 4 pore volumes of oil were injected after the leak was fixed. Pressures for oil flood after the leak fix are plotted in **Figure 3.56**. The pressures show that there was no leak in any section. Flood was stopped after the water cut was below 1%.

Waterflood of core #37 was performed at 46.1 C at a flow rate of 0.3mL/min. Pressures were measured during the flood (**Figure 3.57**). Leaks occurred again during waterflood at the pressure ports. The waterflood was stopped and ports fixed. FEP ports were replaced with stainless steel ports. These ports made a good bond with epoxy and did not leak again.

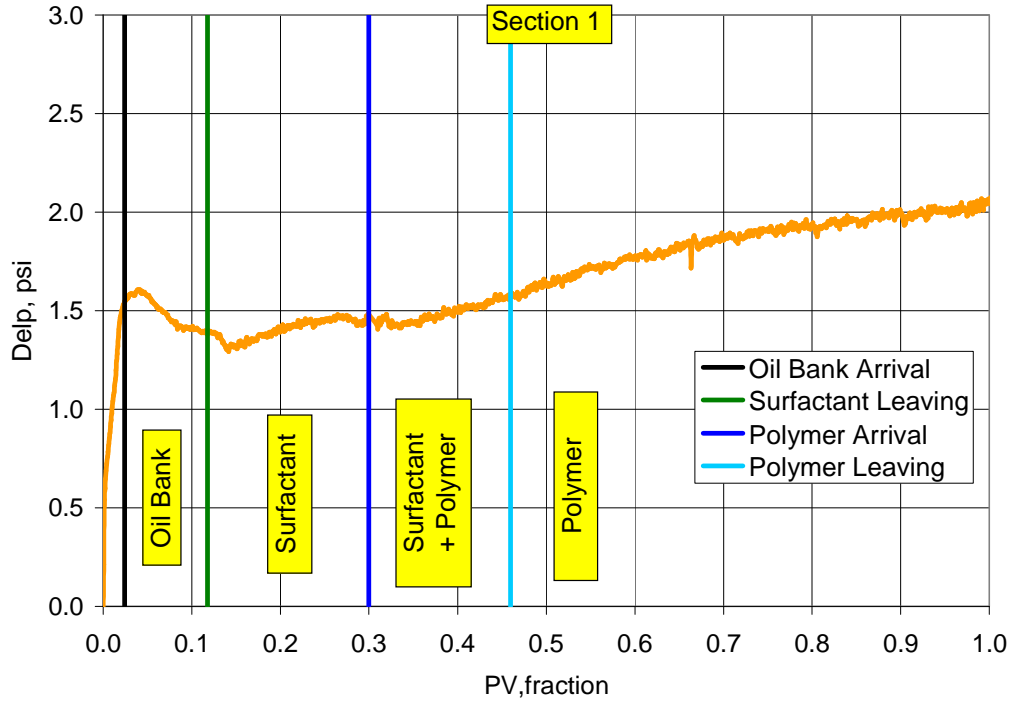


**Figure 3.48:** Section 1 pressure during ASP T-3 with identification of fluid regions using dimensionless velocities and pressure analysis.

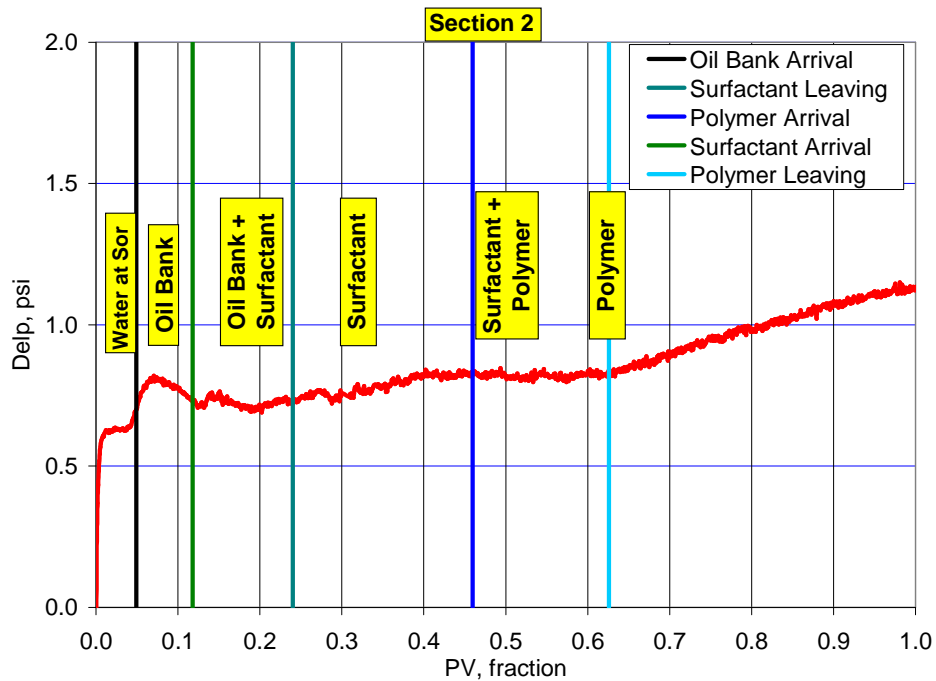


**Figure 3.49:** Section 2 pressure during ASP T-3 with identification of fluid regions using dimensionless velocities and pressure analysis.

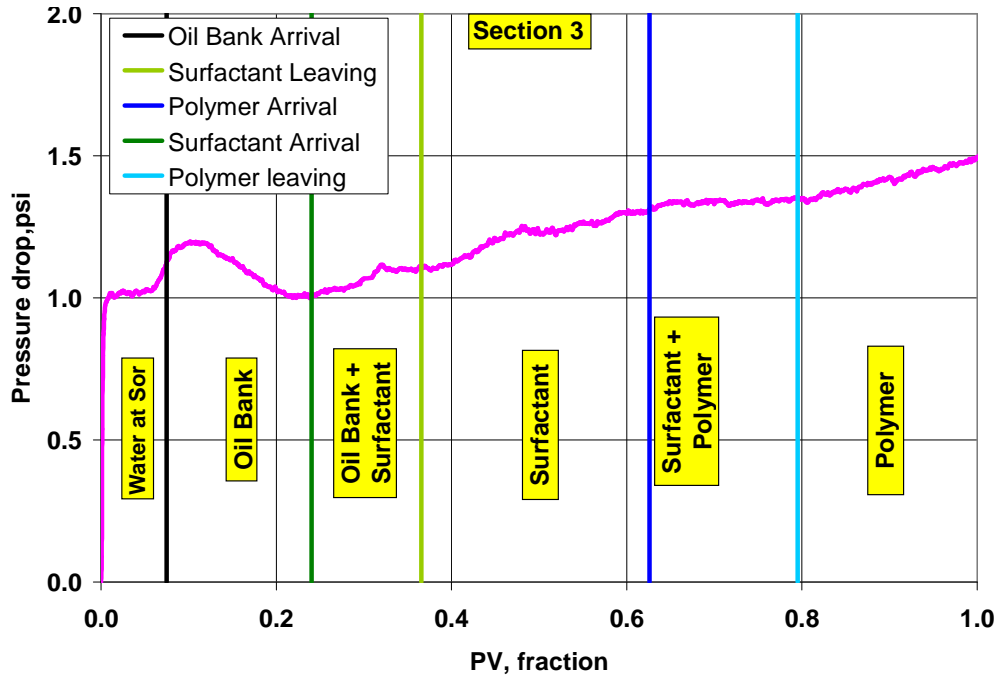


Figure 3.50: Section 3 pressure during ASP T-3 with identification of fluid regions using dimensionless velocities and pressure analysis.

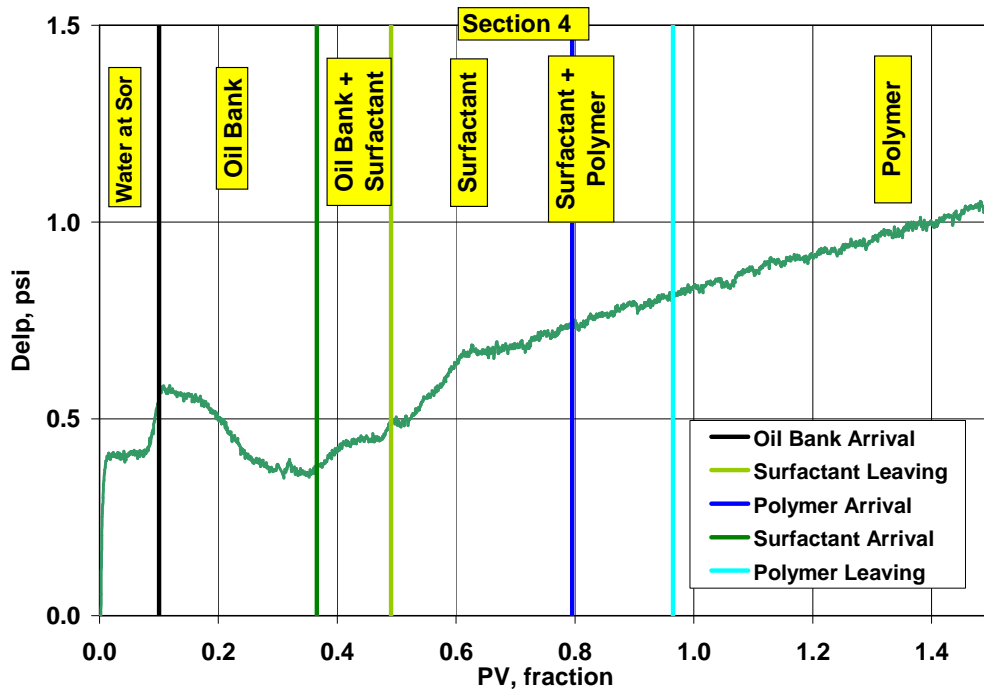
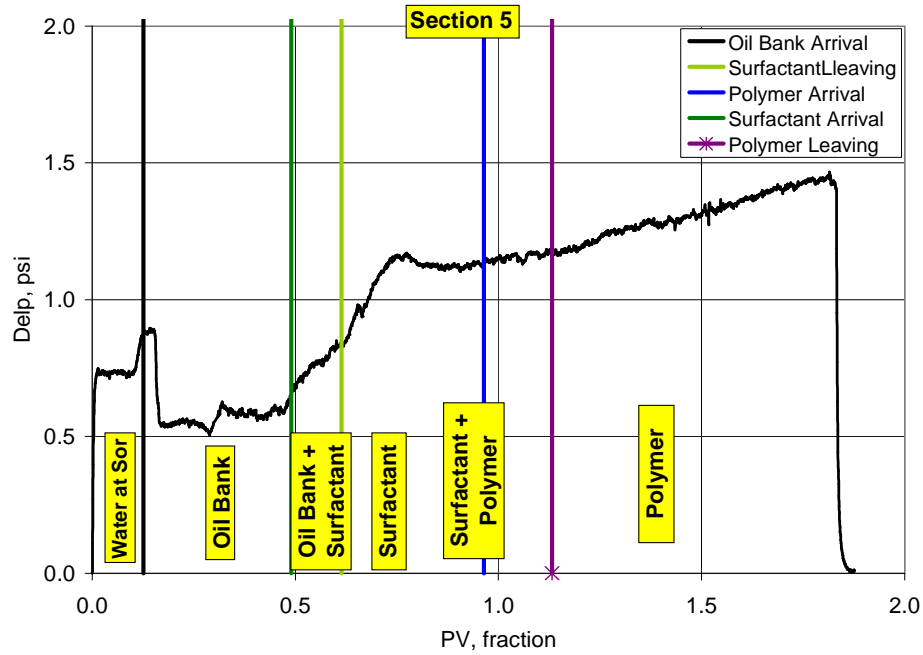
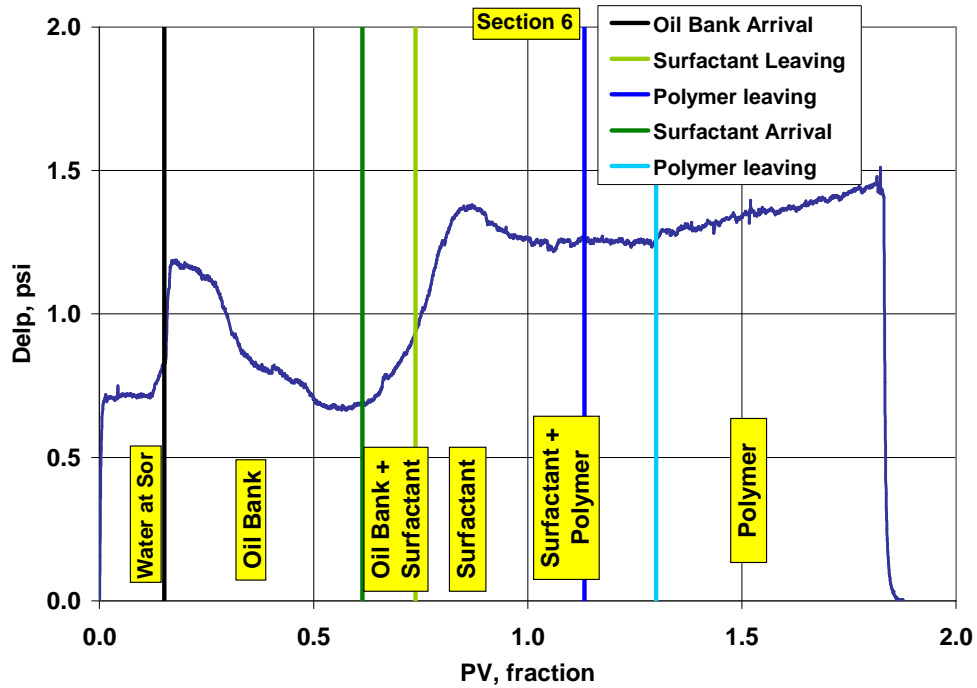


Figure 3.51: Section 4 pressure during ASP T-3 with identification of fluid regions using dimensionless velocities and pressure analysis.





**Figure 3.52:** Section 5 pressure during ASP T-3 with identification of fluid regions using dimensionless velocities and pressure analysis.



**Figure 3.53:** Section 6 pressure during ASP T-3 with identification of fluid regions using dimensionless velocities and pressure analysis.

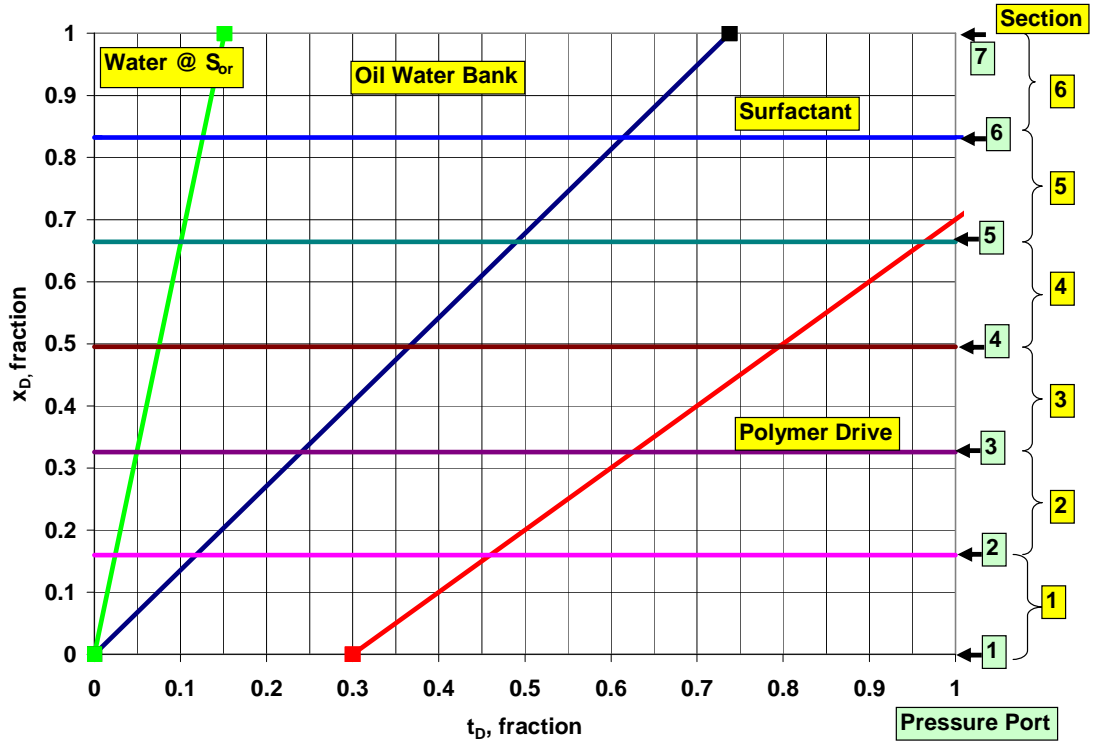


Figure 3.54: Dimensionless distance versus dimensionless time plot for ASP T-3.

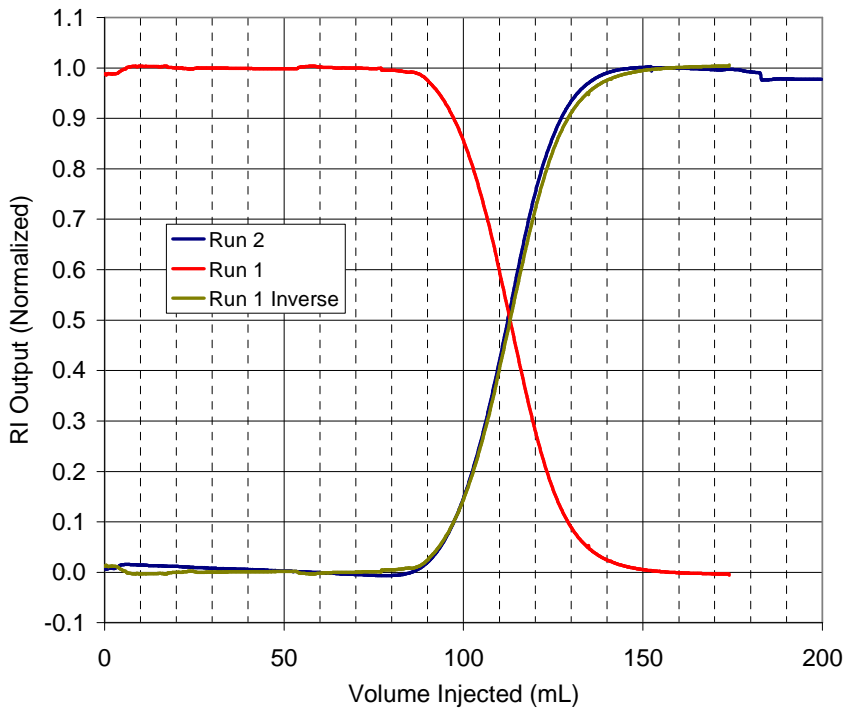
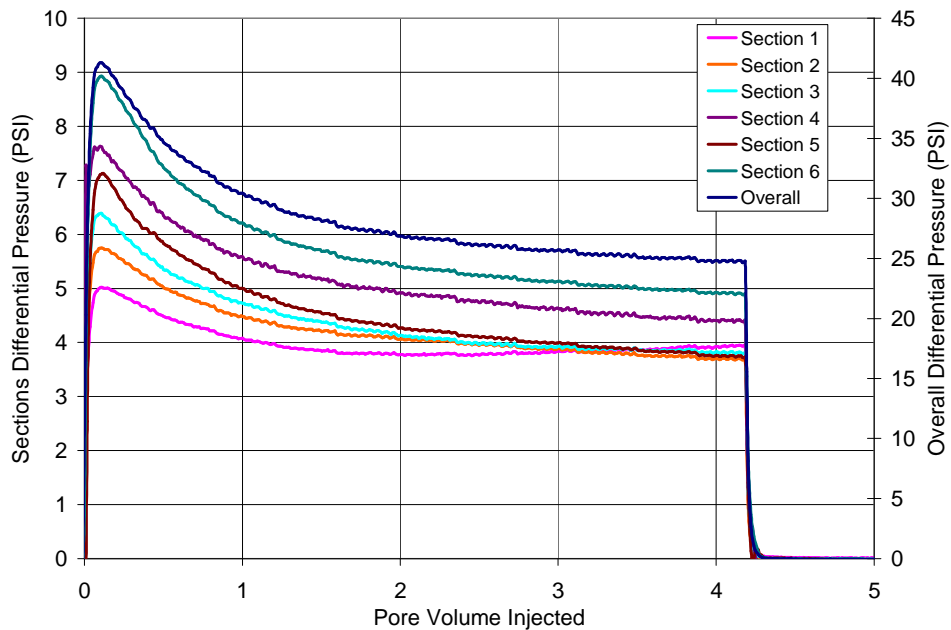
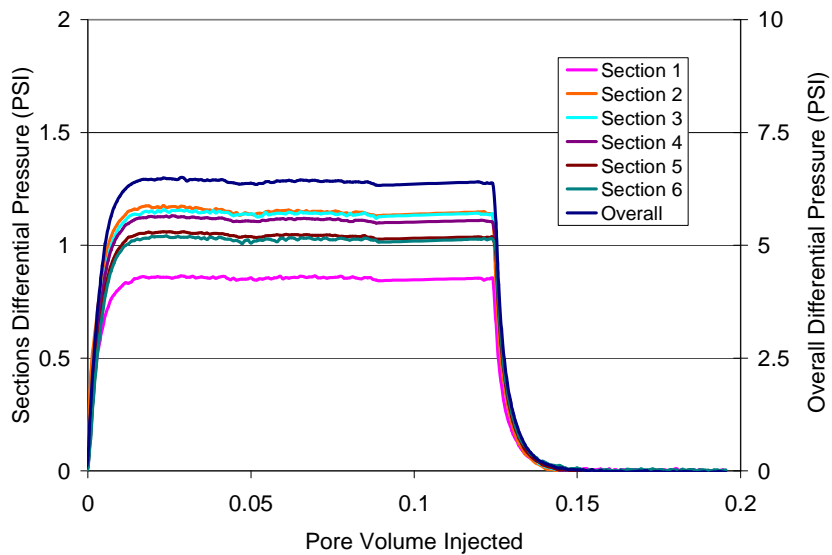


Figure 3.55: Dispersion characterization of Core #37 for core flood T-8.



**Figure 3.56:** Oil flood differential pressures for Core #37 for core flood T-8. Only pressures after the leak had been fixed are plotted. This data was used for end point relative permeabilities.



**Figure 3.57:** Waterflood differential pressures for Core #37 for core flood T-3. Pressures shown are after the leak was fixed. The data was used for estimating end point relative permeabilities.

Pressures shown are after fixing the leak.  $k_{rw}^o$  was determined to be 0.054 from overall pressure at end of waterflood.

Final oil saturation in the core was determined by running tracer through the core. No oil was produced during the tracer run and therefore oil phase was immobile. Oil volume in core was determined to be 38.3 mL, that gave a final saturation of,  $S_{or}=0.383$ .

#### *Surfactant and Polymer Slug*

Surfactant slug contained 0.625 wt% Petrostep S-1, 0.375 wt% Petrostep S-2, 2 wt% SBA, 1 wt%  $\text{Na}_2\text{CO}_3$  and 2200 ppm Flopaam SNF 3330S. To select the salinity of the surfactant slug, phase behavior experiments were performed to determine optimum salinity and the microemulsion phase transition boundaries at WOR of 1 to 9 (**Figure 3.58**). The figure shows that the optimum and the phase transition salinity ( $\text{NaCl} + \text{Na}_2\text{CO}_3$ ) increase with decreasing oil WOR (oil concentration). The range of interest was 40% to 0% oil concentration as the initial oil saturation was 38% oil. As the WOR changed from 1.5 (40% oil concentration) to 9 (10% oil concentration), the optimum salinity changed from 5 wt% TDS ( $\text{NaCl} + \text{Na}_2\text{CO}_3$ ) to 5.5 wt% TDS. If the slug salinity was chosen as 5 wt% TDS based on initial oil saturation in the core, microemulsion would become Type I at 15 wt% oil concentration in core. The correct salinity would be such that the phase behavior would remain in the Type III region at all oil concentrations. From the figure, 5.6 wt% TDS was determined to be this salinity as shown by the blue dotted arrow in the figure. The viscosity of the surfactant slug was 21 cp measured at  $1 \text{ s}^{-1}$  with Bohlin rheometer (**Figure 3.59**).

Polymer slug salinity was determined from study of the effect of dilution of surfactant slug by polymer drive. Optimum salinity and microemulsion phase transition boundaries versus surfactant concentration are plotted in **Figure 3.60**. The figure shows that as the surfactant concentration is reduced, the optimum and transition salinities are reduced. A salinity lower than 4.6 wt% TDS would be required to ensure microemulsion became Type I gradually. Therefore, 4.5 wt% NaCl was chosen as the polymer slug salinity; the blue dotted line shows the phase behavior of the microemulsion phase as it would be diluted by the polymer drive during the ASP flood. This was 80% of surfactant slug. Polymer concentration was 2450 ppm that gave the slug similar viscosity as the surfactant slug, 21 cp @  $1 \text{ s}^{-1}$  (**Figure 3.59**).

#### *Chemical Flood & Oil Recovery*

Core #37 was flooded at 0.15mL/min (2.1 ft/day) with 0.3 pore volume (PV) of surfactant slug and followed by 1.4 PV polymer drive. Oil bank arrived at 0.19 PV and surfactant breakthrough occurred at 0.78 PV. Oil cut dropped below 1% after 91% residual oil recovery. **Figure 3.61** compares the oil recovery from ASP floods T-3 and T-8. Recovery of the flood T-8 was good and slightly better than ASP T-3. Oil bank of T-8 was narrower but taller. T-8 oil cut tail was comparatively longer to T-3, which is the source of the extra oil recovered in comparison to T-3. A maximum oil cut of 0.55 was observed in the oil bank. Oil cut stayed constant at 0.15 from 0.80 PV to 1.15 PV. In the vials, in this range, type III microemulsion phase were observed (see **Figure 3.62**).

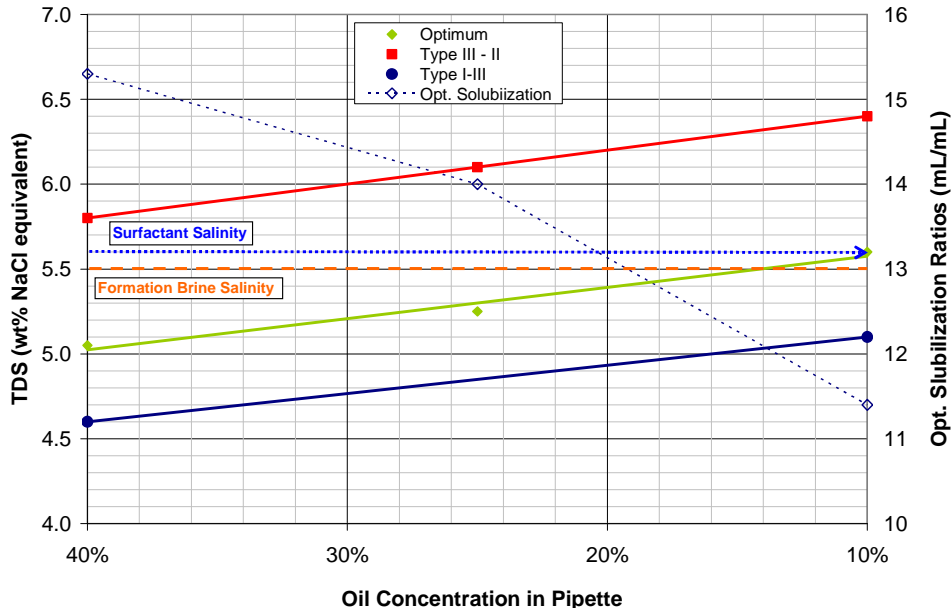


**Figure 3.58:** Optimum equivalent salinity and phase transition boundaries for 1 wt% surfactant formulation X-1 for ASP T-8 (Core 39) versus different oil percent in pipettes for Trembley. Equivalent salinity of surfactant slug (NaCl + Na<sub>2</sub>CO<sub>3</sub>) and formation brine are indicated by the blue arrow and orange line respectively.

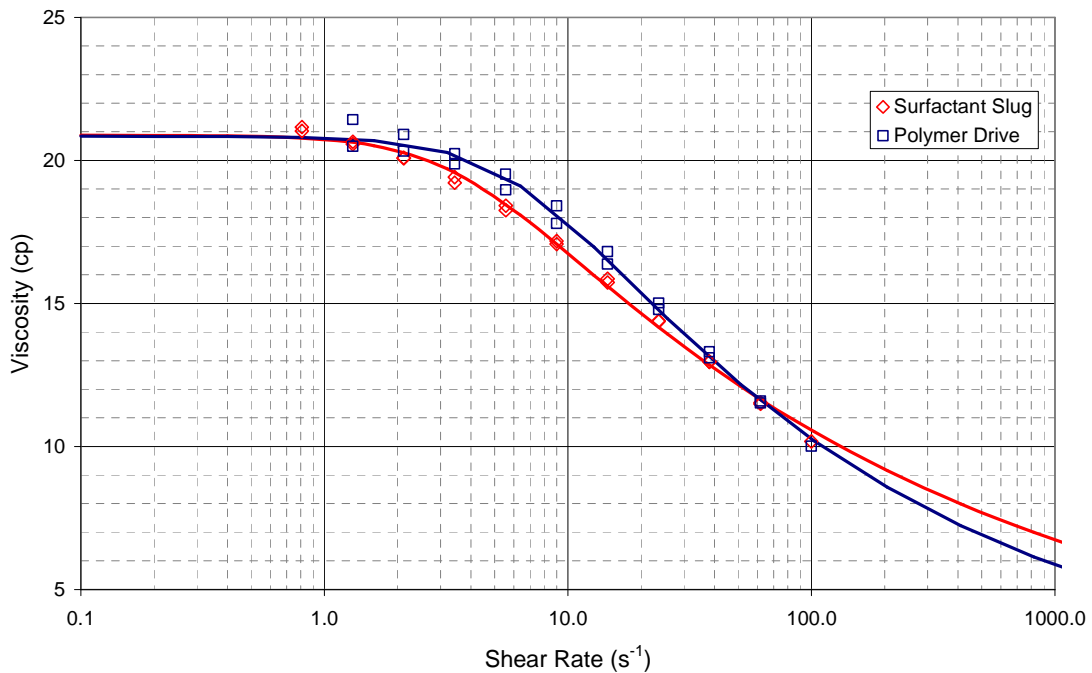


**Figure 3.59:** Viscosities of surfactant and polymer slug for core flood T-8 (Core #37)

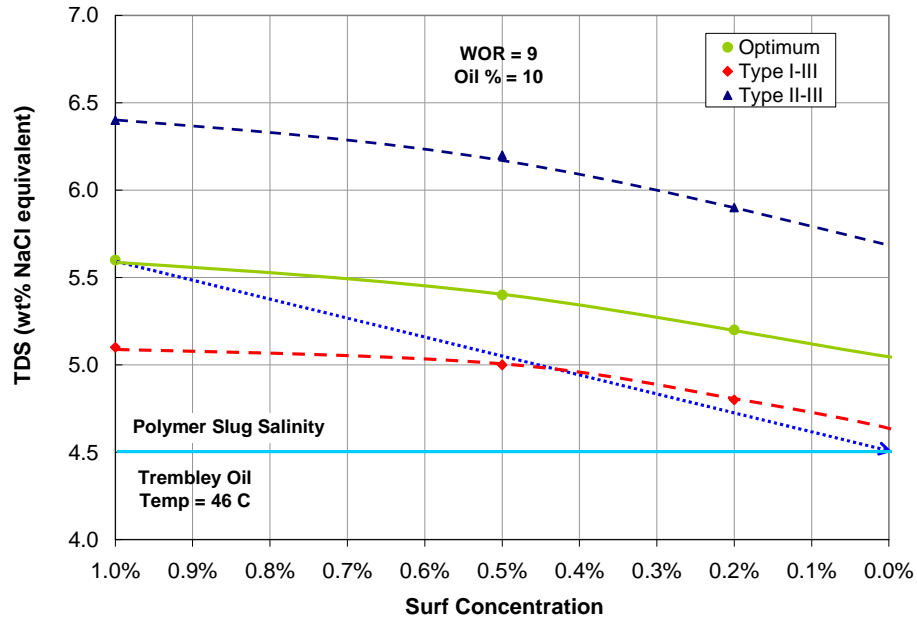


**Figure 3.60:** Optimum equivalent salinity and phase transition boundaries for surfactant concentration range 0 wt% to 1 wt% for Formulation X-1 are plotted. The curves were interpolated and extrapolated to cover the entire range. The dilution of surfactant at the back of surfactant bank and corresponding equivalent salinity (NaCl + Na<sub>2</sub>CO<sub>3</sub>) change is shown by the dotted blue arrow. A polymer salinity of 4.5 wt% for ASP-T-8 would ensure a slow transition to Type I microemulsion.

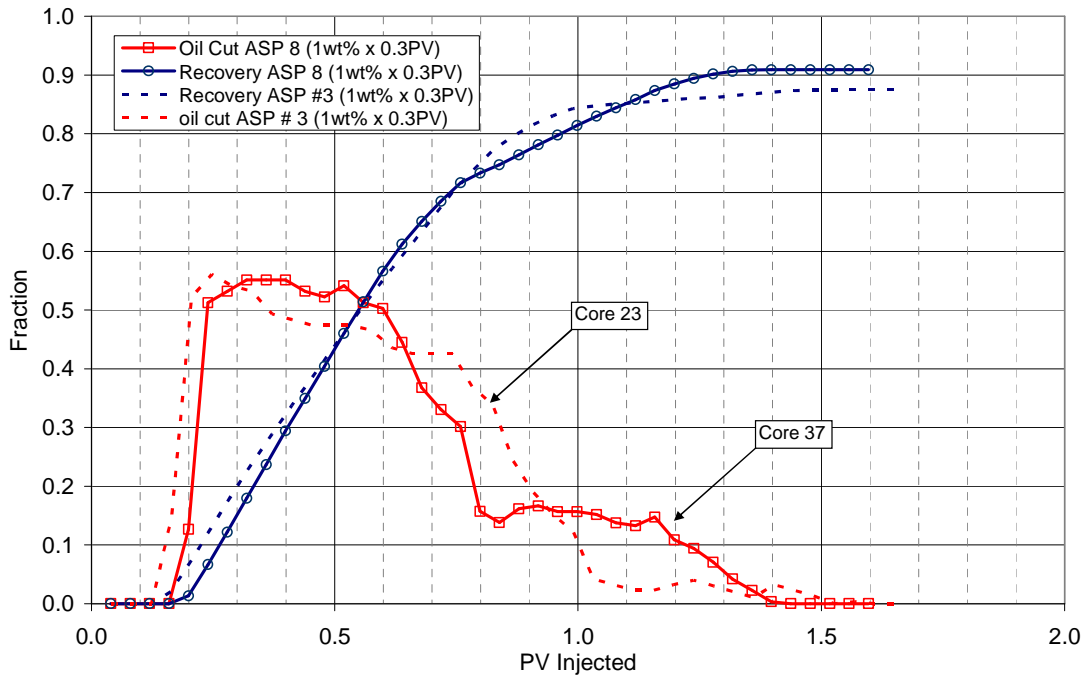


**Figure 3.61:** Oil cut and oil recovery for ASP flood T-8 (Core #37) is compared with ASP T-3 (Core #23).

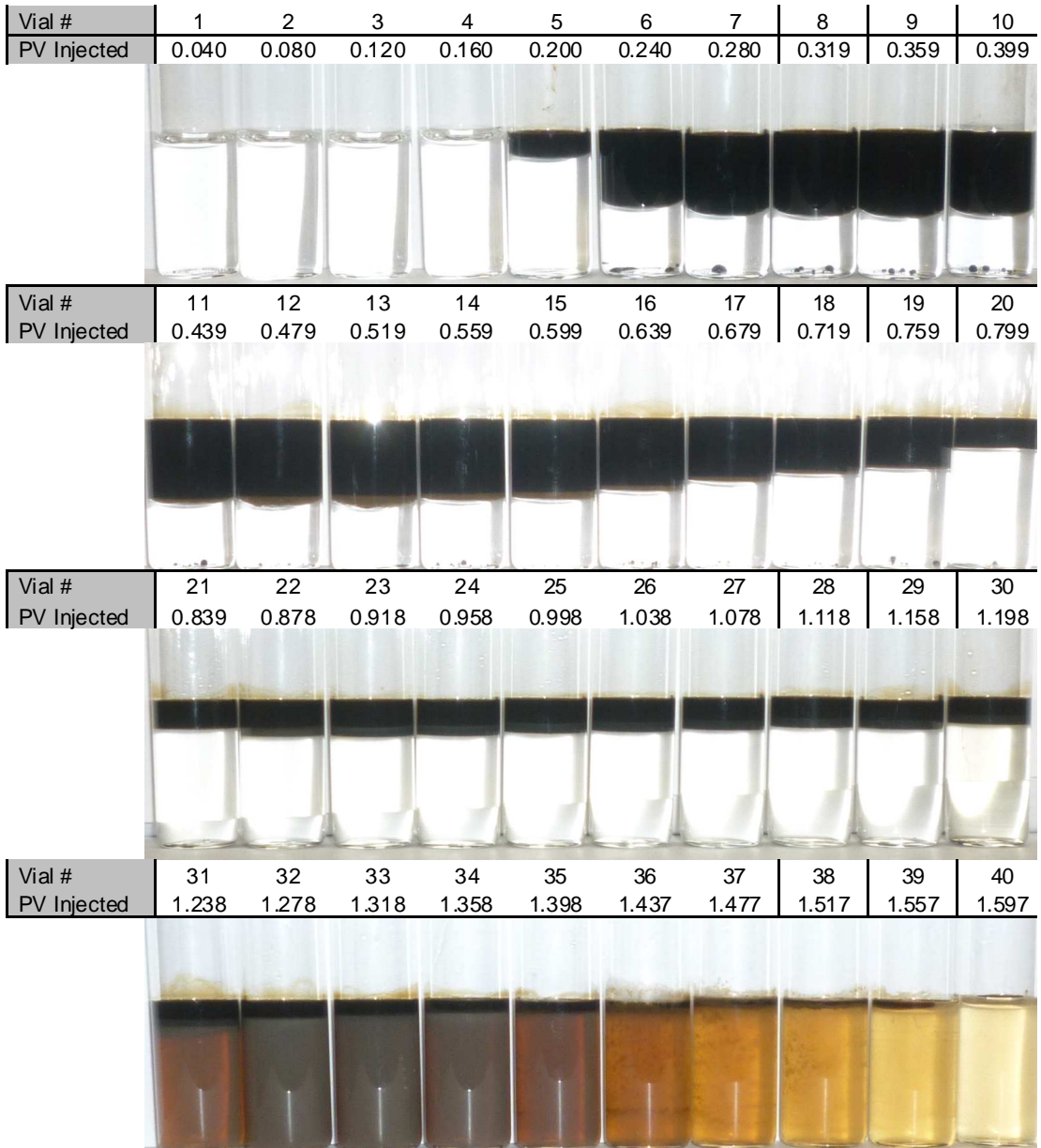


**Figure 3.62:** Photo of effluent vials from ASP T-8 (core #37) with formulation X-1 @ 46.1 °C after equilibrating for 3 days.

### *Effluent Analysis*

Effluent samples were equilibrated for 3 days at reservoir temperature and then evaluated. They are shown in **Figure 3.62**. Visual observations were used to determine the microemulsion type in vials. Vials 20-21 showed a flat interface between oil and water but it couldn't be ascertained if they contained type II microemulsion. Vials 22-30 contain type III microemulsion and vials 31 onwards are type I microemulsion as indicated by the dirty color of the aqueous phase. Therefore, Type III→Type I transition was achieved with the salinity design used.

Viscosity and salinity of aqueous phase of the effluent samples were measured and are presented in **Figure 3.63**. Salinities and viscosities of surfactant and polymer slugs were also measured with the same instruments and are indicated on the graph. Microemulsion phase types indicated on the graph were determined from visual inspection of vials.

Salinity in the aqueous phase at surfactant breakthrough (0.76 PV) was 5.4 wt% TDS, which was above the optimum salinity of the formulation (5 wt% TDS) as measured by the conductivity instrument. Salinity dropped gradually due to smaller difference between salinity of formation brine, surfactant slug and polymer drive Type III region was approximately 0.35 PV long by the time it reached the end of core. This was relatively larger than the previous ASP floods as a result of use of phase behavior relationship for ascertaining salinities for the slug. This helped improve oil recovery.

Viscosity of the aqueous phase increased sharply after oil breakthrough indicating that the polymer did not degrade. It also indicates that the oil bank and surfactant bank interface was sharp.

Pressure drop measured across the core and each section are plotted in **Figure 3.64**. All sections experienced capillary pressure effects from 0 PV to 0.2 PV. Section 1 pressure reached very high plateau compared to other sections. This could have been caused by polymer plugging the pores in the first section. Sections 1, 2, and 3 pressures seemed nearing a plateau towards the end of flood whereas the last three sections' pressures were still ascending but reaching towards a plateau. Section 6 peaked at 0.78 PV. The 2<sup>nd</sup> peak of individual section pressure curves got progressively higher from section 3 to 6. The second peak starts when surfactant hits each section. The increase in peaks height in subsequent sections indicates that the front part of the surfactant slug got progressively inefficient at mobilizing residual oil as it progressed in the core. This is thought to be the result of surfactant front mixing with formation brine and producing type II conditions, as well as dilution of surfactant slug. Oil was mobilized slowly and therefore the pressures at first rose on seeing surfactant slug and then peaked and decreased as oil continued to be mobilized.

Pressures of individual sections (**Figure 3.66 to Figure 3.71**) were analyzed using **Figure 3.65** to determine mobilities of oil bank and surfactant bank. Mobility of oil bank could only be ascertained for last three sections which saw oil bank for the entire length, or at least most part of it. Mobility for oil was estimated at the pore volume at which surfactant arrived and



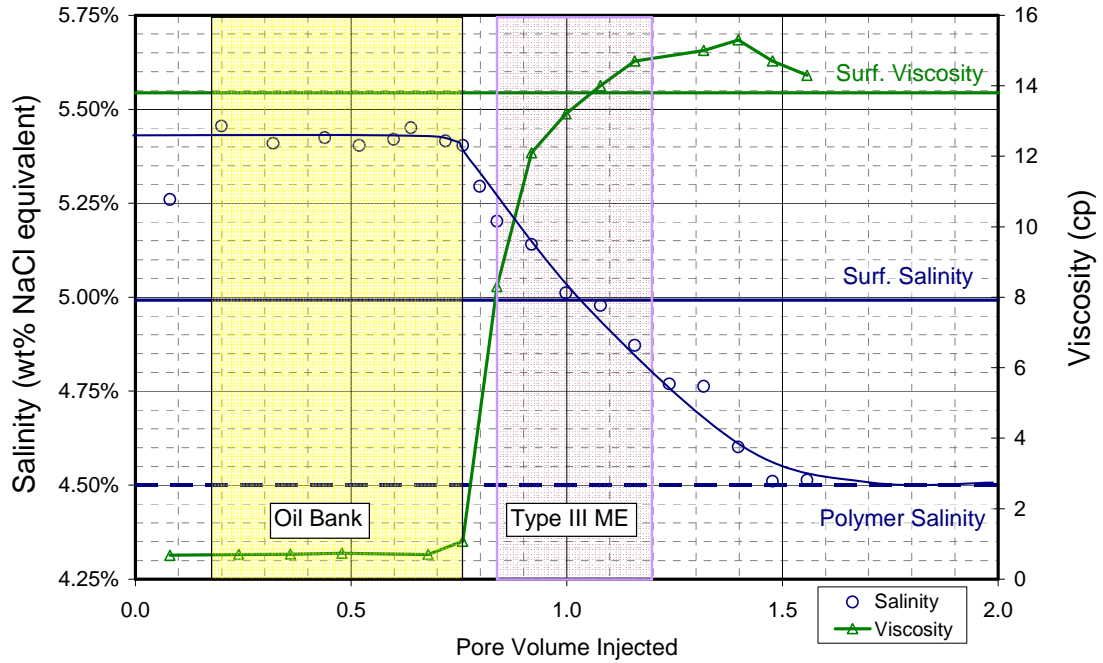


**Figure 3.63:** Viscosity and salinity of aqueous phase in effluent vials from ASP T-8. Viscosity was measured at 46.1 °C with variable shear rates ranging between 37.5 – 75 s<sup>-1</sup> on Brookfield rheometer.

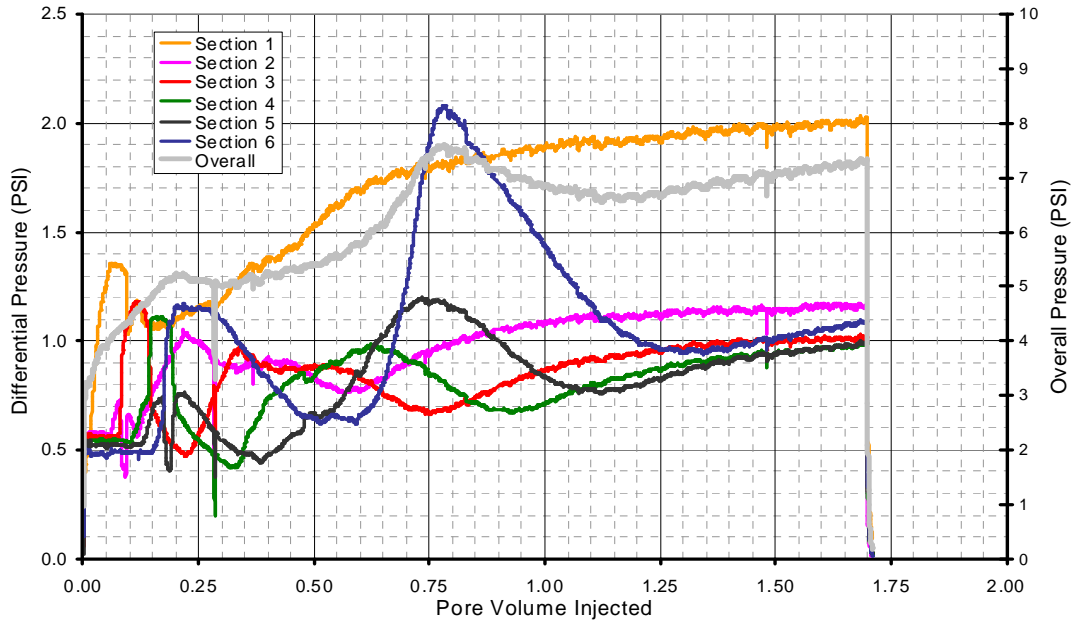


Figure 3.64: Overall core and section pressures during ASP T-8.

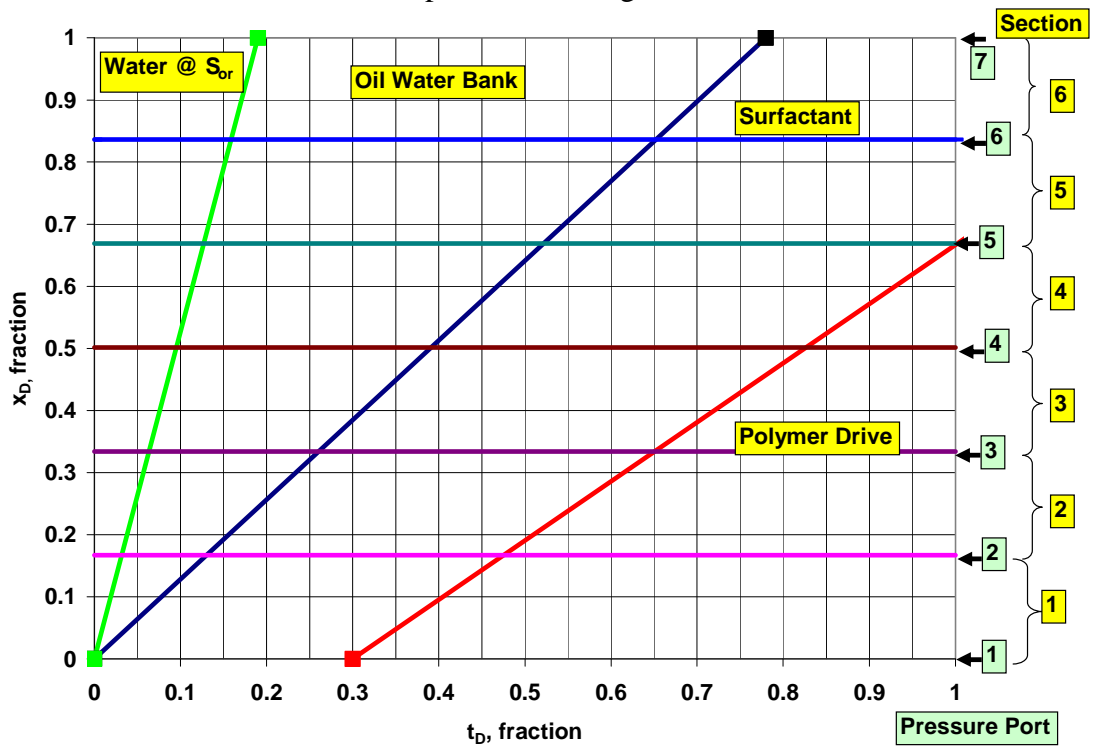
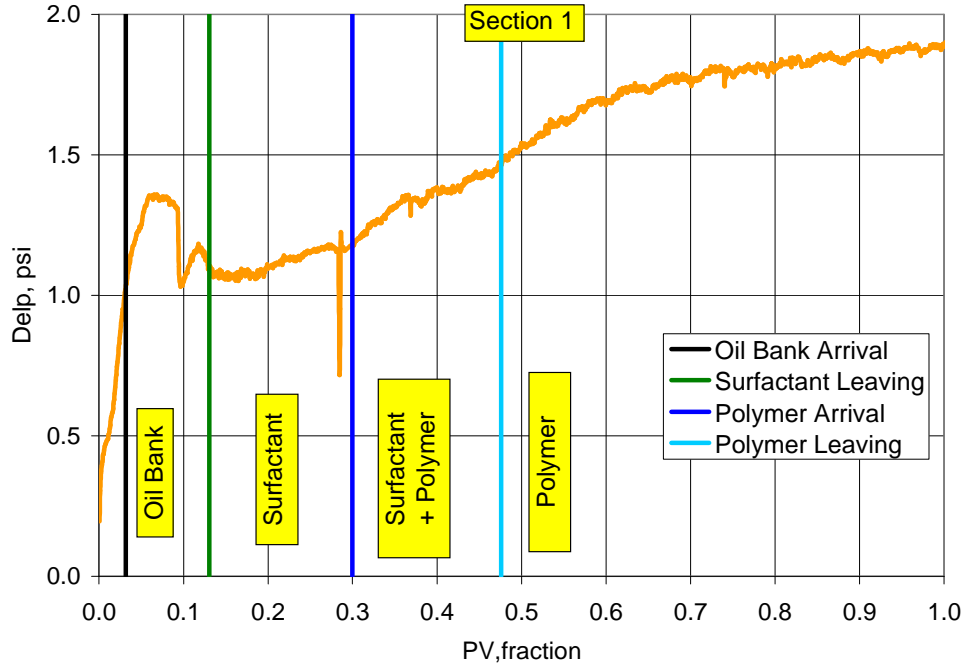
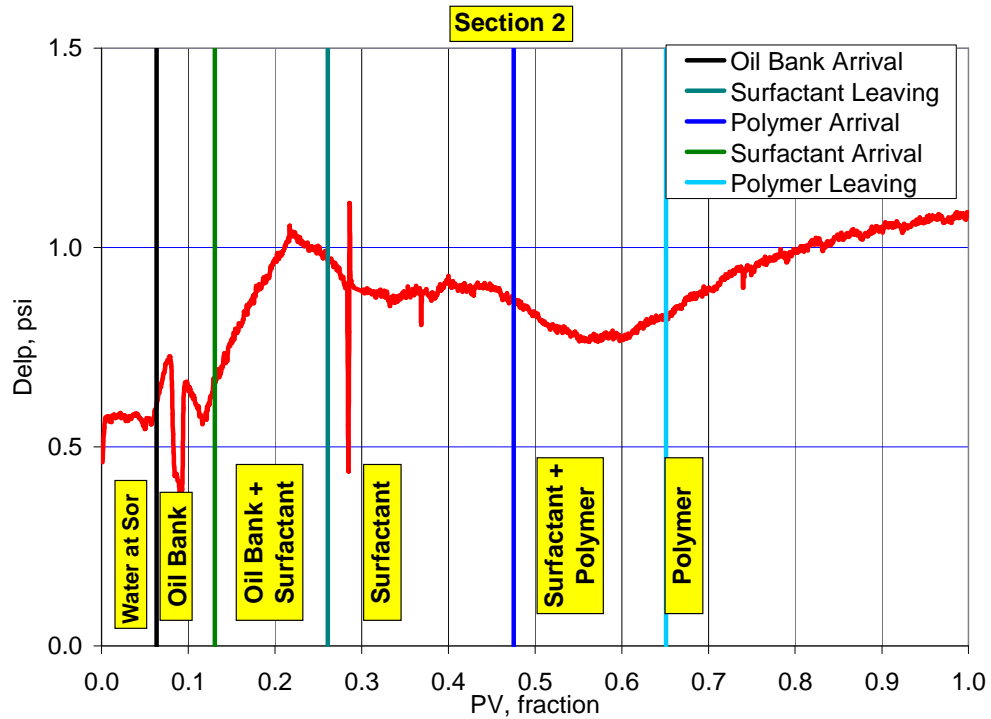


Figure 3.65: Dimensionless distance versus dimensionless time plot for ASP T-8.



**Figure 3.66:** Section 1 pressure during ASP T-8 with identification of fluid regions using dimensionless velocities and pressure analysis.



**Figure 3.67:** Section 2 pressure during ASP T-8 with identification of fluid regions using dimensionless velocities and pressure analysis.

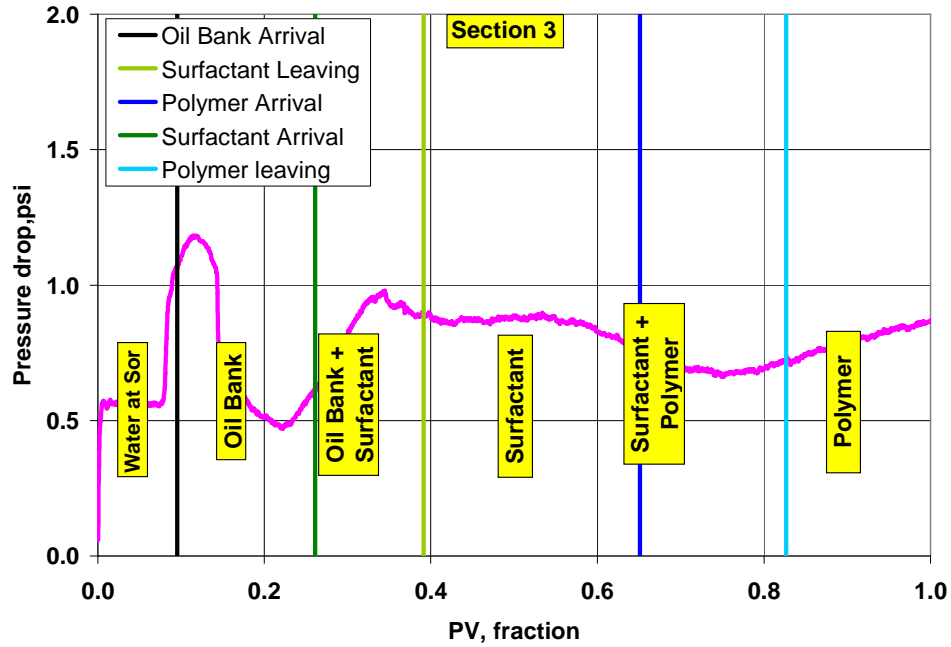


**Figure 3.68:** Section 3 pressure during ASP T-8 with identification of fluid regions using dimensionless velocities and pressure analysis.

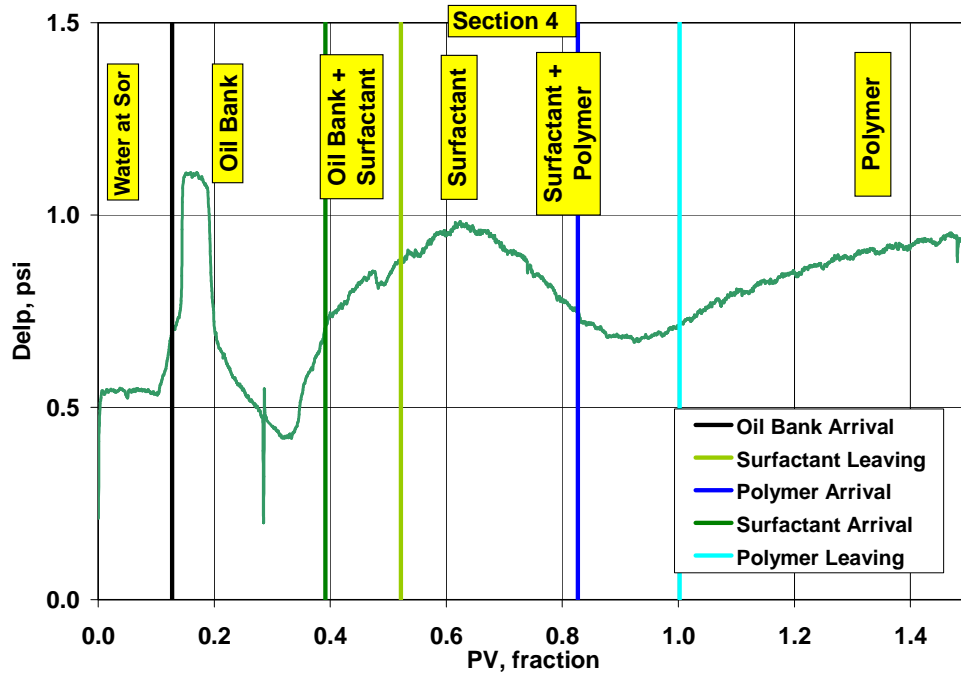


**Figure 3.69:** Section 4 pressure during ASP T-8 with identification of fluid regions using dimensionless velocities and pressure analysis.

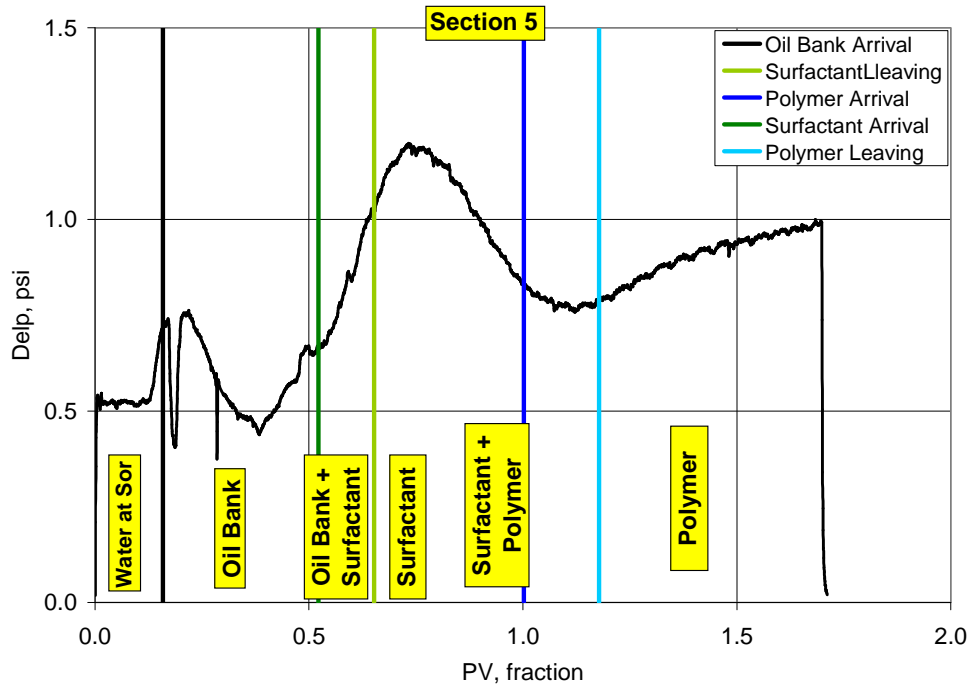


**Figure 3.70:** Section 5 pressure during ASP T-8 with identification of fluid regions using dimensionless velocities and pressure analysis.

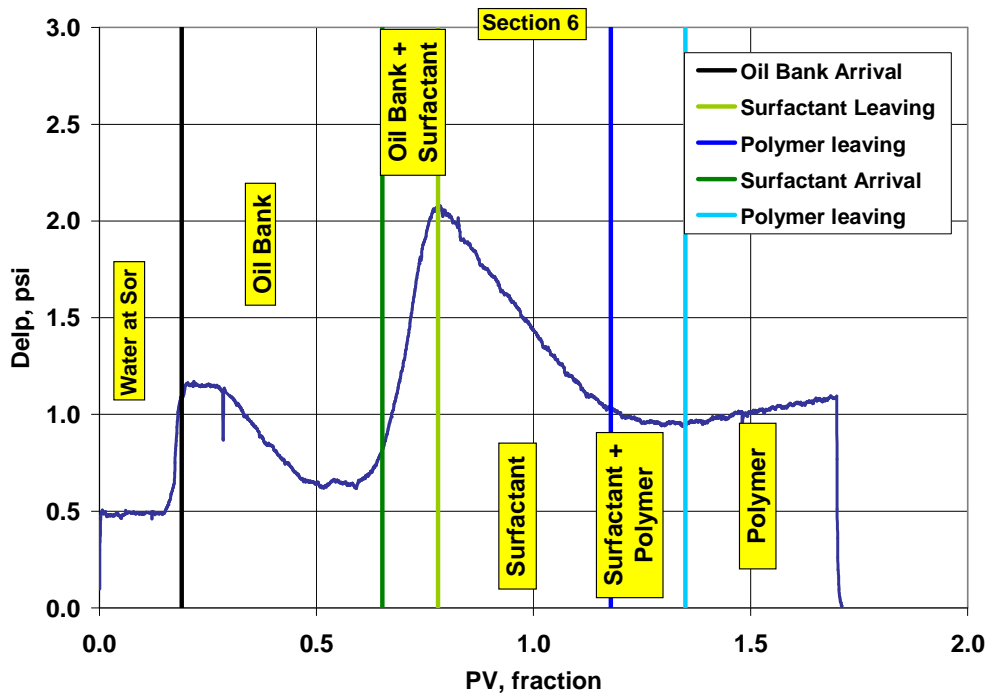


**Figure 3.71:** Section 6 pressure during ASP T-8 with identification of fluid regions using dimensionless velocities and pressure analysis.

mobility of surfactant slug was ascertained at the pore volume at which polymer arrived in a particular section. The estimations are tabulated in **Table 3.18**. For T-8 ASP (core #37), mobility of surfactant slug was lower than the oil bank in the last three sections, indicating good mobility control. Therefore polymer in surfactant slug proved sufficient.

#### ***Core Flood T-9 (Core #39)***

Core flood T-9 (Core #39) was performed to test formulation X-1 with synthetic field brine (SFB) as the formation brine in the core. SFB composition was based on analysis of a field brine sample from Trembley lease (**Table 3.19**). SFB contained 154,591 ppm TDS (15.5 wt% TDS), which were significantly higher than the formation brine TDS in previous floods (4.2 wt% NaCl to 5.5 wt% NaCl). In addition, the SFB contained a significant proportion in divalent cations (Ca<sup>++</sup>, Mg<sup>++</sup> and Sr<sup>++</sup>), a fifth of total cations, which make it considerably hard. Composition of SFB prepared for T-9 is presented in **Table 3.20**. Surfactant slug and polymer slug compositions were similar to ASP T-8, only salinities of the surfactant and polymer were reduced by 0.2 wt% NaCl and 0.3 wt% NaCl. Rationale and methodology followed select the salinities was the same as for T-8.

#### ***Core Characterization***

Core #39, sandstone, was set up for flooding in vertical orientation. Its diameter was 5.08 cm. The length and permeabilities of each section and overall are given in **Table 3.16**. Its dispersion was measured (**Figure 3.72**). Pore volume was determined from tracer curve integration and gravimetric method, and was 110 mL. Overall permeability of the core was 232 md and was determined with the synthetic formation brine. Flow rate used was 6 mL/min (84 ft/day). SFB viscosity was 0.87 cp at 46.1 °C.

#### ***Brine Flood/Oil Flood/Waterflood***

Brine flood was carried out with synthetic formation brine (SFB). The field brine composition and the SFB compositions are tabulated in **Tables 3.19** and **3.20**, respectively. Salts of Barium, Iron, Bicarbonate, Carbonate and Sulfate had to be eliminated to avoid precipitate formation while formulation of SFB. Brine was brought to reservoir temperature (46 °C) and agitated to dissolve all the salts. The brine still had an insignificant amount of precipitate that was filtered out using a 0.45 micron disc filter.

Oil flood on core #39 was run at 49 ft/day (3.5mL/min) and at 46.1 C.  $S_{oi}$  at the end of oil flood was 0.65 and  $k_{ro}^o$  was measured to be 0.74. 5 pore volumes of oil were injected and oil saturation became stabilized (**Figure 3.73**). Pressures during the oil flood are plotted in **Figure 3.74**.

Waterflood was performed at 46.1 C at a flow rate of 0.3mL/min. Pressures were measured during the flood (**Figure 3.75**). Waterflood was conducted until the oil saturation in the core became stable (**Figure 3.76**).  $k_{rw}^o$  was determined to be 0.043 from overall pressure at end of waterflood. Final oil saturation left in the core was 36.7 %.

#### ***Surfactant and Polymer Slug***

Surfactant slug contained 0.625 wt% Petrostep S-1, 0.375 wt% Petrostep S-2, 2 wt% SBA, 1 wt% Na<sub>2</sub>CO<sub>3</sub>, 4.4 wt% NaCl and 2450 ppm Flopaam SNF 3330S. The viscosity of the

**Table 3.19:** Composition of Trembley field brine sample.

Trembley Field Brine Composition					
Cations	mg/L	meq/L	Anions	mg/L	meq/L
Sodium	45663.6	1986.3	Chloride	95139.0	2683.5
Magnesium	2509.0	206.4	Bicarbonate	92.0	1.5
Calcium	8823.0	440.3	Carbonate	0.0	0.0
Srontium	2024.0	46.2	Sulfate	137.0	2.85
Barium	7.5	0.1			
Iron	20.0	0.7			
Potassium	309.0	7.9			

**Table 3.20:** Synthetic formation brine composition used for brine flood of core #39 (T-9). Brine was formulated to mimic concentrations of actual field brine sample but salts of Barium, Iron, Bicarbonate, Carbonate and Sulfate had to be eliminated to avoid precipitate formation.

Trembley Synthetic Field Brine Composition					
<u>Cations</u>	<u>mg/L</u>	<u>meq/L</u>	<u>Anions</u>	<u>mg/L</u>	<u>meq/L</u>
Sodium	45664	1986	Chloride	95263	2686
Magnesium	2509	206			
Calcium	8823	440			
Srontium	2024	46			
Potassium	309	8			
Total	154591	mg/L			

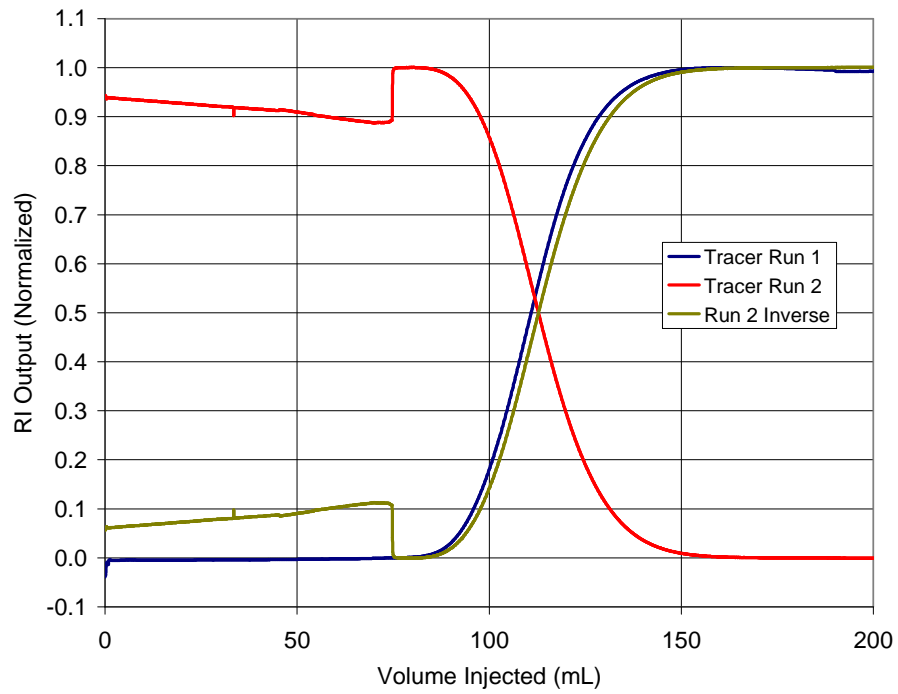


**Figure 3.72:** Dispersion characterization of Core #39 for core flood T-9.

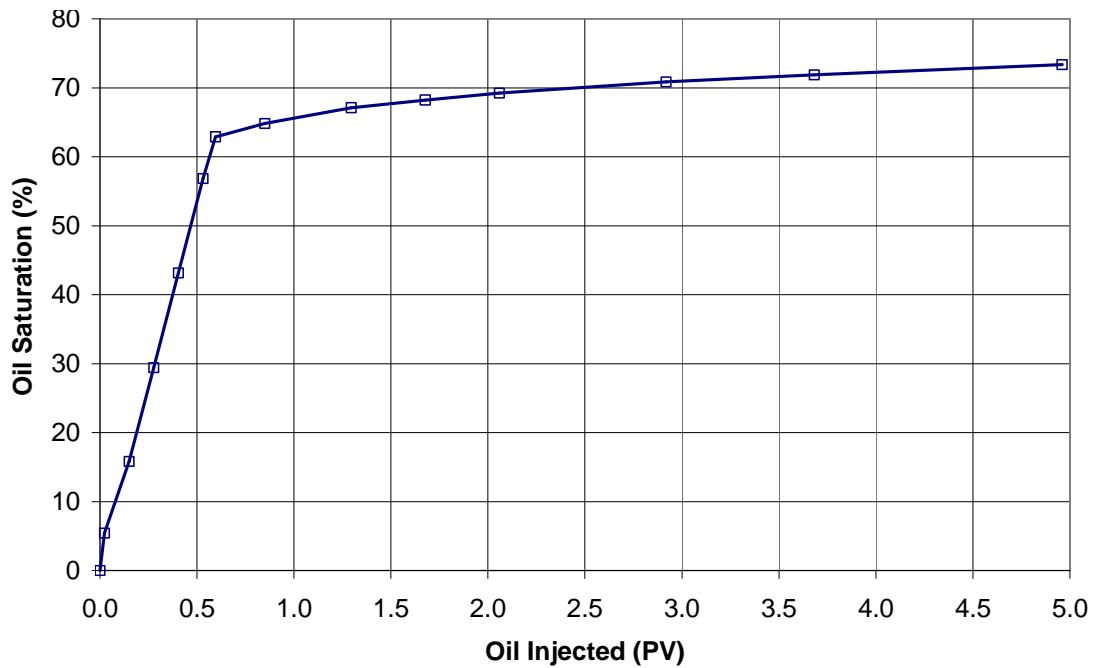


**Figure 3.73:** Oil saturation change in the core during oil flood on core #39.



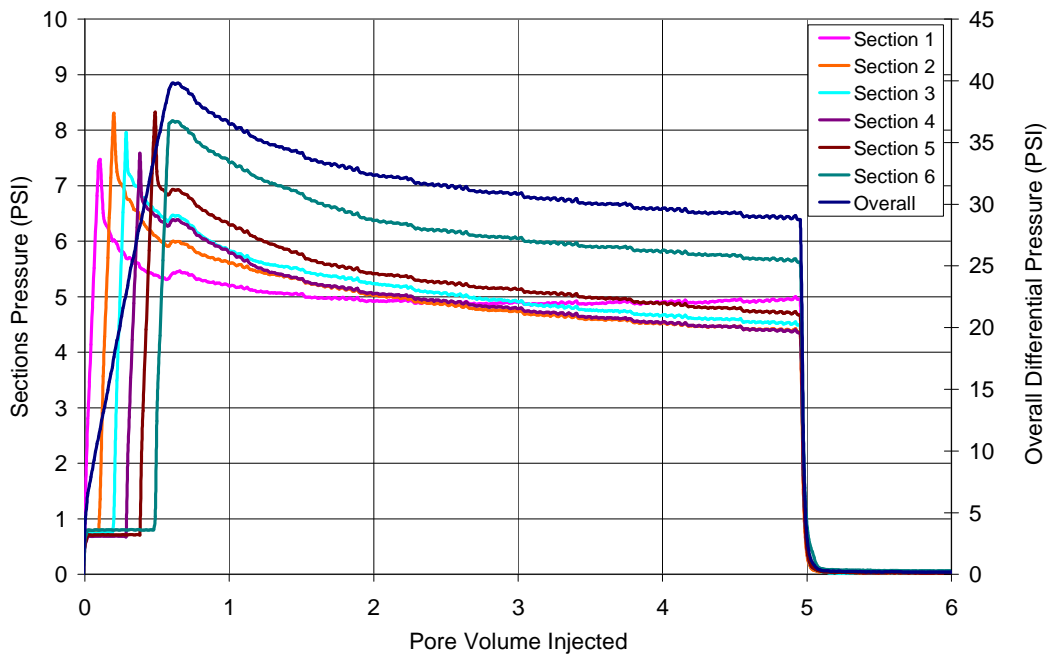


**Figure 3.74:** Oil flood differential pressures for Core #39 for core flood T-9.

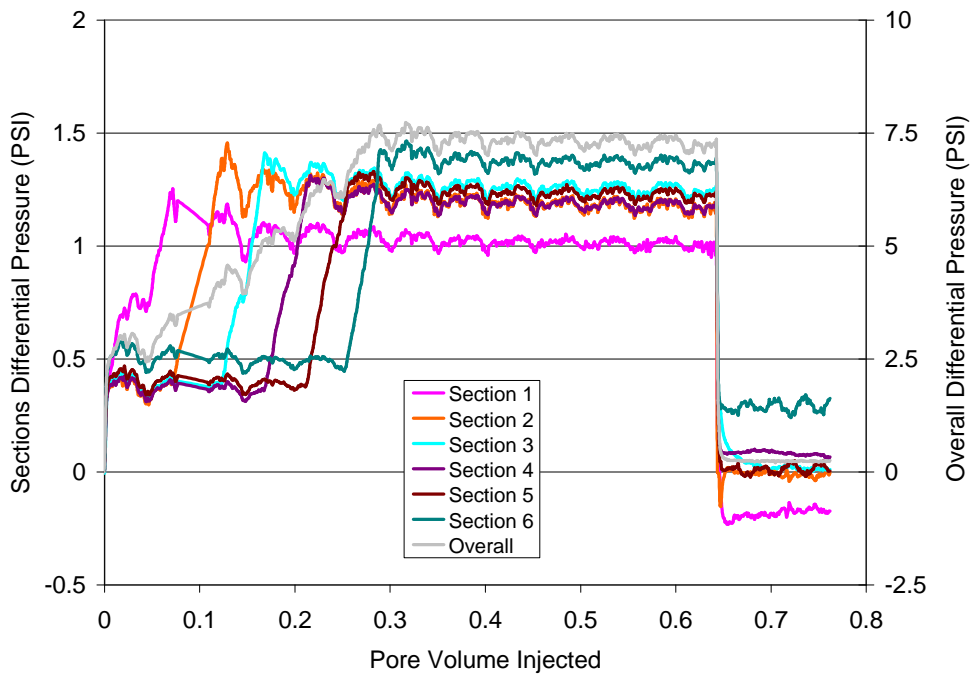


**Figure 3.75:** Waterflood differential pressures for Core #39 for core flood T-9.

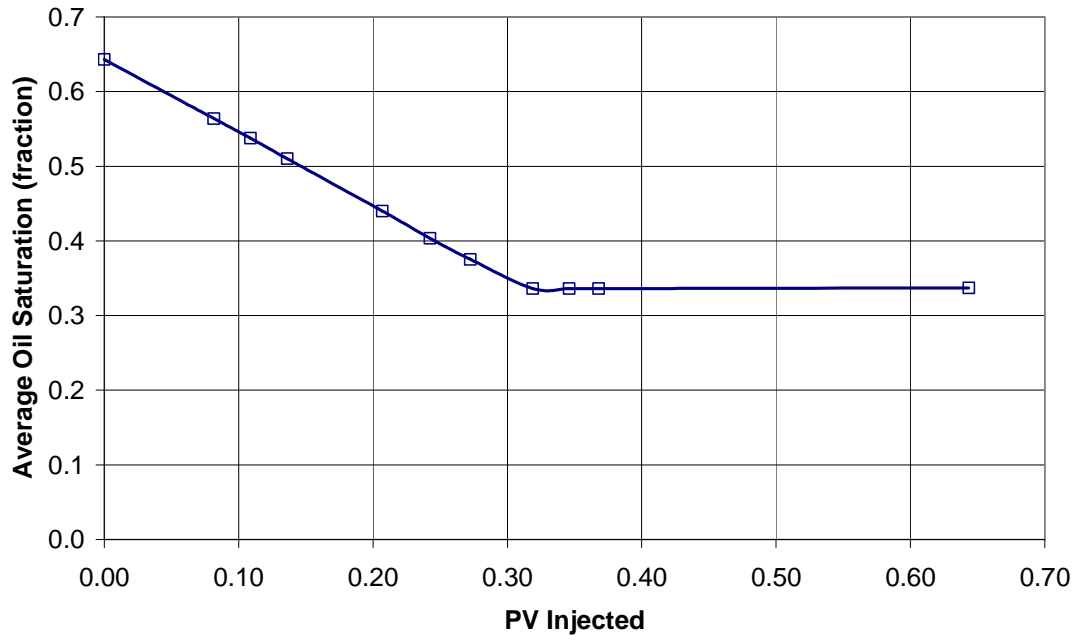


**Figure 3.76:** Oil saturation change in the core during waterflood on core #39.

surfactant slug was 14 cp measured at  $38 \text{ s}^{-1}$  with Brookfield DV-I+. Salinity of the surfactant slug was selected after studying the relationship between optimum salinity and microemulsion Type phase transition boundaries of formulation X-1 with WOR (**Figure 3.77**). The figure shows, that 5.4 wt% equivalent salinity ( $\text{NaCl} + \text{Na}_2\text{CO}_3$ ) would keep the microemulsion in Type III phase at all oil saturations from 36% to 0%.

Salinity of the formation brine was significantly higher than the surfactant salinity and APSL of the system (**Figure 3.77**). Upon mixing with the formation brine in the core, the surfactant slug would potentially become unstable i.e. separate into two phases or precipitate. Even if it was assumed that the high salinity would render the surfactant ineffective at mobilizing oil, it should be for very short period. The slug should displace the formation brine completely and would start mobilizing the oil. As the surfactant slug would travel in the core, the salinity at the front of the slug would become higher than Type III salinity range. This should take Type III microemulsion phase to Type II microemulsion phase. The stability of surfactant slug would not be a problem for this scenario since the surfactant molecules would already be entrapped in the micelles interface; the surfactant would not separate out. In phase behavior experimentation, where the samples were above APSL for the formulation and oil was added to pipettes, clear single aqueous phase and Type II microemulsion phase were observed after mixing.

4.1% NaCl was chosen as the polymer slug salinity, which is 76% of surfactant slug salinity. **Figure 3.78** shows that as the surfactant slug diluted to below 0.7 wt% surfactant concentration, it would become Type I microemulsion. Since the salinity of formation brine was much higher than the surfactant slug salinity, the salinity in the surfactant slug would eventually become higher than the optimum due to dispersion during displacement. Therefore, the figure would not hold true for the entire length of the core flood. Polymer concentration in the polymer slug was 2450 ppm that gave the slug similar viscosity as the surfactant slug, 14 cp @  $38 \text{ s}^{-1}$ .

#### *Chemical Flood & Oil Recovery*

Core #39 was flooded at 0.15mL/min (2.1 ft/day) with 0.3 pore volume (PV) of surfactant slug and followed by 1.7 PV polymer drive. Oil bank arrived at 0.24 PV and surfactant breakthrough occurred at 0.95 PV. Oil cut dropped below 1% after 86% residual oil recovery. **Figure 3.79** compares the oil recovery from ASP floods T-9 and T-8. Recovery of the flood T-9 was good but slightly less than T-8. The oil bank of T-9 (Core #39) did not reach as high oil cut as T-8 (Core #37). The oil bank showed two plateaus i.e. oil cut fraction was constant from 0.3-0.6 PV at 0.42 and then from 0.7-0.9 PV at 0.32. Oil bank was delayed as well as extended in the case of T-9. High salinity of SFB seemed to have caused this.

#### *Effluent Analysis*

Effluent samples were equilibrated for 3 days at reservoir temperature and then evaluated. They are shown in **Figure 3.80**. Salinity and viscosity of the aqueous phase of the effluent along with the oil bank region are presented in **Figure 3.81**. Vials 7-23 (0.24PV-0.93PV) contained oil bank. A distinctive emulsion was observed below the oil phase in vials 16-23 (0.65 PV to 0.93 PV) which suggested that some surfactant might be present. This would not be inconsistent considering that the other ASP core floods showed surfactant slug

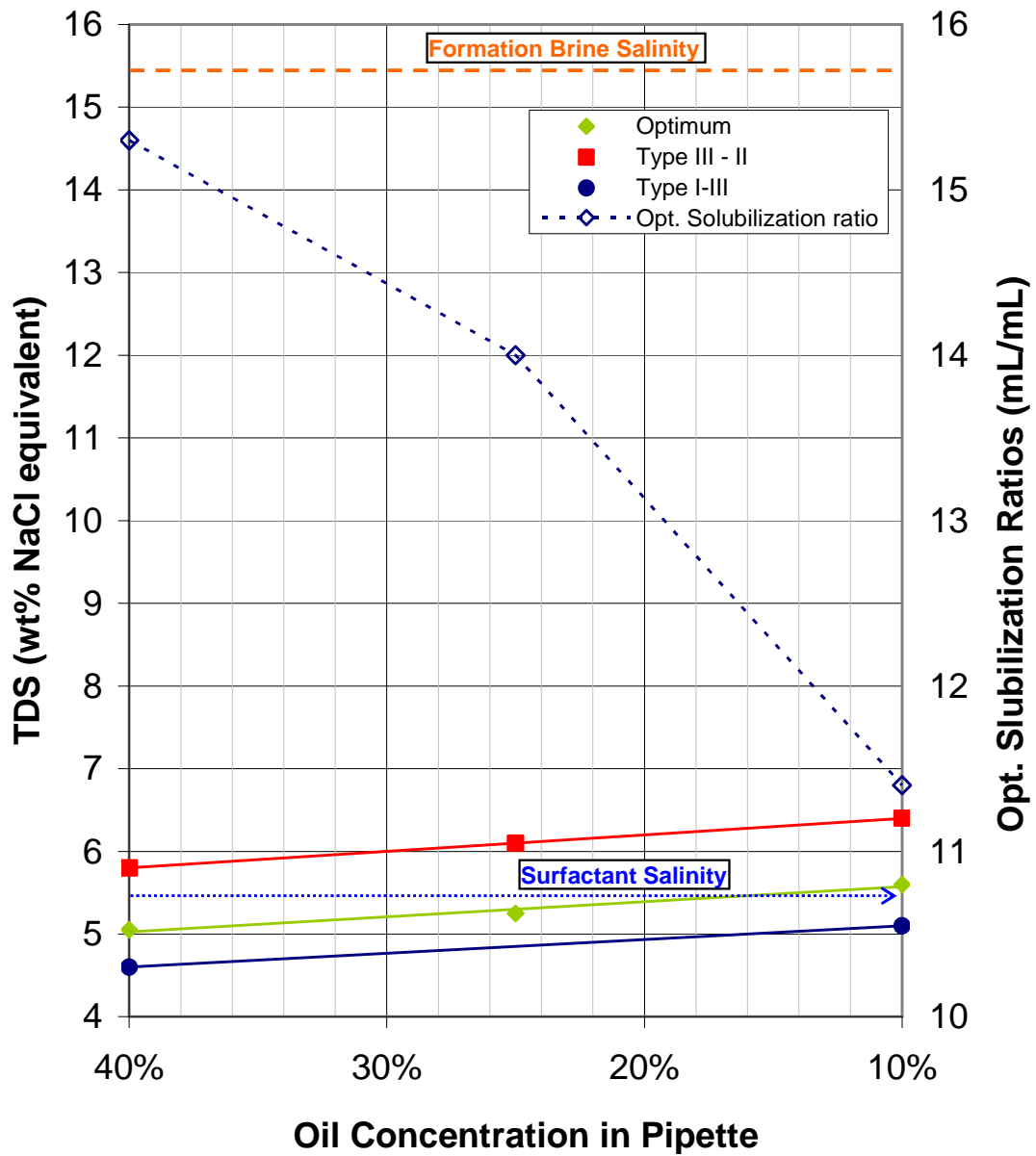


**Figure 3.77:** Optimum equivalent salinity and phase transition boundaries for 1 wt% surfactant formulation X-1 for ASP T-9 (Core 39) versus different oil percent in pipettes for Trembley. Equivalent salinity of surfactant slug (NaCl + Na<sub>2</sub>CO<sub>3</sub>) is indicated by the blue arrow.

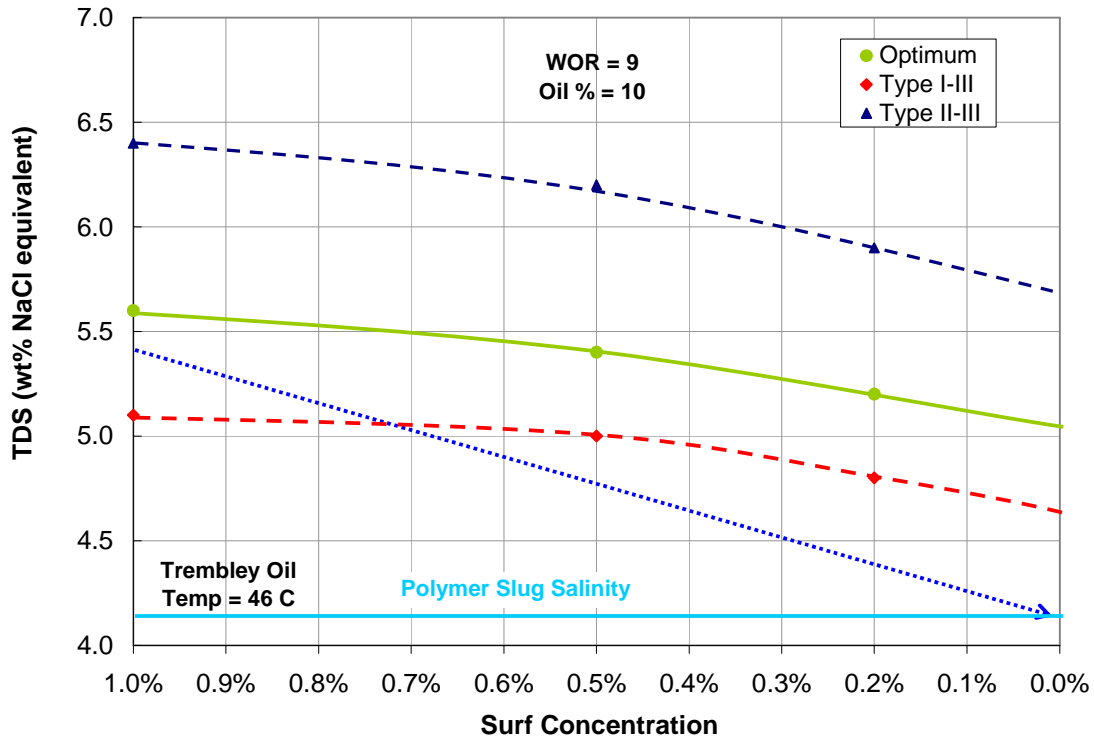


**Figure 3.78:** Optimum equivalent salinity and phase transition boundaries for surfactant concentration range 0 wt% to 1 wt% for Formulation X-1 are plotted. The curves were interpolated and extrapolated to cover the entire range. A polymer salinity of 4.1 wt% was used for ASP-T-9. The dilution of surfactant at the back of surfactant bank and corresponding equivalent salinity (NaCl + Na<sub>2</sub>CO<sub>3</sub>) change is shown by the dotted blue arrow.

Residual Oil Recovered in Trembley ASP Cor 23 and Core 39

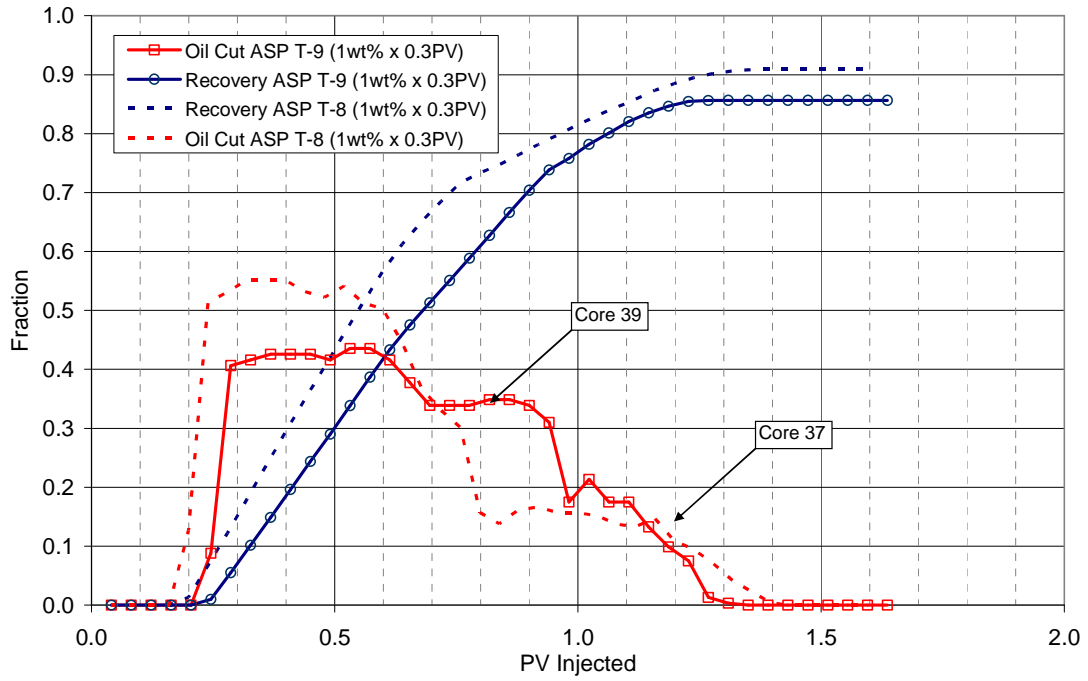
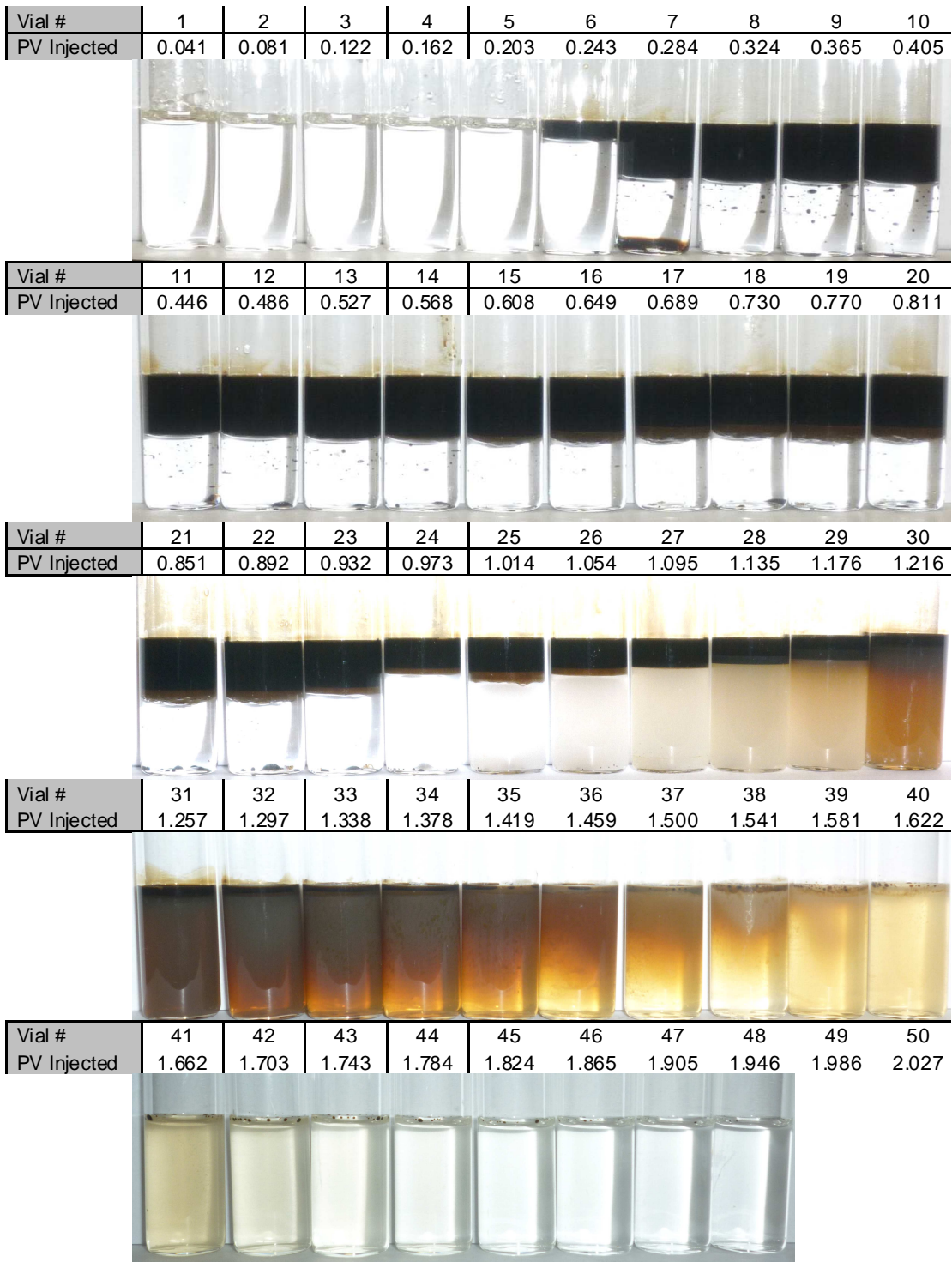
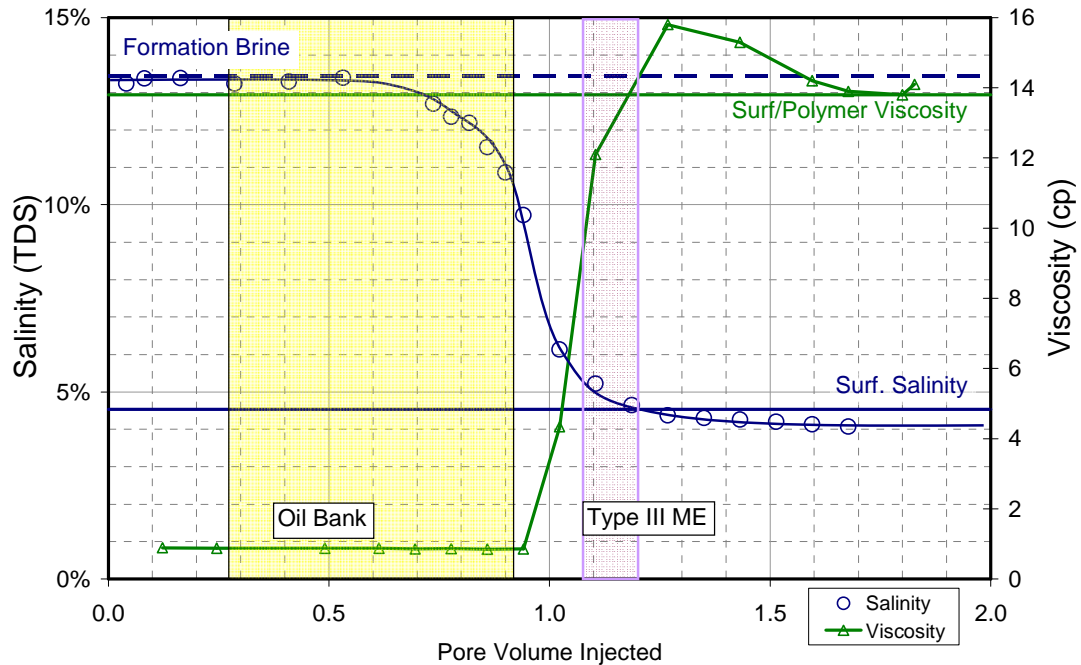


Figure 3.79: Oil cut and oil recovery for ASP flood T-8 (Core #37) is compared with ASP T-3 (Core #23).



**Figure 3.80:** Photo of effluent vials from ASP T-9 (core #39) with formulation X-1 @ 46.1 °C after equilibrating for 3 days.



**Figure 3.81:** Viscosity and salinity of aqueous phase in effluent vials from ASP T-9. Viscosity was measured at 46.1 °C. Shear rates ranged between 37.5 – 75 s<sup>-1</sup> on Brookfield rheometer



breakthrough around 0.65-0.70 PV, however to confirm presence of surfactant, a measurement of surfactant in the aqueous phase may need to be performed. Vial 23-26 (0.93 PV-1.05 PV) showed a drop in oil cut, implying the end of oil bank and surfactant breakthrough.

Whether there was any surfactant present in these vials could not be proven without measurement but the emulsion at the oil and water interface appeared to be due to surfactant. Similar emulsion had been observed in phase behavior studies for Type II microemulsion systems. If there was surfactant present, then the vials were predicted to be Type II microemulsion inferring from their salinity. Salinity in the vials was higher than 6.0 wt% NaCl equivalent. According to **Figure 3.77** and **Figure 3.78**, this should be high enough to give Type II microemulsion, considering both a 20% oil concentration and surfactant concentrations to be around 0.5wt% (assumption). Visually, Type II microemulsion was not possible to differentiate. However, Type III microemulsion was easily recognizable by the middle phase in vial-27, just one vial downstream. Vials 27 to 29 (1.09 PV to 1.18 PV) contained type III microemulsion. Vial 30 and onward (1.22 PV onwards) contained type I microemulsion phase as these vials did not have a middle phase but showed dirty aqueous phase. In this flood, there was evidence that Type II→Type III→Type I transition was achieved with the salinity design used.

Comparing to ASP T-8, the only major difference in ASP T-9 was the type of formation brine. SFB used in T-9 had much higher salinity and also contained divalent cations. **Figure 3.83** compares the effluent salinity of T-8 and T-9. There was an 8 wt% TDS difference in the formation brine salinities as measured by the conductivity instrument. For both cores, Core 37 and 39 salinities dropped at 0.7 PV indicating the emergence of surfactant slug. In T-8 the salinity decline coincided with the end of oil bank. However, Core 39 effluent showed persistent oil cuts until 0.93 PV which suggested the oil bank had not ended at 0.7 PV. Decline in salinity happened at the same pore volume at which the tracer curve took off. The contrast between surfactant slug salinity and formation brine salinity was considerably large for T-9. At approximately 1.1 PV, the effluent salinities of both floods were equal, which should represent the complete evacuation of formation brine from the core.

**Figure 3.84** compares viscosity of effluent aqueous phase from ASP T-8 and T-9. T-9 showed a delayed rise in viscosity compared to T-8 by 0.2 PV. The delay suggested polymer was retained in the core due to the presence of divalent cations and high salinity of the brine. End of oil bank and polymer breakthrough coincided at 0.92 PV. This indicated that mobility control in the surfactant slug decreased because polymer in the surfactant slug was retained. It was possible that the oil bank was drawn out and thus had lower oil cuts due to the delayed polymer breakthrough

T-9 (Core 39) effluent showed a lower pH in the effluent brine compared to T-8 (Core 38) (**Figure 3.85**). pH of the aqueous phase for Core 39 remained under 9 until 1.15 PV, whereas Core 37 effluent got above 9 pH at 0.8 PV. Alkali was consumed by SFB or retained in the core which could have had an impact on the phase behavior in the core. Loss of alkali would be undesirable for limestones as that would cause retention of surfactant.

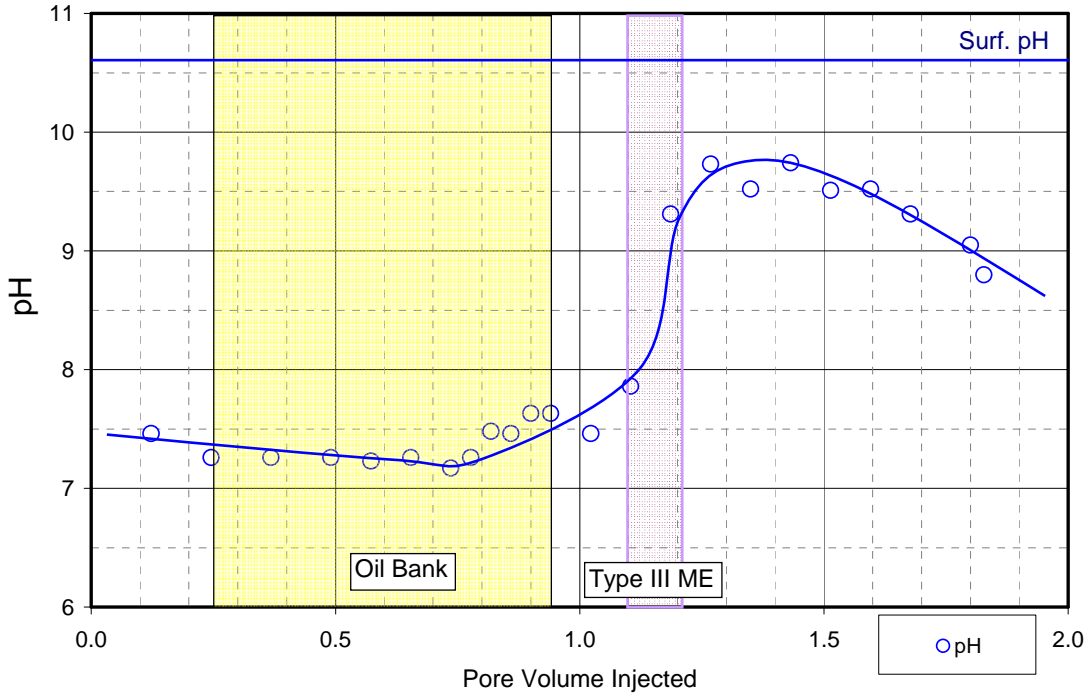


Figure 3.82: pH of aqueous phase in effluent vials from ASP T-9.

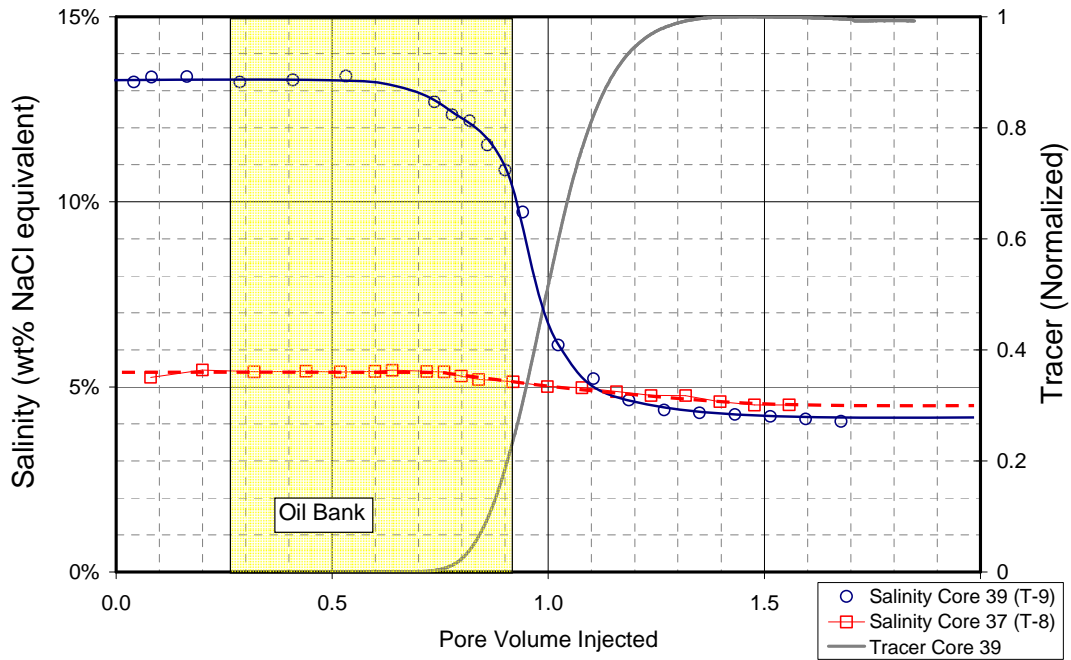
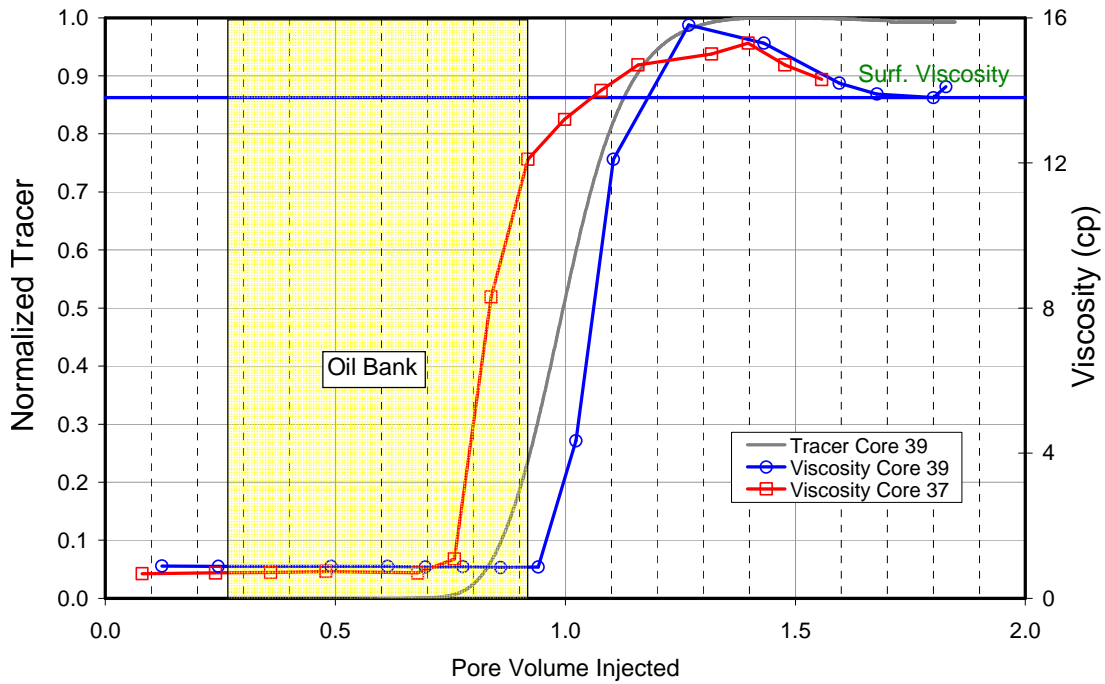
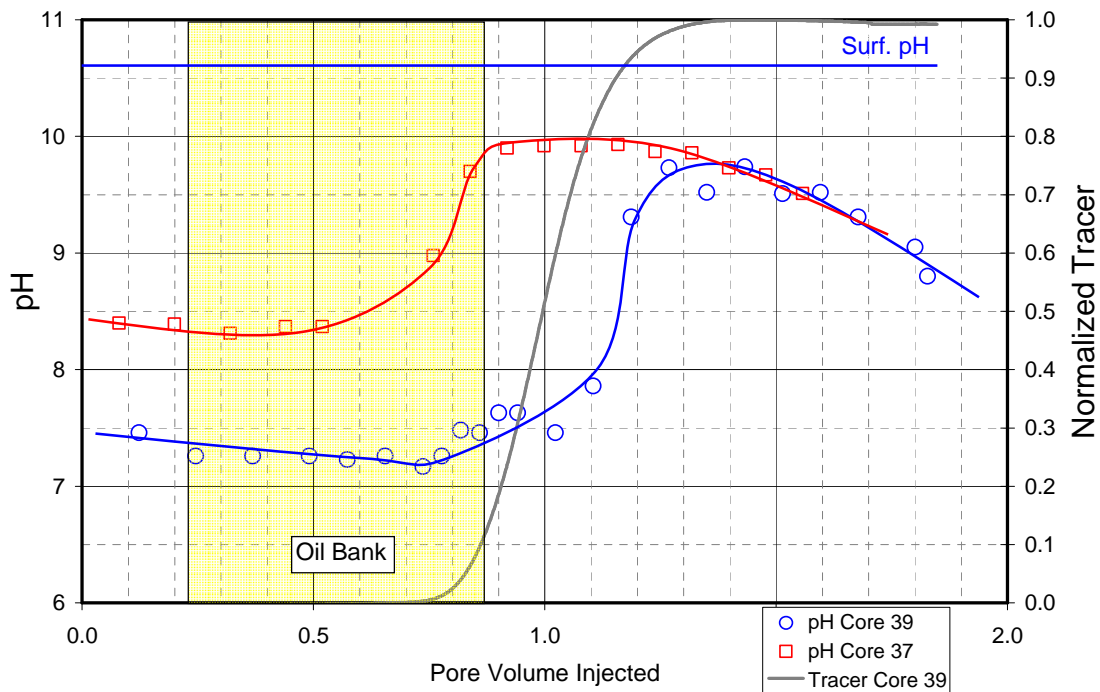


Figure 3.83: Comparison of ASP T-8 (Core 37) and ASP T-9 (Core 39) effluent salinities.



**Figure 3.84:** Comparison of ASP T-8 (Core 37) and ASP T-9 (Core 39) effluent viscosities at  $T_{res}$ . Shear rates ranged between  $37.5 - 75 \text{ s}^{-1}$  on Brookfield rheometer



**Figure 3.85:** Comparison of ASP T-8 (Core 37) and ASP T-9 (Core 39) effluent pH.

### *Pressure Analysis*

Pressure drop measured across the core and each section are plotted in **Figure 3.86**. Sections 2, 3 and 4 experienced capillary pressure effects from 0.15 PV to 0.2 5PV. Section 1 pressure reached a higher plateau compared to other sections. This could have been caused by polymer plugging the pores in the first section. All sections reached a plateau towards the end of flood at 2.0 PV. All sections show pressure spikes which were caused when surfactant slug entered the section. This was thought to be the result of surfactant front mixing with formation brine and producing type II conditions, as well as dilution of surfactant slug. Oil was mobilized slowly and therefore the pressures at first rose on seeing surfactant slug. As Type III conditions followed and oil continued to be mobilized the pressures peaked and decreased. Overall pressure in the core was 9.5 psi/ft at 2 ft/day flow rate, which equated to 4.25 psi/ft at 1 ft/day. This is high in terms of what can be sustained in the field.

Pressures of individual sections (**Figure 3.88** to **Figure 3.93**) were analyzed using **Figure 3.87** to determine mobilities of oil bank and surfactant bank. The estimations are tabulated in **Table 3.18**. For ASP T-9 (core #39), mobility of surfactant slug was lower than the oil bank in the last three sections, which indicated good mobility control. The effluent analysis had shown that there was polymer retention in the core which had delayed the polymer breakthrough. Due to this delay, the mobility behind the oil bank was momentarily lost which caused the oil bank to become extended relative to typical floods. However, once the polymer regained viscosity, it effectively displaced the oil bank ahead as oil bank recovery was still good.

Pressures were a direct reflection of the dynamic changes in viscosity during the core flood. Dimensionless velocities of the phases are estimated based on the breakthrough of the phases at the end of the core and pressure behavior in the last section, section 6. The predicted surfactant phase arrival and exit using dimensionless velocities for earlier sections, Sections 1-4, was later than the actual. This mismatch was caused by the retention of polymer which resulted in loss of viscosity as the SFB got dispersed with the surfactant slug. Earlier sections show quicker arrival of surfactant compared to later sections because the retention and in turn the viscosity loss became progressively worse with pore volume injected.

### **Core Flood T-4 (Core #26) with Formulation X-2**

Surfactant slug designed after formulation X-2 contained 0.31 wt% Petrostep S-1, 0.19 wt% Petrostep S-2, 1.25 wt% SBA, 1 wt% Na<sub>2</sub>CO<sub>3</sub>. NaCl concentrations were chosen at WOR of 1.5. Polymer used was SNF 3330 polymer for both surfactant and polymer slugs. Total surfactant concentration was 0.5 wt%, half of formulation X-1. Only one ASP flood, T-4 (Core #26) was performed with this formulation. The purpose for the flood was to test the efficacy of 0.5wt% surfactant and 0.3 PV surfactant slug size. Chemical flood was performed at reservoir temperature, 46.1 °C but the core was saturated with soft brine (NaCl only) that had similar TDS to surfactant slug. This was done to ensure that the optimum salinity was maintained in slug and it wasn't affected by divalent cations.

### *Core Characterization*

Core #26, sandstone, was set up for flooding in horizontal orientation. First its dispersion was characterized and was found similar to typical sandstone cores (**Figure 3.94**). A pore volume

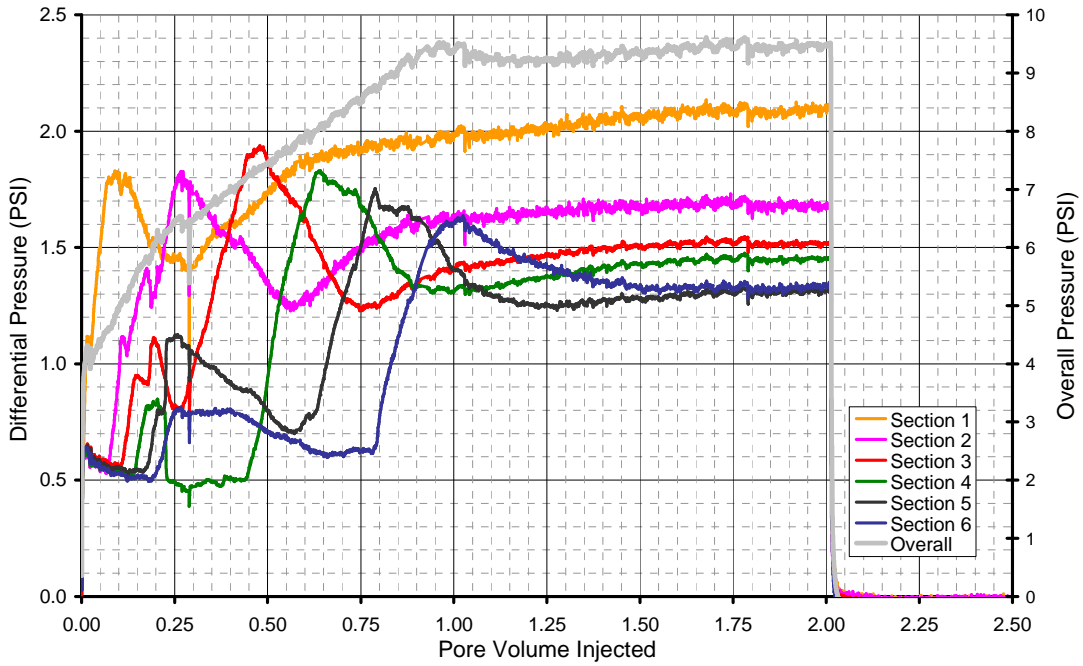


Figure 3.86: Overall core and section pressures during ASP T-9.

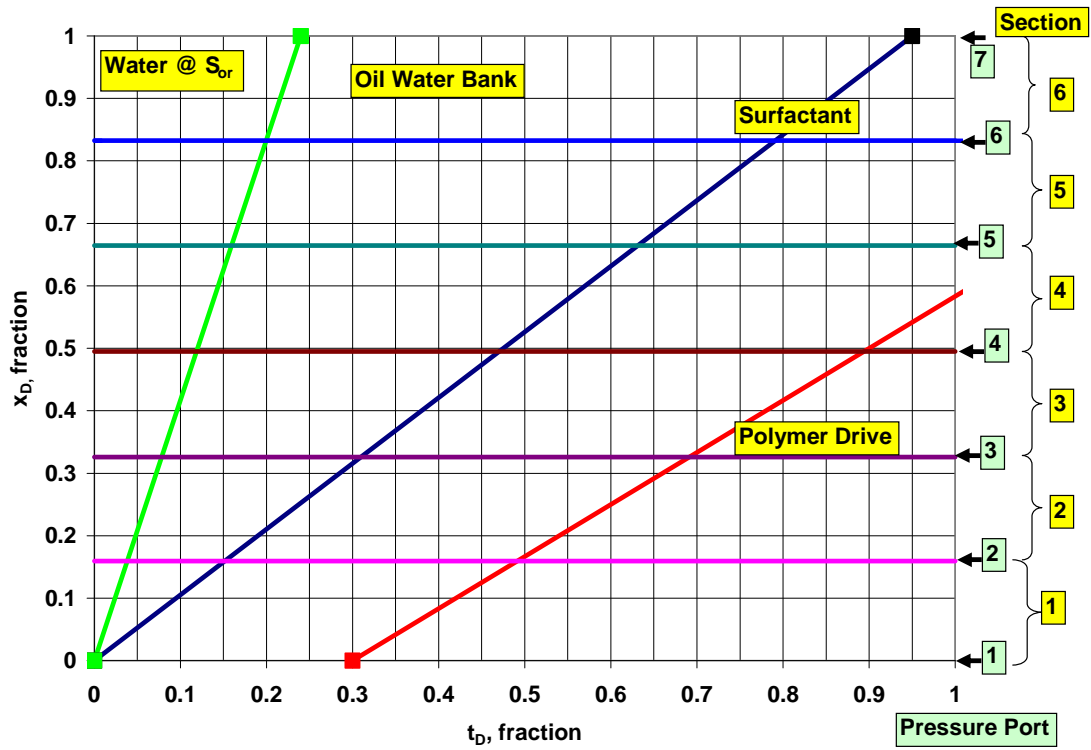
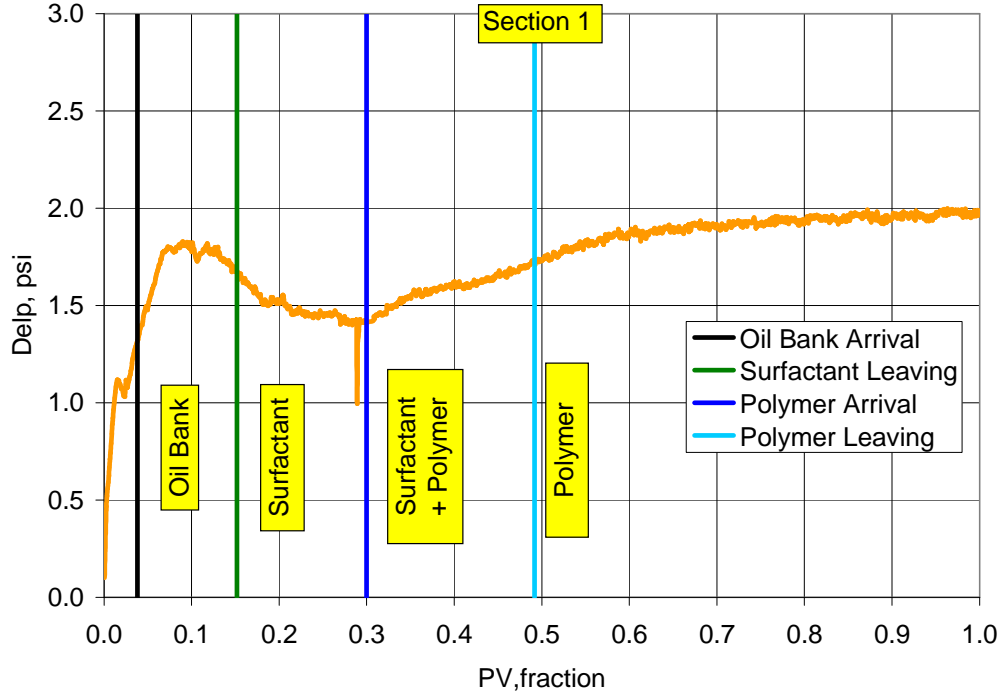
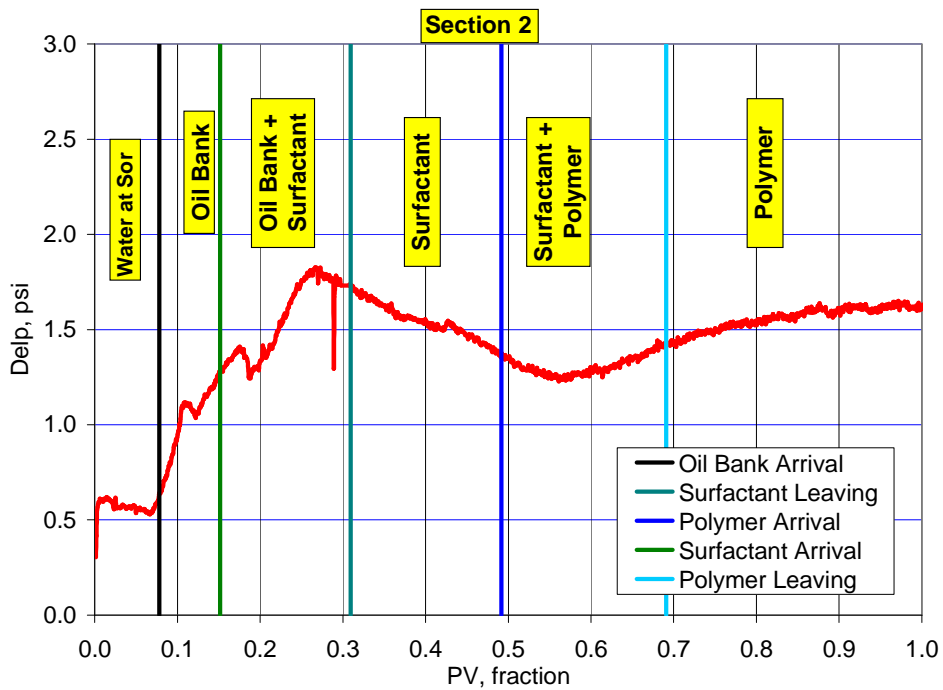


Figure 3.87: Dimensionless distance versus dimensionless time plot for ASP T-9.



**Figure 3.88:** Section 1 pressure during ASP T-9 with identification of fluid regions using dimensionless velocities and pressure analysis.



**Figure 3.89:** Section 2 pressure during ASP T-9 with identification of fluid regions using dimensionless velocities and pressure analysis.

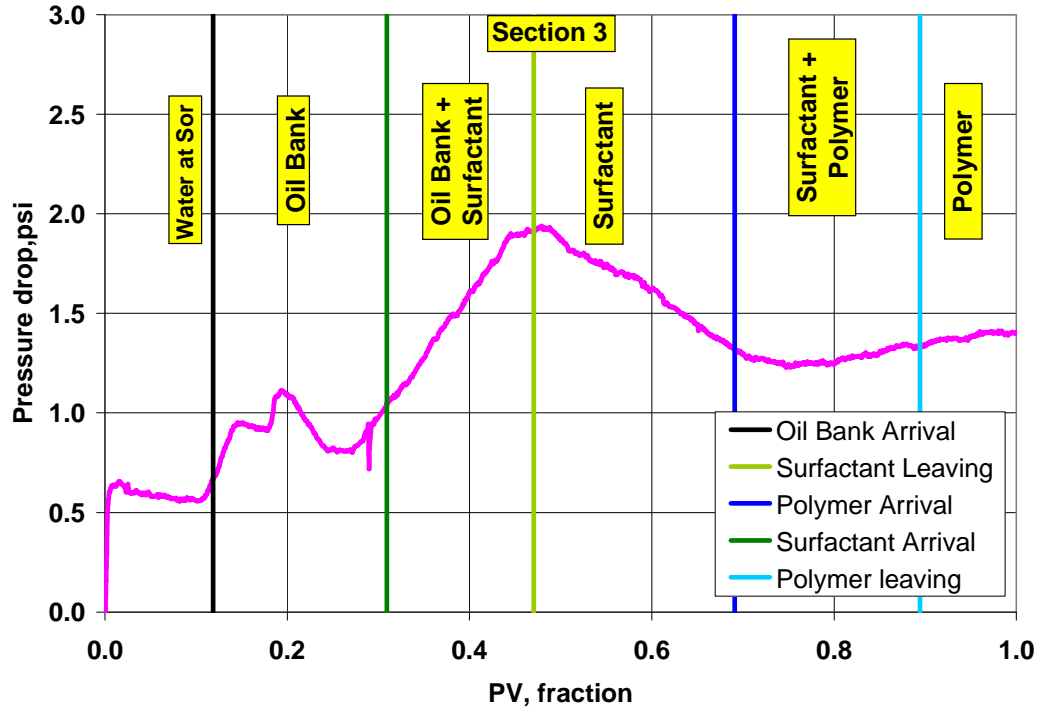


**Figure 3.90:** Section 3 pressure during ASP T-9 with identification of fluid regions using dimensionless velocities and pressure analysis.

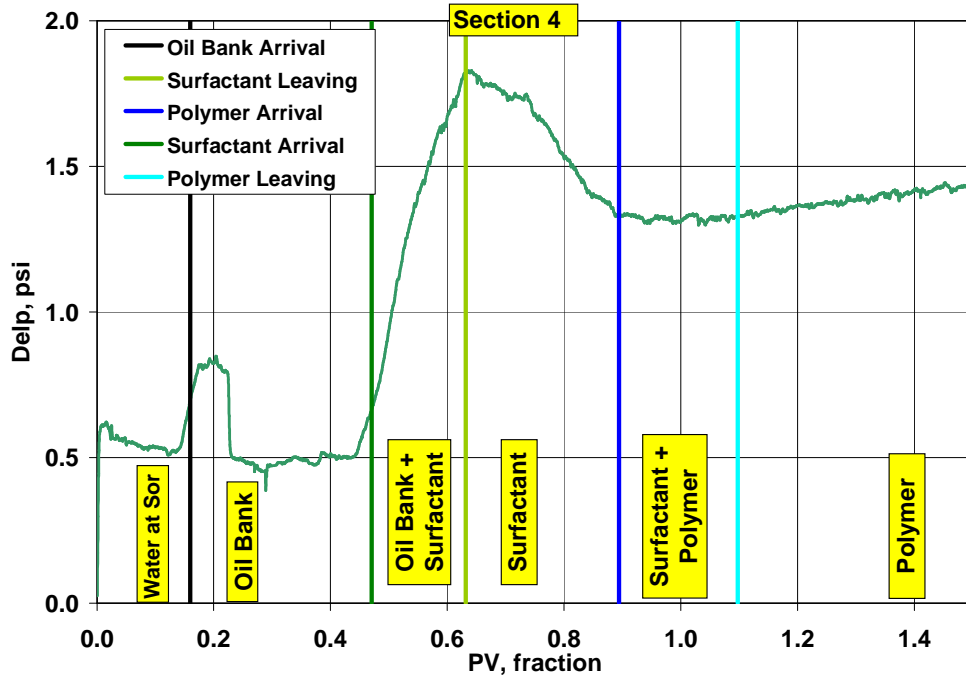


**Figure 3.91:** Section 4 pressure during ASP T-9 with identification of fluid regions using dimensionless velocities and pressure analysis.

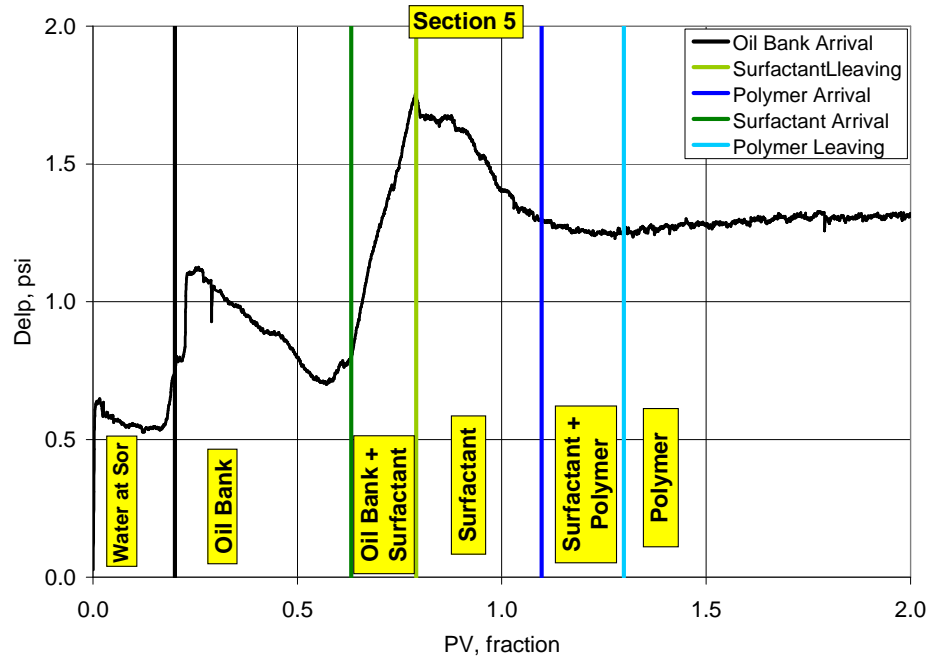


**Figure 3.92:** Section 5 pressure during ASP T-9 with identification of fluid regions using dimensionless velocities and pressure analysis.

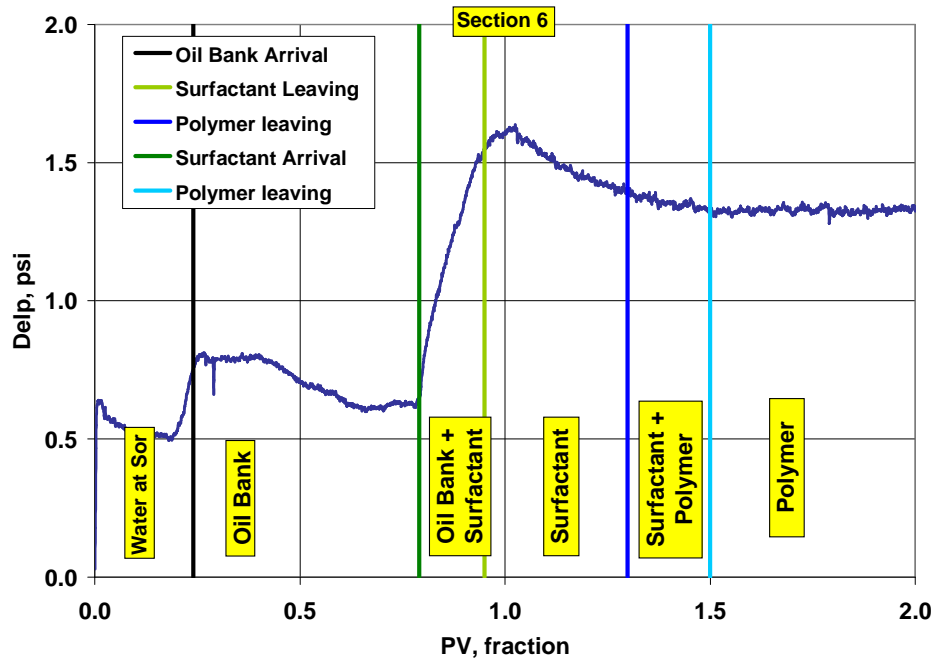


**Figure 3.93:** Section 6 pressure during ASP T-9 with identification of fluid regions using dimensionless velocities and pressure analysis.



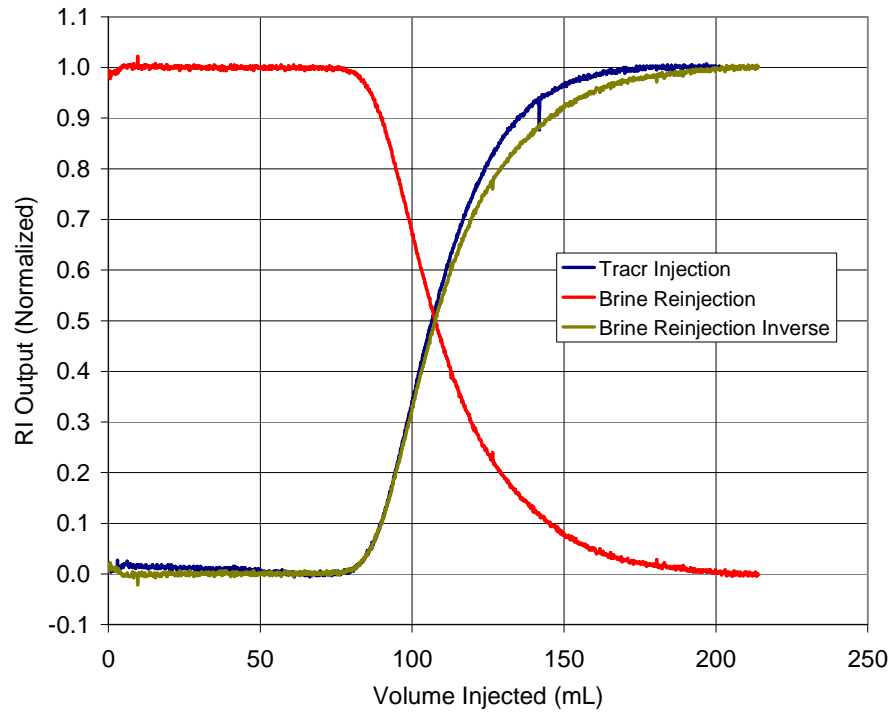


**Figure 3.94:** Dispersion characterization of Core #26 for core flood T-4.

of 109 mL was determined from tracer curve integration and gravimetric method. Permeabilities of the core and sections were determined next and are tabulated in **Table 3.16**. Overall permeability of the core was 150 md, which is low.

#### *Brine Flood/Oil Flood/Waterflood*

Brine flood was carried out with 5 wt% NaCl, soft brine. The salinity matched the surfactant slug optimal salinity at WOR of 1.5.

Oil flood for core #26 was run at 35 ft/day (2.5 mL/min) and at 46.1 °C. Approximately 5 pore volumes of oil were injected.  $S_{oi}$  at the end of oil flood was 0.64 and  $k_{ro}^o$  was measured to be 0.82. Pressures during the oil flood are plotted in **Figure 3.95**.

Waterflood was performed at 46.1 C at a flow rate of 0.3mL/min. Pressures were measured during the flood (**Figure 3.96**). Waterflood was conducted until the oil saturation in the core became stable.  $k_{rw}^o$  was determined to be 0.044 from overall pressure at end of waterflood. Final oil saturation left in the core was 38.9 %.

#### *Surfactant and Polymer Slug*

Surfactant slug contained 0.31 wt% Petrostep S-1, 0.19 wt% Petrostep S-2, 1.25 wt% SBA, 1 wt% Na<sub>2</sub>CO<sub>3</sub>, 4.25 wt% NaCl and 2250 ppm Flopaam SNF 3330S. The viscosity of the surfactant slug was 19 cp measured at 1 s<sup>-1</sup> with Bohlin rheometer (**Figure 3.97**). The optimum salinity of surfactant slug was determined at WOR =1.5.

Polymer slug salinity was 3.33% NaCl, 63% of surfactant slug. This salinity gradient was selected from previous experience of ASP floods T-2 and T-3, in which 60% step down in salinity had given good recovery but slightly smaller type III region. The salinity drop in polymer drive was sufficiently low to give type I microemulsion at the end of the ASP flood. Polymer concentration was 2250 ppm that gave the slug similar viscosity as the surfactant slug, 21cp @ 1 s<sup>-1</sup>(**Figure 3.97**).

#### *Chemical Flood & Oil Recovery*

Core #26 was flooded at 0.15mL/min (2.1 ft/day) with 0.3 pore volume (PV) of surfactant slug and followed by 1.5 PV polymer drive. Oil bank arrived at 0.21 PV and surfactant breakthrough occurred at 0.74 PV. Oil cut dropped below 1% after 60% residual oil recovery. **Figure 3.98** shows the oil cut and residual oil recovery from the ASP flood. Recovery was poor and majority of the oil was recovered in oil bank. Maximum oil cut in the oil bank was 40% only. After, surfactant breakthrough, the oil cut dropped sharply.

#### *Effluent Analysis*

Effluent samples from the coreflood are shown in **Figure 3.99** at room temperature. Vials 5-17 (0.21PV-0.70PV) contained oil bank. Type I microemulsion is observed in vials 18 (0.74 PV) onwards. Since the photo was taken at room temperature, the microemulsion phases are not representative of the conditions in the core.

Salinity, viscosity and pH of aqueous phase of the effluent samples were measured and are presented in **Figure 3.100**. Salinity in the oil bank remained at 5 wt% NaCl, which was equal

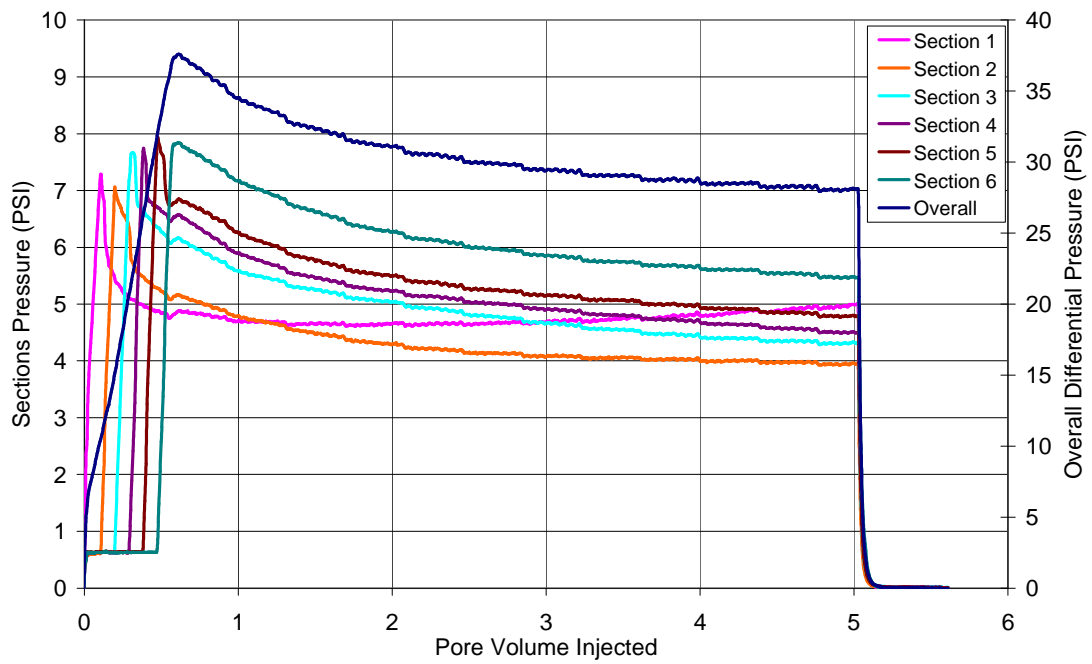


**Figure 3.95:** Oil flood differential pressures for Core #26 for core flood T-4.

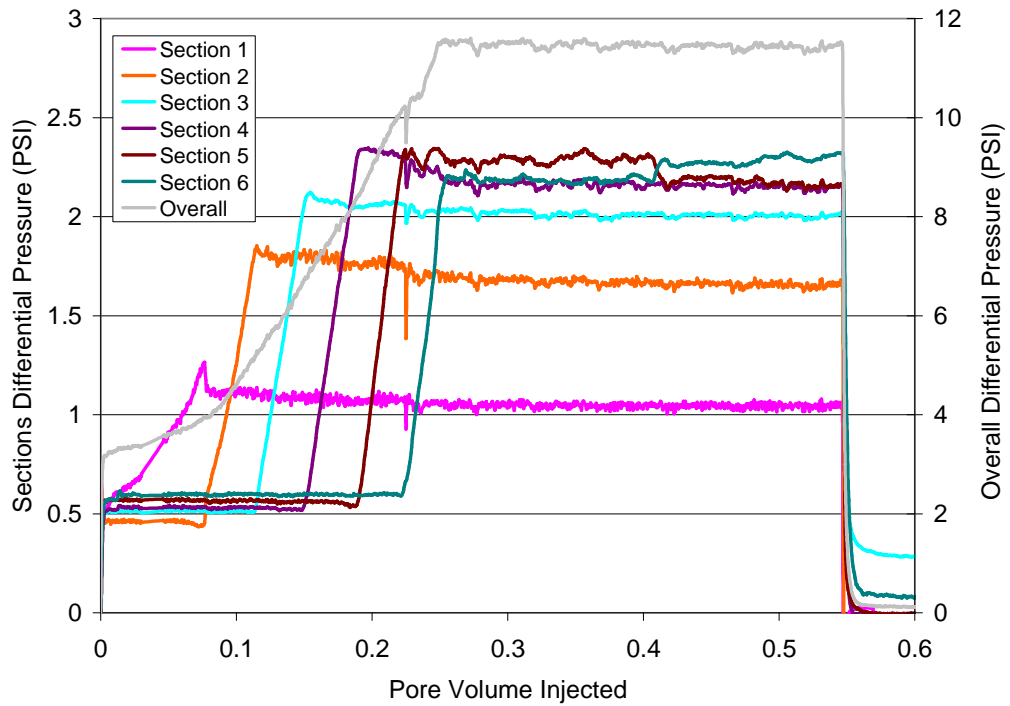


**Figure 3.96:** Waterflood differential pressures for Core #26 for core flood T-4.

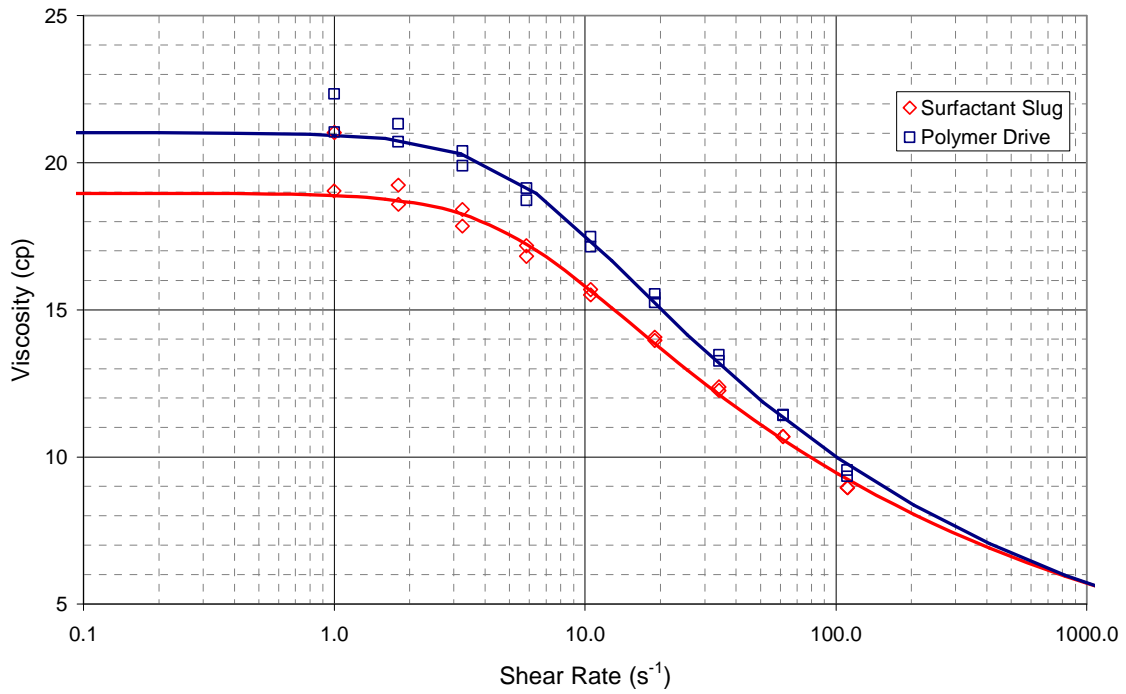


**Figure 3.97:** Viscosities of surfactant and polymer slug for core #26 (T-4) at 46.1°C.

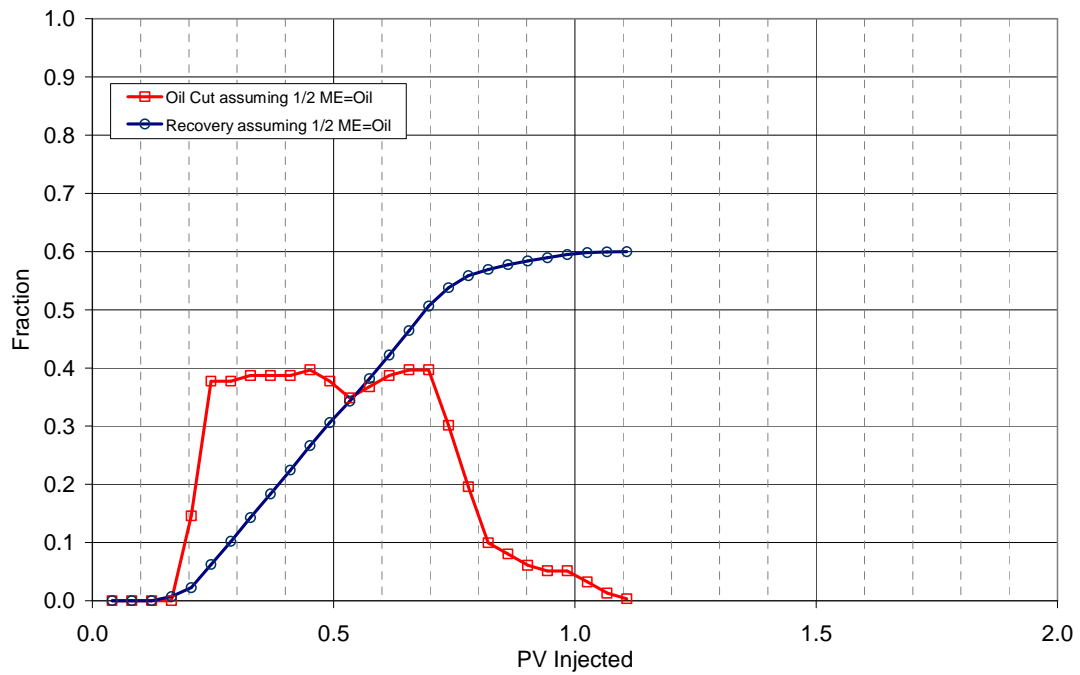


**Figure 3.98:** Oil cut and oil recovery for ASP flood T-4 (Core #26).

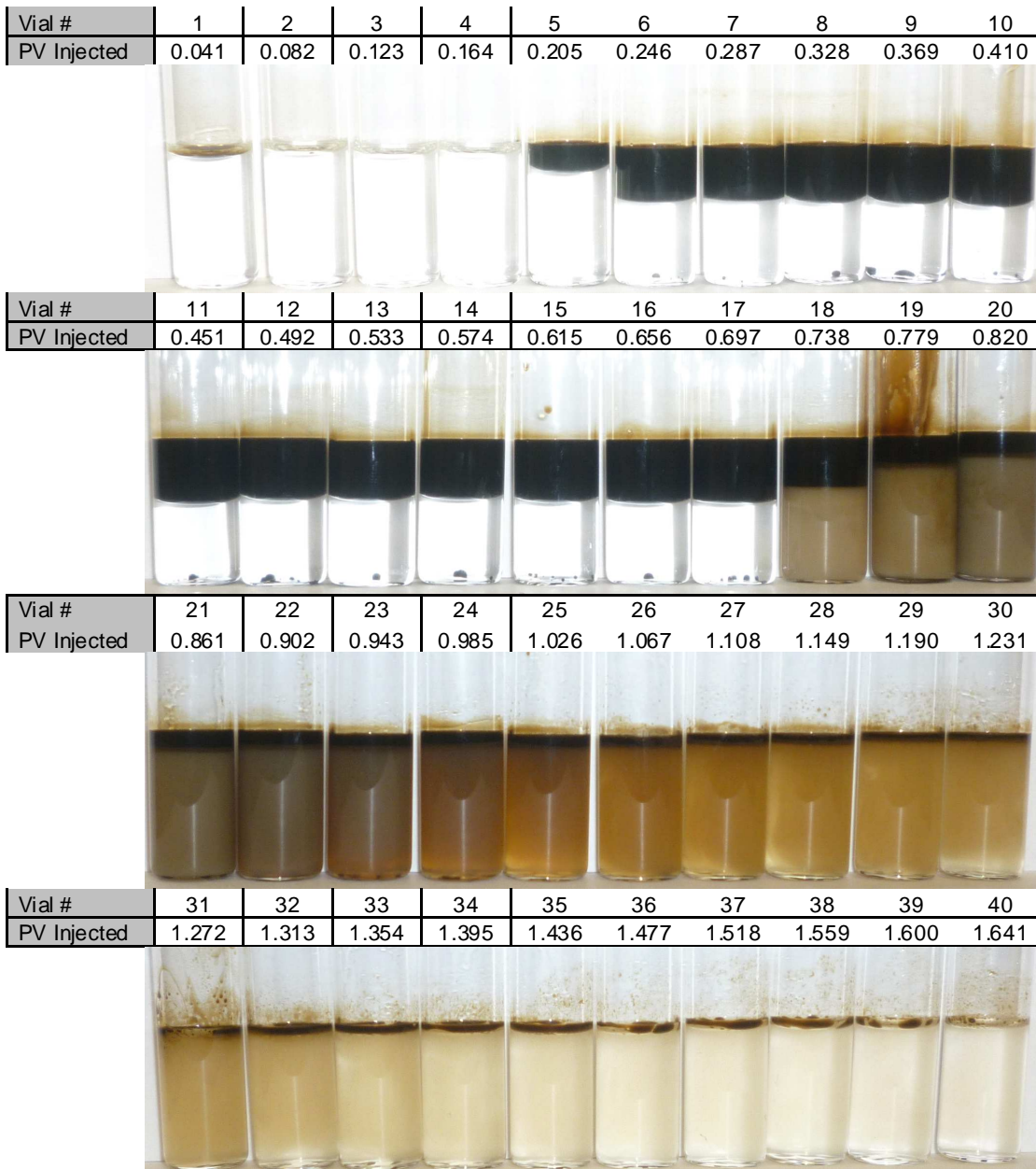


**Figure 3.99:** Photo of effluent vials from ASP T-4 (core #26) with formulation X-2 @ 46.1 °C after equilibrating for 3 days.

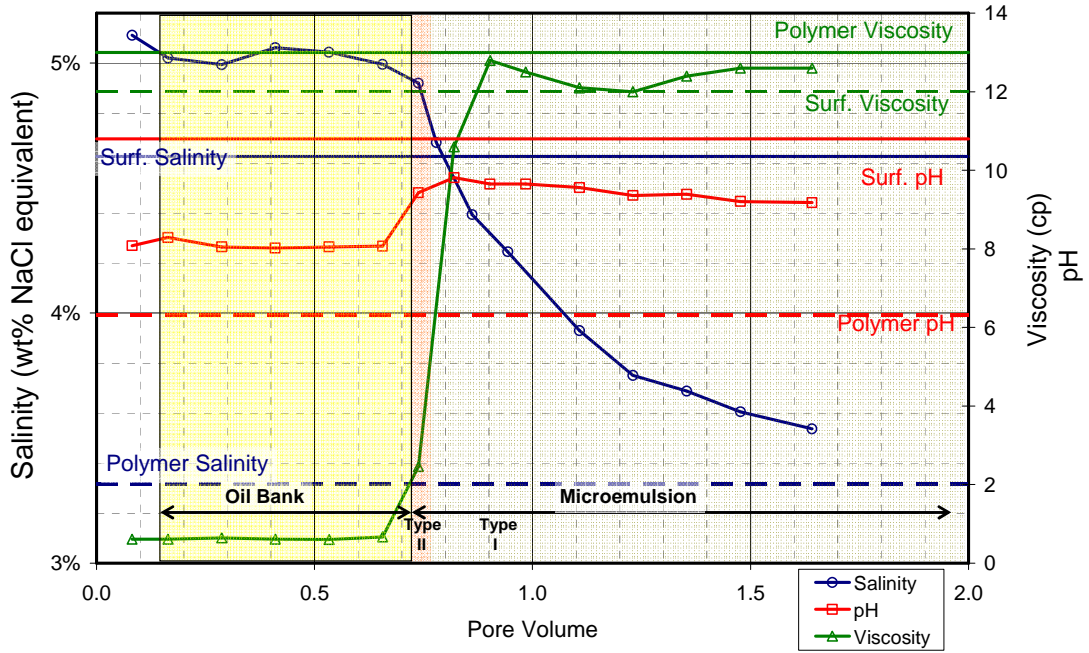


**Figure 3.100:** Viscosity, salinity and pH of aqueous phase in effluent vials from ASP T-4 (Core #26). Viscosity was measured at  $37.5 \text{ s}^{-1}$  and  $46.1 \text{ }^\circ\text{C}$ .

to the formation brine salinity. After surfactant breakthrough, salinity declined sharply. The salinity gradient proved drastic and did not maintain Type III microemulsion for an extended time period in the core.

Viscosity rose sharply at surfactant breakthrough at 0.72 PV, which suggests that a sharp interface existed between oil bank and surfactant bank, and polymer was not retained. pH rose sharply at around surfactant breakthrough and after peaking declined gradually. pH value crossed 9 at surfactant breakthrough which meant that alkali was sufficient.

#### *Pressure Analysis*

Pressure drops measured across the core and each section are plotted in **Figure 3.101**. During the ASP flood, all sections saw dominating pressure spike that started at surfactant entrance into the section. In addition, the final sections pressure drops range between 2.7-4.0 psi, which were substantially higher than seen in other core floods. The later sections showed higher final pressure drops. The spikes suggest that the formulation was inefficient in mobilizing the oil and therefore the pressure rose when higher viscosity surfactant and polymer slugs entered the sections. The subsequent decline in pressures suggests that the oil continued to be mobilized, albeit slowly, and resulted in higher relative permeability to aqueous phase. Three reasons were associated for the inefficiency of the formulation. First, relatively high viscosity of the microemulsion formed by the formulation X-2 as observed in the phase behavior studies. Second, small slug size (0.3 PV); total surfactant was not enough to form enough microemulsion phases to mobilize all the oil. Thirdly, the salinity gradient used behind the surfactant slug was too steep, and resulted in a small type III region passing through to the end of the core.

Pressures of individual sections were analyzed to determine mobilities of oil bank and surfactant bank. The estimations are tabulated in **Table 3.18**. Mobility of surfactant slug was lower than the oil bank in the last three sections, indicating good mobility control. Therefore polymer in surfactant slug proved sufficient.

#### **Core Floods with Formulation X-3**

Surfactant slug designed after formulation X-3 contained 0.31 wt% Petrostep S-1, 0.19 wt% Petrostep S-2, 1.375 wt% DGBE, 1 wt% Na<sub>2</sub>CO<sub>3</sub>. NaCl concentrations were 5.00 wt% – 5.05 wt% NaCl determined from the activity diagram. Polymer used was SNF 3330 polymer for both surfactant and polymer slugs. Total surfactant concentration was 0.5 wt%, same as X-2 but half of formulation X-1. Only difference between formulation X-2 and X-3 was the cosolvent type and concentration. SBA was replaced with DGBE to give more fluidity to the Type III microemulsion phase and also slightly higher optimum solubilization ratios.

A total of 3 ASP floods, T-5(core #27), T-6(core #31) and T-7(core #32) were performed with formulation X-3. T-5 used a 0.3 PV surfactant slug size while T-6 and T-7 used 0.6 PV surfactant slug size. The purpose for the flood was to test the efficacy of 0.5 wt% surfactant with 0.3 PV and 0.6 PV surfactant slug sizes.

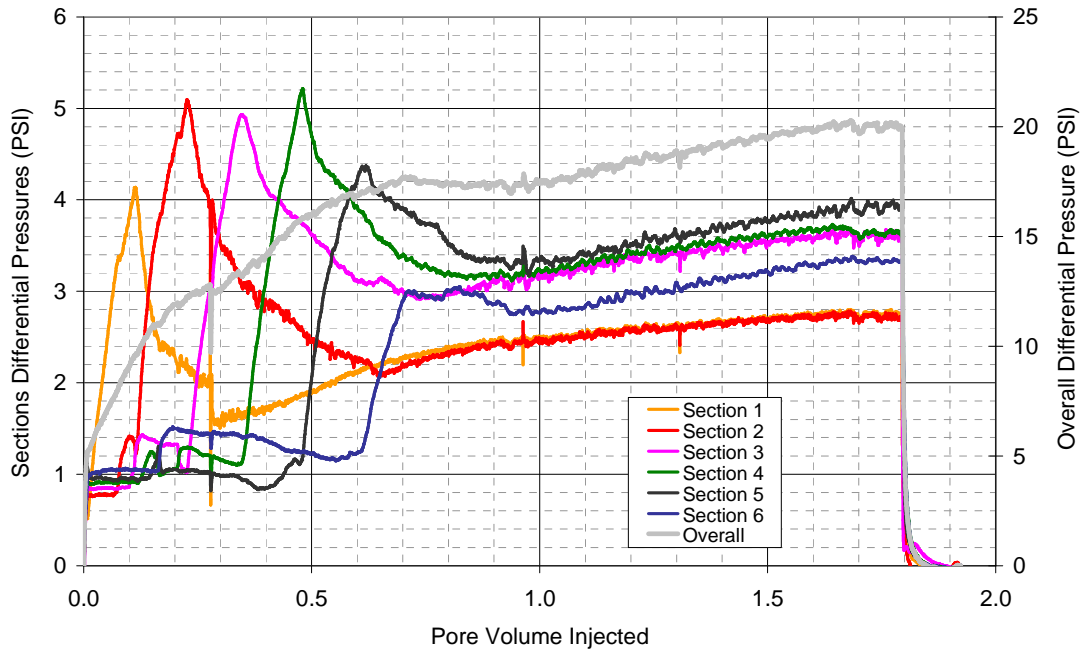


**Figure 3.101 - Overall core and section pressures during ASP T-4 (Core #26).**



### ***Core Flood T-5 (Core #27)***

T-5 was performed to test formulation X-3 with a 0.3 PV surfactant slug size. It was hoped that changing the co-solvent to DGBE and increasing the concentration slightly would work more efficiently. The formulation X-3 gave good phase behavior results, satisfying all the criteria for successful screening results. Chemical flood was performed at reservoir temperature, 46.1 °C, but the core was saturated with soft brine (NaCl only) that had slightly higher TDS than the surfactant slug.

### ***Core Characterization***

Core #27, sandstone, was set up for flooding in horizontal orientation. First its dispersion was characterized (**Figure 3.102**) and was found to be that of typical sandstone cores. A pore volume of 107 mL was determined from tracer curve integration and gravimetric method. Permeabilities of the core and sections were determined next and are tabulated in **Table 3.16**. Overall permeability of the core was 141 md, which is low.

### ***Brine Flood/Oil Flood/Waterflood***

Brine flood was carried out with 6.5 wt% NaCl. The salinity was kept slightly higher than the surfactant slug optimal salinity in order to give a suitable negative salinity gradient for Type II→Type III→Type I microemulsion transition.

Oil flood for core #27 was run at 35 ft/day (2.5 mL/min) and at 46.1 C. 4 pore volumes of oil were injected.  $S_{oi}$  at the end of oil flood was 0.63 and  $k_{ro}^o$  was measured to be 0.85. These values were very similar to core #26. Pressures during the oil flood and average oil saturation in the core versus the pore volumes of oil injected are plotted in **Figure 3.103** and **Figure 3.104**, respectively.

Waterflood was performed at 46.1 C at a flow rate of 0.3 mL/min. pressures were measured during the flood (**Figure 3.105**). Waterflood was conducted until the oil saturation in the core became stable (**Figure 3.106**).  $k_{rw}^o$  was determined to be 0.047 from overall pressure at end of waterflood. Final oil saturation remaining in the core was 38.4 %.

### ***Surfactant and Polymer Slug***

Surfactant slug contained 0.31 wt% Petrostep S-1, 0.19 wt% Petrostep S-2, 1.375 wt% SBA, 1 wt% Na<sub>2</sub>CO<sub>3</sub>, 5.0 wt% NaCl and 2250 ppm Flopaam SNF 3330S. Salinity of surfactant slug was selected from salinity scans of formulation X-3 (0.5 wt% total surfactant) at oil concentrations ranging between 50% and 10% (**Figure 3.107**). The curves for optimum salinity and microemulsion phase transition boundaries were extrapolated from two to three data points. An optimum salinity of 6 wt% TDS (5 wt% NaCl + 1 wt% Na<sub>2</sub>CO<sub>3</sub>) in surfactant slug would give Type III microemulsion for the entire range of oil concentrations. This salinity was well under the APSL for Formulation X-3, which was 7.4 wt% TDS (6.4 wt% NaCl + 1.0 wt% Na<sub>2</sub>CO<sub>3</sub>). Viscosity of the surfactant slug was 18 cp measured at 1 s<sup>-1</sup> with Bohlin rheometer (**Figure 3.109**).

Polymer slug salinity was 4.9 wt% NaCl, 82% of surfactant slug. This salinity gradient was selected from dilution studies of surfactant with polymer drive (**Figure 3.108**). 4.9 wt% NaCl

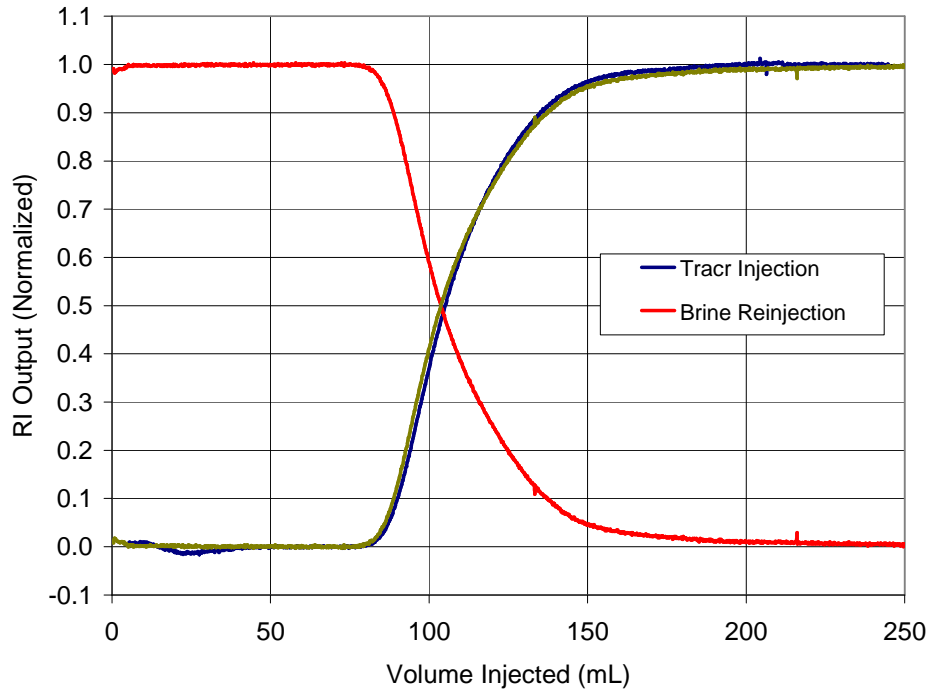


**Figure 3.102:** Dispersion characterization of Core #27 for core flood T-5.

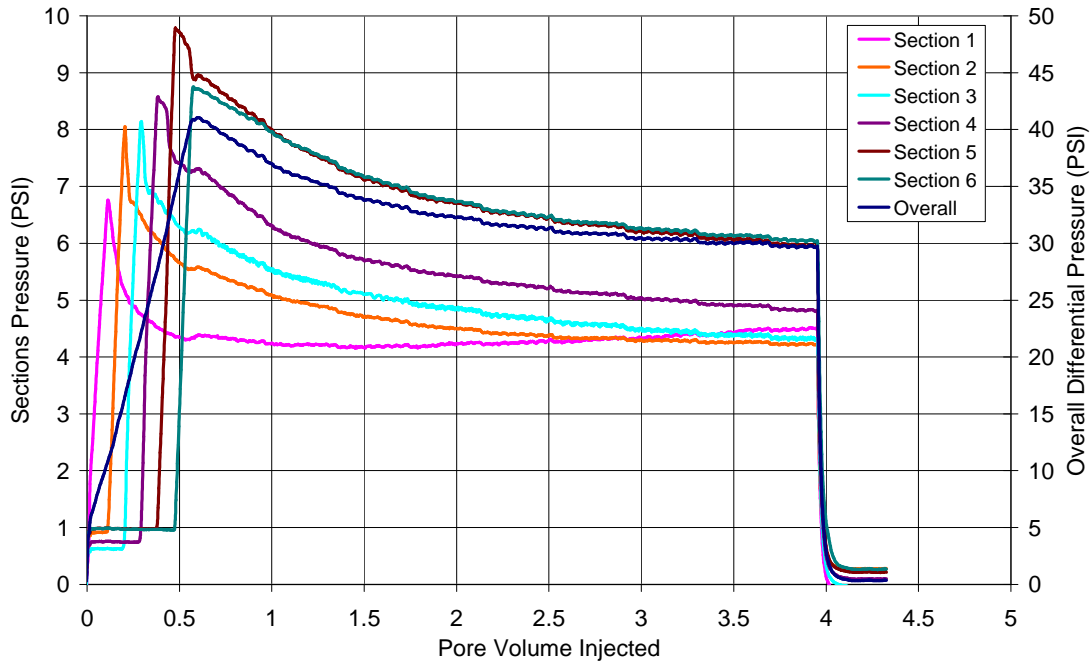


**Figure 3.103:** Oil flood differential pressures for Core #27 for core flood T-5.

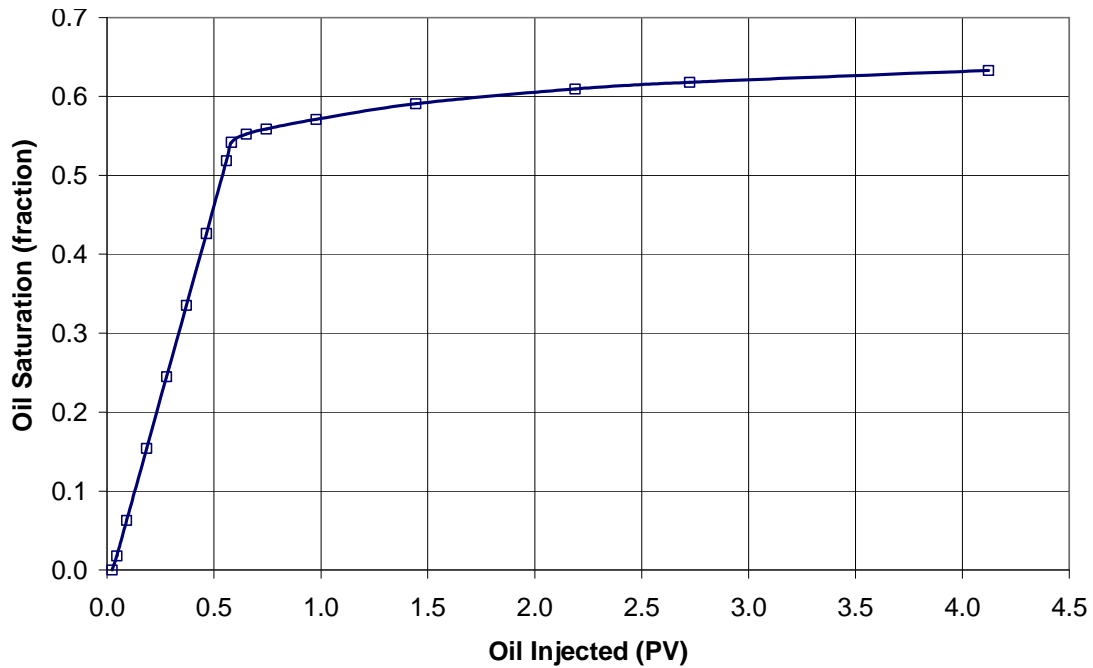


**Figure 3.104:** Oil saturation change in the core during oil flood on core #27.

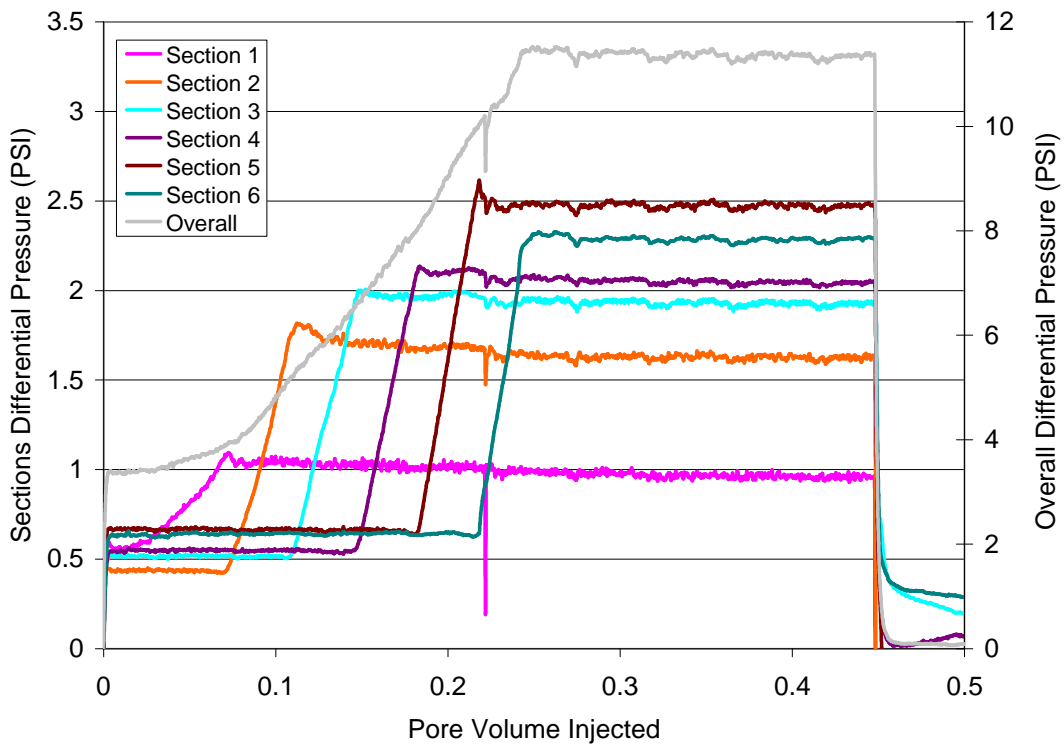


**Figure 3.105:** Waterflood differential pressures for Core #27 for core flood T-5.

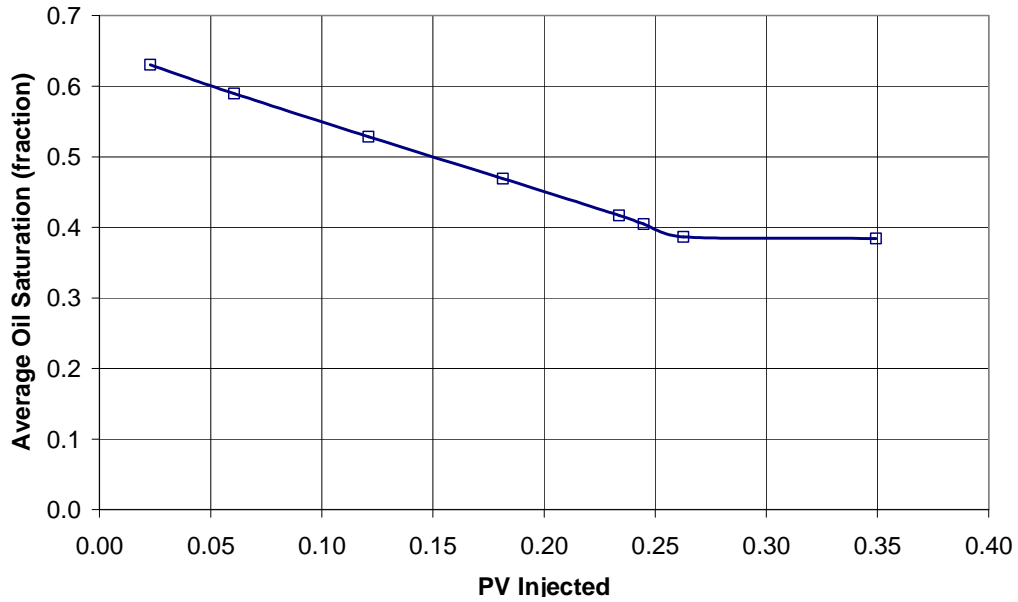


**Figure 3.106:** Oil saturation change in the core during waterflood on core #27.

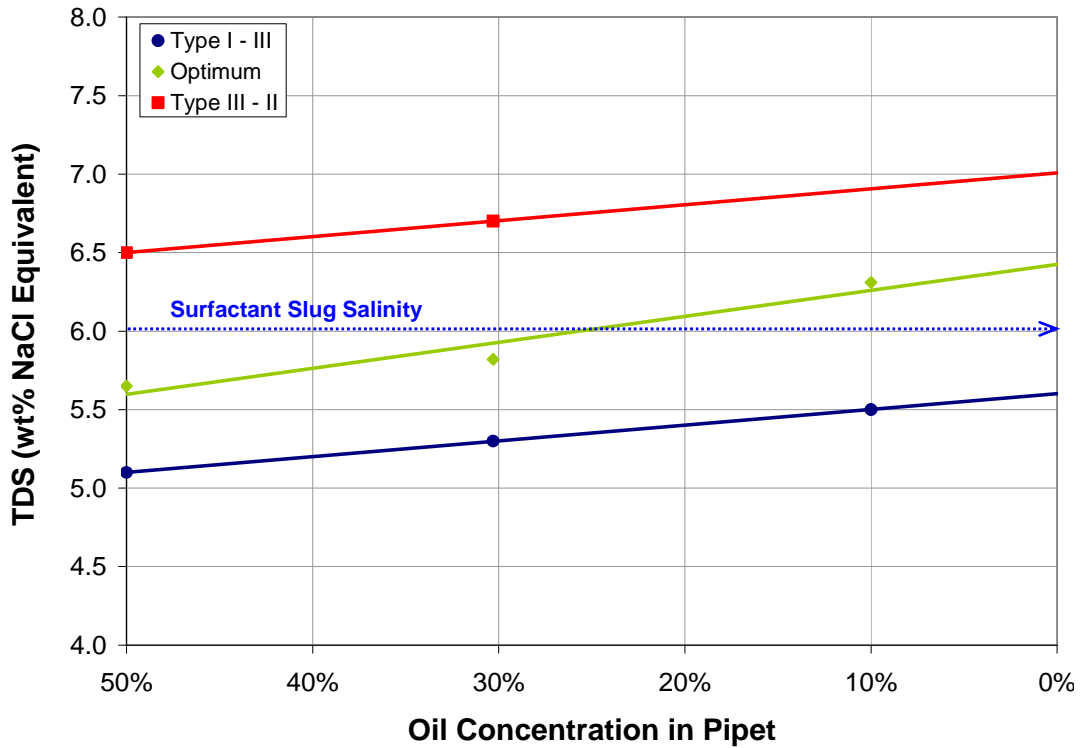


**Figure 3.107:** Optimum salinity and Type III microemulsion phase boundaries for Formulation X-3 (0.5 wt% total surfactant concentration) at oil concentration range of 50% to 10%. A salinity of 6 wt% TDS was selected because it gave Type III microemulsion at all oil concentrations. APSL for this system was 7.4 wt% TDS (6.4 wt% NaCl + 1.0 wt% Na<sub>2</sub>CO<sub>3</sub>)

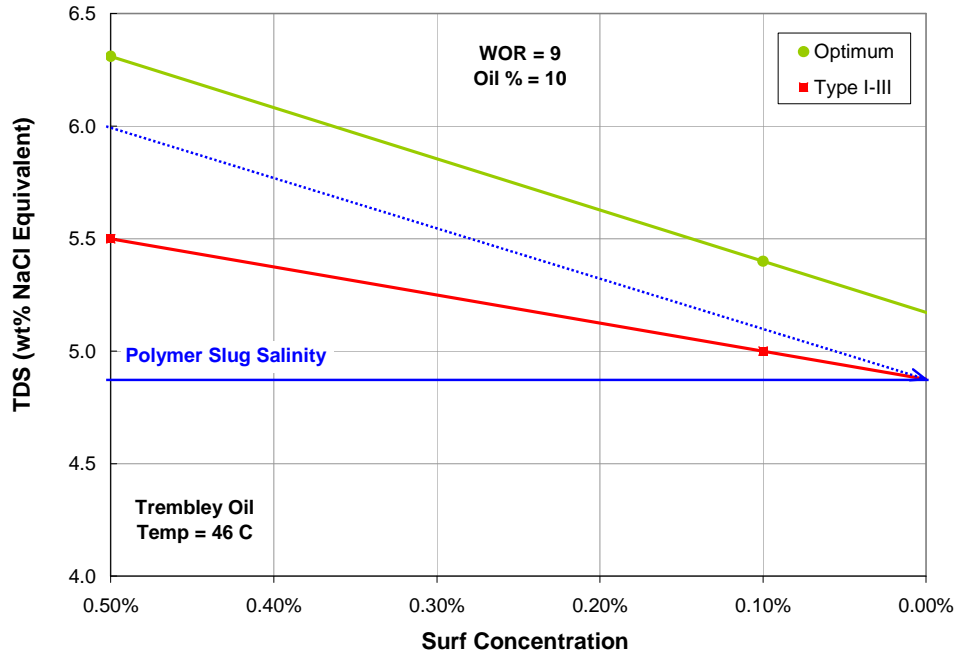


**Figure 3.108:** Optimum equivalent salinity and phase transition boundaries for surfactant concentration range 0 wt% to 0.5 wt% for Formulation X-3 are plotted. The curves were interpolated and extrapolated to cover the entire range. A minimum polymer salinity of 4.9 wt% would be necessary to cause a transition to Type I microemulsion phase. The dilution of surfactant at the back of surfactant bank and corresponding equivalent salinity (NaCl + Na<sub>2</sub>CO<sub>3</sub>) change is shown by the dotted blue arrow.

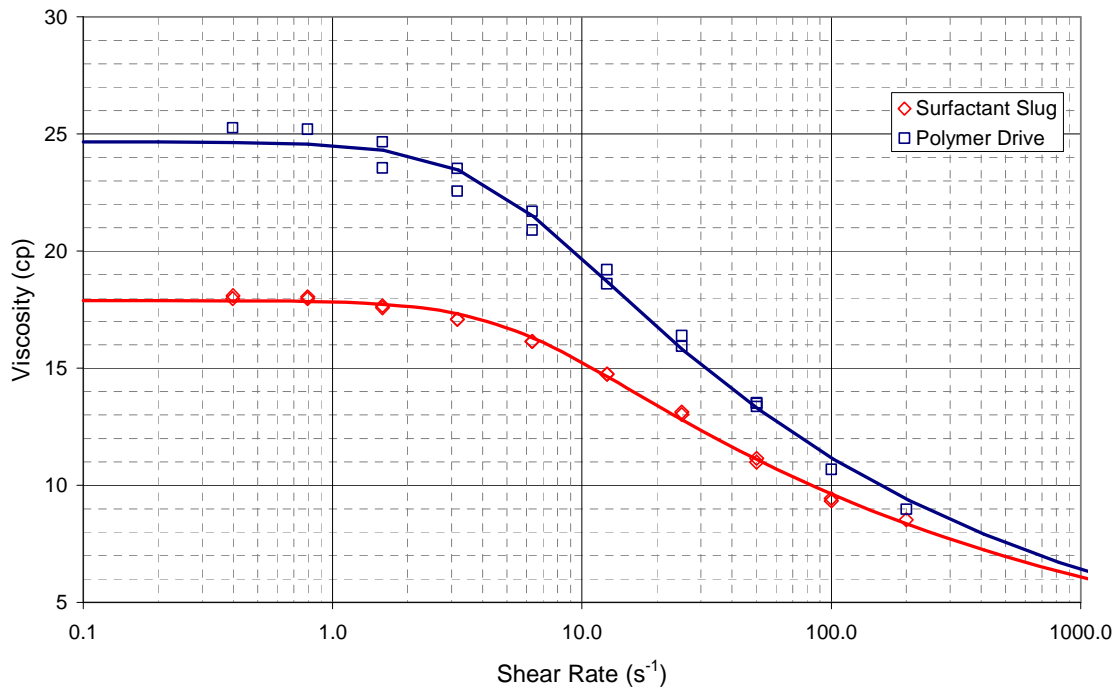


**Figure 3.109:** Viscosities of surfactant and polymer slug for core #27 (T-5) at 46.1°C.

was low enough to give Type I microemulsion at the back end of surfactant slug. Polymer concentration was 2250 ppm that gave the polymer drive higher viscosity than surfactant slug, 25cp @ 1 s<sup>-1</sup>(**Figure 3.109**).

#### *Chemical Flood & Oil Recovery*

Core #27 was flooded at 0.15mL/min (2.1 ft/day) with 0.3 pore volume (PV) of surfactant slug and followed by 1.35 PV polymer drive. Oil bank arrived at 0.18 PV and surfactant breakthrough occurred at 0.71 PV. Oil cut dropped below 1% after 62% residual oil recovery. **Figure 3.** shows the oil cut and residual oil recovery from the ASP flood. Recovery was poor and majority of the oil was recovered in oil bank. Maximum oil cut in the oil bank was 45%. After, surfactant breakthrough, the oil cut dropped sharply. The oil recovery from ASP flood T-5 (core #27) was not much better than T-4 (core #26). However, the oil cut in the beginning of the oil bank was improved from 38% to 45%. The surfactant slug did not prove sufficient.

#### *Effluent Analysis*

Effluent samples from the core flood are shown in **Figure 3.111** at reservoir temperature after 3 days of equilibration. Vials 5-17 (0.18 PV-0.71 PV) contained oil bank. Microemulsion phase of any type could not be detected after the oil bank. This was attributed to the low concentration of surfactant present in those vials as most of the surfactant was consumed in the core or diluted due to dispersion.

Salinity, viscosity and pH of aqueous phase of the effluent samples were measured and are presented in **Figure 3.112**. Salinity in the oil bank remained at 6.4 wt% NaCl, which was equal to the formation brine salinity (slight difference than the actual (6.5 wt% NaCl) is due to measurement inaccuracy). After surfactant breakthrough, salinity declined gradually to reach the polymer salinity.

Viscosity rose sharply at surfactant breakthrough and reached the full value of surfactant slug. This suggests that a sharp interface existed between oil bank and surfactant bank, and polymer retention did not affect mobility control in the surfactant slug. pH rose at around surfactant breakthrough and after peaking declined gradually. pH value remained above 9 after surfactant breakthrough which meant that alkali was sufficient.

#### *Pressure Analysis*

Pressure drops measured across the core and each section are plotted in **Figure 3.113** and give us further insight into the ASP flood performance. Similar to T-4 (core #26), pressure spikes were observed when surfactant reached each section. Section 4, 5 and 6 had noticeably high peaks, in fact, the peak grew progressively from sections 4 to 6. The peaks were caused by the high viscosity of surfactant slug entering the sections. The high peaks in section 4, 5 and 6 relative to the earlier sections suggest that the surfactant slug became less effective with injected volume due to dispersion and adsorption of surfactant in the core. Eventually, sections 5 and 6 pressure leveled out at much higher value compared to other sections suggesting that the oil was trapped in these sections. A bigger slug would be needed to mobilize the oil in all sections.

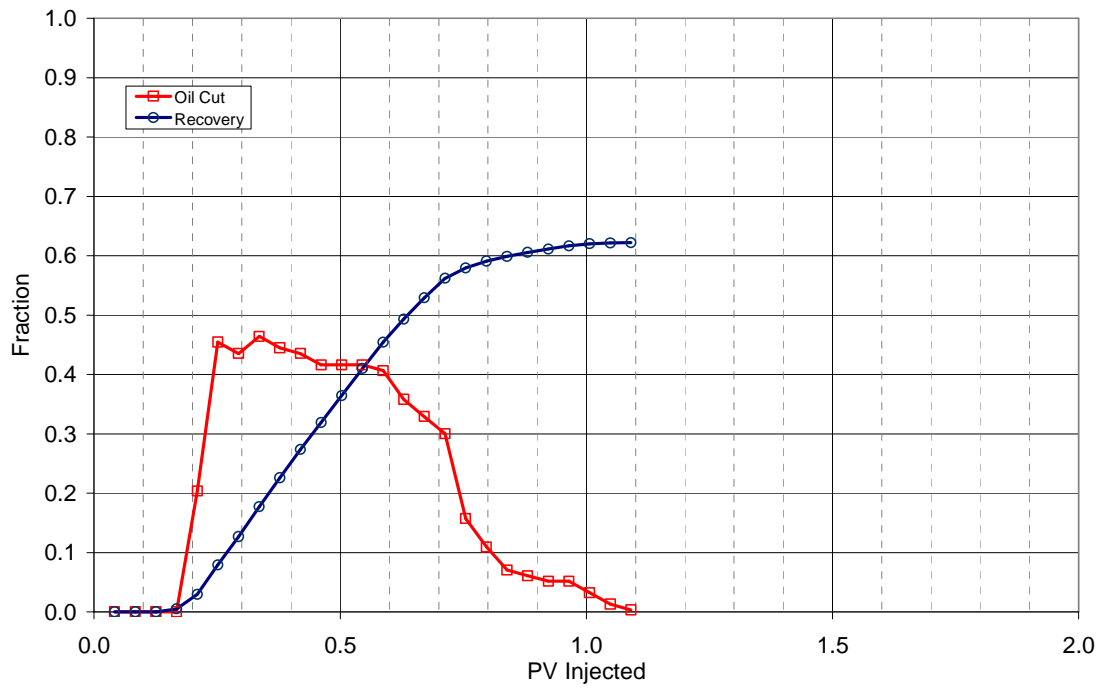


**Figure 3.110** Oil cut and oil recovery for ASP flood T-5 (Core #27).

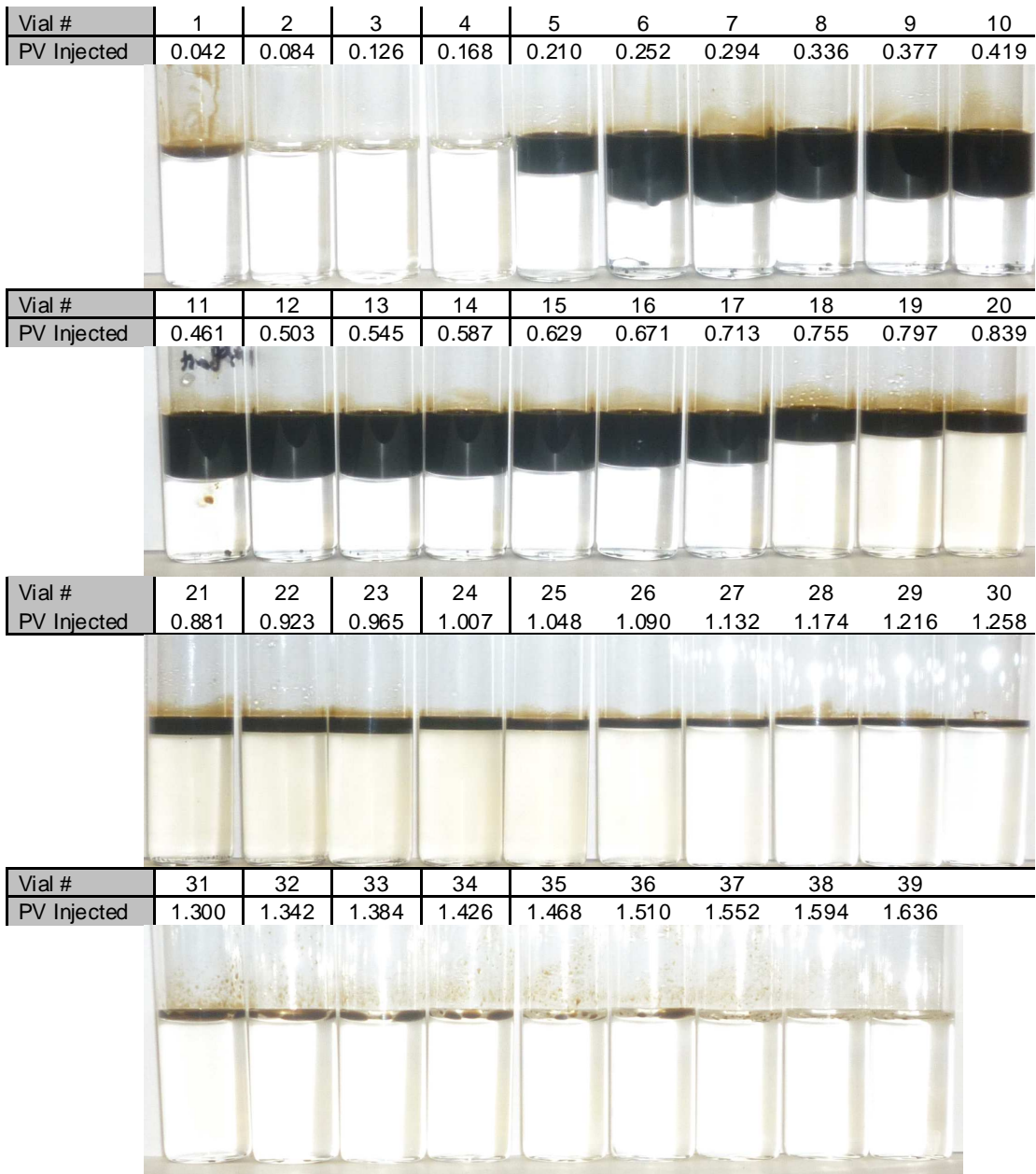


**Figure 3.111:** Photo of effluent vials from ASP T-5 (core #27) with formulation X-3 @ 46.1 °C after equilibrating for 3 days.



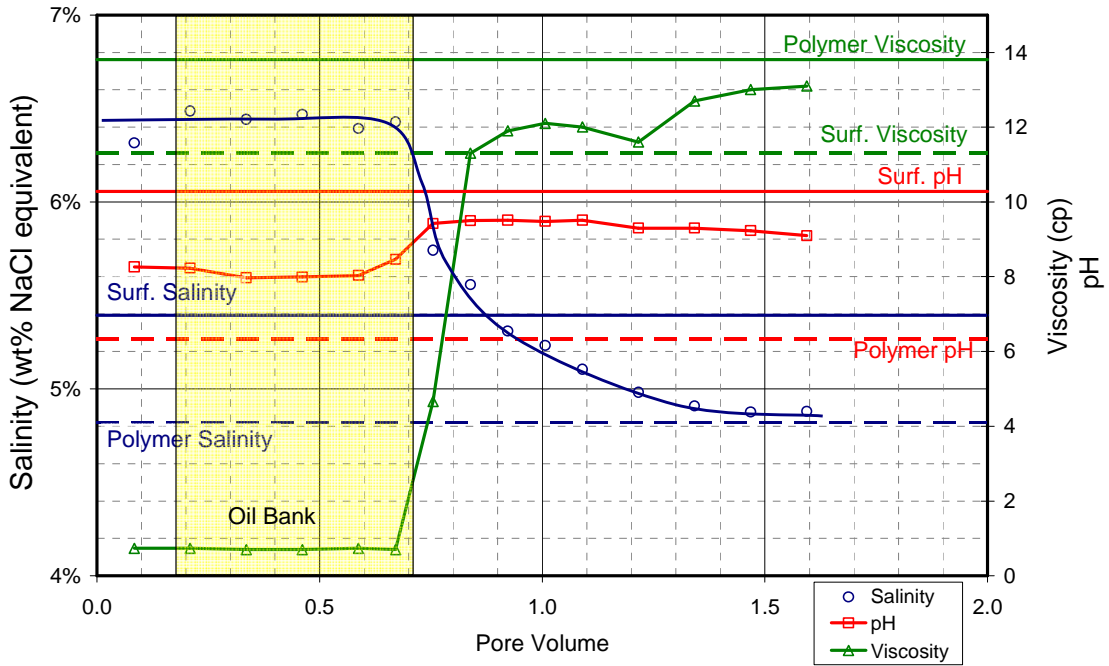


**Figure 3.112:** Viscosity, salinity and pH of aqueous phase in effluent vials from ASP T-5 (Core #27). Viscosity was measured at  $37.5 \text{ s}^{-1}$  and  $46.1 \text{ }^\circ\text{C}$ .

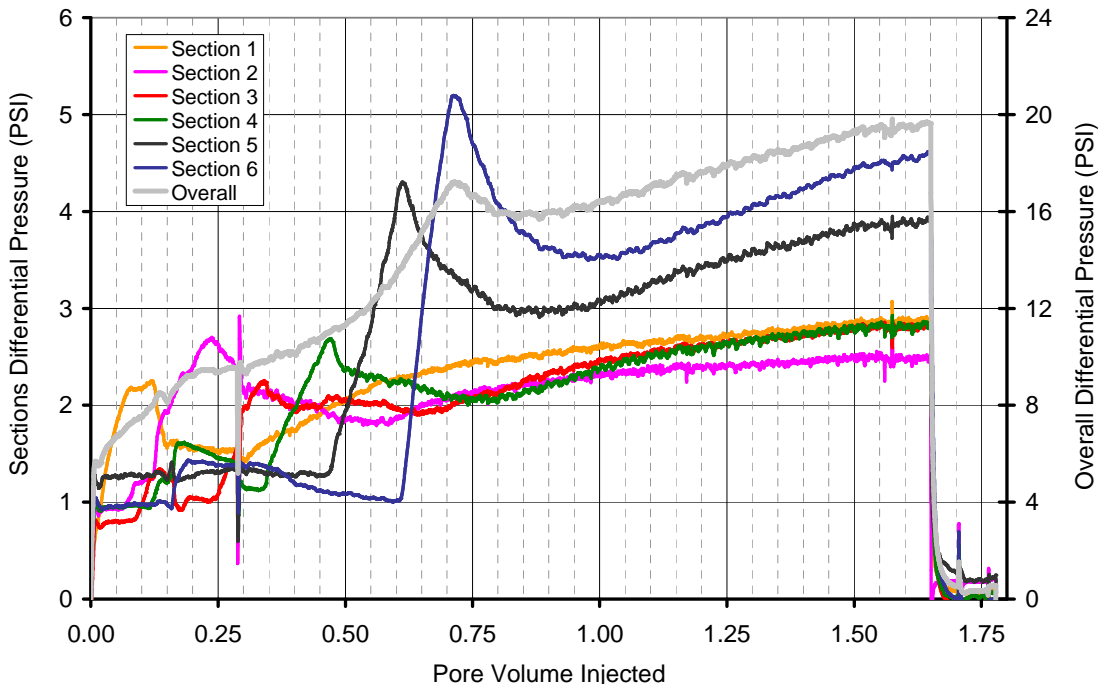


**Figure 3.113:** Overall core and section pressures during ASP T-5 (Core #27).

Pressures of individual sections were analyzed to determine mobilities of oil bank and surfactant bank. The estimations are tabulated in **Table 3.18**. Mobility of surfactant slug was lower than the oil bank in the last three sections, indicating good mobility control. Therefore polymer in surfactant slug proved sufficient.

#### ***Core Flood T-6 (Core #31)***

From ASP flood T-5 (Core #27), it was concluded that 0.3 PV surfactant slug size of Formulation X-3 was inadequate to recover residual oil efficiently, particularly from the later sections, sections 4, 5 and 6. T-6 was performed to test Formulation X-3 with a larger 0.6 PV surfactant slug size.

#### ***Core Characterization***

Core #31, sandstone, was set up for flooding in horizontal orientation. First its dispersion was characterized (**Figure 3.114**) and was found to be abnormal. The tracer profile showed a long tail and the tail had a kink and waviness. The tracer took 250 mL to reach 100% concentration, which was quite long compared to typically observed tracer profile for other cores. A pore volume of 117 mL was determined from tracer curve integration and gravimetric method. Permeabilities of the core and sections were determined next and are tabulated in **Table 3.16**. Overall permeability of the core was 195 md. Section 2 showed abnormally high permeability relative to other sections which cast further doubts about the integrity of this core.

#### ***Brine Flood/Oil Flood/Waterflood***

Brine flood was carried out with 6.1 wt% NaCl, soft brine. The salinity was kept slightly higher than the surfactant slug optimal salinity in order give a suitable negative salinity gradient.

Oil flood for core #31 was run at 37.5 ft/day (2.75 mL/min) and at 46.1 C. 4.5 pore volumes of oil were injected.  $S_{oi}$  at the end of oil flood was 0.64 and  $k_{ro}^{\circ}$  was measured to be 0.91. Pressures during the oil flood and average oil saturation in the core versus the pore volumes of oil injected are plotted in **Figure 3.115** and **Figure 3.116**, respectively.

Waterflood was performed at 46.1 C at a flow rate of 0.3mL/min. pressures were measured during the flood (**Figure 3.117**). The pressures in sections showed abnormal behavior. The arrival of the water front did not give a steep pressure rise in Sections 3, 4, 5 and 6, which suggested that the water front was not sharp as observed in other cores. This could have been caused by the same phenomenon that caused the abnormally high dispersion in tracer run. The waterflood was conducted until the oil saturation in the core became stable (**Figure 3.118**).  $k_{rw}^{\circ}$  was determined to be 0.050 from overall pressure at end of waterflood. Final oil saturation remaining in the core was 38.6 %.

#### ***Surfactant and Polymer Slug***

Surfactant slug contained 0.31 wt% Petrostep S-1, 0.19 wt% Petrostep S-2, 1.375 wt% SBA, 1 wt% Na<sub>2</sub>CO<sub>3</sub>, 5.0 wt% NaCl and 2000 ppm Flopaam SNF 3330S. Viscosity of the surfactant slug was 16 cp measured at 1 s<sup>-1</sup> with Bohlin rheometer (**Figure 3.119**).

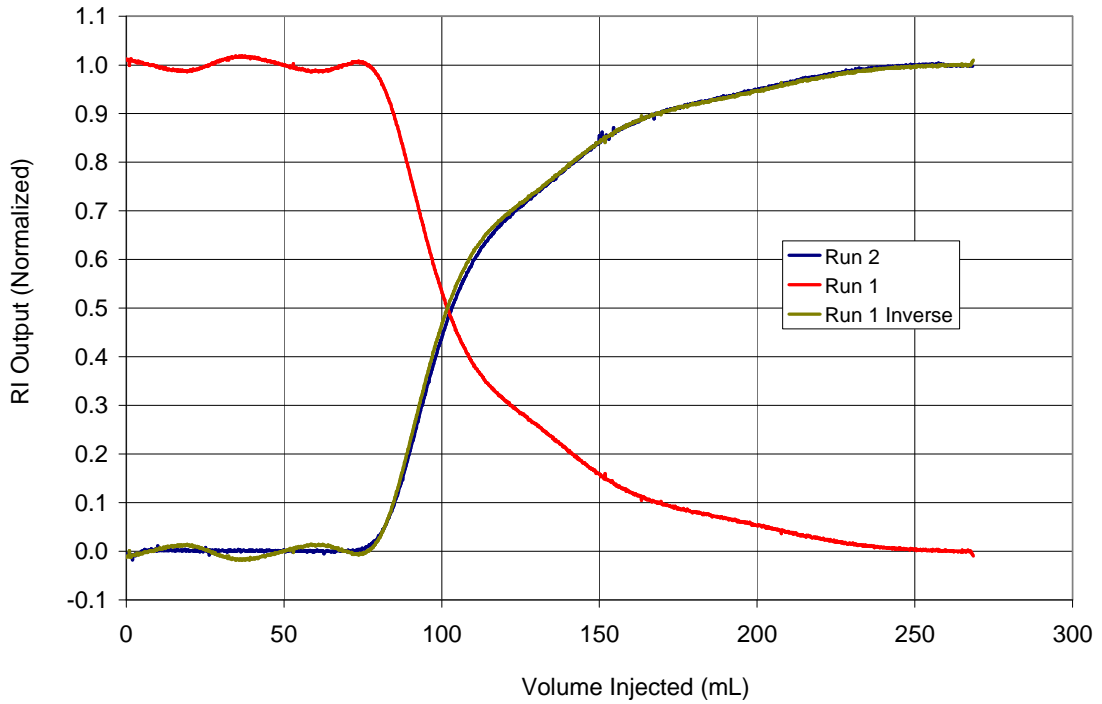


**Figure 3.114:** Dispersion characterization of Core #31 for core flood T-6.

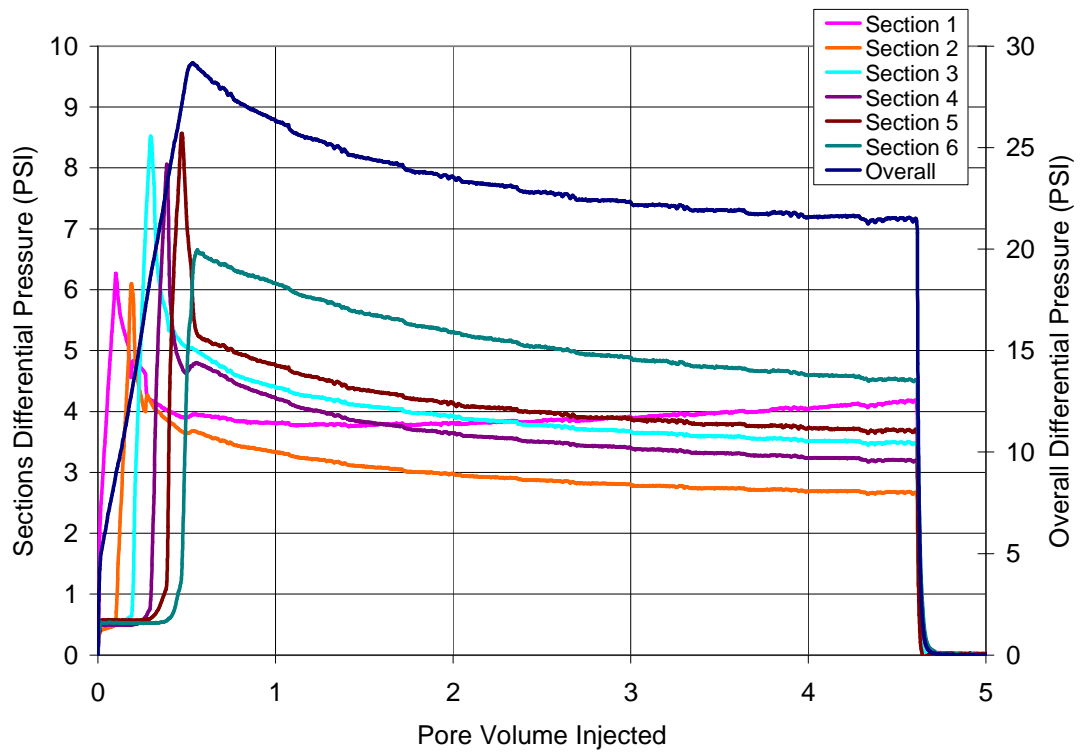


**Figure 3.115:** Oil flood differential pressures for Core #31 for core flood T-6.

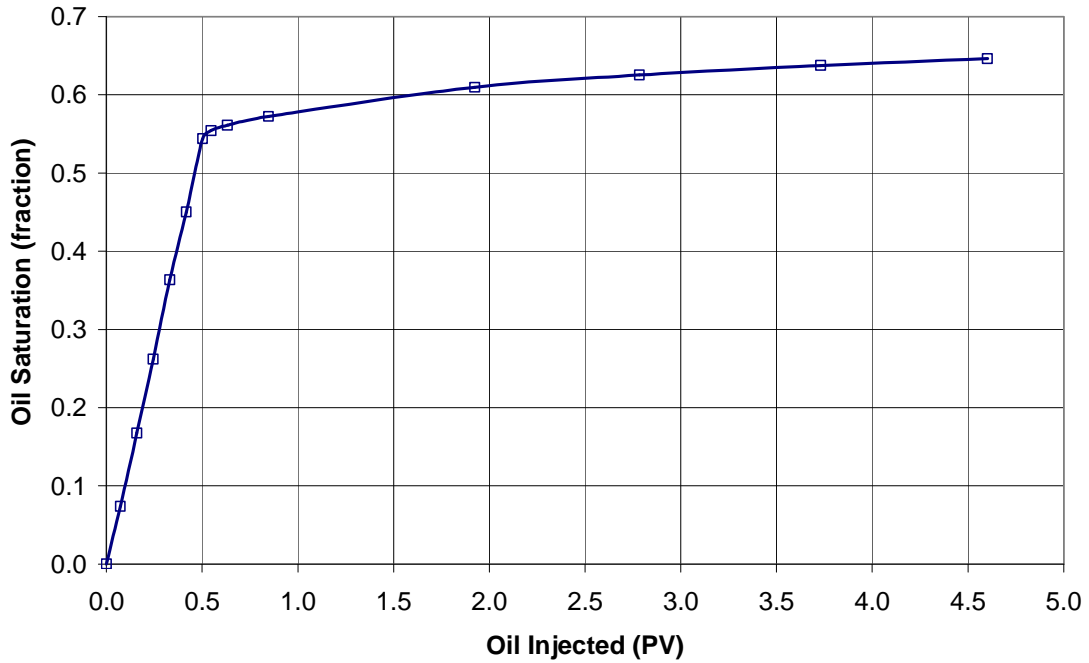


**Figure 3.116:** Oil saturation change in the core during oil flood on core #31.

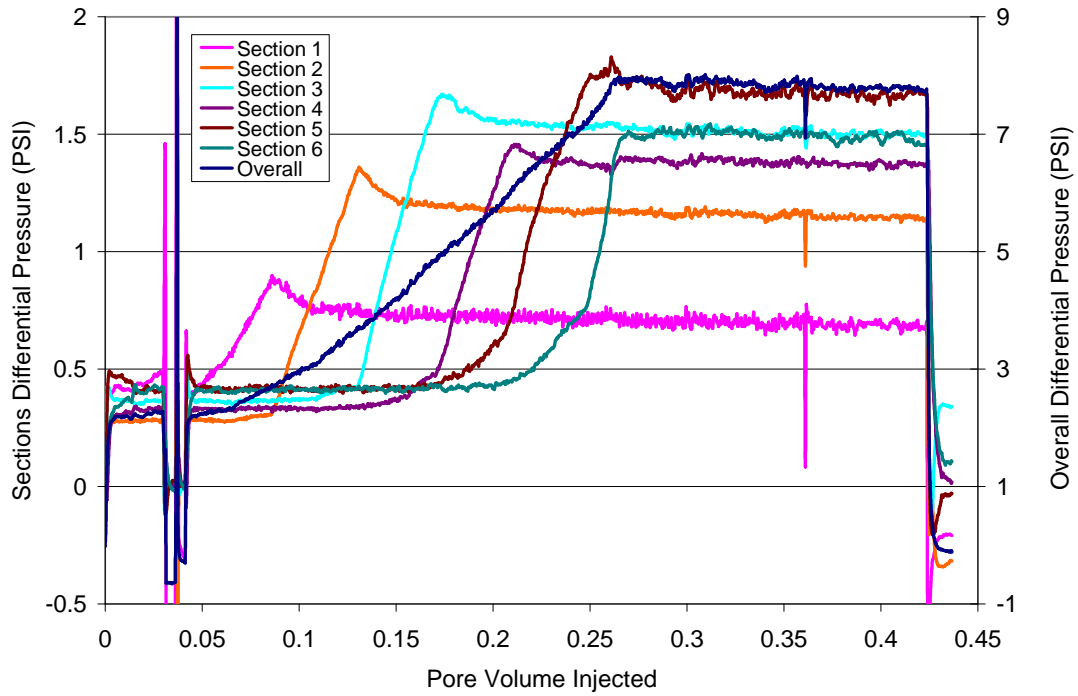


**Figure 3.117:** Waterflood differential pressures for Core #31 for core flood T-6.

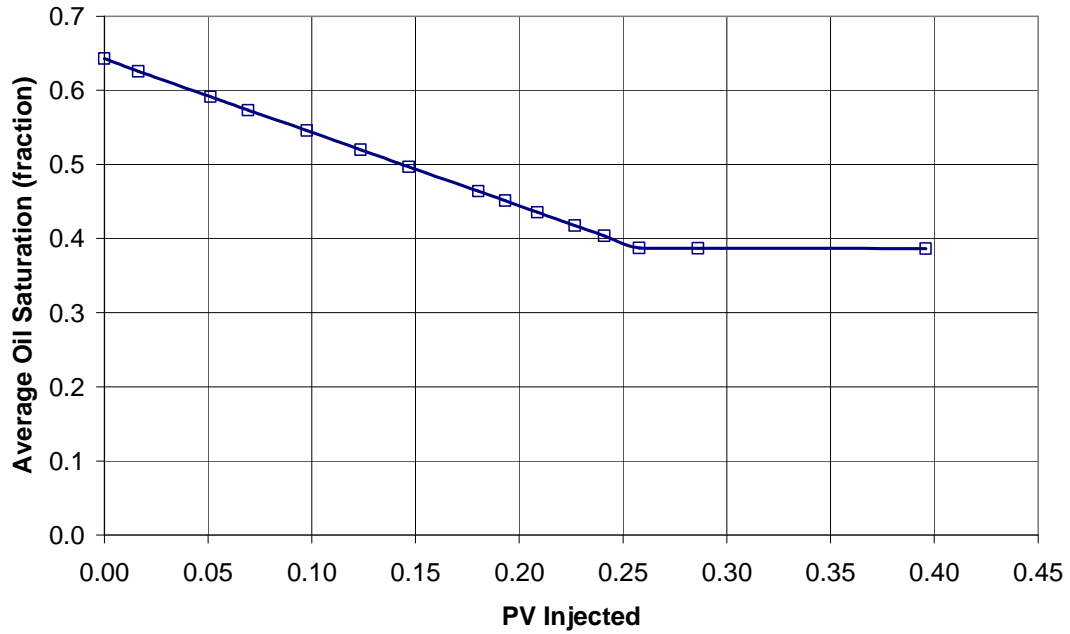


**Figure 3.118:** Oil saturation change in the core during waterflood on core #31.

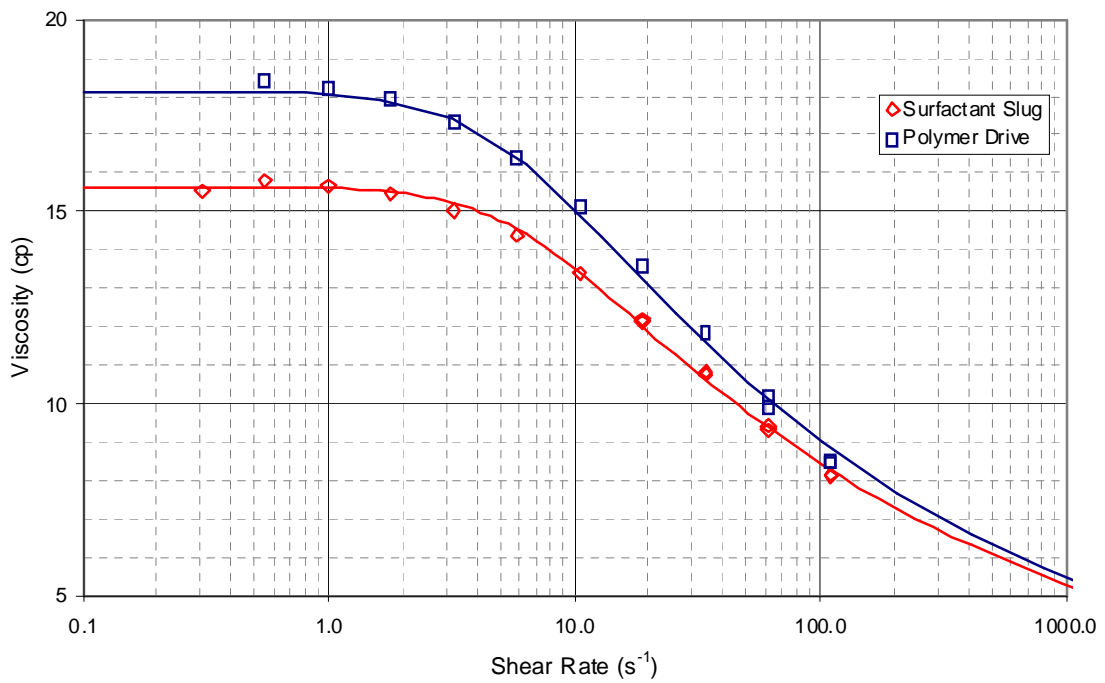


**Figure 3.119:** Viscosities of surfactant and polymer slug for core #31 (T-6) at 46.1°C.

Polymer slug salinity was 4.3% TDS (NaCl only), 70% of surfactant slug. The salinity was lower than the minimum needed to give Type I microemulsion at back of the surfactant slug. Polymer concentration was 2250 ppm that gave the polymer drive higher viscosity than surfactant slug, 18 cp @ 1 s<sup>-1</sup>(**Figure 3.119**).

#### *Chemical Flood & Oil Recovery*

Core #31 was flooded at 0.15mL/min (2.1 ft/day) with 0.6 pore volume (PV) of surfactant slug and followed by 1.2 PV polymer drive. Oil bank arrived at 0.18 PV and surfactant breakthrough occurred at 0.69 PV. Oil cut dropped below 1% after 75% residual oil recovery. **Figure 3.120** shows the oil cut and residual oil recovery from the ASP flood. Oil recovery for ASP T-6 (0.6PV surfactant slug) was greater than T-5 (0.3 PV surfactant slug). Although oil recovered in oil bank for both floods was about 60%, the oil cut in T-6 (0.6 PV) showed a gradual and long decline which was responsible for the incremental oil recovery. Even the maximum oil cut in the oil bank was similar, about 45 %. Still, the incremental recovery was not as good as expected. The long tail in the oil cut profile could also be associated with the abnormally long dispersion profile of the core.

Core #31 was sliced into 6 sections using a saw and then dried to visualize the trapping of oil in the core. Images of the sections are shown in **Figure 3.121**. It can be seen in the images that trapping started in section 2 and became more pronounced in subsequent sections. Trapped oil showed a definite pattern and seemed to grow along the bottom and side of the core in a wedge shape. This phenomenon could be associated with the high dispersion of the core and one cause could be the existence of two different permeability zones in the same core. In the pictures, dark streaks are visible in slices 1 and 2 of cores that run diagonally from top right to bottom of the cores. These streaks appeared to be bedding planes. The oil was trapped to the right of the diagonal streaks which suggested that lower permeability existed to the right side of the core. The trapping of oil was higher in the later sections which appeared to be caused by the decreasing concentrations of surfactant reaching the later section due to retention and diversion to the higher permeability zone.

Gravity override was also examined as a potential cause for the wedge formation in the core. Gravity number was calculated for the chemical system and core as follows:

$$Ng = (4.3957 \times 10^{-6}) \times \frac{(\rho_p - \rho_o) \times \kappa \times g}{\mu_p \times u}$$

Where:

$$\rho_p = \text{polymer\_density} \left( \frac{\text{lbm}}{\text{ft}^3} \right)$$

$$\rho_o = \text{oil\_density} \left( \frac{\text{lbm}}{\text{ft}^3} \right)$$

$$\kappa = \text{permeability}(\text{md})$$

$$g = 9.81 \frac{\text{m}}{\text{s}^2}$$

$$\mu_p = \text{polymer\_viscosity}(\text{cp})$$

$$u = \text{frontal\_velocity} \left( \frac{\text{ft}}{\text{day}} \right)$$

$$Ng = (4.3957 \times 10^{-6}) \times \frac{(64.4 - 52.2) \frac{\text{lbm}}{\text{ft}^3} \times 195 \text{md} \times 9.81 \frac{\text{m}}{\text{s}^2}}{18 \text{cp} \times 2 \frac{\text{ft}}{\text{day}}} = 0.0028$$

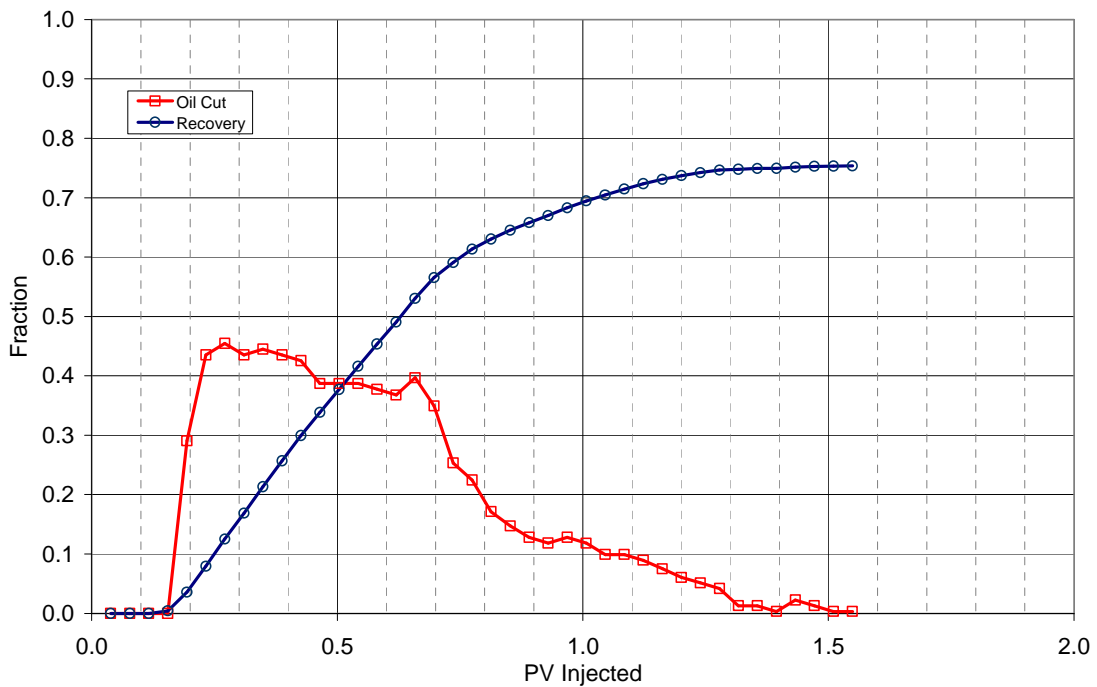


**Figure 3.120:** Oil cut and oil recovery for ASP flood T-6 (Core #31).

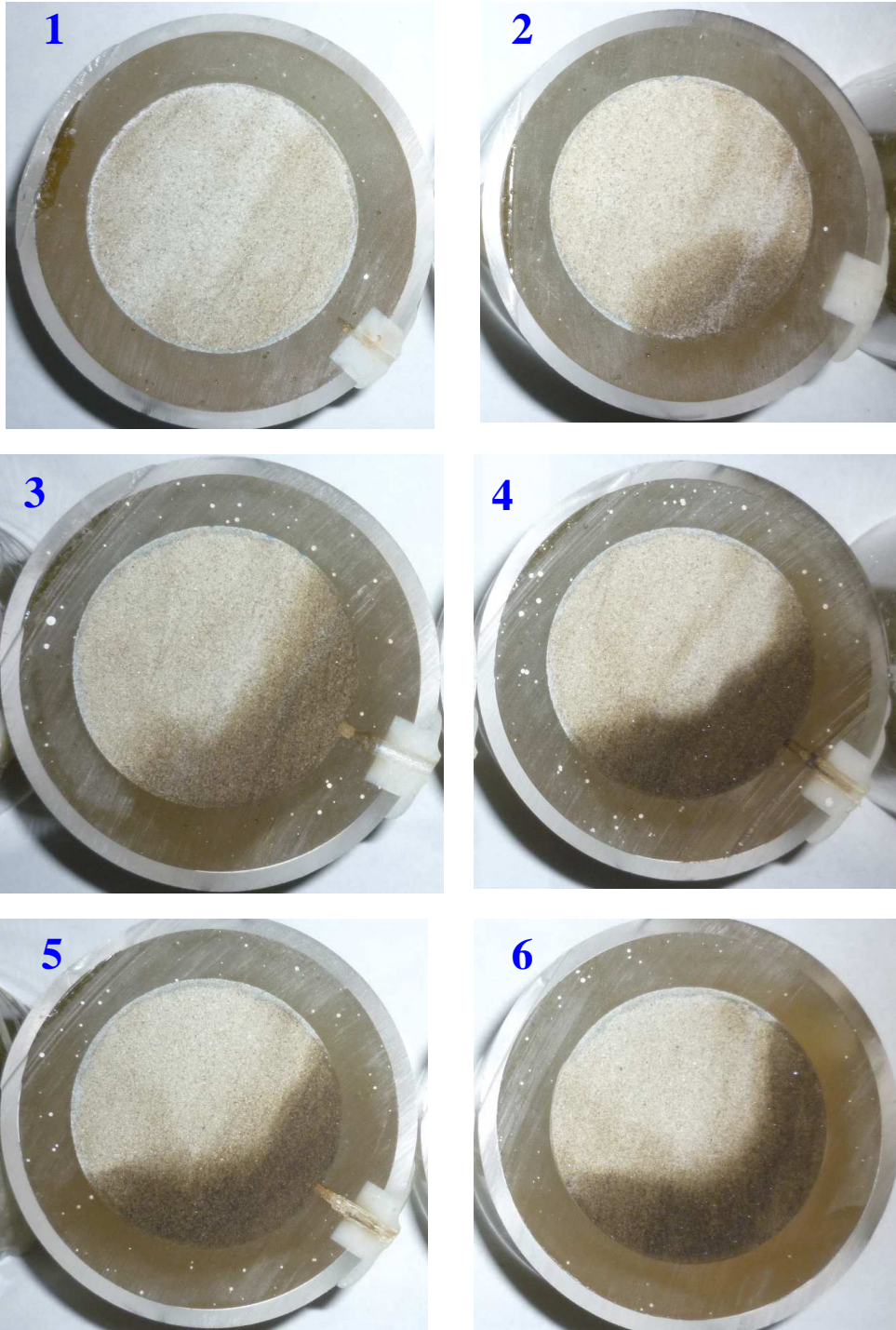


**Figure 3.121:** Sliced view of Core 31 sections after ASP flood. Section numbers given in top left corner. The face shown is the downstream side of section. Oil is trapped at the bottom part of the sections.



Gravity number was found to be 0.0028, which was too small to cause gravity override according to the study by Tham et al. (Tham, Nelson et al. 1983). However, according to the same reference, surfactant concentration if not sufficiently high could also leave a wedge of residual oil. The study referenced pertained to oil wedge at the bottom of the core that were parallel to the horizontal, whereas, Core 31 showed an oil wedge that was not parallel to horizontal. Based on the evidence, dual permeability appeared to be the more likely cause of wedge in this case.

Effect of gravity could be negated by setting up the core in vertical orientation, like in the case of Core 37 and 39.

#### *Effluent Analysis*

Effluent samples from the core flood are shown in **Figure 3.122** at reservoir temperature after 3 days of equilibration. Vials 5-18 (0.18 PV-0.70 PV) contained oil bank. Vials 21-32 (0.81 PV-1.24 PV) have middle phase microemulsion suggesting a long type III region reaching the end of the core. Yet the recovery was low. It could be concluded that in addition to presence of type III microemulsion phase for an extended period, the concentration of microemulsion travelling through the core was also critical for good recovery. The abnormally high dispersion of the core had a further negative effect on the oil recovery as it reduced the surfactant concentration travelling through the core.

Salinity, viscosity and pH of aqueous phase of the effluent samples were measured and are presented in **Figure 3.123**. Salinity started to drop even before surfactant breakthrough because of abnormal dispersion characteristic of the core. Salinity reached a plateau between 0.8 PV and 1.1 PV at 5.2 wt% NaCl concentration, equal to surfactant salinity. The longer slug size enabled maintaining optimum salinity condition for a prolonged period, showing the benefit of bigger slug size. A long Type III microemulsion region was obtained at the end of core as indicated in the figure. After 1.3 PV injected, Type I microemulsion reached the end of core. Type III→Type I microemulsion was completed within 1.3 PV injected.

Viscosity rose sharply at surfactant breakthrough and reached the full value of surfactant slug at 0.9 PV. Viscosity went above polymer drive viscosity momentarily. This would have been caused by the high pH in the surfactant slug mixing with the polymer drive. High pH is known to enhance polymer viscosity.

#### *Pressure Analysis*

Pressure drops measured across the core and each section are plotted in **Figure 3.124**. Pressures were affected by capillary pressure effects and the trapped oil saturation. Regions of oil, surfactant and polymer bank could not be clearly identified for all the sections, which made interpretation of fluid displacement process and mobilities of sections difficult. A maximum overall core pressure of 8.6 PSI was observed at the end of core flood at 2 ft/day. This pressure was much smaller than the peak pressure in core #27 (ASP #T-5). Though core #27 had lower permeability compared to core #31, still longer slug did reduce the high pressure peaks and helped keep the overall pressure lower.

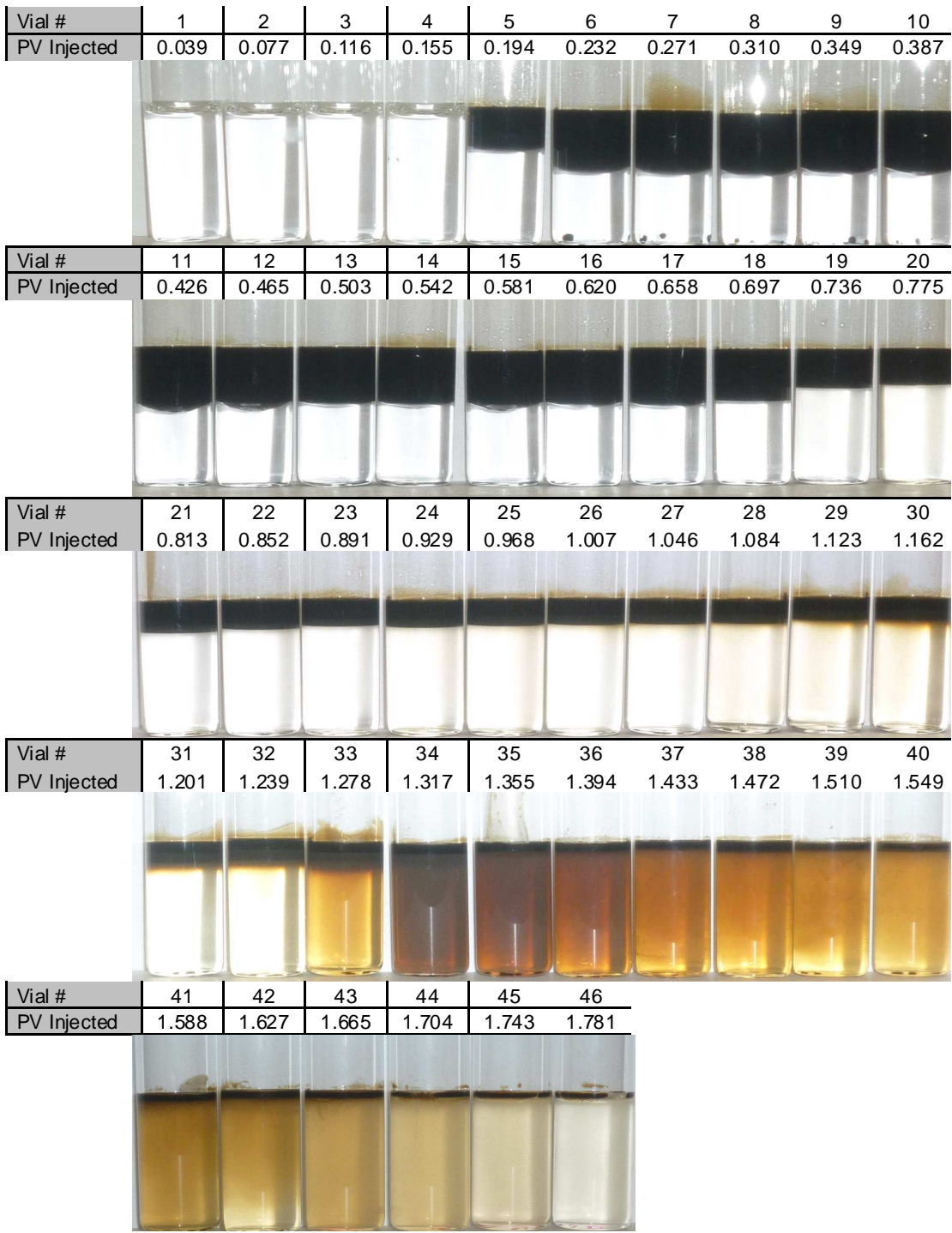


**Figure 3.122:** Photo of effluent vials from ASP T-6 (core #31) with 0.6 PV Formulation X-3 @ 46.1 °C after equilibrating for 3 days.

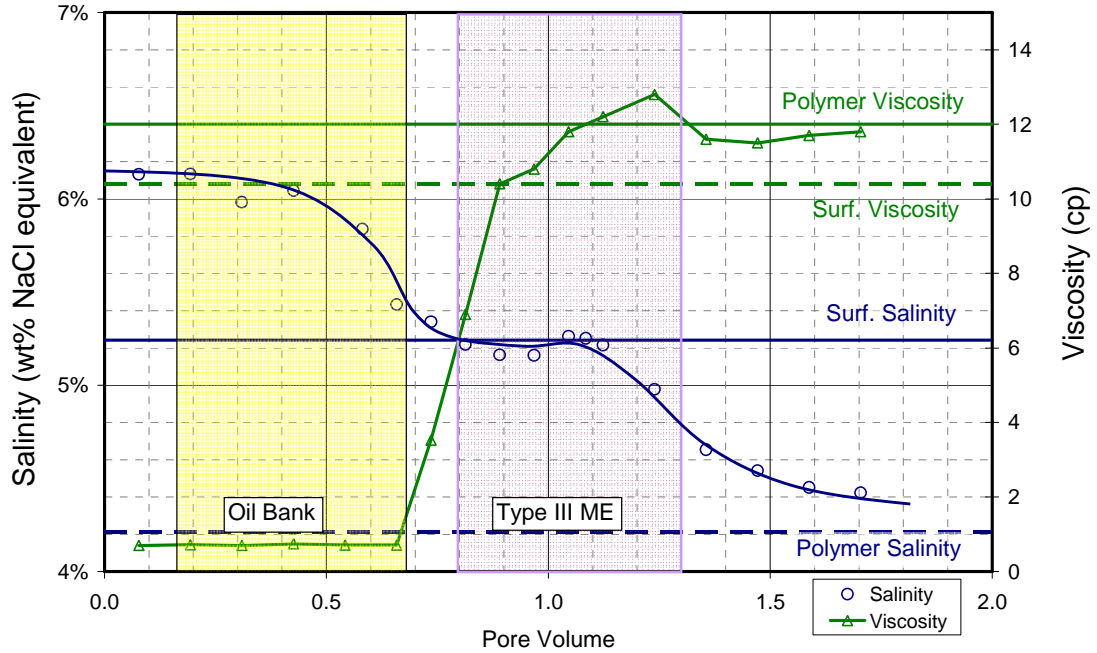


**Figure 3.123:** Viscosity, salinity and pH of aqueous phase in effluent vials from ASP T-5 (Core #27). Viscosity was measured at  $37.5 \text{ s}^{-1}$  and  $46.1 \text{ }^\circ\text{C}$ .

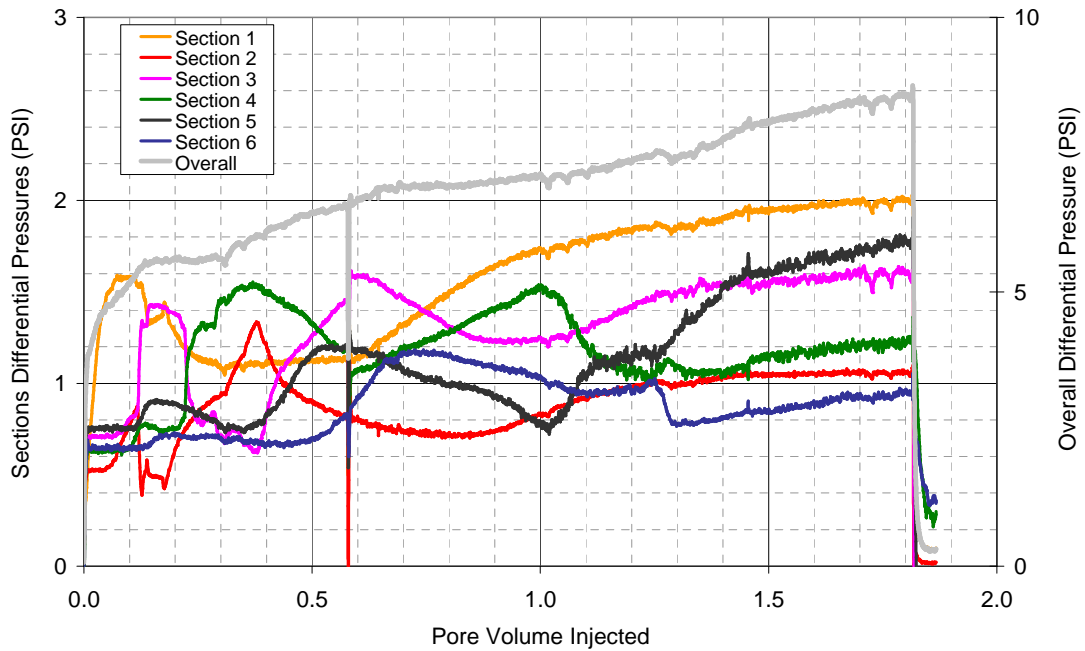


**Figure 3.124:** Overall core and section pressures during ASP T-6 (Core #31).

### ***Core Flood T-7 (Core #32)***

Core flood T-7 was a repeat with the formulation X-3 and a 0.6 PV surfactant slug size. The results of ASP T-6 were confounded by the abnormally high dispersion in the core #31. A new core, core #32, was used for T-7. Before proceeding with the floods, the core was characterized to ensure it showed a dispersion profile consistent with typical sandstone cores. The results would indicate whether dispersion in core could have had an effect on oil recovery in ASP T-6

### ***Core Characterization***

Core #32, sandstone, was set up for flooding in horizontal orientation. First its dispersion was characterized (**Figure 3.125**) and was found consistent with the typical sandstone cores. A pore volume of 110 mL was determined from tracer curve integration and gravimetric method. Permeabilities of the core and sections were determined next and are tabulated in **Table 3.16**. Overall permeability of the core was 120 md. Section 6 had relatively high permeability compared to other sections, 218 md. This was caused by the separation of the epoxy from the core. The separation occurred because the end of core was saturated with soft brine (6% NaCl) accidentally before it was casted in epoxy. NaCl that had precipitated and bonded to the epoxy was dissolved away during brine flood creating gap between the epoxy and rock. The tracer did not seem to get affected by the gap and it was decided to proceed with the core.

### ***Brine Flood/Oil Flood/Waterflood***

Brine flood was carried out with 6.5 wt% NaCl, soft brine. The salinity was kept slightly higher than the surfactant slug optimal salinity in order give a suitable negative salinity gradient.

Oil flood for core #32 was run at 36 ft/day (2 mL/min) and at 46.1 C. 4.0 pore volumes of oil were injected.  $S_{oi}$  at the end of oil flood was 0.63 and  $k_{ro}^{\circ}$  was measured to be 0.85. Pressures during the oil flood and average oil saturation in the core versus the pore volumes of oil injected are plotted in **Figure 3.126** and **Figure 3.127**, respectively. The pressures showed pulses caused by capillary effects. Otherwise, the displacement of brine by oil seemed normal. Section 6 oil flood pressures were low compared to other sections due to the high permeability. The gap between the core and epoxy got saturated with oil when the oil bank reached section 6 (**Figure 3.128**)

A waterflood was performed at 46.1 C at a flow rate of 0.3 mL/min. Pressures were measured during the flood (**Figure 3.129**). Waterflood was conducted until the oil saturation in the core became stable (**Figure 3.130**).  $k_{rw}^{\circ}$  was determined to be 0.042 from overall pressure at end of waterflood. Final oil saturation remaining in the core was 41 %. Again, the pressure in section 6 was low compared to other sections due to higher permeability. The oil that had got trapped in gap between epoxy and core in section 6 was displaced by waterflood (**Figure 3.131**).

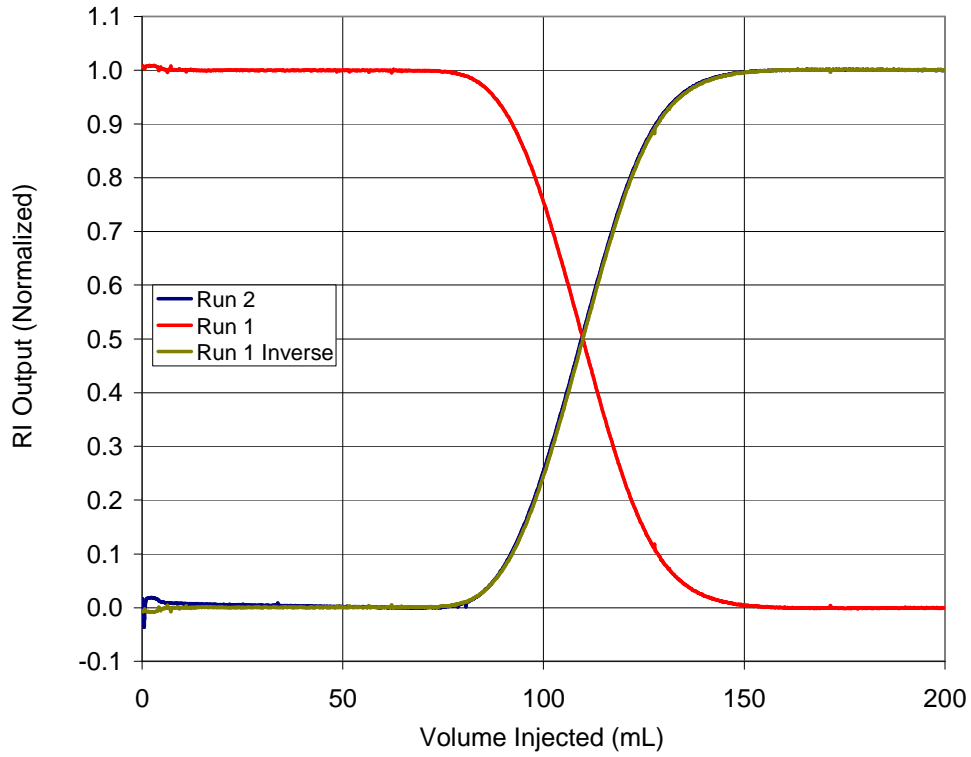


**Figure 3.125:** Dispersion characterization of Core #32 for core flood T-7.

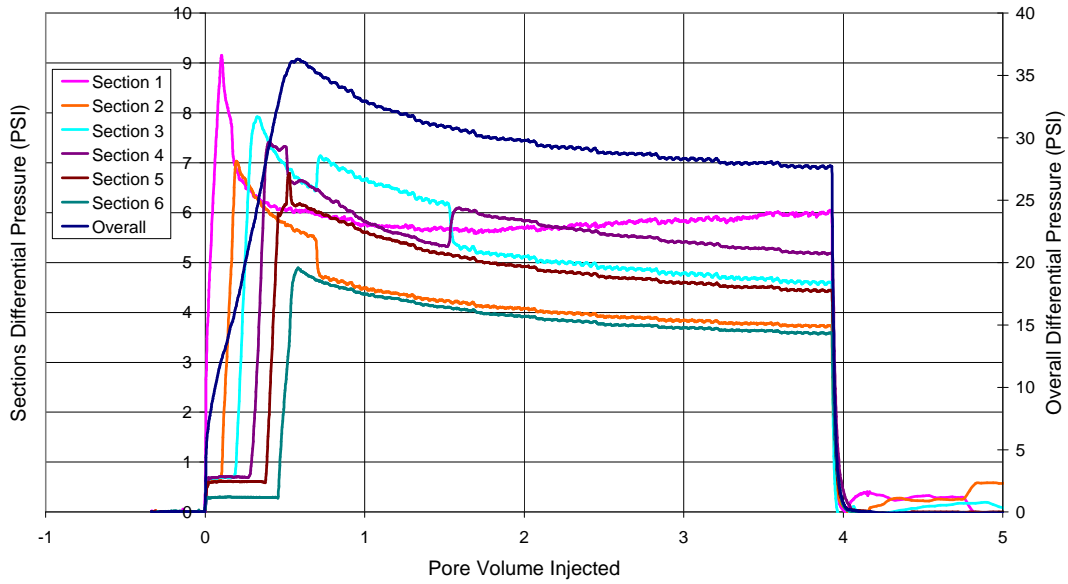


**Figure 3.126:** Oil flood differential pressures for Core #32 for core flood T-7.

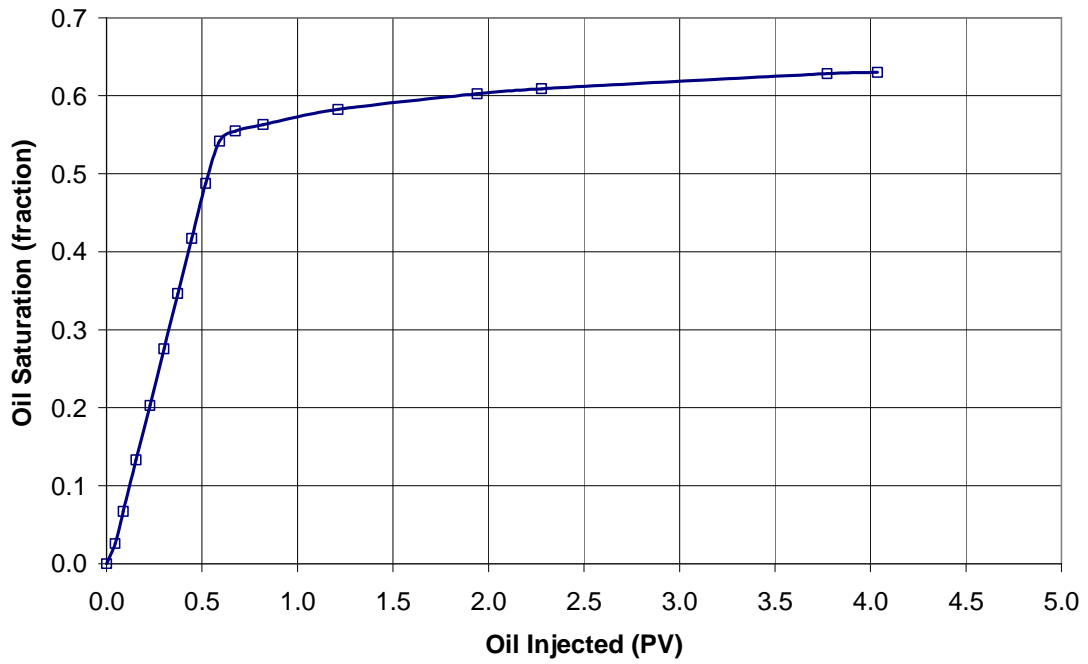


**Figure 3.127:** Oil saturation change in the core during oil flood on core #32.

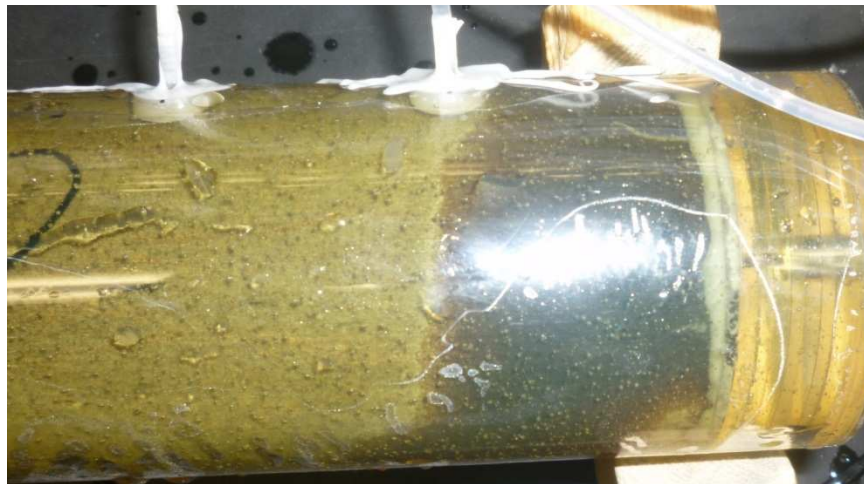


**Figure 3.128:** Core #32 section 6 at the end of oil flood.

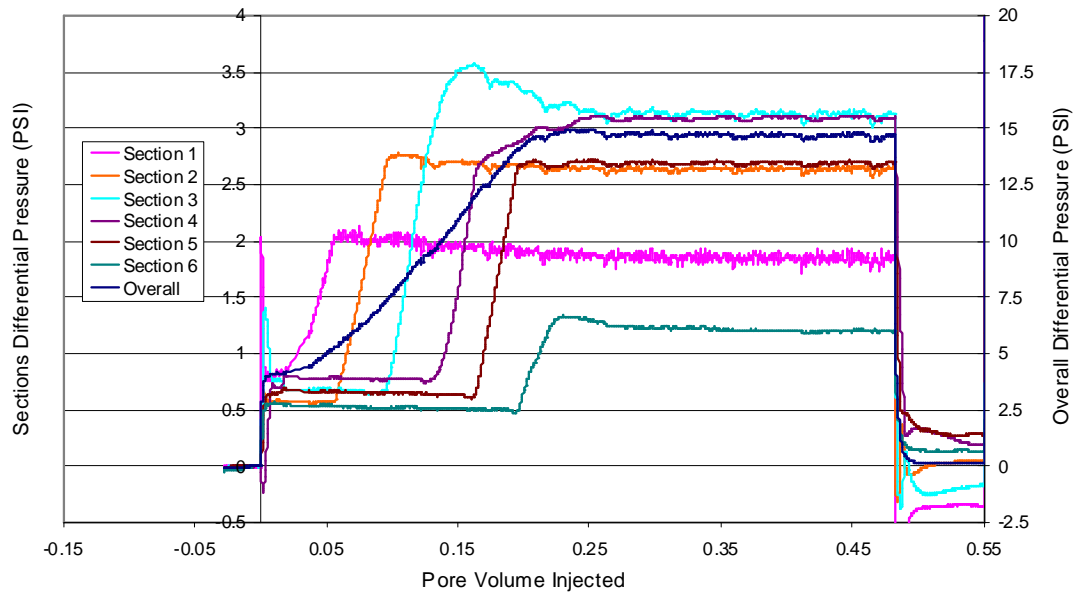


**Figure 3.129:** Waterflood differential pressures for Core #32 for core flood T-7.

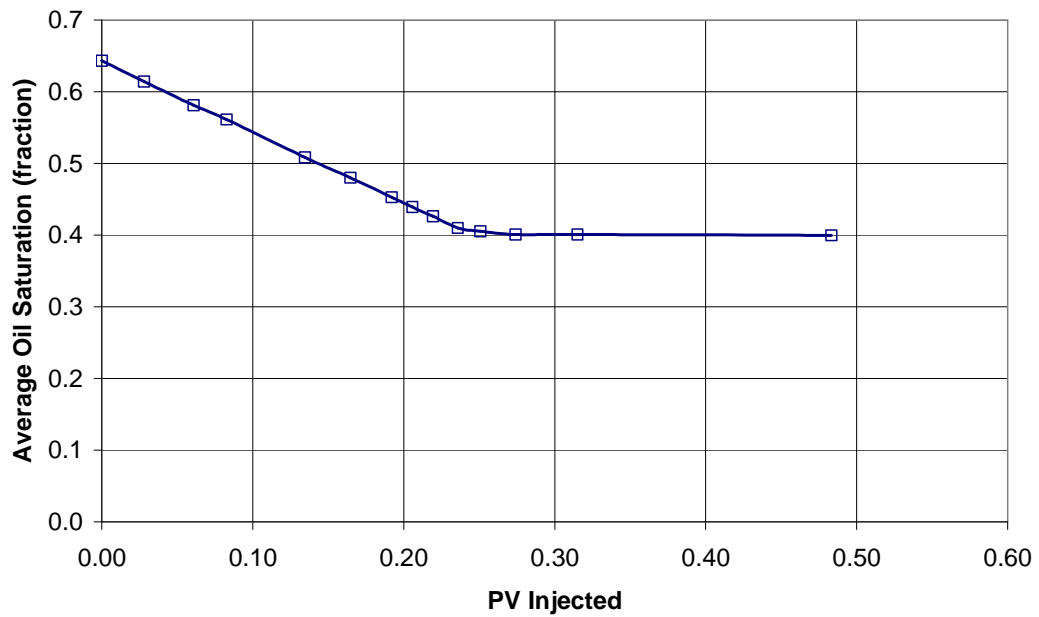


**Figure 3.130:** Oil saturation change in the core during waterflood on core #32.



**Figure 3.131:** Core #32 section 6 at the end of waterflood.



### *Surfactant and Polymer Slug*

Surfactant slug contained 0.31 wt% Petrostep S-1, 0.19 wt% Petrostep S-2, 1.375 wt% SBA, 1 wt% Na<sub>2</sub>CO<sub>3</sub>, 5.05 wt% NaCl and 2200 ppm Flopaam SNF 3330S. Viscosity of the surfactant slug was 18 cp measured at 1 s<sup>-1</sup> with Bohlin rheometer (**Figure 3.132**).

Polymer slug salinity was 4.3% NaCl, 70% of surfactant slug. Salinity of the polymer slug was kept the same as for ASP T-6 as it had worked well. Polymer concentration was 2350 ppm that gave the polymer drive higher viscosity than surfactant slug, 20 cp @ 1 s<sup>-1</sup> (**Figure 3.132**).

### *Chemical Flood & Oil Recovery*

Core #32 was flooded at 0.15 mL/min (2.1 ft/day) with 0.6 pore volume (PV) of surfactant slug and followed by 1.2 PV polymer drive. Oil bank arrived at 0.15 PV and surfactant breakthrough occurred at 0.74 PV. Oil cut dropped below 1% after 82% residual oil recovery. **Figure 3.133** shows the oil cut and residual oil recovery from the ASP flood. Oil recovery for ASP T-7 turned out greater than T-6. The only major difference between the two floods was the dispersion character of the cores used. Oil recovered in oil bank for both floods was about 60%. The maximum oil cut in the oil bank was similar, about 45 %.

Core #32 was sliced into 6 sections using a saw and then dried to visualize the trapping of oil in the core. Images of the sections are shown in **Figure 3.134**. It can be seen in the images that trapping started in section 3 and became more pronounced in subsequent sections. The trend in trapping of oil was similar to Core #31 i.e. it formed a wedge like shape in the core. In this core, the trapping started later than Core #32 and wasn't as severe as Core 31. It could be concluded that dispersion did affect the oil recovery in Core #31 but it wasn't the only cause for trapping of oil. Oil was actually trapped due to inefficient mobilization of oil by formulation X-3, particularly in the later sections. This ineffectiveness was not due to gravity override as the gravity number, Ng, for this core was 0.0016, which was too small to cause gravity override (Tham, Nelson et al. 1983). Also, the wedge was not parallel to the horizontal, as would be the case for gravity override. Surfactant concentration and slug size could be the only reason to cause the ineffective mobilization. This was the second instance of oil wedge which was non-parallel to horizontal. The repetitive occurrence possibly revealed the dynamics of oil trapping in core when surfactant slug was not designed well. A wedge of residual oil could be expected in such cases.

### *Effluent Analysis*

Effluent samples from the core flood are shown in **Figure 3.135** at reservoir temperature after 3 days of equilibration. Vials 4-18 contained oil bank. Vials 20-32 (0.9 PV-1.3 PV) exhibited middle phase, type III, microemulsion, which is quite decent size. It was again proven that a longer slug, even though at smaller surfactant concentration, gave extended type III microemulsion region in the core. However, recovery itself was also dependent on the concentration of microemulsion travelling through the core. Comparing to 1 wt% surfactant formulation, X-1 tested in Core #37 (0.3 PV), the recovery was still low and the sliced core showed trapped oil.

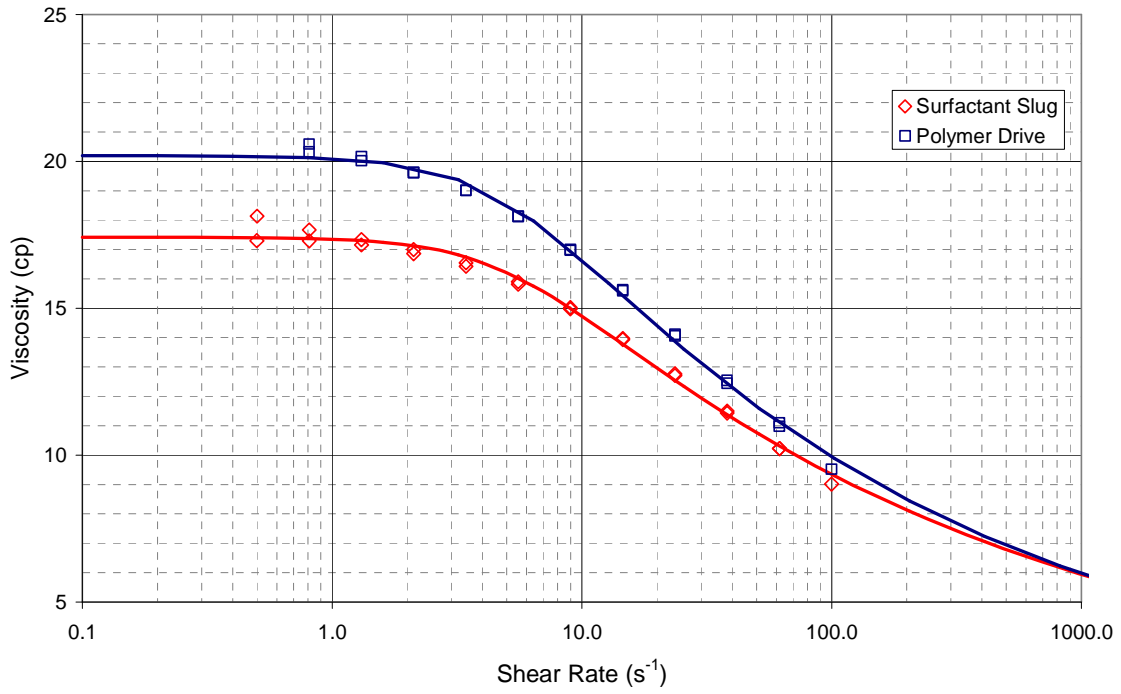


**Figure 3.132:** Viscosities of surfactant and polymer slug for core #32 (T-7) at 46.1°C.

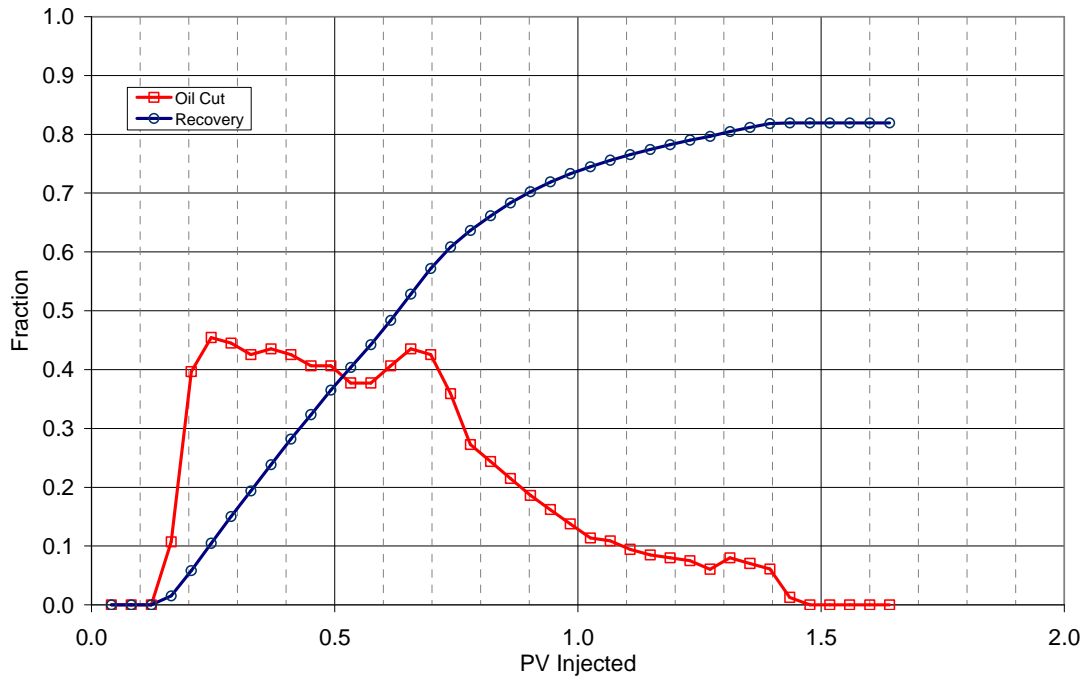


**Figure 3.133:** Oil cut and oil recovery for ASP flood T-7 (Core #32).

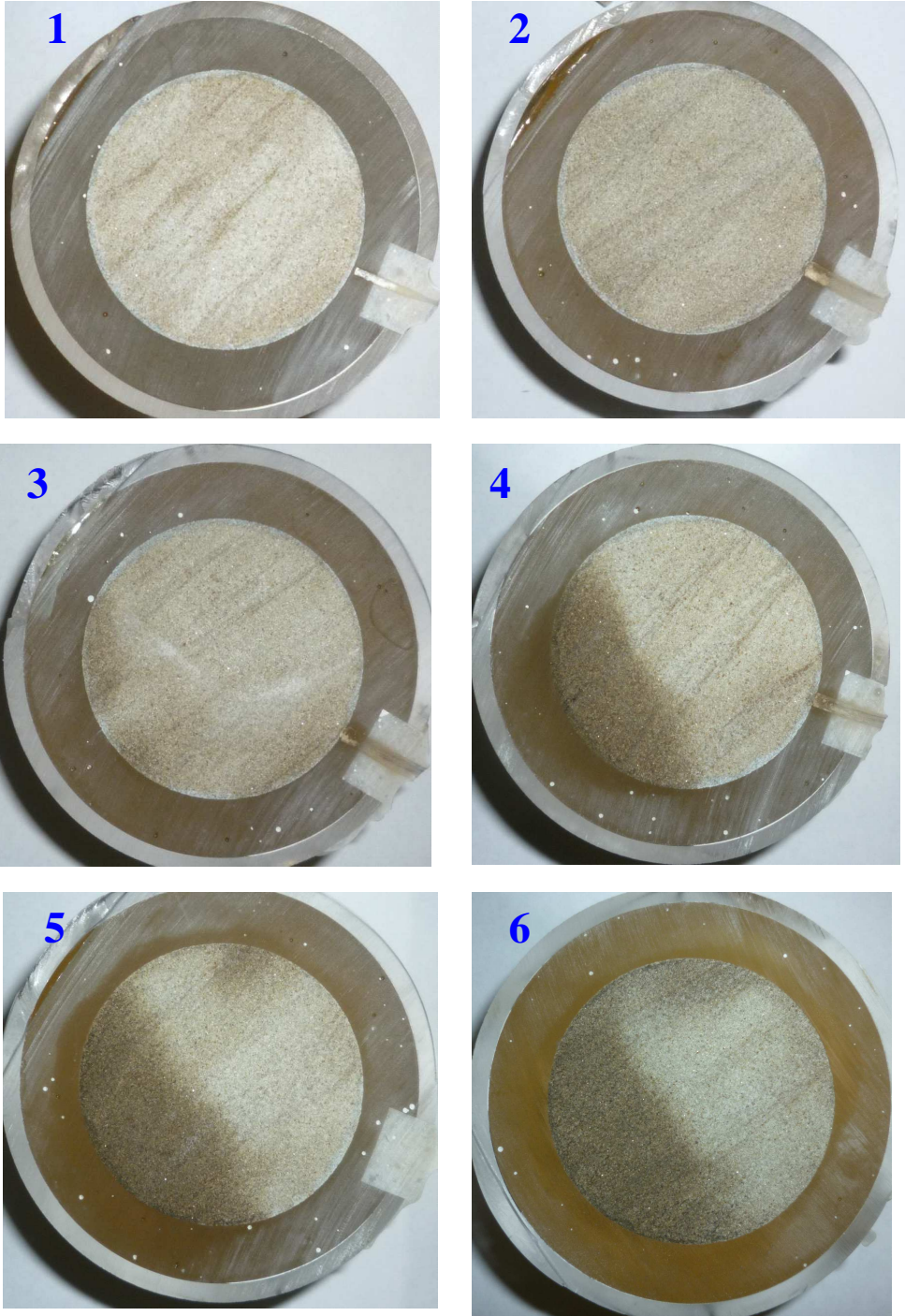


**Figure 3.134:** Sliced view of Core 32 sections after ASP flood. Section numbers given in top left corner. The face shown is the downstream side of section. Oil is trapped at the bottom left part of the sections.

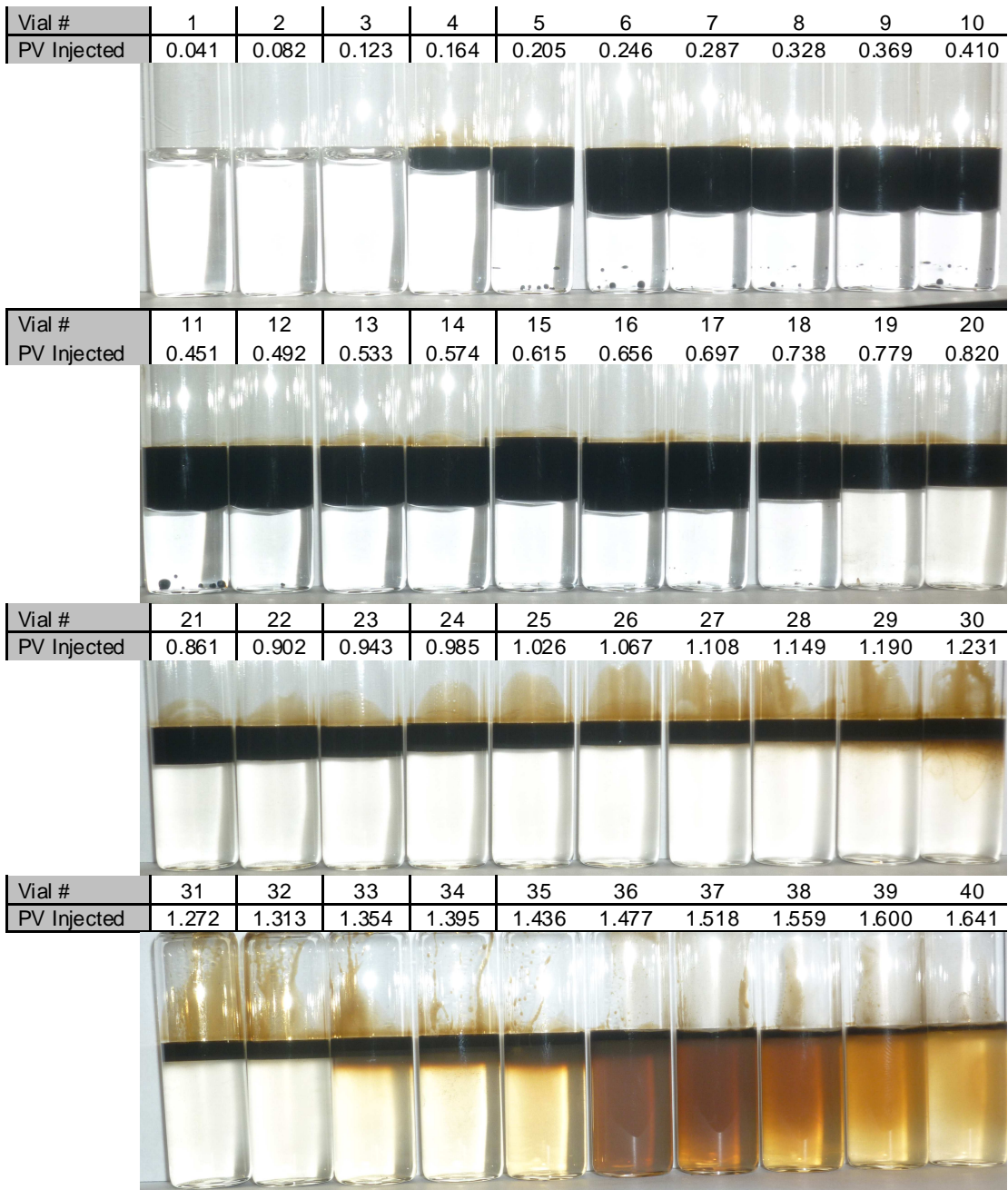


**Figure 3.135:** Photo of effluent vials from ASP T-7 (core #32) with formulation X-3 @ 46.1 °C after equilibrating for 3 days.

Salinity and viscosity of aqueous phase of the effluent samples were measured and are presented in **Figure 3.136**. Salinity started to drop at the end of oil bank. Salinity plateaued from 1.0 to 1.2 PV as a result of the long slug size and the microemulsion remained in type III conditions. As salinity dropped after 1.3 PV, microemulsion changes to type I.

Viscosity rose sharply at surfactant breakthrough and climbed higher than polymer drive viscosity, peaking at 1.3 PV. This would have been caused by the high pH in the surfactant slug mixing with the polymer drive.

#### *Pressure Analysis*

Pressure drops measured across the core and each section are plotted in **Figure 3.137**. The pressure data correlating graph is given in **Figure 3.138** with the pressure data for individual sections in **Figures 3.139** through **3.144**. Overall pressure peaked at the surfactant breakthrough and reached 13.5 PSI. At 1 ft/day, the pressure would be 7 PSI, which was high. The high pressure was a result of the low permeability of the core, 120 md, and the inefficient displacement of oil with the formulation. The pressures resulting from the oil bank were in the range 1.0 to 1.5 PSI in the sections. The pressure spikes caused by the surfactant entrance into each section reached a maximum 2.0-2.5 PSI. As the surfactant continued to displace oil from each section, the pressures subsided and reached a local minimum in the range 1.2-2.0 PSI. Via pressure analysis, the mobilities of oil bank and surfactant bank were compared in each section and are tabulated in **Table 3.18**. It was substantiated by the mobility comparison that good mobility control existed in the last three sections.

#### **SUMMARY OF CORE FLOODS**

A total of nine corefloods were performed to evaluate the waterflood residual oil recovery of the three optimized formulations, X-1, X-2 and X-3. These formulations had successfully fulfilled all the phase behavior screening criteria. All three formulations had similar surfactants, Petrostep S-1 and Petrostep S-2, and surfactant to co-surfactant ratios. Total surfactant concentration in X-2 and X-3 was half of X-1, 1 wt% and 0.5 wt% respectively. X-1 and X-2 used SBA as co-solvent while X-3 used DGBE.  $\text{Na}_2\text{CO}_3$  was used as alkali in all formulations.

Formulation X-1 was tested in 5 core floods. Four cores contained soft brine (NaCl only) prior to chemical flood with salinity equivalent to the optimum salinity, while one flood contained synthetic formation brine (SFB) that mimicked Trembley field brine composition. The injected volume of surfactant slug was 0.3 PV followed by polymer drive for all five floods. The floods with soft brine showed repeatable oil recovery in the range 88%-91% in sandstone cores of varying permeabilities between 180-430 md. The flood with SFB recovered 86% oil, which was slightly less than with soft brine. The effluent properties were evaluated that showed polymer retention for soft brine floods did not prevent attaining mobility control in the surfactant slug. On the other hand, there was evidence that polymer was retained in the presence of high salt concentrations and divalent cations of SFB in the coreflood. Both floods with soft brine and SFB showed a large percentage of oil recovery in the oil bank, 71% and 73% respectively. Maximum pressure drop across the cores, 1 foot long, were in the 6-8 PSI range for soft brine corefloods and in 9-10 PSI range for SFB coreflood at 2 ft/day flow rate.

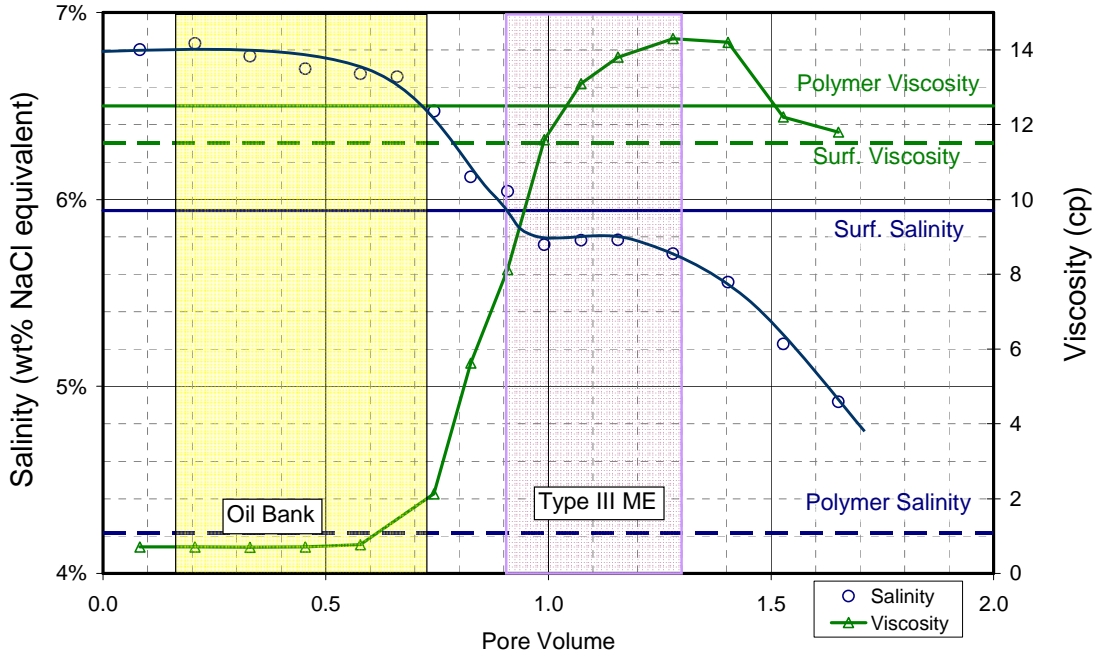


**Figure 3.136:** Viscosity, salinity and pH of aqueous phase in effluent vials from ASP T-7 (Core #32). Viscosity was measured at  $37.5 \text{ s}^{-1}$  and  $46.1 \text{ }^\circ\text{C}$ .

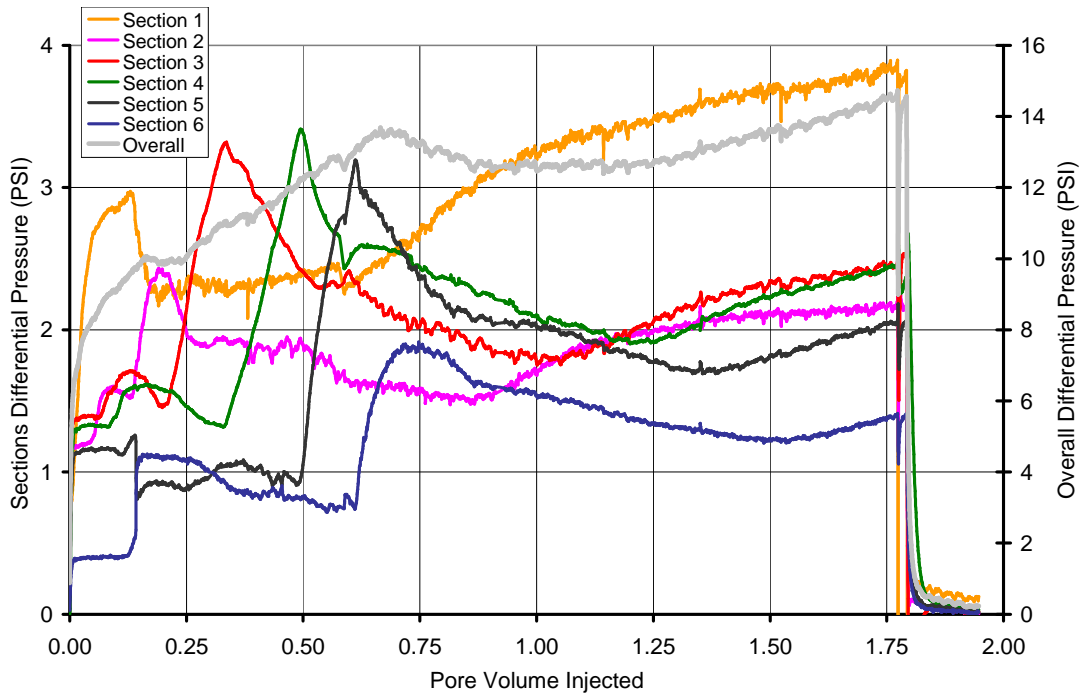


**Figure 3.137:** Overall core and section pressures during ASP T-7 (Core #32).

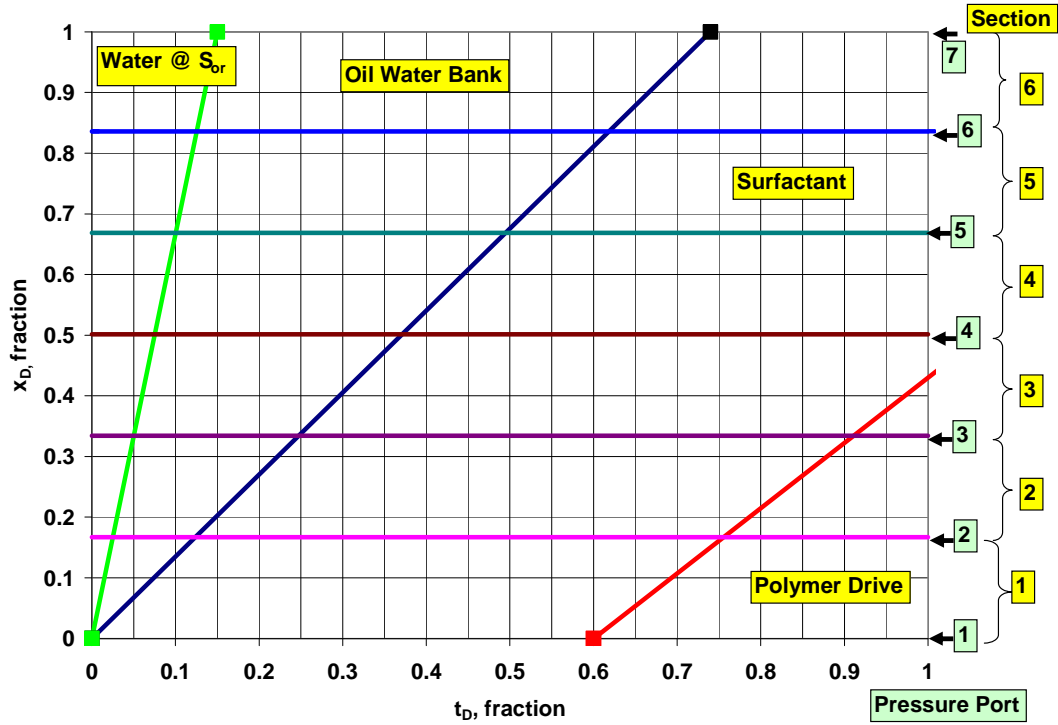


Figure 3.138: Dimensionless distance versus dimensionless time plot for ASP T-7 (core#32).

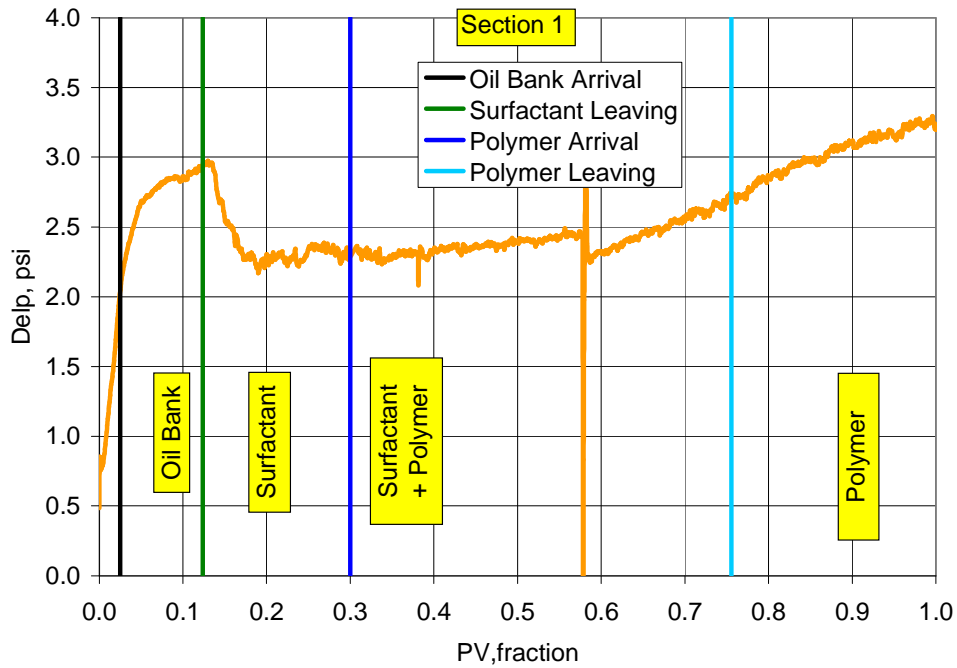
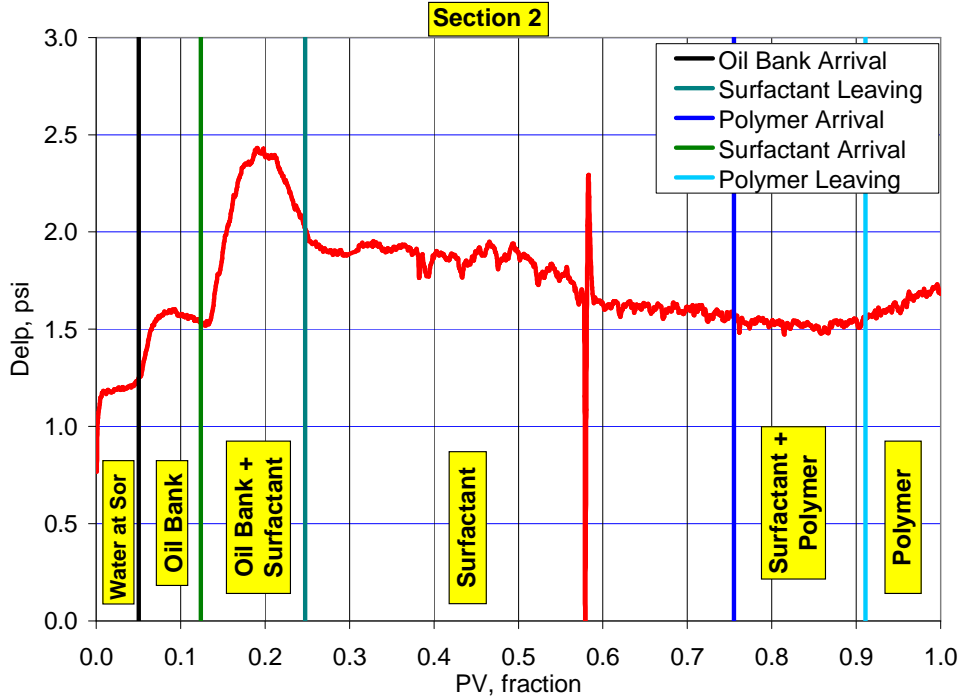
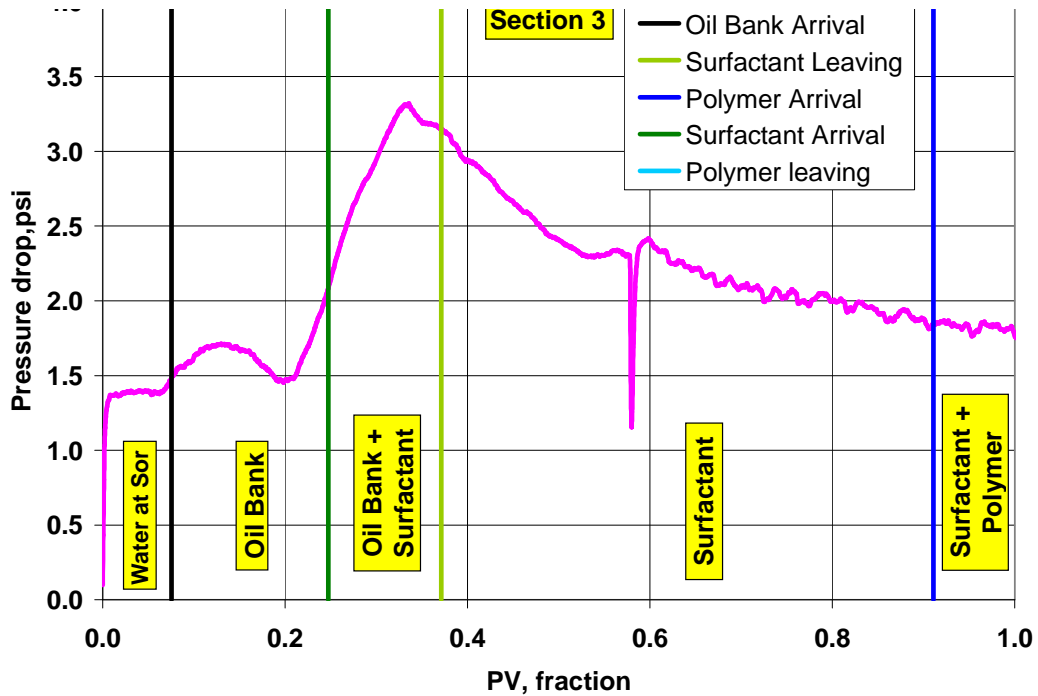


Figure 3.139: Section 1 pressure during ASP T-7 (core#32) with identification of fluid regions using dimensionless velocities and pressure analysis.



**Figure 3.140:** Section 2 pressure during ASP T-7 (core#32) with identification of fluid regions using dimensionless velocities and pressure analysis.



**Figure 3.141:** Section 3 pressure during ASP T-7 (core#32) with identification of fluid regions using dimensionless velocities and pressure analysis.



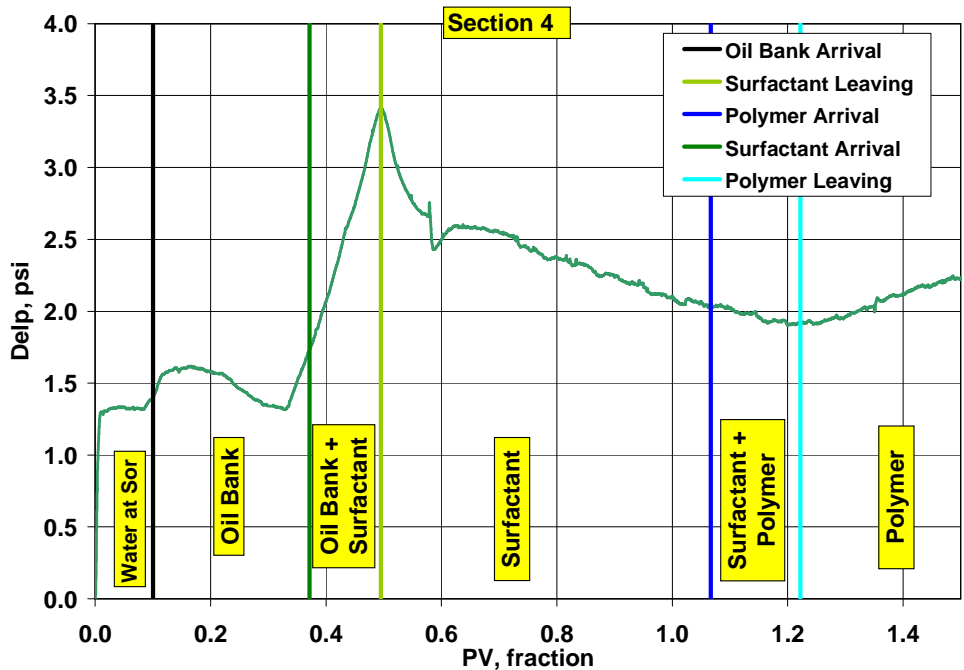


**Figure 3.142:** Section 4 pressure during ASP T-7 (core#32) with identification of fluid regions using dimensionless velocities and pressure analysis.

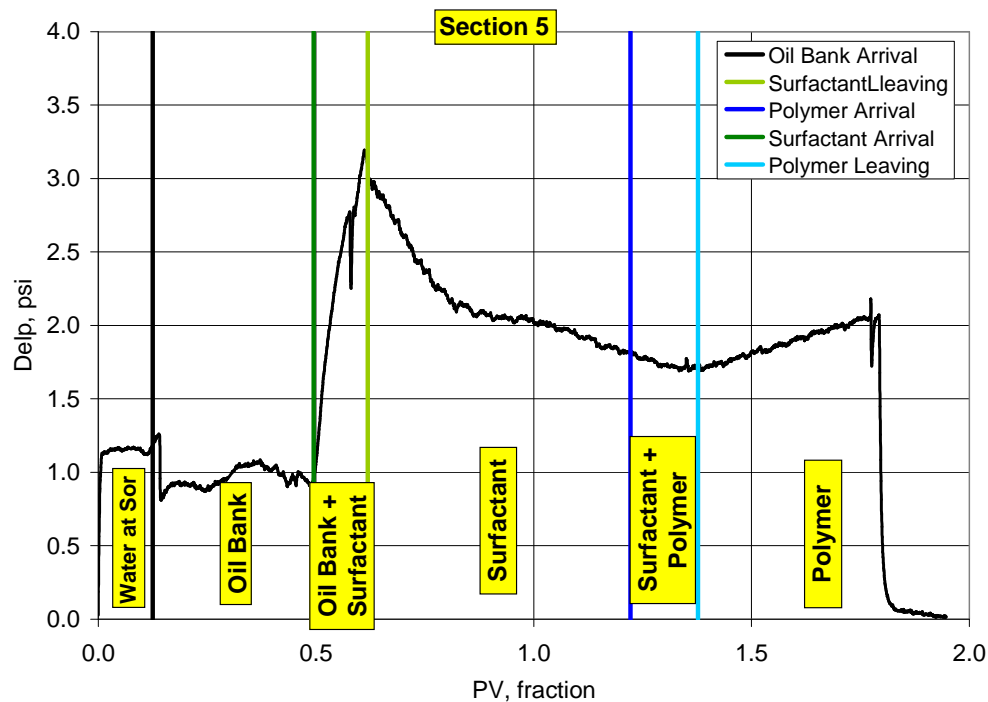


**Figure 3.143:** Section 5 pressure during ASP T-7 (core#32) with identification of fluid regions using dimensionless velocities and pressure analysis.

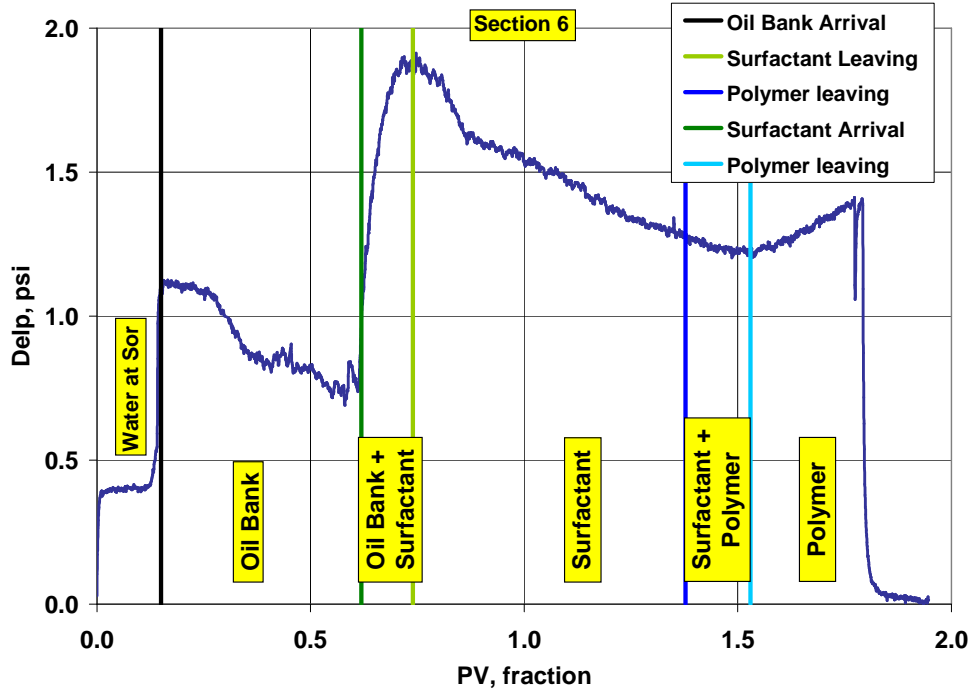


**Figure 3.144:** Section 6 pressure during ASP T-7 (core#32) with identification of fluid regions using dimensionless velocities and pressure analysis.

Formulation X-2 and X-3 were tested once with a 0.3PV surfactant slug size. Only formulation X-3 was tested with 0.6PV slug size, two times. 0.3 PV surfactant slug size gave low oil recoveries ranging between 60%-62% and very high pressure drop across the core reaching 16-20 PSI range at 2 ft/day flow rate for both formulations. 0.6 PV slug size gave improved recovery up to 82% of residual oil for formulation X-3, still lower than formulation X-1. The percentage of oil recovered in oil bank was still low, 57% and 60% for the two floods with 0.6 PV slug size. Pressure drop across the core was in 12-14 PSI range with 0.6 PV slug size, still higher than formulation X-1. It was concluded that lower surfactant concentration in formulations X-2 and X-3 gave lower oil recovery and higher pressure drops compared to formulation X-1. Residual oil was trapped in wedge shape in Core #31 and Core #32, both of which were tested with Formulation X-3. The trapping could not be attributed to gravity override as the gravity numbers calculated for both runs were insignificant. In Core #31, wedge was attributed to dual permeability in core, and in Core #32, the wedge was simply attributed to inefficient surfactant slug.

## **Chapter 4**

### **Reservoir Studies**

Engineering and geological data for each of the ten reservoirs were collected and analyzed. Geological reports for eight of the reservoirs, representing nine leases, are presented in the Appendix. A summary of these reports that evaluates the reservoirs potential for chemical flooding is presented in the following section. Reservoir simulations were conducted for the Trembley Oilfield. Results of history matching the performance of primary and secondary production and prediction of a chemical flooding application in the Trembley oilfield are presented. In the last section of this chapter, economic estimates of chemical flooding applications are presented.

#### **Summary of the Geological Evaluation of Selected Reservoirs for Chemical Flooding**

Geology of the subject reservoir presents a fundamental concern in all enhanced oil recovery processes. At an overriding level for injection EOR processes, of which miscible alkaline-surfactant chemical floods are one, is the drive mechanism, water drive vs. fluid expansion. Injected fluids must raise the pressure to drive oil from the injection wells to the producing wells. Injection-based recovery methods thus require a closed trap with little or no water invasion during production. For this reason, investigators in this project believed that fields that had been successfully waterflooded, where the aim is also to raise field pressure, would be likely candidates for chemical floods.

For chemical floods, key additional questions are the configuration and lithology of the oil reservoir, the amount of remaining oil, and the heterogeneities of fluid saturation, porosity, and permeability across the trap. Here the concerns are fluid-rock interaction, sweep efficiency at a both micro and macro level, and total economic return on the project.

This project was designed to demonstrate feasibility of chemical floods to small, independent operators, especially those in Kansas and surrounding states. As described in the overall report, the first step was to evaluate several fields that might be candidates for chemical floods and to select from among them one or two that might be suitable for a field demonstration project. With two criteria in mind, i.e. small fields that are potentially suitable for chemical flooding, the investigators of the project contacted several of the larger firms that operate in Kansas and asked them to nominate properties for study.

Through this process, ten properties were identified, two of which were contiguous parts of a single filled valley. The candidate fields represented 5 different combinations of stratigraphic intervals and reservoir types: the Middle Ordovician Simpson Sandstone where the reservoir pinches out against an unconformity in an anticlinal structure; a channel sandstone of the Upper Mississippian Chester Stage; a similar sandstone-filled channel of the Lower Pennsylvanian Morrowan Stage or perhaps the Atokan Stage; the Middle Pennsylvanian Cherokee Group sandstones of eastern Kansas; and the several limestone beds of the Cherokee Group, Marmaton Group, and Lansing-Kansas City interval (LKC) of Middle and Late Pennsylvanian age. Much of the production from each of those stratigraphic units in Kansas is by waterflood.

Geological studies were intended to complement the laboratory studies to identify candidate fields for a demonstration project. They used data provided by operators and that publicly available to summarize the lithology, configuration, petrophysics, and production history of the fields in question. Design of the geological studies anticipated that future implementation of a field demonstration would require further characterization of the reservoir rock itself, petrophysics, numerical modeling of the production characteristics of the fields, and tests of injectivity and fluid pathways within the reservoir before implementation of an actual field demonstration.

**Methods.** Operators provided well logs, either digital or raster; drill-stem tests; production history data, ideally of oil, gas, and water on a well-by-well basis; and any earlier reports of engineering or petrophysical analysis. The Kansas Geological Survey (KGS) website posts reports and logs for all wells in Kansas, tabulates picked tops for wells, even those where geophysical logs are unavailable, and provides production history of all oil leases. For the Stewart Field in particular, data were available from studies conducted by the KGS and KU's Tertiary Oil Recovery Project (TORP; Green et al., 2000).

Many of the fields studied had complex histories of ownership and efforts to optimize production. The records provided by the companies or the reports on the KGS website may not reflect the full history of ownership, but they were sufficient to identify the current operator. Commonly, it was necessary to interpret the patterns of production and the history of individual wells or leases to determine when waterflood operations began.

Well data, such as locations, depths, spud or completion dates, elevations, tops, and logs were entered into Petra™, a subsurface GIS program that was granted by IHS to the Department of Geology at the University of Kansas for educational and research purposes. Most wells had logs that showed curves for natural gamma ray, neutron response, and deep resistivity; the so-called RAG logs. Some wells had more modern dual porosity logs and multiple curves for resistivity. Formation tops, whether from the KGS or interpreted from logs, were used to make structural contour maps in Petra of the reservoir itself or an appropriate horizon that mimicked the configuration of the producing interval. Porosity and fluid saturations were determined for most fields from digitized logs. Thickness of the productive interval was determined using the logs and cut-offs of about 8% porosity and 50% oil saturation. Production data from the operators was supplemented by that from the KGS website.

Two cores were available for the Mississippian sandstone-filled channel in the Pleasant Prairie field, where two firms operate adjacent properties. Fortunately, the core reports were available. After matching the core depth to the log depth, plots of core porosity vs. core permeability along with study of the cores themselves permitted recognition of several lithofacies within the cores, and characterizing their petrophysical relations. Subsequently, it was possible to use data from the cored wells to establish a firm relationship between porosity measured on logs with that measured on the cores for the several lithofacies. This relationship, along with log character, was used to determine the lithofacies at 0.5' intervals in each of the logged wells and estimate the permeability at each well. This process was conducted on a stochastic basis and involved using a neural network (Senior, 2012).

With measurements of porosity and fluid saturations, and with statistical characterization of lithology and permeability at each well in the sandstone-filled channel in the Pleasant Prairie field, multiple realizations of the distribution of petrophysics and saturations throughout the field were calculated with Petrel, which was provided by Schlumberger, Inc. Accuracy of those realizations was checked against the original oil in place estimated by volumetric means and well-by-well production (Senior, 2012). On-going numerical modeling studies by other investigators of the reservoir will ultimately determine the distribution of remaining oil in place.

For the Stewart field, the analysis was based upon information from the website, from the operator, PetroSantander, from the KGS database, and from earlier reports (Green et al., 2000) without making maps or measuring petrophysical properties.

**Results.** The eight fields were described in individual reports that were submitted as part of the quarterly reports on this grant, and are attached as an appendix to the report. Additional information has become available for some of the fields after the time they were first examined by participants in the project. That new information is included where it was drawn upon. Some of the fields proved to be inappropriate for chemical flooding, while others are suitable, but of lower priority, as indicated in the discussion below. Key features of each field are summarized in **Tables 4.1 and 4.2.**

**Beaver Creek Field.** Beaver Creek oil field is a small field, 3 producing wells and one injector, in Rawlins County, Kansas. It produces from grainstone of the J-zone of the Kansas City Group, but there are significant shows in or production from other units in field wells and in other wells nearby, specifically the D and G zones of the Kansas City Group. The field lies on a NNE-directed anticlinal nose on the flank of the linear NNW-SSE anticline that underlies the Wilhelm, Wilhelm East, Wicke, and Kompus fields 3 to 5 miles to the west. While the anticlinal nature of the nose is obvious to the north, east, and south, it could not be determined whether the field has closure to the SW onto the anticline because of sparse well control. The operator indicates that 3D seismic is available for the area, however, the fine-scale structure is not completely defined (Bill Horigan, personal communication, 2010). Careful material balance would also reveal the scale of the accumulation.

The field was discovered in 1993 and has produced 184,518 bbls of oil through 3/2012. Production peaked at 17,800 bbls/year in 1997. It declined to 8038 bbls in 2000 before the waterflood was installed in 2001, which raised production to 12,762 bbls in 2002. Production has since declined, reaching 4636 bbls in 2011, the last year for which full production figures are available at the KGS website. The waterflood has been successful, but not spectacularly so, perhaps because it was installed while potential primary production remained.

The field is a potential target for chemical-flood enhanced recovery. Ambiguities about its volume may be resolved by straightforward geophysical and engineering studies. Like so many other fields in the Lansing-Kansas City interval, it is a successful waterflood, and would be a

**Table 4.1 - List of selected properties, their location, and current operators.**

Field or Unit Name	Lease Names	Location:		Date of Discovery	Current operator
		County	Legal		
Beaver Creek field	Wahrman 'B', Wahrman 'E' 1, Wicke (injection only)	Rawlins	1S-32W: S/2 25, N/2 36.	7/13/93	Vess Oil Corporation.
Celia South unit. Includes parts of Celia and Celia South fields unitized for production from a limestone bed in the Cherokee Group.	Celia South waterflood unit, Hubbard (KS Dept of Revenue lease code 120082), Hubbard (119845), Hubbard (120791), Officer, Powell 'A', Fisher 'V', Fisher 'K', Hubbard-Powell, Kehlbeck 1-D	Rawlins	3S-36W: SW 27, S/2 28, SE 29, 32, N/2 & SW 33; 4S-36W NE 5.	8/4/83	Murfin Drilling Co.
Missouri Flats Waterflood Unit	Beesley B Coberly II, Coberly T, Coberly JJ, Coberly U & Missouri Flats NE Unit.	Gove	T14S R28W: S/2 S/2 16, N/2 & N/2 SE 21, NW & N/2 SW 22.	Missouri Flats NE: 12/1973; Missouri Flats NW: 8/20/1975. First well in waterflood unit: 6/18/75.	Merit Energy Corp. sold to Cisco Operating, LLC on 7/1/2010.
Muddy Creek southwest unit (includes Muddy Creek SW and Bruce East oil fields).	Bush, Erbs, & Muddy Creek SW unit.	Butler	T29S R4E: E/2 & SW NW, W/2 & NE SW 26, E/2 SE 27, NE & N/2 SE 34, E/2 NW & NW SW 35.	Muddy Creek SW: early 1981; Bruce East: May 1983. First well in current waterflood unit: 9/25/1981. Waterflooding began in 1987.	Stelbar Oil Corp., Wichita.
Pleasant Prairie field: Chester waterflood unit and Pleasant Prairie Chester unit.	Mary Jones, Federal, Jones, Kuhn, KC Feedlot, Snyder, Moody, Engler.	Finney & Haskell	T27S R34W: parts of Sections 3, 10, 15, 22, & 27		Cimerex and OXY, USA.
Stewart field	Many	Finney	T22S R31W: SE 35; T23S R30W: SW 5, 6, N/2 & SW 7, NE 8; T23S R31W 1, 2 S/2 & NE 3, S/2 4 NE 9, N/2 & SE 10, 11, N/2 & SW 12.	Sandstone reservoir was discovered in 1967.	PetroSantander (USA)
Tobias Simpson waterflood unit	Tobias Simpson waterflood unit.	Rice	T20S R9W: SE 23, SW 24, S/2 & NW 26, E/2 and E/s SW 26, S/2 & NE 35, 36; T21S R9W 2, 3, N/2 & E/2 SE 10, 11.	1961	Berexco, LLC
Trembley field	Trembley leases in section 27 and 34, Trembley 'A' and Trembley 'B'	Reno	T24S R8W: SW 27, W/2 & W/2 NE 34. Trembley Unit includes SW 27 and all of 34 in 24S 8W.	1978	Berexco, LLC.
Woodhead unit within the Vinland field	Woodhead	Douglas	T14R R20E. Vinland Field is S/2 3, 10, S/2 11, N/2 14, E/2 15. Woodhead unit: NW 14.	KGS reports first wells in field in 1983; lease drilled out in 1984-85.	Colt Oil Co.

**Table 4.2 - Stratigraphy, Traps, and waterfloods on selected properties**

Field Name	Producing Unit Stratigraphy	Producing Unit Lithology	Trap structure	Production (bbls, latest available figures, KGS)	Waterflood installed	Waterflood response
Beaver Creek field	Kansas City Group, J zone. Other zones have shows of oil.	Limestone, intergranular to vuggy porosity	Small anticline or nose off larger structure.	184,016 through 2/12	2001	Favorable: ~50% increase.
Celia South unit. Includes parts of Celia and Celia South fields unitized for Lansing B production.	Cherokee, & Marmaton groups & Lansing Group, B-zone. Waterflood the Cherokee Group.	Bioclastic grainstone.	Local anticline. May have several culminations.	2,182,083 through 2/12	1990	Very favorable: Nearly 600% increase from trough (1989) to peak (1991).
Missouri Flats Waterflood Unit. Includes parts of the Missouri Flats NE and NW fields.	Kansas City Group, I, J, K, and L zones.	All zones are limestone. I: fossiliferous LS with intercrystalline porosity. J: Oolitic to oolmolitic LS., K: fossiliferous, "reefy" LS with intercrystalline porosity; L: fossiliferous and oolitic LS.	ESE-plunging anticlinal nose with subtle separate closures.		1981	Very favorable, ~700% increase with waterflood.
Muddy Creek southwest unit.	Cherokee Group sandstone, listed as Bartlesville (Bluejacket in KGS stratigraphy), but probably Cattlemans	Friable, micaceous, coarse- to fine-grained sandstone in a fining-upward succession. Limy with black shale streaks.	Elongate, linear sandstone fills valley incised into earlier units and extends NNE beyond edge of unit. Slopes down to the SSW.	1,221,840 through 2/12	February 1987	Waterflood response was visible, but not pronounced.
Pleasant Prairie field	Chesterian Stage rocks of the Hugoton Embayment.	Sandstone in incised valley fill.	Stratigraphic & unconformity: Valley walls define limit of porous sandstone; up dip the pre-Pennsylvanian unconformity truncates the valley fill & Morrowan shale beds provide the seal.	52,171 bbls in 2011, last full year of data. Total production to date: 4,472,501 bbls through 2/2012.	1999	This field has been an excellent waterflood.



**Table 4.2 - Stratigraphy, Traps, and waterfloods on selected properties**

Field Name	Producing Unit Stratigraphy	Producing Unit Lithology	Trap structure	Production (bbls, latest available figures, KGS)	Waterflood installed	Waterflood response
Stewart field	Morrowan Stage (Lower Pennsylvanian). Some argue that it is actually part of the Atokan Stage. Also produces from the Mississippian St. Louis Limestone.	Sandstone in incised valley fill.	Geomorphic and unconformity trap: sides defined by walls of incised valley, up-dip truncation against the pre-Pennsylvanian unconformity.		1995	This field has been an excellent waterflood
Tobias Simpson waterflood unit	Arbuckle Group, Simpson Group, Lansing-Kansas City interval. Simpson Group is the target here.	Simpson Group contains beds of shale & sandstone. Sandstone is quartzarenite; shale is sufficiently carbonaceous to be a potential source rock.	Faulted anticline, partially bald headed in the Simpson. LKC production is in band SW and S of main structure.	For entire field 13,221,405 bbls and nearly 2.5 MMM cu ft gas as of 2/2012. Tobias Simpson unit has produced 70131 bbls from 1990 to 2/2012.	Thunderbird Drilling: 1968-1996 Berexco: 1990 to present	Successful waterflood.
Trembley field	Kansas City Group L-zone (Hertha Limestone)	Oolitic grainstone with oomoldic porosity.	Anticlinal nose extending SE from larger structure under Morton Field. Reduction of permeability of reservoir rock may limit up-dip migration. Internal permeability barrier cuts off part of the reservoir.	539,357 bbls as of 2/2012; 2011 production: 3714	February 1995	Excellent
Woodhead unit within the Vinland field	Cherokee Group; informally named Squirrel sandstone near the top of the Cabaniss Formation.	Sandstone. Part of a coarsening upward succession, perhaps channel fill at top of a prograding shoreline.	Anticlinal nose.	1563 bbls in 2011. Total: 331,359 as of 2/2012.	1990	Very strong.

good demonstration for a large number of other small fields in Kansas and surrounding states. However, it is placed at a lower priority as a demonstration project for several reasons. Waterflood performance was solid and probably profitable, but not as marked as that in other fields. No cores are available for the field, so that petrophysical information is limited. The pattern, with an injector well on the south supporting a linear arrangement of three wells to the north is not closed, and injected fluids could bleed off to the south. Finally, operators may wish to produce oil from other zones before proceeding with EOR on the J-zone.

***Celia South Waterflood Unit.*** Coastal Oil & Gas Co. first found oil in a bioclastic grainstone bed in the Middle Pennsylvanian Cherokee Group in June 1983. The field lies on a local irregular dome in the broad structural low between the Cambridge Arch to the northeast and the Las Animas Arch to the southeast. The dome has over 20' of structural relief, including at least 15 feet of closure and appears to have several culminations of a few feet. Production in the Celia South Field and the nearby Celia Field (where Lansing B-zone production had begun earlier) rose to 379,105 bbls in 1984. The waterflood for the Cherokee limestone was installed in 1990 by OXY USA, after production had declined to 67,695 bbls in 1989. This was a successful waterflood, with production rising to 383,525 bbls in 1992. Murfin Drilling Co. of Wichita, Kansas, now operates the waterflood unit. In the Celia South waterflood unit total production in 2011, the last year with full data available, was 14,519 bbls and cumulative production through February 2012 is 2,182,083 bbls. Six of the wells in the field were cored and thus provide better petrophysical information than that available for most of the fields considered in this study. These permitted determining the relationship of core permeability to core porosity and then core permeability to log porosity, so that both porosity and permeability could be mapped across the field. Furthermore, using a field-specific value of the Archie exponent  $m$  allowed calculation of the original water saturation in the field more accurately. Generally, the oil saturation declined from high wells to lower ones. Several factors identify this field as a strong candidate for a chemical flood EOR process: The structure and the petrophysics are well defined by numerous wells and several cores, respectively. The field has produced about 29.2% of OOIP through primary and secondary production to date, with the waterflood actually raising production to a level above the highest rate recorded on primary production. A small production increment of 5 to 10% of OOIP could yield nearly half a million to a million bbls, justifying significant investment in installing and operating such a flood. The several structural culminations could be flooded separately, so that the demonstration could be carried out with a small number of wells, if desired. The one factor arguing against using the Celia South waterflood as demonstration is the fact that it is in the limestone of the Cherokee Group. While bioclastic grainstone of the Cherokee probably has similar properties as far as production is concerned as those in the more common grainstone reservoirs of the LKC interval, the results of a demonstration chemical flood in the Celia South unit would have some ambiguity in their application across the several stratigraphic units where grainstone is common.

***Missouri Flats NE Waterflood Unit.*** First production from the Missouri Flats NE field began in 1973; the first wells into the area of the waterflood unit itself were drilled in 1975. The unit was formed and waterflooding began in 2002. The Missouri Flats NE Unit produces from lime grainstones of the I, J, K, and L zones of the Kansas City Group. These units and other grainstones of the Lansing-Kansas City interval are characteristically waterflooded after an

episode of primary production. Limestone beds of the Marmaton Group, and even those of the Cherokee Group in western Kansas, are similar reservoirs. Hence a successful demonstration in this field would have implications for a large number of other oilfields in Kansas, Nebraska, and Colorado.

The trap is a NW-SE-oriented linear structure with a number of culminations and that extends beyond the margins of the waterflood unit itself, so that in the immediate area of the field, a number of other properties could benefit from what is learned from a chemical flood of the Missouri Flats NE unit. There may be variations of permeability along the axis of the play that segment the areas of production. The unit had a strong response to waterflooding, with production increasing from nearly 9900 bbls/year in 2001 to nearly 74,400 bbls/year in 2005 after the waterflood was installed. In 2011, production remained at over 20,400 bbls/year, a level over twice that in 2001. All of these factors suggest that the unit might be a candidate for a proven chemical-injection technique in the future.

On the other hand, several factors mitigate its potential for this demonstration project. The multiple completion zones, with not all wells completed in the same combination of intervals, would make the evaluation of the individual zones subject to considerable uncertainty, and the flow path of any injected fluid might be complex. The effort necessary to characterize the reservoir and that necessary to make any recompletions or other adjustments to production before a demonstration project could begin, would add expense to the project and would likely make the results ambiguous. Furthermore, Merit Energy Co., who operated the field when it was accepted into the project, has since transferred it to Cisco Operating, LLC, on July 1, 2010, adding an additional layer of uncertainty. For these reasons, the Missouri Flats NE Unit is not recommended as a demonstration project even though it is a strong candidate for an alkaline surfactant flood.

***Muddy Creek Southwest Unit.*** The Muddy Creek SW unit produces from 5 producing and two injection wells in Butler County, Kansas. The field lies in the western part of the Cherokee basin, just 2 miles east of the Nemaha fault zone. The reservoir is an elongate, roughly linear sandstone lens that extends from the SSW end of production in the unit to the NNE across the length of the unit and beyond onto an adjacent production unit. Structure contours show the top of the reservoir dipping to the south or south-southwest, so the sandstone lens may extend farther to the SSW just as it does to the NNE. Distribution of oil may be controlled by the elevation of the top of the sandstone bed.

The reservoir sandstone bed apparently truncates the Scammon Coal Bed and the Chelsea Sandstone Bed below it and rests on the Tebo Coal Bed (with an associated black shale bed) of the Cabaniss Formation of the Cherokee Group. The lithology of the reservoir is described as a fining-upwards succession from coarse to fine sand. Core (5 cores) analysis shows that the average porosity is 16.9% and permeability averages 30.9 md. The average water saturation ranged from 27.1 to 40.1% in five different wells when sampled.

The first wells were drilled into the Muddy Creek field in 1981. The maximum rate of production was in 1983, when 176,407 bbls were produced. This rate had declined to 16,040 in 1987, just before waterflooding commenced. Production under waterflood peaked at 70,708 bbls

in 1993 and since has fallen to 6765 bbls in 2011, the last year for which full production statistics are available. Total production from the Muddy Creek SW waterflood was 1,221,840 bbls through February 2012.

Several features of the Muddy Creek Southwest unit indicate that it would be a suitable candidate for an EOR demonstration project of chemical flooding. In eastern Kansas, the part east of the Humboldt fault zone along the east side of the Nemaha uplift, much of the production is by waterflood of linear sandstone bodies in the Cherokee Group. This unit and the example (below) from the Vinland Field are both representative of a large number of operations in the eastern part of the state, in northeastern Oklahoma, and, to a lesser extent, in Missouri. The unit has been a successful waterflood for a quarter of a century. Initial oil saturation averaged about 65 to 70 percent, so despite producing over 1.2 MMbbls of oil, a considerable amount of oil remains. The producing reservoir lies at a depth of 2850 to 2900', generally shallower than the reservoirs of western Kansas. Shallow depth will reduce the costs of any wells drilled in the process of implementing the flood. However, while a demonstration in fluvial reservoirs of eastern Kansas would be useful to the operators in that area, the total volumes of oil production from that unit argue for a demonstration in other stratigraphic horizons.

***Chester Waterflood unit and Pleasant Prairie Chester unit.*** The Chester Waterflood unit and the Pleasant Prairie Chester unit are adjacent production units that produce oil from a Chesterian (Upper Mississippian) sandstone valley-fill deposit. The Pleasant Prairie field is a much larger entity that produces from a large number of stratigraphic units and a large number of leases. These two properties received considerably more attention than the other fields or units that were studied because they had core, 3D seismic, modern well logs, and high production potential. They were the subject of a Master's Thesis (Senior, 2012) and have been also investigated as part of the Kansas Geological Survey's studies of potential carbon use and sequestration in Kansas oil reservoirs (Dubois et al., 2012).

The incised valley fill extends north to south across the SE part of the larger Pleasant Prairie field in T27S R34W Sections 3, 10, 15, & 22. The valley-fill deposit is also the source of oil at other fields, such as the South Eubank, Shuck, and Wide Awake fields along a line that extends across Haskell and Seward counties to the Oklahoma border. Limits to production from this sandstone body in the Pleasant Prairie field are provided by discontinuities within it, the walls of the valley, a down-to-the-basin fault to the south, and the up-dip truncation of the valley fill where it intersects the sub-Pennsylvanian unconformity.

Senior (2012) demonstrated that the valley was filled with fluvial channel and overbank sediments and differs from the fields farther south in the same valley-fill sequence that have a greater influence of tidal processes in their depositional history. Within the reservoir he was able to trace scour surfaces overlain by limestone-clast conglomerates at the base of the succession and at one level near the middle. Other such limestone-clast conglomerates are present, but do not seem to be as continuous. Some areas have a higher concentration of shale and serve to divide the overall succession into two compartments.

Through amalgamated hierarchical clustering of descriptive and log properties in cored wells, Senior (2012) was able to differentiate four lithologies in the valley fill: shale, shaley (basal)

conglomerate, limy conglomerate, and reservoir sandstone. Senior developed core porosity vs. core permeability cross-plots for the different lithofacies he recognized in core. He then demonstrated that core porosity was related to log porosity. He has identified these lithofacies in the wells that are not cored using the properties determined by the statistical analysis. He was then able to define the permeability at each well, based upon the petrophysical correlations. Dubois et al. (2012) have traced the walls of the incised valley in seismic records, so that the extent of the valley fill is defined. Senior (2012) and Dubois et al. (2012) have generated multiple realizations of the distribution of lithofacies and petrophysical properties in the valley fill using the Petrel software package. These have been tested by comparisons to wells that were held out of the modeling process and by comparing modeled and actual production.

Production from the incised valley fill is unitized in two production units, the Pleasant Prairie Chester unit operated by OXY USA, Inc. and the Chester waterflood unit operated by Cimerex. The total production from the two units through February 2012, the latest data available, is over 4,472,000 bbls. During 2011, the last year with full data available, 22,880 bbls were produced in the Chester waterflood and 29,291 bbls in the Pleasant Prairie Chester waterflood for a total of 52171 bbls for the two units together. These values are down from a peak production of 333,720 bbls in 2000 for the Chester Waterflood unit, and 239,284 for the Pleasant Prairie Waterflood unit in 2003.

Several features make the Chesterian valley-filling sandstone in the Pleasant Prairie oil field an attractive target for a chemical flood. It should be pointed out that the Chesterian valley-fill sandstone in the Pleasant Prairie field at least superficially resembles many valley-filling sandstones in the Lower Pennsylvanian Morrowan Stage, or Kearney Formation, of southwestern Kansas and adjacent Oklahoma and Colorado. While Senior (2012) does point out some differences in lithology and petrophysics, the information from an EOR demonstration on the Chesterian valley fill would have obvious relevance to EOR applications in the Morrowan interval. Furthermore, studies of the reservoir have identified its extent and internal structure to a higher degree than any of the other candidates identified in this study. These studies are based on a combination of interpretation of 3D seismic images, on two cores from the field and on modern logs for all of the wells that have been drilled. While beds of less permeable shale and conglomerate subdivide the reservoir sandstone body, the locations of these beds are either determined or predictable. With the potential for generating numerous realizations of the reservoir and other rocks, and modeling the result of an EOR process, it is possible to put statistically valid limits on the costs and returns from an EOR process. This field will probably undergo EOR beyond waterflooding in the future.

***Stewart Field - Morrowan Reservoir.*** Production was established in sandstone of the Stewart field, in Finney County, in 1967, but was not fully developed until 3D seismic identified the incised-valley-filling nature of the reservoir sandstone. Rapid development followed and a waterflood was installed in 1995. The channel-fill has generally been correlated to the Morrowan Stage (or Kearney Formation), but the KGS website identifies its age as Atokan (Late Early Pennsylvanian).

The valley is cut through sandstone and shale beds of Early Pennsylvanian age and into Ste. Genevieve and St. Louis limestones of Mississippian age. Production had been established in the

St. Louis in the field area as early as 1952. The incised valley forms a sinuous feature, extending east to west into the Hugoton embayment. The valley is 400 to 650 m wide and extends about 8 km, although the sinuosity makes the actual sandstone reservoir somewhat longer. Reservoir sandstones range from 6 to 13 m thick. The productive sandstone is bounded by less permeable rocks on either side of the incised valley and passes into marine shale at the western end. The overlying seal is of marine shale of Pennsylvanian age. Internally, the valley fill is complex, with at least 3 stages representing cycles of inundation and erosion owing to relative changes of sea level.

After discovery in 1967, the Morrowan reservoir in Stewart field was most rapidly developed beginning in 1985. After peaking in 1991 at 794,653 bbls, primary production declined to 172,059 bbls in 1995. Waterflooding began in 1995 and production peaked at 998,603 bbls in 1999, showing that this project has been a very successful waterflood. Morrowan production was 104,181 bbls in 2010, and total production from the Morrowan in the field stood at 9,833,207 bbls at the end of 2011.

This field has been extensively studied. Green et al. (2000) report the effort of the KGS and the Tertiary Oil Recovery Project to characterize the field for waterflood. Montgomery (1996) was a report to industry of an important development of exploration and production in the US Mid-continent.

This field has many advantages both as a potential demonstration project for a chemical flood and as an operational EOR project. The first advantage is the extensive data observations that are available for the field. Second, Stewart field has been an excellent waterflood, exceeding the predicted ultimate recovery. Third, it is a type of reservoir that is common in southwestern Kansas and adjacent Colorado: an incised valley filling sandstone. It is likely that this field will undergo enhanced oil recovery in the future, either with CO<sub>2</sub> or an alkaline surfactant.

***Tobias Field.*** The Tobias field is an older field (discovered October 1961) in Rice County that produces from the Lansing-Kansas City interval (LKC), the Pennsylvanian basal conglomerate, the Simpson Group, and the Arbuckle Group. Brewer (1965) provides a nice summary of the structure, stratigraphy, and early history of the Tobias Field. The structure is a faulted anticline, partially baldheaded in the Simpson. Arbuckle production has been strongest on the crest of the anticline and in nearby areas. Conglomerate production comes from the east flank of the field. LKC production is limited to the southern and southwestern part of the field where dips define slopes outward from the flanks of the more pronounced core of the field. Simpson production is from some wells on the crest of the anticline and also from wells off the main structure.

Because the Arbuckle Group displayed a strong water drive, and the Simpson sandstone reservoirs produced by gas solution and fluid expansion drive with some water drive, the two zones were not comingled. In fact, wells were twinned if both Arbuckle and Simpson production was present at their location. The Simpson reservoir was waterflood beginning at least as early as 1968. The current waterflood under consideration is the Tobias Simpson unit, operated by Berexco, LLC, of Wichita. That unit has produced 70,000 bbls of oil since 1990 and in 2011 produced 4950 bbls from 5 wells.

The Tobias Simpson Unit in the Tobias field was not analyzed further because preliminary examination of the data indicated that the distribution of productive wells precluded a demonstration project without drilling additional wells, thereby greatly raising the cost of any demonstration.

***Trembley Field.*** The Trembley field lies on an anticlinal nose extending SE from the large dome that forms the Morton, Morton Southeast and Trembley North fields in T24S R8W in Reno County, Kansas. The field displays closure to the northeast, southeast, and southwest, but not to the northwest. Here either the well control is inadequate to define the closure of the structure or the porosity and permeability decline to the northwest. The well control suggests that the porosity indeed decreases to the northwest, suggesting a stratigraphic trap.

A stratigraphic trap is consistent with the nature of the reservoir. The Hertha Limestone Member, or L-zone of the Kansas City Group, is oolitic grainstone. Such grainstone bodies are known to be discontinuous or to display discontinuous patches of porous rock. Here, the individual oolites are dissolved to create oomoldic porosity, ranging up to about 25%, and good permeability. However, development of porosity is not uniform, and a low permeability barrier separates two formerly productive wells from the rest of the field.

After discovery in 1978, the Trembley field produced as many as 72,006 bbls (1979) but production dropped to less than 10,000 bbls in 1984 and 1943 bbls in 1995. Waterflooding raised production to 72,430 bbls in 1997 after only 2 years. It has since declined; 3714 bbls in 2011, the last full year recorded. Total production has been 539,187 bbls as of February 2012.

Grainstones are common reservoirs in the Lansing and Kansas City group in Kansas and, to a lesser extent, in Nebraska. Grainstone reservoirs, or oolitic grainstone reservoirs in particular, are present in the Marmaton, Douglas, and Shawnee groups as well. Consequently a demonstration of alkaline-surfactant flooding in the Trembley field would inform operators of a large number of oil fields. Like many other LKC fields, the Trembley field has been an excellent waterflood. In addition, the data available is excellent, including logs, cores, core analyses, well production records, a field study related to installation of the waterflood and a speculative study of the potential for CO<sub>2</sub> flooding, and much other information. The field is of small enough size to allow a full-field demonstration of chemical flood technology, but large enough to bear the cost of such of demonstration. All of these factors argue that the Trembley Field should be a strong candidate to be the demonstration project for a chemical flood.

***Vinland Field, Woodhead Lease.*** The Woodhead lease in the Vinland Field is a densely drilled-out waterflood of a kind common in eastern Kansas. The wells are on 2 ½ acre spacings (330' or ~100m apart). The field is developed as a series of regular 5-spot patterns, with most injectors surrounded by 4 producers (and most producers surrounded by 4 injectors). The reservoir lies at a depth of 700', so it is at lower temperature and pressure than the other fields described in this report. Low permeability, high viscosity, and low well costs make production on this spacing both possible and desirable.

The Vinland field lies in the southern part of the subtle Forest City basin. Regional dip is to the northwest. The field appears to lie on a slight anticlinal nose that projects to the west. The

productive sandstone lies at the top of the Cabaniss Formation of the Cherokee Group. It is overlain by the Mulky Coal and by the Excello Shale Bed, which is a dark gray, highly radioactive shale that is considered the top of the Cherokee or the base of the overlying Marmaton Group. The sandstone is the top of a coarsening upward succession that might be a delta front or another form of prograding shoreline.

Primary production peaked at 36,202 bbls in 1985, just after the drilling was complete. It declined to 3911 bbls in 1990 as the waterflood was being installed and rose to a peak of 26,397 bbls in 1995.

What is the prospect for this field as a demonstration of the utility of chemical flooding? Clearly, the Vinland Field is a successful waterflood. The waterflood has produced over 13% of OOIP, while primary production produced only about 5.5%. This suggests that 80% or more of the original 1755 M bbls of oil remain in the field as a target for enhanced recovery. Furthermore, a wealth of data is available because wells in eastern Kansas in the past have routinely been cored and the cores analyzed for porosity, permeability, and fluid saturations. Maps of porosity, permeability, and fluid saturation were developed for this field and are included in the report in the Appendix. Despite the abundant core data, logs are not in modern format: Most of the logs for the field are un-scaled gamma-neutron logs upon which quantitative calculations are not easily accomplished. However, on balance, this field and many like it in eastern Kansas may be candidates for proven, low-cost, easily operated enhanced oil recovery techniques as they become available.

The overall reasons not to continue with this field as a demonstration of chemical floods at this time are twofold: It is not representative of a large untapped resource, and production rates and volumes of production from individual fields and particular wells are small. Eastern Kansas has been producing oil since the 1880s and much of it has come from fields similar in some respect to the Vinland field. However, the overall target is small relative to that in the Lansing-Kansas City interval or the Chesterian-Morrowan-Atokan succession of western Kansas. Wells commonly come in at about 10 bbls per day and continue to be produced at 1 bbls per day or less while producing great amounts of water. Good wells produce 25,000 bbls of oil, much smaller volumes than good western Kansas wells.

**Conclusions.** Primary production and waterflooding, or secondary production, can combine to remove about 1/3 or somewhat more or less of the original oil in place in oil fields with fluid expansion drive. A successful waterflood at its economic limit might leave up to 2/3 of the oil in place, trapped behind barriers of interfacial tension and reservoir heterogeneity. Heterogeneities will remain the bane of oil producers, because the macroscopic reduce sweep efficiency but are not predictable or subject to amelioration.

On the other hand, alkaline surfactants can reduce interfacial tension, allowing a higher percentage of oil to be recovered. How much is not clear, and will have to await a series of well-documented demonstrations of well-characterized oil fields. Many of the small oil fields in Kansas where fluid-expansion drive is predominant are ideal subjects for such a demonstration because of the scale of the operations, because many fields that are under waterflood lie near



their economic limit, and because of the potential for technology transfer to other operators in nearby fields.

This study examined fields representing several stratigraphic units in which fluid expansion drive reservoirs are common: the Simpson Sandstone (Tobias Field), Chesterian incised valley fill deposits (Pleasant Prairie field) and the similar Morrowan or Atokan incised-valley-fill deposits of the Stewart field, the smaller incised valley fills of the Cherokee Group in eastern Kansas (the Woodhead lease of the Vinland field and the Muddy Creek SW unit in the Muddy Creek field), and grainstone reservoirs in limestone members of the Cherokee, Kansas City, and Lansing groups in the Beaver Creek oil field, the Celia South Unit, the Missouri Flats waterflood unit, and Trembley field. All of the fields examined were successful waterfloods and are likely to be subject to miscible alkaline-surfactant chemical flooding, if a cost-effective method can be established.

Of the types studied, the incised valley fills of the Chesterian and Morrowan-Atokan and the grainstone accumulations of the Lansing-Kansas City interval are the most productive overall in Kansas. It is recommended that a field from one of those stratigraphic intervals be selected for a demonstration project.

### **Simulation of Chemical Flooding**

Several of the nine fields studied became potential candidates for chemical flood application. Discussions were conducted with the operators and the Trembley field rose to the top as the most immediately available field. The Trembley Oilfield is a good candidate for several reasons – a great deal of data exists for the field in the form of electric logs, core analysis, and previous reports studying alkali-polymer flooding and CO<sub>2</sub> flooding, it is small and is believed to be well-contained, and it showed an excellent response to waterflood.

Computer Modelling Group's (CMG) suite of simulation programs was selected to simulate both the laboratory corefloods and the expected operation of the field. These software tools include IMEX for black-oil simulation, STARS for simulation of chemical floods, CMOST for automated history matching, and RESULTS for post-simulation visualization. The 2010 version of these tools was used.

The general procedure for building simulation models is to develop a geological model that describes the reservoir as a grid that is populated with data for reservoir and fluid properties. Not all of these properties are measured and some must be assumed or extracted from a history match. Relative permeability functions are one example. Geological models were prepared for both the laboratory coreflood and the Trembeley Oilfield.

The coreflood model was used to history match the waterflood in order to determine the relative permeability functions of the core sample. These relative permeability curves are then incorporated into the model and history matching of the chemical flood results was conducted to determine correlation parameters that model the ability of the chemical slugs to mobilize and

displace oil. The correlation parameters determined in the coreflood are used in simulations of chemical floods in the field model.

Simulations using the geological model for the field were performed to history match the historic primary and secondary production data. The history match provided parameters for the relative permeability curves for oil, water and gas. Simulations of the chemical flood in the field are then performed using the correlation parameters for the chemical slugs determined from the corefloods.

**Laboratory Coreflood Simulations.** The laboratory coreflood using Core #2 with the Trembley crude oil was selected for the simulation study. The laboratory setup is described in Chapter 2 and detail experimental results are described in Chapter 3. A square end-section core grid with pore volume identical to the actual round laboratory core was created because the software allows greater flexibility visualizing this arrangement. The end section was 4.5cm on a side and the grid was set to 27.53 cm in length. Since homogeneity is assumed for the core properties no layering was specified. The length was divided into 102 segments. The first and last segments were sized to accommodate the injection and production wells and the 100 central segments were all of the same length. The injection and production wells were modeled using the built-in Tube-End Linear Flow model. Other core properties are summarized in the following **Table 4.3**. Fluid saturation and relative permeability endpoint data are summarized in **Table 4.4**.

**Table 4.3** – Coreflood parameters for simulation runs.

Description	Value	Units
Pore Volume	93.4	ml
Porosity	0.1674	
Permeability to Air	430	mD
Brine Viscosity	0.75	cp
Oil Viscosity	4.06	cp
Surfactant Slug Viscosity	10	cp
Polymer Slug Viscosity	10	cp
Waterflood Flow Rate	0.15	ml/min
ASP Flow Rate	0.15	ml/min
Polymer Slug Flow Rate	0.15	ml/min

**Table 4.4** – Fluid saturations and relative permeabilities of the coreflood that were used for history-matching simulations.

Description	Value
Initial Water Saturation	0.4068
Initial Oil Saturation	0.5932
Relative Permeability to Oil at Residual Water Saturation	1.0
Post-Waterflood Water Saturation	0.6467
Post-Waterflood Oil Saturation	0.3533
Relative Permeability to Water at Residual Oil Saturation	0.0482
Post-ASP Flood Water Saturation	0.9648
Post-ASP Flood Oil Saturation	0.0352

The Trembley oil had a viscosity 4.06 cp at reservoir temperature of 110 °F. Brine properties from the correlations present in the CMG software were used. Rate-time data for oil and water production and water injection were inputs for the simulations.

CMOST history-matching tool was used to determine the relative permeability parameters for the waterflood. Oil production rate and the cumulative oil production were history matched and the results are compared in **Figure 4.1** for the waterflood that is represented in the first 300 minutes on the graph. Although this match is not exact it does represent the general trends fairly well. The relative permeability parameters for the match of the waterflood are given in **Table 4.5**.

Using the parameters determined for the waterflood match, chemical floods were conducted to match the parameters for interfacial tension and capillary number correlations that are used to describe the mobilization of oil by chemical flooding. Oil production for the chemical flood match is shown in **Figure 4.1** where the chemical flood began at 300 minutes. The chemical flood fluid correlations were used for the field simulations.

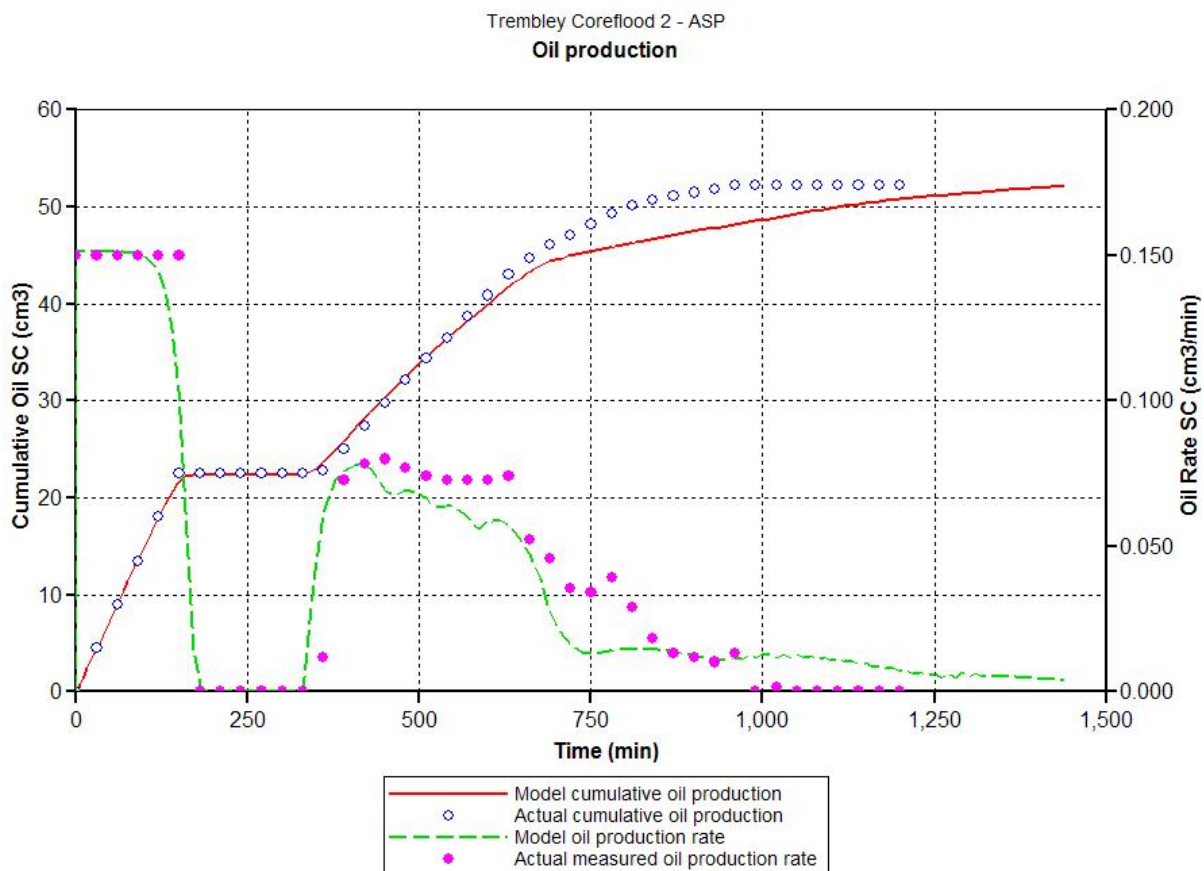


**Figure 4.1** – Comparison of simulated and experimental oil production of coreflood. Water flood between 0 and 300 minutes; Chemical flood from 300 minutes on.

**Table 4.5** – Relative permeability parameters for the coreflood simulations.

Description	Value	Description	Value
Swcon	0.41	Krocw	1.00
Swcrit	0.41	Krwiro	0.048218
Soirw	0.35	Krgcl	0.90
Sorw	0.35	Nw	1.0
Soirg	0.35	No	0.5
Sorg	0.35	Nog	4.0
Sgcon	0.00	Ng	2.5
Sgcrit	0.06		

**Trembley Oilfield Simulations.** A geologic report of the Trembley field is presented in the Appendix. For the purpose of simulation a grid was exported from data stored in IHS’s Petra software representing the physical layout of the reservoir (areal extent and thickness). A permeability barrier is believed to exist separating the southern two wells from the rest of the reservoir. Those southern two wells have since been plugged and will not be available to participate in any future field work. Since those two wells are thought to contribute only to the primary production, are not currently available, and complicate the model without material contribution, they have been eliminated from the model and their production has been eliminated from the appropriate data streams. Porosity and water saturation estimates are available from open-hole electric log interpretation and can be compared with two lab core analyses available from this field. Maps of the geological model of the Trembley Oilfield are depicted in **Figures 4.2 through 4.4** that present the reservoir thickness, porosity and oil saturation. It is apparent from these maps that the southern area has been effectively eliminated by making the porosity and oil saturation zero. The model grid was 116 blocks in both the X and Y direction. No attempt was made to model layers in the thickness of the model so although the thickness is not uniform across the reservoir there are no layers present in the model.

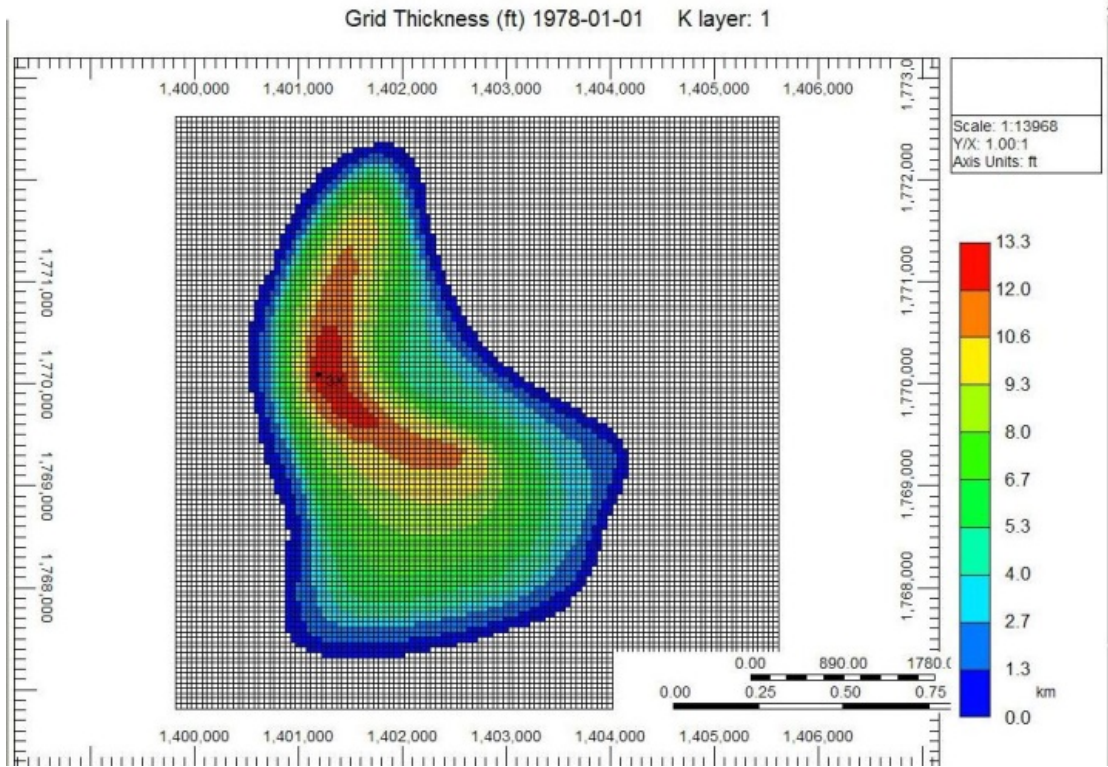


Figure 4.2 – Reservoir thickness of the Trembley Oilfield.

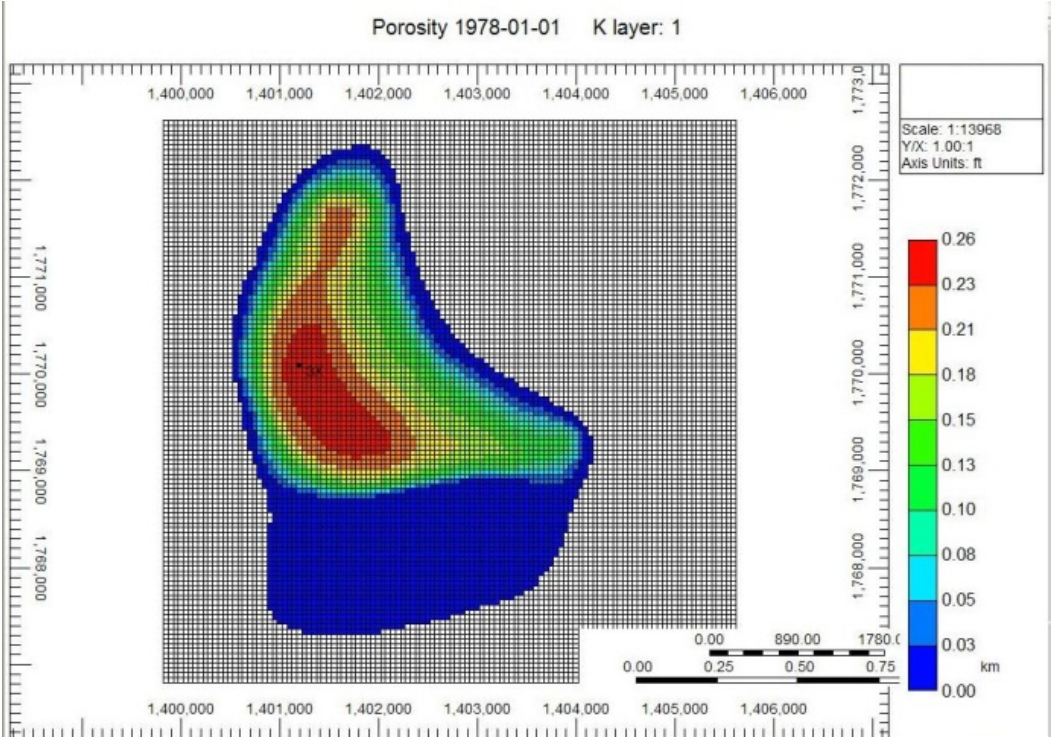
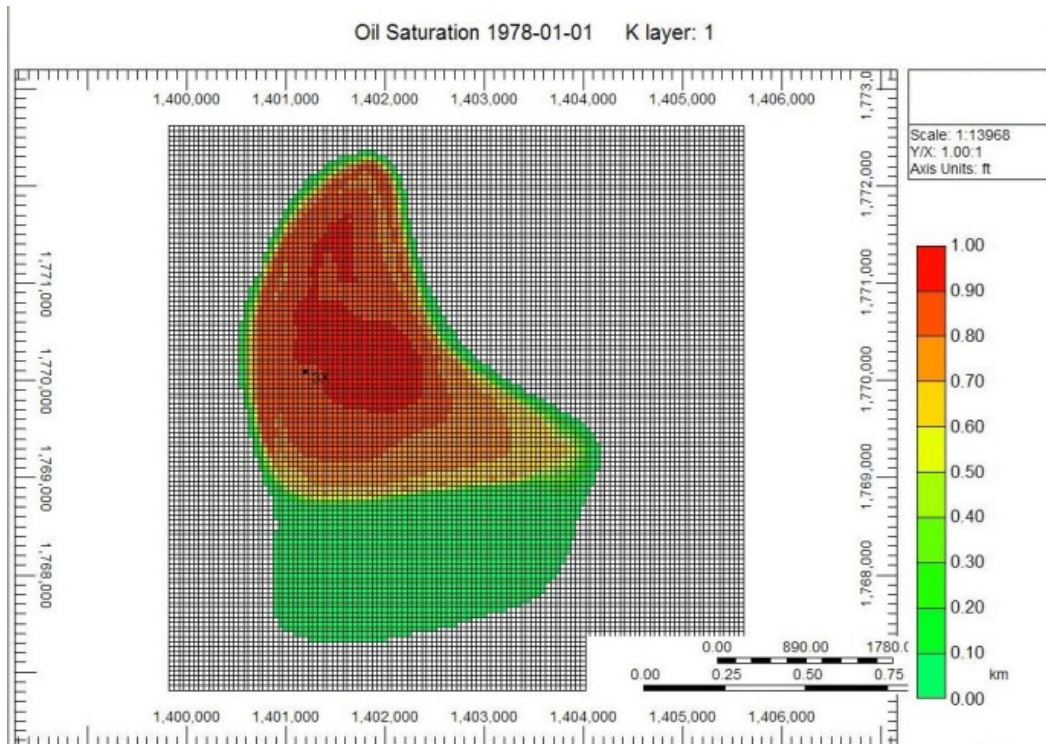


Figure 4.3 – Porosity of the Trembley Oilfield.



**Figure 4.4** – Initial oil saturation of the Trembley Oilfield.

Primary and secondary production data were entered into the model and a CMOST history-match file was created to automatically fit the relative permeability parameters that are presented in **Table 4.6**. Oil production rate and the cumulative oil production for the history match of primary and secondary production is shown in **Figure 4.5**.

**Table 4.6** – Parameters for the relative permeability correlation for the Trembley Oilfield.

Description	Value		Description	Value
Swcon	0.20		Krocw	0.85
Swcrit	0.20		Krwiro	0.75
Soirw	0.20		Krgcl	1.0
Sorw	0.20		Nw	2.0
Soirg	0.10		No	3.0
Sorg	0.20		Nog	0.5
Sgcon	0.00		No	3.0
Sgcrit	0.06			

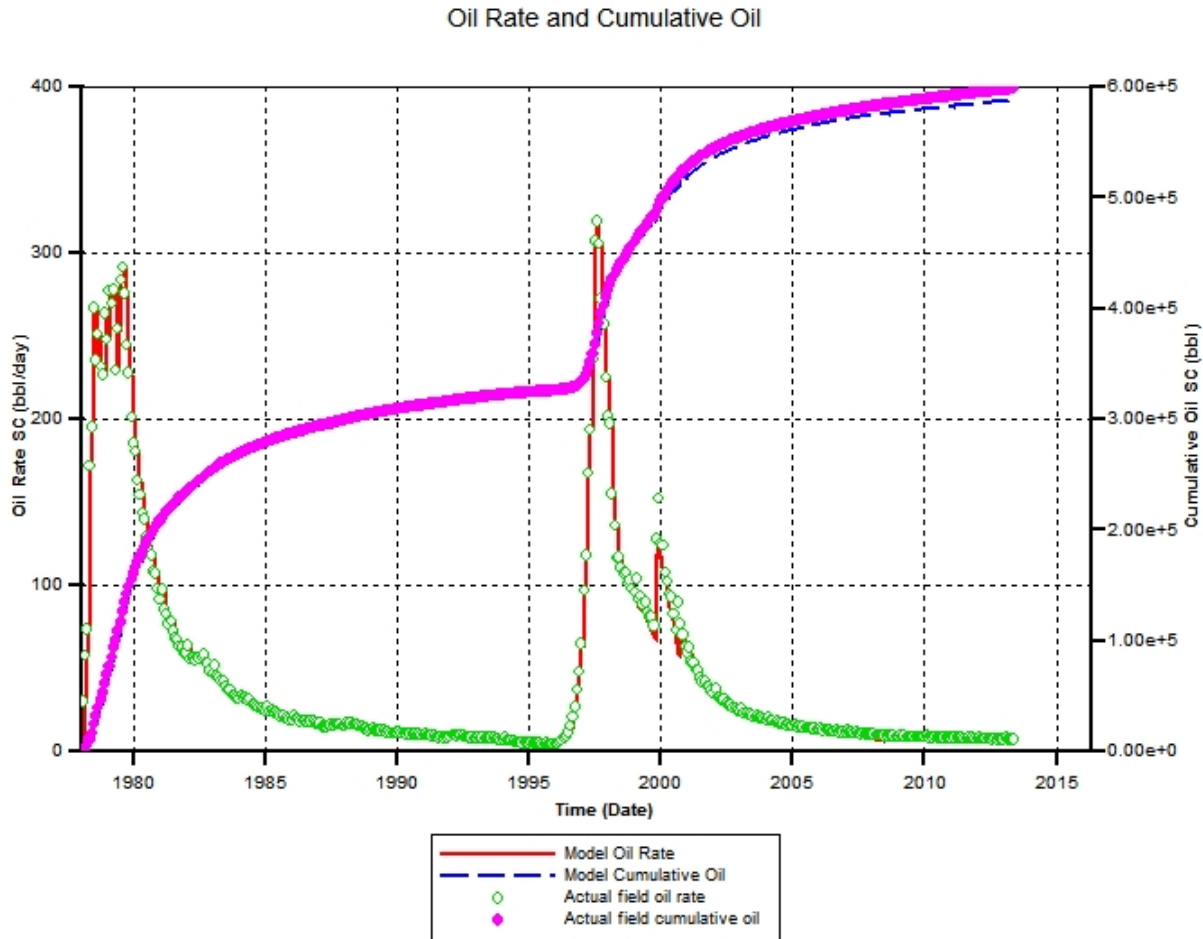


**Figure 4.5** – Comparison of simulated and actual oil production during primary and secondary operations of the Trembley Oilfield.

A chemical flood of the Trembley Oilfield was simulated using the relative permeability parameters from the history match and the chemical slug parameters derived from the coreflood. A chemical slug was injected in the three injection wells for 24 months starting in July 2013. The volume of chemical slug injected was approximately 30% of the reservoir pore volume. The chemical slug was displaced by injection of a polymer drive for 24 months, followed by water injection.

Oil rate and cumulative oil production for the Trembley Oilfield, both historical data and simulation runs are shown in **Figure 4.6**. The simulated chemical flood produced an oil bank but the cumulative amount of oil produced was less than both the primary and secondary operations. The lower oil production during the chemical flood was due to the failure of the chemical slug to mobilize oil in the reservoir away from the injection well. This is shown in **Figure 4.7** where the oil saturation of the reservoir is shown at the end of the simulation. Oil production values from this simulation were used for estimating economics of the process in the following section.

The simulation of the chemical flood is a great tool for designing a chemical flood in terms of visualizing reservoir fluid flow. But it is not without its shortcomings. Incorporation of

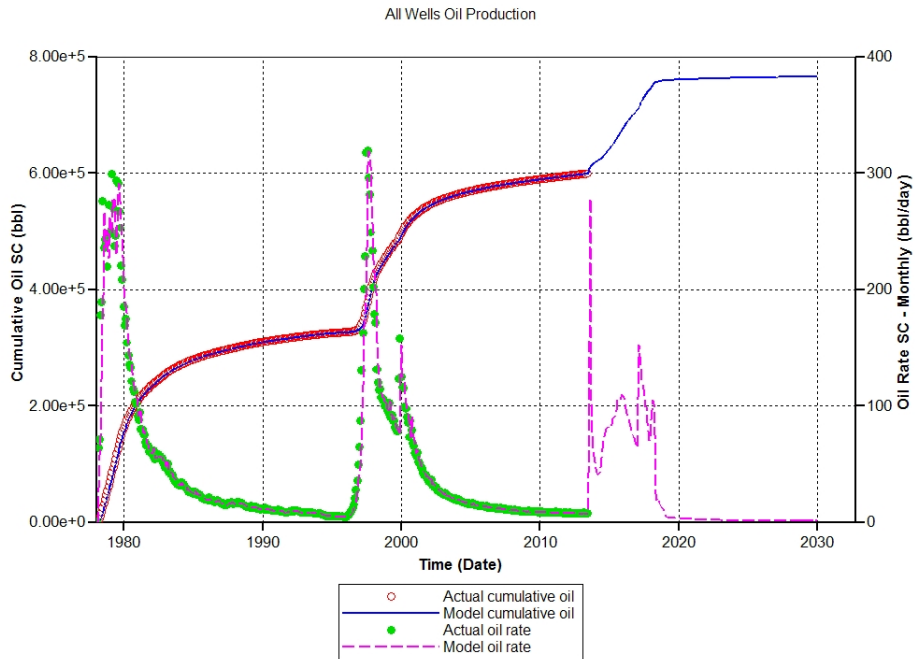


**Figure 4.6** – Oil production of the simulated chemical flood of the Trembley Oilfield. Simulated and actual oil production during primary and secondary operations are shown for comparison.

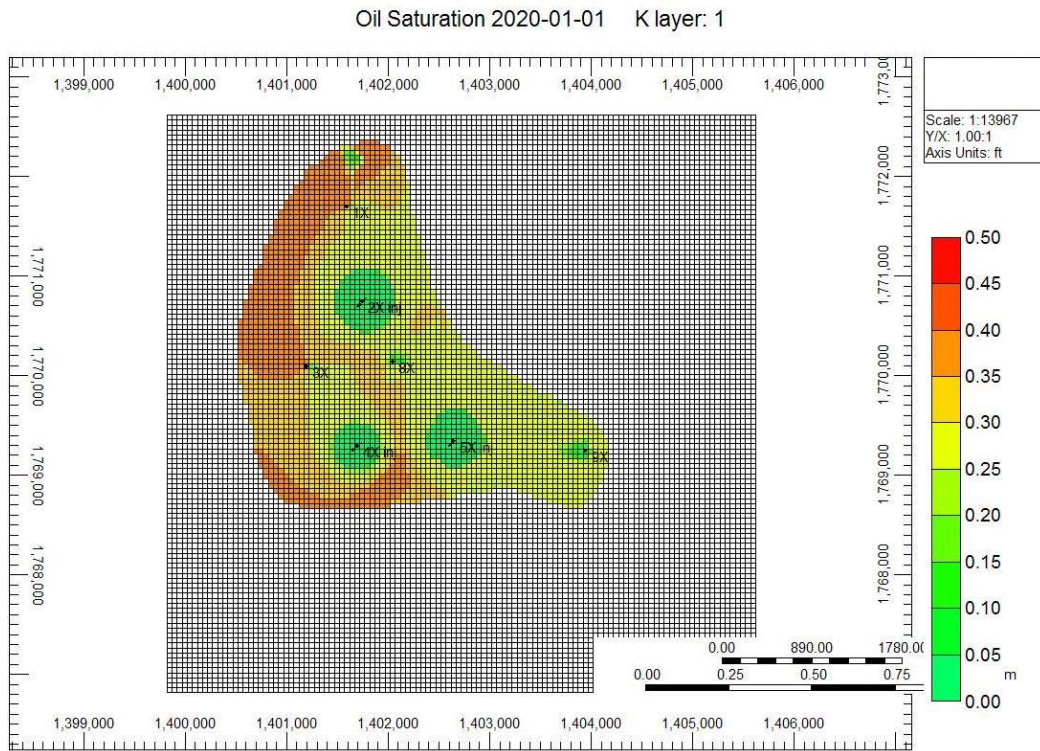


**Figure 4.7** – Oil saturation of the Trembley Oilfield after simulated chemical flood.



additional data like a field tracer study would improve the geological model and history matches of primary and secondary productions. Additionally, correlations for the efficacy of the chemical slug need to be improved which can be accomplished with addition laboratory and field data.

### **Economics of Field Applications of Chemical Floods**

Economics estimates of field applications of chemical floods were prepared in order to determine if a field applications could be conducted with an expectation of economic success. Chemical formulations identified from the laboratory studies, field data that was collected and analyzed, and results from the simulation of the chemical flood were used for the estimates.

***Economic Estimates by Material Balances.*** Chemical costs are the major expense of a chemical flooding application. Capital costs and operating expenses are important and their percentage of the portion of costs is reduced with the size of a project. Initial economic estimates were performed by applying laboratory coreflood data to field scale to determine the magnitude of the investment (chemical costs) required for field applications. Economic evaluations are estimated using the *chemical costs per barrel of oil produced* result.

A spreadsheet was developed to perform material balance and economic calculations. A print of a portion of the spreadsheet is shown as **Table 4.7** for seven of the oilfields in this study. Field data was analyzed to determine reservoir volumes and historic oil saturations. Laboratory results for the chemical formulations and oil recoveries were used for chemical flooding. Unit chemical costs and oil price are given in **Table 4.8**.

**Table 4.8** – Unit chemical costs for economic evaluations.

Surfactant (\$/lb)	3.25
Alcohol (\$/lb)	1.50
Alkali cost (\$/lb)	0.40
Polymer cost (\$/lb)	1.75
Gross Oil Price (\$/bbl)	80.00

Chemical costs per barrel of oil recovered ranged from \$17 to \$40. Lower oil recoveries from the chemical flood or low oil saturations calculated after waterflooding were the cause of the higher values. The magnitude of these results for several of the oilfields that range from \$17 to \$24 indicates that a chemical flood would likely be an economic success. This conclusion requires the chemical flood to technically successful. Improved economics can be achieved by optimizing the chemical formulations. Other surfactants could reduce chemical loadings, particularly by reduction of the alcohol concentrations that were required for the systems formulated in this study.

Results of successful field applications are not publicly available. Pilot floods are needed to test and improve technical issues of chemical flooding applications. A second spreadsheet was developed to determine the magnitudes of investment required to test chemical flooding in a

**Table 4.7 – Economic estimates of field application of chemical flooding.**

Field name	Trembley	Beaver Creek	Celia South	Pleasant Prairie		Vinland	Muddy Creek SW
Gross Pore Volume (bbl)	2,025,800	313,814	9,937,700	18,082,000	6,648,800	1,241,250	4,777,146
Initial Oil Saturation	0.90	0.90	0.70	0.75	0.90	0.85	0.63
Original Oil in Place (bbl)	1,823,220	282,433	7,004,091	13,561,500	5,983,920	1,055,063	3,015,669
Primary Production (bbl)	350,500	47,450	754,000	449,850	395,190	109,091	412,269
Remaining Oil Saturation	0.73	0.75	0.63	0.73	0.84	0.76	0.54
Waterflood PV (bbl)	1,038,300	208,000	6,558,882	11,497,500	4,227,650	827,500	2,834,373
Available Oil (bbl)	754,825	155,750	4,125,060	8,337,086	3,553,603	630,648	1,544,648
Secondary Prod. (bbl)	234,800	56,600	1,395,750	2,022,000	1,461,100	216,145	671,806
Remaining Oil (bbl)	520,025	99,150	2,729,310	6,315,086	2,092,503	414,503	872,842
(Saturation)	0.50	0.48	<b>0.42</b>	0.55	0.49	0.50	<b>0.31</b>
Chemical System:							
Surfactant %	1.00	0.50	0.50	0.50	0.50	0.50	0.50
Alcohol %	1.38	1.75	2.00	1.75	1.75	2.00	2.00
Alkali %	1.0	1.0	1.0	1.0	1.0	1.0	1.0
Chemical Slug size (PV)	0.30	0.60	0.60	0.60	0.60	0.60	0.60
Polymer ppm	2,250	2,000	2,500	2,500	2,500	2,500	2,500
Lab Oil Rec (	0.88	0.97	0.77	0.98	0.98	<b>0.50</b>	0.99
Est. Volumetric Sweep	0.80	0.80	0.80	0.80	0.80	0.80	0.80
Saturation at the end of Tertiary recovery	0.15	0.11	0.16	0.12	0.11	0.30	0.06
Tertiary Oil recov. (bbl)	366,098	76,940	1,681,255	4,951,028	1,640,522	165,801	691,291
Surfactant Required (lb)	873,439	174,974	5,517,461	9,671,925	3,556,383	696,109	2,384,331
Alcohol Required (lb)	1,200,978	612,408	22,069,846	33,851,736	12,447,340	2,784,438	9,537,324
Alkali (lb)	873,439	349,947	11,034,923	19,343,849	7,112,766	1,392,219	4,768,662
Polymer Required (lb)	655,079	116,649	4,597,884	8,059,937	2,963,652	580,091	1,986,943
Surfactant cost	2,838,675	568,665	17,931,750	31,433,755	11,558,244	2,262,355	7,749,076
Alcohol cost	1,801,467	918,612	33,104,768	50,777,604	18,671,010	4,176,656	14,305,986
Alkali cost	349,375	139,979	4,413,969	7,737,540	2,845,106	556,888	1,907,465
Polymer cost	1,146,388	204,136	8,046,298	14,104,890	5,186,392	1,015,160	3,477,149
Total Chemical Costs	6,135,906	1,831,392	63,496,785	104,053,789	38,260,752	8,011,059	27,439,677
Oil Revenue (0.875 WI)	25,626,849	5,385,802	117,687,849	346,571,940	114,836,554	11,606,075	48,390,345
Gross Profit	19,490,943	3,554,411	54,191,064	242,518,151	76,575,802	3,595,016	20,950,669
chemical cost / bbl recovered	16.76	23.80	37.77	21.02	23.32	48.32	39.69
Ratio of Est Gross Profit to Total Chemical Costs	3.18	1.94	0.85	2.33	2.00	0.45	0.76

pilot, or demonstration, project. A print of that exercise is shown in **Table 4.9** for a flood pattern in the oilfields where the opportunity to conduct a project was indicated through discussions with the operating oil producers. Chemical costs for a full-pattern flood in these reservoirs are too high for an oil operator to embrace for testing purposes. Improved designs with lower chemical loadings, partial-pattern flooding and/or government assistance will be required for testing chemical flooding in Kansas.

**Table 4.9** - – Economic estimates of pilot application of chemical flooding.

Oilfield	Trembley	Beaver Creek	Celia South	Pleasant Prairie -OXY	Vinland
∅·h·A (ac-ft)	67.45	26.81	54.00	240.53	8.25
Pattern Pore Volume (bbl)	523,268	208,000	418,921	1,865,950	64,000
Remaining Oil Sat (C13)	0.50	0.48	0.42	0.49	0.50
Chemical System:					
Surfactant (%)	1.00	0.50	0.50	0.50	0.50
Alcohol (%)	2.00	1.75	1.75	1.75	2.00
Alkali (%)	1.0	1.0	1.0	1.0	1.0
Chemical Slug size (PV)	0.30	0.60	0.60	0.60	0.60
Polymer (ppm)	2,250	1,800	3,500	2,500	2,500
Lab (microscopic) Recovery	0.88	0.97	0.77	0.98	0.50
Estimated Volumetric Sweep	1.00	0.80	0.80	0.80	0.80
Avg saturation at the end of Tertiary recovery	0.06	0.11	0.16	0.11	0.30
Tertiary Oil recovered (bbl)	230,626	76,940	107,383	724,074	12,823
Surfactant Required (lb)	550,230	174,974	352,404	1,569,674	53,838
Alcohol Required (lb)	1,048,846	583,686	1,175,566	5,236,186	205,253
Alkali (lb)	1,397,584	888,868	1,790,214	7,973,944	273,498
Polymer Required (lb)	123,802	62,991	246,683	784,837	26,919
Est Surfactant cost (\$)	1,788,247	568,666	1,145,314	5,101,440	174,974
Est Alcohol cost (\$)	1,573,269	875,529	1,763,349	7,854,278	307,879
Est Alkali cost (\$)	559,033	355,547	716,086	3,189,577	109,399
Est Polymer cost (\$)	216,653	110,234	431,695	1,373,465	47,108
Total Chemical Costs (\$)	4,137,202	1,909,975	4,056,444	17,518,761	639,361
Est Oil Revenue (0.875 WI)	16,143,843	5,385,811	7,516,812	50,685,191	897,633
Est Gross Profit (\$)	12,006,642	3,475,836	3,460,367	33,166,430	258,272
chemical cost (\$/ bbl oil)	17.94	24.82	37.78	24.19	49.86
Ratio of Est Gross Profit to Total Chemical Costs	2.90	1.82	0.85	1.89	0.40
Ratio of Est Oil Revenue to Total Chem Cost	3.90	2.82	1.85	2.89	1.40

***Economic Estimates using Simulation Results.*** A discounted cashflow spreadsheet was developed to allow for a closer discrimination of the economics involved in a chemical flooding application. This spreadsheet requires as inputs the oil production over time, water production, and water disposal requirements. The fluid production streams are intended to come from simulations of the chemical flooding process. The user also estimates capital outlays, operating costs and overhead associated with the project. An escalation factor for inflation is also included.

The detailed Economic Estimation spreadsheet contains several tabs to organize the input data. Screen-shots of the spreadsheet worksheets are presented here for illustration. The spreadsheet was designed to accommodate changes and is customizable. The *Intro* worksheet is shown in **Figure 4.8** and is provided to reacquaint the user with the individual components. Capital expenses and operating costs are entered in the worksheets shown in **Figure 4.9** and **Figure 4.10**, respectively. Monthly rates of oil, water, and gas production and monthly rates for water injection with chemical concentrations for the chemical flood are entered in the *Prod & Inj* worksheet as shown in **Figure 4.11**. Results are presented in the *Economics* worksheet as shown in **Figure 4.12**. (The tables in Figures 4.11 and 4.12 are truncated; the project life was 68 months.) The final worksheet presents a cash flow discount table with the internal rate of return for the project. The results are on a before-taxes basis.

**Figures 4.9** through **4.12** present a chemical flooding project for the Trembley Oilfield using the simulation results presented in this chapter. The project was ended after 68 months when the cash flow became negative. This analysis calculated an internal rate of return of 32% indicating the economic success possible with chemical flooding.

## General Guide to the tabs in this Worksheet

Notice that there are 7 tabs at the bottom of this spreadsheet window. The tab names correspond to the descriptions listed here. The purpose of the tabs is to collect related data onto one sheet for each general category of information input and to keep the actual Economics sheet as focused on the final numbers as possible. All subsidiary sheets flow into the main Economics sheet.

### Intro

This sheet - overview of subsequent material

### Capital Expenses

Well workovers  
Build the Chemical Plant  
Upgrade facilities

### Operating Costs

Electricity and maintenance for the Chemical plant  
Producing well operating and maintenance  
Injection well operating and maintenance  
Other surface equipment operating and maintenance  
Water disposal costs  
Pumper and Field management wages  
Office overhead

### Production & Injection (Prod & Inj)

Estimated oil production  
Estimated gas production  
Estimated water production  
Estimated water injection  
Estimated water disposal  
Provide chemical schedule over time  
Provide chemical costs  
Calculate monthly volumes of chemical from the recipe

Bring these values in from a model

### Economics

Combine the preceding items and shake out a discounted gross profit

### Discount Table

The "Gross Profit" column from the Economics sheet is discounted at several rates

### Note:


The .xlsm version of the spreadsheet (the "macro-enabled version") will automatically run a GoalSeek on the Discount Table tab

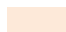
You can manually run a GoalSeek (Data / What-If Analysis / GoalSeek) by

"Set Cell" is the summation at the bottom of the far-right column

"To Value" = 0

"By Changing Cell" is the interest rate at the top of the far-right column

 Fields in Green like this are for Data Entry  
Please be sure to fill these in with values relevant to your project

 Fields in light orange like this are headings (and similar)  
This is meant solely to separate the heading from the data for readability

 Fields in Yellow like this are calculated and highlighted to catch the user's attention

Please look over the Economics results row by row to see where the Gross Profit turns **negative**

Decide in which month to stop the project

Enter this month in the upper left hand corner of the **Discount Table**

**Figure 4.8** – *Intro* worksheet of the Surfactant Flooding Economics spreadsheet.

Capital Equipment							
Category	Description	cost	units	Qty	Extended		
Spec					parts	labor	
<b>Chemical Plant site</b>							
	site prep, est. 30'x60'x6"	4,000	each	1		4,000	
	gravel/chat (~ 36 yards)	30	ton	54	1,620		
	Building	10	ft2	1,800	18,000		
	Heat & A/C	10,000	each	1	10,000		
	Installation	5	ft2	1,800		9,000	
	Electrical	40,000	each	1	40,000		
	Installation	50	hr	50		2,500	
<b>Chemical Plant equipment</b>							
	Polymer hydration & metering	36,500	each	2	73,000		
	Alkali hydration & metering	25,000	each	1	25,000		
	Surfactant prep & metering	10,000	each	3	30,000		
	Filter, In-line mixer, Meter	8,500		1	8,500		
	PLC control	50,000		1	50,000		
	Safety shower/Eye wash	3,000	each	1	3,000		
	Fabrication	60	hr	1000			
	Installation	50	hr	40		2,000	
	Installation	1,000	each	1		labor to plumb crane to set	
	Misc	9,000	each	1		9,000	
	Freight	1,800		1	1,800		
<b>Plant water input</b>							
	Water supply well workover						
	Input water treatment/softening	7,000		1	7,000		
	Input water storage	5,000	each	1	5,000		
	Installation	50	hr	20		1,000	
	Plumbing	1.50	ft	1000		1,500	
<b>Chemical Plant output</b>							
	Storage	5,000		1	5,000		
	Mixing	3,500	each	1	3,500		
	Plumbing	1,500		1		1,500	
	Injection pump	20,000	each	1	20,000		
<b>Workover Injectors</b>							
<b>Workover Producers</b>							
<b>Surface Production Handling equipment</b>							
	Separation						
	De-emulsification	10,000	each	1	10,000		
	Engineering Design and Consulting fees	15,000	each	1		15,000	
					311,420	45,500	356,920

**Figure 4.9** – *Capital Expenses* worksheet of the Surfactant Flooding Economics spreadsheet.

Operating Expenses - monthly					
Category	Description	cost	units	Qty	Extended
Chemical Plant	Electricity	0.08	\$/kWh	126720	10,138
	Labor				
	Maintenance	0.004167	% of capital c	356,920	1,487
Injection Plant	Electricity	0.08	\$/kWh	308,160	24,653
	Labor				
	Maintenance				
Producers	Electricity	0.08	\$/kWh	43,700	3,496
	Pulling/Maintenance				
	Pull to replace downhole pump				
	Pull to replace rods				
	Pull to replace tubing				
	Casing corrosion chemical treat	200	each	8	1,600
Injectors	Maintenance/MIT	85	5 years	3	255
Other Surface Equip	Free-Water knockout				
	Gunbarrel				
	Stock tanks				
	De-emulsification chemical	200	per month	1	200
Water Disposal	Pumper	2,000	month	1	2,000
	Foreman	500	month	1	500
	Office Overhead	500	month	1	500

Figure 4.10 – Operating Costs worksheet of the Surfactant Flooding Economics spreadsheet.

Estimated Production and Injection volumes				Chemical Costs in \$/active lb											
				349.9860	Injected slug density in lb/bbl			3.00	3.50	5.00	1.50	0.40	1.75		
Month	Production			Injected Liquid	ChemFlood Recipe and Time Schedule					Calculated chemical injection amounts					
	Oil bbl/mo	Water bbl/mo	Gas MMscf/mo		Surf 1	Surf 2	Surf 3	Alcohol	Alkali	Polymer	Surf 1	Surf 2	Surf 3	Alcohol	Alkali
1	1,255.8	25,704	0	9,000	0.65	0.25	0.10	1.0	0.20	20,474	7,875	3,150	0	31,498	6,300
2	8,630.4	30,328	0	18,600	0.65	0.25	0.10	1.0	0.20	42,313	16,274	6,510	0	65,097	13,019
3	3,245.1	24,212	0	18,600	0.65	0.25	0.10	1.0	0.20	42,313	16,274	6,510	0	65,097	13,019
4	2,244.1	21,904	0	18,000	0.65	0.25	0.10	1.0	0.20	40,949	15,749	6,300	0	62,998	12,600
5	1,871.4	21,562	0	18,600	0.65	0.25	0.10	1.0	0.20	42,313	16,274	6,510	0	65,097	13,019
6	1,548.2	20,580	0	18,000	0.65	0.25	0.10	1.0	0.20	40,948	15,749	6,300	0	62,997	12,599
7	1,435.3	21,106	0	18,600	0.65	0.25	0.10	1.0	0.20	42,313	16,274	6,510	0	65,097	13,019
8	1,308.1	20,508	0	18,600	0.65	0.25	0.10	1.0	0.20	42,314	16,274	6,510	0	65,098	13,020
9	1,132.0	18,051	0	16,800	0.65	0.25	0.10	1.0	0.20	38,218	14,699	5,880	0	58,797	11,759
10	1,298.4	19,517	0	18,600	0.65	0.25	0.10	1.0	0.20	42,313	16,274	6,510	0	65,097	13,019
11	1,414.3	18,504	0	18,000	0.65	0.25	0.10	1.0	0.20	40,948	15,749	6,300	0	62,997	12,599
12	1,715.5	18,833	0	18,600	0.65	0.25	0.10	1.0	0.20	42,313	16,274	6,510	0	65,097	13,019
13	1,903.6	18,008	0	18,000	0.65	0.25	0.10	1.0	0.20	40,948	15,749	6,300	0	62,997	12,599
14	2,207.8	17,972	0	18,600	0.65	0.25	0.10	1.0	0.20	42,313	16,274	6,510	0	65,097	13,019
15	2,376.1	17,324	0	18,600	0.65	0.25	0.10	1.0	0.20	42,313	16,274	6,510	0	65,097	13,019
16	2,392.6	16,341	0	18,000	0.65	0.25	0.10	1.0	0.20	40,949	15,749	6,300	0	62,998	12,600
17	2,515.1	16,681	0	18,600	0.65	0.25	0.10	1.0	0.20	42,313	16,274	6,510	0	65,097	13,019
18	2,437.6	16,086	0	18,000	0.65	0.25	0.10	1.0	0.20	40,948	15,749	6,300	0	62,997	12,599
19	2,502.2	16,671	0	18,600	0.65	0.25	0.10	1.0	0.20	42,313	16,274	6,510	0	65,097	13,019
20	2,526.7	16,791	0	18,600	0.65	0.25	0.10	1.0	0.20	42,313	16,274	6,510	0	65,097	13,019
21	2,362.3	15,246	0	16,800	0.65	0.25	0.10	1.0	0.20	38,218	14,699	5,880	0	58,798	11,760
22	2,754.9	16,767	0	18,600	0.65	0.25	0.10	1.0	0.20	42,313	16,274	6,510	0	65,097	13,019
23	2,703.2	15,958	0	18,000	0.65	0.25	0.10	1.0	0.20	40,948	15,749	6,300	0	62,997	12,599
24	2,816.8	16,328	0	18,600	0.65	0.25	0.10	1.0	0.20	42,313	16,274	6,510	0	65,097	13,019
25	2,886.9	16,186	0	18,000					0.20	0	0	0	0	0	12,599
26	3,274.4	16,845	0	18,600					0.20	0	0	0	0	0	13,019
27	3,246.3	16,254	0	18,600					0.20	0	0	0	0	0	13,019
28	3,157.1	15,211	0	18,000					0.20	0	0	0	0	0	12,599
29	3,337.7	15,853	0	18,600					0.20	0	0	0	0	0	13,019
30	3,294.6	15,330	0	18,000					0.20	0	0	0	0	0	12,599
31	3,328.3	15,675	0	18,600					0.20	0	0	0	0	0	13,019
32	3,182.9	15,521	0	18,600					0.20	0	0	0	0	0	13,019
33	2,841.8	14,477	0	17,400					0.20	0	0	0	0	0	12,180
34	2,897.2	15,550	0	18,600					0.20	0	0	0	0	0	13,019
35	2,721.2	15,346	0	18,000					0.20	0	0	0	0	0	12,599
36	2,664.6	16,144	0	18,600					0.20	0	0	0	0	0	13,019
37	2,461.9	15,814	0	18,000					0.20	0	0	0	0	0	12,599
38	2,456.1	16,534	0	18,600					0.20	0	0	0	0	0	13,019
39	2,368.3	16,738	0	18,600					0.20	0	0	0	0	0	13,019

Figure 4.11 – Prod and Inj worksheet of the Surfactant Flooding Economics spreadsheet. Project life of table is truncated.

\$ per active pound				\$ Monthly Expense with Yearly % Increase								Oil Price		Discount			
3.33	1.50	0.40	1.75	11,625	500	5,096	100	100	100	2500	500	80	15%				
0.00%	0.00%	0.00%	0.00%	5.000%	2.000%	6.000%	5.000%	6.000%	3.000%	2.000%	2.000%	Increase 2.000%					
												NRI	0.875				
Expenses												Revenue		Total			
Chemical (costs)				Operating Costs								Prod & Inj		(from below)			
Prod & Inj (volumes)														1,071,391			
Month	Capital Expense	Surfactant	Alcohol	Alkali	Polymer	Chemical Plant	Injection Plant	Producers	Injectors	Other Surface Equip	Water Disposal	Pumper & Foreman	Office Overhead	Total Costs	Oil Revenue	Gross Profit	Discounted Profit
0	356,920													356,920		-356,920	-356,920
1		104,732	0	12,599	11,024	11,673	0	5,121	100	101	100	2,504	501	148,456	88,049	-60,407	-59,662
2		216,449	0	26,039	22,784	11,722	0	5,147	101	101	101	2,508	502	285,453	606,142	320,689	312,819
3		216,447	0	26,039	22,784	11,771	0	5,173	101	102	101	2,513	503	285,532	228,292	-57,240	-55,146
4		209,468	0	25,199	22,049	11,820	0	5,199	102	102	101	2,517	503	277,060	158,139	-118,921	-113,156
5		216,449	0	26,039	22,784	11,869	0	5,225	102	103	101	2,521	504	285,697	132,096	-153,601	-144,350
6		209,467	0	25,199	22,049	11,918	0	5,251	103	103	102	2,525	505	277,221	109,461	-167,760	-155,710
7		216,449	0	26,039	22,784	11,968	0	5,277	103	104	102	2,529	506	285,860	101,645	-184,215	-168,873
8		216,450	0	26,039	22,784	12,018	0	5,303	103	104	102	2,534	507	285,945	92,797	-193,148	-174,876
9		195,501	0	23,519	20,579	12,068	0	5,330	104	105	102	2,538	508	260,353	80,437	-179,916	-160,885
10		216,449	0	26,039	22,784	12,118	0	5,357	104	105	103	2,542	508	286,109	92,412	-193,697	-171,069
11		209,467	0	25,199	22,049	12,169	0	5,383	105	106	103	2,546	509	277,635	100,828	-176,808	-154,225
12		216,449	0	26,039	22,784	12,220	0	5,410	105	106	103	2,550	510	286,277	122,509	-163,768	-141,087
13		209,467	0	25,199	22,049	12,270	0	5,437	106	107	103	2,555	511	277,804	136,165	-141,638	-120,516
14		216,449	0	26,039	22,784	12,322	0	5,465	106	107	104	2,559	512	286,446	158,192	-128,253	-107,780
15		216,447	0	26,039	22,784	12,373	0	5,492	106	108	104	2,563	513	286,529	170,531	-115,997	-96,277
16		209,468	0	25,199	22,049	12,424	0	5,519	107	108	104	2,568	514	278,061	172,002	-106,059	-86,941
17		216,449	0	26,039	22,784	12,476	0	5,547	107	109	104	2,572	514	286,702	181,114	-105,588	-85,486
18		209,467	0	25,199	22,049	12,528	0	5,575	108	109	105	2,576	515	278,231	175,826	-102,405	-81,886
19		216,449	0	26,039	22,784	12,580	0	5,603	108	110	105	2,580	516	286,874	180,784	-106,091	-83,786
20		216,449	0	26,039	22,784	12,633	0	5,631	109	110	105	2,585	517	286,961	182,858	-104,103	-81,201
21		195,502	0	23,519	20,579	12,685	0	5,659	109	111	105	2,589	518	261,377	171,247	-90,130	-69,434
22		216,449	0	26,039	22,784	12,738	0	5,687	110	112	106	2,593	519	287,136	200,042	-87,094	-66,267
23		209,467	0	25,199	22,049	12,791	0	5,715	110	112	106	2,598	520	278,667	196,611	-82,056	-61,663
24		216,449	0	26,039	22,784	12,845	0	5,744	110	113	106	2,602	520	287,312	205,212	-82,100	-60,994
25		0	0	0	22,049	12,898	0	5,773	111	113	106	2,606	521	44,178	210,676	166,498	122,049
26		0	0	0	22,784	12,952	0	5,802	111	114	107	2,611	522	45,002	239,348	194,346	140,703
27		0	0	0	22,784	13,006	0	5,831	112	114	107	2,615	523	45,092	237,688	192,596	137,715
28		0	0	0	22,049	13,060	0	5,860	112	115	107	2,619	524	44,447	231,547	187,101	132,134
29		0	0	0	22,784	13,115	0	5,889	113	116	108	2,624	525	45,272	245,198	199,926	139,448
30		0	0	0	22,049	13,169	0	5,918	113	116	108	2,628	526	44,628	242,438	197,810	136,269
31		0	0	0	22,784	13,224	0	5,948	114	117	108	2,632	526	45,454	245,325	199,871	135,989
32		0	0	0	22,784	13,279	0	5,978	114	117	108	2,637	527	45,545	234,996	189,451	127,308
33		0	0	0	21,314	13,334	0	6,008	115	118	109	2,641	528	44,167	210,165	165,998	110,171
34		0	0	0	22,784	13,390	0	6,038	115	118	109	2,646	529	45,729	214,617	168,888	110,705
35		0	0	0	22,049	13,446	0	6,068	116	119	109	2,650	530	45,087	201,915	156,829	101,531
36		0	0	0	22,784	13,502	0	6,098	116	120	109	2,654	531	45,915	198,043	152,128	97,272

Figure 4.12 – Economics worksheet of the Surfactant Flooding Economics spreadsheet.



## **Chapter 5**

### **Technology Transfer**

Results of this investigation have presented to the producers and the oil industry by oral presentations, poster presentations and written articles. These presentations and articles are listed.

#### **Presentations**

Stan McCool, “Chemical Flooding,” monthly meeting of the Wichita Section of the Society of Petroleum Engineers, Wichita, KS (December 10, 2008).

Stan McCool, “Chemical Flooding in Kansas,” Eighteenth Oil Recovery Conference, Tertiary Oil Recovery Project, Wichita, KS (April 1-2, 2009).

Stan McCool, “Chemical Flooding Designs for Kansas,” monthly meeting of the Wichita Section of the Society of Petroleum Engineers, Wichita, KS (March 15, 2011).

Stan McCool, “Chemical Flooding in Kansas,” Nineteenth Oil Recovery Conference, Tertiary Oil Recovery Project, Wichita, KS (April 6-7, 2011).

#### **Poster presentations**

Stan McCool and Mark Ballard, “Bridging the Gap Between Chemical Flooding and Independent Oil Producers,” poster presentation, 72nd Annual Meeting of the Kansas Independent Oil and Gas Association (KIOGA), Wichita, KS (August 16-17, 2009).

Mark Ballard, “Bridging the Gap Between Chemical Flooding and Independent Oil Producers,” poster presentation, 73rd Annual Meeting of the Kansas Independent Oil and Gas Association (KIOGA), Wichita, KS (August 15-16, 2010).

Stan McCool and Mark Ballard, “Bridging the Gap Between Chemical Flooding and Independent Oil Producers,” poster presentation, 74th Annual Meeting of the Kansas Independent Oil and Gas Association (KIOGA), Wichita, KS (August 21-22, 2011).

Mark Ballard and Stan McCool, “Bridging the Gap Between Chemical Flooding and Independent Oil Producers,” poster presentation, 75th Annual Meeting of the Kansas Independent Oil and Gas Association (KIOGA), Wichita, KS (August 19-20, 2012).

Senior, P. J. and Walton, A.W., 2011, Depositional Environment, Reservoir Characteristics, and EOR Potential of an incised valley fill: Pleasant Prairie field, Haskell County, Kansas: AAPG Search and Discovery Article #90133©2011 American Association of Petroleum Geologists Mid-Continent Section Meeting, Oklahoma City, Oklahoma [Awarded Roger N. Planalp Memorial Award for best poster; [http://www.searchanddiscovery.com/documents/2011/50515senior/ndx\\_senior.pdf](http://www.searchanddiscovery.com/documents/2011/50515senior/ndx_senior.pdf)] (1-4 October 2011).

### **Graduate Student thesis**

Shahab Ahmed, “Methodology for Designing and Evaluating Chemical Systems for Improved Oil Recovery,” MS thesis, Department of Chemical and Petroleum Engineering, The University of Kansas (2012).

Zhijun Liu, “Experimental Evaluation of Surfactant Application to Improve Oil Recovery ,” MS thesis, Department of Chemical and Petroleum Engineering, The University of Kansas (2011).

Peter Senior, “Depositional Environment, Reservoir Properties, and EOR Potential of an Incised-Valley-Fill Sandstone, Pleasant Prairie Oilfield, Haskell County, Kansas,” MS thesis, Department of Geology, The University of Kansas (2012).

### **Articles**

Stan McCool “Let’s recover that oil that is left behind with Chemical Flooding,” Kansas Geological Society Bulletin, Vol. 84, No. 1, Kansas Geological Society, Wichita, KS (January-February 2009).

Stan McCool and Ginny Weyland, “Designing chemical floods for Kansas reservoirs,” *World Oil*, pg. 107-110 (April 2011).

Quarterly Technical Reports for this project and this Final Report are available at [www.torp.ku.edu](http://www.torp.ku.edu).

## **Chapter 6**

### **Summary and Relevancy of Results**

Chemical flooding using surfactants, polymers and alkali has the potential to significantly increase oil production from reservoirs that would otherwise be abandoned after primary and secondary production operations. The purpose of this investigation was to introduce chemical flooding and to promote field testing to independent oil producers (IOPs) in Kansas and beyond. This purpose was achieved by providing preliminary designs of chemical floods for selected applications through formulation of reservoir-specific chemical systems and by providing estimated economics of field applications. The results of this investigation are used to encourage IOPs to participate in field testing of the technology. Only when field results show technical success and indicate economical application will IOPs embrace and apply chemical flooding technology.

Most candidate reservoirs for chemical flooding in the US are operated by independent oil producers (IOPs). Delays in implementing chemical flooding or other enhanced oil recovery techniques could permanently leave recoverable oil in the ground due to well plugging and higher costs involved to upgrade the additional deterioration of wells and infrastructure that occur.

The work described in Chapters 1 through 5 demonstrates the potential of “next generation” chemical flooding processes and provides the design work necessary for Independent Oil Producers to make an informed assessment for implementation of a pilot or demonstration project. Ten Kansas oil reservoirs/leases were selected for study by assessing the potential performance of chemical flooding through geological and engineering characteristics. The reservoirs/leases surveyed represented about 45% of past Kansas oil production. Reservoirs/leases that have been efficiently waterflooded have the highest performance potential for chemical flooding.

Laboratory work to identify efficient chemical systems and to test the oil recovery performance of the systems was the major effort of the project. Efficient chemical systems were identified for crude oils from nine of the reservoirs/leases through phase behavior studies where the behavior of various aqueous surfactant/polymer systems is observed before and after they are mixed with a crude oil. Efficient chemical systems met a set of formalized criteria. Most of the Kansas crude oils responded favorably to chemical systems that contained two surfactants: an alcohol propoxy sulfate and an internal olefin sulfonate. This system also required relatively high concentrations of alcohol solvents. The performance of the chemical systems in phase behavior studies was enhanced with the addition of sodium carbonate (alkali). All of the crude oils had low acid numbers, negating the use of alkali in the chemical system for soap production.

Oil recovery performance of the identified chemical systems was tested in coreflood experiments using quarried Berea sandstone and Indiana limestone rocks. Performance was measured as the percentage of oil recovered from cores initially at a waterflooded residual saturation. Chemical formulations recovered 90% or more of the residual oil for seven crude oils in Berea sandstone cores. Oil recoveries increased with the amount of chemical injected for floods conducted in Berea sandstone cores.

Chemical floods were conducted with formulations for the Wahrman crude oil in Indiana limestone cores. Oil recoveries were 50% or less in the Indiana limestone cores for the same chemical formulation that had 90+ % recoveries in Berea sandstone cores. An alternate system containing an alcohol propoxy sulfate and an ethoxylated alcohol without alcohol co-solvent recovered 80% of the Wahrman crude from a limestone core. Tracer experiments showed significantly larger mixing zones in the limestone cores. Dilution of the chemical slug due to greater mixing in the limestone rocks contributed to the lower oil recoveries.

Geological evaluations were used in the selection of the ten reservoirs/leases for study. Geological studies for nine of the oil reservoirs were prepared and the Pleasant Prairie, Trembley, Vinland and Stewart Oilfields were showed to be the most favorable for a pilot chemical flood from geological considerations.

Simulation software was used to model the performance of a laboratory coreflood and predict the performance of a field application of chemical flooding for the Trembley Oilfield. Economics estimates of field applications indicated chemical flooding is a viable technology for oil recovery. Laboratory, simulation and economic results have and will be dispersed through technical papers and presentations to independent oil operators.

Chemical flooding technology works well in the laboratory. However, there have been limited field tests and very little field data for chemical flooding applications using next-generation chemical systems. What little information that has been publicly available for field tests, technical issues have occurred. This is not to say that successful applications have not been conducted but, if so, these field results have been kept confidential. Field testing with publicly available results is paramount to the advancement of chemical flooding.

Field tests are being designed and implement by major oil companies but the results have been confidential. Field testing is too expensive to be undertaken by most independent oil producers (IOPs). For results to be public, field projects that are partially funded by government agencies like the Department of Energy (DOE) are needed.

The Tertiary Oil Recovery Project at the University of Kansas has and will pursue and encourage field tests of chemical flooding. This is the intended progression of the work conducted for this project. A proposal to perform a chemical flooding test in the Trembley Oilfield, Reno County, KS was submitted to the Research Partnership to Secure Energy for America (RPSEA), a subcontractor to DOE. As of this writing, the proposal has been selected for negotiations of a research contract. The implementation of this field project, and possibly others, will be the result of the research work conducted for this project. Only with successful field results will chemical flooding technology be advanced to recover oil from mature producing regions before the fields are plugged and abandoned.

## References

Ahmed, Muhammad Shahab: "Methodology for Designing and Evaluating Chemical Systems for Improved Oil Recovery," MS thesis, University of Kansas, Lawrence, KS 2012.

Aoudia, M., W. H. Wade, et al. (1995). "Optimum Microemulsions Formulated with Propoxylated Guerbet Alcohol and Propoxylated Tridecyl Alcohol Sodium Sulfates." *Journal of Dispersion Science and Technology* **16**(2): 115 - 135.

Barnes, J. R., J. Smit, et al. (2008). Development of Surfactants for Chemical Flooding at Difficult Reservoir Conditions. SPE/DOE Symposium on Improved Oil Recovery. Tulsa, Oklahoma, USA.

Bennett, K. E., C. W. Macosko and L. E. Scriven (1981). Microemulsion Rheology: Newtonian and Non-Newtonian Regimes. SPE Annual Technical Conference and Exhibition. San Antonio, Texas, 1981 Copyright 1981, Society of Petroleum Engineers.

Bourrel, M. and R. S. Schechter (1988). Microemulsions and related systems : formulation, solvency, and physical properties. New York, M. Dekker.

Brewer, J.E. , 1965, The Tobias field: Kansas Geological Society, Kansas Oil and Gas Fields, vol. 4, pp. 255-268 .

Dubois, M.K., Senior, P.R., Williams, E., and Hedke D.E., 2012, Reservoir Characterization and Modeling of a Chester Incised Valley Fill Reservoir, Pleasant Prairie South Field, Haskell County, Kansas, Kansas Geological Survey, Downloaded June 25, 2012.

Eicke, H.-F., Parfitt, G. D. (1987). Interfacial Phenomena in Apolar Media. New York, M. Dekker.

Flaaten, A., Q. P. Nguyen, G. A. Pope and J. Zhang (2008). A Systematic Laboratory Approach to Low-Cost, High-Performance Chemical Flooding. SPE/DOE Symposium on Improved Oil Recovery. Tulsa, Oklahoma, USA, Society of Petroleum Engineers.

Flaaten, A., Q. P. Nguyen, et al. (2009). "A Systematic Laboratory Approach to Low-Cost, High-Performance Chemical Flooding." *SPE Reservoir Evaluation & Engineering* 12(5).

Green, D. W. and G. P. Willhite (1998). Enhanced Oil Recovery. Richardson, TX, Society of Petroleum Engineers.

Flaaten, Adam Knut, "Experimental Study of Microemulsion Characterization and Optimization in Enhanced Oil Recovery: A Design Approach for Reservoirs with High Salinity and Hardness", M.S. Thesis, University of Texas at Austin, (December 2007).

Green, D. W. and G. P. Willhite (1998). Enhanced Oil Recovery. Richardson, TX, Society of Petroleum Engineers.

Green, D.W., Willhite, P.G., Reynolds, R.R., McCune, A.D., Michnick, M.J., Walton, A.W., and Watney, W.L. (2000) Improved oil recovery in fluvial-dominated deltaic reservoirs of Kansas – Near term, Final Report: Prepared by The University of Kansas Center for Research, Inc., for U.S. Department of Energy, published by National Petroleum Technology Office, U.S. Department of Energy, Tulsa, Oklahoma.

Healy, R. N. and R. L. Reed (1974). "Physicochemical Aspects of Microemulsion Flooding." 14(5): 491-501.

Healy, R. N., R. L. Reed, and D.G. Stenmark (1976). "Multiphase Microemulsion Systems." SPE Journal 16(3): 147-160.

Hirasaki, G. J., C. A. Miller, et al. (2008). Recent Advances in Surfactant EOR. SPE Annual Technical Conference and Exhibition. Denver, Colorado, USA, Society of Petroleum Engineers.

Hirasaki, G. J., G. A. Pope, et al. (2004). Surfactant Based Enhanced Oil Recovery and Foam Mobility Control, 1st Annual Technical Report to DOE, DE-FC26-03NT15406, June.

Hirasaki, G. J., G. A. Pope, et al. (2005). Surfactant Based Enhanced Oil Recovery and Foam Mobility Control, 2nd Annual Technical Report to DOE, DE-FC26-03NT15406, July.

Hirasaki, G. J., G. A. Pope, et al. (2006). Surfactant Based Enhanced Oil Recovery and Foam Mobility Control, Final Report to DOE, DE-FC26-03NT15406, June.

Hirasaki, G. J., H. R. van Domselaar, et al. (1983). "Evaluation of the Salinity Gradient Concept in Surfactant Flooding." 23(3).

Huh, C. (1979). "Interfacial tensions and solubilizing ability of a microemulsion phase that coexists with oil and brine." Journal of Colloid and Interface Science 71(2): 408-426.

Jackson, A. C. (2006). Experimental Study of the Benefits of Sodium Carbonate on Surfactants for Enhanced Oil Recovery. Petroleum Engineering. Austin, TX, The University of Texas at Austin. MS.

Levitt, D., A. Jackson, C. Heinson, L. N. Britton, T. Malik, V. Dwarakanath and G. A. Pope (2006). Identification and Evaluation of High-Performance EOR Surfactants. SPE/DOE Symposium on Improved Oil Recovery. Tulsa, Oklahoma, USA, Society of Petroleum Engineers.

Levitt, D., A. Jackson, et al. (2009). "Identification and Evaluation of High-Performance EOR Surfactants." SPE Reservoir Evaluation & Engineering 12(2): pp. 243-253.

Liu, S, Li R.F., Miller C.A and Hirasaki, G.J.: "ASP Processes: Wide Range of Conditions for Good Recovery," SPE 113936, presented at the 2008 SPE/DOE Improved Oil Recovery Symposium, Tulsa, OK (19-23 April 2008).

Liu, Zhijun: "Experimental Evaluation of Surfactant Application to Improve Oil Recovery," MS thesis, University of Kansas, Lawrence, KS, 2011.

Lopez-Salinas, J. L., C. A. Miller, et al. (2009). Viscometer for Opaque, Sealed Microemulsion Samples. SPE International Symposium on Oilfield Chemistry. The Woodlands. Texas, Society of Petroleum Engineers.

Montgomery, S.L., 1996, Stewart Field, Finney County, Kansas: Seismic definition of thin channel reservoirs: AAPG Bulletin, v. 80, no. 12, p. 1833-1844.

Nelson, R. C. (1982). "The Salinity-Requirement Diagram - A Useful Tool in Chemical Flooding Research and Development." 22(2).

Nelson, R. C. and G. A. Pope (1978). "Phase Relationships in Chemical Flooding." Society of Petroleum Engineers 18(5): 325-338.

Prince, L. M. (1977). Microemulsions Theory and Practice. L. M. Prince. New York, Academic Press, Inc.

Pope, G. A. (2007). Overview of Chemical EOR. Casper EOR Workshop. Casper.

Pope, G. A., B. Wang, et al. (1979). "A Sensitivity Study of Micellar/Polymer Flooding." 19(6). Prince, L. M. (1977). Microemulsions Theory and Practice. L. M. Prince. New York, Academic Press, Inc.

Sahni, V., R. M. Dean, et al. (2010). The Role of Co-Solvents and Co-Surfactants in Making Chemical Floods Robust. SPE Improved Oil Recovery Symposium. Tulsa, Oklahoma, USA.

Salager, J.-L., R. Antón, et al. (2005). "Enhancing solubilization in microemulsions—State of the art and current trends." Journal of Surfactants and Detergents 8(1): 3-21.

Salter, S. J. (1977). The Influence Of Type and Amount of Alcohol On Surfactant-Oil-Brine Phase Behavior and Properties. SPE Annual Fall Technical Conference and Exhibition. Denver, Colorado, 1977 Copyright 1977, American Institute of Mining, Metallurgical, and Petroleum Engineers, Inc.

Schoeling, L. G., D. W. Green, et al. (1989). "Introducing EOR Technology to Independent Operators." SPE Journal of Petroleum Technology 41(12).

Senior, P.J. (2012) Depositional Environment, Reservoir Properties, and EOR Potential of an Incised Valley- fill Sandstone, Pleasant Prairie Oilfield, Haskell County, Kansas: MS Thesis, The University of Kansas.

Stegemeier, G. L. (1977). *Mechanisms of Entrapment and Mobilization of Oil in Porous Media. Improved Oil Recovery by Surfactants and Polymer Flooding*. D. O. Shah and R. S. Schechter. New York, Academic Press.

Taber, J. J. (1969). "Dynamic and Static Forces Required To Remove a Discontinuous Oil Phase from Porous Media Containing Both Oil and Water." 9(1).

Tham, M. J., R. C. Nelson, et al. (1983). "Study of the Oil Wedge Phenomenon Through the Use of a Chemical Flood Simulator." *Society of Petroleum Engineers Journal* 23(5): 746-758.

Winsor, P. A. (1954). *Solvent properties of amphiphilic compounds*. London, Butterworths Scientific Publications.

Zhang, D., S. Liu, et al. (2006). *Favorable Attributes of Alkali-Surfactant-Polymer Flooding*. SPE/DOE Symposium on Improved Oil Recovery. Tulsa, Oklahoma, USA, Society of Petroleum Engineers.



**BEAVER CREEK FIELD, RAWLINS COUNTY, KANSAS**  
**Peter Senior & Anthony Walton<sup>1</sup>**

**1. INTRODUCTION**

Surfactant flooding, like all enhanced oil recovery (EOR) operations, requires knowledge of the nature and properties of both the reservoir and the fluids within it as well as the injected fluids and the interactions among them. While much of the research on the project *Bridging the Gap between Chemical Flooding and Independent Oil Producers* is devoted to studying the interactions of potential EOR fluids, reservoir oils, and connate water, it is also necessary to understand the extent of the reservoir, its potential for additional recovery, its configuration, any heterogeneity, and the potential for interaction between EOR fluids and reservoir rocks. For this reason this project includes a program of geological and engineering characterization and evaluation of candidate reservoirs has been undertaken in parallel with the efforts at characterizing fluid-fluid interactions in laboratory experiments.

During the fall of 2009, workers on this project began the process of characterizing candidate reservoirs. Below is very preliminary geological report on one field, the Beaver Creek field in Rawlins County, Kansas. This report is from a training effort on one of the smaller fields that had been identified for study. This effort brought the student who was undertaking the study up to speed with the avenues of investigation, sources of data and methods appropriate for the characterization of the fields.

The Beaver Creek oil field produces from three wells completed in the J-zone of the Kansas City Group and has one injector. The report includes a gazette of wells in the field and the local area, listing of the kinds of data available and what is missing, a type log, cross-sections and maps of the field, some description of the productive rocks, some petrophysical information and appraisal of the potential of this field as a demonstration project for surfactant flood in light of its geology and the information available for reservoir characterization.

---

<sup>1</sup> Department of Geology, The University of Kansas, 1475 Jayhawk Blvd., Suite 120, Lawrence, Kansas 66045. Contact e-mail: twalton@ku.edu

## 2. LOCATION

Beaver Creek field is located in northeastern Rawlins County, in far northwest Kansas (Figure 1). The field occupies the southern half of Section 25 and northern half of Section 36, T1S R32W. The field lies in a valley with approximately 100 feet of relief (Figure 2).

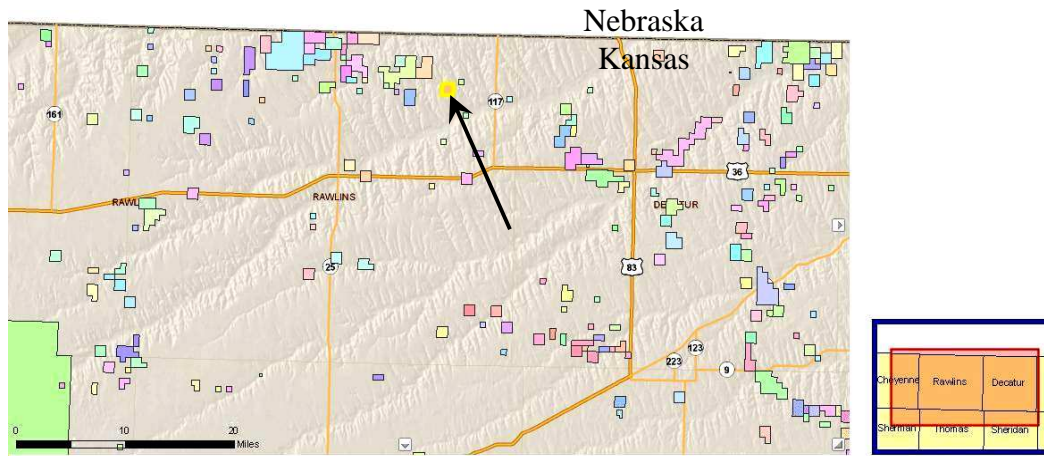


Fig. 1: Colored polygons show oilfields in Rawlins County, Kansas; Beaver Creek field indicated by arrow and highlighted yellow. Modified from <http://maps.kgs.ku.edu/oilgas/> on Dec. 20 2009.

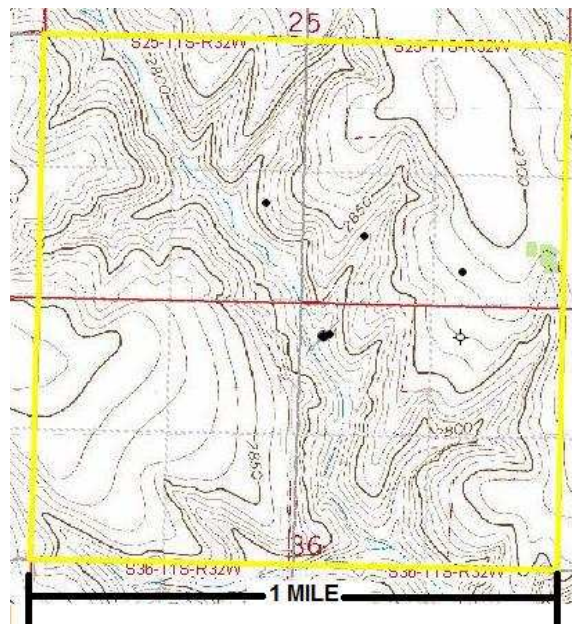


Fig. 2: Topography of field area. Beaver Creek field is outlined in yellow. Black dots are oil wells. Modified from <http://maps.kgs.ku.edu/oilgas/> on Dec. 20 2009.

### 3. METHODS

This report was the result of analysis of data in the public domain and that provided by the field operators directly to the investigators. The major methods were use of well logs to determine the configuration of key horizons and the thickness and porosity distribution within the reservoir. The data and logs were imported into Petra, a subsurface GIS program and analyzed using standard techniques.

### 4. DISCOVERY AND EARLY HISTORY

Thunderbird Drilling spudded the discovery well for Beaver Creek, Wahrman B #1, on July 6, 1993 and discovered oil in the J-Zone of the Lansing-Kansas City interval on July 13 (Figure 3). Initial production was 95 barrels of oil per day with no water. After drilling two dry holes in March and July of 1994<sup>2</sup>, Thunderbird Drilling successfully completed the Wahrman B #2 well just slightly northwest of the original discovery well. This well produced 56, 62, and 67 barrels of oil plus a barrel of water per day in its first three days after completion. Thunderbird Drilling completed another successful well in October of 1995, the Wicke #2, which produced 46 barrels of oil and a trace of water its first day before dropping to 21 and then 17 barrels plus a trace of water on its second and third days. The Thunderbird Wahrman E #1 well, completed in June of 1996, flowed 50, 49, and 50 barrels of oil with no water in its first three days. Sovereign Energy drilled the last well in the Beaver Creek field, the Wahrmann 22-25, a dry hole, in March of 1997. Vess Oil Corporation is currently waterflooding the field, using the

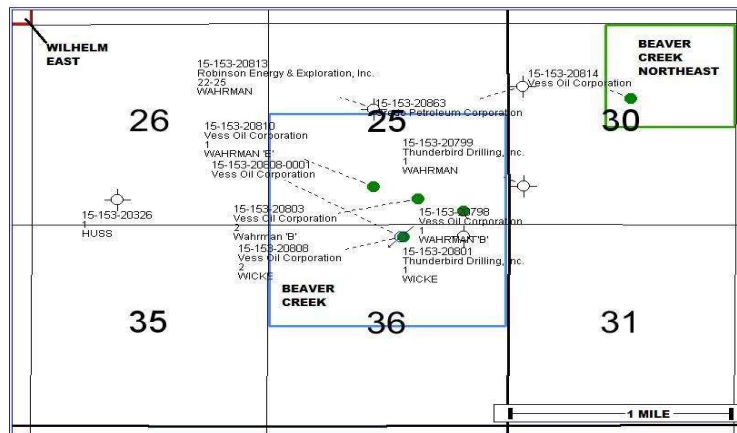


Figure 3. Wells in the Beaver Creek oil field and surrounding areas in T1S R32W, Rawlins County, Kansas.

<sup>2</sup> The later well, the Wicke 1, had a good show, recovering 20' of oil and 10' of oil-cut mud on the drill-stem test.

**Table 1: Wells in Beaver Creek oil field and selected others used in this report. Data retrieved from the Kansas Geological Survey website [www.kgs.ku.edu](http://www.kgs.ku.edu) on December 20, 2009**

API NUMBER	LEASE	WELL	FIELD	SECTION - TOWNSHIP - RANGE	SPOT	CURRENT OPERATOR	SPUD	COMPLETION	STATUS OR PLUGGING DATE
15-153-20109	PITNER	1	WILDCAT	14-2S-32W	E2 W2 NW SE	unavailable	26-Mar-71	2-Apr-71	2-Apr-71
15-153-20113	H. J. WICKE	1	WICKE	17-1S-32W	C SE SW	Philpott Oil & Gas Co Inc	4-May-71	22-Jun-71	Abandoned oil producer, plugged 18-Sep-98
15-153-20326	HUSS	1	WILDCAT	26-1S-32W	C SE SW	unavailable	21-Jun-78	26-Jun-78	26-Jun-78
15-153-20342	FRANKE	1	HERNDON	36-1S-31W	SE SE SW	unavailable	22-Dec-78	11-Apr-79	Oil Producer
15-153-20436	FRANKE	2	HERNDON	36-1S-31W	SE NE SW	unavailable	18-Dec-81	24-Dec-81	30-Dec-81
15-153-20798	WAHRMAN 'B'	1	BEAVER CREEK	25-1S-32W	SW SE SE	Vess Oil Corporation	6-Jul-93	30-Jul-93	Oil Producer
15-153-20799	WAHRMAN	1	BEAVER CREEK	30-1S-31W	NW SW SW	Thunderbird Drilling, Inc.	21-Mar-94	28-Mar-94	27-Mar-94
15-153-20801	WICKE	1	BEAVER CREEK	36-1S-32W	NW NE NE	Thunderbird Drilling, Inc.	5-Jul-94	11-Jul-94	11-Jul-94
15-153-20803	Wahrman 'B'	2	BEAVER CREEK	25-1S-32W	C SW SE	Vess Oil Corporation	7-Jun-95	26-Jun-95	Oil Producer
15-153-20808	WICKE	2	BEAVER CREEK	36-1S-32W	NW NW NE	Vess Oil Corporation	8-Oct-95	4-Jan-96	Water injection well.
15-153-20810	WAHRMAN 'E'	1	BEAVER CREEK	25-1S-32W	NE SE SW	Vess Oil Corporation	21-Jun-96	27-Jun-96	Oil Producer
15-153-20813	WAHRMAN	22-25	BEAVER CREEK	25-1S-32W	N2 SE SE NW	Robinson Energy & Exploration, Inc.	14-Mar-97	20-Mar-97	20-Mar-97
15-153-20814	BASGALL 'C'	1	BEAVER CREEK NORTHEAST	30-1S-31W	W2 SW NE	Vess Oil Corporation	22-Jan-98	10-Mar-98	Oil producer
15-153-20863	Wahrman	1-30	N/A	30-1S-31W	NW SW NW	Credo Petroleum Corporation	7-Jul-08	19-Jul-08	19-Jul-08

Table 2: Reservoir, log, and DST data from wells in Beaver Creek field and selected others used in construction of this report; data retrieved from Kansas Geological Survey website Dec. 20, 2009.(Continues on following page)

API NUMBER	DEPTH	PRODUCING FORMATION & THICKNESS (FEET)	RESERVOIR THICKNESS (FEET)	LOGS & CORES	DRILL-STEM TESTS
15-153-20109 Pinter 1	3945			RA GUARD LOG	
15-153-20113 H.J. Wicke 1	4170			RA GUARD LOG	
15-153-20326 Huss 1	4165				
15-153-20342 Frank 1	4440			GAMMA RAY NEUTRON CALIPER; INDUCTION ELECTRIC LOG	
15-153-20436 Frank 2	3994				
15-153-20798 Wahrman 'B' 1	4100	LKC J-ZONE; 21	6	NEUTRON DENSITY POROSITY LOG; SONIC CEMENT BOND LOG; RA GUARD LOG	#1 - OREAD & LKC A-ZONE (3748-3850), 90' MUD, 30/30/30/30 IFP 39-68 FFP 68-78, SIP 1210-1190; #2 - LKC D-ZONE (3844-3910), 20' OIL CUT MUD (10% OIL), 30/30/30/30, IFP 29-29, FFP 39-39, SIP 986-916; #3 - LKC H-ZONE (3935-3995), 60' MUD W/SCUM OF OIL, 420' SALTWATER, 30/60/45/60, IFP 68-136, FFP 146-244, SIP1122-1043; #4 - LKC J-ZONE (3986-4030), 339' OIL 36°API, 120' MUD CUT OIL (60& OIL), 30/60/45/60, IFP 39-97, FFP 117-205, SIP1338-1309
15-153-20799 Wahrman 1	4120			RA GUARD LOG; GEOLOGISTS REPORT	#1 - LKC D-ZONE (3878-3920), 691' SALT WATER, 30/60/45/60, IFP 68-146, FFP 166-332, SIP 1141-1141; #2 - LKC G-ZONE (3922-3970), 120' WATER, 20/30/0/0 IFP 58-68, SIP1151; #3 - LKC H-ZONE (3970-4010), 10' MUD, 30/30/30/30, IFP 48-48, FFP 48-48, SIP 1072-1003; #4 - LKC J-ZONE (4010-4050), 10' MUD, 30/30/0/0, IFP 38-38, SIP 38
15-153-20801 Wicke 1	4080			RA GUARD LOG; NEUTRON DENSITY POROSITY LOG; GEOLOGISTS REPORT	#1 - LKC A-ZONE (3780-3830), 150' MUDDY WATER, 45/45/45/45, IFP 48-48, FFP 78-78, SIP 1190-731; #2 - LKC D-ZONE (3830-3880), 10' OIL, 65' OIL CUT MUDDY WATER, 45/45/45/45 IFP 29-29, FFP 48-48, SIP 731-634; #3 - LKC H-ZONE (3940-3980), 210' MUDDY WATER W/FEW OIL SPECKS, 30/60/45/60, IFP 39-48, FFP 58-87, SIP 1240-1210; #4 - LKC J-ZONE (3968-4015), 20' OIL, 10' OIL CUT MUD, 30/30/30/30, IFP 19-19, FFP 24-24, SIP 507-488
15-153-20803 Wahrman 'B' 2	4042	LKC J-ZONE; 20	5	NEUTRON DENSITY POROSITY LOG; GEOLOGISTS REPORT; RA GUARD LOG; SONIC CEMENT BOND LOG	#1 - OREAD (3700-3750), 5' WATER CUT OIL (95% OIL), 186' OIL SPECKED WATER, 45/45/45/45, IFP 48-69, FFP 77-117, SIP 1151-1122; #2 - LKC D-ZONE (3784-3840), 2' OIL, 65' OIL CUT MUD, 45/45/45/45, IFP 48-48, FFP 68-68, SIP 877-809; #3 - LKC H-ZONE (3885-3930), 5' OIL SPECKED MUD, 30/30/30/30, IFP 39-39, FFP 39-39, SIP 58-48; #4 - LKC J-ZONE (3925-3965), 120' GAS, 60' OIL, 60' OIL CUT MUD, 30/60/45/60, IFP 48-48, FFP 73-73, SIP 575-566

API_NUMBER	DEPTH	PRODUCING FORMATION & THICKNESS (FEET)	RESERVOIR THICKNESS (FEET)	LOGS & CORES	DRILL-STEM TESTS
15-153-20808 Wicke 2	4004	LKC J-ZONE; 20	5	GEOLOGISTS REPORT; CEMENT BOND LOG;	#1 - LKC D-ZONE (3745-3800), 20' HEAVILY OIL CUT MUD (35° API), 30/30/30/30, IFP 26-28, FFP 36-34, SIP 765-428; #2 - LKC J-ZONE (3880-3925), 200' GAS, 50' CLEAN GASSY OIL, 50' MUDDY OIL (75% OIL), 30/30/45/60, IFP 28-30, FFP 42-50, SIP 528-615
15-153-20810 Wahrman 'E' 1	4032	LKC J-ZONE; 20	5	NEUTRON DENSITY POROSITY LOG; RA GUARD LOG; SONIC CEMENT BOND LOG; GEOLOGISTS REPORT	#1 - OREAD (3680-3720), 62' THIN MUD W/SCUM OF OIL, 496' SALTWATER, 30/60/45/60, IFP 73-104, FFP 209-240, SIP 1200-1170; #2 - LKC G-ZONE (3817-3870), 496' GAS, 372' OIL (34° API), 124' GASSY OIL CUT MUD (40% OIL), 30/60/45/60, IFP 85-106, FFP 149-181, SIP 1212-1170; #3 - LKC J-ZONE (3903-3950), 2' OIL, 15' OIL CUT MUD (5% OIL), 30/60/30/60, IFP 53-53. FFP 53-53, SIP 1086-1012
15-153-20813 Wahrman 22-25	4125			GEOLOGISTS REPORT; RA GUARD LOG; DUAL INDUCTION LOG; NEUTRON DENSITY POROSITY LOG	#1 - LKC G-ZONE (3913-3961), 15' MUD, 30/45/30/45, IFP 29-29, FFP 29-29, SIP 1046-1026; #2 - LKC J-ZONE (4004-4050), 5' MUD W/SHOW OF OIL, 30/60/30/60, IFP 23-24, FFP 24-25, SIP 78-43
15-153-20814 Basgall 'C' 1	4034	LKC J-ZONE		GEOLOGISTS REPORT; DENSITY POROSITY LOG; RA GUARD LOG	#1 - LKC D-ZONE (3780-3835), 186' GAS, 186' CLEAN GASSY OIL, 62' MUD CUT GASSY OIL, 124' OIL CUT GASSY MUD, 125' SLIGHTLY OIL AND WATER CUT GASSY MUD, 62' MUDDY WATER, 30/60/45/60, FP 39-137 & 177-246, SIP 1116-1086; #2 - LKC J-ZONE (3920-3970) 10' CLEAN OIL, 80' OIL CUT MUD, 30' MUDDY WATER, FP 74-74 & 117-117, SI 1278-1278, HYDROSTATIC PRESSURE 2061-2029.
15-153-20863 Wahrman 1-30	4163				

converted Wicke #2 as an injection well. The six-section area centering on the Beaver Creek field contains 10 wells, including one producing well in the Beaver Creek NE field in the northeast quarter of Section 30 as well as the 3 producers and one injector in the Beaver Creek Field itself (Figure 3, Table 1, 2).

## 5. PRODUCTION HISTORY

After completion in 1993 the Wahrman B #1 well produced 7,665 bbls with production increasing in 1994 and 1995, the latter year supplemented by successful completion of the Wahrman B 2 well (Table 3). With completion of the Wicke #2 and Wahrman E #1 in 1996, field production rose to 15318 bbls and peaked at 17810 bbls in 1997. The Wicke well was shut in during 1998 and subsequently converted to an

injection well as field production began its decline. An increase in production in 2001, peaking in 2002 is the result of implementing the waterflood using the now-converted Wicke #2 well. Production hit another secondary peak in 2006, interrupting an otherwise monotonic decline (Table 3, Figure 4).

Table 3: Annual and cumulative production data for entire Beaver Creek field (includes Wahrman B, Wahrman 'E' 1, and Wicke leases. Data retrieved from Kansas Geological Survey website Dec. 20, 2009<sup>1</sup>.

Year	Annual Production	Cumulative Production	Number of wells
1993	7655	7655	1
1994	11980	19,635	1
1995	13810	33,455	1
1996	15317	48,772	4
1997	17810	66,582	4
1998	13486	80,245	4
1999	9195	89,245	3
2000	8038	97,283	3
2001	10192	107,475	3
2002	12762	120,237	3
2003	9333	129,570	3
2004	8412	137,982	3
2005	8328	146,310	3
2006	9664	155,974	3
2007	7109	163,083	3
2008	5714	168,797	3
2009	3580	172,377	3

<sup>1</sup>Data for 2009 incomplete at time of download

#### 4. GEOLOGY

The important stratigraphic interval in Beaver Creek field is the Upper Pennsylvanian, which includes the Lansing Group and the Kansas City Group. These lithologically similar groups consist largely of vertically alternating limestone and shale units throughout the state of Kansas, and Beaver Creek field is no exception; they are commonly lumped together as the Lansing-Kansas City interval. Within the field, total thickness ranges from 261 to 266 feet in different wells. Limestone units within the Lansing-Kansas City interval are conventionally labeled alphabetically as “zones”, beginning with the A-zone as the stratigraphically highest unit (Morgan, 1953). The Beaver Creek field produces oil from the J-zone limestone, which is the limestone bed

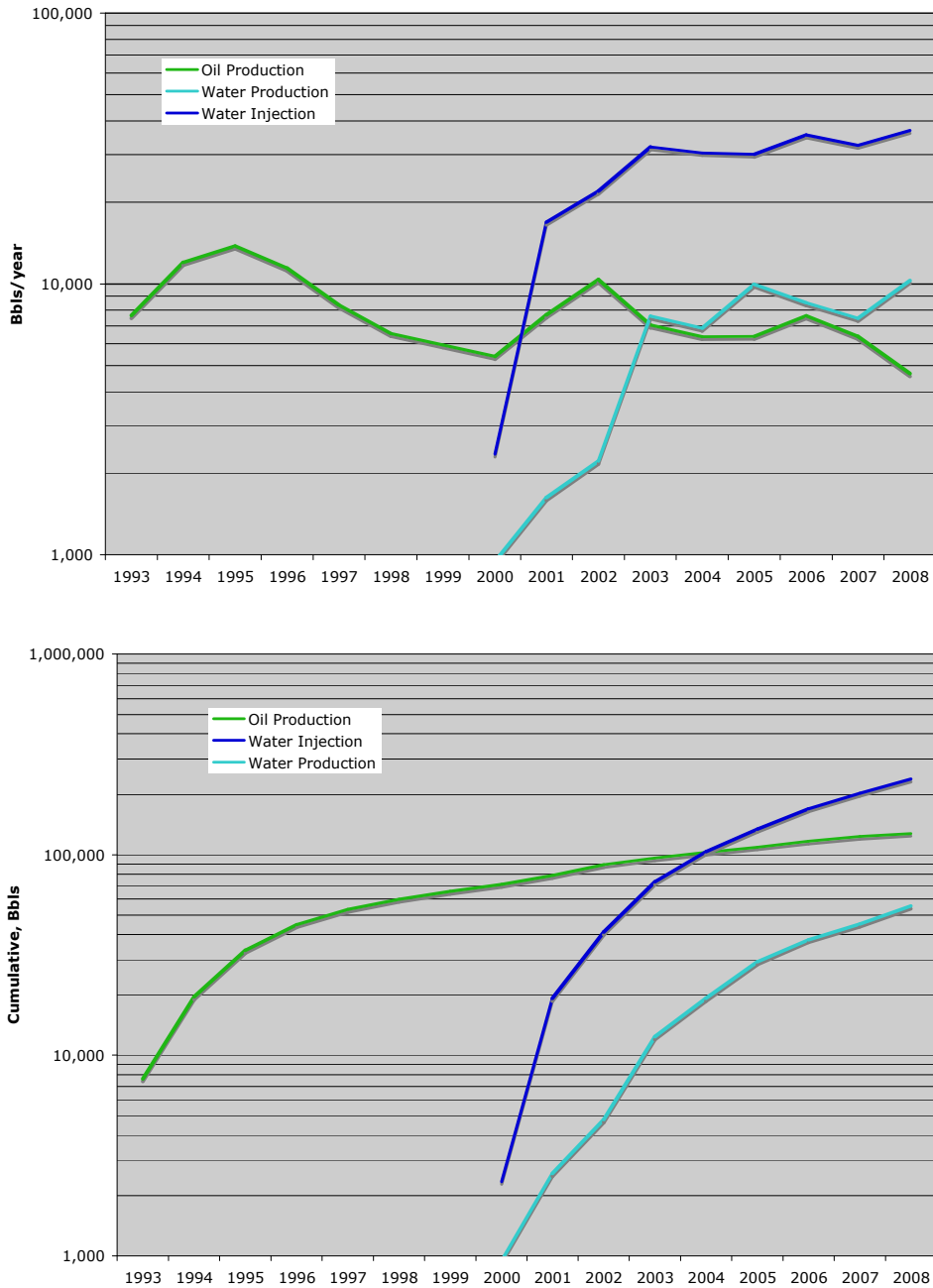


Figure 4. Annual (top) and cumulative production (bottom) from the Wahrman B Lease in the Beaver Creek oil field, Rawlins County Kansas. Two of the three producing wells in the field and the single injector are included in this data. Results for 2009 were incomplete at the time of reporting.

directly above the Stark Shale Member, a highly radioactive bed that is an excellent correlation marker, and stratigraphically equivalent to the Winterset Limestone Member of the Dennis Limestone of the outcrop belt around Kansas City.

The geologist's log from the Wahrman B 2 well gives lithologic descriptions of the section. Figure 5 shows this log along with the gamma ray, neutron, and induction



logs from the Wahrman B 2 well as an illustration of the stratigraphy of Beaver Creek field. Many of the alphabetically labeled zones of limestone within the Lansing-Kansas City interval can be picked out on the geophysical log. Drill-stem tests conducted in

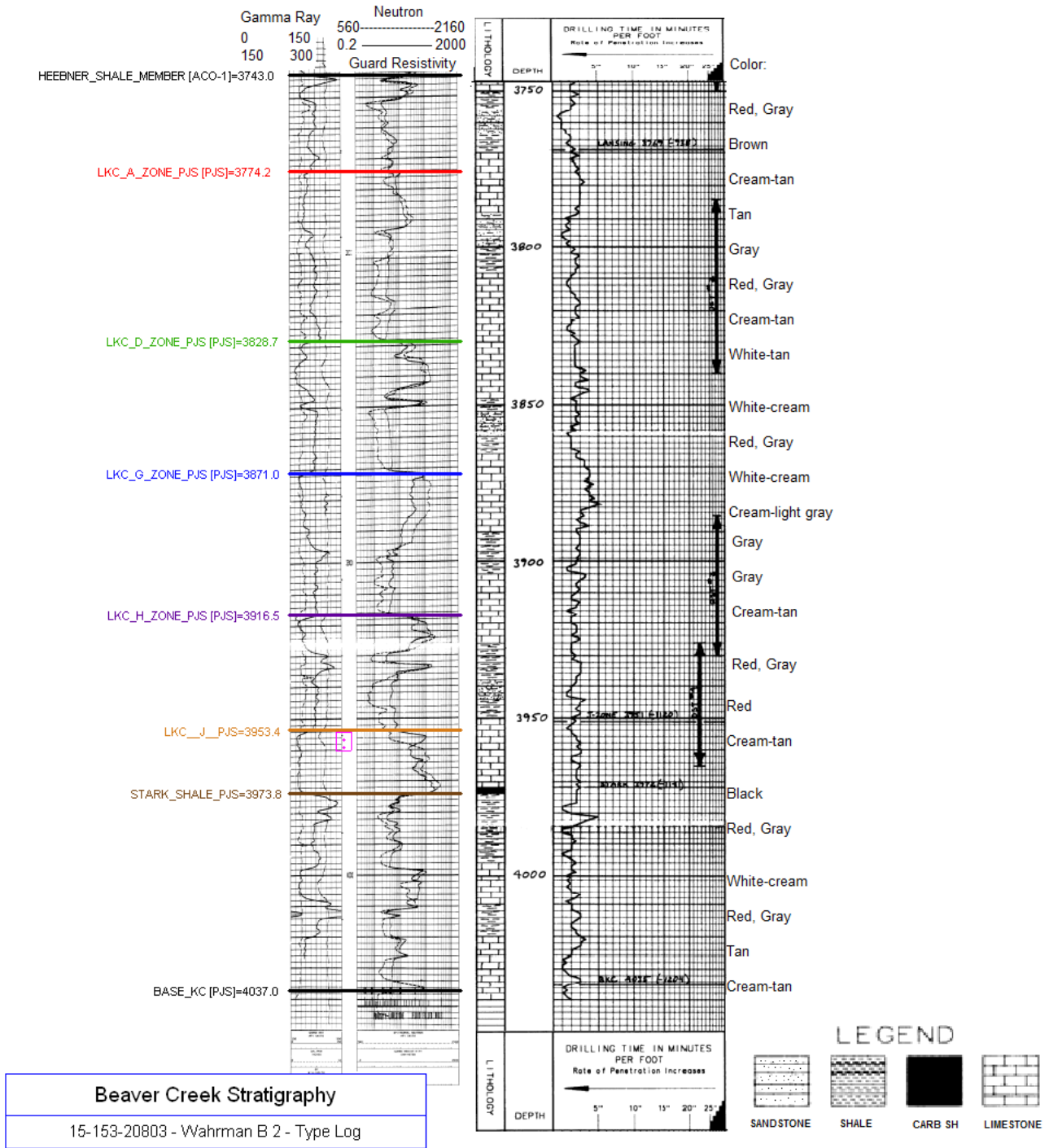


Figure 5. Stratigraphy of Beaver Creek field in the Wahrman B 2 well. Left: RAG log with gamma-ray, neutron, and induction logs, pink box in the depth track shows the perforations at the top of the J-zone. Right: Geologist's log of the well by C.W. Todd Adkins III.

wells in Beaver Creek field revealed the presence of oil in the D, G, H, and J-zones. The J-zone is the only one from which oil has been produced.

The Lansing-Kansas City J-zone is of relatively uniform thickness in the Beaver Creek field, especially in the productive wells. Geologist's logs from the Beaver Creek field describe the J-zone as a slightly fossiliferous limestone with vuggy porosity near the top, and some intergranular porosity. The color is described as white to cream, cream to light gray, or cream to tan, and it is described as chalky to finely crystalline in texture. Figure 4 is a bubble map showing the thickness of the J-Zone in and around Beaver Creek field.

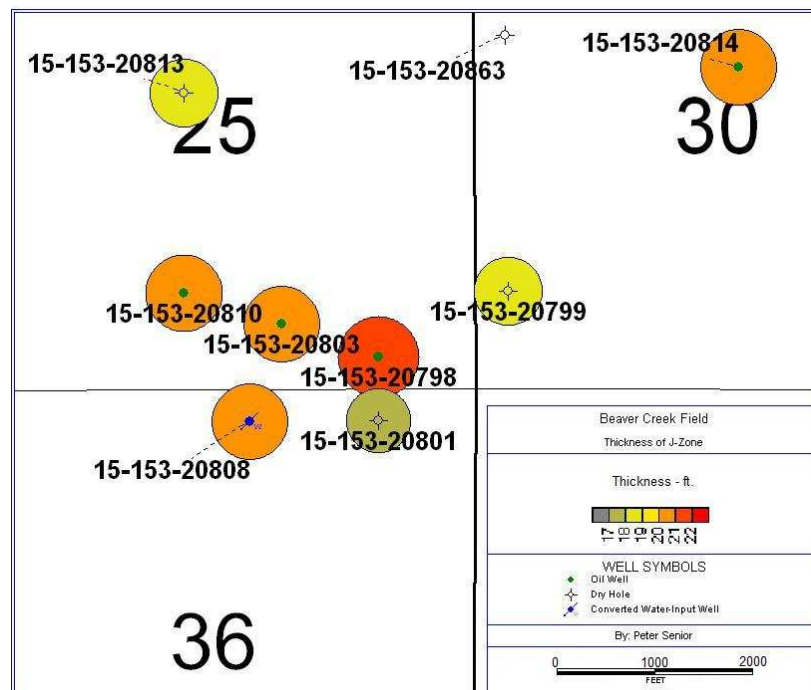


Figure 6. Thickness of the J-zone of the Kansas City Group in the area of the Beaver Creek field.

There is little variation of thickness, especially among the productive wells. The only notable trend seems to be that the three dry holes visible on the map show slightly less thick values. Within the J-Zone, the producing interval is a zone of porous rock at the top of the limestone; it averages five feet in thickness. Figure 7 is a bubble map showing the thickness of this interval in the producing wells of Beaver Creek field.

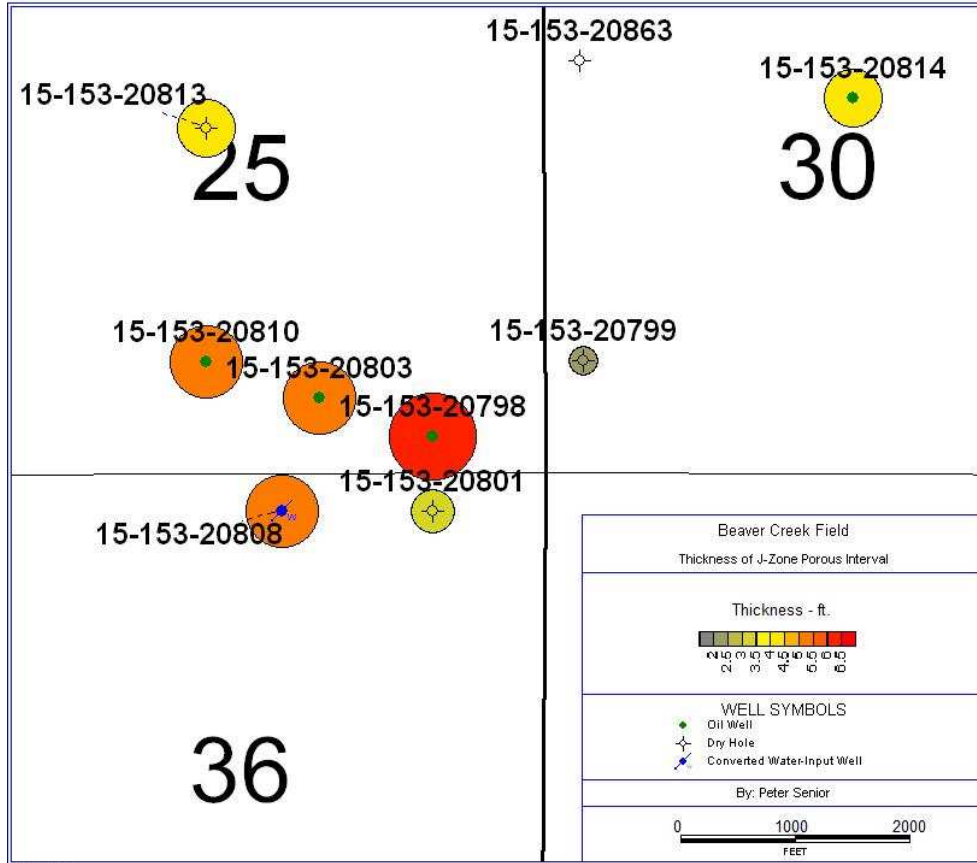


Figure 7: Thickness of the productive interval in the J-zone of the Beaver Creek field.

The structural map of the top of the Lansing-Kansas City interval in northeast Rawlins County shows the large Wilhelm, Wicke, and Wilhelm East oil fields (Figure 8). Beaver Creek field is indicated by the blue circle. The map shows that the larger fields occupy the high areas of a large northwest-southeast trending anticline, and that Beaver Creek lies at a break in slope of a slight bench along the eastern flank of the anticline. In a close-up view, the field is seen to occupy a small protrusion or nose along the eastern flank of the larger anticlinal subsurface feature (Blue rectangle in Figure 9). The nose juts out to the north off the flank, and appears to continue up dip into the southwest corner of section 36.

The three producing wells are aligned NW-SE on a line nearly perpendicular to the structural nose (Figure 10). The cross-section shows a slight high in the J-zone among these three wells. The cross-section in Figure 11 is approximately normal to that in Figure 10. It also shows a slight rollover, but like the section in Figure 10, is not

optimally positioned or oriented because of the distribution of available wells. Although the structural trend is upwards to the right (southwest) of well #15-153-20808, which

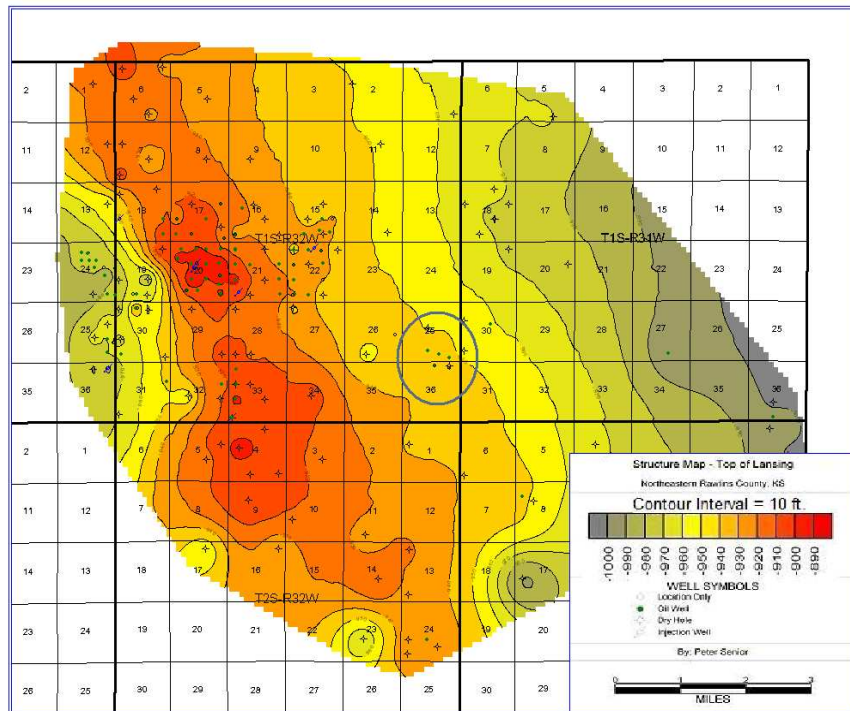


Figure 8. Structure contour map of the top of the Lansing Group. Beaver Creek field lies in the blue circle .

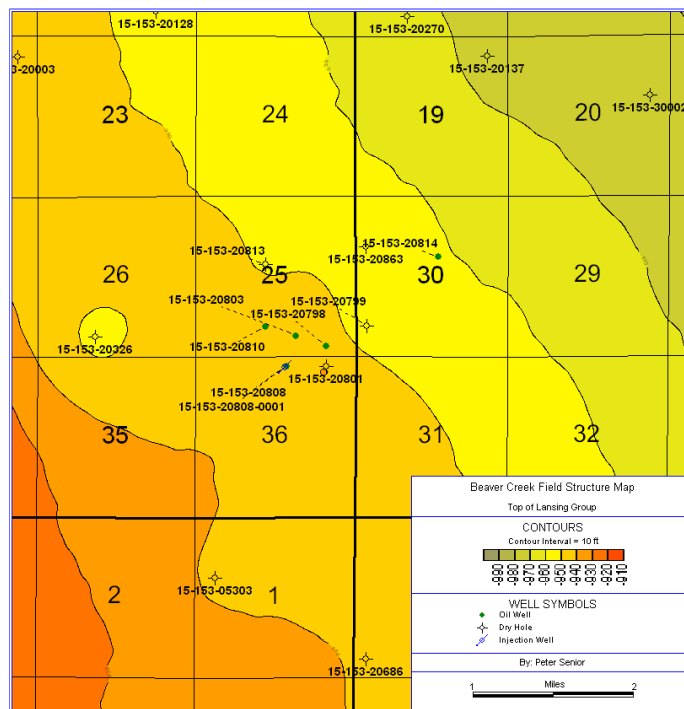


Figure 9. Detail of Figure 8 showing the minor nose on the NE flank of the Wilhem-Wicke anticline.

produces oil, if another well existed immediately to the southwest it could show whether the anticlinal feature has closure or extends slightly farther southwest than is seen in Figure 10. It is possible that the Beaver Creek Field is a small anticline with 360° closure.

However, it is also possible that it represents a local patch of porous, permeable rock with no structural closure at all. The productive interval within the J-zone of the Lansing-Kansas City interval is most porous in the area of the Beaver Creek field (Figure 12; c.f. Figs 4, 7). For the map, porosity was estimated from neutron logs at each two-foot interval, then added together and averaged over the thickness of the J-zone. Taking the values of net reservoir thickness as the thickness of the porous zone and multiplying by the average porosity of this zone (porosity readings estimated from logs at two-foot intervals, added and averaged), an estimate of net reservoir porosity feet can be obtained (Table 4).

Two dry holes immediately northeast of the productive wells provide a good constraint on the extent of the field in that direction. The Wicke 1 well immediately to the southeast of the productive wells had a good show of oil in the drill-stem test (Table 2), but its porosity is somewhat lower than the most productive wells to the northwest. As noted above, no wells have been drilled immediately southwest of Beaver Creek, and so the extent of the reservoir is unknown in that direction. As neither the porosity pinch-out nor the structural closure is defined from available data to the west, south or southeast, only additional investigation can define the extent of the field.

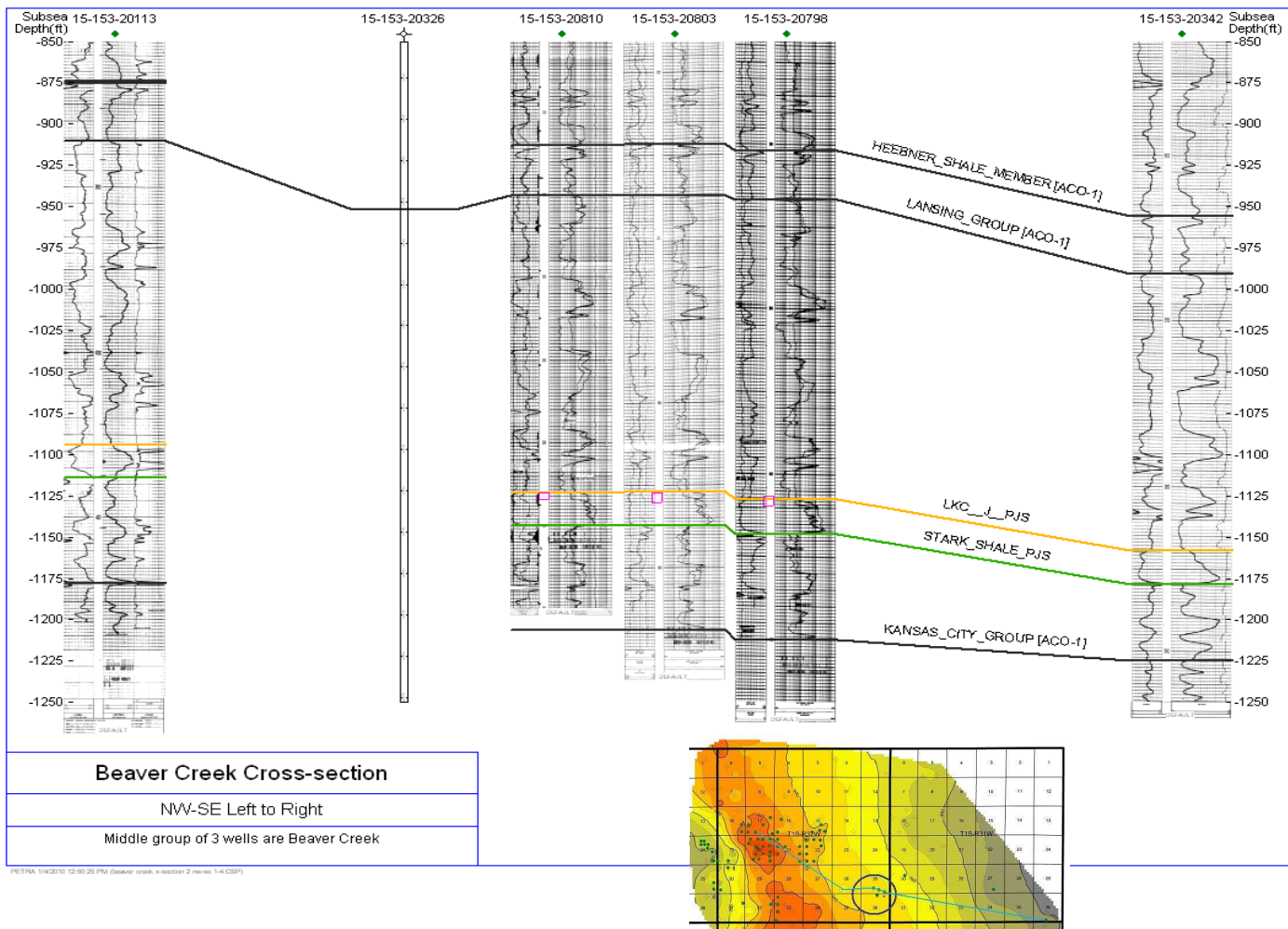


Figure 10. NW-SE cross-section roughly perpendicular to the axis of the structural nose, showing a few feet of rollover. Well 15-153-20326 has no log, but the top of the Lansing Group was picked. Inset shows line of section, with Beaver Creek field circled.

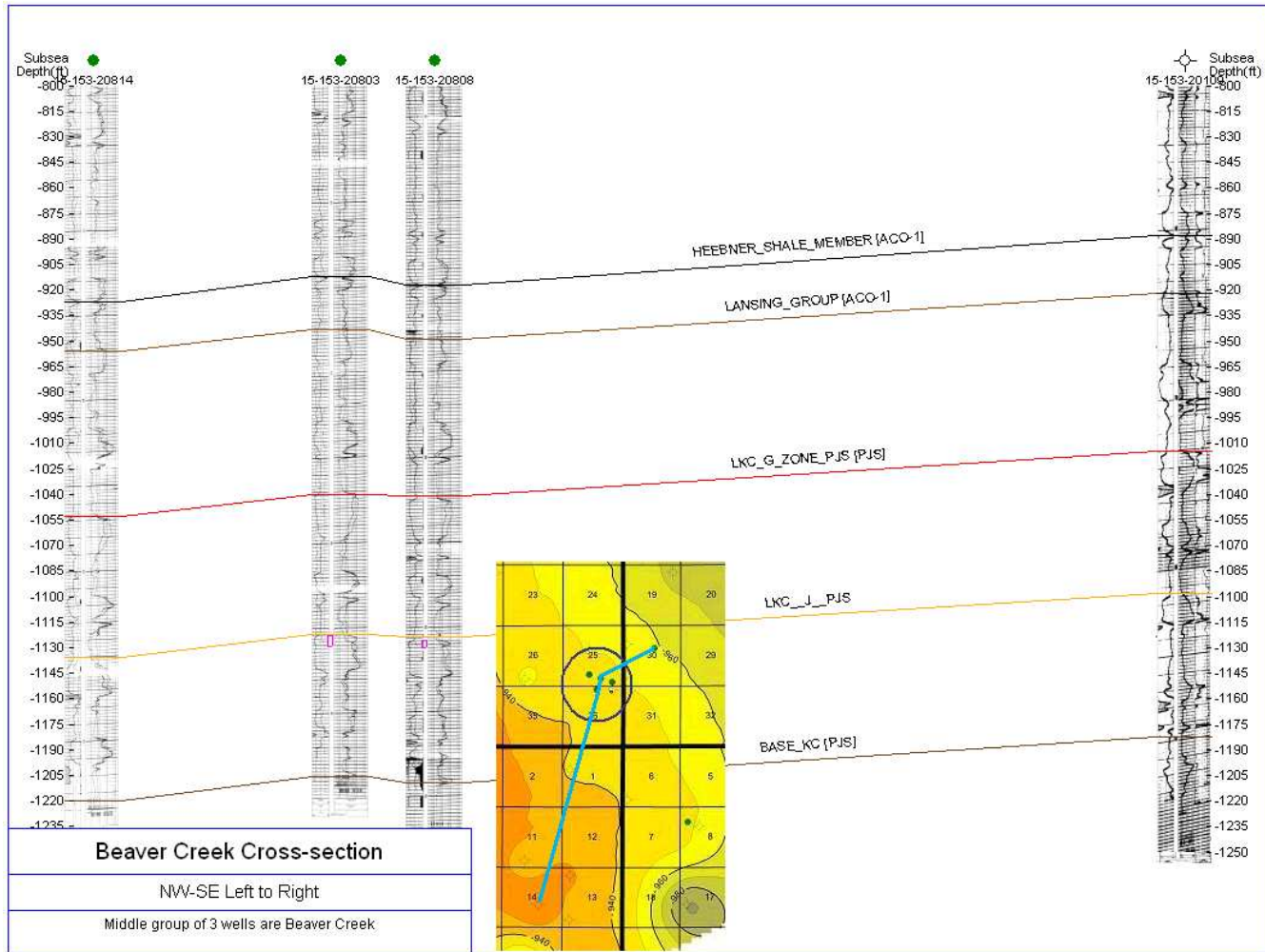


Figure 11, NNE (left)-SSW (right) cross-section through the Beaver Creek field. This section shows a slight rollover, as does Figure 10, suggesting a low degree of closure to the structure, although neither cross-section is optimally located, owing to well distribution. Blue line on insert is the line of section, with Beaver Creek Field circled.

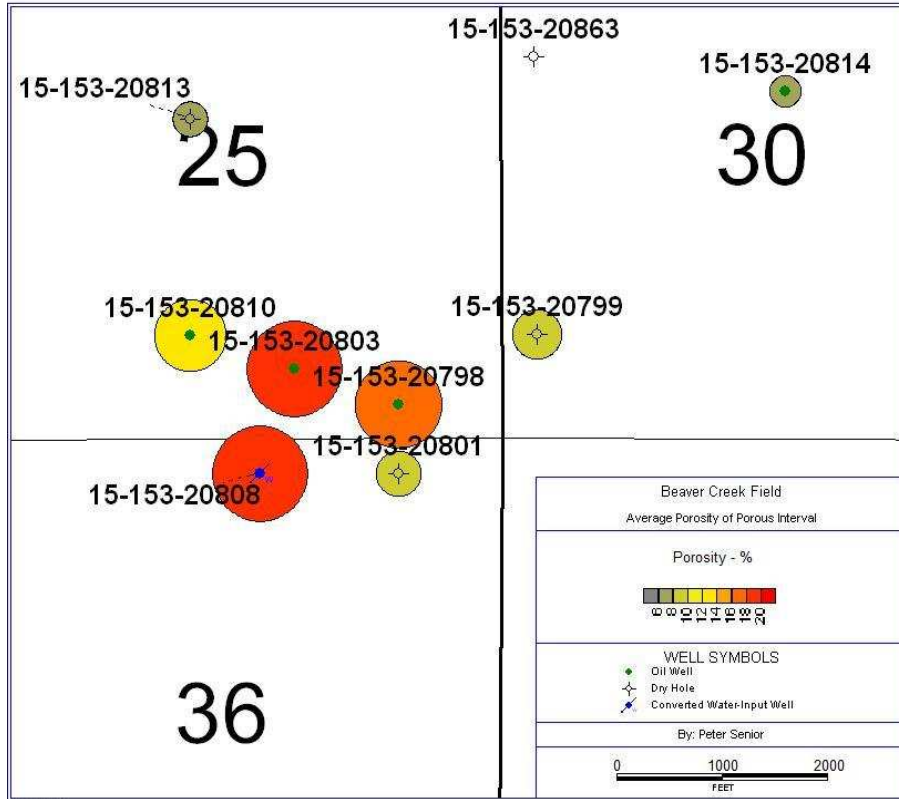


Figure 12: Bubble map showing porosity (%) of productive interval of the J-zone of the Kansas City Group in wells in the area of the Beaver Creek field. Highest porosity lies on the structural nose defined in the structure contour map.

**Table 4: Net porosity feet for producing wells in the Beaver Creek field.**

WELL API NUMBER	NET RESERVOIR THICKNESS (FEET)	AVERAGE RESERVOIR POROSITY (DECIMAL)	NET RESERVOIR POROSITY FEET
15-153-20798	6	0.165	0.99
15-153-20803	5	0.18	0.9
15-153-20808	6	0.18	1.08
15-153-20810	5	0.13667	0.68335

## 5. DATA AVAILABILITY

Lease production figures (Monthly), analyses of produced and make-up water, and basic oil properties are available from Vess Petroleum Corp., the field operator. The operator's production figures and those posted on the KGS website, which were reported to the Kansas Corporation Commission, do not agree exactly, but are close. The operators have also provided samples of recovered oil for analysis of its fluid properties and its reactivity with potential EOR chemicals. Basic geologic data including completion reports, logs, and summaries of drill-stem tests are available from the Kansas Geological Society website and the Kansas Corporation



Commission as well as the operator. However, distribution of wells leaves the trapping mechanism and extent of the field ambiguous. Furthermore, no wells were cored, and drill-stem test results are not in the public domain, other than initial and final pressures and fluid recovery. Core petrophysics (permeability, permeability-porosity equation, relative permeability) may be available from nearby fields. Information on pressure status before waterflood operations must come from the operators. While the operators have provided considerable data and are very interested in successful conclusion of the project, unless more key data are available it will be difficult to establish the target amount of remaining oil.

## **6. CONCLUSION**

The Beaver Creek field lies on a subtle structural nose where porosity is developed in the J-zone of the Lansing-Kansas City interval. Well distribution does not permit analysis of whether the field is trapped by structural closure or permeability pinchout, and no wells lie immediately up regional dip of the field limit. Since discovery in 1993, production peaked in 1997 at 17,800 bbls from three producers. The field is now under waterflood and is producing at about 5000 bbls/year.

The size of the field and the fact that it may be similar to a large number of other Lansing-Kansas City waterfloods suggest it could be an attractive target for a prototype chemical flood. Many Lansing or Kansas City oil fields have been successfully waterflooded. The mineralogy of the reservoirs, calcite and some dolomite, with little clay or quartz, is well known. While field operators can provide information on rates, quantities, and pressures of water injection and production of oil, water, and gas (if any) from individual wells. None of the wells was cored, so full petrophysical analysis must be by analogue with other Lansing-Kansas City fields in the area. If pressure history and closure of the trap cannot be determined, the amount of original oil in place must be estimated volumetrically with key variables assumed. Lacking the key variables, numerical modeling of the field production either under waterflood or as part of an enhanced oil recovery project would be problematic at best.

## 7. REFERENCE CITED

Morgan, J.V., (1953) Correlation of radioactive logs of the Lansing and Kansas City groups in central Kansas [with discussion]: *Journal of Petroleum Technology*, vol. 4, no. 4, pp. 111-118 (also avail. as *Am. Inst. Min. Eng. Trans.*, vol. 195, pp. 111-118).

## 8. ADDITIONAL BIBLIOGRAPHY

The following works describe aspects of the Lansing-Kansas City interval in northwestern Kansas, or aspects of the petroleum geology of the region.

Anderson, J.E.(1989) Diagenesis of the Lansing and Kansas City groups (Upper Pennsylvanian), northwestern Kansas and southwestern Nebraska: unpubl. M.S. thesis, Department of Geology, University of Kansas, Lawrence, Kansas, 259 p. (avail. as *Kans. Geol. Survey, Open-file Rept.*, no. 89-14).

Ben Omran, Abdelmoneim (1972) A geological study of the oil fields in Rawlins County, Kansas: unpubl. M.S. thesis, Department of Geology, Wichita State University, Wichita, KS, 55 p.

Ross, J.A.; Lee, S.B.; and Beene, D.L. (1993) Oil and gas fields, Goodland quadrangle in Kansas: *Kansas Geological Survey, Map Series*, no. 34-1, 1 sheet, scale 1:250,000.

Watney, W.L. (1980) Cyclic sedimentation of the Lansing-Kansas City groups in northwestern Kansas and southwestern Nebraska; a guide for petroleum exploration: *Kansas Geological Survey, Bulletin*, no. 220, 72 pages,

<http://www.kgs.ku.edu/Publications/Bulletins/220/index.html>  
<<http://www.kgs.ku.edu/Publications/Bulletins/220/index.html>>

Watney, W.L.(1985) Origin of four Upper Pennsylvanian (Missourian) cyclothems in the subsurface of western Kansas; application to search for accumulation of petroleum: Unpubl. Ph.D. dissertation, Department of Geology, University of Kansas, Lawrence, KS, 524 pages (avail. as *Kans. Geol. Survey, Open-file Rept.*, no. 85-2).

# **CELIA SOUTH WATERFLOOD UNIT, RAWLINS COUNTY, KANSAS**

**Peter Senior & Anthony W. Walton<sup>1</sup>**

## **1. INTRODUCTION**

Celia South waterflood unit is currently operated by Murfin Drilling Company, Inc. of Wichita, Kansas. The unit covers parts of the Celia and Celia South oilfields and currently comprises 31 wells – 23 producers and 8 injectors. Wells were drilled from the early 1970's to late 1980's. Oil is produced from a limestone near the top of the Middle Pennsylvanian Cherokee Group at measured depths of around 4,650 feet. Cumulative oil production from 1983 to July 2011 from both fields is 2,805,206 barrels, with annual production in 2010 of 15,767 barrels.

## **2. LOCATION**

Celia and Celia South oilfields are in western Rawlins County, Kansas less than one mile south of the town of McDonald, Kansas (Figure 1, 2). The Celia South waterflood unit occupies 2240 acres, covering parts of sections 20, 21, and 27, all of section 28, and parts of sections 29, 32, and 33, Township 3 South, Range 36 West (Figure 2). A topographic map shows that the northern part of the unit spans a valley, which has nearly 100 feet of relief (Figure 3).

---

<sup>1</sup> Department of Geology, The University of Kansas, 1475 Jayhawk Blvd., Suite 120, Lawrence, Kansas 66045.  
Contact e-mail: twalton@ku.edu

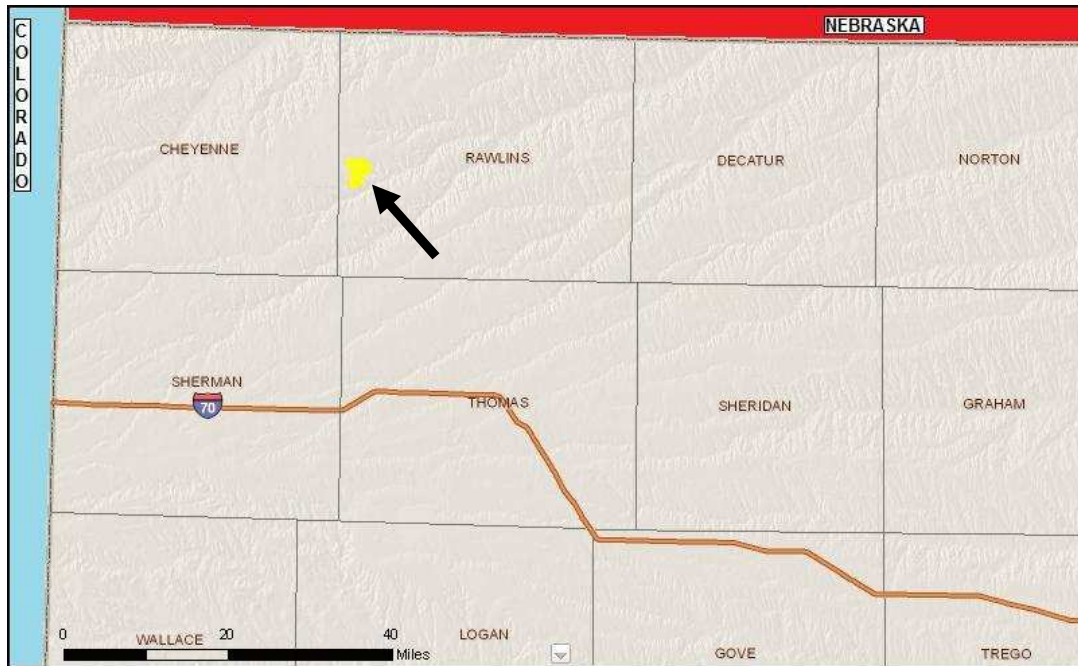


Fig. 1: Regional map showing location of Celia South waterflood unit, modified from KGS website.

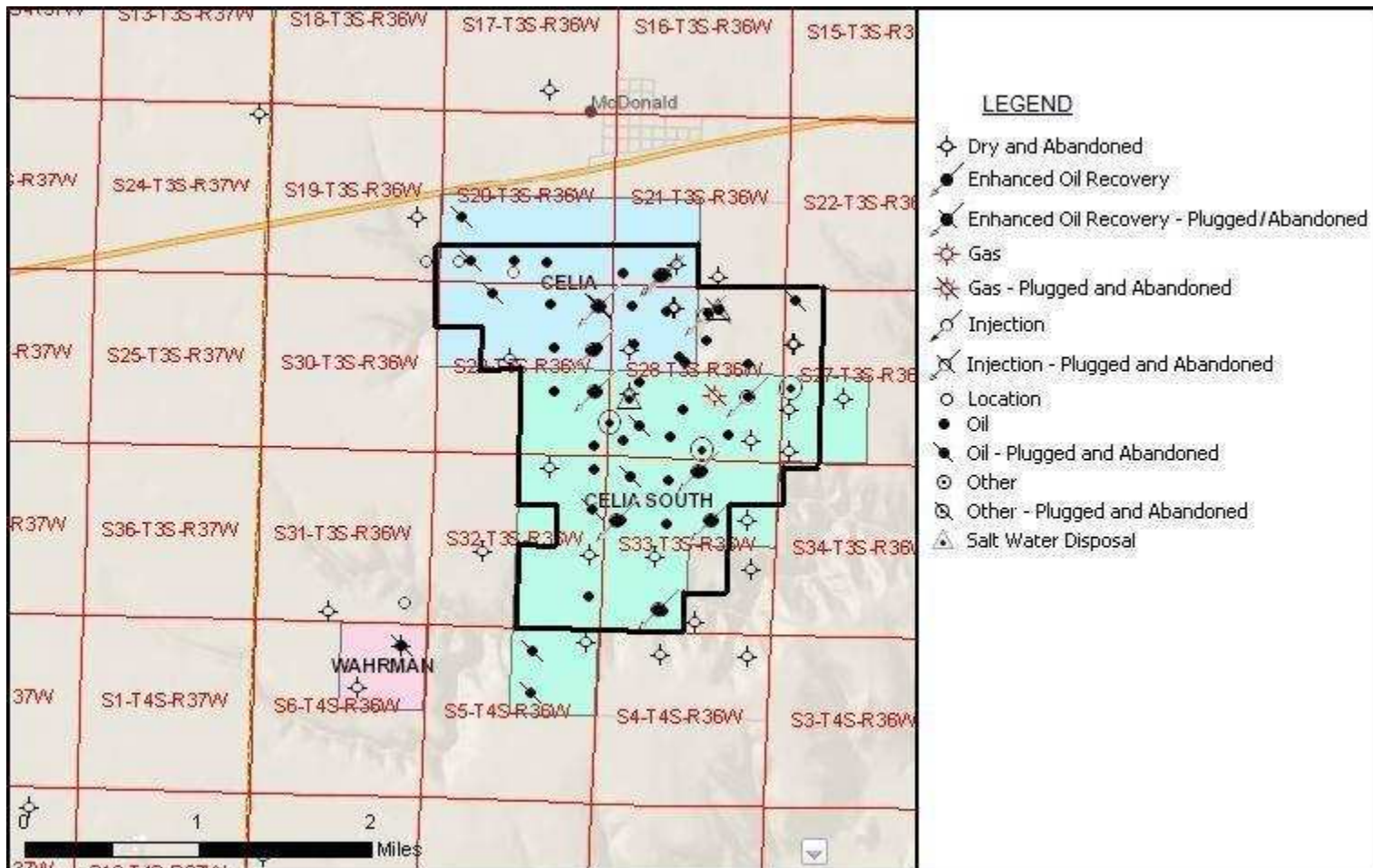


Fig. 2: Sub-regional map of Celia South waterflood unit, outlined in black, and associated oilfields, modified from KGS website.

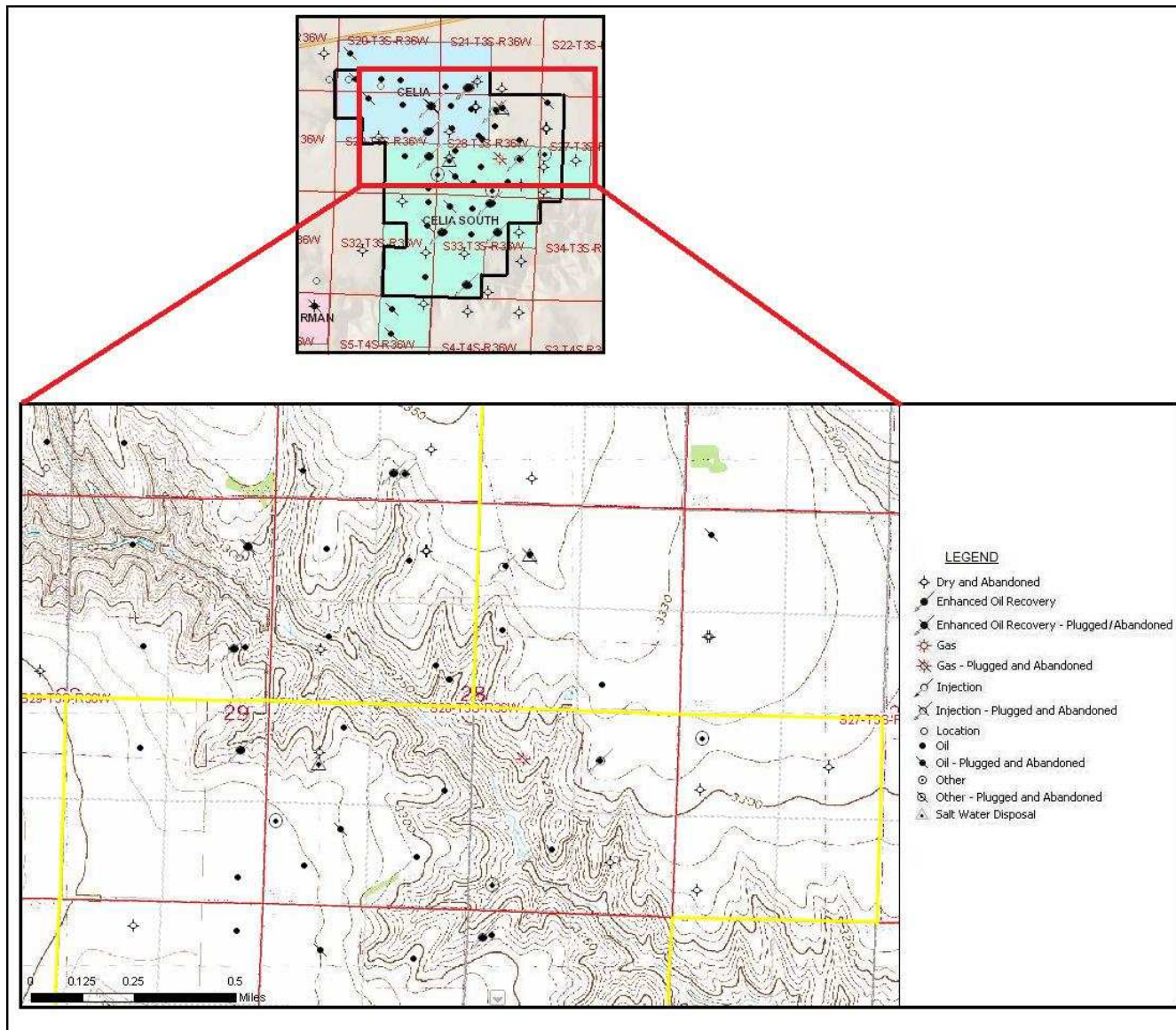


Fig. 3: Topographic map of Celia South waterflood unit area from KGS website. Bold contour lines are at 50 foot intervals, indicating the valley on the map has around 100 feet of relief.

### **3. METHODS**

This report was constructed by analyzing data in the public domain and posted on the Kansas Geological Survey (KGS) website (<http://www.kgs.ku.edu>), along with data provided by the field operator directly to the investigators. The major methods were use of well logs to determine the configuration of key horizons to create geologic maps and cross-sections of the reservoir. The data and logs were imported into Petra™, a subsurface GIS program, and analyzed using standard techniques. Logs of porosity and resistivity were digitized in Petra™ so that the Archie Equation could be used to calculate fluid saturations. Production history, quantities, and rates were downloaded from the KGS website.

### **4. DISCOVERY & DEVELOPMENT HISTORY**

Coastal Oil & Gas Corporation completed the discovery well, the Hubbard 1-28V (API# 15-153-20477), in June 1983. Drill-stem testing recovered 22 barrels of oil and 1/2 barrel of oil-cut mud from a limestone in the Cherokee Group. Pressures from the drill-stem test were as follows: IFP 117#-383#, ISIP 383#-1338#, FFP 417#-832#, FSIP 832#-1330#. According to an internal Coastal Oil & Gas Corporation report (Amonsens, D.R., et al., 1987) the well had initial production rate of 138 barrels of oil per day (BOPD). Development of the reservoir through drilling of further wells spanned the decade of the 1980s. Of the 55 additional wells drilled after discovery, 42 were successful, according to the KGS database. A number of companies besides Coastal Oil & Gas Corporation were involved in development of the reservoir, including Magnus Oil & Gas and Cities Service Co., as well as independent operators such as Ed Cahoj, Bruce Clark, James Dillie, and Paul Prijatel. Murfin Drilling Company, Inc. is the current operator of the ongoing waterflood of the reservoir. Table 1 provides information on locations, statuses, and relevant dates associated with wells in the Celia and Celia South oilfields.

Prior to completion of the discovery well for the Cherokee Group reservoir, the Cahoj 2 well (API# 15-153-20365) produced oil from a shallower reservoir in the Lansing Group. The Coastal Oil & Gas Hubbard 7 (API#15-153-20517) produced from both the Lansing and Cherokee reservoirs, but was later plugged back to produce only from the Lansing, and has since been plugged and abandoned. No commingling of production currently exists between the two reservoirs.

Table 1: Summary of wells in the Celia and Celia South oilfields, compiled from from KGS.

API NUMBER	LEASE	WELL	FIELD	TWP-RGE-SEC	SPOT	CURRENT OPERATOR	SPUD	COMPL	PLUG	RECOMPL	TYPE
15-153-20149, -0001	HUBBARD	9 SWD	CELIA	3S-36W-28	N2 S2 NW SW	Coastal Oil & Gas Corp.	23-Feb-73	4-Mar-73	4-Mar-73	App withdrawn	SWD
15-153-20286, -0001	CAHOJ	1	CELIA	3S-36W-28	C NE NW	Clark B and Cahoj E	26-May-77	4-Jun-77	4-Jun-77	18-Apr-80	D&A, RECOMPL-P&A
15-153-20365	CAHOJ	2	CELIA	3S-36W-28	C NW NE	unavailable	17-Nov-79				OIL
15-153-20387	HENRY CAHOJ	1	CELIA	3S-36W-21	C SE SW	unavailable	7-Jul-80	8-Aug-80	8-Aug-80		D&A
<b>15-153-20477</b>	<b>HUBBARD</b>	<b>1-28V</b>	<b>CELIA SOUTH</b>	<b>3S-36W-28</b>	<b>S2 SE NE SW</b>	<b>Murfin Drilling Co. Inc.</b>	<b>22-May-83</b>	<b>17-Jun-83</b>			<b>OIL ***Discovery Well</b>
15-153-20479	CAHOJ 'A'	1	CELIA	3S-36W-28	SE SE NW	Clark B and Cahoj E	22-Jun-83	30-Jul-83			OIL
15-153-20480, -0001	CAHOJ 'B'	2	CELIA	3S-36W-28	NW SW NE	Murfin Drilling Co. Inc	15-Aug-83	30-Oct-83		7-Mar-90	OIL CONV TO EOR
15-153-20481	CAHOJ	27-13A	CELIA SOUTH	3S-36W-27	SW SW SW	MAGNUS O&G	18-Jul-83	24-Jul-83	24-Jul-83		D&A
15-153-20485, -0001, also listed as 15-153-90099	HENRY CAHOJ 'C'	1	CELIA	3S-36W-21	SW SE SW	Murfin Drilling Co. Inc	27-Jul-83	16-Aug-83		7-Mar-90	OIL CONV TO EOR
15-153-20486, -0001	CAHOJ	27-12A	CELIA SOUTH	3S-36W-27	NW NW SW	MAGNUS O&G	26-Jul-83	2-Aug-83	2-Aug-83	1-May-84	D&A, RECOMPL-P&A
15-153-20487	HUBBARD	2-28V	CELIA SOUTH	3S-36W-28	NE NW SW	Murfin Drilling Co. Inc.	22-Aug-83	9-Sep-83			OIL
15-153-20489	CAHOJ 'B'	1	CELIA	3S-36W-28	SW NW NE	Murfin Drilling Co. Inc	15-Aug-83	12-Sep-83			OIL
15-153-20492	HUBBARD	3-28V	CELIA SOUTH	3S-36W-28	C NW SE	COASTAL O&G	1-Sep-83	16-Sep-83	31-Mar-99		GAS-P&A
15-153-20493	HUBBARD	4-28V	CELIA SOUTH	3S-36W-28	C SE SW	Murfin Drilling Co. Inc.	22-Oct-83	8-Nov-83			OIL
15-153-20494	HUBBARD	5-28V	CELIA SOUTH	3S-36W-28	E2 SW SE	Murfin Drilling Co. Inc.	9-Oct-83	25-Oct-83			OIL
15-153-20495	CAHOJ 'A'	2	CELIA	3S-36W-28	N2 SW NW	Murfin Drilling Co. Inc	24-Oct-83	2-Feb-84			OIL
15-153-20496	CAHOJ 'A'	3	CELIA	3S-36W-28	W2 NE NW	Murfin Drilling Co. Inc	4-Dec-83	8-Feb-84			OIL
15-153-20497	CAHOJ 'B'	3	CELIA	3S-36W-28	SW SE NE	Murfin Drilling Co. Inc	10-Sep-83	30-Oct-83			OIL
15-153-20515	CAHOJ 'A'	4	CELIA	3S-36W-28	C NW NW	Murfin Drilling Co. Inc	15-Nov-83	1-Feb-84			OIL



Table 1 (cont.): Summary of wells in the Celia and Celia South oilfields, compiled from from KGS.

API NUMBER	LEASE	WELL	FIELD	TWP-RGE-SEC	SPOT	CURRENT OPERATOR	SPUD	COMPL	PLUG	RECOMPL	TYPE
15-153-20516, -0001	HUBBARD	6-28V	CELIA SOUTH	3S-36W-28	W2 NE SE	Murfin Drilling Co. Inc.	30-Oct-83	14-Nov-83	8-Aug-90		OIL CONV TO EOR
15-153-20517, -0001	HUBBARD	7-28V	CELIA SOUTH	3S-36W-28	NE SW SW	COASTAL O&G	7-Nov-83	21-Nov-83	31-Mar-99	27-Jun-85	OIL CONV TO EOR, P&A
15-153-20520	FISHER	2-33V	CELIA SOUTH	3S-36W-33	NW NW NE	Murfin Drilling Co. Inc.	15-Nov-83	9-Dec-83		20-Jan-90	OIL CONV TO EOR
15-153-20522	CAHOJ	27-14A	CELIA SOUTH	3S-36W-27	C NE SW	MAGNUS O&G	19-Nov-83	25-Nov-83	25-Nov-83		D&A
15-153-20528	Henry Cahoj 'C'	2	CELIA	3S-36W-21	SW SW SW	Murfin Drilling Co. Inc	26-Dec-83	1-Mar-84			OIL
15-153-20530	HUBBARD	1-33V	CELIA SOUTH	3S-36W-33	C NE NW	Murfin Drilling Co. Inc.	14-Jan-84	31-Jan-84			OIL CONV TO EOR
15-153-20531	HUBBARD	2-29V	CELIA	3S-36W-29	NE SE NE	Coastal Oil & Gas Corp.	5-Jan-84	25-Jan-84			OIL
15-153-20532	FISHER	5-33V	CELIA SOUTH	3S-36W-33	SE NW SE NE	COASTAL O&G	18-Dec-83	3-Jan-84	31-Jan-84		D&A
15-153-20533	JOE CAHOJ 'D'	1	CELIA	3S-36W-21	S2 SW SE	JAMES DILLIE	20-Jan-84	1-May-84	22-Dec-88		D&A
15-153-20537, -0001	HUBBARD	3-29V	CELIA SOUTH	3S-36W-29	NE NE SE	Murfin Drilling Co. Inc.	10-Mar-84	29-Mar-84		7-Mar-90	OIL CONV TO EOR
15-153-20538	HUBBARD	4-29V	CELIA	3S-36W-29	NE NE NE	Coastal Oil & Gas Corp.	19-Feb-84	7-Mar-84	31-Mar-99		OIL-P&A
15-153-20538, -0001	HUBBARD	4-29V	CELIA	3S-36W-29	NE NE NE	Coastal Oil & Gas Corp.	19-Feb-84	7-Mar-84	31-Mar-99	7-Mar-90	OIL CONV TO EOR, P&A
15-153-20540	HUBBARD	8-28V	CELIA SOUTH	3S-36W-28	E2 SW SE SE	COASTAL O&G	1-Mar-84	30-Mar-84	30-Mar-84		D&A
15-153-20541, -0001	FISHER	3-33V	CELIA SOUTH	3S-36W-33	S2 N2 SW NE	Murfin Drilling Co. Inc.	23-Jun-84	13-Jul-84		13-Jan-90	OIL CONV TO EOR
15-153-20569	FISHER	7-33S	CELIA SOUTH	3S-36W-33	C NE SE	COASTAL O&G	24-Aug-84	30-Aug-84	30-Aug-84		D&A
15-153-20575	HUBBARD 'C'	1	CELIA	3S-36W-29	W2 E2 NW NE	Murfin Drilling Co. Inc	25-Sep-84	6-Nov-84			OIL
15-153-20576	HUBBARD-POWELL 'A'	1	CELIA SOUTH	3S-36W-33	SW NE NW NW	Murfin Drilling Co. Inc.	13-Oct-84	14-Nov-84	26-Jan-99		OIL-P&A
15-153-20579	CELIA	27-1	CELIA	3S-36W-27	E2 NW SW NW	IREX OPERATING	30-Oct-84	3-Nov-84	3-Nov-84		D&A

Table 1 (cont.): Summary of wells in the Celia and Celia South oilfields, compiled from from KGS.

API_NUMBER	LEASE	WELL	FIELD	TWP-RGE-SEC	SPOT	CURRENT OPERATOR	SPUD	COMPL	PLUG	RECOMPL	TYPE
15-153-20586	HUBBARD	6-29V	CELIA SOUTH	3S-36W-29	E2 NW SE	Murfin Drilling Co. Inc.	14-Dec-84	4-Jan-85			OIL
15-153-20592	POWELL 'A'	1	CELIA SOUTH	3S-36W-32	NE NE NE	Murfin Drilling Co. Inc.	19-Jan-85	6-Mar-85			OIL
15-153-20594	Henry Cahoj	1-D	CELIA	3S-36W-20	E2 SE SW	JAMES DILLIE	31-Jan-85	18-Feb-85			OIL
15-153-20595	HUBBARD 'C'	2	CELIA	3S-36W-29	E2 SW NE	Murfin Drilling Co. Inc	9-Mar-85	3-Apr-85			OIL
15-153-20596	HUBBARD	1-20K	CELIA	3S-36W-20	C SW SE	Murfin Drilling Co. Inc	3-Mar-85	23-Mar-85			OIL
15-153-20597	Kehlbeck	1-D	CELIA SOUTH	3S-36W-5	C NW NE	James Dillie Oil & Gas	20-Mar-85	19-Apr-85	6-Jul-87		OIL-P&A
15-153-20598	CAHOJ 'A'	5	CELIA	3S-36W-28	NW SE SE NW	Clark B and Cahoj E	15-Apr-85	8-May-85			OIL
15-153-20604	HUBBARD	5-29-S	CELIA SOUTH	3S-36W-29	SE SE SE	Murfin Drilling Co. Inc.	2-May-85	17-May-85			OIL
15-153-20606	CELIA SOUTH WATER FLOOD UNIT, was HUBBARD 'D'	1	CELIA	3S-36W-29	NW NE NW	Murfin Drilling Co. Inc	9-May-85	13-Aug-85	29-Apr-09		OIL-P&A
15-153-20609	POWELL 'A'	2	CELIA SOUTH	3S-36W-32	NE NW NE	OXY USA Inc.	29-May-85	5-Jun-85	5-Jun-85		D&A
15-153-20611	HUBBARD	10-28V	CELIA SOUTH	3S-36W-28	NE SW SW SW	Murfin Drilling Co. Inc.	11-Jun-85	22-Jun-85			OIL
15-153-20613	HENRY CAHOJ	3-D	CELIA	3S-36W-20	C NW SW	Cahoj H Drilling	3-Jul-85	21-Aug-85	6-Mar-91		OIL-P&A
15-153-20619, -0001	HUBBARD-POWELL 'A'	2	CELIA SOUTH	3S-36W-33	SE NW SW NW	Murfin Drilling Co. Inc.	22-Jul-85	22-Aug-85		7-Mar-90	OIL CONV TO EOR
15-153-20621, -0001	FISHER	4-33K	CELIA SOUTH	3S-36W-33	C SE SW	OXY USA Inc.	3-Aug-85	19-Aug-85		30-Nov-95	OIL CONV TO EOR
15-153-20624	CELIA SOUTH G was POWELL 'A' 3	4	CELIA SOUTH	3S-36W-32	NE SE NE	Murfin Drilling Co. Inc.	2-Aug-85	15-May-86	26-May-10		OIL-P&A
15-153-20625	OFFICER	32-43A	CELIA SOUTH	3S-36W-32	NE NE SE	J D P CORP	13-Nov-85	16-Feb-86	16-Feb-86		D&A

Table 1 (cont.): Summary of wells in the Celia and Celia South oilfields, compiled from from KGS.

API_NUMBER	LEASE	WELL	FIELD	TWP-RGE-SEC	SPOT	CURRENT OPERATOR	SPUD	COMPL	PLUG	RECOMPL	TYPE
15-153-20626	OFFICER	32-44A	CELIA SOUTH	3S-36W-32	NE SE SE	Murfin Drilling Co. Inc.	13-Nov-85	3-Jan-86			OIL
15-153-20636	HUBBARD	2-33K	CELIA SOUTH	3S-36W-33	C SE NW	Murfin Drilling Co. Inc.	25-Sep-85	16-Oct-85			OIL
15-153-20637	FISHER	6-33K	CELIA SOUTH	3S-36W-33	SW SW SE	COASTAL O&G	3-Oct-85	11-Oct-85	11-Oct-85		D&A
15-153-20641	HENRY CAHOJ	2-D	CELIA	3S-36W-20	E2 SW SW	Cahoj H Drilling	29-Nov-85	7-Jan-86	2-Sep-99		OIL-P&A
15-153-20643	WEBB	19-43	CELIA	3S-36W-19	C NE SE	Murfin Drilling Co. Inc	8-Dec-85	15-Dec-85	15-Dec-85		D&A
15-153-20646	VOLENTINE HUBBARD	1-4K	CELIA SOUTH	3S-36W-4	C NE NW	COASTAL O&G	15-Dec-85	22-Dec-85	11-Mar-86		D&A
15-153-20648	KEHLBECK	2-D	CELIA SOUTH	3S-36W-5	NE NE NE	James Dillie Oil & Gas	20-Jan-86	27-Jan-86	28-Jan-86		D&A
15-153-20726	KEHLBECK	3	CELIA SOUTH	3S-36W-5	C SW NE	PRIJATEL PAUL	31-Dec-88	1-Feb-89	4-Aug-89		OIL-P&A
15-153-20741	CELIA SOUTH UNIT	E-5-S	CELIA SOUTH	3S-36W-28	NW NW SW SW	Murfin Drilling Co. Inc.	25-Oct-89	31-Jan-90			WATER SUPPLY, INAC.
	CELIA S	F-5	CELIA SOUTH	3S-36W-33	SW NE NW NW	Murfin Drilling Co. Inc.			12-Jan-99		OIL

## 5. PRODUCTION HISTORY

Annual oil production data from the KGS shows a primary combined production peak for Celia and Celia South oilfields in 1984 of 379,105 barrels. This peak was followed by a period of steep decline to a low of 67,695 barrels in 1989. Oil production in 1990 rose to 118,596 barrels and peaked in 1991 at 383,525 BBLs as a result of waterflooding. Since that time annual production has declined to a total production in 2010 of 15,767 barrels. Cumulative production as of July, 2011 is 2,805,206 barrels. Table 2 and Figures 4 and 5 provide numerical and graphical summaries of production data.

From the peak annual production in 1984 to the low point in 1989, oil production had declined over 80 percent. Waterflooding of the reservoir provided a rapid, significant increase in production; 1990 annual oil production was over 175 percent of the previous year's total. Peak annual production from the waterflood was actually slightly above peak annual primary production. From the peak annual waterflood production in 1991 to the last complete year's production in 2010, annual oil production decline has been over 95 percent. Decline in production on an annual basis was in the 20 to 30 percent range through the end of the 1990s, but has since reduced to a level where year-on-year declines in production are commonly less than 10 percent. Current production rates for wells in the unit are in the 2-5 BOPD range, generally with a few hundred barrels of water per well.

The report by Amosen et al. (1987, p. 7) estimated original oil in place (OOIP) of approximately 9.6 million barrels of oil (9.6 MMBO). The current cumulative production of 2,805,206 BBLs indicates to a recovery factor of 29.2% of OOIP. Cumulative primary production, from 1983 to 1989 was 13% of OOIP, while cumulative secondary production from 1990 to present has been 16.2% of OOIP. Taking the OOIP estimate minus cumulative production gives an estimated amount of oil remaining of approximately 6.79 MMBO. If a tertiary recovery phase could recover an additional 5-10% of OOIP, incremental production would be 480,000 to 960,000 BBLs.

Table 2: Annual and cumulative oil production data for Celia and Celia South oilfields, from KGS. 2011 oil production data is incomplete. Production from Lansing reservoir not included.

Year	Celia South		Celia		Both Fields	Both Fields
	Production (bbls)	Cumulative (bbls)	Production (bbls) minus LKCprod.	Cumulative (bbls) minus LKCprod.	Annual (bbls)	Cumulative (bbls)
1983	41,963	41,963	60,920	60,920	102,883	102,883
1984	177,800	219,763	201,305	262,225	379,105	481,988
1985	167,716	387,479	154,534	416,759	322,250	804,238
1986	100,205	487,684	91,171	507,930	191,376	995,614
1987	65,994	553,678	46,619	554,549	112,613	1,108,227
1988	35,452	589,130	33,930	588,479	69,382	1,177,609
1989	52,153	641,283	15,542	604,021	67,695	1,245,304
1990	112,711	753,994	5,885	609,906	118,596	1,363,900
1991	378,008	1,132,002	5,517	615,423	383,525	1,747,425
1992	234,462	1,366,464	5,523	620,946	239,985	1,987,410
1993	165,392	1,531,856	4,552	625,498	169,944	2,157,354
1994	120,599	1,652,455	4,525	630,023	125,124	2,282,478
1995	73,833	1,726,288	1,761	631,784	75,594	2,358,072
1996	49,562	1,775,850	1,085	632,869	50,647	2,408,719
1997	42,952	1,818,802	1,227	634,096	44,179	2,452,898
1998	36,128	1,854,930	1,099	635,195	37,227	2,490,125
1999	37,458	1,892,388	839	636,034	38,297	2,528,422
2000	34,404	1,926,792	18	636,052	34,422	2,562,844
2001	33,727	1,960,519			33,727	2,596,571
2002	31,527	1,992,046			31,527	2,628,098
2003	30,361	2,022,407			30,361	2,658,459
2004	28,692	2,051,099			28,692	2,687,151
2005	24,111	2,075,210			24,111	2,711,262
2006	20,300	2,095,510			20,300	2,731,562
2007	19,044	2,114,554			19,044	2,750,606
2008	19,593	2,134,147			19,593	2,770,199
2009	15,585	2,149,732			15,585	2,785,784
2010	15,767	2,165,499			15,767	2,801,551
2011	3,655	2,167,767			3,655	2,805,206

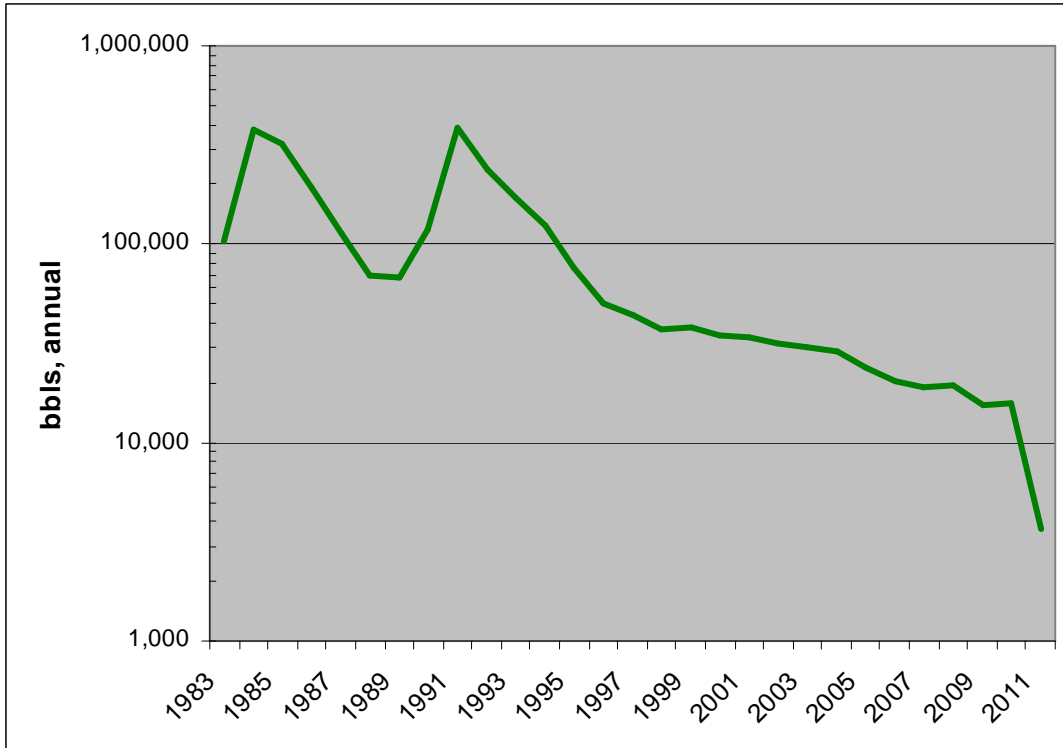


Fig. 4: Annual oil production data for Celia and Celia South oilfields. Total oil production in 2010 was 15,767 bbls, all from the Celia South field. Steep drop at end of graph indicates incomplete data for year 2011.

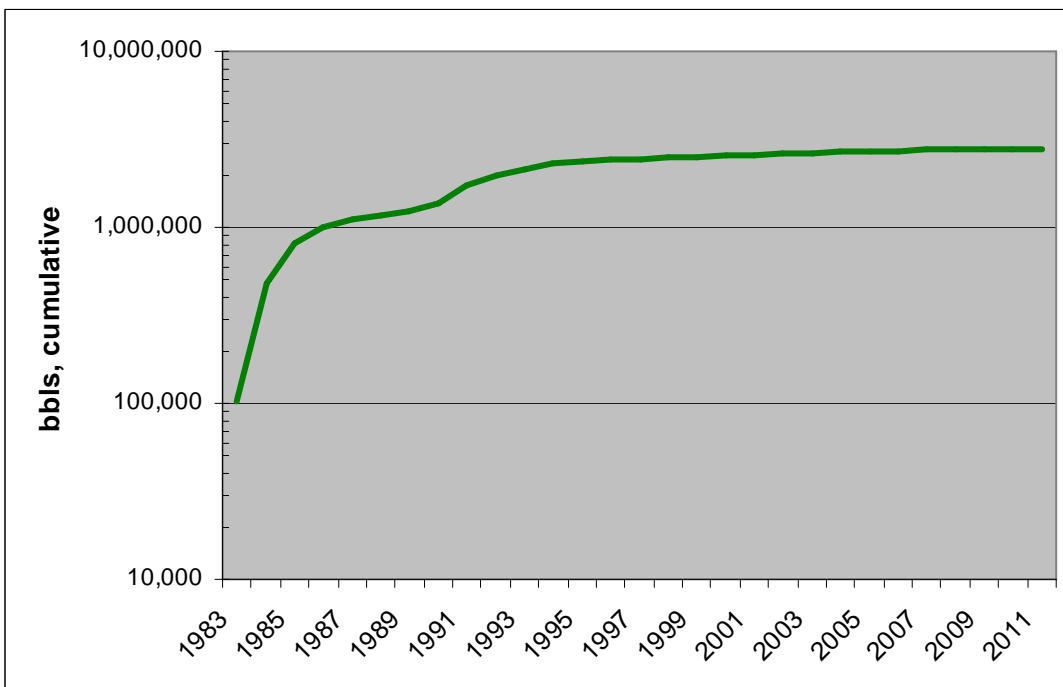


Fig. 5: Cumulative oil production for Celia and Celia South oilfields. Cumulative oil production, through 12/2010 was 2,805,826 bbls.

The last fifteen years (1996-2010) of annual production data show a fairly consistent decline. Using this data and choosing an arbitrary production limit, a simple decline curve analysis can be carried out to predict the reservoir's future performance. The fifteen years of production data are plotted on a semi-log graph and an exponential trend line curve is fitted to the data in Microsoft Excel (Figure 6). If an arbitrary production limit of 1 BOPD per well is chosen as the point below which production is economically unfeasible, annual production is calculated as: 23 producing wells \* 1 BOPD \* 365 days/year = 8395 barrels of oil. Figure 6 shows that, given the trend of the last ten years, this limit would be reached in 2018. The function for the exponential trend line is:

$$y = (157336302247939.0 * 10^{61}) e^{-0.0813352483941153x}$$

Integrating the function for the exponential trend line from 2011 to 2018 gives a total of 77,391 barrels of oil that would be produced over that time, or 0.8% of OOIP. This number indicates the cumulative production of oil according to the simple decline curve analysis scenario from 2010 to an arbitrary economic limit if the present waterflood continues unchanged. Moving to a surfactant flood could significantly increase future production and prolong the productive life of the reservoir beyond the time calculated in this scenario.

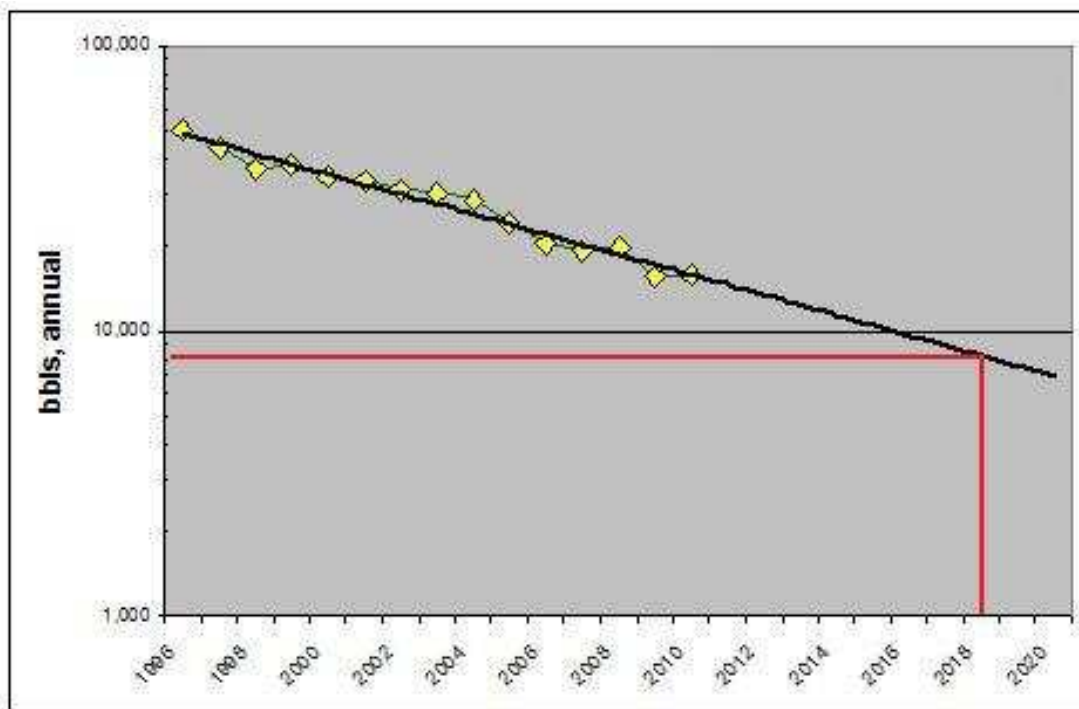


Fig. 6: Simple decline curve analysis of annual production for Celia South waterflood unit. Red line indicates arbitrary economic limit of 1 BOPD per well for the 23 current producers.

## 6. GEOLOGY

The reservoir interval in the Celia South waterflood unit is a limestone in the upper part of the Middle Pennsylvanian Cherokee Group. The reservoir interval lacks formal nomenclature in the KGS stratigraphic column and is referred to as simply Cherokee Lime or Cherokee Pay Zone in well completion forms filed with the Kansas Corporation Commission. Cross-sections in this report label the reservoir “Celia” and it will be referred to herein as the Celia limestone.

The Celia limestone lies below two useful regional markers, both radioactive black shales easily recognizable on well logs – the Excello shale, marking the top of the Cherokee Group, and another, unnamed shale generally about 20 to 30 feet below which immediately overlies the Celia limestone reservoir. The base of the Celia limestone is marked by another, but weaker gamma-ray marker, a less radioactive shale. The Hubbard 5-28V well is taken as a type log for the reservoir area, showing the two shale markers and the Celia limestone (Figure 7).

The type well log from the Celia South waterflood, the Hubbard 5-28V, was correlated with a published stratigraphic type log of Ness County, Kansas (Figure 8; Ramaker, 2007) to make sure stratigraphic tops correlated in the area of this project could be correlated with other published data. The comparison shows a similar pattern of stratigraphic thicknesses above and below the Pawnee Limestone, part of the Marmaton Group. The Pawnee Limestone section is thicker in the Ness County type log. The same pattern of radioactive black shale markers below the Pawnee Limestone is present in both logs; one at the base of the Pawnee Limestone, the Excello Shale marking the top of the Cherokee Group, and the unnamed shale just above the Celia limestone reservoir in the area of this project.

Analysis of six cores from the field shows that the Celia limestone is a bioclastic grainstone (Amonsén, D.R., et al., 1987). Bioclasts include mainly algal fragments, with some crinoid, echinoid, gastropod, ostracode, and brachiopod fragments, as well as forams. The depositional environment is interpreted to have been a shallow marine carbonate bank or shoal, and laminations present in core indicate the possibility that the rock may have been deposited as part of a stromatolitic bioherm (Amonsén, D.R., et al., 1987). Primary interparticle porosity is best near the top of the limestone and decreases downward as micrite matrix becomes more abundant and the rock grades downward to a wackestone-packstone. This phenomenon is interpreted to result from wave action washing out muds in the shallowest parts of the original depositional setting, leaving more mud in deeper areas.



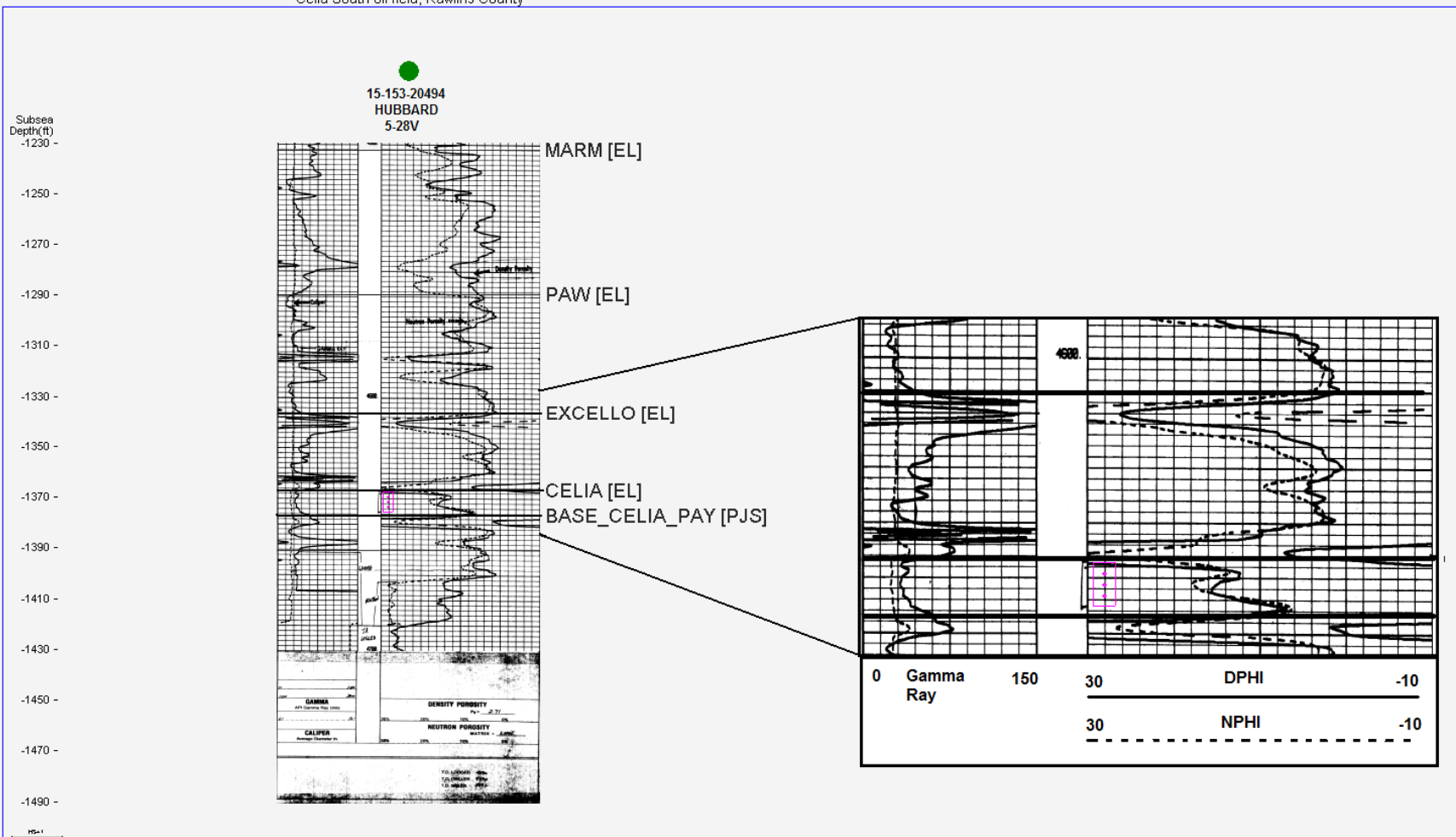


Fig. 7: Type well log in Celia South waterflood unit.

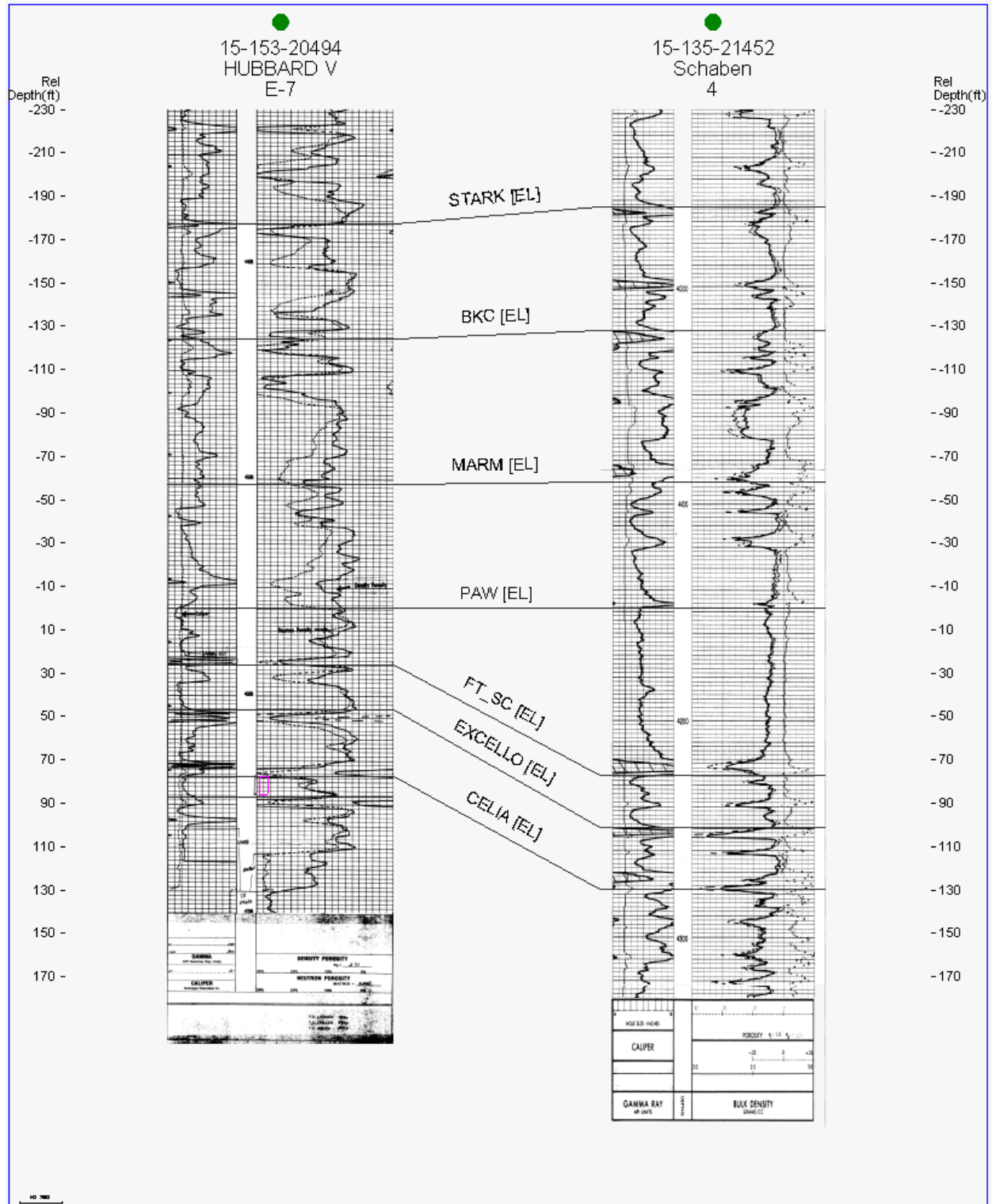


Fig. 8: Comparison of type well log from the Celia South waterflood unit with published stratigraphic type log for Ness County from Ramaker, 2007.

A basement structure map of the region (Figure 9; Cole, 1976) shows a high area trending from northwest to southeast, and dipping to the southwest, across Rawlins County. This trend is part of the Cambridge Arch, which extends into Kansas from Nebraska and continues to the southeast as the Central Kansas Uplift, a major structural feature in Kansas that is associated with significant oil and gas production in the State. The Celia South waterflood unit does not, however, lie on this structural trend. Instead it lies across a subtle structural low between the Cambridge Arch and another, locally significant structural trend that rises to the west-southwest. This trend is part of the Las Animas Arch, which extends into Kansas from Colorado. The trend is discernable in Figure 9, especially in western Cheyenne County, but a regional structure map of the top of the Cherokee Group (Figure 10) provides a clearer illustration, showing the Celia South waterflood unit situated on a northeast-trending protrusion. A sub-regional Cherokee Group structure map (Figure 11) shows more clearly the northeast-trending structural protrusion, with the Celia South waterflood unit lying on the eastern flank.

A Cherokee Group structure map focused on the Celia South waterflood unit shows a main structural dome feature centered in Section 28, T3S-R36W, with a smaller associated dome feature immediately to the south (Figure 12). Structural closure is indicated around the Celia South waterflood unit by dry holes in Sections 19-21, 27, 29, 32, 34 T3S-R36W, and 4-5 T4S-R36W. Structural closure is most apparent on the eastern and northern sides where the structure falls off steeply. To the northwest a dry hole in Section 19 T3S-R36W shows approximately 10 feet of closure in cross-sectional view (Figure 13), and a structurally low area is developed to the southwest in Section 32 T3S-R36W (Figures 12, 14). The main structural dome feature is separated from the smaller one to the south by a saddle in Section 33 T3S-R36W, which is penetrated by a dry hole (Figure 12), indicating a lack of communication between the reservoirs in the two structures.

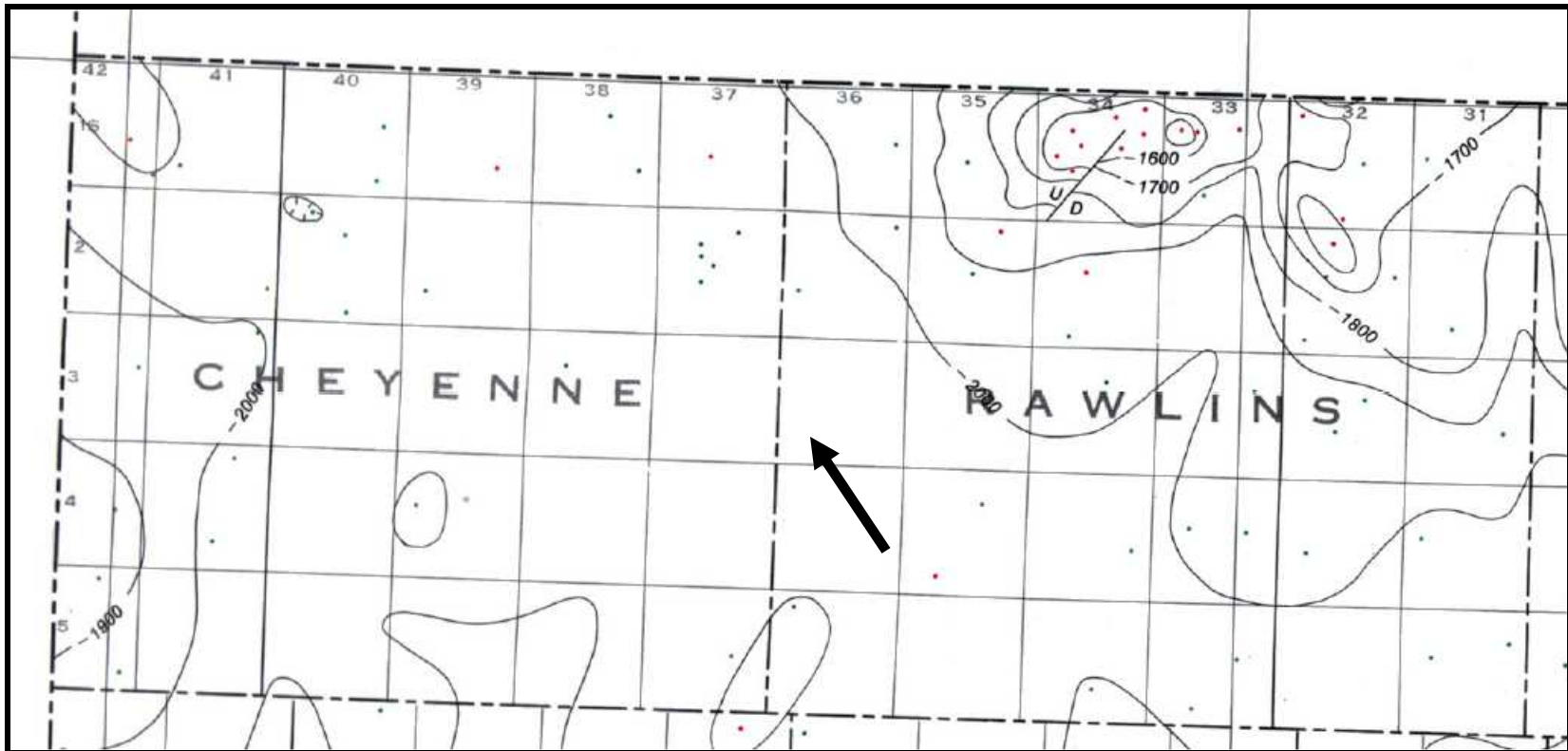


Fig. 9: Basement structure map of northwest Kansas from Cole (1976). Contours are in feet below sea level. Dots indicate wells used in mapping, and arrow indicates location of Celia South waterflood unit. Compare to Figure 10.

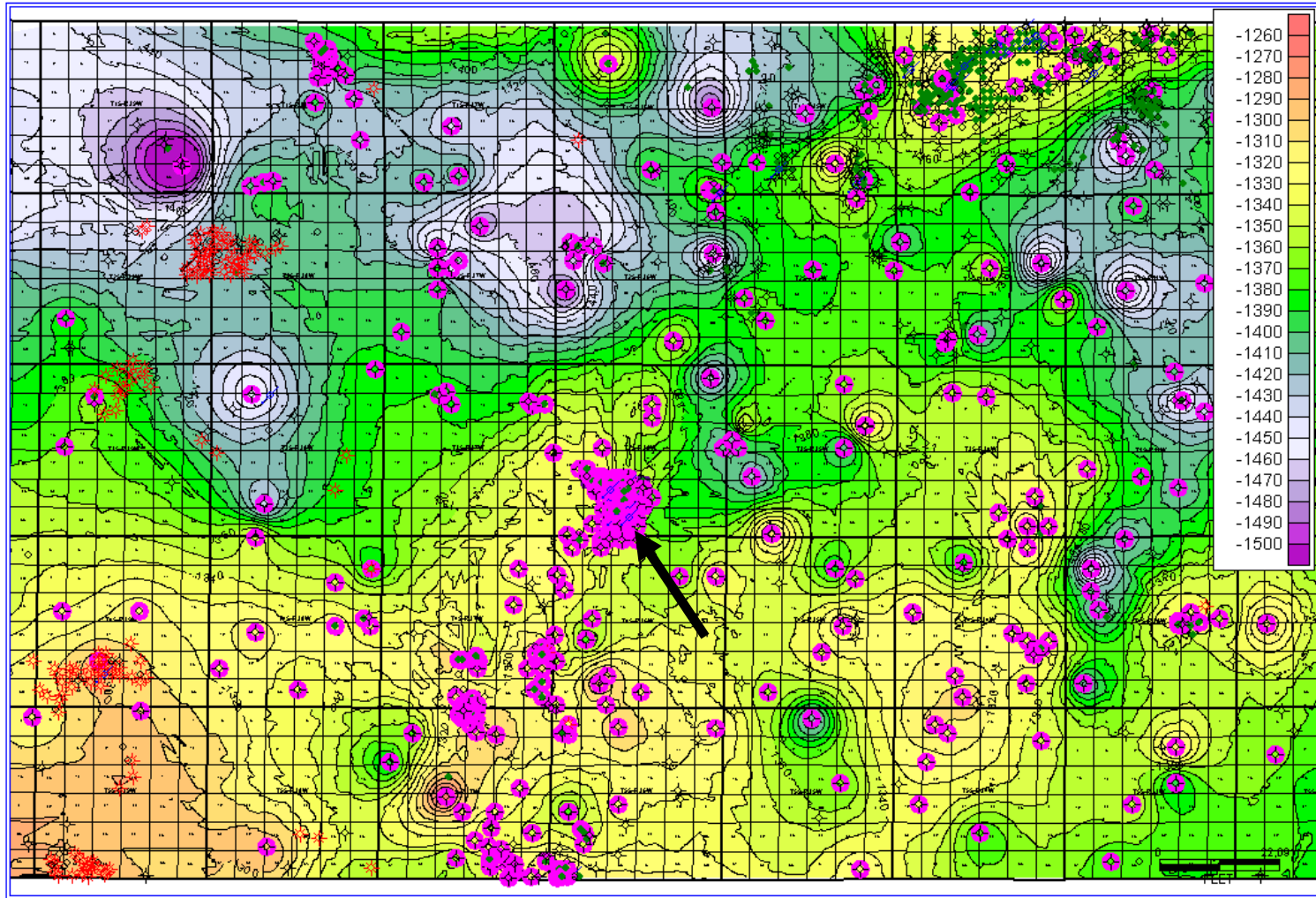


Fig. 10: Regional structural map of the top of the Cherokee Group. Contours are in feet below sea level. Highlighted wells indicate data points. Arrow indicates Celia South waterflood unit.

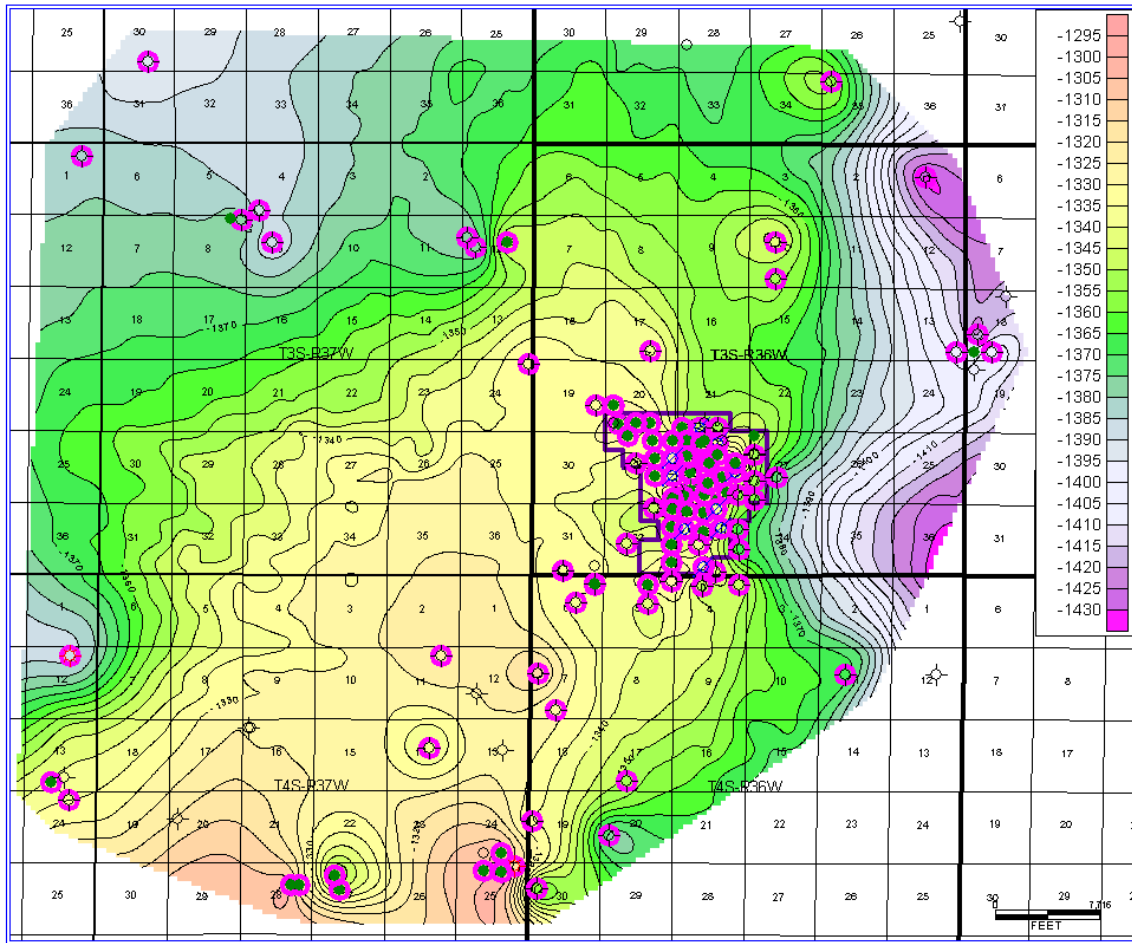
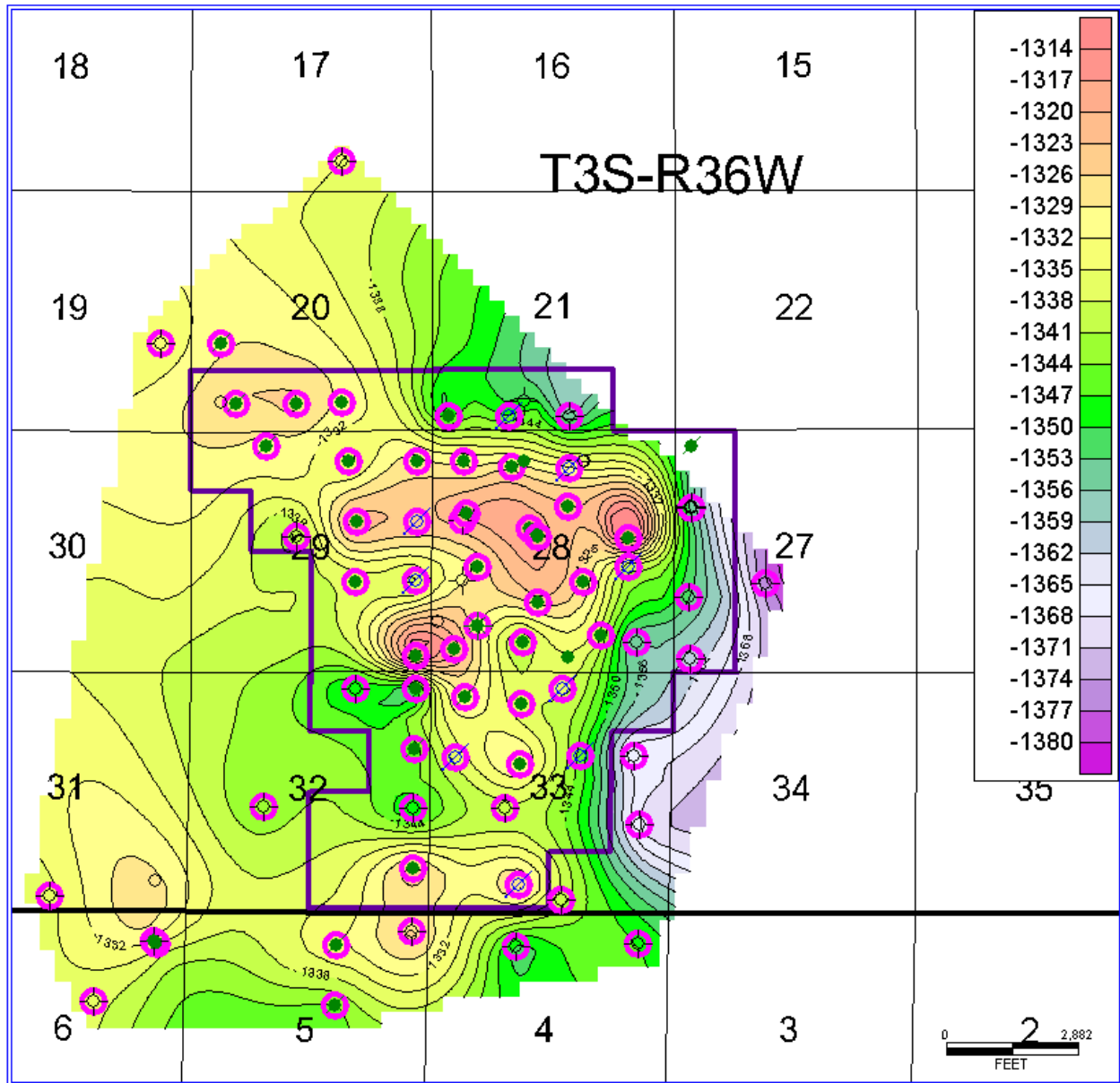


Fig. 11: Subregional structural map of the top of the Cherokee Group. Contours are in feet below sea level. Highlighted wells indicate data points.



PETRA 01/2011 1:06:48 PM

Fig. 12: Structural map of the top of the Cherokee Group in and around Celia South waterflood unit. Contours are in feet below sea-level. Highlighted wells indicate data points.

Celia South oil field, Rawlins County

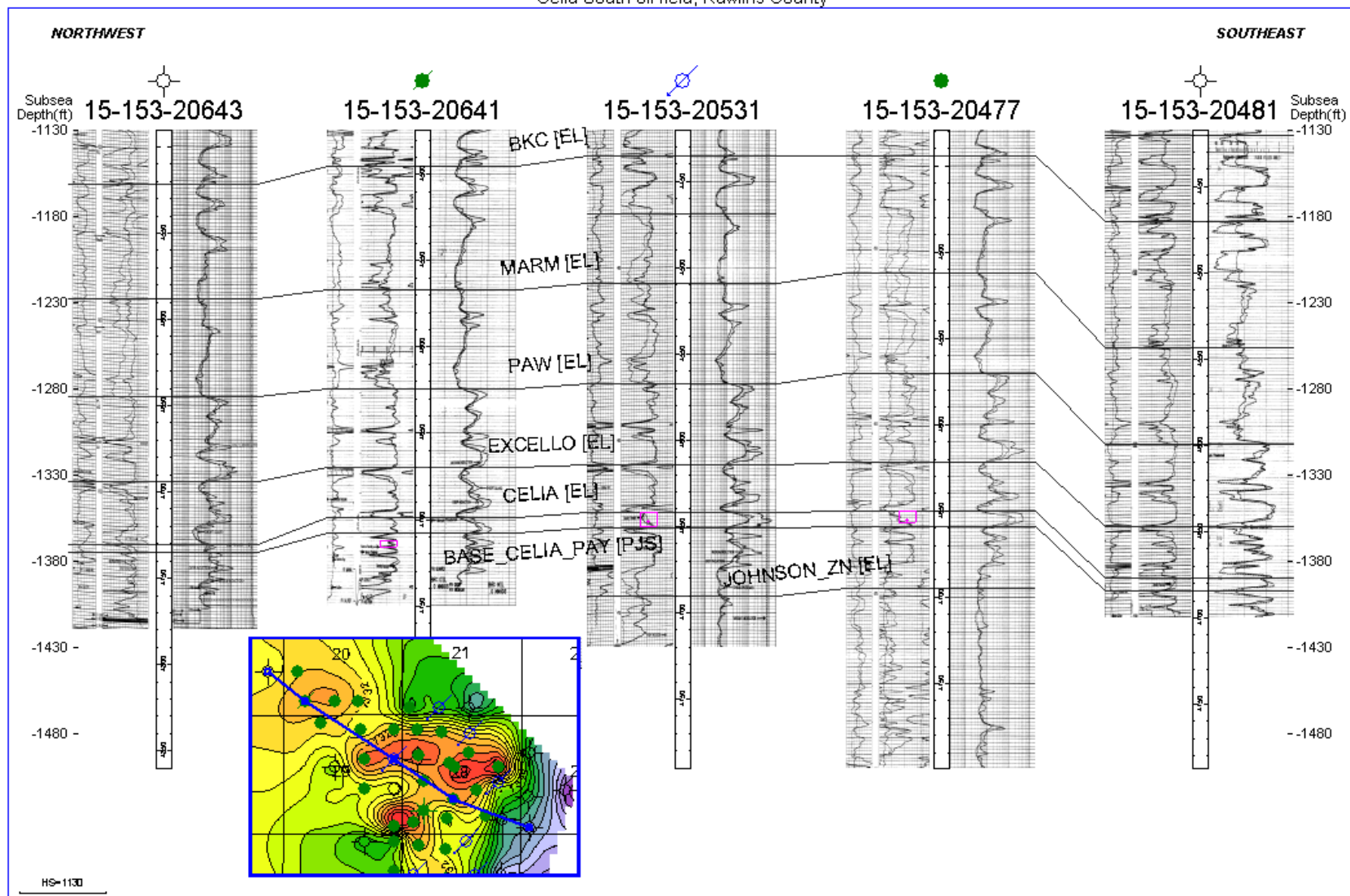


Fig. 13: Structural cross-section through Celia and Celia South showing structure from southwest to northeast. Well logs on the right of the depth tracks are gamma ray and neutron-density, with resistivity logs on the left of the depth tracks.



Celia South oil field, Rawlins County

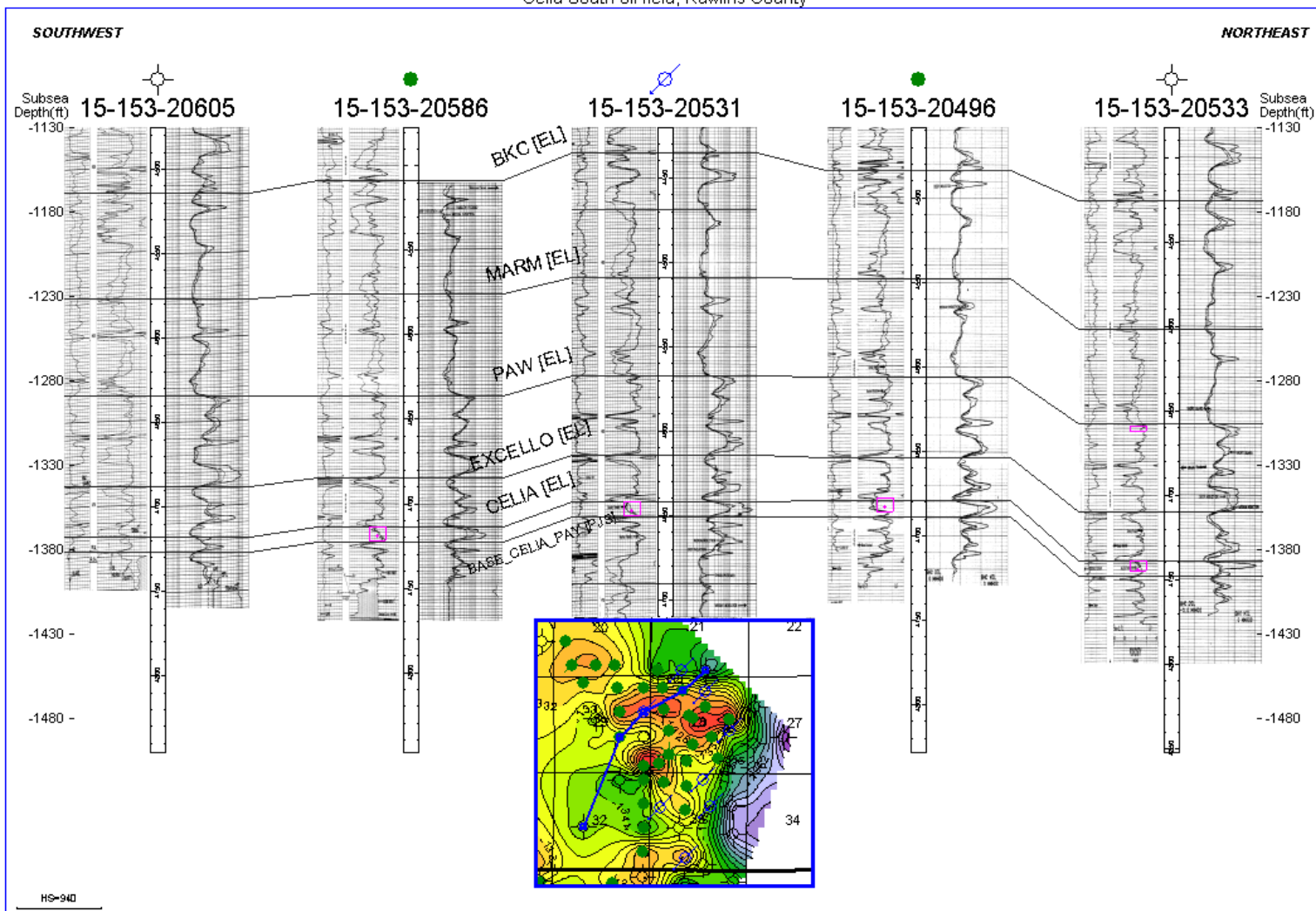


Fig. 14: Structural cross-section through Celia and Celia South showing structure from northwest to southeast. Well logs on the right of the depth tracks are gamma ray and neutron-density, with resistivity logs on the left of the depth tracks.

## 7. PETROPHYSICS

The cementation exponent, 'm' in the Archie Equation, was calculated from core analysis of the Hubbard 4-28V (API # 15-153-20493) well. This well was chosen from among the six cores available in the region (Figure 15) because the initial fluid saturation calculations were reasonable, core and log porosity matched well, and the resistivity log provided a clear indicator as to where fluid saturations might change from oil-water mixture to just water. After depth-shifting the core porosity data to most closely match well log porosity, back-calculation for cementation exponent 'm' was performed by setting water saturation to 100 percent at each sampled interval. Values for 'm' ranged from 1.27 to 3.84 over the cored interval. Next, it was necessary to select a reasonable estimated depth of 100 percent water saturation. Examining the resistivity log data provided the best estimate of this depth. There is a sharp drop off in the deep resistivity log from values over 100 ohm·m to 54 ohm·m at 4684 to 4685 feet measured log depth, indicating a change in rock fluids, which is interpreted to be from a more resistive oil-water mixture to less resistive water. When this depth is interpreted as 100 percent water saturation a cementation exponent 'm' of 1.627 is calculated. This value for 'm' was used in the Archie Equation to calculate fluid saturations, resulting in a map of averaged oil saturation in the Celia limestone pay interval (Figure 16).

Porosity logs run in the Celia South waterflood unit were scaled to a limestone matrix. A map of average well-log porosity of the Celia limestone made using the neutron porosity log NPHI (Figure 17) shows that generally the highest porosity corresponds to the area of the main structural dome feature. An isopach map of the Celia limestone (Figure 18) shows little variation in thickness in the main structural dome feature; most thicknesses there are in the 9 to 10 foot range. Multiplying oil saturation, porosity, and isopach thickness at each well gives a value of hydrocarbon feet (Figure 19). Highest values in the Celia South waterflood unit are found in the southern half of Section 28 and southeastern corner of Section 29, reflecting the structural dome of the field.

Porosity and permeability data from the six cored wells are reproduced in Table 3. A porosity-permeability cross-plot was created using the data from these six wells (Figure 20). A power trend line in the cross-plot relates porosity to permeability with an R-squared value of 0.7584. The equation from the trend line was used to calculate permeability from the log porosity curve NPHI, and a map of average permeability of the Celia limestone was created

(Figure 21). This map shows highest permeability in the southeast quarter of Section 28, with significant decrease in permeability away from the area of the main structural dome feature, especially to the southwest.

At the time of discovery the reservoir was undersaturated with respect to gas, and production was driven by fluid and rock expansion. After pressure had decreased below the bubble point production was solution-gas driven (Amonsens et al, 1987).

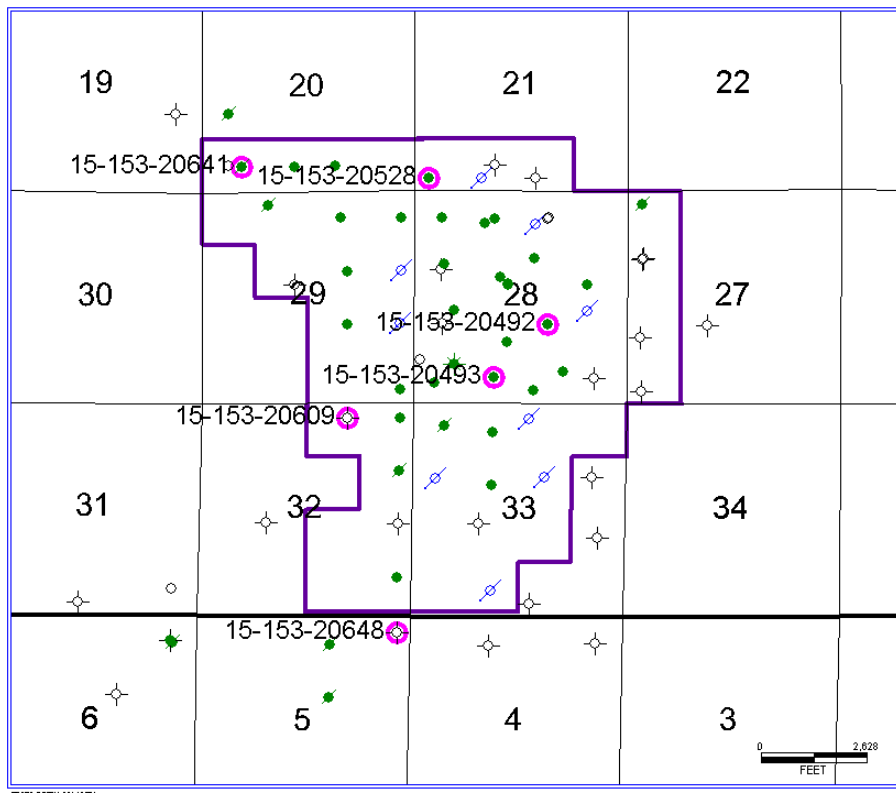


Fig. 15: Locations of cored wells (highlighted and labeled) in and around Celia South waterflood unit

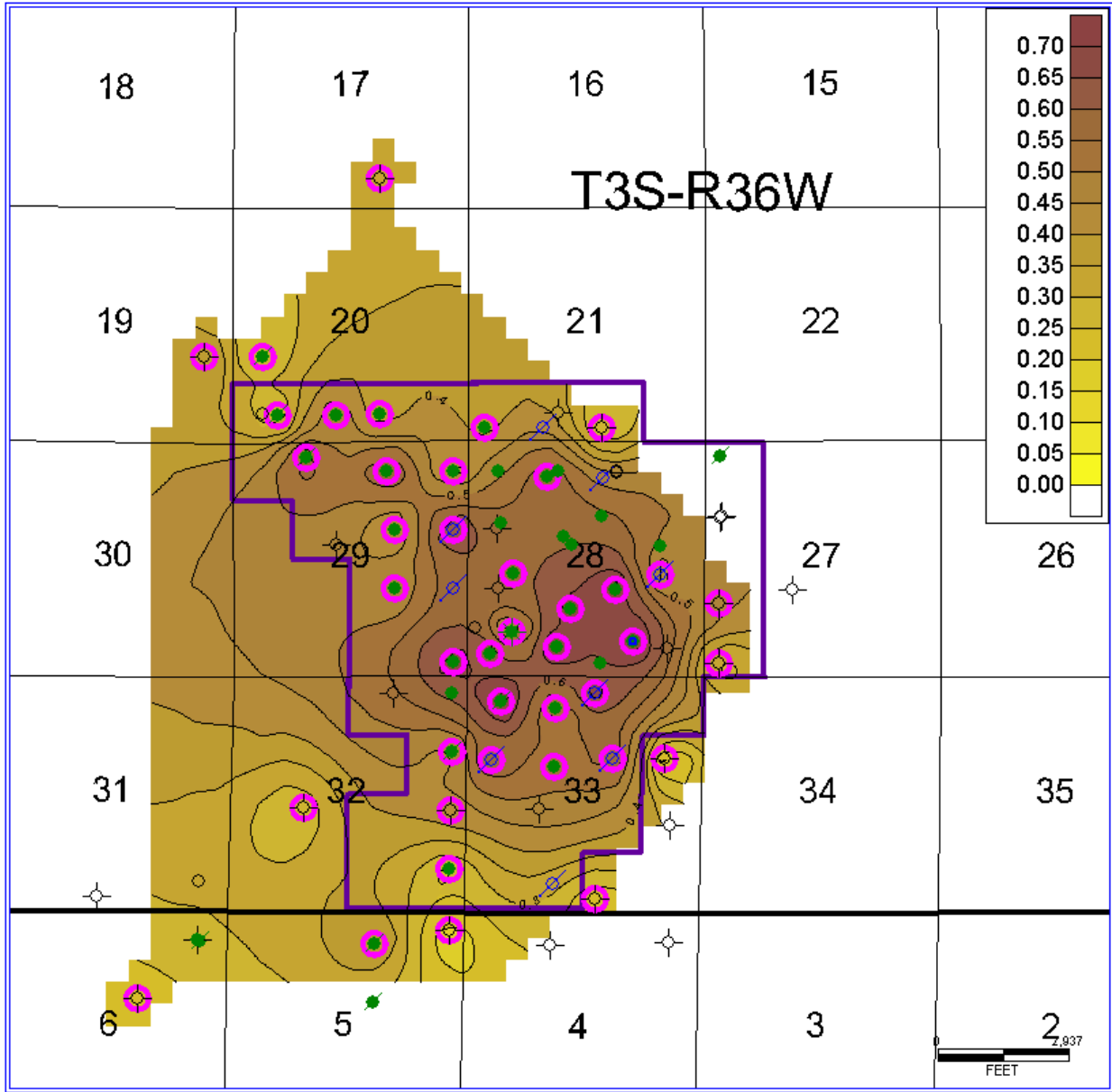


Fig. 16: Averaged oil saturation map of Celia limestone in Celia South waterflood unit. Highlighted wells indicate data points and contours are percent oil saturation. Data for remaining non-highlighted wells was not available for further investigation.

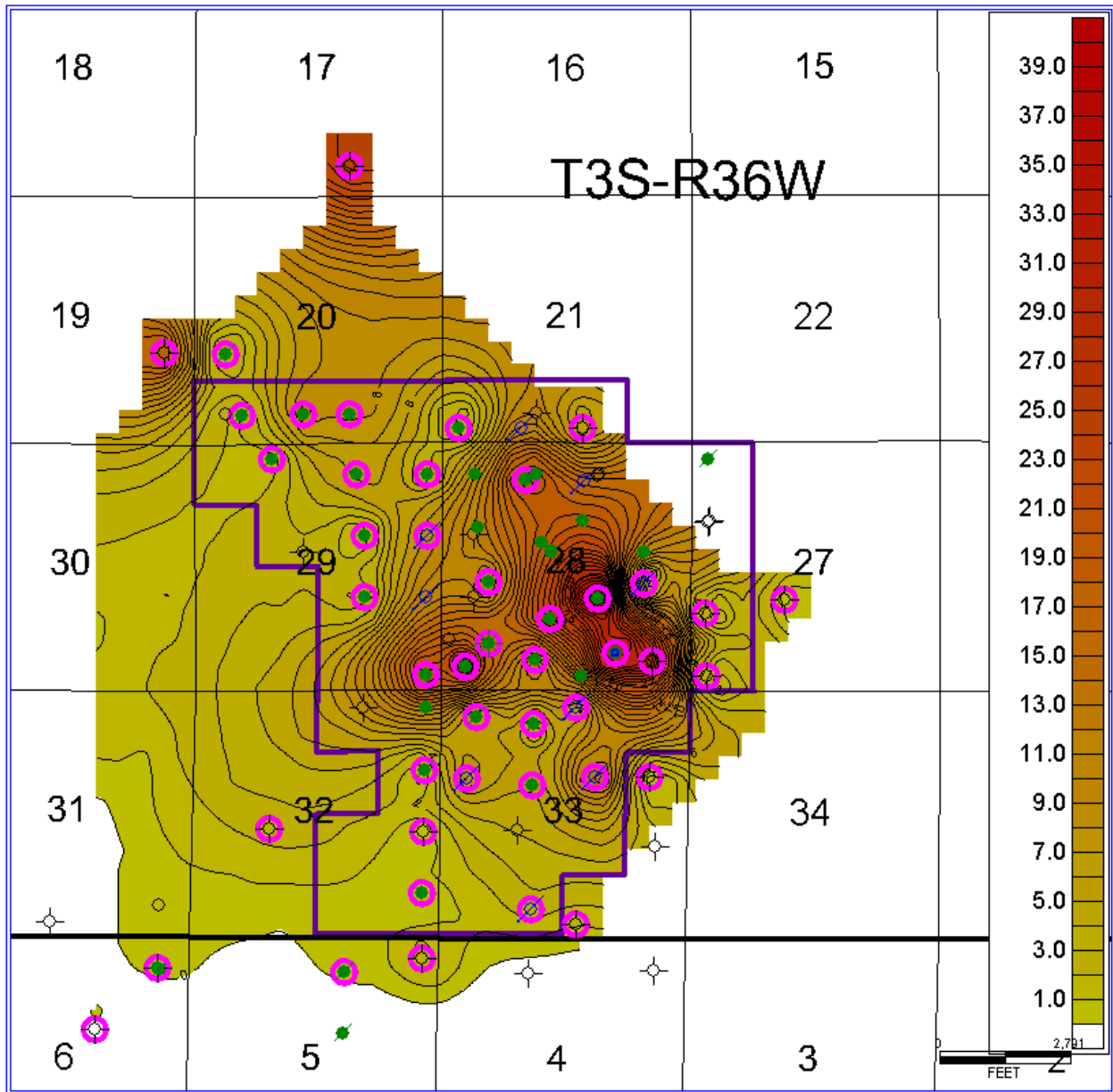
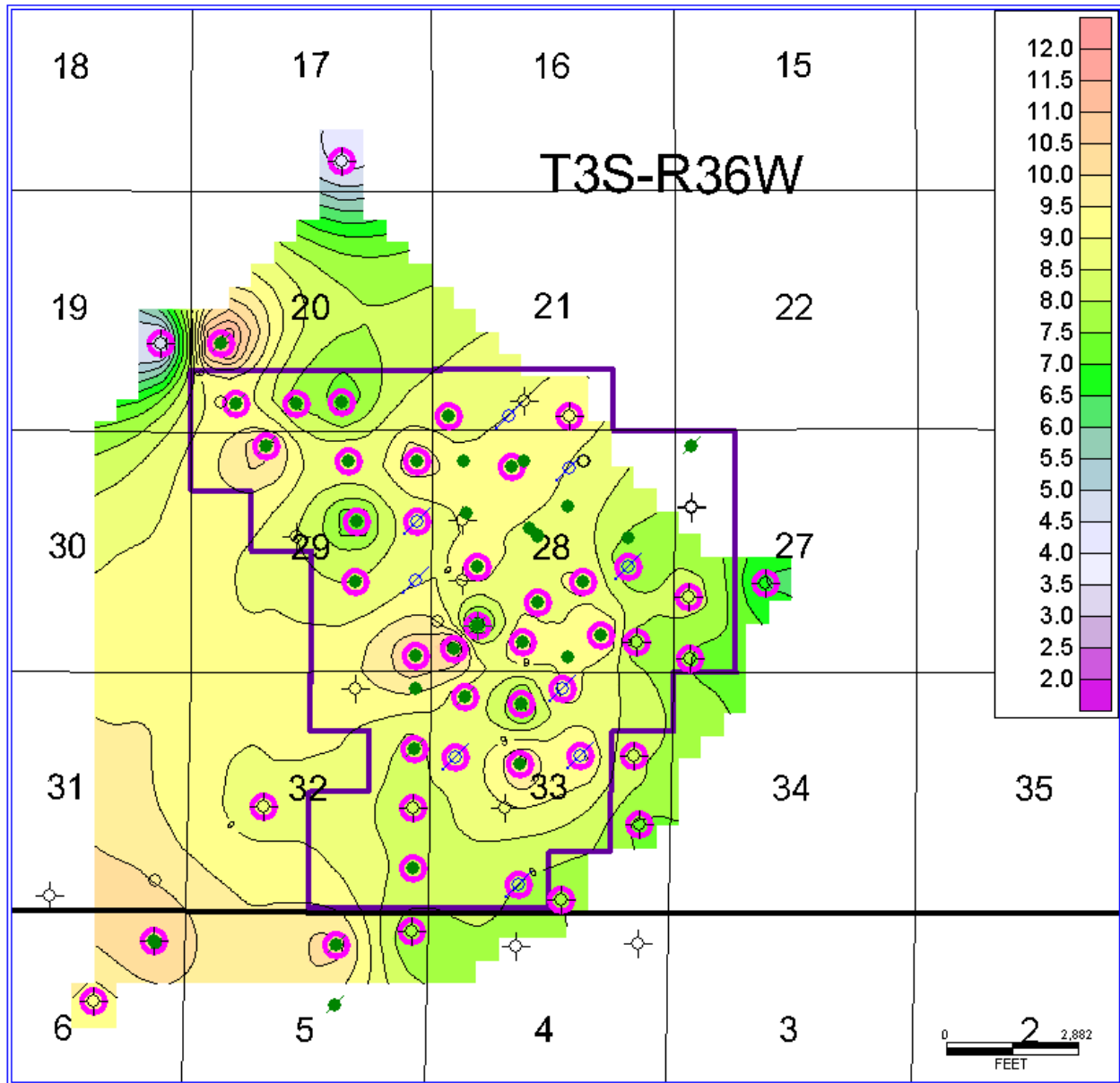


Fig. 17: Average porosity map of Celia limestone in and around Celia South waterflood unit. Highlighted wells indicate data points and contours represent percent porosity.



PETRA 01/20/11 7:12:36 PM

Fig. 18: Thickness map of Celia limestone in and around Celia South waterflood unit. Highlighted wells indicate data points and contours are feet thickness.

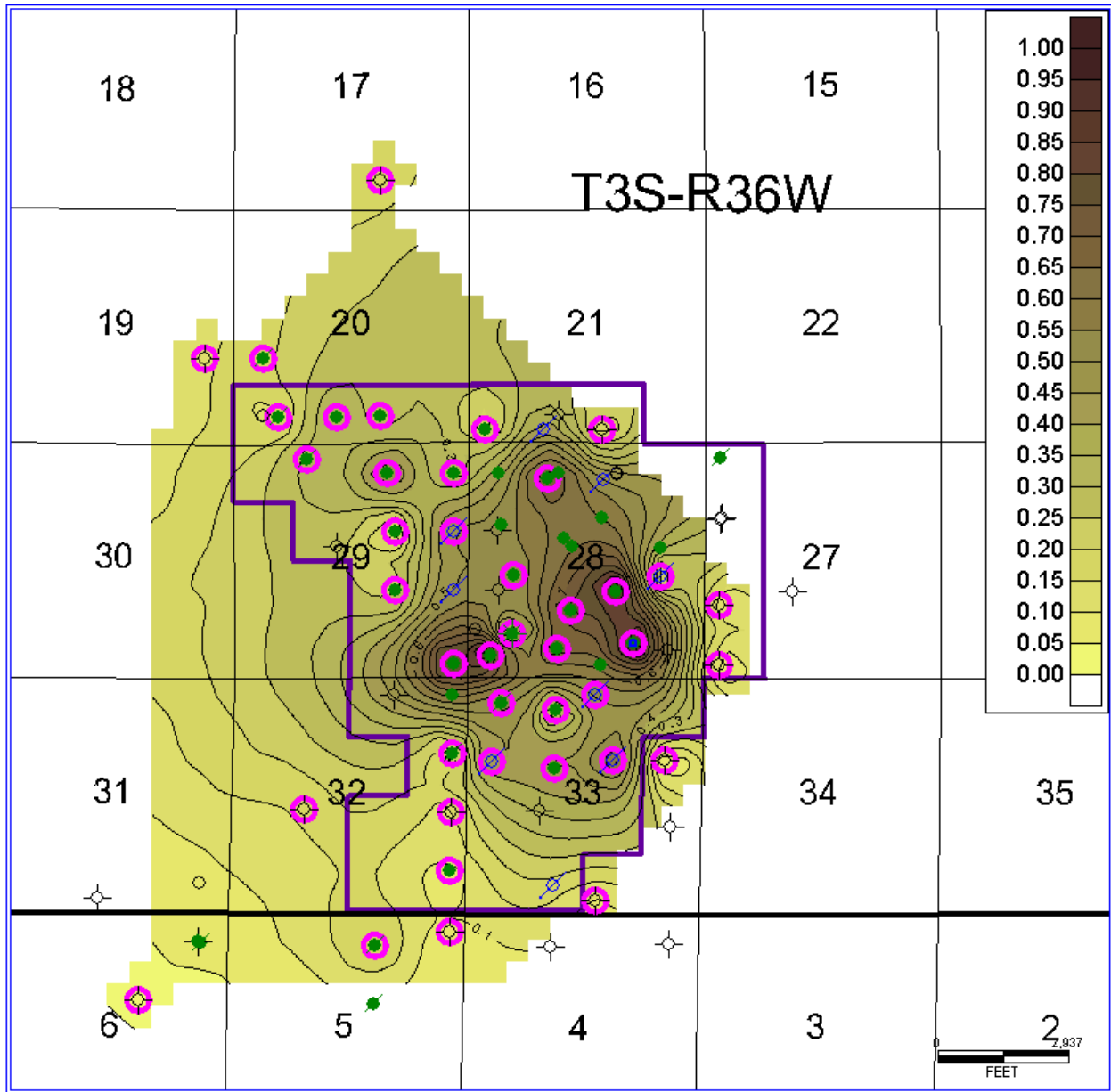


Fig. 19:  $S_o$ - $\Phi$ - $h$  map (oil saturation times porosity times thickness) of Celia limestone. Highlighted wells indicate data points.

Table 3: Summary of core porosity and permeability data from six wells in Celia South waterflood unit.

API#	Well	Depth	Porosity %	Air Permeability md
1515320492	Hubbard #3	4633	22.3	1250
1515320492	Hubbard #3	4635	25.2	496
1515320492	Hubbard #3	4636	23.1	1149
1515320492	Hubbard #3	4638	11.6	32.5
1515320492	Hubbard #3	4639	15.7	184
1515320492	Hubbard #3	4640	8.8	28.3
1515320492	Hubbard #3	4642	2.6	0.92
1515320528	H Cahoj C-2	4601	1.7	0.01
1515320528	H Cahoj C-2	4602	2	0.03
1515320528	H Cahoj C-2	4603	0.7	0.01
1515320528	H Cahoj C-2	4679	1.2	0.01
1515320528	H Cahoj C-2	4679.5	3	6.4
1515320528	H Cahoj C-2	4680	5.1	0.02
1515320528	H Cahoj C-2	4680.5	3.1	0.02
1515320528	H Cahoj C-2	4681	1.4	0.01
1515320528	H Cahoj C-2	4681.5	2	0.01
1515320528	H Cahoj C-2	4682	1	0.01
1515320528	H Cahoj C-2	4682.5	0.9	0.01
1515320528	H Cahoj C-2	4683	1.5	0.03
1515320528	H Cahoj C-2	4683.5	1.8	0.01
1515320528	H Cahoj C-2	4684	1.9	0.01
1515320528	H Cahoj C-2	4684.5	0.5	0.01
1515320641	Henry Cahoj 2-D	4702	2.9	0.65
1515320641	Henry Cahoj 2-D	4703	2.2	0.03
1515320641	Henry Cahoj 2-D	4704	2.2	0.01
1515320641	Henry Cahoj 2-D	4705	1.6	0.08
1515320641	Henry Cahoj 2-D	4706	3.5	0.22
1515320641	Henry Cahoj 2-D	4707	1.7	0.15
1515320641	Henry Cahoj 2-D	4708	0.4	0.01
1515320641	Henry Cahoj 2-D	4714	10.3	54
1515320641	Henry Cahoj 2-D	4715	10.1	413
1515320641	Henry Cahoj 2-D	4716	2	0.01
1515320641	Henry Cahoj 2-D	4717	1.9	0.01



Table 3 (cont.): Summary of core porosity and permeability data from six wells in Celia South waterflood unit.

API#	Well	Depth	Porosity %	Air Permeability md
1515320609	Powell A-2	4737.8- 4738.3	7.1	7.5
1515320609	Powell A-2	4738.3- 4738.9	11	13
1515320648	Kehlbeck2-D	4697	5.5	0.04
1515320648	Kehlbeck2-D	4698	5.4	1.6
1515320648	Kehlbeck2-D	4699	2.6	0.01
1515320648	Kehlbeck2-D	4700	4.4	0.34
1515320648	Kehlbeck2-D	4701	2	0.01
1515320648	Kehlbeck2-D	4702	3.4	0.01
1515320648	Kehlbeck2-D	4703	3.5	0.01
1515320648	Kehlbeck2-D	4704	0.4	0.01
1515320493	Hubbard #4	4670	14.6	427
1515320493	Hubbard #4	4671	17.7	125
1515320493	Hubbard #4	4672	20.8	120
1515320493	Hubbard #4	4673	12.2	99
1515320493	Hubbard #4	4674	4.2	6.7
1515320493	Hubbard #4	4675	9.8	77
1515320493	Hubbard #4	4676	16.4	75
1515320493	Hubbard #4	4677	6.5	0.74
1515320493	Hubbard #4	4678	2.6	0.03
1515320493	Hubbard #4	4679	2.2	1.5
1515320493	Hubbard #4	4680	1.2	0.15
1515320493	Hubbard #4	4681	5.3	1.2

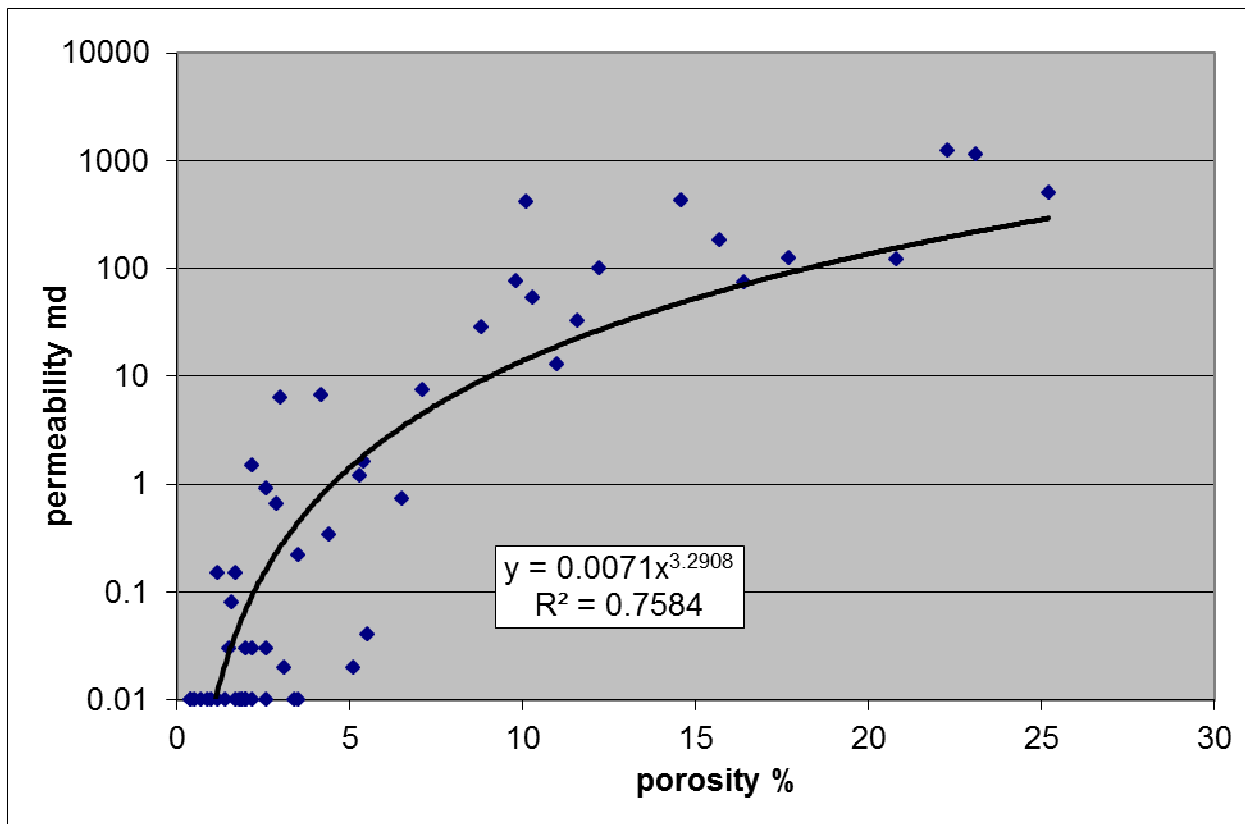


Fig. 20: Cross-plot of porosity and permeability data from cores in Celia South waterflood unit with trendline and equation, generated in Microsoft Excel.

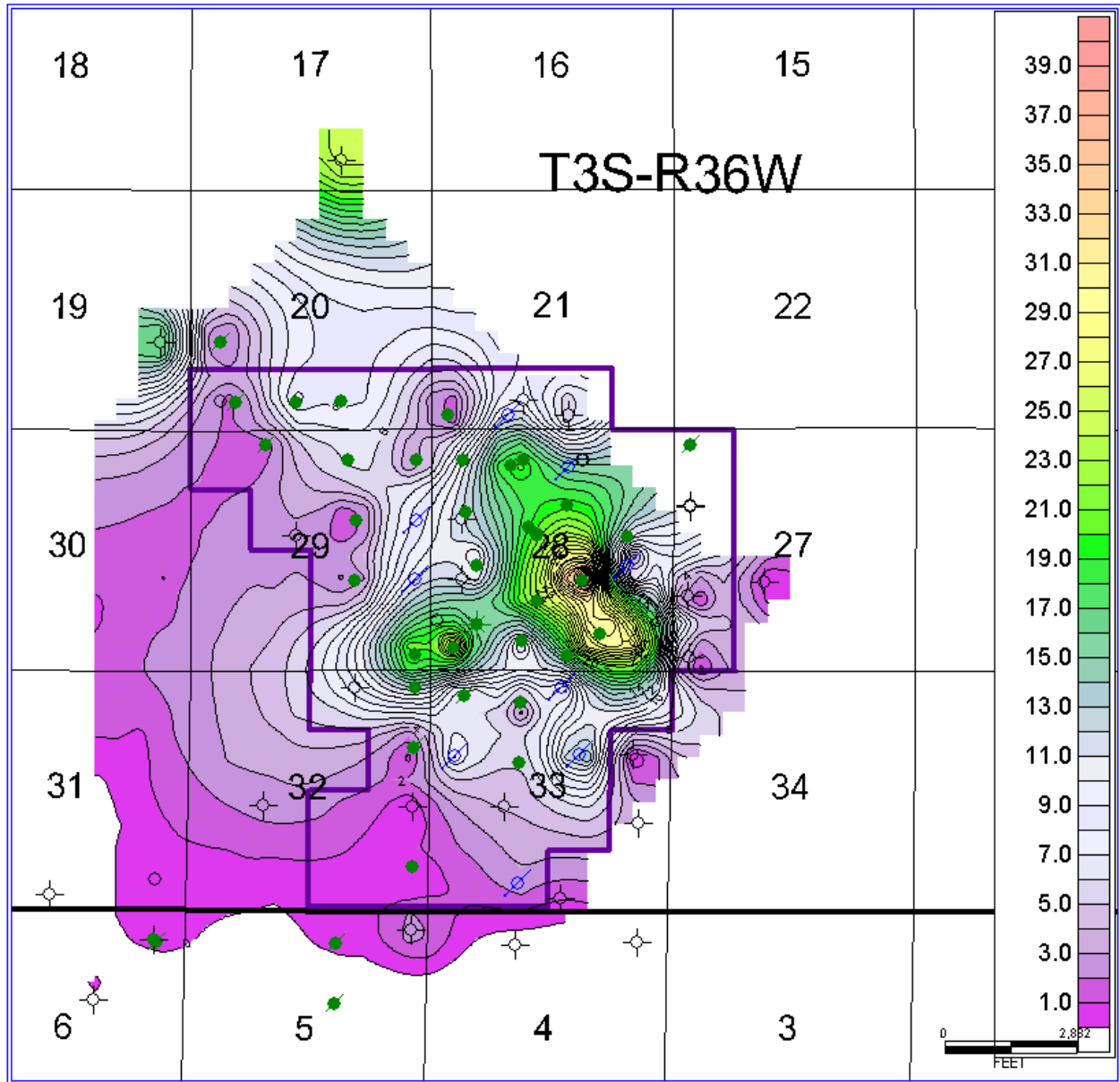


Fig. 21: Average permeability (millidarcies) map of Celia limestone. Highlighted wells indicate data points and contours represent permeability to air in millidarcies.

## **8. DATA AVAILABILITY**

Abundant useful data are available for evaluating the geology of the Celia South waterflood unit. Core reports taken on six wells allow a mathematical relationship to be developed between porosity and permeability, which allows mapping of permeability in the reservoir. Neutron-density logs were collected for almost all of the wells, so not only is log coverage of the unit extensive, it is consistent. The extent of well-log control allows the structural nature of the reservoir to be delineated with a good degree of certainty, and shows that the oil is structurally trapped in a dome. Oil production data for the Celia and Celia South oilfields are available at the KGS website [www.kgs.ku.edu](http://www.kgs.ku.edu), along with scanned logs for many wells. Oil production data for the two oilfields are also available by lease at the KGS website.

## **9. SUITABILITY FOR ENHANCED RECOVERY**

Three important factors establish the Celia South waterflood unit as a good candidate for a tertiary recovery project. Cumulative recovery of oil to date stands at 29.2%, leaving a significant amount that could potentially be recovered with a tertiary recovery phase; incremental recovery of 5-10% of OOIP amounts to 480,000-960,000 barrels. The structural nature of the reservoir is well delineated by mapping; dry holes constrain its limits and provide a clear picture of a dome-shaped structural trap. The field has several separate culminations, one of which, the southern one, appears to be isolated from the rest of the field by a low saddle. The reservoir experienced a massive increase in annual production after initiation of waterflooding in 1989; production nearly doubled from 1989 to 1990, then more than tripled from 1990 to 1991. Significant remaining oil in place indicates potential for increasing production and prolonging the life of the reservoir. A well-defined reservoir with a clear structural trap gives a high degree of confidence that injected surfactants will not bypass the reservoir and go to waste. Rapid and favorable response to waterflooding is desirable when considering tertiary recovery because it means a comparably short response time may be expected when switching to a surfactant flood.

One further characteristic of the Celia South waterflood unit that is important to consider for this project, which seeks to demonstrate the effectiveness of surfactant flooding, is the configuration of the waterflood. The Celia South waterflood unit currently operates on a

peripheral pattern, with injectors concentrated around the edge of the field rather than distributed throughout it. The operator might choose to use all injectors in the current peripheral pattern at the Celia South waterflood unit, which would provide a better opportunity for demonstrating the effectiveness of surfactant flooding than using just one or a few injectors in the current pattern. If the unit operator is not amenable to switching the entire flood over to surfactants, some pattern modification may be necessary. In a peripheral waterflood a single injector well at the edge of the reservoir would impact only a few producers. In a restricted demonstration scenario using only part of a field, one or a few 5-spot patterns waterflood could be established to demonstrate the effectiveness of surfactant flooding. The operator should take note of the structural configuration of the reservoir, with its separate culminations, in designing any enhanced recovery effort.

## **10. CONCLUSION**

The Celia South waterflood unit covers parts of the Celia and Celia South oilfields in west-central Rawlins County, Kansas. Oil is produced from a limestone in the Middle Pennsylvanian Cherokee Group at measured depths of around 4650 feet (Subsea elevations between -1350' and -1315'). The limestone is a bioclastic grainstone, grading downward into lower porosity wackestone-packstone. The reservoir was discovered in June 1983 with the Coastal Oil & Gas Hubbard 1-28V (API# 15-153-20477) which had initial production of 138 BOPD. Murfin Drilling Company, Inc. of Wichita, Kansas is the current unit operator. Waterflooding began in 1989, and cumulative oil production to July 2011 is 2,805,206 barrels, with annual production for 2010 of 15,767 barrels.

The reservoir is a structural trap, it is a dome-shaped feature with multiple culminations surrounded by dry holes. Potential incremental production of 5-10% of OOIP would amount to 480,000-960,000 barrels. The well-defined nature of the reservoir means that a proposed tertiary recovery project would have little risk of injected surfactants going to waste. Waterflooding of the reservoir provided a significant boost to oil production within one year, demonstrating that injection of fluids can cause a response in this reservoir in a short period of time. The waterflood is currently set up as a peripheral pattern. If the whole pattern could be used a convincing demonstration of the utility of surfactant flooding could be made. However, if only one or a few injectors were available for such a demonstration it might be necessary to adjust the pattern to a

line or 5-spot pattern where several producers surround each injection well. Any such pattern adjustments should consider the irregularity of the dome-like configuration of the reservoir bed, with its separate culminations. The Celia South waterflood unit, based on its significant remaining reserves, structural character and positive response to waterflooding, is a strong candidate to demonstrate to independent producers in Kansas the effectiveness of surfactant flooding.

## 11. REFERENCES

- Amonsens, D.R., Crouch, C.B., Mayes, J., Orsak, R., Douglass, T., Raymondetta, P., Yaeger, D., Cahoj, E., Dillie, J., and Park, T., 1987, Technical committee report for South Celia (Cherokee) Unit: Coastal Oil & Gas Corporation report submitted to Working Interest Owner's Committee, South Celia (Cherokee) Field
- Cole, V.B., 1976, Configuration of the top of Precambrian rocks in Kansas: Kansas Geological Survey, Map Series, no. M-7, 1 sheet, scale 1:500,000 (available online at [http://www.kgs.ku.edu/Publications/Bulletins/Map7/ks\\_precambrian\\_map.pdf](http://www.kgs.ku.edu/Publications/Bulletins/Map7/ks_precambrian_map.pdf))
- Kansas Geological Survey website: <http://www.kgs.ku.edu>
- Ramaker, B.J., 2007, Type log showing stratigraphic horizons for Ness County, Kansas Kansas Geological Survey, Open-file Report, no. 2007-16 (available online at [http://www.kgs.ku.edu/PRS/publication/2007/OFR07\\_16/index.html](http://www.kgs.ku.edu/PRS/publication/2007/OFR07_16/index.html))

# **MISSOURI FLATS WATERFLOOD UNIT, GOVE COUNTY, KANSAS: GEOLOGY, HISTORY, PRODUCTION, AND ENHANCED OIL RECOVERY**

Peter J. Senior and Anthony W. Walton, Department of Geology,  
The University of Kansas, Lawrence, Kansas.

## **1. INTRODUCTION**

The Missouri Flats Waterflood Unit, operated by Merit Energy Company of Dallas, Texas, covers parts of the Missouri Flats Northeast and Missouri Flats Northwest oilfields in Gove County, Kansas. Most of the wells in this unit date from the mid 1970's, and Merit acquired ownership in 2008. The unit produces oil from four Upper Pennsylvanian limestone zones near the base of the Kansas City Group. Waterflooding began in 2002, and 2009 annual oil production is still more than two times the amount it was before the waterflood. This report provides a summary of information on the field location, drilling and production history, geology, and suitability for enhanced recovery.

## **2. LOCATION**

Missouri Flats Northeast and Northwest are adjacent fields located in the northwestern part of Kansas in Gove County (Figure 1). The two fields span parts of five sections in T14S R28W, completely covering three (Figure 2). The Missouri Flats Waterflood Unit includes parts of the Missouri Flats Northeast oil field and the Missouri Flats Northwest field (Figure 3; Merit Energy Company, 2008).

## **3. METHODS**

This report was constructed by analyzing data provided by the field operators directly to the investigators along with that in the public domain and posted on the website of the Kansas Geological Survey (KGS). The major methods were use of well logs to determine the configuration of key horizons to create geologic maps and cross-sections of the reservoir. The data and logs were imported into Petra™, a subsurface GIS program and analyzed using standard techniques. Production history, quantities, and rates were downloaded from the website of the KGS.

#### **4. DISCOVERY & DEVELOPMENT HISTORY**

The earliest discovery well in the Missouri Flats Northeast oilfield was completed in the Marmaton Group in December 1973 (Coberly #1, API# 15-063-20197), and the second was completed in the K-zone of the Lansing-Kansas City interval in July 1974 (R.S. Coberly #1, API# 15-063-20214). Five more development wells drilled in 1974 resulted in two more producers, two dry holes, and a water supply well. A further fifteen wells were drilled in 1975, of which ten were productive and five were dry holes. A single, unproductive well was drilled in 1977, and the decade of the 1980s saw three productive wells drilled along with two dry holes. One unproductive well was drilled in 1990, followed by single productive wells in 2005 and 2007. Completion of the well in 2007 marks the end of development in the field so far, although Merit Energy Company (2008) had planned to drill another well in 2008, the Beesley B #2 (API# 15-063-21733).

The adjacent Missouri Flats Northwest field is considerably smaller than Missouri Flats Northeast. Only five wells have been drilled as part of the field; three wells were dry and two were productive. Merit currently operates both of the successful wells in the field as part of the waterflood unit; one well has been converted to an injection well.

Table 1 provides a summary of information on all the wells in the waterflood unit. Vintage Petroleum, Inc. of Tulsa, Oklahoma, converted all of the injection wells from producers in 2002. Vintage completed a productive well in 2005, and Cordillera Energy Partners, LLC completed the last productive well so far in 2007. Merit Energy Company subsequently acquired the Missouri Flats Waterflood Unit in 2008, including all of the wells listed in Table 1.





Fig. 1: Regional map showing location of adjoining Missouri Flats Northeast and Missouri Flats Northwest oilfields in Gove County, Kansas, modified from [www.kgs.ku.edu](http://www.kgs.ku.edu) 6-2-10.

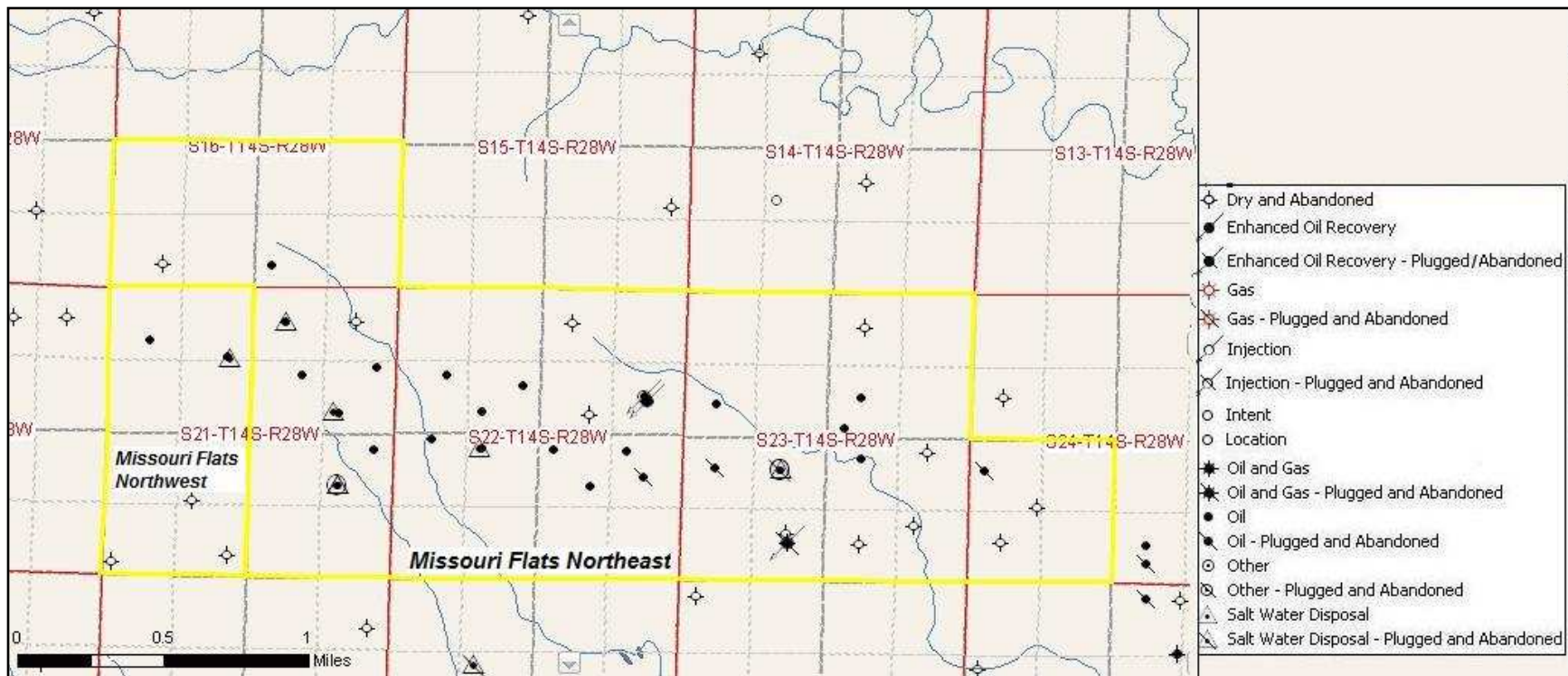


Fig. 2: Sub-regional map of Missouri Flats Northeast (larger yellow polygon) and Missouri Flats Northwest (smaller, adjacent yellow polygon in section 21), from [www.kgs.ku.edu](http://www.kgs.ku.edu) 6-2-10.

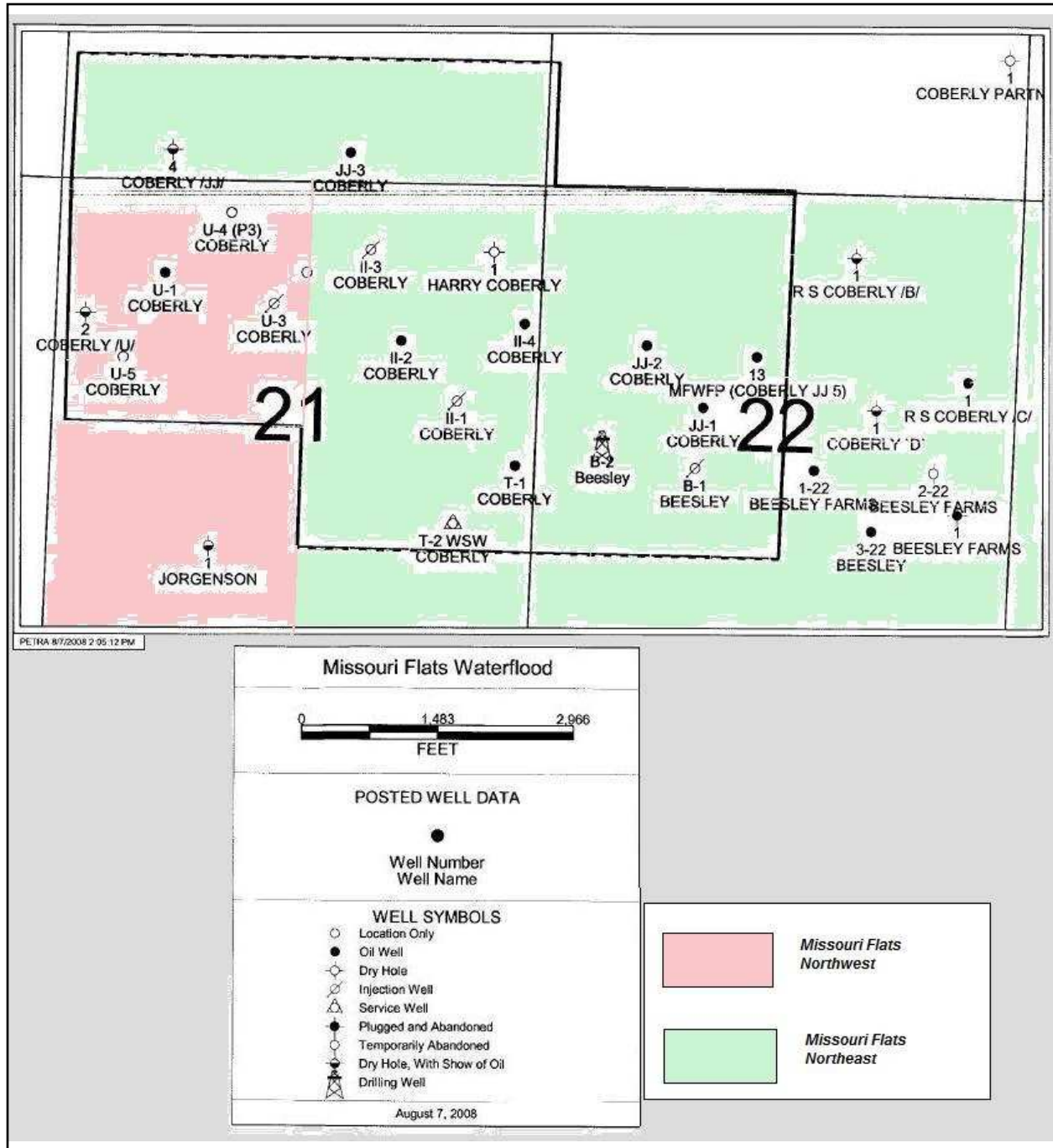


Fig. 3: Map of Missouri Flats Waterflood Unit, included in Intent to Drill Form with the Beesley B2 well (API# 15-063-21733), from [www.kgs.ku.edu](http://www.kgs.ku.edu) 6-2-10.

## 5. PRODUCTION HISTORY

The Missouri Flats Waterflood Unit comprises six leases in two different oilfields (Table 2). Oil production dates back to 1975 and continues to the present, with a cumulative total of just

over 1.3 million barrels produced as of the end of 2009 (Table 3). The greatest annual production was achieved in 1976, with 175,219 barrels of oil. Annual production steadily declined after 1976, except for minor increases from 1991-1992 and 1996-1997. A significant increase in production from 2000 to 2004 indicates the effect of waterflooding (Figure 4, 5). Several wells were converted to injectors in late 2002 and a significant rise in annual oil production occurred in 2003. Waterflooding successfully boosted oil output from its low point of 9,957 barrels in 2000 to 74,396 barrels in 2004. Output in 2009 remains at 23,468 barrels, still significantly higher than the low point reached before waterflooding began.

## **6. GEOLOGY**

The Missouri Flats Waterflood Unit produces from multiple, closely spaced limestone horizons of the Upper Pennsylvanian Kansas City Group. Four zones are perforated in the B. Beesley #1 well (API# 15-063-20257), and other wells for which perforation data are available show from one to three zones perforated. No geologist's reports are available in wells in the Missouri Flats Northeast or Missouri Flats Northwest fields, although one is available from a wildcat well drilled in 2000 immediately to the northeast of the waterflood unit (Coberly Partnership #1, API# 15-063-21546). This geologist's report, partially reproduced in Figure 6, shows the I, J, K, and L limestone zones of the Kansas City Group; these limestone zones are the reservoir intervals in the waterflood unit, which are referred to in well-completion forms as the LKC 160, 180, 200, and 220 zones, respectively. The limestone reservoir zones are stratigraphically clustered around the Stark Shale, near the base of the Kansas City Group. The I-zone (LKC 160) and the J-Zone (LKC 180) lie directly above the Stark Shale; the K-zone (LKC 200) lies directly below the Stark Shale and is separated from the underlying L-zone (LKC 220) by the Hushpuckney Shale.

Cores were not taken from any wells in the Missouri Flats Northwest or Missouri Flats Northeast fields, but the geologist's report cited above provides a thorough lithologic description of each of the reservoir zones. The I-zone (LKC 160), stratigraphically the highest, is described as white to cream to tan, finely crystalline, dense, fossiliferous limestone, chalky in places and cherty in places, with primary crystalline porosity, a trace of vugs and pinpoint porosity. The J-zone (LKC 180), the second highest, is described as white to cream, oolitic to slightly oomoldic, fossiliferous, finely crystalline limestone, with primary crystalline porosity. The K-zone (LKC 200) is described as white to cream-colored, fine-to-medium crystalline

**Table 1: Summary of wells in the Missouri Flats Waterflood Unit, compiled from [www.kgs.ku.edu](http://www.kgs.ku.edu) 5-31-10.**

API NUMBER	LEASE and WELL NUMBER	SECTION-TOWNSHIP-RANGE	SPOT	ORIGINAL OPERATOR	PERMIT	COMP.	TYPE
15-063-20247 15-063-20247-0001	Coberly, I.I. 1	21-14S-28W	SW SE NE	SLAWSON DONALD C Vintage Petroleum, Inc.		18-Jun-75 10-Oct-02	OIL Inj
15-063-20252	J. J. COBERLY 1	22-14S-28W	SW SE NW	SLAWSON & BRUCE ANDERSON		17-Jun-75	OIL Prod
15-063-20255	Coberly, T. 1	21-14S-28W	NE NE SE	SLAWSON DONALD C		17-Jun-75	OIL Prod
15-063-20257 15-063-20257-0001	B. BEESLEY 1	22-14S-28W	NW NE SW	SLAWSON DONALD C Vintage Petroleum, Inc.		22-Aug-75 18-Oct-02	OIL Inj
15-063-20259	J. J. COBERLY 2	22-14S-28W	NE SW NW	SLAWSON, DONALD C.		20-Aug-75	OIL Prod
15-063-20262	Coberly, I.I. 2	21-14S-28W	NE SW NE	SLAWSON DONALD C		20-Aug-75	OIL Prod
15-063-20268 15-063-20268-0001	Coberly, I.I. 3	21-14S-28W	C NW NE	SLAWSON DONALD C Vintage Petroleum, Inc.		6-Oct-75 25-Sep-02	OIL Inj
15-063-20271	COBERLY 'JJ' 3	16-14S-28W	SW SW SE	SLAWSON DRLG & ANDERSON		6-Oct-75	OIL Prod
15-063-20326 15-063-20326-0001 15-063-20326-0002	Coberly, T. 2	21-14S-28W	SW NE SE	SLAWSON DONALD C Vintage Petroleum, LLC Vintage Petroleum, Inc.		15-Feb-77 14-Jun-01 11-Nov-02	SWD SWD Water
15-063-20487 15-063-20487-0001	Coberly, U. 3	21-14S-28W	E2 E2 NW	SLAWSON DONALD C Vintage Petroleum, Inc.		23-Jan-81 10-Sep-02	OIL Inj
15-063-21602	Coberly, I.I. 4	21-14S-28W	NE SE NE	Vintage Petroleum, Inc.	8-Sep-05	18-Oct-05	OIL Prod
15-063-21672	MISSOURI FLATS, NE UNIT 13	22-14S-28W	NE SE NW	Cordillera Energy Partners II, LLC	16-Jul-07	27-Aug-07	OIL Prod
15-063-20260	Coberly, U. 1	21-14S-28W	SE NW NW	SLAWSON DONALD C		20-Aug-75	OIL Prod
15-063-21733	BEESLEY B-2	22-14S-28W	NW SW	Merit Energy Company	11-Aug-08		Expired Intent to drill

**Table 2: Names and corresponding well API numbers for six leases comprising Missouri Flats Waterflood Unit, compiled from [www.kgs.ku.edu](http://www.kgs.ku.edu) 5-31-10.**

MISSOURI FLATS NORTHEAST LEASES					MISSOURI FLATS NORTHWEST LEASE
COBERLY II	COBERLY T	COBERLY JJ	MISSOURI FLATS, NE UNIT	BEESLEY B	COBERLY U
15-063-21602 15-063-20268 -0001 15-063-20262 15-063-20247 -0001	15-063-20255 15-063-20326 -0001 -0002	15-063-20271 15-063-20252 15-063-20259	15-063-21672	15-063-20257 -0001	15-063-20260 15-063-20487 -0001

**Table 3: Combined cumulative and annual oil production data for the six leases comprising the Missouri Flats Waterflood Unit, compiled from [www.kgs.ku.edu](http://www.kgs.ku.edu) 5-31-10. Data incomplete for 2010.**

YEAR	BBLs	CUM BBLs	YEAR	BBLs	CUM BBLs
1975	129,705	129,705	1993	13,850	873,803
1976	175,219	304,924	1994	12,199	886,002
1977	120,247	425,171	1995	12,805	898,807
1978	72,408	497,579	1996	11,539	910,346
1979	52,471	550,050	1997	13,189	923,535
1980	41,841	591,891	1998	11,789	935,324
1981	41,957	633,848	1999	10,535	945,859
1982	33,770	667,618	2000	9,957	955,816
1983	29,900	697,518	2001	10,410	966,226
1984	24,990	722,508	2002	10,331	976,557
1985	22,656	745,164	2003	22,383	998,940
1986	20,144	765,308	2004	74,396	1,073,336
1987	18,699	784,007	2005	71,886	1,145,222
1988	16,494	800,501	2006	62,483	1,207,705
1989	16,082	816,583	2007	40,286	1,247,991
1990	15,156	831,739	2008	38,589	1,286,580
1991	13,964	845,703	2009	23,468	1,310,048
1992	14,250	859,953	2010***	1,720	1,311,768

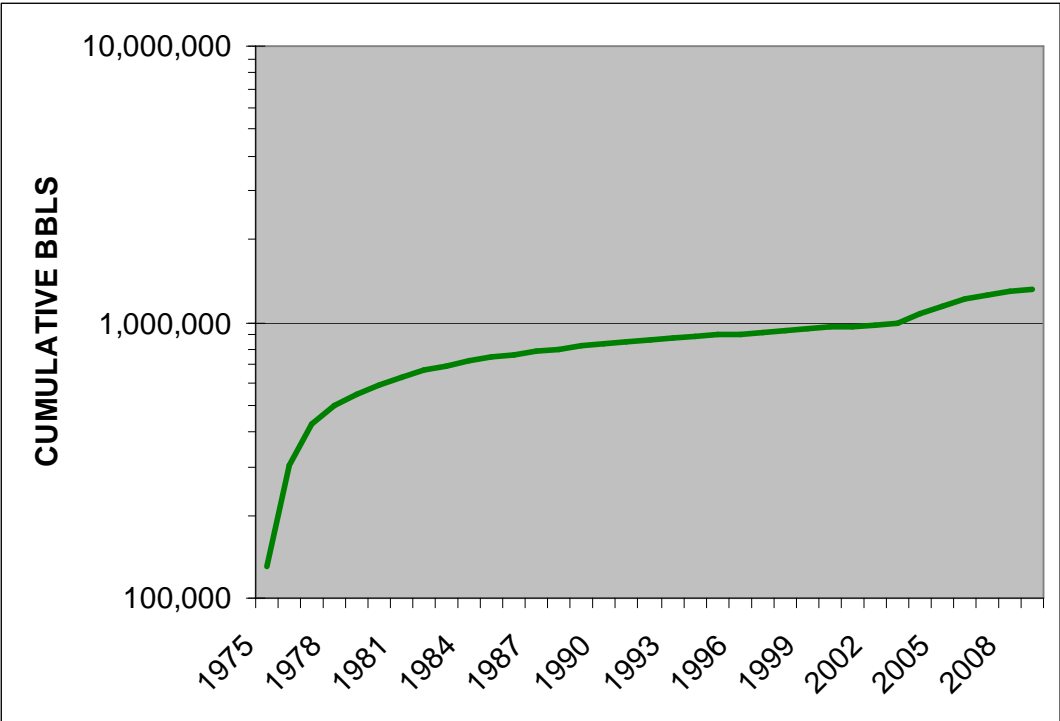


Fig. 4: Cumulative oil production data for the Missouri Flats Waterflood Unit, from [www.kgs.ku.edu](http://www.kgs.ku.edu) 5-31-10.

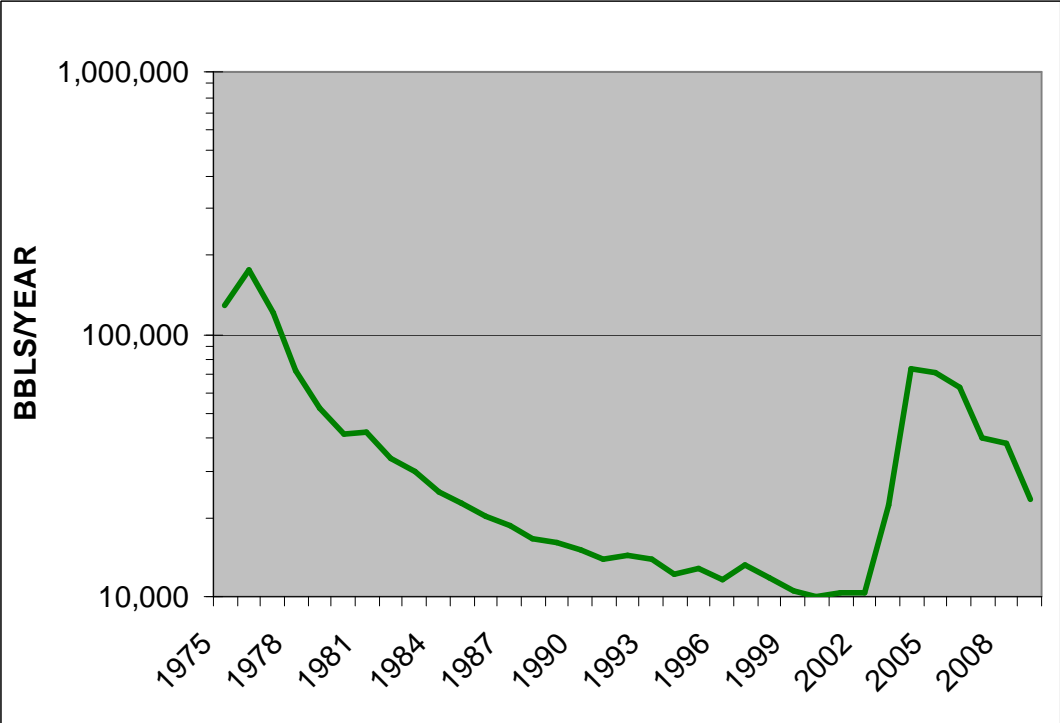


Fig. 5: Annual oil production data for the Missouri Flats Waterflood Unit, from [www.kgs.ku.edu](http://www.kgs.ku.edu) 5-31-10.

<b>M. BRADFORD RINE</b> <i>Certified Petroleum Geologist - R.A.S.G.P. 138897</i> 100 S. Main Suite 415 Wichita, Ks 67202 (316)252-5418		RECEIVED REGISTRATION COMMISSION APR 3 1 2000 WICHITA, KANSAS
<b>GEOLOGIST'S REPORT</b>		
COMPANY <u>Connelly Exploration, Inc.</u> LEASE <u>Coberly Partnership #1</u> FIELD <u>Wildcat</u> LOCATION <u>SE-NE-SE</u> SECTION <u>15</u> TOWNSHIP <u>16S</u> RANGE <u>28W</u> COUNTY <u>Gore</u> STATE <u>Kansas</u>	API: <u>15-063-21546-0000</u> ELEVATIONS KR <u>2590</u> FEET DR <u>2388</u> FEET GI <u>2382</u> FEET MEASUREMENTS ARE ALL FROM <u>K8</u>	CONVEYANCE DIVISION WICHITA, KANSAS
CONTRACTOR <u>Discovery Drilling Co.</u> COMMENCED DRILLING <u>April 17, 2000</u> COMPLETED DRILLING <u>April 26, 2000</u> RTD <u>4475</u> FEET LTD <u>4475</u> FEET MUD UP AT <u>3500</u> FEET MUD TYPE <u>Chem</u>	CASING <u>8518m-244@27K18</u> P&A	ELECTRICAL SURVEYS <u>D/N/IND/5/GR</u>
SAMPLES SAVED FROM <u>3500</u> FEET TO <u>4475</u> FEET DRILLING TIME KEPT FROM <u>3500</u> FEET TO <u>4475</u> FEET SAMPLES EXAMINED FROM <u>3600</u> FEET TO <u>4475</u> FEET GEOLOGICAL SUPERVISION FROM <u>3600</u> FEET TO <u>4475</u> FEET	NOTES: Please note additional geological and drilling information on the following "header" pages.	

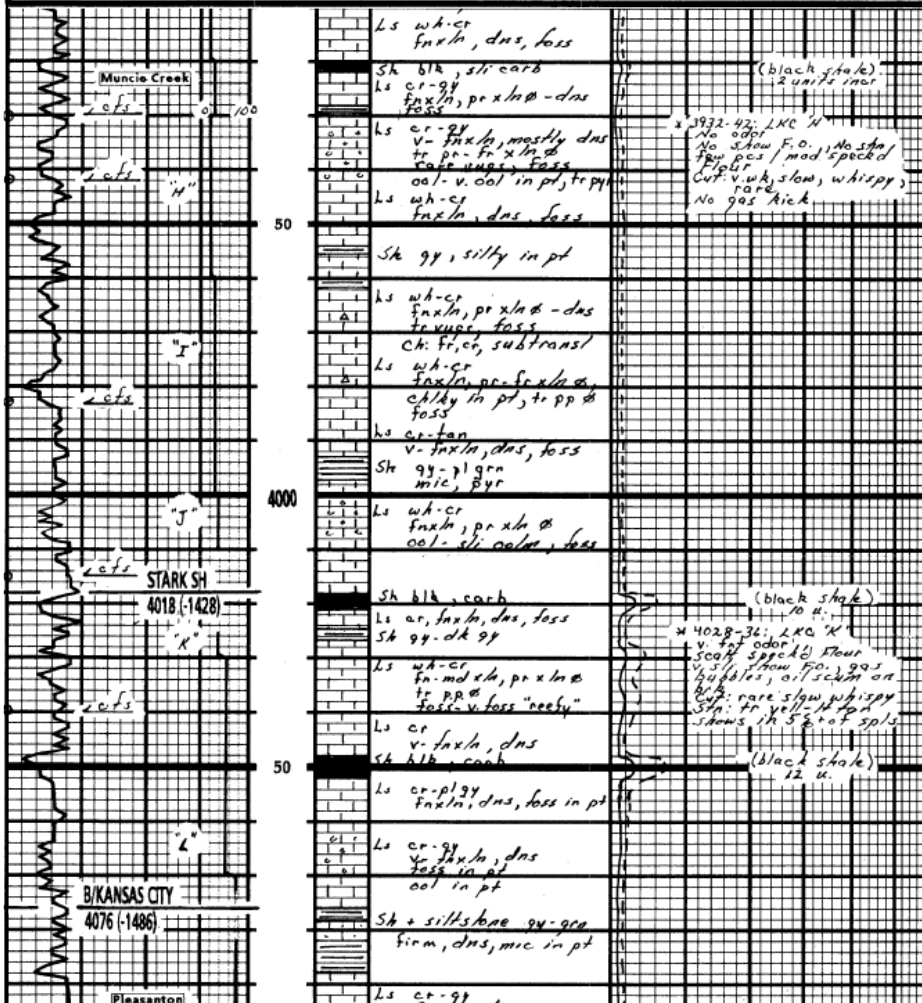


Fig. 6: Geologist's report constructed by M. Bradford Rine, from the Coberly Partnership #1 well (API# 15-063-21546), a dry wildcat well immediately northeast of the waterflood unit. The I, J, K, and L zones of the Kansas City Group produce oil in the Missouri Flats Unit. From [www.kgs.ku.edu](http://www.kgs.ku.edu) 6-3-10.



limestone, with traces of pinpoint porosity, and primary crystalline porosity; it is very fossiliferous, and is called “reefy”. The L-zone (LKC 220), the lowest, is described as cream to pale gray, dense, fine-to-very-fine crystalline limestone, fossiliferous in places and oolitic in places. The well from which the geologist’s report came was a dry hole; it is structurally lower than the productive wells in the waterflood unit and has lower porosity in the reservoir zones, but the descriptions in the report are useful as an indication of the character of the reservoir rocks in the productive wells.

An east-southeast plunging anticline characterizes the waterflood unit, and a similar structure runs parallel south of it (Figure 7, 8). Cross-sections of the waterflood unit show good overall structural closure in three directions – northeast, southeast, and southwest. A northeast-southwest cross-section (Figure 9) shows good structural closure. Cross-sectional views running the length of the structure reveal a more complex situation (Figure 10, 11). While the general structural trend rises from the southeast to the northwest, the rise is not uniform; dips in the structure define separate subtle closures (Figure 11). Two dry wells forming the northwest end of the cross-sections in Figures 10 and 11 are somewhat low, compared to the core of the field, but not low enough to create full structural closure, given that lower wells to the southeast are productive.

Loss of porosity to the northwest completes the trap at the waterflood unit. Figure 12 compares the two northwestern-most well logs from the cross-section in Figure 10, illustrating significantly reduced porosity in the in the dry well, which is farther to the northwest than the productive well (now used as a water injector). The northwestern-most wells in Figure 11 show a similar pattern, which can be seen in the cross-section. The Coberly U #1 (API # 15-063-20260) is perforated in the J-zone or LKC 180, and close examination of the log in Figure 11 shows good porosity, while the Coberly AE #1 well (API # 15-063-20492) shows very low porosity in all four zones toward the NW of Coberly U #1.

Figures 13–16 are a series of maps showing thickness and average porosity in the net pay intervals of the four reservoir zones in the waterflood unit. Net pay intervals were defined using perforation data and well-log cutoffs of having at least 10% porosity and less than 60 API units on the gamma-ray log. The wells perforated in each zone are highlighted on the maps. Porosity maps of the LKC 160 (I), 180 (J), and 200 (K) zones show highest porosity generally in the east-central to northeastern part of section 21, but beyond this general resemblance there seems to be

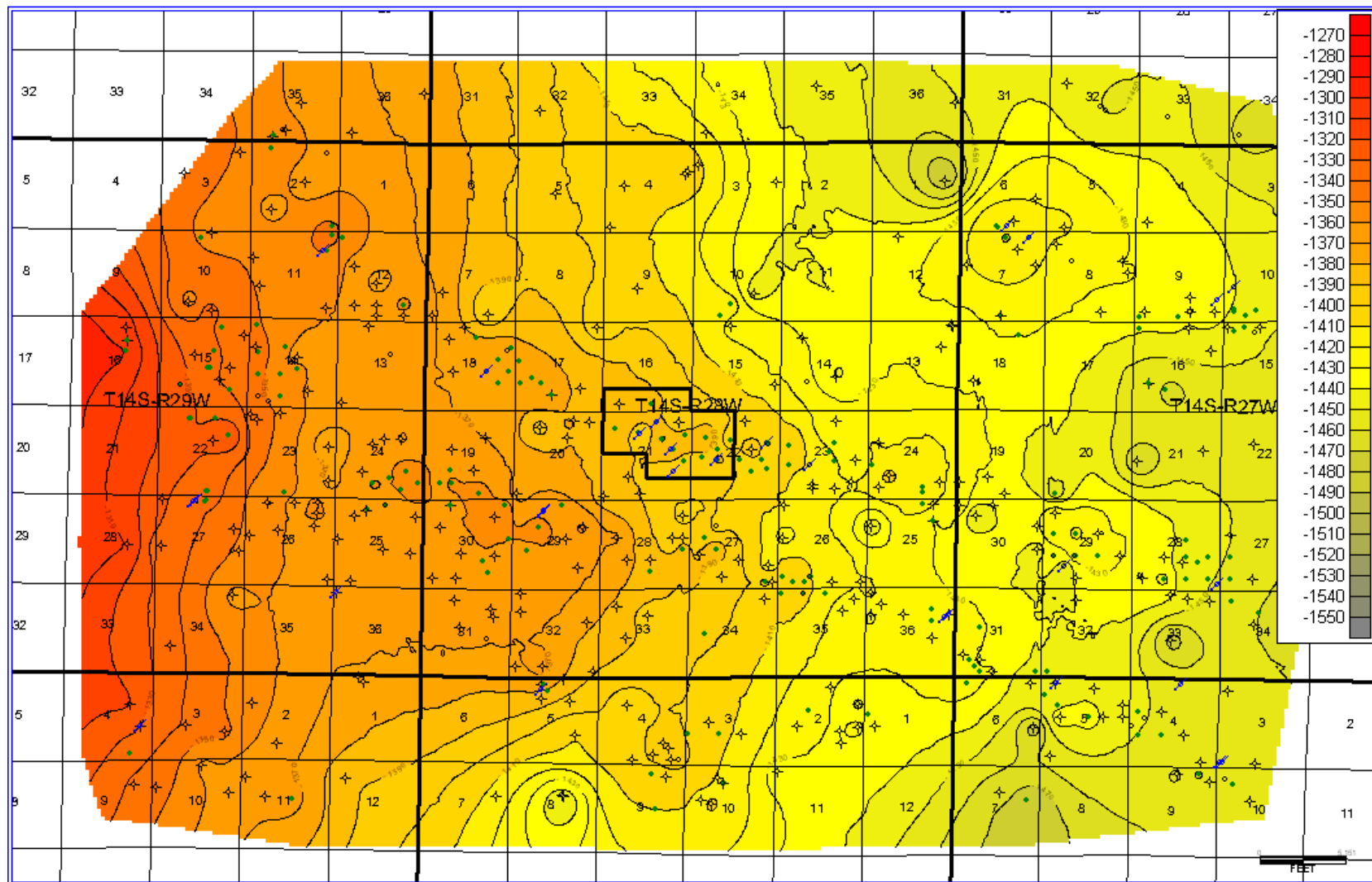


Fig. 7: Regional structural map of the top of the Stark Shale, with Missouri Flats Waterflood Unit indicated with black polygon. The MFwu lies on a SSE-plunging anticline that is parallel to a similar structure lying to the south. Elevation contours are in feet, and datum is sea level.

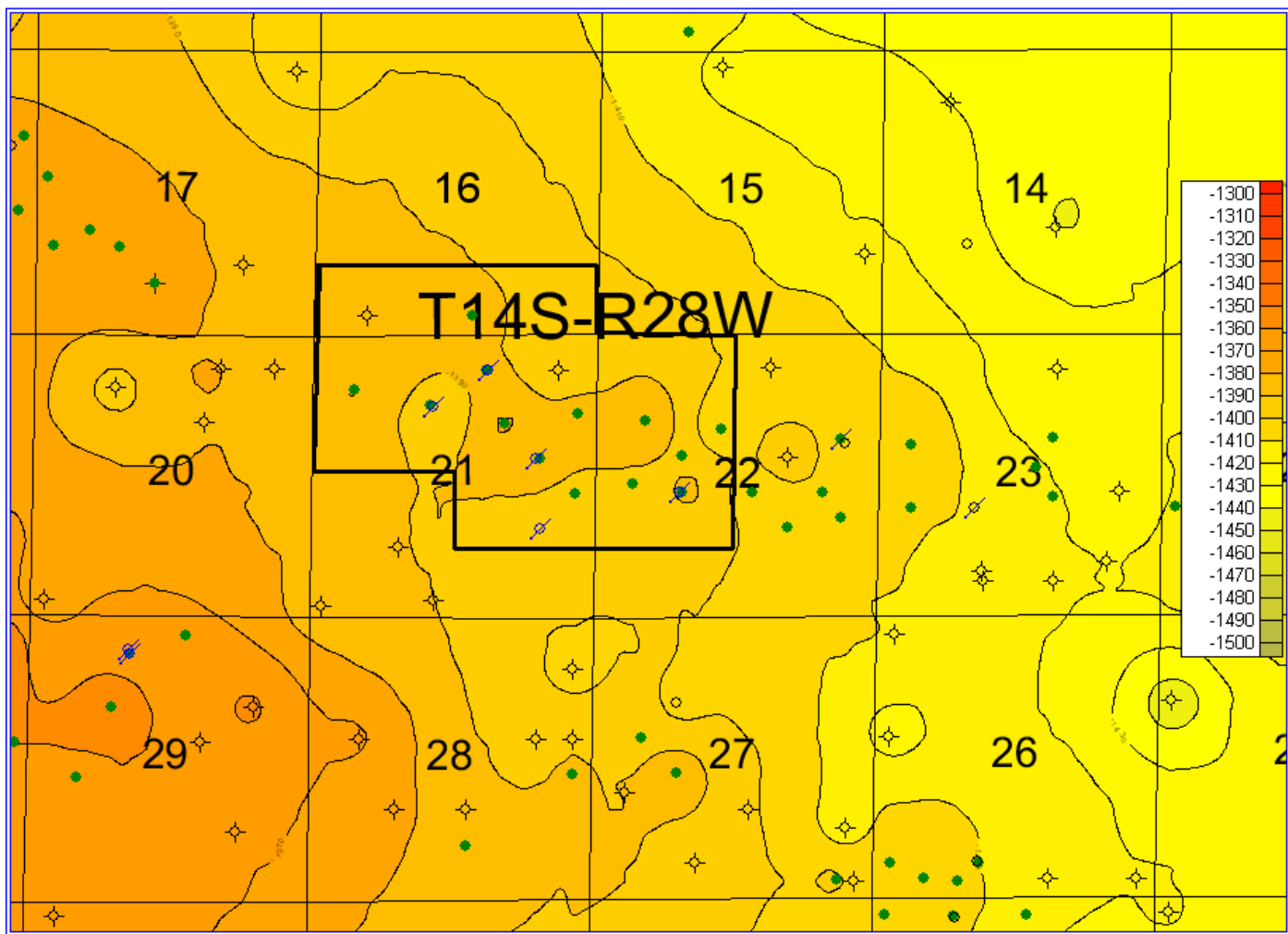


Fig. 8: Sub-regional structural map of the top of the Stark Shale, with Missouri Flats Waterflood Unit indicated by black polygon. Contours show subtle but distinct culminations of the crest of the anticline, but productive wells to the southeast are structurally lower than those to the NW, indicating a lack of overall closure in the field. Elevation contours are in feet, and datum is sea level.

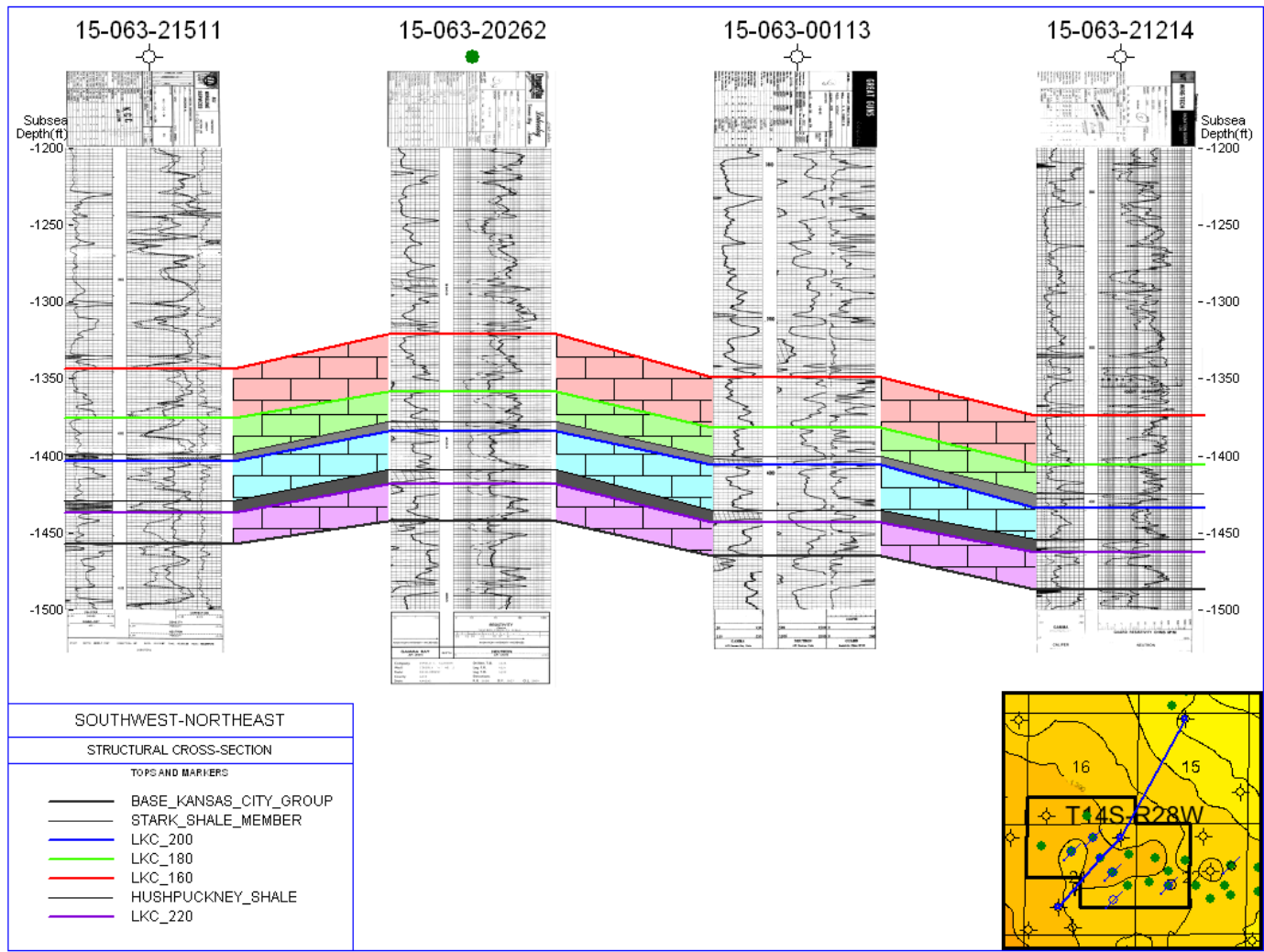


Fig. 9: Southwest-northeast cross-section through Merit Energy Company Missouri Flats Waterflood Unit, with inset map showing orientation. Polygons in depth tracks indicate perforations.

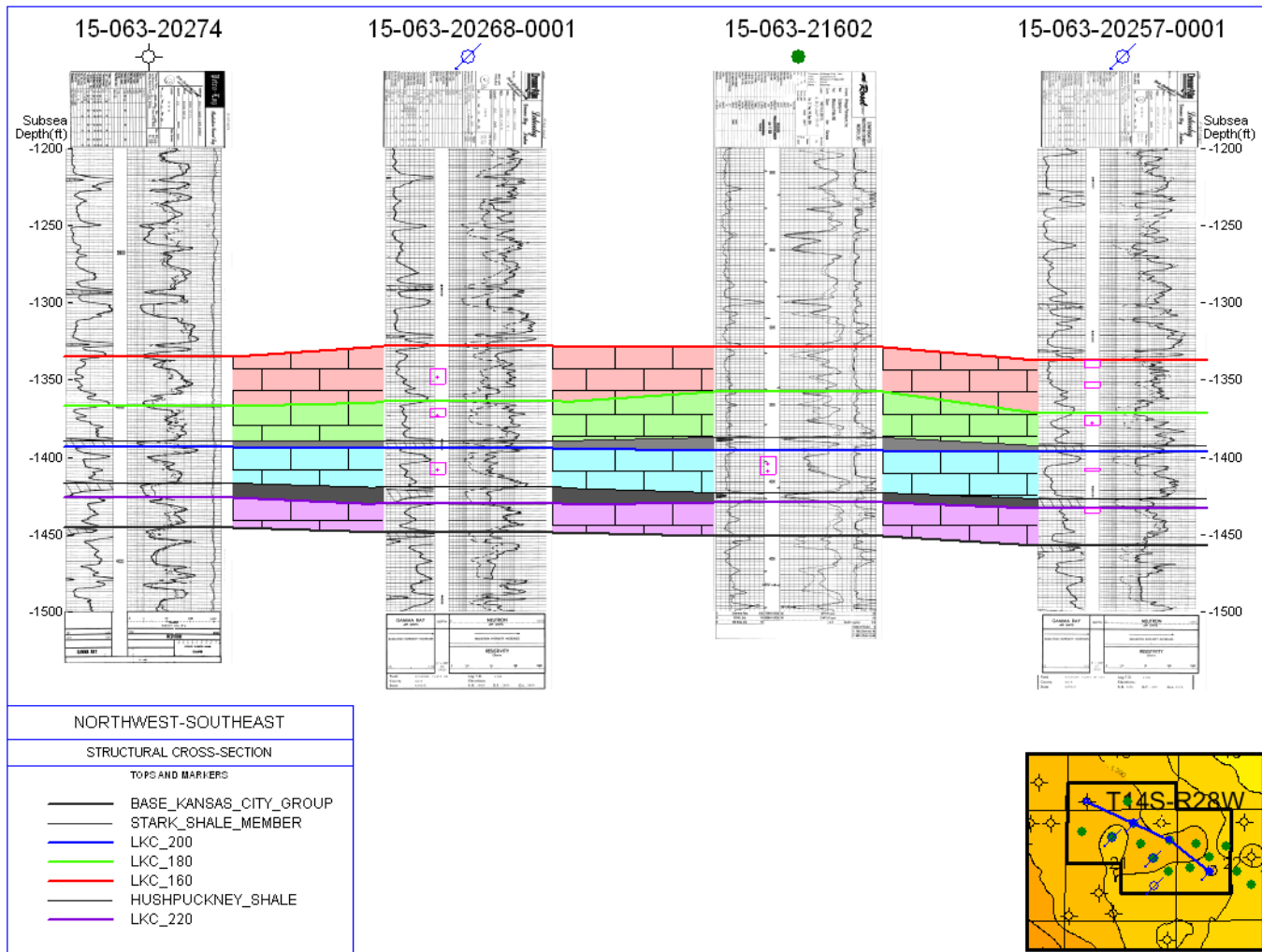


Fig 10: Northwest-southeast cross-section through Merit Energy Company Missouri Flats Waterflood Unit, with inset map showing orientation. Polygons in depth tracks indicate perforations. The southeastern-most well on the right is structurally lower than the non-productive well on the left (northwest). However, the logs show little porosity in the northwest well.

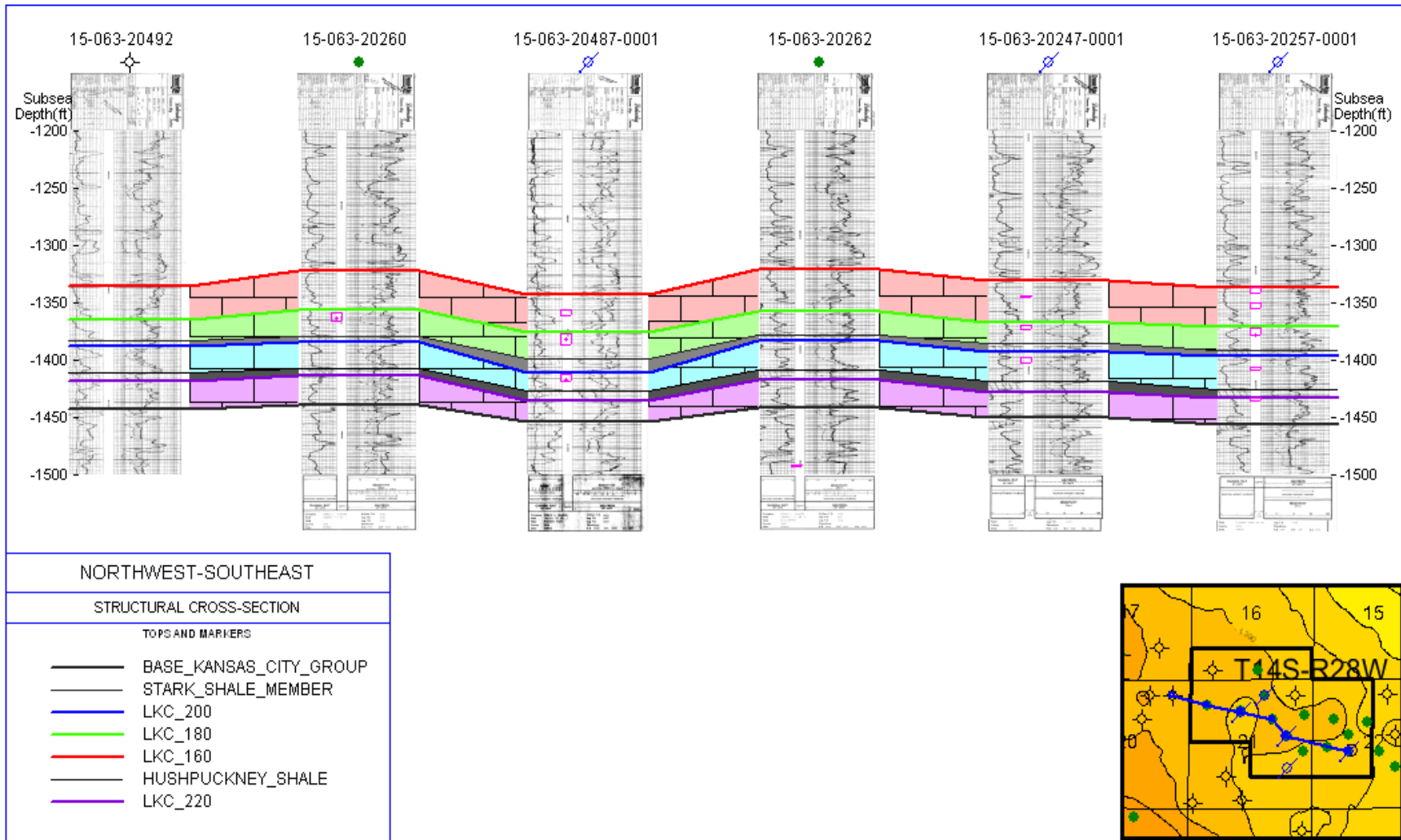
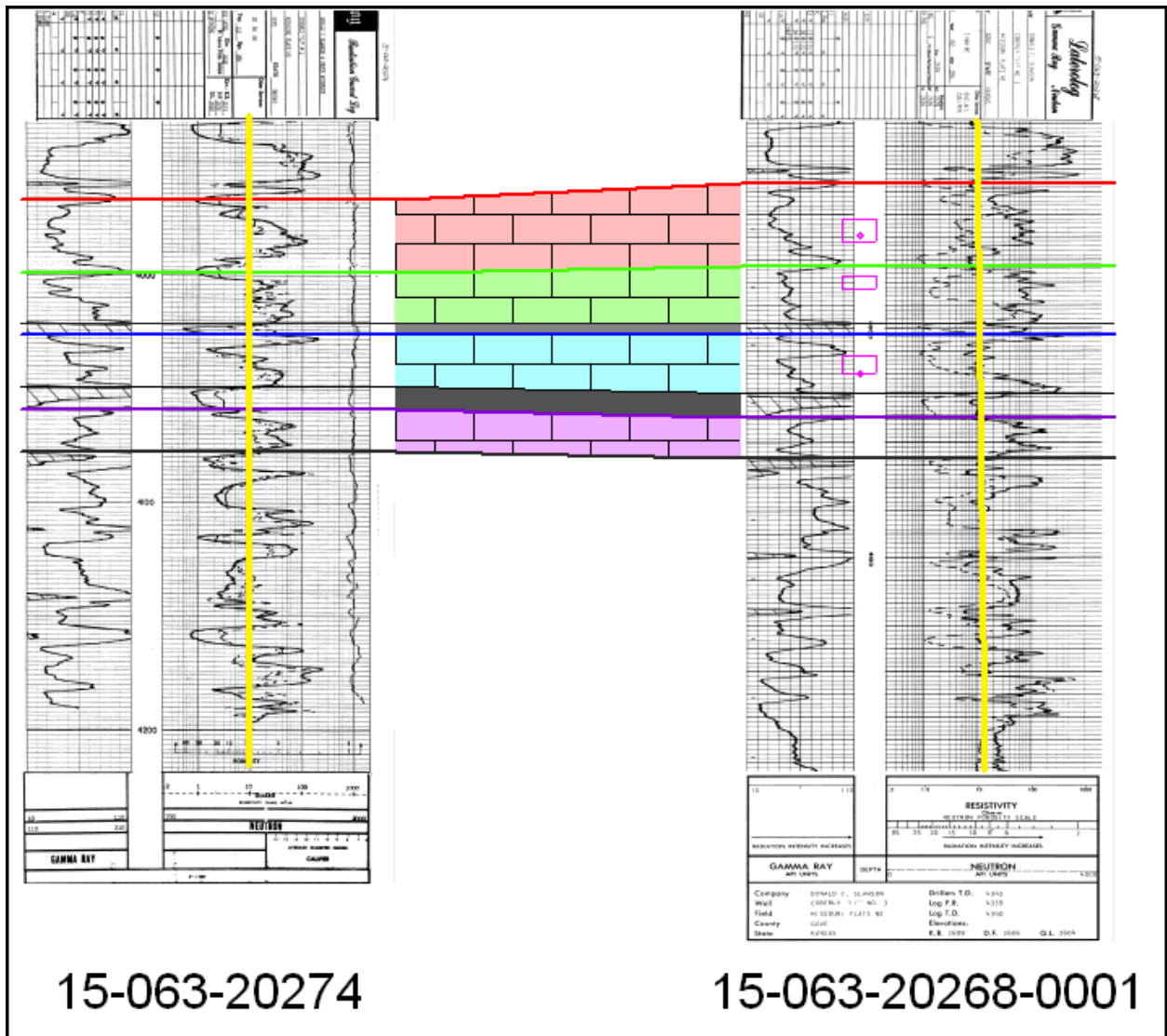


Fig 11: Northwest-southeast cross-section through Merit Energy Company Missouri Flats Waterflood Unit, with inset map showing orientation. This cross-section shows the separate but subtle closures along the crest of the anticline. Again, the well on the left (northwest) is structurally higher than wells to the southeast, but lacks development of pores. Polygons in depth tracks indicate perforations.



15-063-20274

15-063-20268-0001

Fig. 12: Comparison of porosity in two northwestern-most wells from cross-section in Figure 11. Porosity is in right-hand track of each log; solid line in left log, dashed line in right. Vertical lines indicate 10% porosity – less to the right, greater to the left. The I, J, and K zones are porous in the well on the right, but not in that on the left. Polygons in depth tracks indicate perforations.

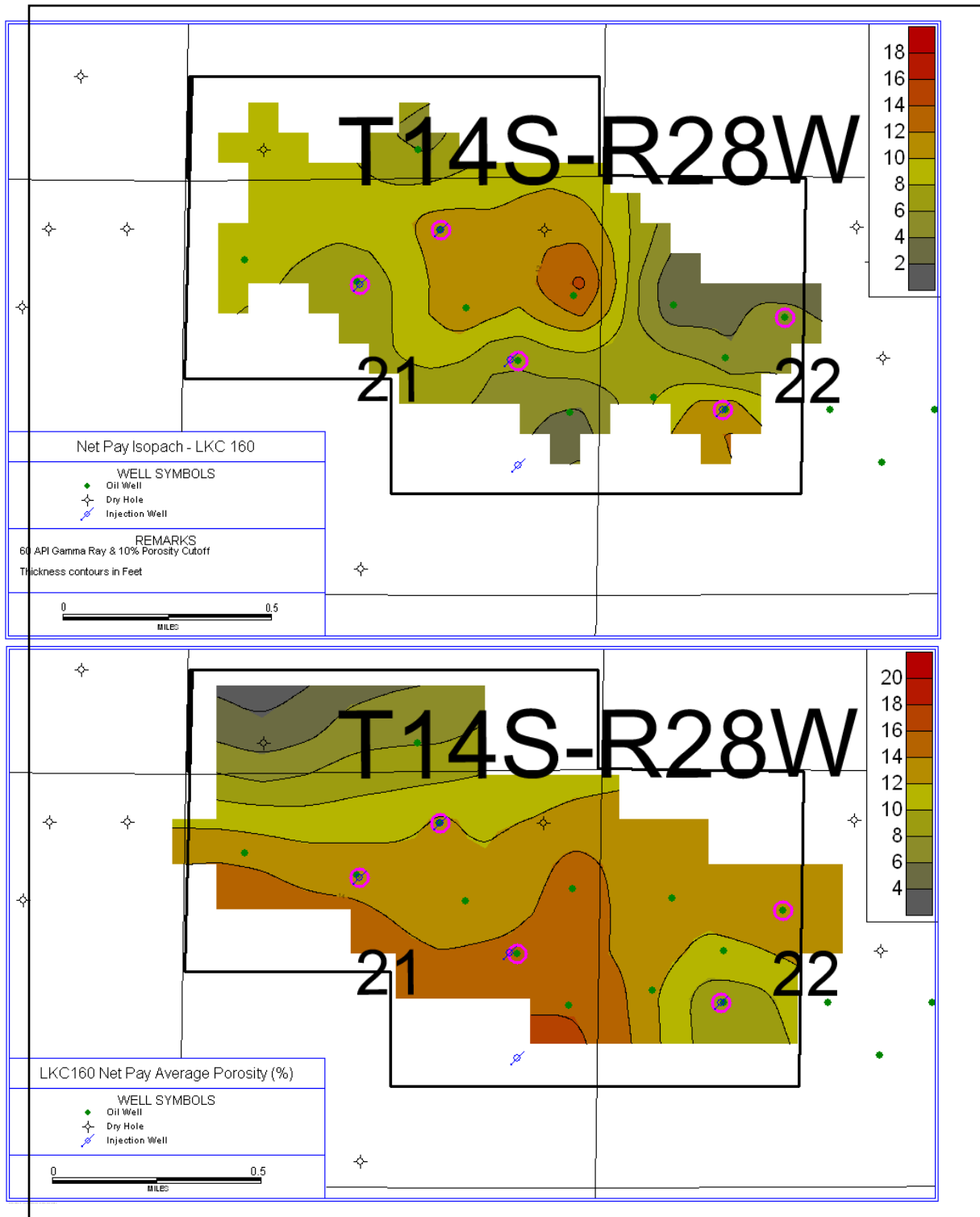


Fig. 13: Thickness (upper) and average porosity (lower) maps of net pay in the LKC 160 (I-zone) in the Waterflood Unit. Porosity is well developed in the area of thickest reservoir, but declines to the north and east. Highlighted wells completed in the I-zone.



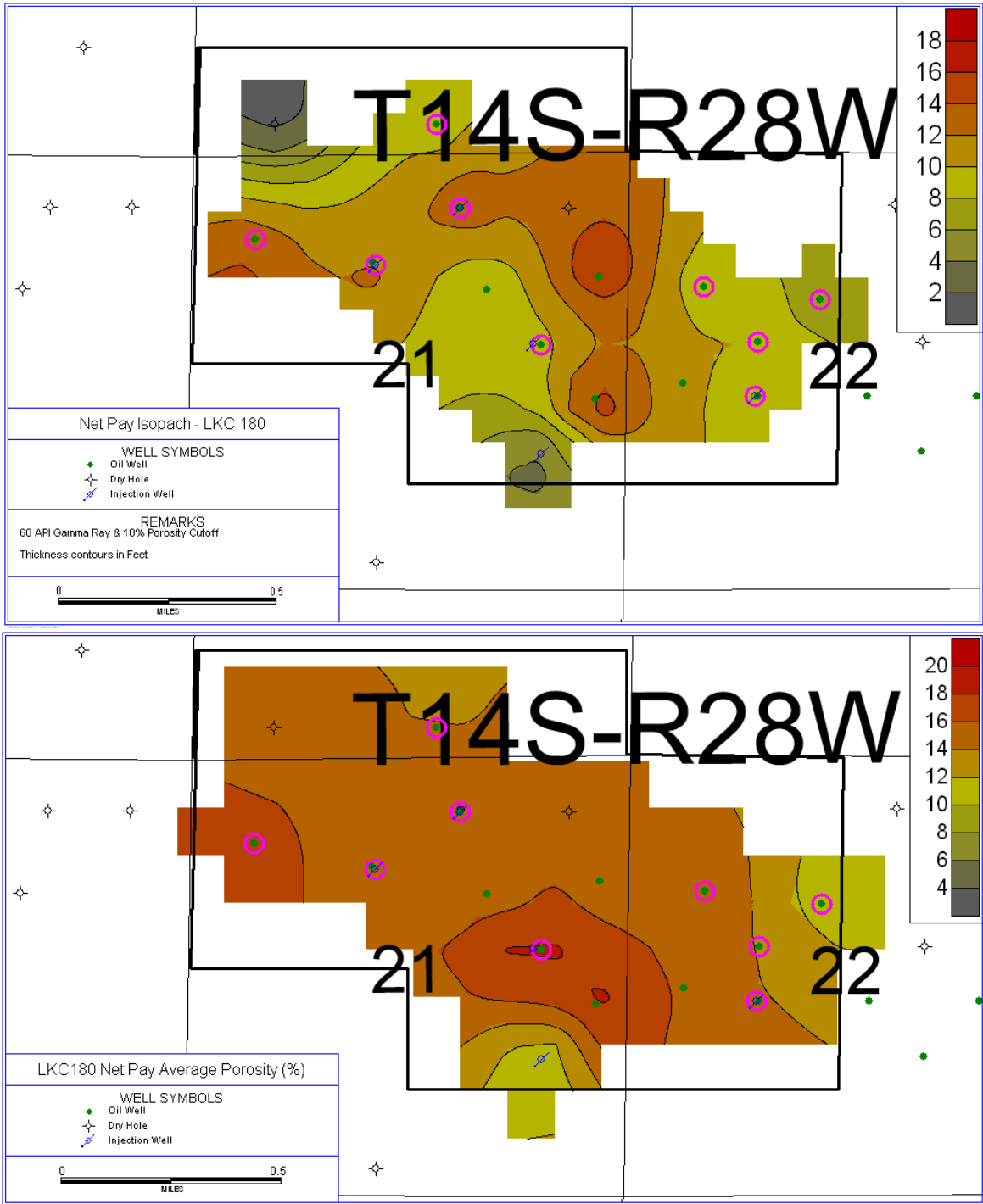


Fig. 14: Thickness (upper) and average porosity (lower) maps of net pay in the LKC 180 (J-zone) in the Waterflood Unit. Area of greatest thickness roughly underlies the area of greatest thickness in the I zone. Highlighted wells completed in the J-zone.

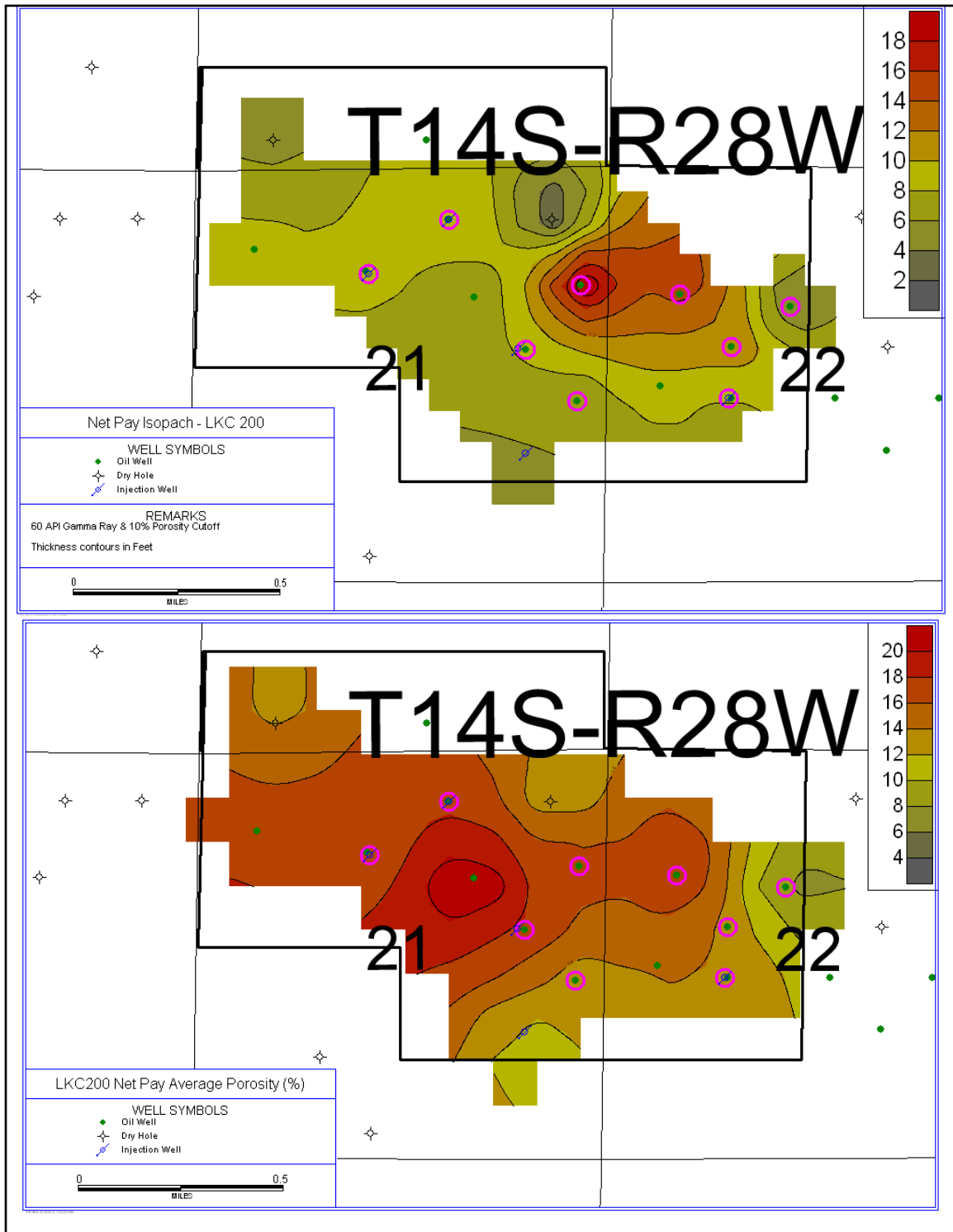


Fig. 15: Thickness (upper) and average porosity (lower) maps of net pay in the LKC 200 (K-zone) in the Waterflood Unit. Greatest thickness is somewhat east of that in I and J zones but overlapping. Highlighted wells completed in the K-zone.

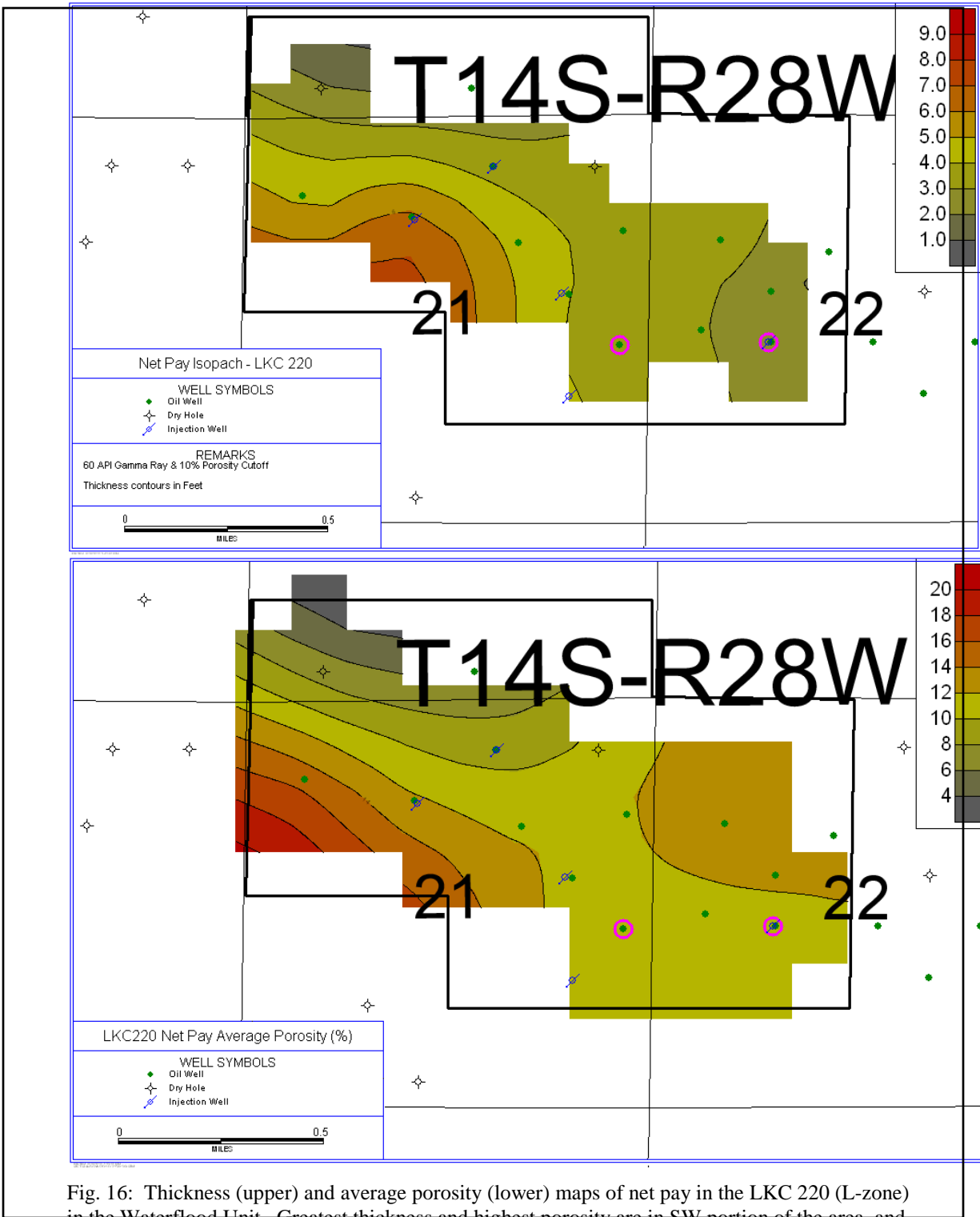


Fig. 16: Thickness (upper) and average porosity (lower) maps of net pay in the LKC 220 (L-zone) in the Waterflood Unit. Greatest thickness and highest porosity are in SW portion of the area, and do not coincide with high porosity and great thickness in the I, J, and K zones. Highlighted wells completed in the L-zone.

no definable overall spatial trend to porosity in the waterflood unit. The LKC 220 or L zone, the lowest zone, has much lower net pay thicknesses than the other three zones.

## **8. DATA AVAILABILITY**

Oil production data for the Missouri Flats Northeast and Missouri Flats Northwest oilfields is available online at the KGS website [www.kgs.ku.edu](http://www.kgs.ku.edu), including annual and cumulative data for the entire field, production for individual leases, and number of producing wells in each year. Well logs, formation top data, and well completion forms, which include perforation data, are also available online from the KGS. Data on water injection and production were not available for consideration in constructing this report nor was information on well-by-well production; presumably such data are available from the operators. Core data are not available, although existing correlations might allow estimation of permeability from porosity. No pressure data or estimates of original oil in place were provided.

## **9. SUITABILITY FOR ENHANCED RECOVERY**

Although oil production numbers show that the waterflood in the Missouri Flats Waterflood Unit has been successful, no water injection or production data are available to the investigators. The unit has four reservoir zones, and most of the wells in the unit are not completed in all four of them. Without more data it is not possible to allocate oil production among the various zones and wells. Without such allocation, and also allocation of injected and produced water, accurate calculations of remaining oil in place for the several zones are not possible. Comparison of water injection to production could provide insight into other important factors that affect the viability of the unit for a surfactant-flooding demonstration project, such as the presence of permeability barriers or whether injected water flowed out of the unit in places.

In the current arrangement with co-mingled production, any injected chemical surfactants would be dispersed and produced unevenly, thus lowering the efficiency of flooding. Alternatively, one zone of the four could be proposed for a demonstration project, but this would require records, tests, or modeling to discover which of the four zones had the most oil left. Perforations in the other three zones would need to be squeezed off, perhaps leaving producible oil behind. Co-mingling of production is an undesirable characteristic in a candidate for a chemical flooding demonstration project, because it is not possible to determine where

concentrations of remaining oil reside. Ideally, a single, well-defined reservoir interval is sought for the demonstration project as this would assure maximum effectiveness of flooding.

## **10. CONCLUSION**

The Missouri Flats Waterflood Unit covers parts of two oilfields and produces oil from four Upper Pennsylvanian limestone reservoir zones. Production began in 1975 and cumulative production is over 1.3 million barrels of oil. Merit Energy Company has owned the unit since 2008. The reservoir zones are on local structural high of an east-southeast plunging anticline that displays a porosity seal as it rises to the northwest. Net pay thickness of individual reservoir zones reaches a maximum of 20 feet based on 10% porosity cutoff. Waterflooding successfully boosted oil production starting in 2003, but oil production data and water injection and production data on a well-by-well and zone-by zone basis were unavailable at the time this report was written.

Although waterflooding has been a demonstrated success, the unit is not a strong candidate for any surfactant flooding demonstration project. The presence of multiple reservoir zones, not perforated in all wells, would lead to decreased efficiency of surfactant flooding compared to a field with a single reservoir zone. A single reservoir zone could be chosen out of the four in the unit, but this would require testing to decide which one to use, and shutting off the other three zones. While surfactant flooding may be deemed viable for this unit in the future, the present project seeks to demonstrate the effectiveness of surfactant flooding as efficiently as possible and so a stronger candidate for the project would ideally have a single, well defined reservoir zone in order to assure a greater chance of maximum efficiency of the demonstration.

## **11. REFERENCE**

Merit Energy Co., 2008, Intent to Drill Form, Beesley B2 Well (API# 15-063-21733), retrieved from [http://www.kgs.ku.edu/PRS/Documents2/2008\\_08\\_01\\_KCC/081108\\_Beesley\\_B\\_2.pdf](http://www.kgs.ku.edu/PRS/Documents2/2008_08_01_KCC/081108_Beesley_B_2.pdf) 6-4-2010.

# CHESTERIAN VALLEY-FILLING SANDSTONE, PLEASANT PRAIRIE OIL FIELD, HASKELL AND FINNEY COUNTIES, KANSAS

Peter Senior and A.W. Walton<sup>1</sup>

## 1. INTRODUCTION

The Chester Waterflood (operated by Cimarex Energy Co.) and Pleasant Prairie Chester Unit (operated by OXY USA Inc. or OXY) are adjacent units producing from the same sandstone reservoir within the Pleasant Prairie oilfield in southwestern Kansas. The Pleasant Prairie oilfield covers parts of three counties, (Figure 1) and has been productive since 1954. Many companies operate leases within the field and several stratigraphic intervals produce oil and gas. This particular report emphasizes only a part of the field, two waterflood units that produce from a linear sand body in the Chesterian Shore Airport Formation that fills a valley incised into older rocks.

## 2. LOCATION

The area of interest to this project lies in the eastern end of the Pleasant Prairie oilfield and is marked by a north-south line of wells drilled into a Late Mississippian Chesterian Stage channel-filling or ‘shoestring’ sand body extending through six sections in Haskell and Finney counties. Cimarex’s Chester Waterflood is the northern part of the sand body and OXY’s Pleasant Prairie Chester Unit is the southern part (Figure 1, 2, 3).

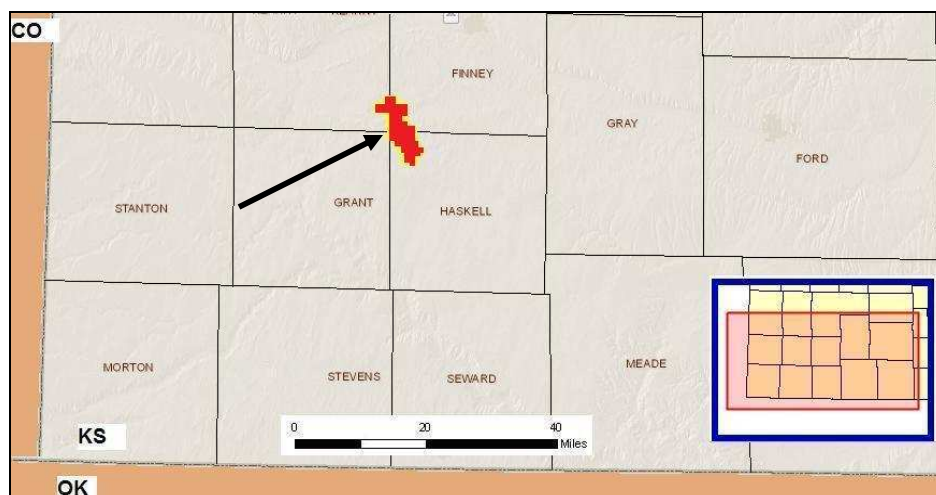


Fig 1: Map of southwestern Kansas showing location of the Pleasant Prairie oilfield (colored polygon) indicated by arrow. Modified from [www.kgs.ku.edu](http://www.kgs.ku.edu) March 9, 2010.

<sup>1</sup> Department of Geology, The University of Kansas, 120 Lindley Hall, 1475 Jayhawk Blvd, Lawrence, Kansas. [twalton@ku.edu](mailto:twalton@ku.edu).

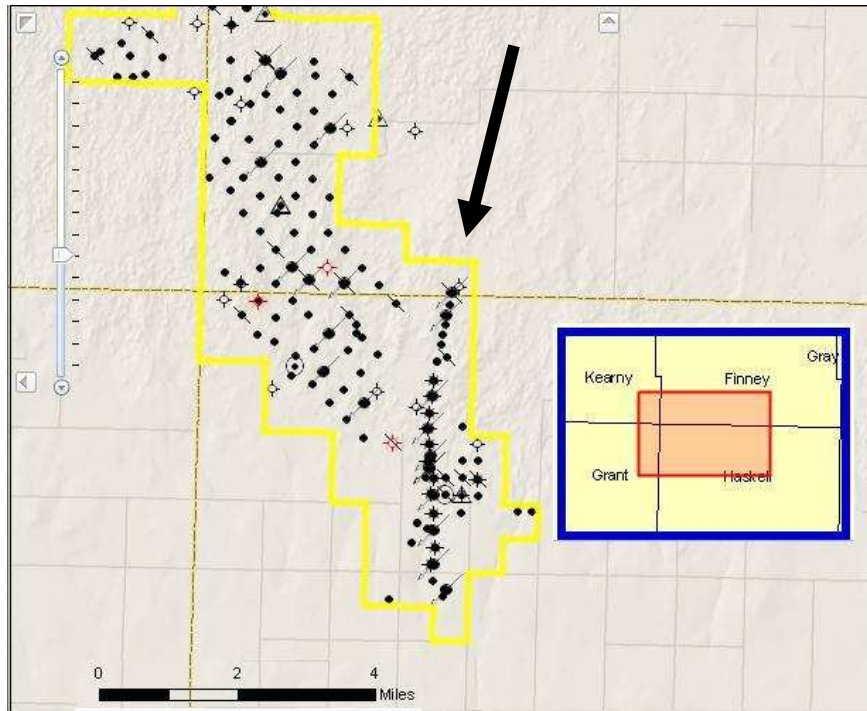


Fig. 2: Enlarged view of Pleasant Prairie oilfield with wells. Note linear trend of wells at eastern end, indicated by arrow, representing the shoestring sand of interest to this project. Modified from [www.kgs.ku.edu](http://www.kgs.ku.edu) March 9, 2010.

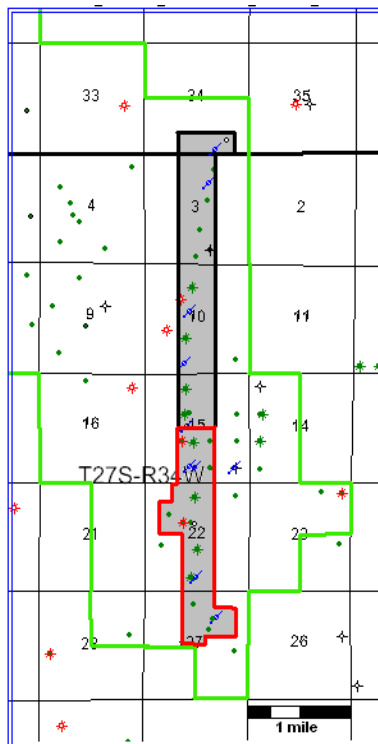


Fig. 3: Detail of Pleasant Prairie oilfield showing approximate boundaries of Oxy USA's Pleasant Prairie Chester unit (red) and Cimarex's Chester Waterflood unit (black) producing from Chesterian shoestring sand.

### **3. METHODS**

This report was constructed by analyzing data in the public domain and posted on the website of the Kansas Geological Survey (KGS) with that provided by the field operators directly to the investigators. The major methods were use of well logs to determine the configuration of key horizons and the thickness distribution within the reservoir. The data and logs were imported into Petra, a subsurface GIS program and analyzed using standard techniques. Production history, quantities, and rates were provided by the operators or downloaded from the website of the KGS.

### **4. DISCOVERY & EXPLORATION HISTORY**

Production from the Chesterian sandstone began in 1990 with the Kearny County Feedlot #1 well, which was completed in October of that year by Helmerich & Payne ([www.kgs.ku.edu](http://www.kgs.ku.edu) March 9, 2010). Exploration was slow for the next nine years with only three more wells drilled, one in 1991 and two in 1996. The years 1999 through 2001 were very active, with a total of eighteen wells drilled; four of these were later converted to injection wells. Cimarex completed one new water injection well in 2004 and two in 2005, followed by a new oil well in 2006. OXY completed a new oil well in their Pleasant Prairie Chester Unit in late 2008, but data from it remain confidential. However, the targeted formation on the Intent to Drill form filed with the Kansas Corporation Commission is listed as St. Louis Limestone, which is stratigraphically lower than the Chesterian, while the Well Completion Report lists the producing formation as Morrowan, which is stratigraphically above the Chesterian. This well represents the latest drilling activity in the Chesterian shoestring sand body in the Pleasant Prairie oilfield. Given the spacing and position of the wells in the Chesterian sandstone, it is thoroughly explored. Table 1 provides a summary of all the wells operated by Cimarex and OXY in the Chester Waterflood and Pleasant Prairie Chester Unit.



**Table 1: List of wells in Chesterian sandstone in Pleasant Prairie oilfield. Data retrieved from [www.kgs.ku.edu](http://www.kgs.ku.edu) March 19, 2010.**

API NUMBER	LEASE	WELL	SEC -TOW-RG	SPOT	CURRENT OPERATOR	SPUD	COMPLETION	STATUS
15-081-20639	KEARNY CO. FEEDLOT	1	15-27S-34W	C SE NW	Cimarex Energy Co.	29-Aug-90	5-Oct-90	Producing
15-081-20690	ENGLER	2-15	15-27S-34W	C SW SE	C & R Petroleum Co.	26-Jun-91	7-Aug-91	Plugged and Abandoned 27-Apr-98
15-081-20883	KUHN	2-10	10-27S-34W	SE SE SW	Cimarex Energy Co.	11-Nov-94	17-Feb-96	Converted to EOR Well
15-081-21006	KUHN	4-10	10-27S-34W	SE SE NW	Cimarex Energy Co.	11-Mar-96	30-Apr-96	Producing
15-081-21006-0001	KUHN	4-11	10-27S-34W	SE SE NW	Cimarex Energy Co.			EOR - UIC Application Dismissed
15-081-21235	Berger 'A'	1	22-27S-34W	NE SE SW	Oxy USA, Inc.	1-Mar-99	28-Mar-99	Converted to EOR Well
15-081-21237	Berger 'A'	2	22-27S-34W	SW NW SE	Oxy USA, Inc.	23-Apr-99	1-Jun-99	Well Drilled
15-081-21253	KEARNY CO. FEEDLOT	2	15-27S-34W	SE NE NW	Cimarex Energy Co.	8-Oct-99	2-Dec-99	Producing
15-081-21256	Kuhn	6-10	10-27S-34W	NW SE NE SW	Cimarex Energy Co.	21-Oct-99	5-Dec-99	Producing
15-081-21254	Moody 'D'	1	15-27S-34W	E2 E2 NE SW	Oxy USA, Inc.	12-Oct-99	13-Dec-99	Producing
15-081-21255	MOODY 'D'	2	15-27S-34W	NE SE SW	Oxy USA, Inc.	15-Nov-99	18-Dec-99	Converted to EOR Well
15-081-21295	GARRISON 'B'	1	22-27S-34W	NE SE NE NW	Oxy USA, Inc.	30-Mar-00	20-Apr-00	Producing
15-081-21296	Garrison B	2	22-27S-34W	NE SE NW	Oxy USA, Inc.	29-Apr-00	27-May-00	Converted to EOR Well
15-081-21306	Schuh A	1	27-27S-34W	NE SE NE NW	Oxy USA, Inc.	9-May-00	23-Jun-00	Producing
15-081-21313	Garrison 'C'	1	22-27S-34W	NE NE SW NW	Oxy USA, Inc.	27-May-00	15-Jul-00	Well Drilled
15-081-21302	MARY JONES	1	3-27S-34W	SW SW NE	Cimarex Energy Co.	22-Jun-00	26-Jul-00	Producing
15-081-21322	Kells 'D'	1	27-27S-34W	NE NE SW NE	Oxy USA, Inc.	17-Jun-00	28-Jul-00	Converted to EOR Well
15-081-21334	MARY JONES	2	3-27S-34W	NW SE NW NE	Cimarex Energy Co.	31-Jul-00	10-Sep-00	Producing
15-081-21313-0001	PLEASANT PRAIRIE UNIT	201	22-27S-34W	NE SW NW	Oxy USA, Inc.	9-Oct-00	16-Oct-00	Inactive Well
15-081-21332	FEDERAL	2	3-27S-34W	SW NW SE	Cimarex Energy Co.	22-Sep-00	2-Nov-00	Producing
15-081-21363	Kuhn	7-10	10-27S-34W	SE NE NW	Cimarex Energy Co.	29-Jan-01	23-Feb-01	Producing
15-081-21333	FEDERAL	3	3-27S-34W	SE SE SW	Helmerich & Payne, Inc.	7-Mar-01	9-May-01	Well Drilled
15-081-20690-0001	PPCU	001S	15-27S-34W	SW SE	Oxy USA, Inc.	17-Jul-01	10-Aug-01	Well Drilled
15-081-21322-0001	PLEASANT PRAIRIE UNIT	601W	27-27S-34W	NE SW NE	Oxy USA, Inc.	24-Aug-01	27-Aug-01	Authorized Injection Well
15-081-21296-0001	PLEASANT PRAIRIE UNIT	302-W	22-27S-34W	SE SE NW	Oxy USA, Inc.	28-Aug-01	30-Aug-01	Authorized Injection Well
15-081-21255-0001	Pleasant Prairie Unit	102-W	15-27S-34W	NE SE SW	Oxy USA, Inc.	30-Aug-01	4-Sep-01	Authorized Injection Well
15-081-21235-0001	PLEASANT PRAIRIE UNIT	401W	22-27S-34W	SE SE SW	Oxy USA, Inc.	20-Sep-01	24-Sep-01	Authorized Injection Well
15-081-21500	MARY JONES	4	3-27S-34W	NW SW NE	Cimarex Energy Co.	30-Dec-03	20-Jan-04	Authorized Injection Well
15-081-21566	KEARNY CO. FEEDLOT	3	15-27S-34W	SW SE SE NW	Cimarex Energy Co.	22-Jan-05	5-Feb-05	Authorized Injection Well
15-081-21588	KEARNY CO. FEEDLOT	4	15-27S-34W	NE SE NW	Cimarex Energy Co.			Expired Intent to Drill (C-1)
15-055-21879	MARY JONES	5	34-27S-34W	SW SE SW SE	Cimarex Energy Co.	3-Aug-05	29-Aug-05	Plugged and Abandoned
15-081-21656	KC FEEDLOT	5	15-27S-34W	SE NE SE NW	Cimarex Energy Co.	22-Apr-06	10-May-06	Producing
15-081-21658	KC Feedlot	4	15-27S-34W	SW SE SE NW	Cimarex Energy Co.	14-Jul-06	10-Aug-06	Authorized Injection Well
15-081-21854	PLEASANT PRAIRIE CHESTER UNIT	602	27-27S-34W	NW SW NE	Oxy USA, Inc.	14-Nov-08	30-Dec-08	Producing

The reservoir has been under waterflood since at least October of 2001, which is the earliest date of water injection data provided by OXY. Cimarex and OXY are both currently waterflooding the reservoir. Cimarex is using a total of four injectors to go along with nine producers. OXY is also using a total of four injection wells and currently runs five producers not including the PPCU 602 well, which may be producing from a Morrowan rather than Chesterian reservoir. Both companies have set up the waterflood to have injection wells alternating with producing wells down the length of the shoestring sand (Figures 4 and 5).

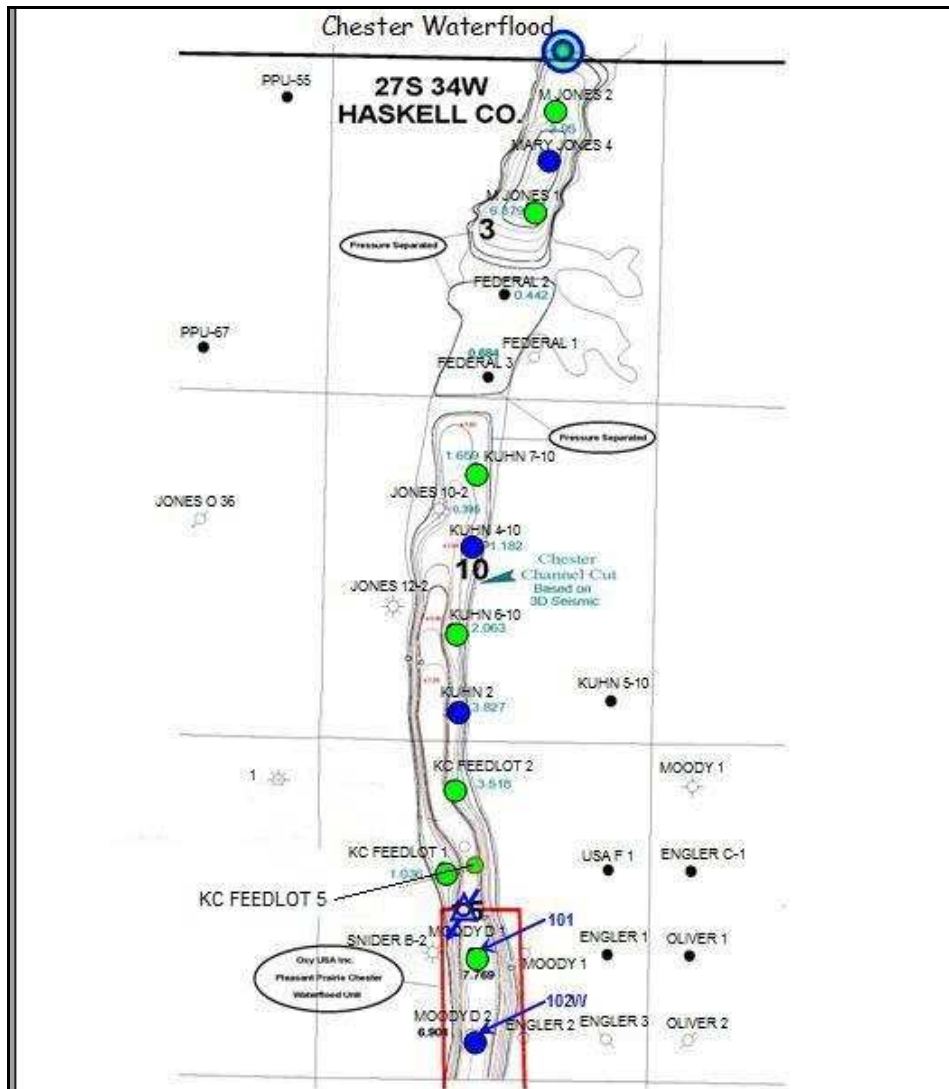


Fig. 4: Map of Cimarex's Chester Waterflood showing outline of Chesterian sandstone and locations of wells. Blue indicates injector wells, green and black indicate oil producers. Modified from original provided by Cimarex Energy Co.

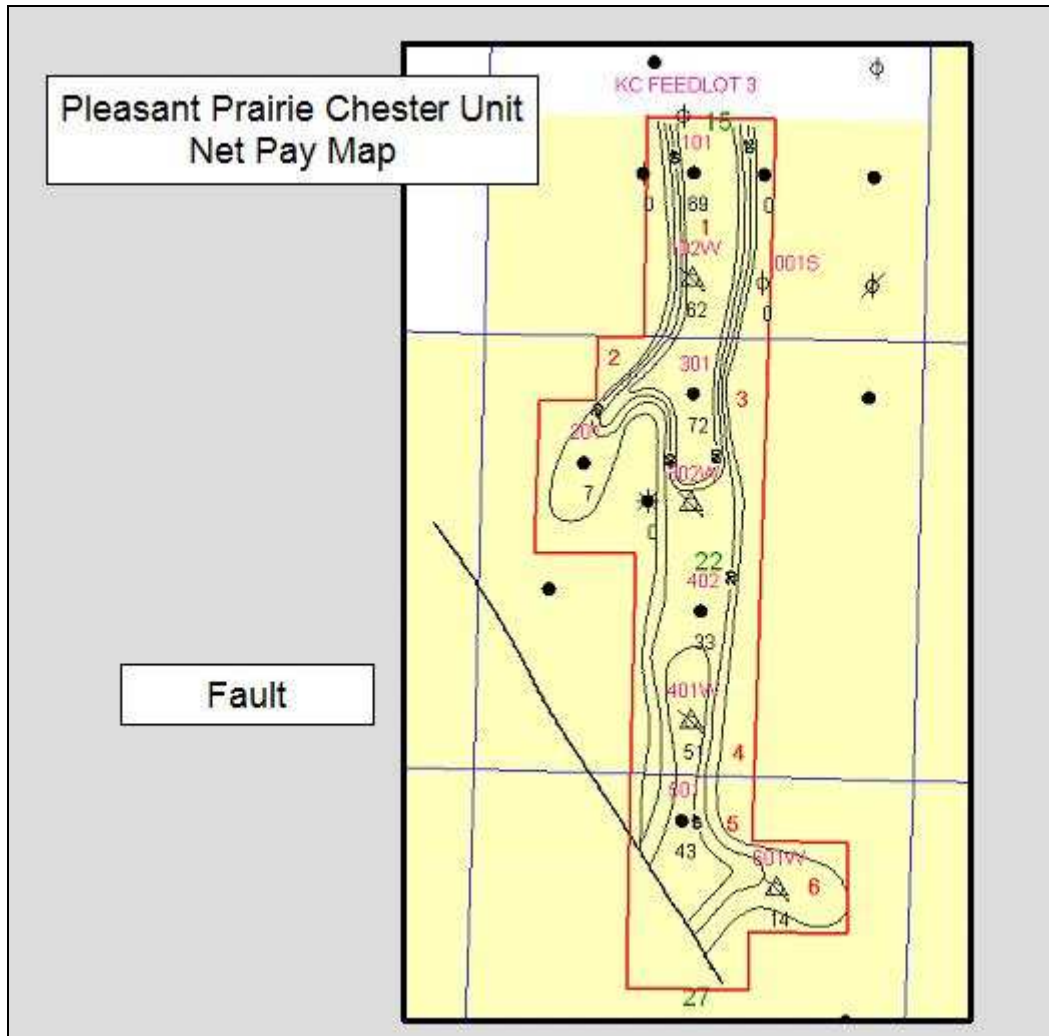


Fig. 5: Map of Pleasant Prairie Chester Unit showing outline of Chesterian sandstone and locations of wells; note fault truncating southern end of reservoir. Triangles indicate injector wells and black indicates oil producers; legal boundary in red. Modified from original provided by OXY USA Inc.

## 5. PRODUCTION HISTORY

The most recent year for which complete production data are available is 2008. Total cumulative production of oil for the Chester Waterflood is 2,380,091 barrels at the end of 2008, while the Pleasant Prairie Chester Unit has produced a cumulative total of 1,837,066 barrels as of the end of 2008. Data on water injection and production were unavailable for the Chester Waterflood, but were provided by OXY for the Pleasant Prairie Chester Unit. Cumulative oil production since waterflooding commenced on the Pleasant Prairie Chester Unit is 1,204,260 barrels. Peak annual production for the

Pleasant Prairie Chester Unit occurred in 2000 with 337,847 barrels of oil. The Chester Waterflood experienced an early peak in 2000, when 333,720 barrels of oil were produced, but that total was later surpassed with 386,246 barrels in 2004. Cimarex has provided a graph showing daily oil production over the period from 2003 to 2008, reproduced below. Annual and cumulative production data for both the Chester Waterflood and the Pleasant Prairie Chester Unit are summarized below in Table 2.

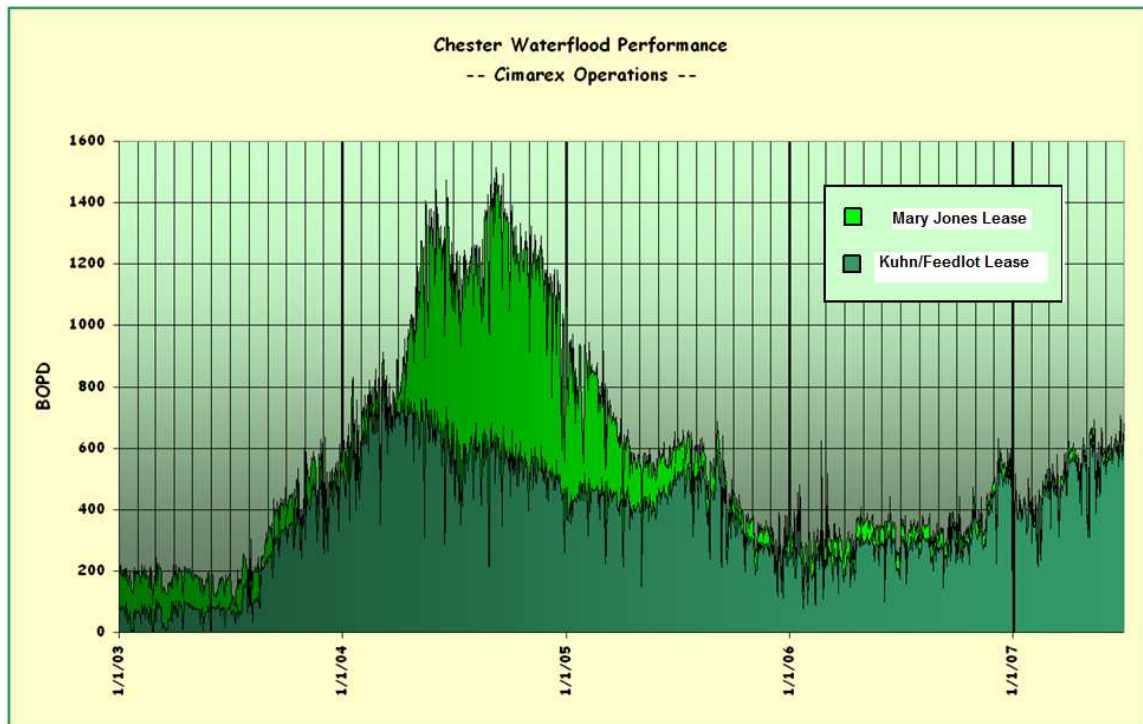


Fig. 6: Graph of daily oil production vs. time for the Chester Waterflood, modified from original provided by Cimarex Energy Co. Note the spike in production beginning in late 2003. Although no quantitative data were available regarding water injection into this lease, the production spike likely represents a response of the reservoir to increased waterflooding.

Cumulative and annual oil production are compared graphically to water injection and production for the Pleasant Prairie Chester Unit below in Figures 7 and 8. Cumulative oil production seems to be leveling off while cumulative totals of water injection and production continue to rise, indicating lessening amounts of oil being swept out by the ongoing waterflood. Trends in the graph comparing annual oil production to annual water production and injection confirm that the waterflood is losing effectiveness. Oil production is on a significant decline since 2006 despite continual injection of relatively steady amounts of water since then. The Pleasant Prairie Chester Unit

responded well to the waterflood from 2002 and 2003, where production increased dramatically as can be seen in Figure 8 and Table 2.

YEAR	CHESTER WATERFLOOD		PLEASANT PRAIRIE CHESTER UNIT	
	ANNUAL OIL PRODUCTION	CUMULATIVE OIL PRODUCTION	ANNUAL OIL PRODUCTION	CUMULATIVE OIL PRODUCTION
1990	13,722	13,722	-	-
1991	45,560	59,282	-	-
1992	38,745	98,027	-	-
1993	34,761	132,788	-	-
1994	31,821	164,609	-	-
1995	75,966	240,575	-	-
1996	70,244	310,819	-	-
1997	65,952	376,771	-	-
1998	49,617	426,388	-	-
1999	120,981	547,369	58,945	58,945
2000	333,720	881,089	337,847	396,792
2001	230,175	1,111,264	236,014	632,806
2002	124,991	1,236,255	135,844	768,650
2003	115,126	1,351,381	239,284	1,007,934
2004	386,246	1,737,627	208,935	1,216,869
2005	204,857	1,942,484	230,873	1,447,742
2006	124,844	2,067,328	206,694	1,654,436
2007	188,254	2,255,582	111,634	1,766,070
2008	124,509	2,380,091	70,997	1,837,066

Table 2: Annual and cumulative oil production data for the Chester Waterflood and Pleasant Prairie Chester Unit

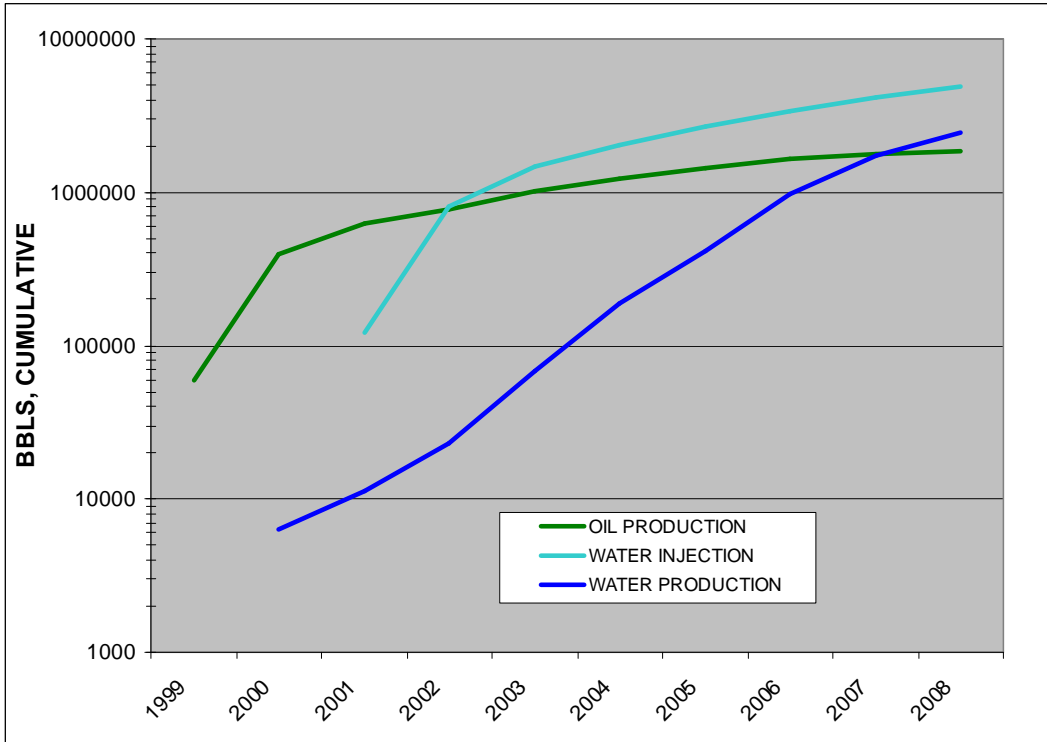


Fig. 7: Cumulative injection and production data for the Pleasant Prairie Chester Unit.

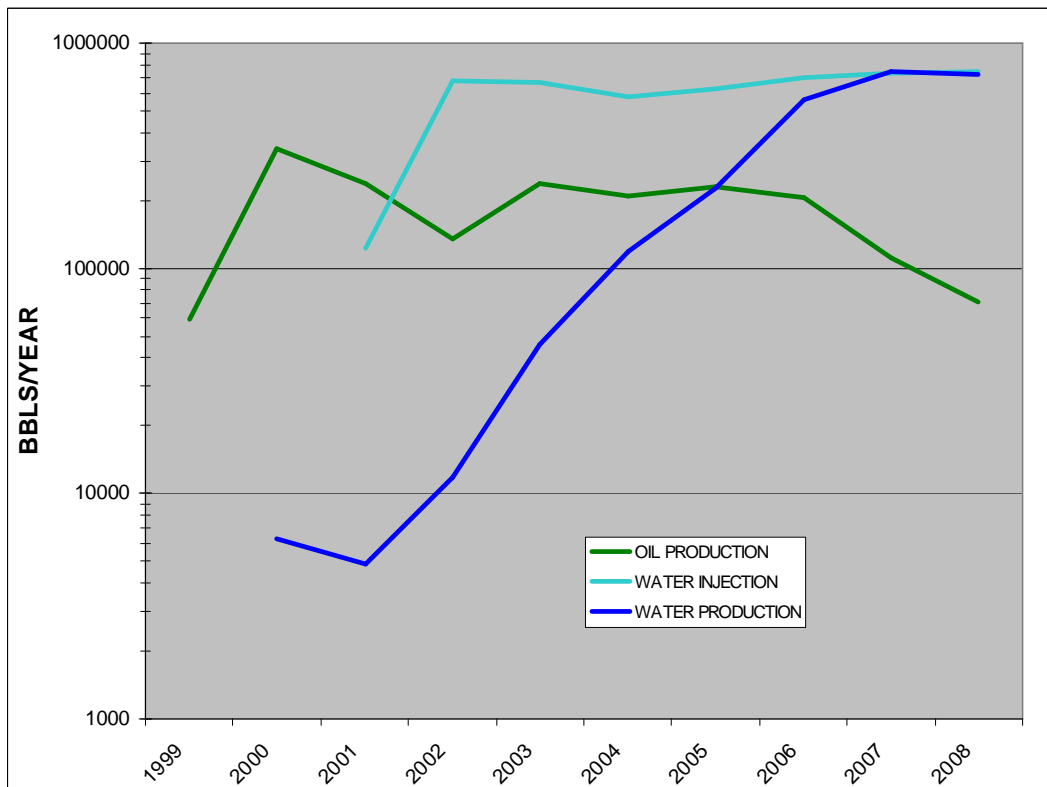


Fig. 8: Annual injection and production data for the Pleasant Prairie Chester Unit.

## 6. GEOLOGY

The Chesterian Stage is the youngest part of the Mississippian Series in southwestern Kansas. The end of the Mississippian Series in Kansas is marked by an unconformity of great areal extent that is a very useful marker for subsurface mapping and stratigraphy. The unconformity truncates Chesterian rocks across southwestern Kansas; they thin progressively northward from the Oklahoma border and ultimately disappear from the subsurface not far north of Pleasant Prairie oilfield. During Chesterian time, sand was deposited in a channel cut into underlying limestones of the Meramecian Stage (Figures 9 and 10). The channel in Pleasant Prairie oilfield is part of an incised valley trend extending south to Oklahoma and containing several Chesterian sandstone reservoirs. Previous studies indicate Chesterian sands south of Pleasant Prairie in this incised valley trend were deposited in an estuarine environment with tidal influence (Cirilo, 2002; Montgomery and Morrison, 1999; Shonfelt, 1988).

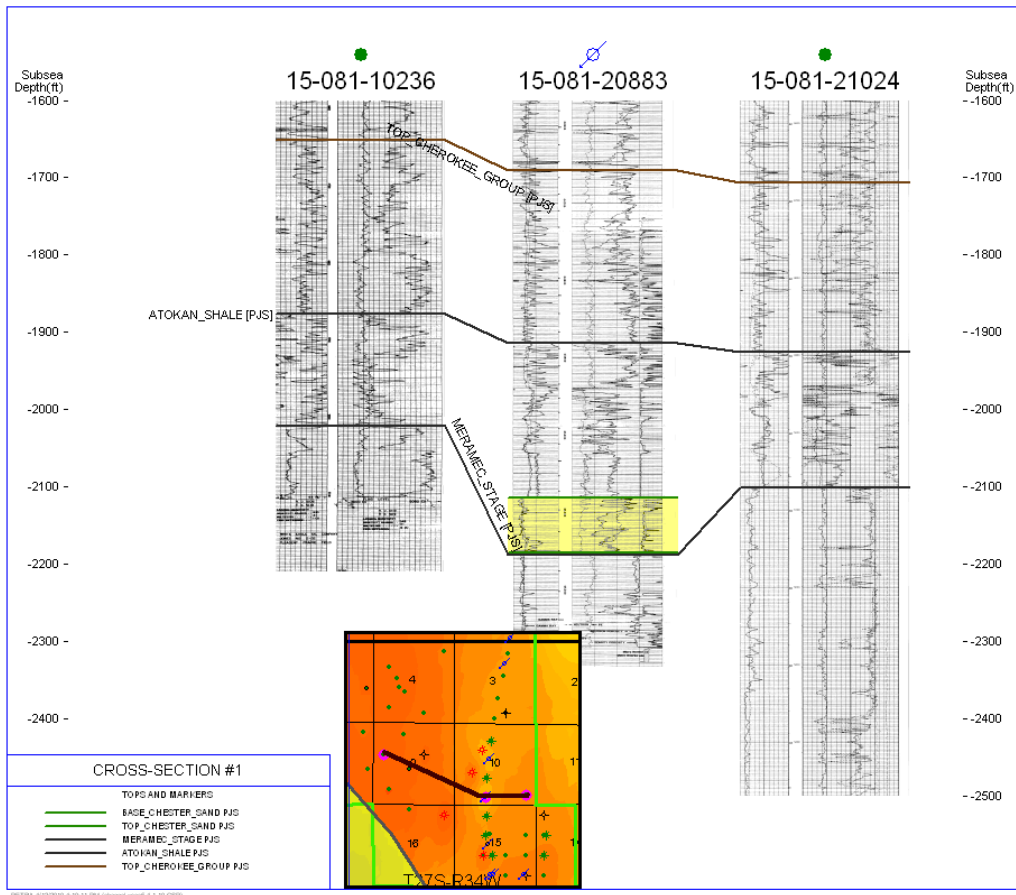


Fig. 9: Cross-section showing distinct channel structure of Chesterian sandstone (highlighted yellow) in Cimarex's Chester Waterflood lease.

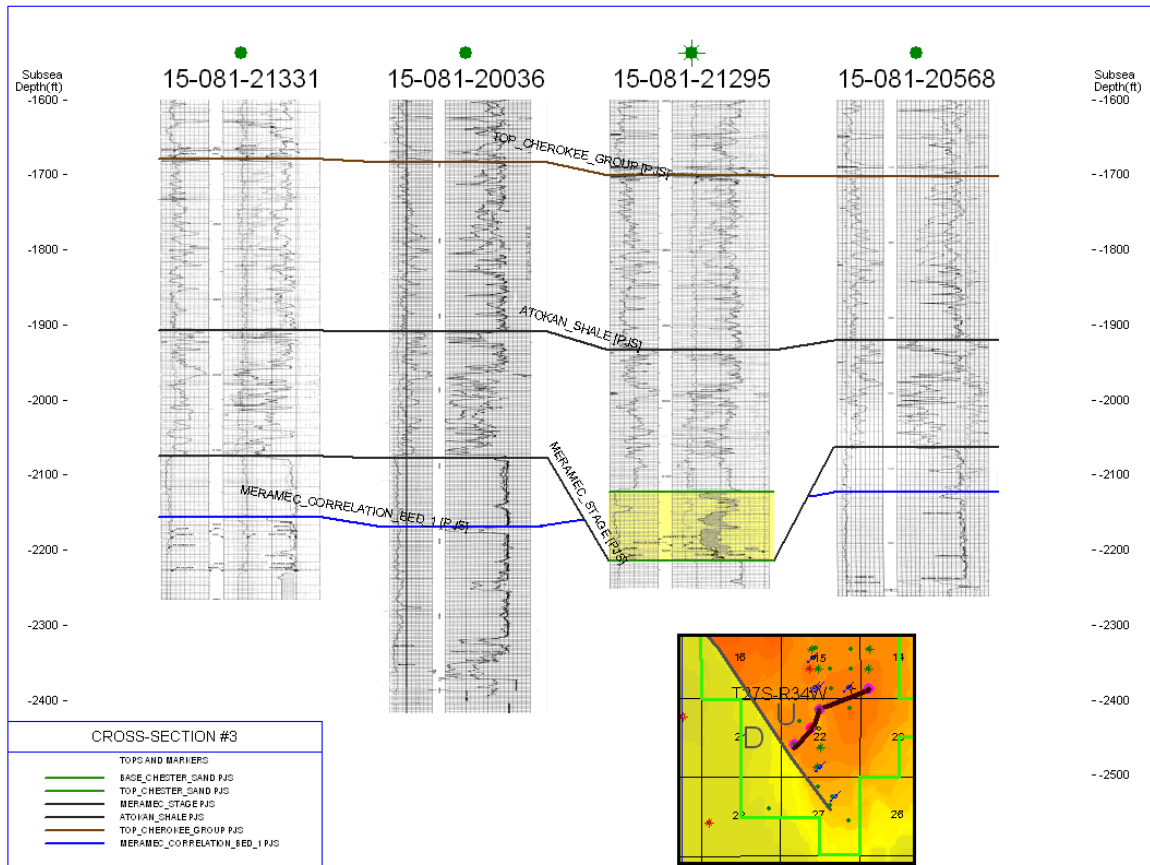


Fig. 10: Cross-section showing distinct channel structure of Chesterian sandstone (highlighted yellow) OXY's Pleasant Prairie Chester Unit.

The sandstone reservoir rock is described in geologist's logs as fine to very-fine grained, sub-angular, well sorted, and moderately friable with calcareous cement and intergranular porosity (e.g. OXY's Moody D #1, 15-081-21254, by Craig Corbett, accessed at [www.kgs.ku.edu](http://www.kgs.ku.edu)). Color is variously described in geologist's logs as tan, gray, white, and frosty (e.g. OXY's Schuh A #1, 15-081-21306, by Craig Corbett, accessed at [www.kgs.ku.edu](http://www.kgs.ku.edu)). A typical log response and stratigraphic section through the reservoir shows a low gamma ray and neutron-density crossover characteristic of sandstone, with sharp boundaries above and below (Figure 11). The lower part of the sandstone body in Figure 11 appears to have streaks of clay, and the intensity of gamma radiation decreases slightly, but irregularly, upwards, suggesting somewhat less clay in the top of the bed.



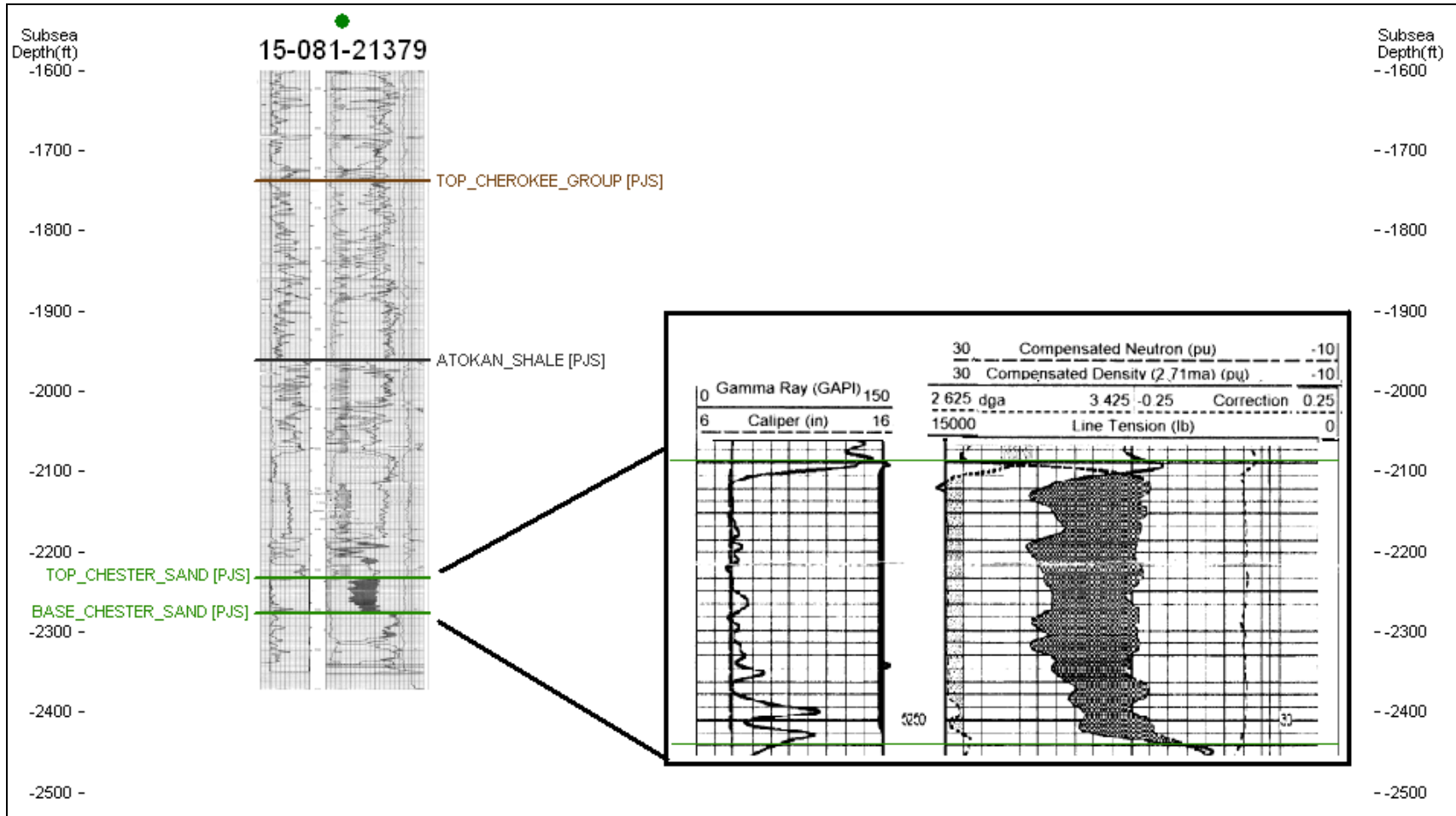


Fig. 11: Typical well log response through reservoir.

Regional tectonic deformation occurred during mid-Pennsylvanian time (Rascoe and Adler, 1983), and is likely responsible for the fact that the Chesterian shoestring sandstone in Pleasant Prairie oilfield appears to cut across a structurally higher nose of older Meramecian Stage rocks projecting to the southeast (Fig. 12). The fault which cuts across the southern end of the oilfield is also likely due to mid-Pennsylvanian tectonism.

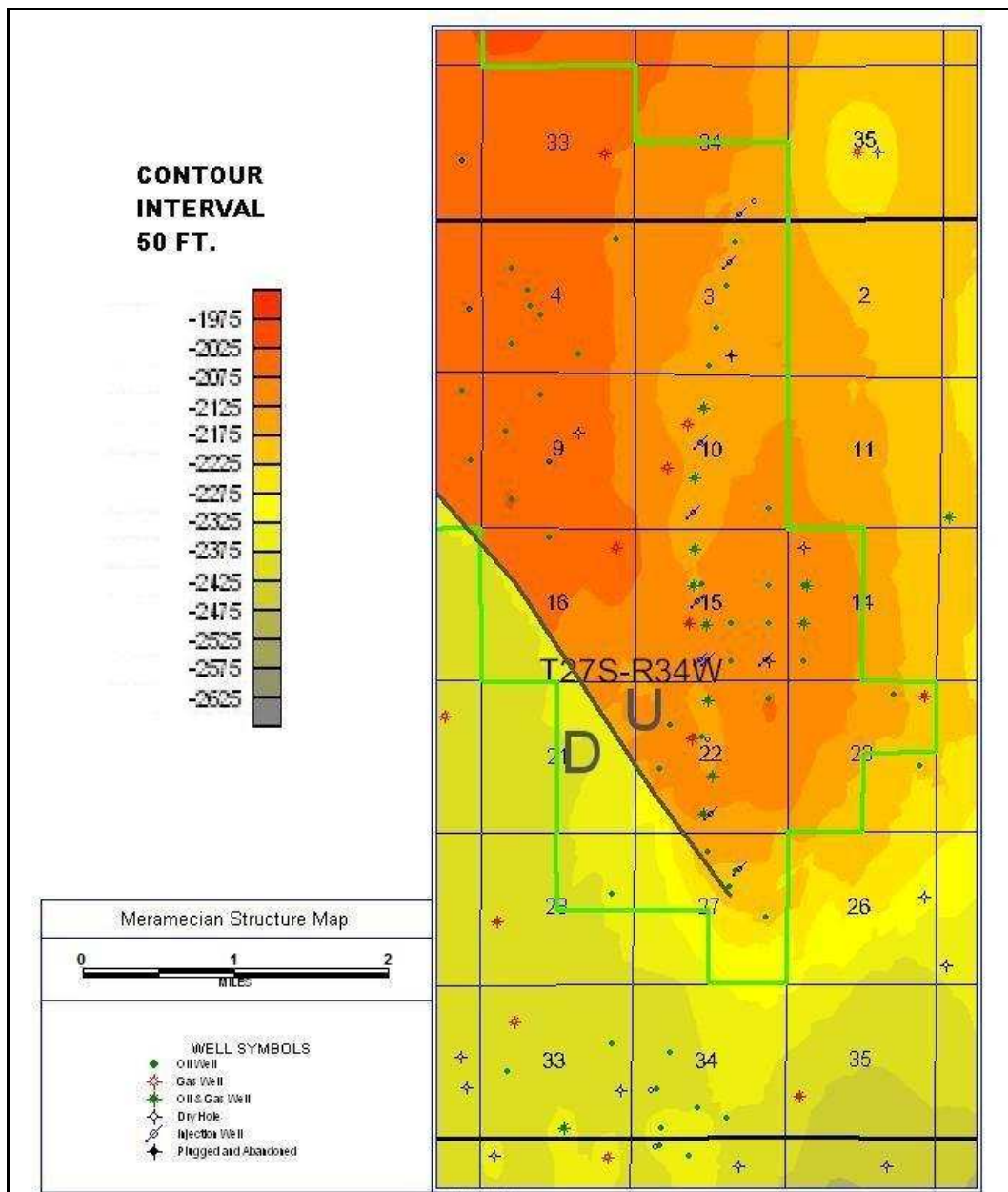


Fig. 12: Structure map of the top of the Meramecian Stage. The incised channel of Chesterian sandstone runs north-south through sections 3, 10, 15, and 22.

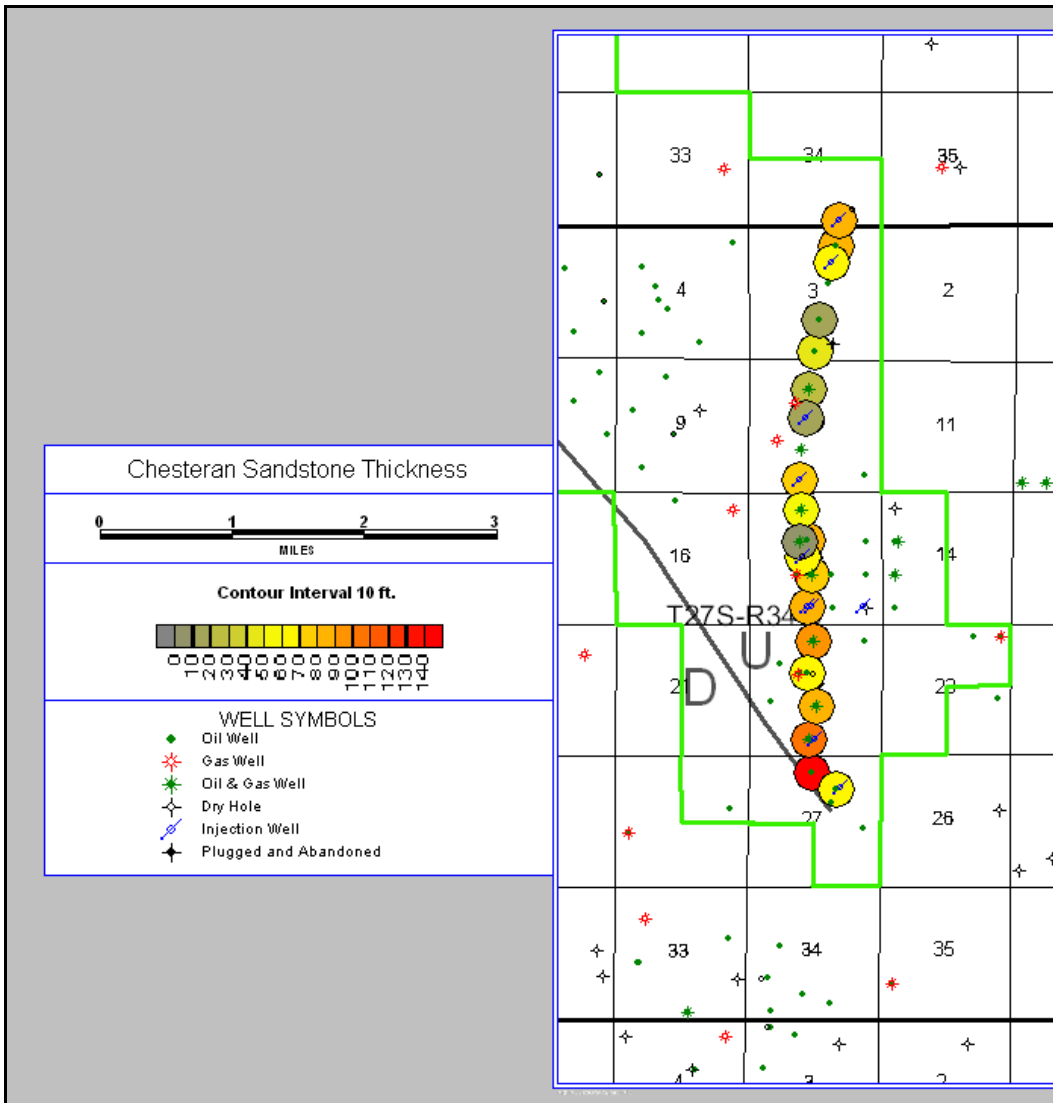
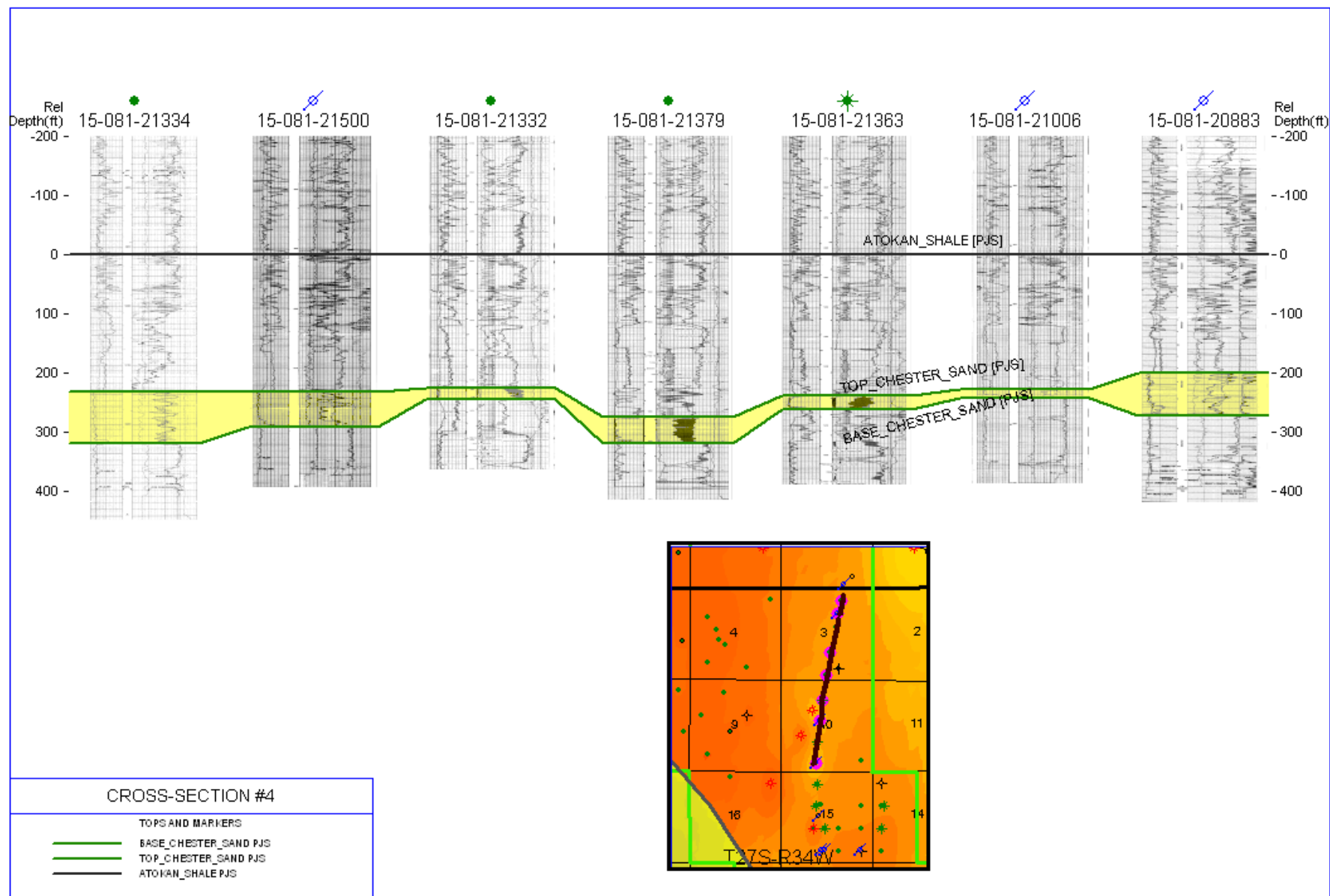


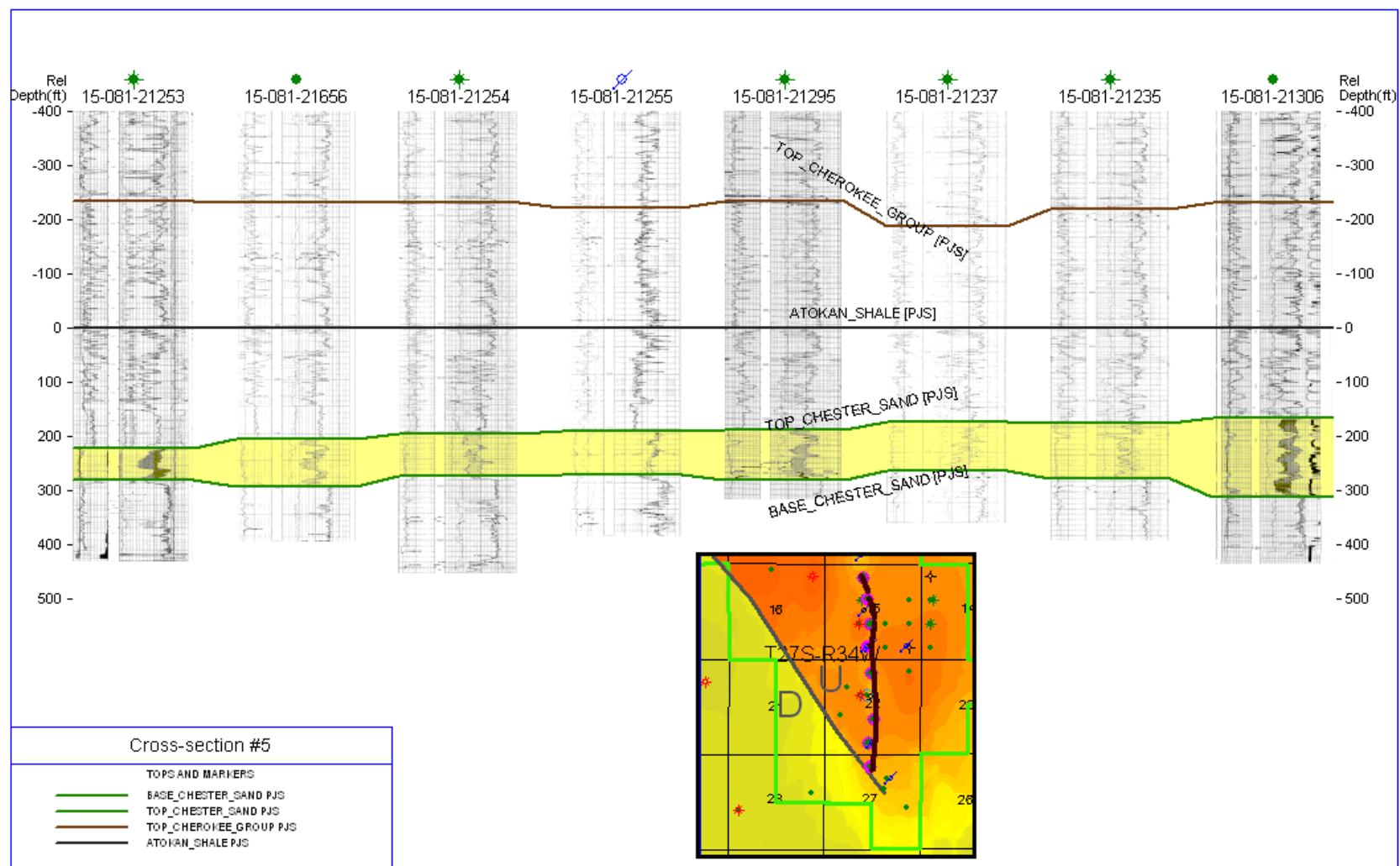
Fig. 13: Bubble map showing thickness of Chesterian sandstone. Thicknesses were measured from tops picked on available well logs.

The gross thickness of the sand in wells varies greatly (Figure 13). Some wells in the Chester Waterflood lease did not penetrate the thickest part of the channel (Figure 4), resulting in a longitudinal profile (Figure 14) with considerable variation in gross thickness of the sandstone. A longitudinal profile of the southern end of the channel (Figure 15) shows more consistent gross thickness of sandstone, with an overall trend of thickening to the south.



PETRA 4/12/2010 3:52:12 PM (channel\_xsec3 4-1-10.CSP)

Fig. 14: Longitudinal north-south stratigraphic cross-section through Chester Waterflood wells. Flattened on Atokan shale bed in attempt to show profile of channel closer to time of deposition.



PETRA 4/12/2010 4:03:20 PM (channel\_xss04-4-1-10.CSP)

Fig. 15: Longitudinal north-south stratigraphic cross-section through Pleasant Prairie Chester Unit wells. Flattened on Atokan shale bed in attempt to show profile of channel closer to time of deposition.

## **7. DATA AVAILABILITY**

Production data for both the Chester Waterflood and Pleasant Prairie Chester Unit are available online at the KGS website [www.kgs.ku.edu](http://www.kgs.ku.edu). OXY also provided their own production data, which confirmed and slightly modified that of the KGS. Both Cimarex and OXY provided maps of their respective leases, both of which are reproduced in this report. Well logs and completion reports are available online from the KGS, and OXY provided logs from several of their wells for use in this report.

## **8. TERTIARY RECOVERY SUITABILITY**

Because the reservoir is a channel sandstone, it is spatially compact and well defined. As such, it is a good candidate for chemical flooding: If the reservoir were extremely large, chemical flooding would take a longer time to be effective, and if the boundaries were nebulous the likelihood of success would be lower due to an increased possibility of injected chemicals not staying in the reservoir.

The successful implementation of waterflooding in both units and the fact that the reservoir is well explored further strengthens the candidacy of this channel-filling sandstone for a tertiary recovery demonstration. If waterflooding had been ineffective in the reservoir, then chemical flooding would not be likely to significantly enhance oil production either. Good well control throughout the reservoir means a greater ability to monitor the effectiveness of chemical flooding.

Figure 15 shows that the Chesterian sandstone from which the Pleasant Prairie Chester Unit and Chester Waterflood produce is a single body of rock. The reservoir is continuous across the lease boundary, which means communication of fluids between the leases exists. The important implication is that surfactant injection into one lease could impact production in both leases. The continuity of the reservoir across lease boundaries does not diminish its suitability for tertiary recovery, it only means more than one operator would be involved in any tertiary recovery project.

One important consideration not covered in this report is the amount of remaining reserves. This is important to consider because there must be sufficient oil in the reservoir to make a tertiary recovery project economically feasible. To explore this, estimates of original oil in place need to be made available for comparisons to cumulative production.

## **9. CONCLUSION**

The Chesterian sandstone reservoir in Pleasant Prairie oilfield is an elongate sandstone body deposited in a channel incised into underlying rocks during late Mississippian time. The reservoir resembles the incised-valley-fill sandstones in the overlying Morrowan Stage rocks, such as those in the Steward, Minneola, and Congdon oilfields. It is important to test whether Chesterian valley-fill rocks have similar facies and petrophysical properties. If they do, knowledge and experience from the Morrowan will apply to the Chesterian, and demonstration of the utility of chemical flooding in enhanced recovery activity in Pleasant Prairie oilfield will apply to Morrowan fields as well.

The Pleasant Prairie Chester Unit and Chester Waterflood are two leases of the same contiguous sandstone reservoir in the Pleasant Prairie oilfield. If a tertiary recovery program is implemented in one lease, it could affect the reservoir in the other lease. Waterflooding proved to be an effective method of recovering oil from the reservoir in both leases. Because it is well-defined spatially, has excellent well control throughout, and has demonstrated good response to waterflooding, the Chesterian sandstone in Pleasant Prairie oilfield merits serious consideration as a candidate for chemical flooding.

## **10. REFERENCES CITED**

- Cirilo, L. L., 2002, Transgressive estuarine fill of an incised paleovalley, Upper Mississippian Chesterian Series, Shuck field area, Seward County, Kansas: Unpublished M.S. thesis, University of Houston, Houston, TX, 194 p.
- Montgomery, S. L., and Morrison, E., 1999, South Eubank Field, Haskell County, Kansas: A Case of Field Redevelopment Using Subsurface Mapping and 3-D Seismic Data: AAPG Bulletin, v. 83, no. 3, p. 393-409.
- Rascoe B., and Adler F. J., 1983, Permo-Carboniferous hydrocarbon accumulations, mid-continent, U.S.A.: AAPG Bulletin, v. 67, no. 6, p.979-1001.
- Shonfelt, J. P., 1988, Geologic heterogeneities of a Chesterian sandstone reservoir, Kinney-Lower Chester field, Stevens and Seward counties, Kansas, and their affect on hydrocarbon production: Unpublished M.S. thesis, Wichita State University, Wichita, KS, 206 p.

# **TREMBLEY OILFIELD, RENO COUNTY, KANSAS**

Peter J Senior and Anthony W. Walton  
Department of Geology, The University of Kansas

## **1. INTRODUCTION**

Trembley oilfield is a small field that covers 560 acres in two sections in Reno County in central Kansas. The field was discovered in 1978, and production continues to the present. Berexco Inc. is the current operator. Trembley oilfield produces from the Hertha Limestone Formation of the Upper Pennsylvanian Kansas City Group at an average depth of 3491 feet. The OOIP has been estimated at 2,049,759 barrels. No water influx into the reservoir was apparent during primary production, indicating a fluid-expansion drive (Waterflood Feasibility Study, 1989). This report provides a summary of information on the field location, drilling and production history, geology, and suitability for enhanced recovery.

## **2. LOCATION**

Trembley oilfield lies approximately sixty miles northwest of Wichita and twenty miles southwest of Hutchinson (Figure 1). The small town of Arlington lies just to the southeast, and the north fork of the Ninnescah River flows through the field. Figure 2 shows the Trembley field in relation to surrounding fields. The defined field occupies the SW quarter of Section 27 and in Section 34, it occupies the west half of the section, plus the west half of the NE quarter (Kansas Geological Survey (KGS) website, <http://www.kgs.ku.edu/>, 7/17/10). The Trembley Unit, operated by Berexco, encompasses 800 acres: all of the Trembley field, plus the rest of Section 34 (Figure 2, 3). Documents limit the effective area of the waterflood to the SESW Section 27 and the E/2 NW and SWSWNE Section 34, T24SR8W, with a total area of 148 acres with greater than 4' of net pay thickness (CO<sub>2</sub> EOR Demonstration Proposal, 1999).

## **3. METHODS**

This report was constructed by analyzing data in the public domain and posted on the website of the Kansas Geological Survey (KGS) along with that provided by the field operators directly to the investigators. The major methods were use of well logs to determine the



configuration of key horizons to create geologic maps and cross-sections of the reservoir. The data and logs were imported into Petra™, a subsurface GIS program and analyzed using standard techniques. Production history, quantities, and rates were provided by the operators or downloaded from the website of the KGS.



Fig. 1: Regional map indicating location of Trembley oilfield. Modified from [www.kgs.ku.edu](http://www.kgs.ku.edu) 5-5-2010.

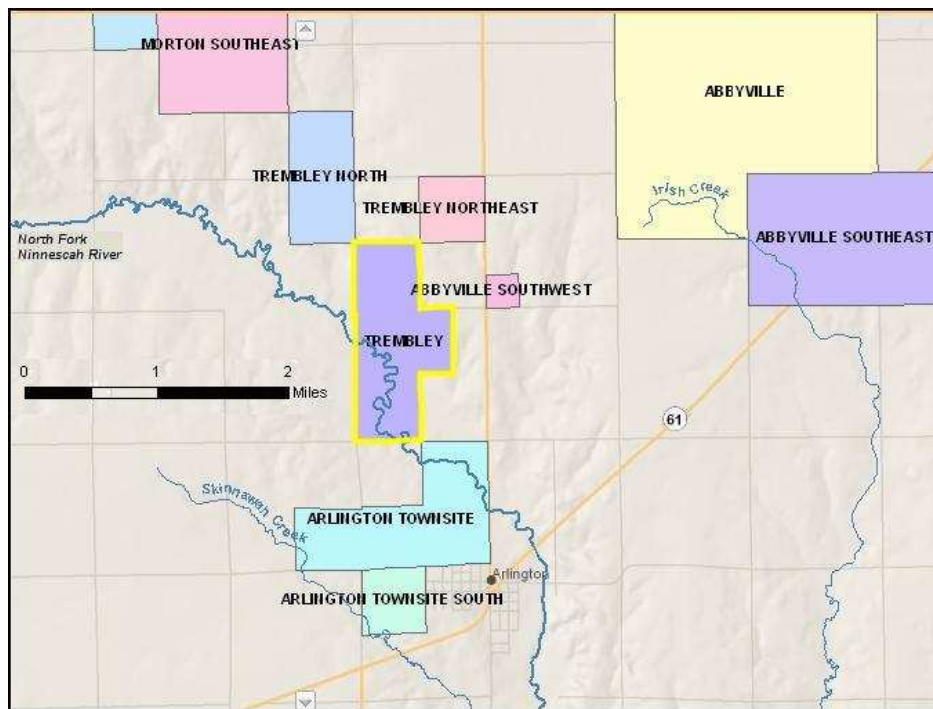


Fig. 2: Sub-regional locator map for Trembley oilfield, from [www.kgs.ku.edu](http://www.kgs.ku.edu) 5-5-2010.

#### **4. DISCOVERY & DEVELOPMENT HISTORY**

Discovery of the field occurred with completion of the Trembley #1 well (API # 15-155-20477) in February 1978 by National Cooperative Refinery Association (NCRA). The discovery well was tested at 192 BOPD from perforations in the Hertha Limestone at 3482 to 3492 feet. Subsequent exploratory drilling in 1978 saw completion of four new producing wells and three dry holes. Development drilling in the Trembley field in 1979 resulted in one new oil well and three more dry holes. The decade of the 1980s saw one oil well completed in 1982 and dry holes drilled in 1983 and 1984. In 1993 a dry hole was drilled, and in October of 1999 one new oil well was completed. Since 1999 no new wells have been drilled.

An older well was recompleted in 1999: the Trembley Unit 'X' 9 (API # 15-155-20582-0001) was originally the Barnes 3 well, a dry hole that was drilled as a step-out from the nearby Abbyville Southwest field (Table 1). The result of over twenty years of development drilling, from 1978 to 1999, has been a good definition of the spatial extent of the reservoir; dry holes delineate the area within which productive reservoir rock is found, especially around the northern part of the field (Figure 3).

#### **5. PRODUCTION HISTORY**

Over three decades of oil production from Trembley oilfield, 1978 to 2010, have resulted in a cumulative total of 528,340 barrels of oil produced (Table 2 and Figure 4), or 25.8% of the OOIP reported in the Waterflood Feasibility Study (1989). The primary phase of production lasted from discovery in 1978 to February 1995, when waterflooding began. Primary recovery was initially highly successful, with annual production reaching 72,006 barrels from four wells in 1979, but production dropped rapidly to below 10,000 barrels per year by 1984. Annual production numbers continued to decline until 1995 when it hit a low point, with only 1,943 barrels. The secondary recovery phase has also proven highly successful. The reservoir showed a strong initial response to waterflooding, reaching an all-time high in annual oil production of 72,430 barrels in 1997. Two wells in the southern part of the field however, the Trembley Unit 'X' 6 and 'X' 7 (API # 15-

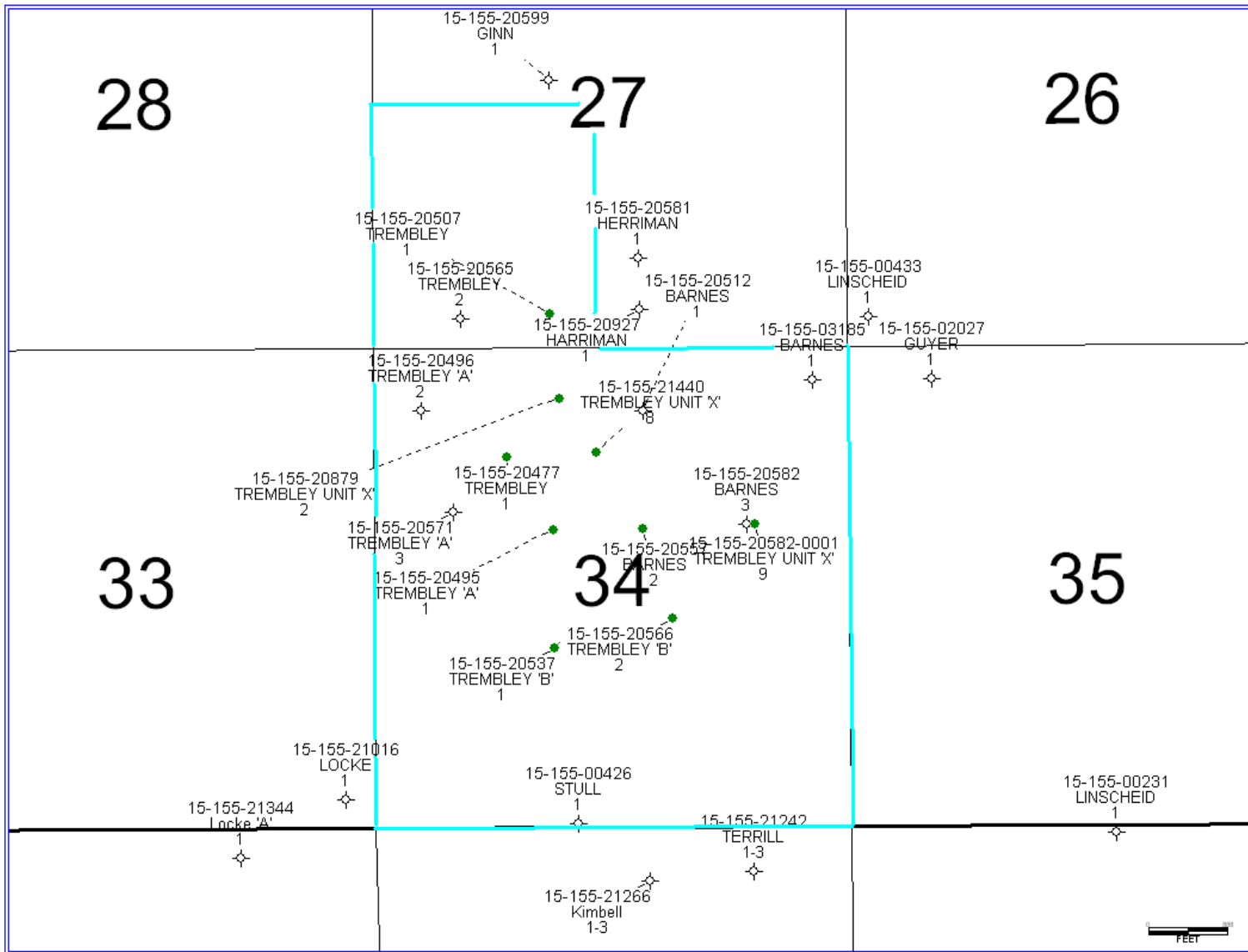


Fig. 3: Distribution of wells in and around Trembley oilfield. Blue outline shows approximate unit boundary.

Table 1: Wells in Trembley oilfield, from [www.kgs.ku.edu](http://www.kgs.ku.edu) 5-5-10. Wells in Berexco's Trembley Unit are highlighted. In yellow

API NUMBER	LEASE & WELL #	SECTION-TOWNSHIP-RANGE	SPOT	ORIGINAL OPERATOR	COMPLETION	PLUG DATE	TYPE	STATUS
15-155-20477	TREMBLEY 1 TREMBLEY UNIT 'X' 3	34-24S-8W	SW SW NE NW	National Cooperative Refinery Association (NCRA)	23-Feb-78		OIL	Producing
15-155-20495 ****CORED**** 15-155-20495-0001	TREMBLEY 'A' 1 TREMBLEY UNIT 'X' 4	34-24S-8W	C SE NW	NCRA Berexco, Inc.	10-May-78	5-Feb-90	OIL- P&A EOR	Converted to EOR Well Authorized Injection Well
15-155-20496 ****CORED****	TREMBLEY 'A' 2	34-24S-8W	E2 W2 NW NW	NCRA	21-Apr-78	18-Apr-78	D&A	Plugged and Abandoned
15-155-20507	TREMBLEY UNIT 'X' 1	27-24S-8W	S2 SE SW	HINKLE OIL CO.	12-Jul-78		OIL	Producing
15-155-20512	BARNES 1	34-24S-8W	W2 NW NE	NCRA	23-May-78	12-May-78	D&A	P&A
15-155-20537 15-155-20537-0001	TREMBLEY 'B' 1 TREMBLEY UNIT 'X'6	34-24S-8W	C NE SW	NCRA Berexco, Inc.	25-Sep-78	12-Dec-08	OIL EOR	Converted to EOR Well P&A
15-155-20557 15-155-20557-0001	BARNES 2 Trembley Unit 'X'5	34-24S-8W	W2 SW NE	NCRA Berexco Inc.	14-Dec-78		OIL EOR	Converted to EOR Well Authorized Injection Well
15-155-20565	TREMBLEY 2	27-24S-8W	SE SW SW	HINKLE OIL & NCRA	18-Dec-78	18-Dec-78	D&A	Plugged and Abandoned
15-155-20566 ****CORED**** 15-155-20566-0001	TREMBLEY 'B' 2 TREMBLEY UNIT 'X'7	34-24S-8W	W2 NE NW SE	NCRA Berexco, Inc.	29-Mar-79		OIL EOR	Converted to EOR Well Authorized Injection Well
15-155-20571 ****CORED****	TREMBLEY 'A'3	34-24S-8W	SW NE SW NW	NCRA	27-Feb-79	27-Feb-79	D&A	Plugged and Abandoned
15-155-20599	GINN 1	27-24S-8W	S2 SE NW	L G STEPHENSON & CO., INC.	16-Jul-79	16-Jul-79	D&A	Plugged and Abandoned
15-155-20581	HERRIMAN 1	27-24S-8W	NW SW SE	NCRA	22-Jul-79	22-Jul-79	D&A	P&A
15-155-20879 15-155-20879-0001	TREMBLEY UNIT 'X' 2	34-24S-8W	NE NE NW	NCRA Berexco, Inc.	14-Jul-82		OIL EOR	Converted to EOR Well Authorized Injection Well
15-155-20927	HARRIMAN 1	27-24S-8W	SW SW SE	QUIVERA EXPL	21-Feb-83	21-Feb-83	D&A	P&A
15-155-21016	LOCKE 1	33-24S-8W	SE SE SE	MALLONEE- WARREN LTD	23-Sep-84	23-Sep-84	D&A	Plugged and Abandoned
15-155-21266	Kimbell 1-3	3-24S-8W	SE NW NW NE	Stelbar Oil Co.	1-Jul-93	1-Jul-93	D&A	P&A
15-155-21440	TREMBLEY UNIT 'X'8	34-24S-8W	SE SE NE NW	BEREXCO INC	13-Oct-99		OIL	Producing
15-155-20582-0001	TREMBLEY UNIT 'X' 9	34-24S-8W	W2 SE NE	BEREXCO INC.	16-Oct-99		OIL	Producing
15-155-01019-0001	FOSTER 2	27-24S-8W	NE NE NE	HONEY OIL CO., INC.		13-Dec-01	SWD	P&A
15-155-19028-0001	TREMBLEY 'X' 3	34-24S-8W	SESENWNE	Berexco, Inc.	1-Dec-55		OIL	Producing

Table 2: Annual and cumulative oil production data, from [www.kgs.ku.edu](http://www.kgs.ku.edu), 5-5-10. 2008 is the most recent year for which complete data were available.

Year	Oil			Year	Oil		
	Production (bbls)	Wells	Cumulative (bbls)		Production (bbls)	Wells	Cumulative (bbls)
1978	60,233	4	60,233	1995	1,943	5	284,854
1979	72,009	4	132,242	1996	2,274	6	287,128
1980	41,367	4	173,609	1997	72,430	6	359,558
1981	23,812	4	197,421	1998	45,799	6	405,357
1982	17,889	5	215,310	1999	33,545	6	438,902
1983	13,511	5	228,821	2000	29,404	6	468,306
1984	9,916	5	238,737	2001	15,512	6	483,818
1985	8,197	5	246,934	2002	10,271	6	494,089
1986	6,131	5	253,065	2003	9,269	6	503,358
1987	5,465	5	258,530	2004	6,536	6	509,894
1988	5,191	5	263,721	2005	4,961	6	514,855
1989	4,383	5	268,104	2006	4,844	5	519,699
1990	3,975	5	272,079	2007	4,714	4	524,413
1991	3,071	5	275,150	2008	3,927	4	528,340
1992	2,814	5	277,964	2009*	3,406	4	531,746
1993	2,222	5	280,186	2010	170	4	531,916
1994	2,725	5	282,911				

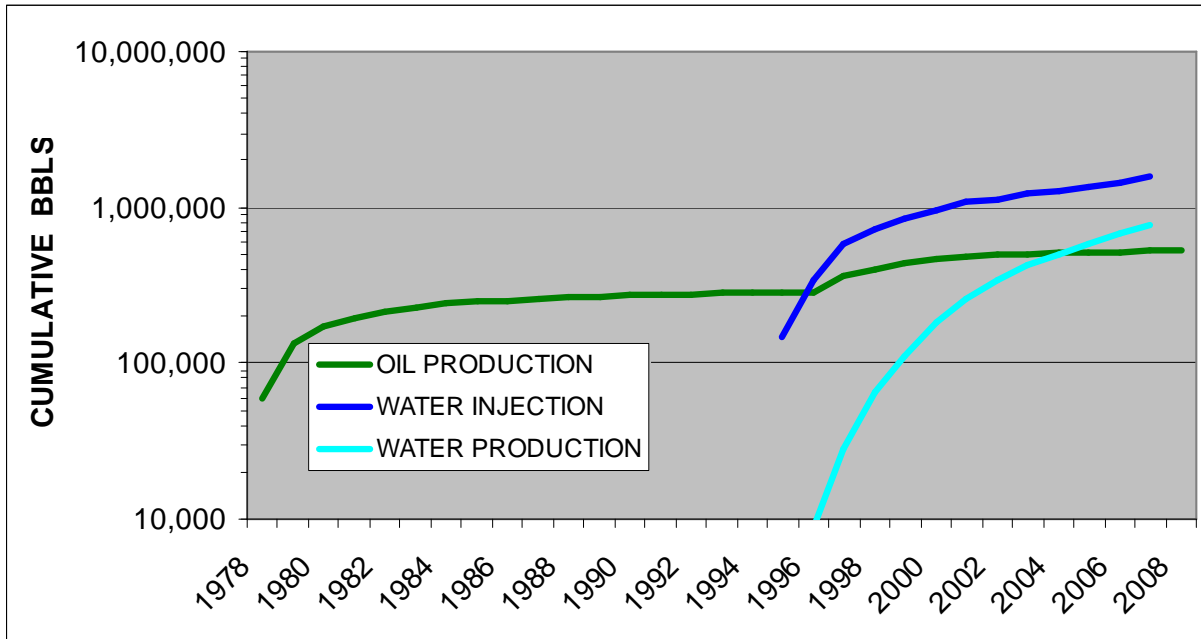


Fig. 4: Cumulative oil production and water injection for Trembley oilfield. Water injection and production data from the field operator, oil production data from the KGS.

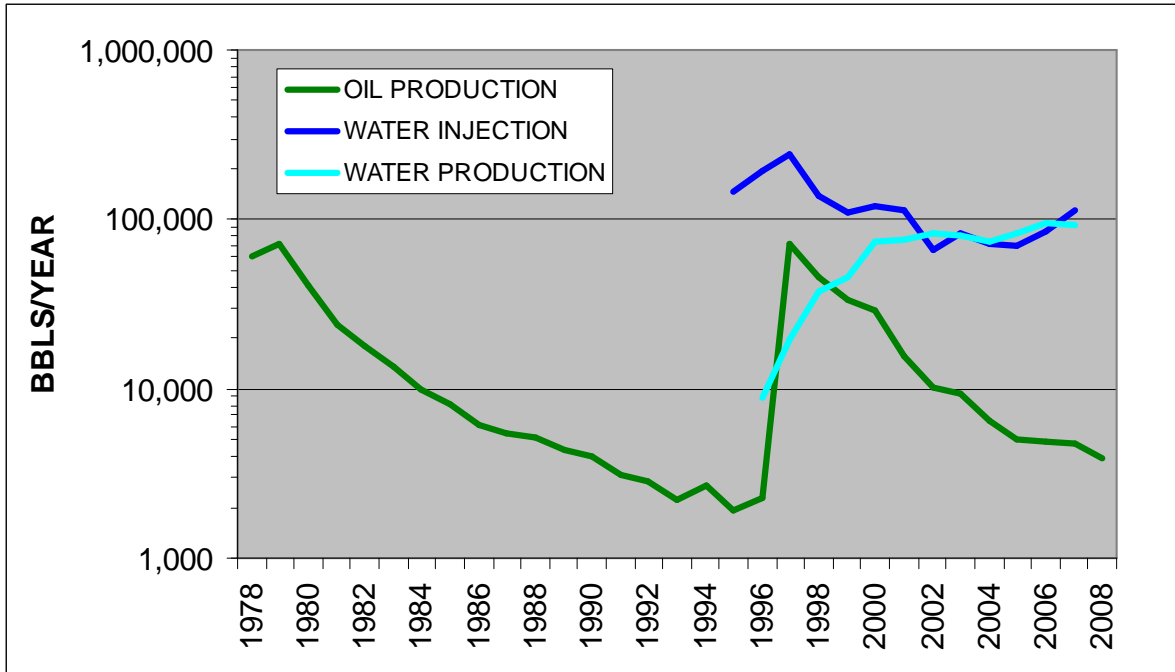


Fig. 5: Annual oil production and water injection for Trembley oilfield. Water injection and production data from the field operator, oil production data from the KGS.

155-20537 and 15-155-20566) have been abandoned due to poor performance. The Trembley 6X was temporarily abandoned in October 1999 and the 7X in April 2007 according to information provided by Berexco Inc. These wells apparently lie south of a permeability barrier in the field, which limits their communication with the wells to the north (CO<sub>2</sub> EOR Demonstration Proposal, 1999). Since 2001, annual production of water in the field has been close to annual injection, and annual oil production has tapered off continuously since 1997 (Figure 5), but still remains considerably higher than the previous low point.

## 6. GEOLOGY

The reservoir rock at the Trembley oilfield is the Hertha Limestone, the basal formation of the Upper Pennsylvanian Kansas City Group in Kansas (Figure 6). In the field area the Hertha is an oolitic limestone, with moldic porosity development resulting from diagenetic dissolution of ooids (Waterflood Feasibility Study, 1989). Connectivity between the moldic pores results in permeability in the reservoir. Figure 7 shows a typical well-log response of the Hertha at

Trembley oilfield. Neither the top of the Hertha Limestone nor the prominent markers of the Stark and Hushpuckney shale members have been picked in most of the wells used for mapping in this report. However, the Hertha Limestone is near the base of the Kansas City Group, so structural maps of that horizon are a close approximation of the structure of the Hertha Limestone (Figures 8 and 9).

A large dome-shaped structural high covers about nine sections in Township 24 South, Range 8 West and contains the Morton and Morton Southeast oilfields at its highest part; Trembley oilfield lies on the southeastern extension of this larger structure (Figure 8). The structural trend of Trembley is a southeast-plunging anticlinal nose (Figure 9) that shows good structural closure in three directions. Cross-sectional views through Trembley show that the structure is closed to the southwest and northeast (Figure 10), and to the southeast, but not to the northwest (Figure 11).

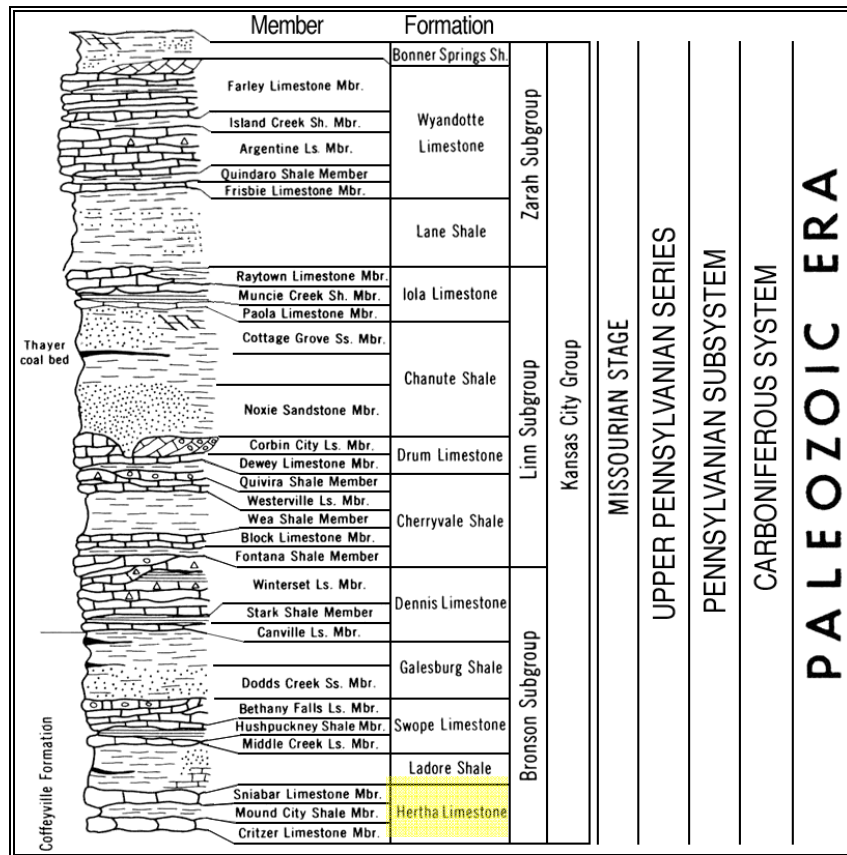


Fig. 6: Stratigraphy of the Upper Pennsylvanian Kansas City Group in Kansas, from , <http://www.kgs.ku.edu/PRS/petroDB.html>, 5-5-10.

COMPANY NATIONAL COOPERATIVE REFINERY ASSOCIATION  
 WELL TREMBLY #1 "A" T.D. LOGGED 3699'  
 FIELD T.D. DRILLER 3700'  
 COUNTY RENO STATE KANSAS T.D. WELEX 3700'

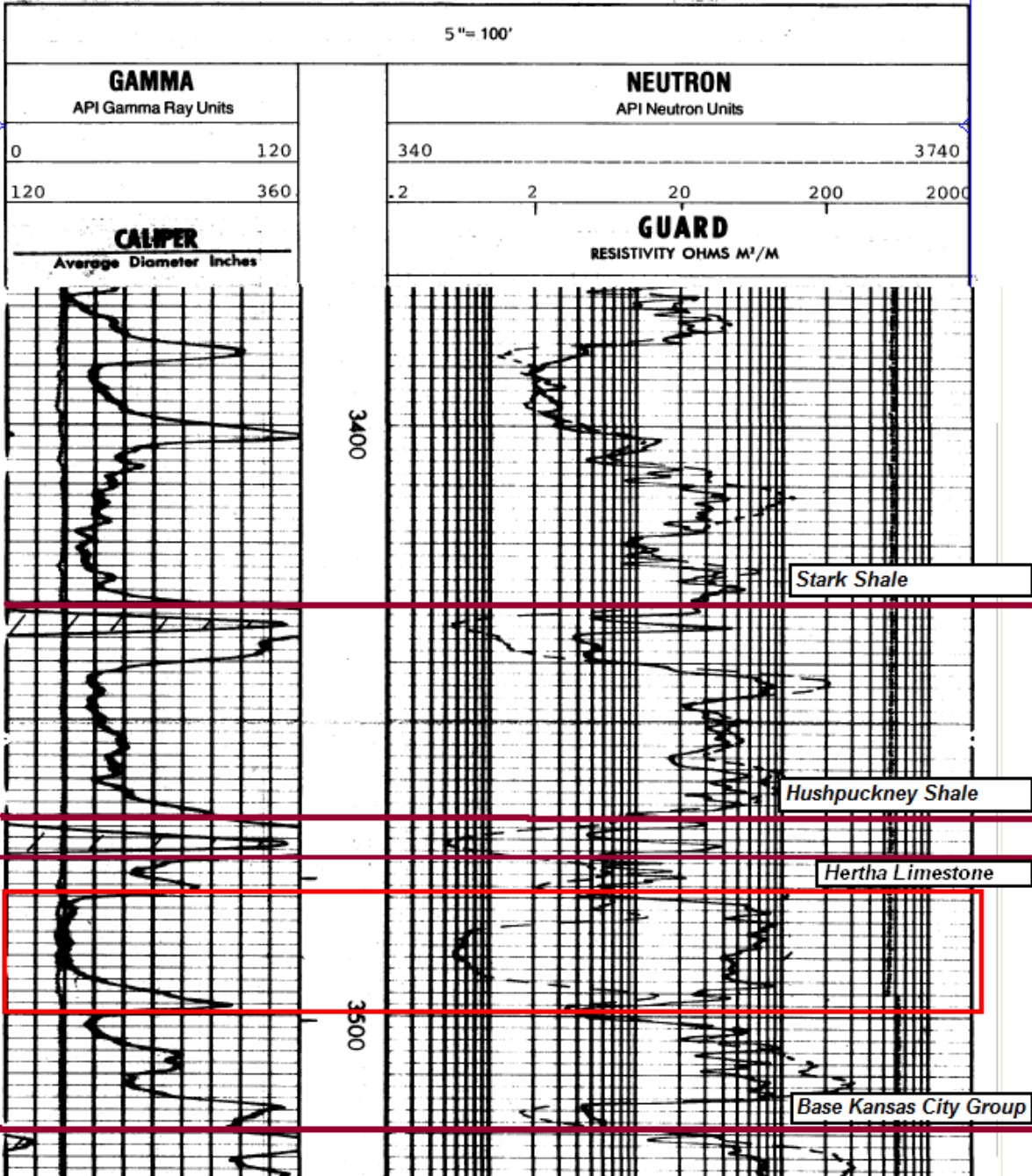


Fig. 7: Well-log showing gamma ray, neutron, and resistivity curves through the reservoir interval in the Hertha Limestone (red box) in the Trembley 'A' 1 well (API # 15-155-20495), <http://www.kgs.ku.edu/PRS/petroDB.html>.



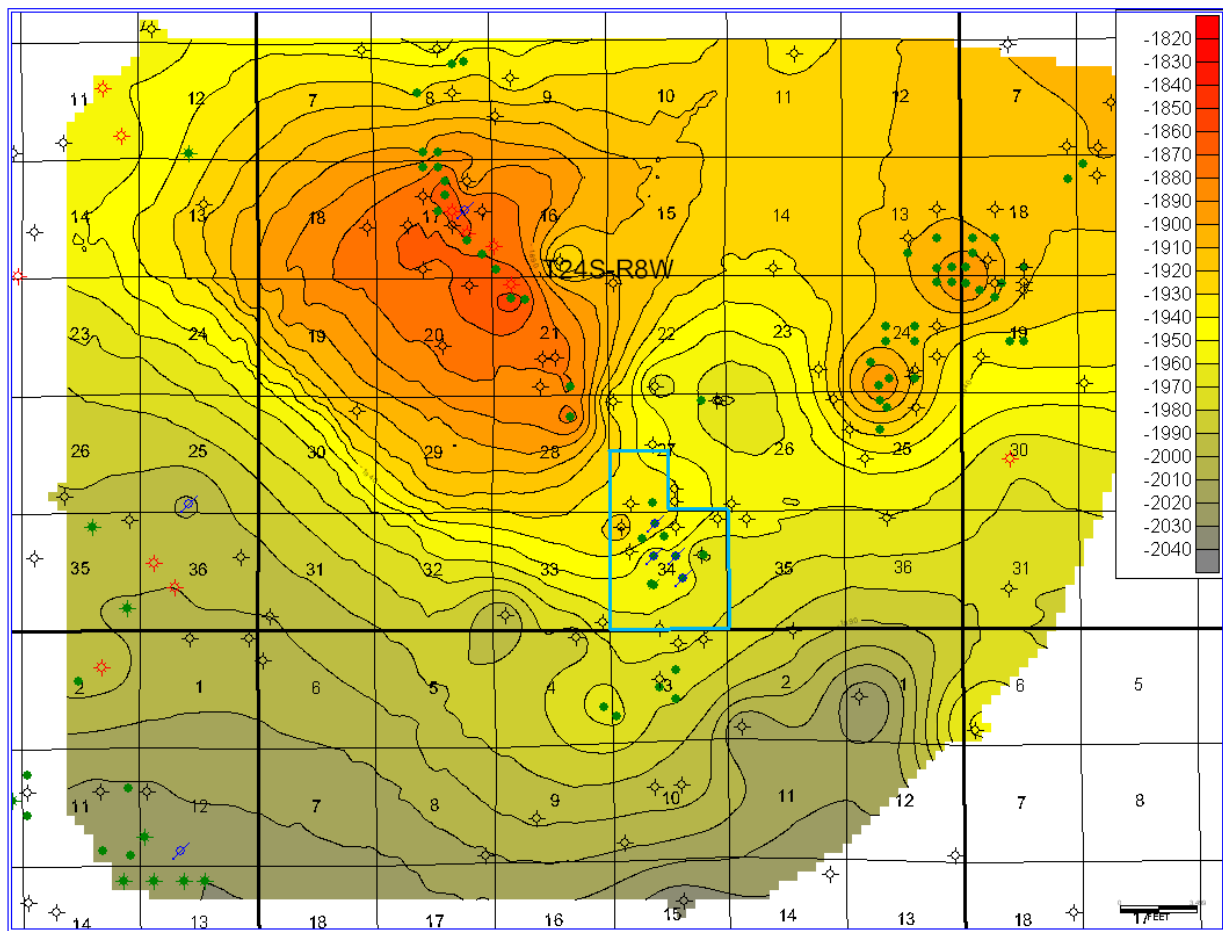


Fig. 8: Structure map of the base of the Kansas City Group in the Trembley field area. Elevation contours are given in feet; datum is sea level. Trembley unit outlined in blue. Trembley North, Morton Southeast, and Morton fields occupy the pronounced anticline centering in Sections 17, 21 and 28; Abbyville field occupies two domes to the NE of Trembley Field.

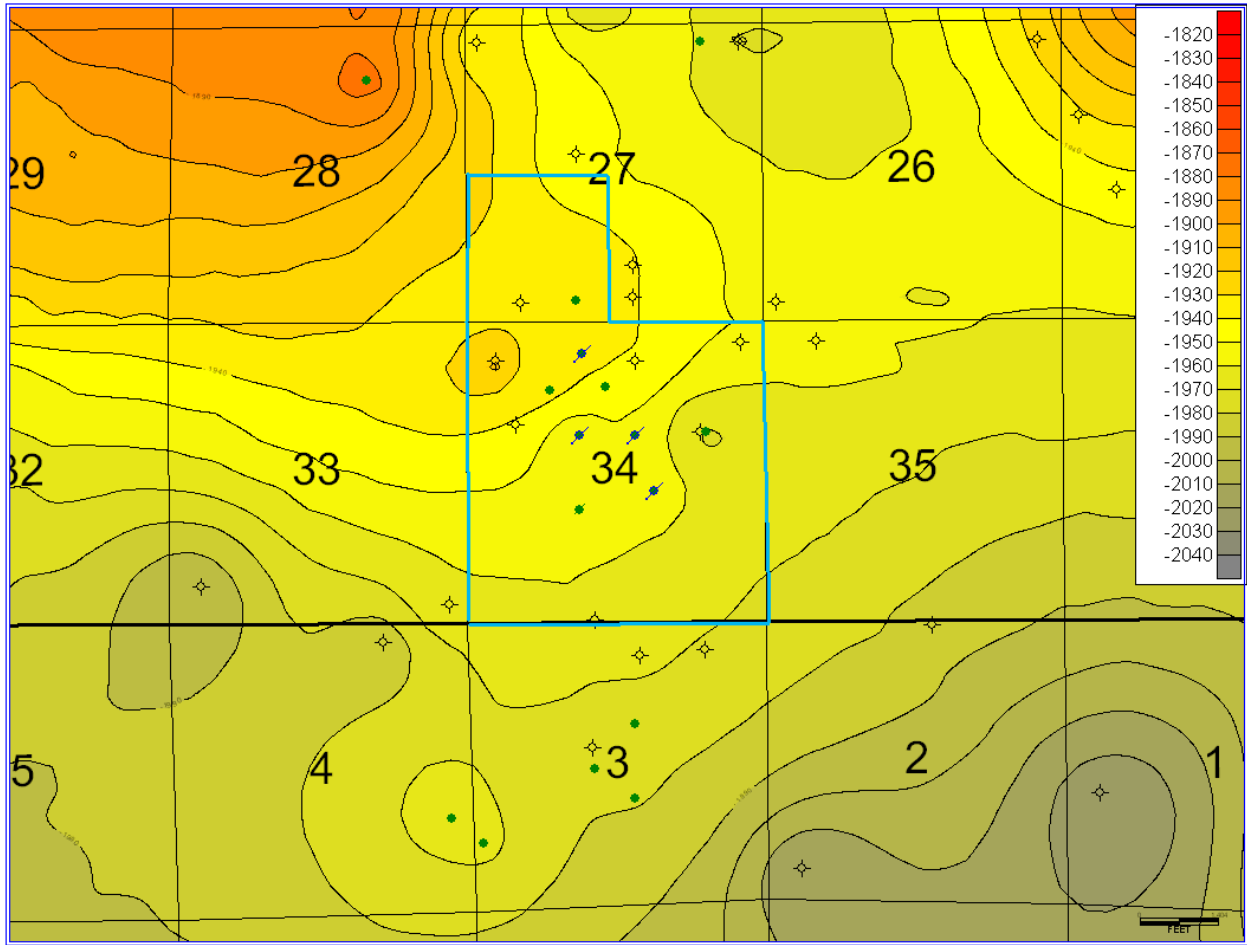


Fig. 9: Close-up view of structure map of the base of the Kansas City Group in the Trembley field area. Trembley unit outlined in blue. Elevation contours are given in feet below sea level.

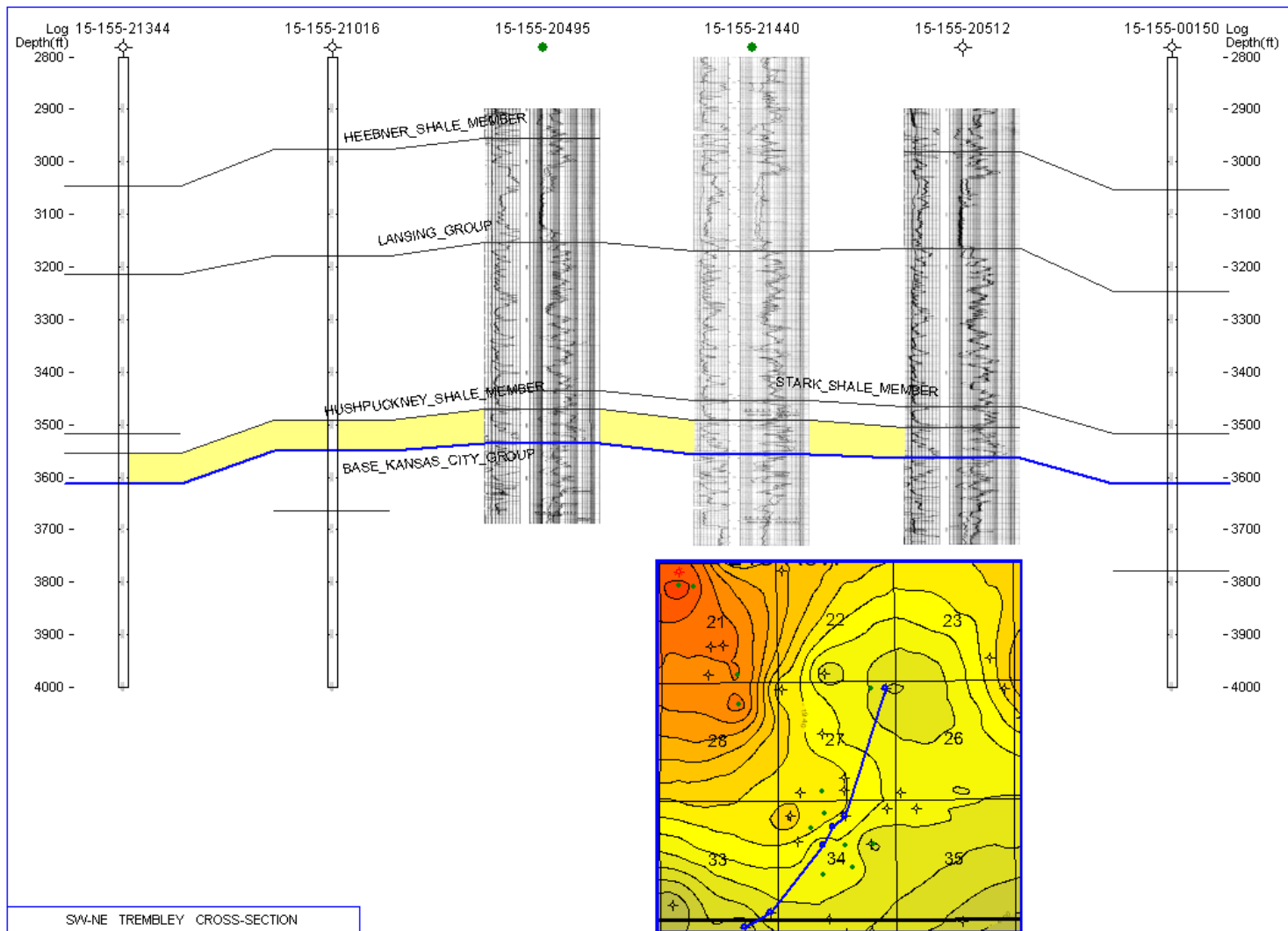


Fig. 10: Southwest-northeast cross-section through Trembley oilfield. Inset map shows location.

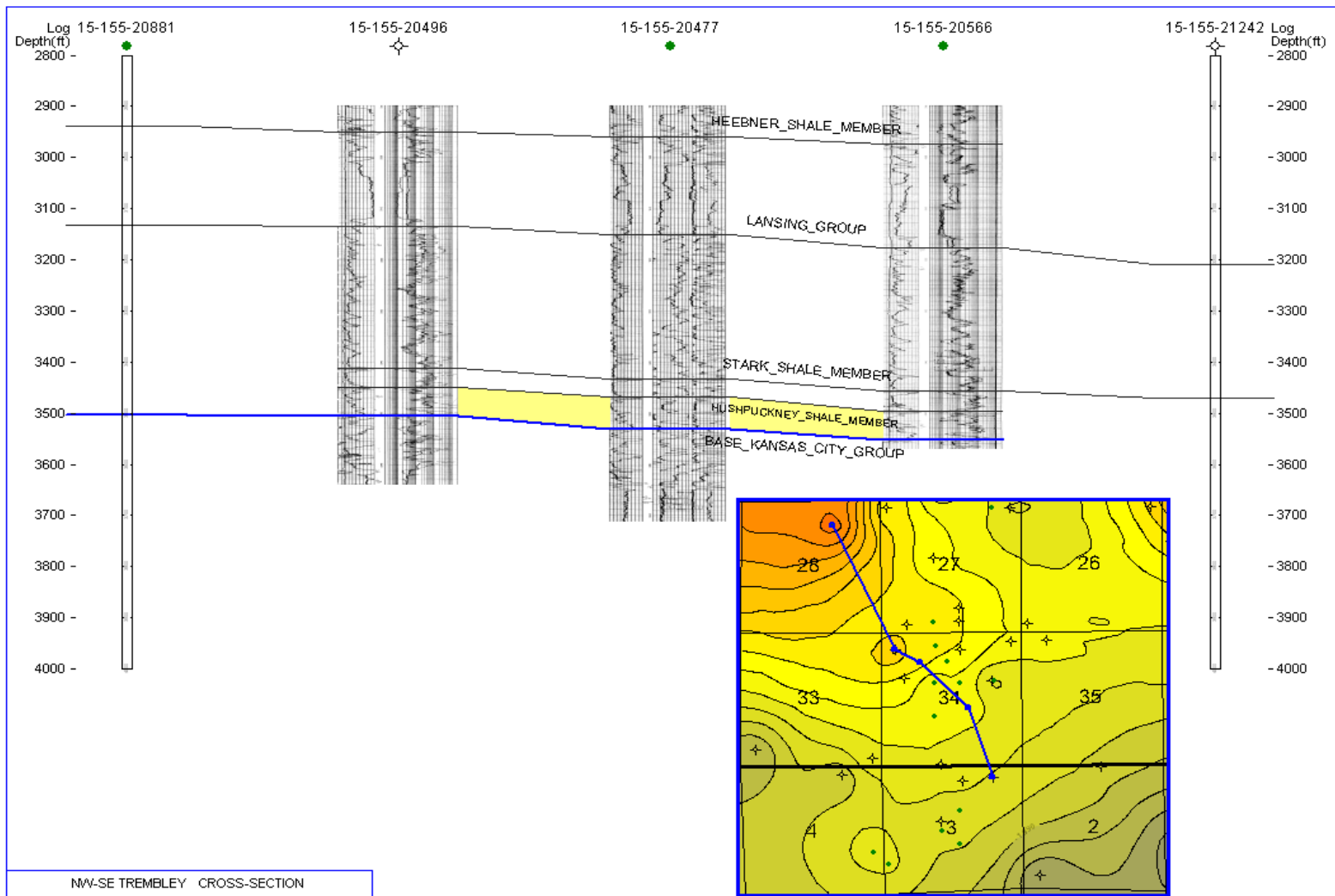


Fig. 11: Northwest-southeast cross-section through Trembley oilfield. Inset map shows location.

If the structural trap is open to the northwest, updip direction, then a stratigraphic effect must have prevented further migration of oil out of the field. A contour map of porosity (Figure 12) and a comparison of well logs (Figure 13) show how porosity pinches out around the reservoir. The porosity pinch-out is especially well constrained by dry holes in the north and northwest of the field. Stratigraphic pinch-out of porosity combines with a structural nose to create a combination anticlinal and stratigraphic trap.

The process of waterflooding in Trembley led to discovery of a permeability barrier in the southern part of the field during secondary recovery (Figure 12). Early in the waterflooding process two injectors, the Trembley 6X and 7X (API #s 15-155-20537-0001 and 15-155-20566-0001) built up pressure faster than expected. During the winter of 1996 a freeze-up stopped the water injection process, and neither well's shut-in pressure dropped appreciably, while other wells saw significant decreases (Berexco Inc. Interoffice Memo, 1996). This difference in pressure decrease indicated a lack of flow from the southern part of the field to the northern part, which could only be explained by some sort of permeability barrier in the reservoir. Due to the presence of this permeability barrier the 6X injection well was converted to a producer for a time before finally being plugged and abandoned in December of 2008. No data considered in preparing this report give any indication of further reservoir compartmentalization.

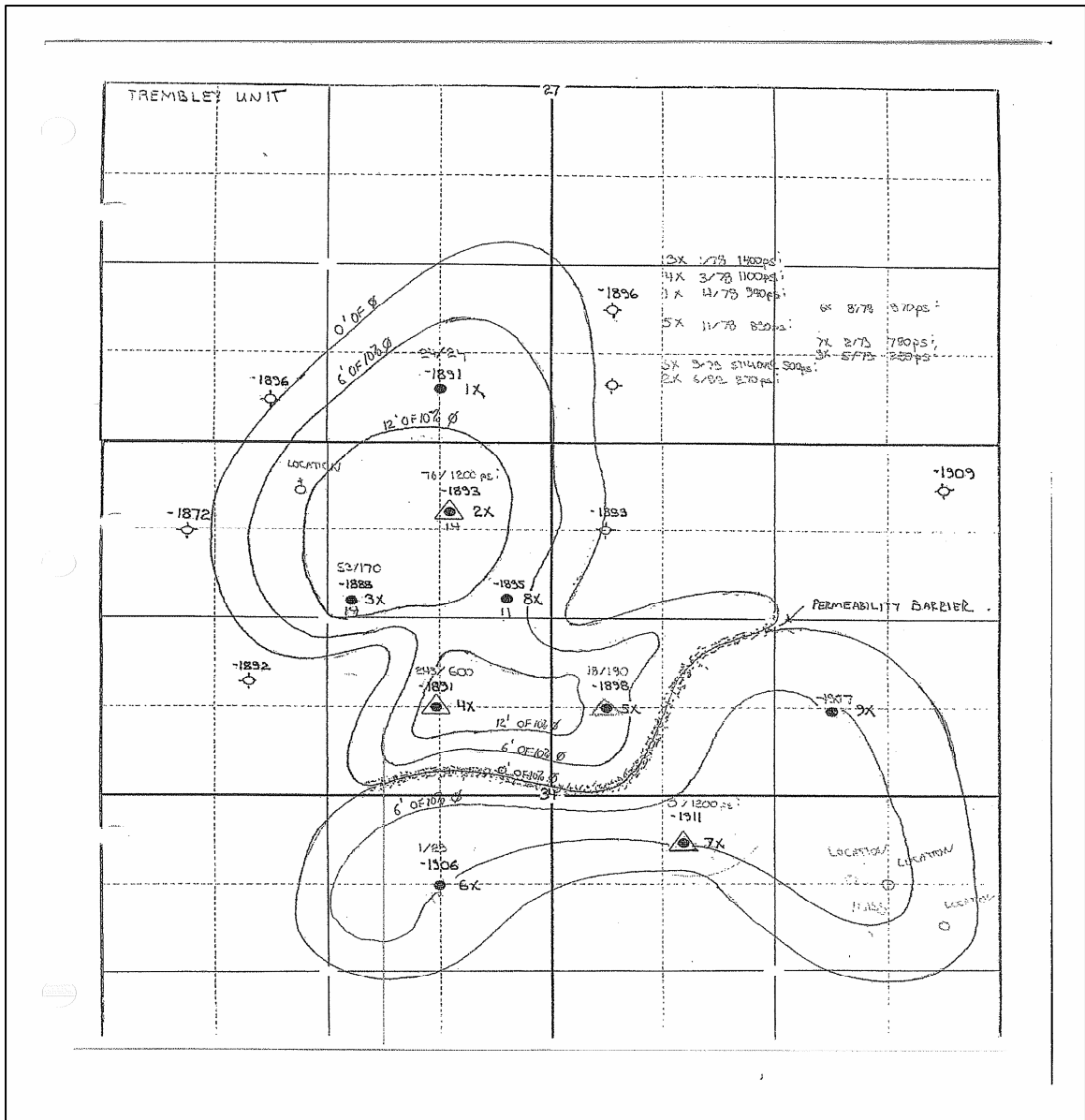


Fig. 12: Porosity isopach map of Trembley oilfield showing thickness of rock with porosity exceeding 10%. Note inferred permeability barrier; refer to text for discussion. Courtesy of Berexco Inc., contour interval of 6 ft.

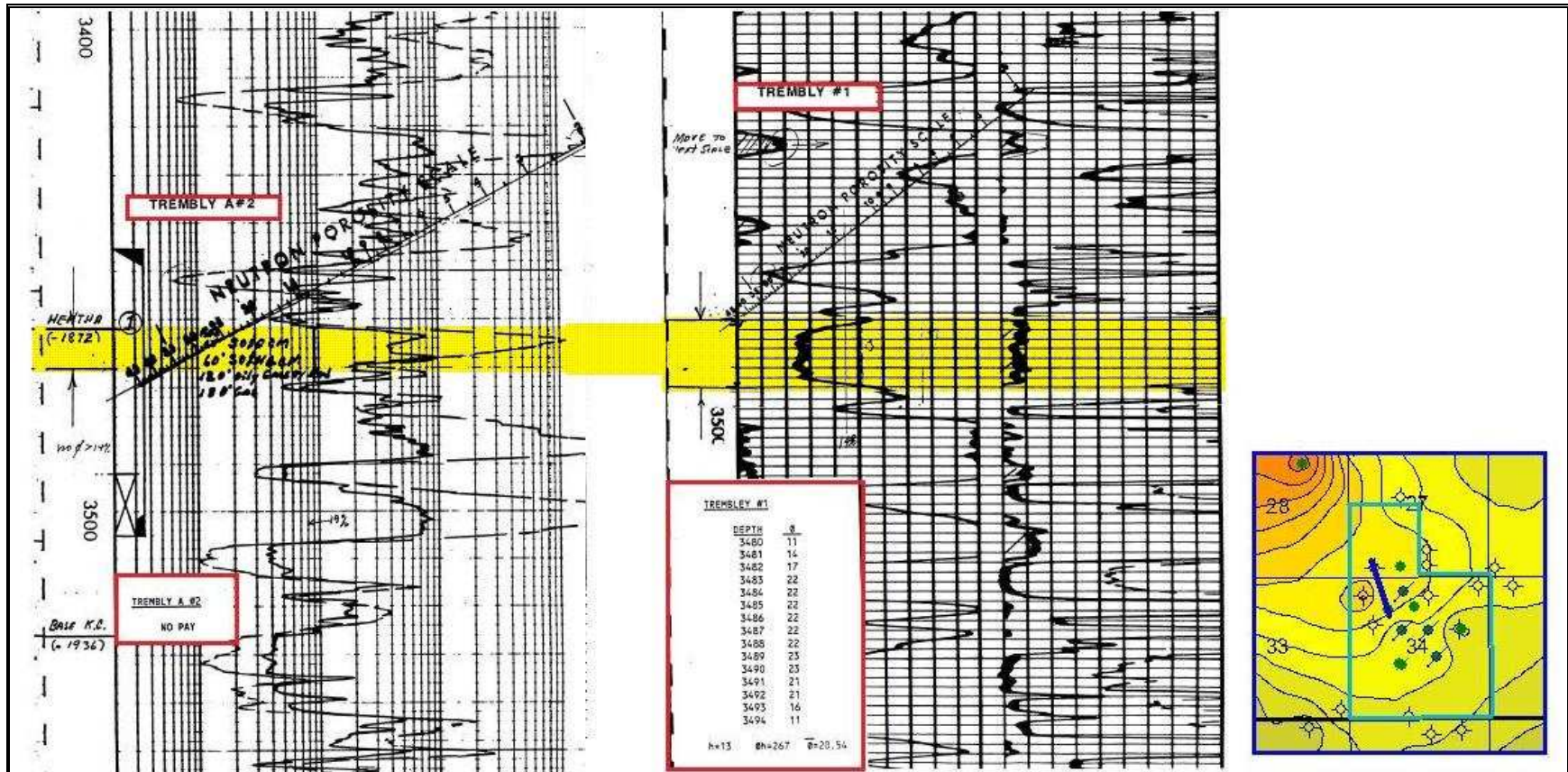


Fig. 13: Comparison of neutron and deep resistivity curves for well logs from the Trembley A#2 and Trembley #1 wells. Inset map shows positions of the two wells. Porosity in the Hertha Limestone pinches out to the northwest, where the Trembley A#2 well shows only 6 to 8% porosity and no pay, while the Trembley #1 to the southeast has 11 to 23% porosity.

## 7. PETROPHYSICS

Table 3 summarizes drill-stem test data were provided by Berexco Inc. Drill-stem tests were interpreted to show an initial reservoir pressure of 946 psig. For petrophysical calculations, initial reservoir temperature was 110° F, and a cementation factor of 2, and  $R_w$  of 0.4 were assumed (Waterflood Feasibility Study, 1989). Volumetric reservoir fluid parameters (Table 4), volumetric and pressure data (Tables 5 and 6), and viscosity data (Table 7) are available. Porosity-permeability relationships from core studies show wide scatter, little correlation, and substantial variation from well to well (Figures 14 and 15). For example in Figure 15 porosity of about 30% shows permeability ranging from just a few to almost 100 millidarcys. Carbonate reservoirs with oomoldic porosity, such as the Hertha Limestone at Trembley, can display great heterogeneity in porosity and permeability, sometimes over very short distances.

In 1980, Exoil Services of Golden, Colorado, ran tests on core samples to simulate flooding the reservoir with different fluids. Two-inch radial discs from cores were prepared by cold-flushing with hexane, drying and then saturating with produced water. Water was displaced with filtered lease crude in a series of injection pulses at elevated pressure and reservoir temperature. After injection with nitrogen to simulate primary production, tests were run to simulate flooding with water, polymer, and caustic-polymer by injecting each of these fluids into the core samples. Caustic-polymer flooding produced the lowest recovery, while waterflooding and polymer flooding recovered approximately equal amounts. Polymer flooding resulted in faster cumulative recovery of the same amount of oil than waterflooding (Waterflood Feasibility Study, 1989).



Well API# and Name	Depth	Remarks
15-155-20507 Trembley 1x	3460-3525	Rec. 3MCF gas, 60' mud, 790' MFO, 124-174, 1103, 331-399, 939
15-155-20879-0001 Trembley 2x	3500-3536	Rec. 60' GCM, 300' HGCM, 165' Froggy Oil, 95-95, 259, 122-109, 273
15-155-20477 Trembley 3x	3465-3500	GTS 12 min., 23.3MCFD, rec. 1800' oil, 118-247, 1421, 296-118, 1401
15-155-20495-0001 Trembley 4x	3469-3501	GTS 35 min., TSTM, rec. 315' OGCM, 310' gas, 310' oil & gas, 1191, 81, 97, 1111
15-155-20557-0001 Trembley 5x	3487-3510	GTS 15 min., rec. 540' HOGCM, 1560' oil
15-155-20537-0001 Trembley 6x	3480-3506	rec. 2950' gas, 110' MCO, 60'OGCM, 30' SOGCM
15-155-20566-0001 Trembley 7x	3488-3520	rec. 120' foamy oil, 60' SOGCM, 60' VHOGCM, FSIP 781psi
15-155-21440 Trembley 8x	3486-3510	rec. 255' CO, 120' GMCO; available at KGS website

Table 3: Summary of drill-stem tests done in eight Trembley wells; data provided by Berexco Inc.

PARAMETER	
SATURATION PRESSURE (BUBBLE POINT PRESSURE)	946 PSIG @ 110°F
SPECIFIC VOLUME AT SATURATION PRESSURE: (FT <sup>3</sup> / LB.)	0.02016 @ 110°F
THERMAL EXPANSION OF SATURATED OIL @ 2000 PSI	VOLUME @ 110°F / VOLUME @ 70°F = 1.01433
COMPRESSIBILITY OF SATURATED OIL AT RESERVOIR TEMPERATURE	FROM 2000 PSI TO 1700 PSI = $7.03 \times 10^{-4}$
	FROM 1700 PSI TO 1500 PSI = $7.36 \times 10^{-6}$
	FROM 1500 PSI TO 946 PSI = $7.64 \times 10^{-6}$

Table 4: Volumetric reservoir fluid parameters calculated from an oil sample from the Trembley #1 well (API # 15-155-20477) by Core Laboratories, Dallas, TX (Waterflood Feasibility Study, 1989).

PRESSURE (PSIG)	RELATIVE VOLUME: $V/V_{sat}$ in barrels at indicated pressure per barrel at saturation pressure (946 PSIG).	Y Function: $(P_{sat}-P)/(P_{abs})(V/V_{sat}-1)$
2000	0.9922	
1700	0.9943	
1500	0.9958	
1400	0.9965	
1300	0.9972	
1200	0.998	
1100	0.9987	
1000	0.9995	
946	1	
938	1.0015	
927	1.0038	
907	1.008	
887	1.0133	
845	1.0239	4.906
778	1.0453	4.682
702	1.0775	4.391
627	1.1208	4.113
545	1.1857	3.856
470	1.2723	3.604
405	1.3811	3.338
350	1.5116	3.192
284	1.7401	2.992
212	2.1663	2.772
155	2.8091	2.572
108	3.8831	2.363

Table 5: Pressure-Volume relations of oil sample from Trembley #1 well (API # 15-155-20477) at 110°F by Core Laboratories, Dallas, TX (Waterflood Feasibility Study, 1989).

DIFFERENTIAL VAPORIZATION @ 110°F							
PRESSURE (PSIG)	SOLUTION GAS/OIL RATIO (1)	RELATIVE OIL VOLUME (2)	RELATIVE TOTAL VOLUME (3)	OIL DENSITY GM/CC	DEVIATION FACTOR Z	GAS FORMATION VOLUME FACTOR(4)	INCREMENTAL GAS GRAVITY
946	192	1.104	1.104	0.7948			
800	177	1.099	1.147	0.7968	0.91	0.01793	0.798
650	160	1.093	1.216	0.7981	0.915	0.0221	0.787
500	141	1.087	1.352	0.7995	0.936	0.02919	0.762
350	118	1.079	1.631	0.8022	0.954	0.04195	0.744
200	90	1.068	2.379	0.8058	0.966	0.07215	0.768
95	62	1.056	4.375	0.8099	0.982	0.14336	0.885
0	0	1.023	3.357	0.8185			1.317
Gravity of Residual Oil: 37.3°API at 60°F							
1: Cubic feet of gas at 14.65 psia and 60°F per barrel of residual oil at 60°F							
2: Barrels of oil at indicated temperature and pressure per barrel of residual oil at 60°F							
3: Barrels of oil plus liberated gas at indicated temperature and pressure per barrel of residual oil at 60°F							
4: Cubic feet of gas at indicated pressure and temperature per cubic foot at 14.65 psia and 60°F							

Table 6: Differential vaporization data for oil sample from Trembley #1 well (API # 15-155-20477) by Core Laboratories, Dallas, TX (Waterflood Feasibility Study, 1989).

PRESSURE (PSIG)	OIL VISCOSITY (CENTIPOISE)	CALCULATED GAS VISCOSITY (CENTIPOISE)	OIL/GAS VISCOSITY RATIO
5000	2.38		
4000	2.17		
3000	1.96		
2000	1.74		
1700	1.68		
1500	1.63		
1100	1.55		
946	1.52		
800	1.54	0.0125	123.2
650	1.58	0.0121	130.6
500	1.64	0.0118	139
350	1.73	0.0116	149.1
200	1.86	0.0112	166.1
95	2	0.0106	188.7
0	2.57	0.009	285.6

Table 7: Viscosity data for oil sample from Trembley #1 well at 110° F (API # 15-155-20477) by Core Laboratories, Dallas, TX (Waterflood Feasibility Study, 1989).

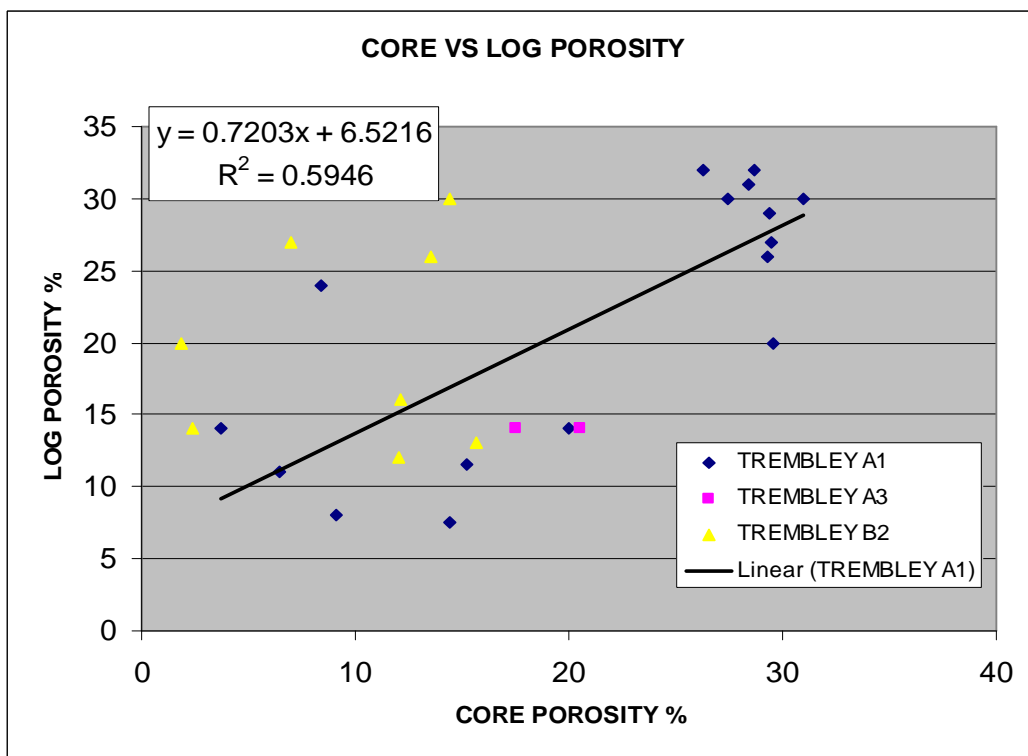
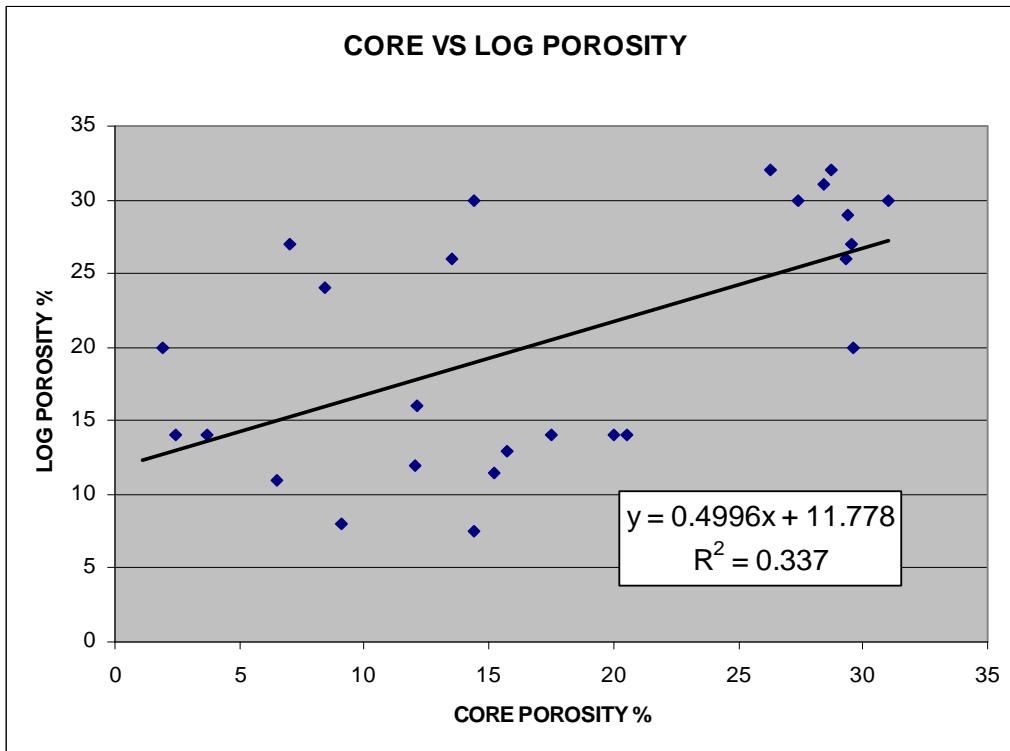


Fig. 14: Core versus log porosity for three cored wells in Trembley oilfield, reproduced from data generated by Core Laboratories, Dallas, TX (Waterflood Feasibility Study, 1989). Trendline in lower figure is for Trembley A1 well data points only.

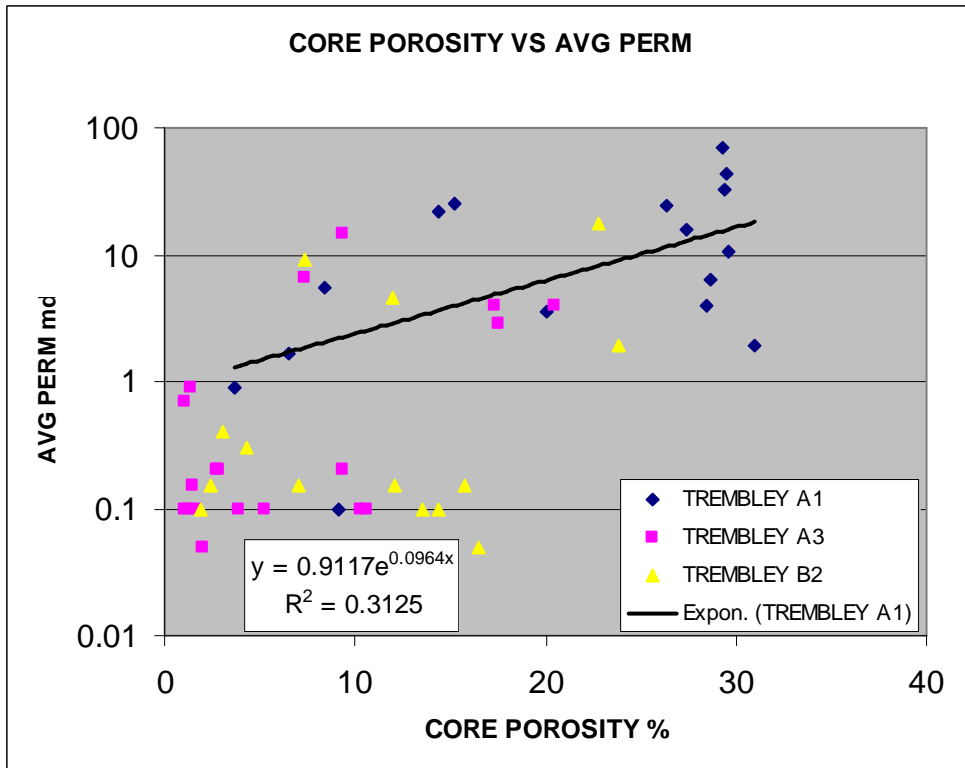
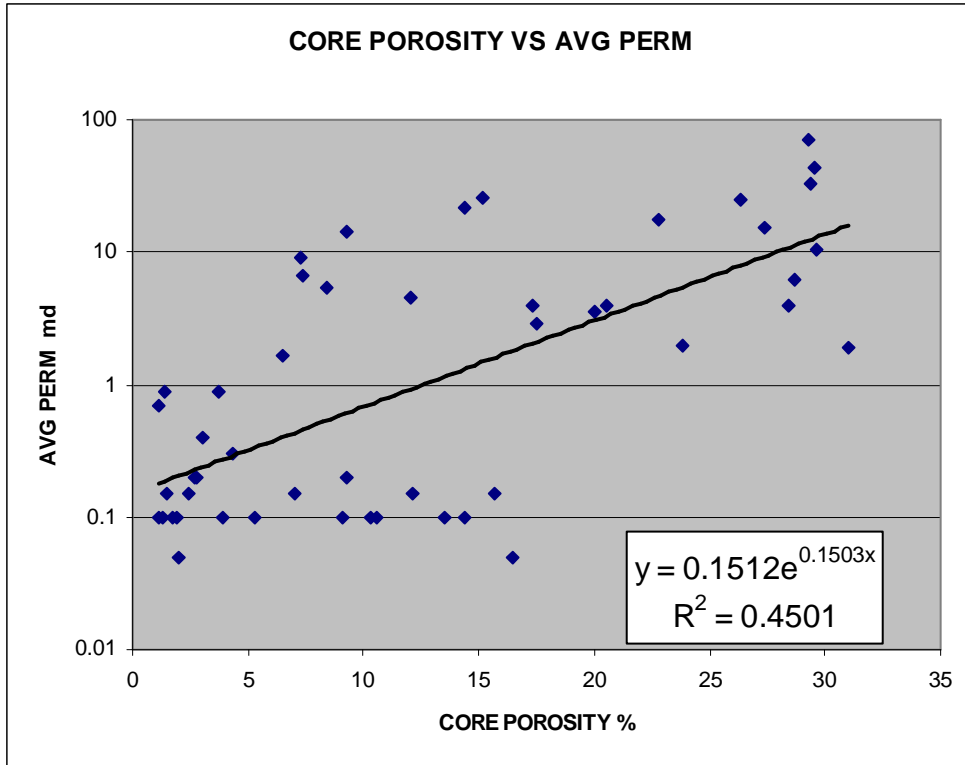


Fig. 15: Core porosity versus average core permeability for three cored wells in Trembley oilfield, reproduced from data generated by Core Laboratories, Dallas, TX (Waterflood Feasibility Study, 1989). Trendline in lower figure is for Trembley A1 well data points only.

## **8. DATA AVAILABILITY**

Oil production data for the Trembley oilfield is available online at the KGS website [www.kgs.ku.edu](http://www.kgs.ku.edu), including annual and cumulative data and number of producing wells in each year. Data made available by the field operator include water injection rates ranging in time from the inception of the waterflood through 2008, primary production data, porosity data from several wells, drill-stem test results, and a general geologic description of the reservoir. Well logs, completion reports, and formation top data are available online from the KGS, and cores from four wells in Trembley are available at the KGS in Lawrence, Kansas.

## **9. SUITABILITY FOR ENHANCED RECOVERY OPERATIONS**

Trembley oil field has both attractive features as a target for enhanced recovery and some questions. Favoring the field as a candidate for EOR are its extent, which is well-defined by wells and subsurface structure, its single reservoir bed, the L-zone or Hertha Limestone of the Kansas City Group, and its good response to waterflooding. Production rose from 1,943 barrels in 1995 to 72,430 bbls in 1997, higher even than during early flush production, after waterflooding began. Flooding tests on cores from the field were favorable. However, the permeability barrier identified during waterflood operations raises the question of whether additional heterogeneities of permeability may exist. The field has produced only 25.8% of the OOIP, despite having been under waterflood for 15 years. Admittedly, it is not clear how much of the OOIP is trapped south of the permeability barrier, and now isolated from the waterflood. This situation may have reduced the apparent recovery factor. More extensive analysis of production is necessary to determine the amount and distribution of remaining oil in place in the active waterflood. The plot of core permeability vs. core porosity shows a low degree of correlation between those properties. This suggests that oil may be trapped in porous, but impermeable rock, and therefore unrecoverable. If so, and if some of that impermeable but oil-saturated rock lies in the area of the waterflood, EOR will not get it out. On balance, however, this field does contain a significant remaining resource, and has many favorable indications for EOR, despite the possibility of heterogeneity.

## **10. CONCLUSION**

The Trembley oilfield in Reno County, Kansas, is a small field that has produced oil from the Hertha Limestone of the Upper Pennsylvanian Kansas City Group for over thirty years. Cumulative production is over 528,000 barrels to the present, which is just over 25% of volumetrically estimated OOIP. The reservoir is a combination structural-stratigraphic trap, with up to 12 feet of net pay based on 10% porosity cutoff. Waterflooding began in February of 1995 and continues to the present.

Several factors indicate that this oilfield merits serious consideration for an enhanced recovery program. Care on the part of the operators has ensured good-to-excellent data availability. Almost 75% of the OOIP remains in the reservoir, simulation showed that polymer flooding was effective, no water influx is apparent, the spatial extent of the reservoir is well defined, and, above all, waterflooding has been successful. The presence of a permeability barrier, highly variable permeability, and rather low primary plus secondary recovery indicate a potential for reservoir compartmentalization and storage of oil in inaccessible pores, which could negatively impact an enhanced recovery program. However, the long term success of waterflooding indicates that no further compartmentalization exists which would adversely affect such a program.

## **10. REFERENCES CITED**

Berexco Inc. Interoffice Memo, dated June 2, 1996, re: Trembley Oilfield.

CO<sub>2</sub> EOR Demonstration Proposal, 1999, CO<sub>2</sub> EOR Demonstration Project, Berexco, Incorporated, Trembley Unit. Document provided by Berexco, Inc.

Waterflood Feasibility Study (1989): Proposed Trembley Waterflood Unit, Hertha (Lansing-Kansas City) Limestone, Reno County, Kansas, Wichita: National Cooperative Refinery Association. (unpublished; provided by Berexco, Inc.).



# WOODHEAD UNIT, VINLAND OIL FIELD, DOUGLAS COUNTY, KANSAS

Peter Senior & Anthony W. Walton

## 1. INTRODUCTION

The Woodhead Unit is part of the Vinland oil field in Douglas County, Kansas. Oil is produced from a sandstone bed in the Middle Pennsylvanian Cherokee Group at measured depths of around 700 feet. The unit comprises 63 wells; all were drilled between 1984 and 1985. The unit has been under waterflood since 1990. Wells are on 2½ acre spacing and the unit covers one quarter section. Colt Energy, Inc. of Fairway, Kansas is the current operator; oil production in 2010, the most recent year for which complete data are available, was 2,199 barrels, and cumulative production is 329,354 barrels.

## 2. LOCATION

Vinland oilfield is located approximately 15 miles southeast of Lawrence in eastern Douglas County, Kansas (Figure 1). The defined field is in T14S, R20E and occupies the south half of sections 3 and section 11, the north half of section 14, the east half of section 15, and all of section 10. Within the field, the Woodhead Unit is the area of interest for this report; it is the part of the field under consideration for a tertiary recovery procedure. The Woodhead lease occupies the NW quarter of section 14 (Figure 2).

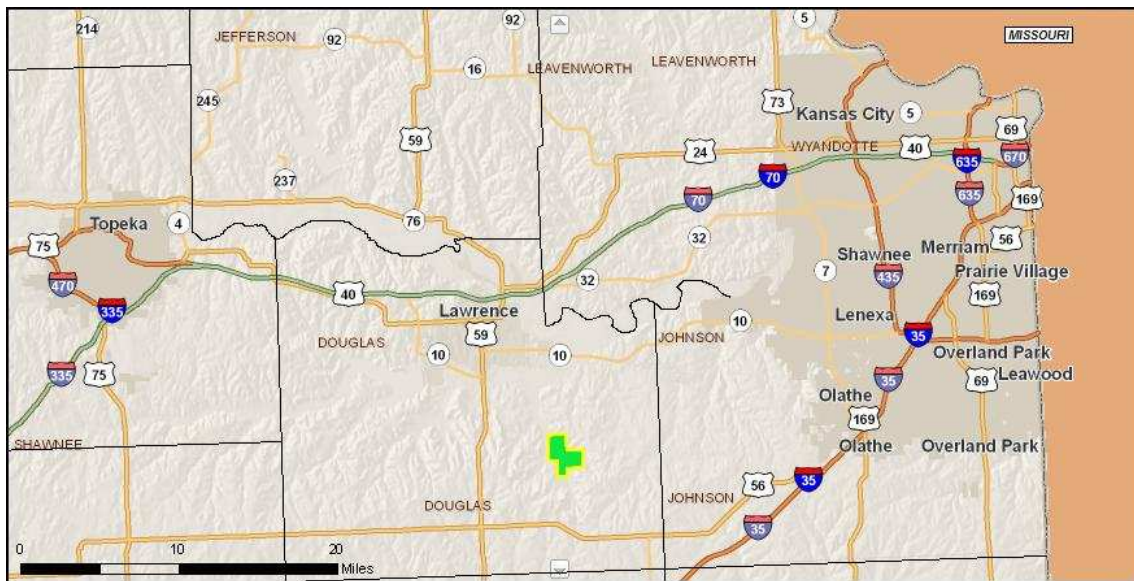


Fig 1: Regional map showing location of Vinland oilfield (green polygon), modified from KGS website.

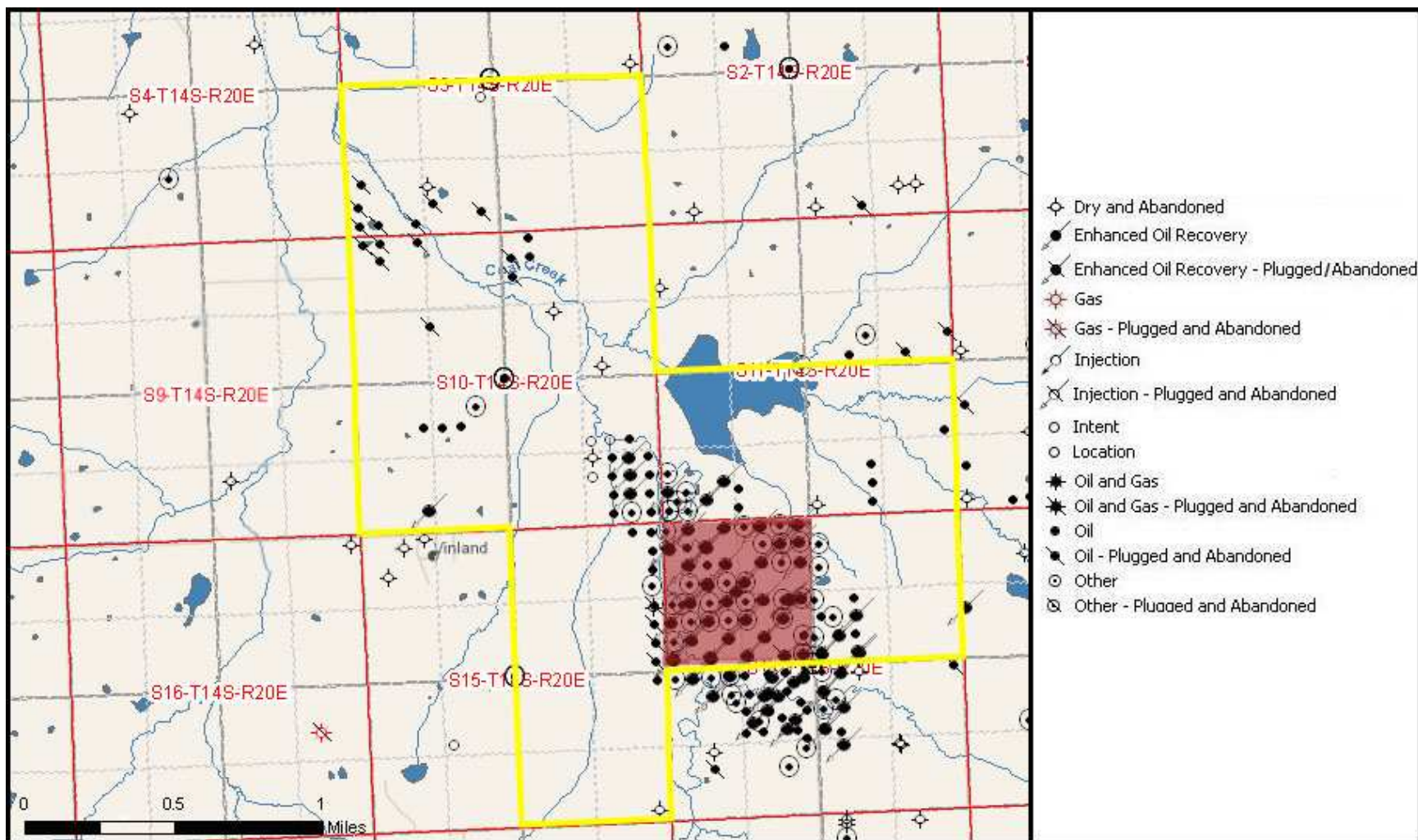


Fig. 2: Sub-regional map of Vinland oilfield, outlined in yellow, with red highlighted area indicating approximate area of Woodhead lease, modified from KGS website.

### **3. METHODS**

This report was constructed by analyzing data in the public domain and posted on the website of the Kansas Geological Survey (KGS), along with data provided by the field operators directly to the investigators. Direct correspondence with Colt Energy, Inc. was especially helpful in clarifying data that were unclear in the KGS database on the status and correct location of several wells. The major methods were use of well logs to determine the configuration of key horizons to create geologic maps and cross-sections of the reservoir and use of core analysis reports to map porosity, permeability, and oil saturation in the field. The data and logs were imported into Petra™, a subsurface GIS program, and analyzed using standard techniques. Production history, quantities, and rates were provided by the operator or downloaded from the KGS website (see references).

### **3. DISCOVERY & DEVELOPMENT HISTORY**

The earliest completed oil well within the bounds of the field is the Wiseman #1 (API# 15-045-20423), completed on January 20, 1984, and the first well completed as part of the Woodhead Unit is Woodhead #1 (API# 15-045-20498), completed May 10, 1984 (KGS website, 2011). Development of the unit was extremely rapid, likely due in to the shallow depth and close spacing of the wells. The wells are drilled on 2½ acre spacing and total depths are in the 700-foot range. By July 1985, 63 wells had been completed as part of the Woodhead Unit.

Well-completion reports indicate that most of the Woodhead wells were initially operated by Kansas Oil Properties, Inc. of Ottawa, Kansas. Colt Energy Inc. of Fairway, Kansas assumed ownership of the unit in 1988 and is the current operator. No new wells have been drilled as part of the Woodhead Unit since 1985, but two wells were drilled in 2009 and one in 2010 just to the west of the unit and completed in the Squirrel sandstone. Well-completion reports list Brett Lee of Boise, Idaho is the operator of the two wells drilled in 2009, one of which is dry and abandoned and the other successfully completed at 5 barrels of oil per day. Petrox, LLC of South Elgin, Illinois is the operator of the well drilled in 2010. The well-completion report indicates this well is a successful oil producer but does not give initial production. The new wells are on the same 2 ½ acre well spacing and are thus quite close to the Woodhead Unit wells. Table 1 lists information about the 63 wells that make up the Woodhead Unit.

Table 1: Summary of wells in the Woodhead Unit, compiled from from KGS and unit operator. Well # indicates well name, e.g. 33 indicates Woodhead 33.

API NUMBER	WELL #	PERMIT	SPUD	COMP	TYPE	STATUS	TOWNSHIP-RANGE-SECTION	SPOT	ORIG OPERATOR	CURR OPERATOR
15-045-20498	1	9-Apr-84	13-Apr-84	10-May-84	OIL	Producer	14S-20E-14	NW SW SW NW	Kansas Oil Properties Inc	Colt Energy Inc
15-045-20499	2	9-Apr-84	19-Apr-84	10-May-84	OIL	Converted to EOR Well	14S-20E-14	SE SW NW NW	KANSAS OIL PROPERTIES	Colt Energy Inc
15-045-20500	3	9-Apr-84	20-Apr-84	10-May-84	OIL	Producer	14S-20E-14	SE NW SW NW	KANSAS OIL PROPERTIES	Colt Energy Inc
15-045-20501	4	9-Apr-84	25-Apr-84	11-May-84	OIL	Converted to EOR Well	14S-20E-14	NW NW SW NW	KANSAS OIL PROPERTIES	Colt Energy Inc
15-045-20532	5	25-Apr-84	26-Apr-84	11-May-84	OIL	Producer	14S-20E-14	NW NE SE NW	KANSAS OIL PROPERTIES	Colt Energy Inc
15-045-20533	6	25-Apr-84	1-May-84	23-May-84	EOR	Recompleted	14S-20E-14	NE NE SE NW	KANSAS OIL PROPERTIES	Colt Energy Inc
15-045-20534	7	25-Apr-84	3-May-84	23-May-84	OIL	Producer	14S-20E-14	NE SE SE NW	KANSAS OIL PROPERTIES	Colt Energy Inc
15-045-20535	8	25-Apr-84	4-May-84	23-May-84	EOR	Recompleted	14S-20E-14	SW SW SE NW	KANSAS OIL PROPERTIES, INC.	Colt Energy Inc
15-045-20548	9	7-May-84	9-May-84	23-May-84	OIL	Converted to EOR Well	14S-20E-14	NW NW SE NW	KANSAS OIL PROPERTIES	Colt Energy Inc
15-045-20552	10	7-May-84	9-May-84	23-May-84	EOR	Recompleted	14S-20E-14	SE NE NE NW	KANSAS OIL PROPERTIES	Colt Energy Inc
15-045-20549	11	7-May-84	10-May-84	23-May-84	OIL	Producer	14S-20E-14	SE SE NW NW	KANSAS OIL PROPERTIES	Colt Energy Inc
15-045-20550	12	7-May-84	11-May-84	23-May-84	OIL	Converted to EOR Well	14S-20E-14	SE NW NE NW	KANSAS OIL PROPERTIES	Colt Energy Inc
15-045-20551	13		14-May-84	9-Jul-84	OIL	Producer	14S-20E-14	SE NW NW NW	KANSAS OIL PROPERTIES	Colt Energy Inc
15-045-20606	14		18-Jul-84	11-Aug-84	OIL	Producer	14S-20E-14	NW NW NE NW	KANSAS OIL PROPERTIES	Colt Energy Inc
15-045-20607	15		18-Jul-84	11-Aug-84	OIL	Converted to EOR Well	14S-20E-14	NW	Colt Energy Inc.	Colt Energy Inc
15-045-20608	16		20-Jul-84	11-Aug-84	OIL	Producer	14S-20E-14	NW NE NE NW	KANSAS OIL PROPERTIES, INC.	Colt Energy Inc
15-045-20609	17	2-Jul-84	24-Jul-84	11-Aug-84	EOR	Recompleted	14S-20E-14	N2 NW SW NW	COLT, MACK C., INC.	Colt Energy Inc

Table 1 (cont.): Summary of wells in the Woodhead Unit, compiled from from KGS and unit operator. Well # indicates well name, e.g. 33 indicates Woodhead 33.

API NUMBER	WELL #	PERMIT	SPUD	COMP	TYPE	STATUS	TOWNSHIP-RANGE-SECTION	SPOT	ORIG OPERATOR	CURR OPERATOR
15-045-20629	18		2-Aug-84	11-Aug-84	OIL	Producer	14S-20E-14	NW SW NW NW	ROLEX, INC.	Colt Energy Inc
15-045-20630	19		11-Sep-84	25-Sep-84	EOR	Recompleted	14S-20E-14	SW SE SW NW	KANSAS OIL PROPERTIES	Colt Energy Inc
15-045-20631	20		13-Sep-84	25-Sep-84	OIL	Producer	14S-20E-14	NW	Colt Energy Inc.	Colt Energy Inc
15-045-20632	21		18-Sep-84	25-Sep-84	OIL	Producer	14S-20E-14	NW	Colt Energy Inc.	Colt Energy Inc
15-045-20685	22	14-Sep-84	19-Sep-84	25-Sep-84	OIL	Producer	14S-20E-14	NW NE SE NW	Colt Energy Inc.	Colt Energy Inc
15-045-20686	23	14-Sep-84	20-Sep-84	2-Oct-84	EOR	Recompleted	14S-20E-14	SW SW SW NW	KANSAS OIL PROPERTIES	Colt Energy Inc
15-045-20687	24		21-Sep-84	2-Oct-84	OIL	Producer	14S-20E-14	NW SW SW NW	KANSAS OIL PROPERTIES, INC.	Colt Energy Inc
15-045-20705	25	21-Sep-84	24-Sep-84	2-Oct-84	OIL	Converted to EOR Well	14S-20E-14	SW SE SE NW	KANSAS OIL PROPERTIES	Colt Energy Inc
15-045-20734	26		24-Oct-84	5-Dec-84	EOR	Recompleted	14S-20E-14	NE SW SW NW	KANSAS OIL PROPERTIES, INC.	Colt Energy Inc
15-045-20735	27		31-Oct-84	5-Dec-84	OIL	Producer	14S-20E-14	SE NW SW NW	KANSAS OIL PROPERTIES	Colt Energy Inc
15-045-20736	28		30-Oct-84	5-Dec-84	OIL	Converted to EOR Well	14S-20E-14	NE SW NE NW	KANSAS OIL PROPERTIES	Colt Energy Inc
15-045-20737	29		29-Oct-84	5-Dec-84	OIL	Producer	14S-20E-14	NE NW SE NW	KANSAS OIL PROPERTIES	Colt Energy Inc
15-045-20742	30		5-Nov-84	29-Nov-84	OIL	Producer	14S-20E-14	NW NE SW NW	KANSAS OIL PROPERTIES	Colt Energy Inc
15-045-20743	31		7-Nov-84	29-Nov-84	EOR	Recompleted	14S-20E-14	NE SE SW NW	KANSAS OIL PROPERTIES, INC.	Colt Energy Inc
15-045-20744	32		8-Nov-84	29-Nov-84	OIL	Producer	14S-20E-14	SE NE SW NW	KANSAS OIL PROPERTIES, INC.	Colt Energy Inc
15-045-20745	33	1-Nov-84	18-Dec-84	9-Jul-85	OIL	Producer	14S-20E-14	NW SE NW NW	KANSAS OIL PROPERTIES	Colt Energy Inc
15-045-20767	33		18-Dec-84		OIL	Producer	14S-20E-14	NE SW NW NW	KANSAS OIL PROPERTIES	Colt Energy Inc

Table 1 (cont.): Summary of wells in the Woodhead Unit, compiled from from KGS and unit operator. Well # indicates well name, e.g. 33 indicates Woodhead 33.

API NUMBER	WELL #	PERMIT	SPUD	COMP	TYPE	STATUS	TOWNSHIP-RANGE-SECTION	SPOT	ORIG OPERATOR	CURR OPERATOR
15-045-20746	34	1-Nov-84	20-Dec-84	6-Aug-85	OIL	Producer	14S-20E-14	SW NE SE NW	Colt Energy Inc.	Colt Energy Inc
15-045-20768	34	17-Dec-84			OIL	Producer	14S-20E-14	SW SW NE NW	Colt Energy Inc.	Colt Energy Inc
15-045-20747	35	1-Nov-84	22-Dec-84	19-Mar-85	OIL	Producer	14S-20E-14	SW NE SW	Colt Energy Inc.	Colt Energy Inc
15-045-20769	35	17-Dec-84			OIL	Producer	14S-20E-14	SW NW SE NW	KANSAS OIL PROPERTIES	Colt Energy Inc
15-045-20748	36	1-Nov-84	26-Dec-84	19-Mar-85	OIL	Converted to EOR Well	14S-20E-14	SW NE SW NW	Colt Energy Inc.	Colt Energy Inc
15-045-20770	36	17-Dec-84			OIL	Producer	14S-20E-14	NW		Colt Energy Inc
15-045-20749	37	1-Nov-84	4-Jan-85	19-Mar-85	OIL	Producer	14S-20E-14	SW NE NE NW	Colt Energy Inc.	Colt Energy Inc
15-045-20771	37	17-Dec-84			OIL	OIL	14S-20E-14	NW NE NE NW	KANSAS OIL PROPERTIES	Colt Energy Inc
15-045-20772	38	26-Dec-84	11-Jan-85	19-Mar-85	OIL	Converted to EOR Well	14S-20E-14	NW NE SW NW	KANSAS OIL PROPERTIES	Colt Energy Inc
15-045-20773	39	26-Dec-84	14-Jan-85	19-Mar-85	OIL	OIL	14S-20E-14	NW NW NE NW	KANSAS OIL PROPERTIES	Colt Energy Inc
15-045-20774	40		13-Jun-85	2-Jul-85	EOR	Recompleted	14S-20E-14	NW	KANSAS OIL PROPERTIES	Colt Energy Inc
15-045-20790	41		18-Jun-85	2-Jul-85	OIL	OIL	14S-20E-14	NW	KANSAS OIL PROPERTIES	Colt Energy Inc
15-045-20791	42		19-Jun-85	2-Jul-85	EOR	Recompleted	14S-20E-14	NW	KANSAS OIL PROPERTIES	Colt Energy Inc
15-045-20792	43		22-Jun-85	9-Jul-85	OIL	Converted to EOR Well	14S-20E-14	NW	KANSAS OIL PROPERTIES	Colt Energy Inc
15-045-20793	44		24-Jun-85	9-Jul-85	OIL	OIL	14S-20E-14	NW	KANSAS OIL PROPERTIES	Colt Energy Inc
15-045-20794	45		28-Jun-85	9-Jul-85	OIL	Converted to EOR Well	14S-20E-14	NW	KANSAS OIL PROPERTIES	Colt Energy Inc
15-045-20795	46		29-Jun-85	9-Jul-85	OIL	Producer	14S-20E-14	NW	KANSAS OIL PROPERTIES	Colt Energy Inc
15-045-20825	47		30-Jun-85	9-Jul-85	OIL	Converted to EOR Well	14S-20E-14	SE SW NW	KANSAS OIL PROPERTIES	Colt Energy Inc

Table 1 (cont.): Summary of wells in the Woodhead Unit, compiled from from KGS and unit operator. Well # indicates well name, e.g. 33 indicates Woodhead 33.

API NUMBER	WELL #	PERMIT	SPUD	COMP	TYPE	STATUS	TOWNSHIP-RANGE-SECTION	SPOT	ORIG OPERATOR	CURR OPERATOR
15-045-20809	48		3-Jul-85	9-Jul-85	EOR	Recompleted	14S-20E-14	NE NW NE NW	KANSAS OIL PROPERTIES	Colt Energy Inc
15-045-20810	49	6-May-85	10-Jul-85	16-Jul-85	OIL	Converted to EOR Well	14S-20E-14	SE NE SW NW	KANSAS OIL PROPERTIES	Colt Energy Inc
15-045-20811	50	6-May-85	11-Jul-85	6-Aug-85	OIL	Producer	14S-20E-14	NW SE NE NW	KANSAS OIL PROPERTIES	Colt Energy Inc
15-045-20812	51		15-Jul-85	6-Aug-85	OIL	Converted to EOR Well	14S-20E-14	NE SW SE NW	KANSAS OIL PROPERTIES	Colt Energy Inc
15-045-20813	52		25-Jul-85	6-Aug-85	OIL	Converted to EOR Well	14S-20E-14	NE NE NE NW	KANSAS OIL PROPERTIES	Colt Energy Inc
15-045-20814	53		5-Jul-85	16-Jul-85	OIL	Converted to EOR Well	14S-20E-14	NE SW SE NW	KANSAS OIL PROPERTIES	Colt Energy Inc
15-045-20815	54		3-Jul-85	16-Jul-85	OIL	Producer	14S-20E-14	NE NE SE NW	KANSAS OIL PROPERTIES	Colt Energy Inc
15-045-20816	55		9-Jul-85	16-Jul-85	OIL	Producer	14S-20E-14	NE NW SE NW	KANSAS OIL PROPERTIES	Colt Energy Inc
15-045-20817	56		8-Jul-85	16-Jul-85	EOR	Recompleted	14S-20E-14	NE SE NW NW	KANSAS OIL PROPERTIES	Colt Energy Inc
15-045-20818	57		27-Jun-85	9-Jul-85	OIL	Producer	14S-20E-14	NW NW NW	KANSAS OIL PROPERTIES	Colt Energy Inc
15-045-20819	58		18-Jul-85	6-Aug-85	EOR	Recompleted	14S-20E-14	NE NW NE NW	KANSAS OIL PROPERTIES	Colt Energy Inc
15-045-20820	59		17-Jul-85	6-Aug-85	OIL	Producer	14S-20E-14	NE NE NW NW	KANSAS OIL PROPERTIES	Colt Energy Inc
15-045-20821	60		29-Jun-85	9-Jul-85	OIL	Producer	14S-20E-14	SE NE NW	KANSAS OIL PROPERTIES	Colt Energy Inc
15-045-20822	61		22-Jul-85	6-Aug-85	OIL	Converted to EOR Well	14S-20E-14	SE SE NW	KANSAS OIL PROPERTIES	Colt Energy Inc
15-045-20823	62	7-May-85	16-Jul-85	6-Aug-85	OIL	Producer	14S-20E-14	SE SE SE NW	KANSAS OIL PROPERTIES	Colt Energy Inc
15-045-20824	63		23-Jul-85	6-Aug-85	OIL	Converted to EOR Well	14S-20E-14	NE SW NE NW	KANSAS OIL PROPERTIES	Colt Energy Inc
15-045-21069	IW				OTHER		14S-20E-14	SW SE SE NW	KANSAS OIL PROPERTIES, INC.	Colt Energy Inc

## 5. PRODUCTION HISTORY

Annual oil production data from both Colt Energy Inc. and the KGS website are in close agreement, with only very minor discrepancies. Colt also provided data on water injection (Figure 3, 4, Table 2). According to well-completion forms, wells in the Woodhead Unit typically had initial production of 10 barrels of oil per day (BOPD) with an oil gravity of 26° or 27°; some wells had initial production of 4 or 5 BOPD. No data are available on water production, although initial water cut was about 0.2%.

Oil production from the unit began in 1984, and the primary production peak was in 1985 at 36,202 barrels per year. A period of steep decline followed, with annual oil production reaching a low point of just 3,911 barrels in 1989. Waterflooding commenced in 1990 and the reservoir response was very rapid. 1990 saw oil production climb from the previous year, therefore the waterflood positively impacted oil production in less than one year. Secondary production peaked at 26,379 barrels in 1995 and, with the exception of 2007-2008 and 2009-2010, has been steadily declining. The increase in 2008 annual oil production over 2007 from the unit was less than 100 barrels total, and 2010 production exceeds 2009 by a similar amount. Annual water injection has declined from over 60,000 barrels in 2000 to less than 30,000 barrels in 2008. Oil production in 2010, the most recent year for which complete data are available, was 2,199 barrels, and cumulative production is 329,354 barrels.



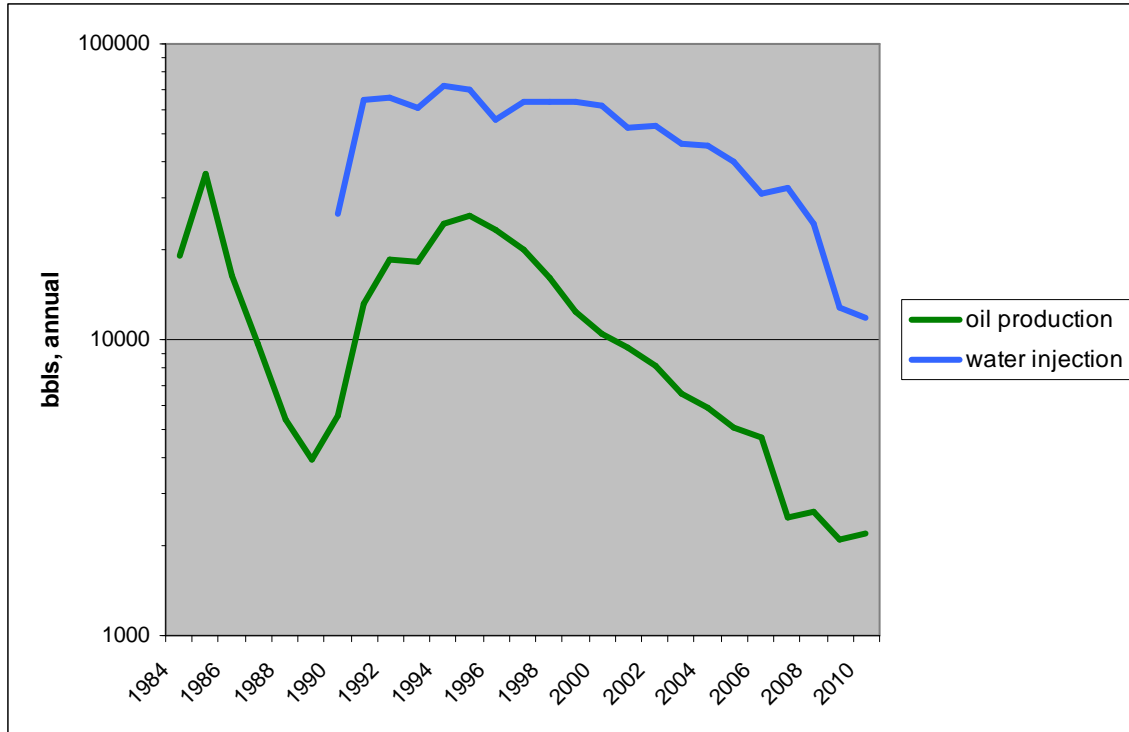


Fig. 3: Annual production and injection data for Woodhead Unit. Oil production in 2010 was 2199 bbls. Oil production and water injection from Colt Energy Inc., oil production in 2009 & 2010 from the KGS website.

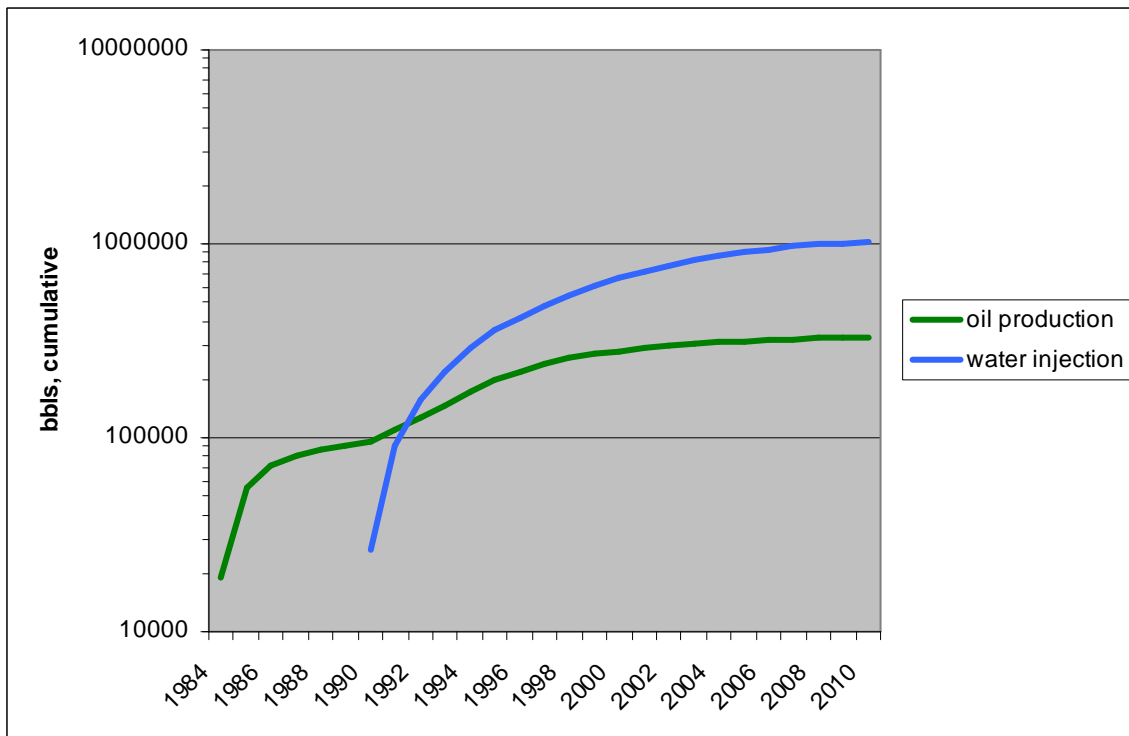


Fig. 4: Cumulative oil production and water injection data for Woodhead Unit compiled from data provided by the field operator and KGS. Cumulative oil production, through 12/2010, was 329,354 bbls.

Table 2: Annual and cumulative oil production and water injection data for Woodhead Unit, Vinland oil field. 2009 and 2010 oil production data from KGS, all other data from Colt Energy Inc.

Year	Oil		Water	
	Production	Cumulative	Injection	Cumulative
1984	19194	19194		
1985	36202	55396		
1986	16458	71854		
1987	9667	81521		
1988	5365	86886		
1989	3911	90797		
1990	5537	96334	26781	26781
1991	13235	109569	64711	91492
1992	18645	128214	66036	157528
1993	18262	146476	60922	218450
1994	24617	171093	71852	290302
1995	26379	197472	69580	359882
1996	23438	220910	55104	414986
1997	20114	241024	63888	478874
1998	16133	257157	63888	542762
1999	12515	269672	63888	606650
2000	10485	280157	61798	668448
2001	9387	289544	52049	720497
2002	8177	297721	52980	773477
2003	6615	304336	46140	819617
2004	5865	310201	45011	864628
2005	5040	315241	39982	904610
2006	4671	319913	30978	935588
2007	2516	322429	32720	968308
2008	2606	325035	24732	993040
2009	2120	327155	12761	1005801
2010	2199	329354	11811	1017612

## 6. GEOLOGY

The reservoir interval of the Woodhead Unit is in the upper part of the Middle Pennsylvanian Cherokee Group. The reservoir is sandstone and occurs near the top of the Cabaniss Formation (Figure 5), just below the Mulky coal bed and the overlying Excello Shale. While the sandstone lacks a formally recognized name in the KGS stratigraphy, it is referred to informally in northeastern Kansas as the Squirrel sandstone. Where this uppermost part of the Cabaniss is limestone or limey sandstone, it is referred to as the Breezy Hill Limestone. One story attributes the origin of the name Squirrel to unknown drillers who are said to have likened the sandstone's unpredictable occurrence in the subsurface to the erratic jumping around of a

squirrel. Other stories attribute the name to discovery of oil on a farm owned by a man named Squirrel.

A typical well log through the reservoir shows a gradual coarsening-upward profile in the gamma-ray log, and further to the southeast, in Greenwood County, Kansas, the pattern through the same stratigraphic interval is much the same (Figure 6). Isolith mapping in the subsurface at a regional scale by R.L. Brenner (1989) and his students reveals a lobate geometry of the sandstone (Figure 7). The lobate geometry, as well as outcrop, well log, and core examination, have led to interpretation of the sandstone as delta deposits (Brenner, 1989). A paleogeographic reconstruction of eastern Kansas by Brenner (1989) shows many delta systems existing in the region during time of deposition of the Squirrel sandstone, including several in Douglas County (Figure 8).

Regional structural dip of rocks is in a northwesterly direction, as mapped both on the base of the Kansas City Group (Figure 9) and on the top of the Squirrel sandstone (Figure 10). The two maps show generally parallel structural dip at the regional scale. The Woodhead Unit is located in the Forest City Basin, which encompasses much of northeastern Kansas, northwestern Missouri, southeastern Nebraska, and southwestern Iowa. A closer view of the structure in the Woodhead Unit shows the same northwesterly dipping trend, with some indication that the top of the Squirrel sandstone may show a small anticlinal nose protruding in a westerly direction (Figure 11). Figure 11 seems to show a steep gradient in the Woodhead Unit at the top of the Squirrel sandstone. However, across approximately three-fourths of section 14 in a north-south direction the contours show an elevation increase from 185 to 220 feet, or 35 feet (10.7 meters) over a distance of 3960 feet (1.2 km). Mathematically this calculates to a slope of about half a degree. The steep-appearing gradient on the maps is just a reflection of the density of formation-top data in the Woodhead Unit.

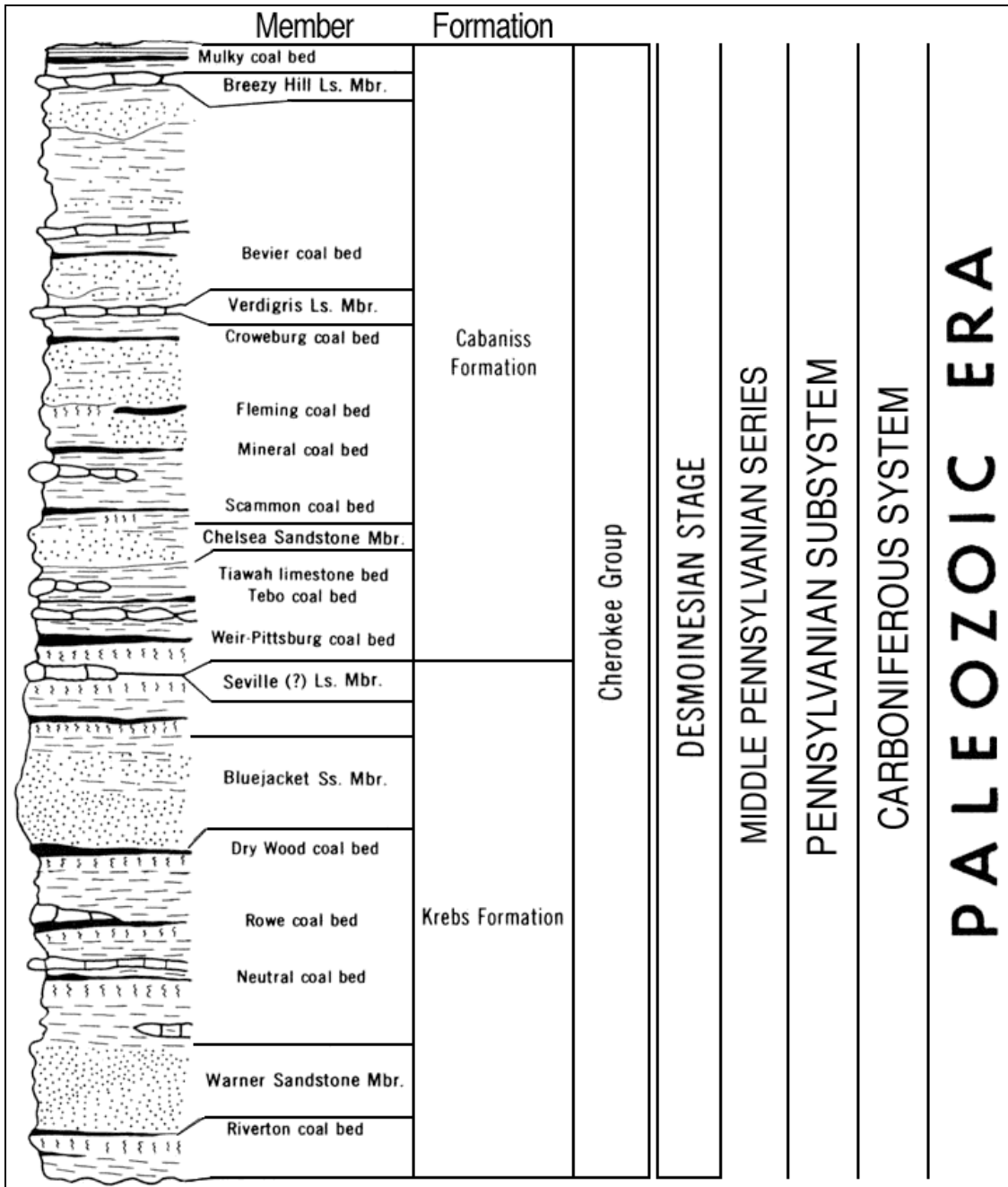


Fig. 5: Stratigraphic column of the Cherokee Group from the KGS. Woodhead Unit reservoir interval is in upper part of Cabaniss Formation.

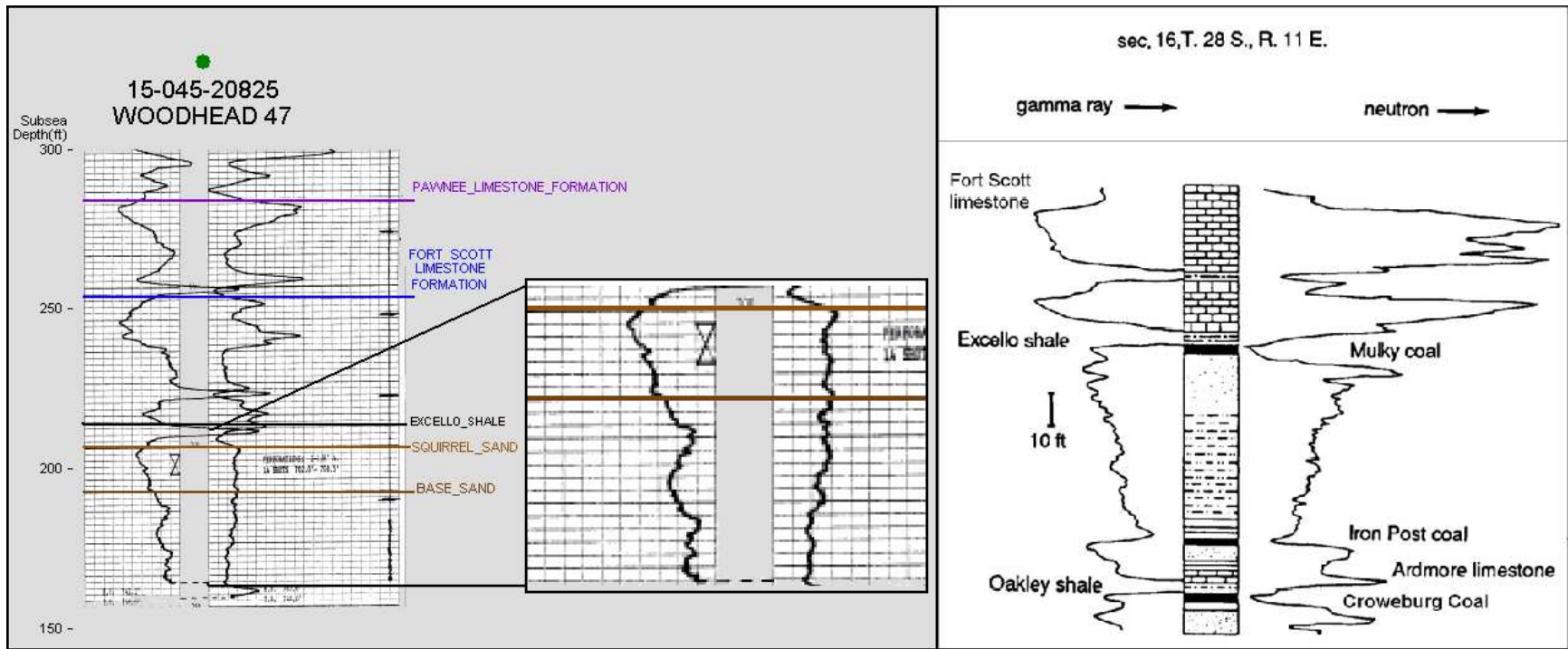


Fig 6: Typical well log through sandstone reservoir in Woodhead Unit showing coarsening-upward gamma-ray profile. Well log displays un-scaled gamma-ray and neutron logs. Compare to log of same interval in Greenwood County, KS on right, modified from Brenner (1989).

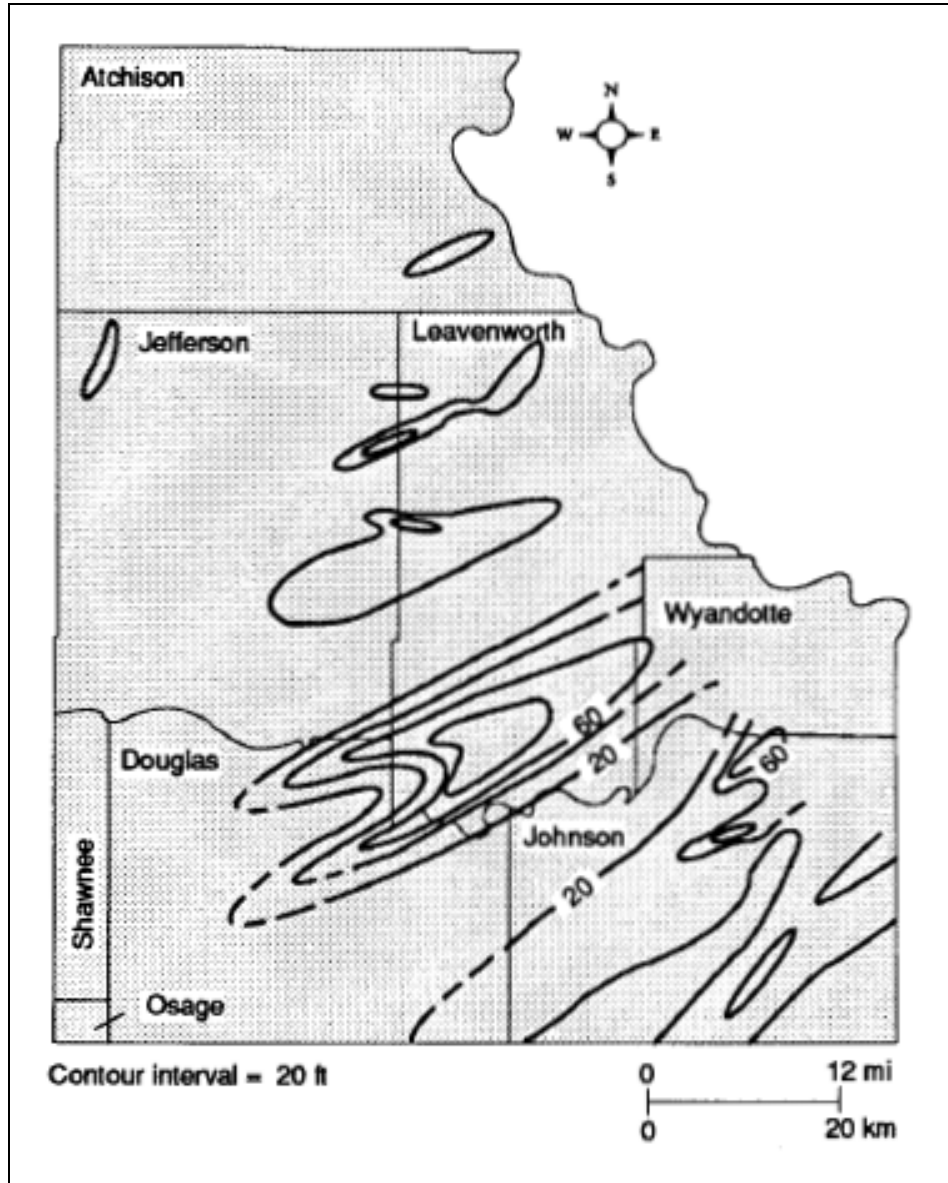


Fig. 7: Sandstone-isolith map showing lobate geometry of sand bodies in subsurface of northeastern Kansas (Brenner, 1989).

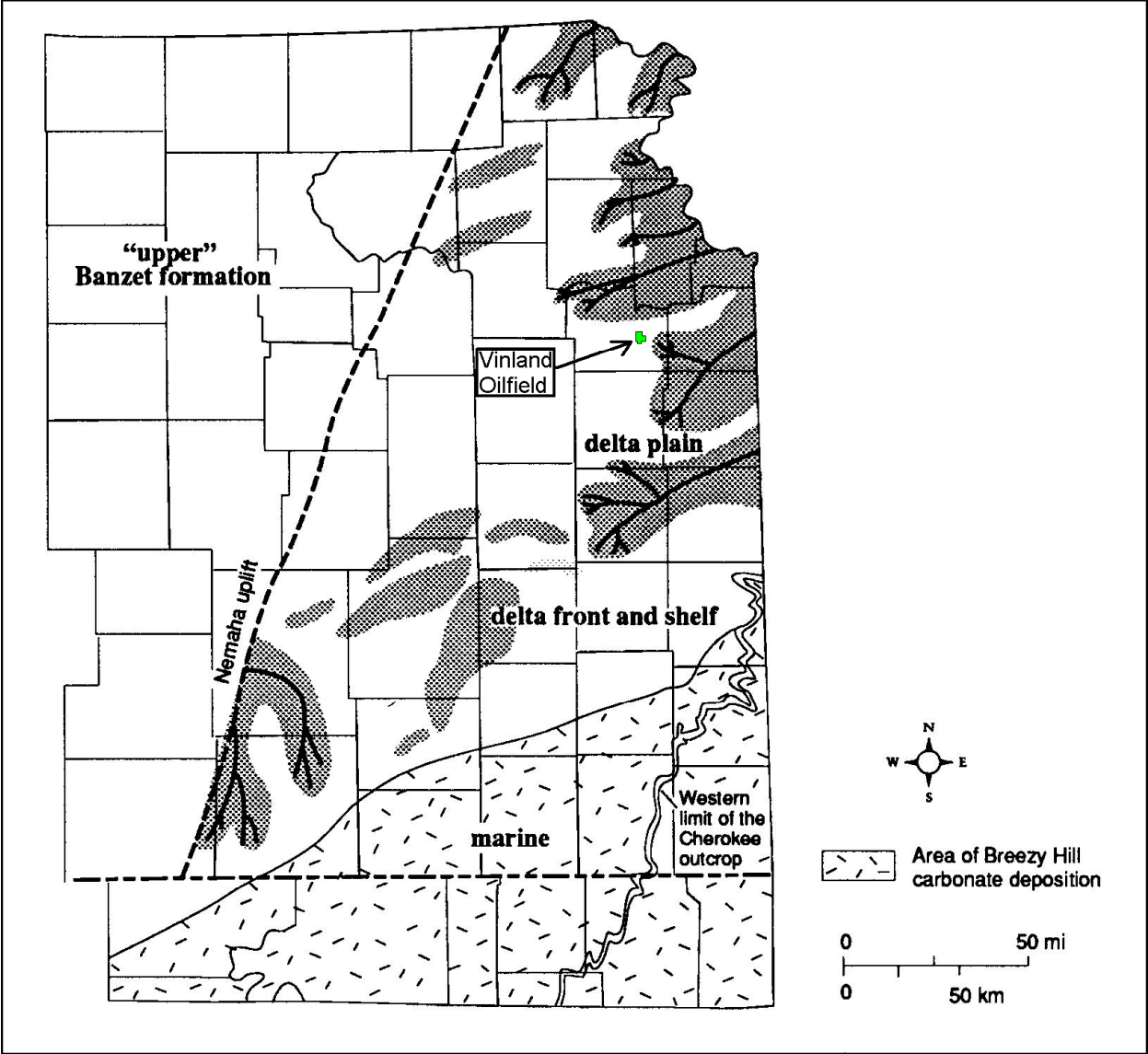


Fig. 8: Paleogeographic reconstruction showing distribution of delta environments during late Middle Pennsylvanian time, with location of Vinland oilfield indicated, modified from Brenner (1989). The Banzet formation as defined by Brenner includes the Squirrel sandstone.

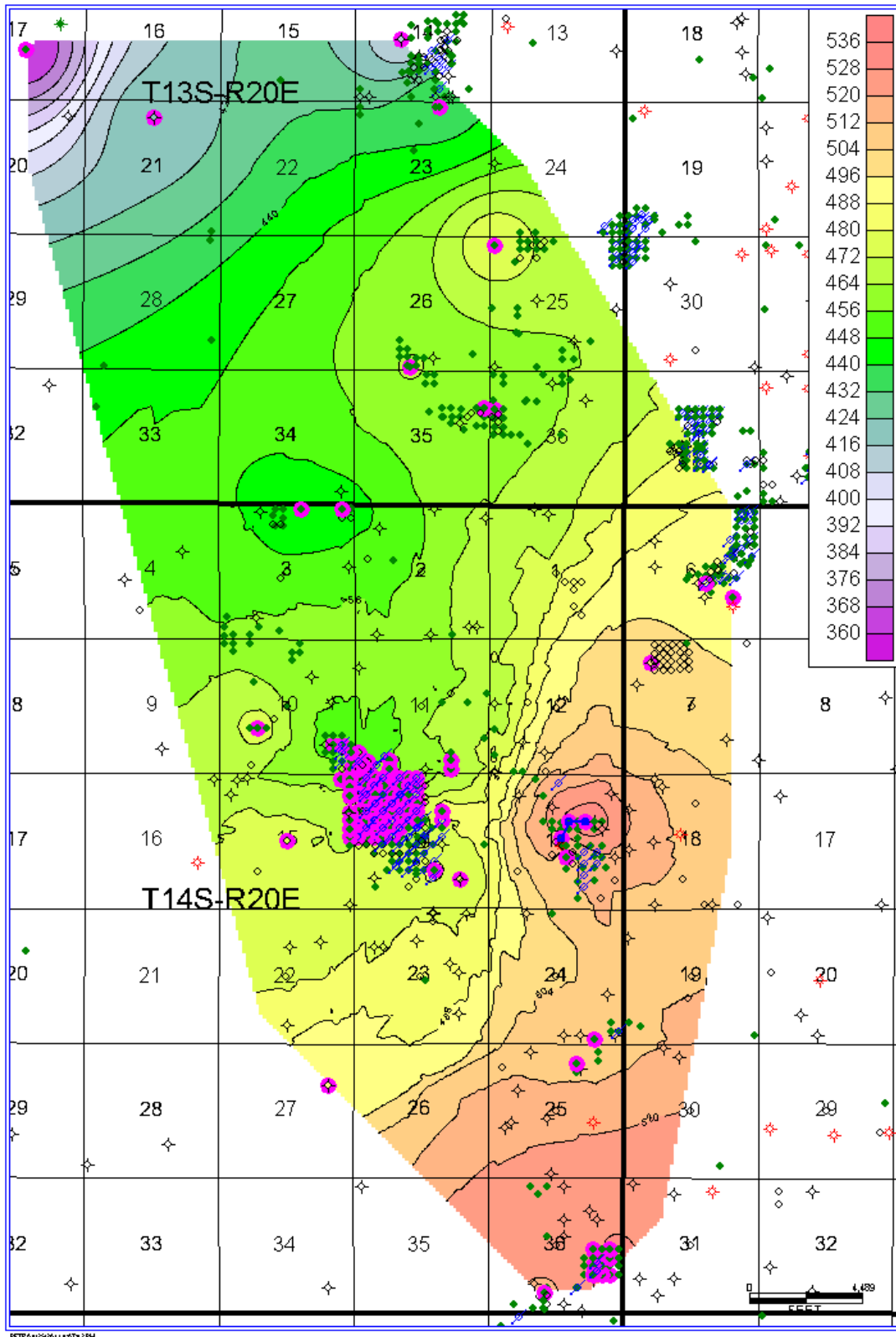


Fig. 9: Regional structural map of the base of the Kansas City Group. Compare to Fig. 10. Contours are in feet above sea level. Highlighted wells indicate data points.



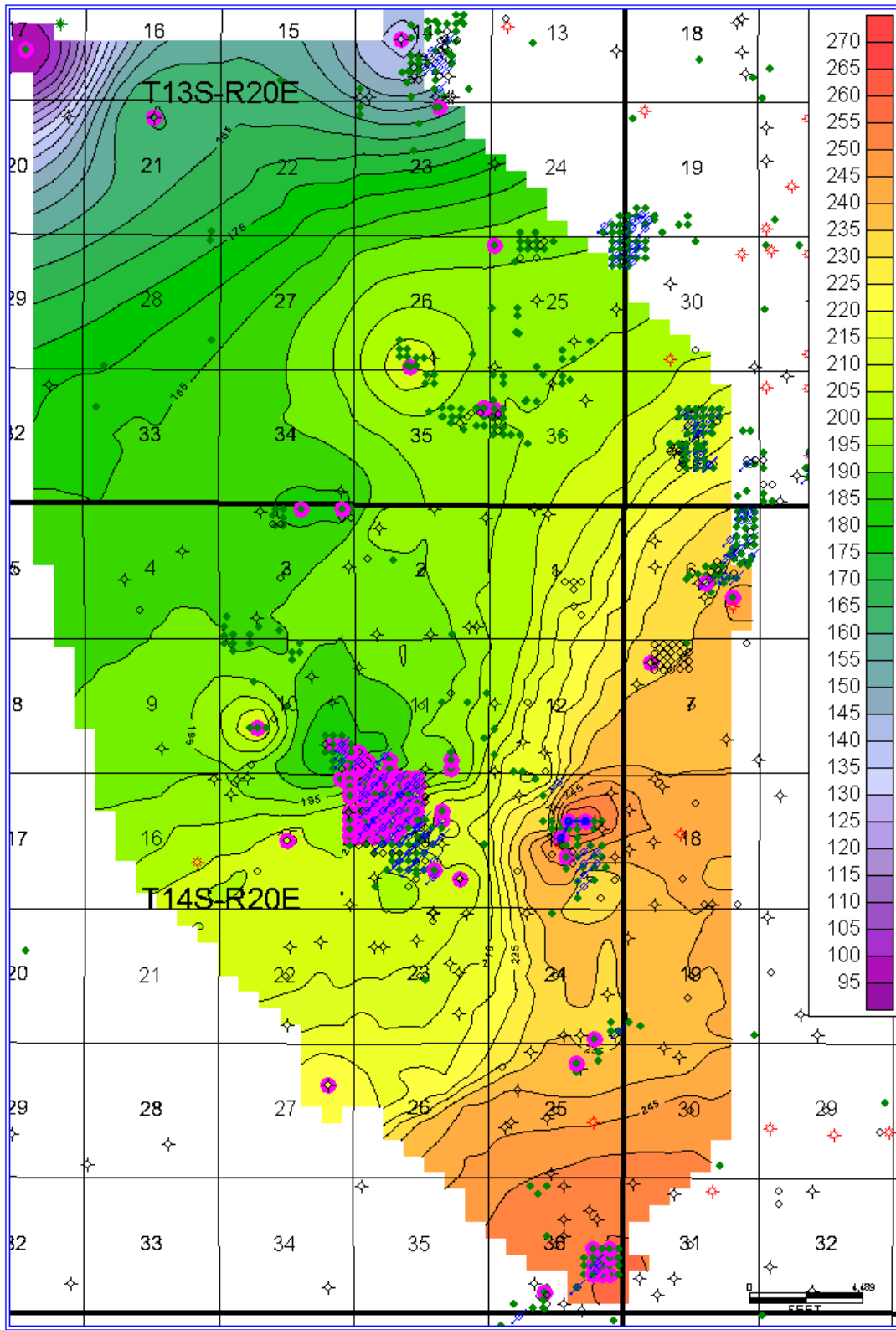


Fig. 10: Regional structural map of the top of the Squirrel sandstone. Compare to Fig. 9. Contours are in feet above sea level. Highlighted wells indicate data points.

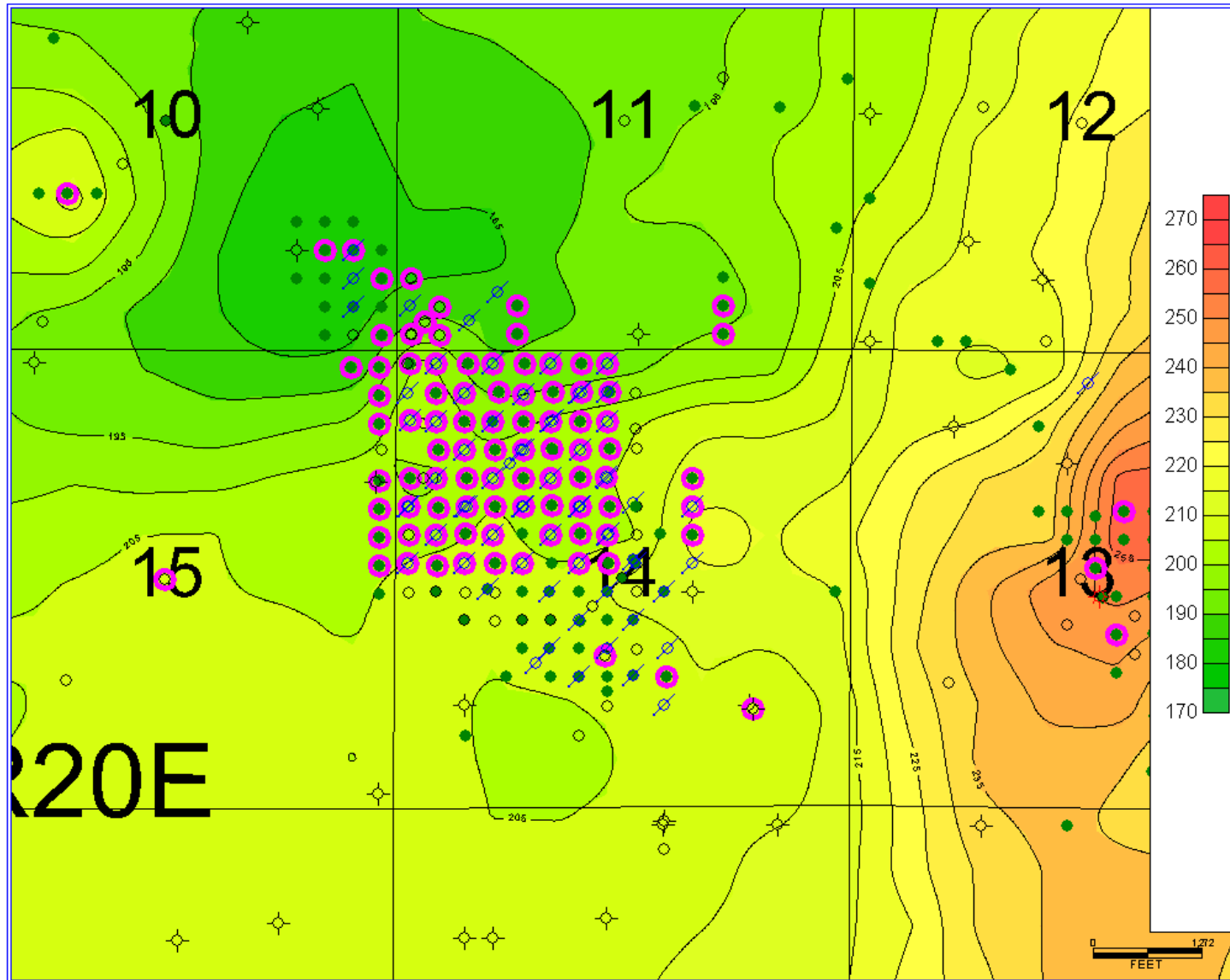


Fig. 11: Subregional structural map of the top of the Squirrel sandstone. Contours are in feet above sea-level

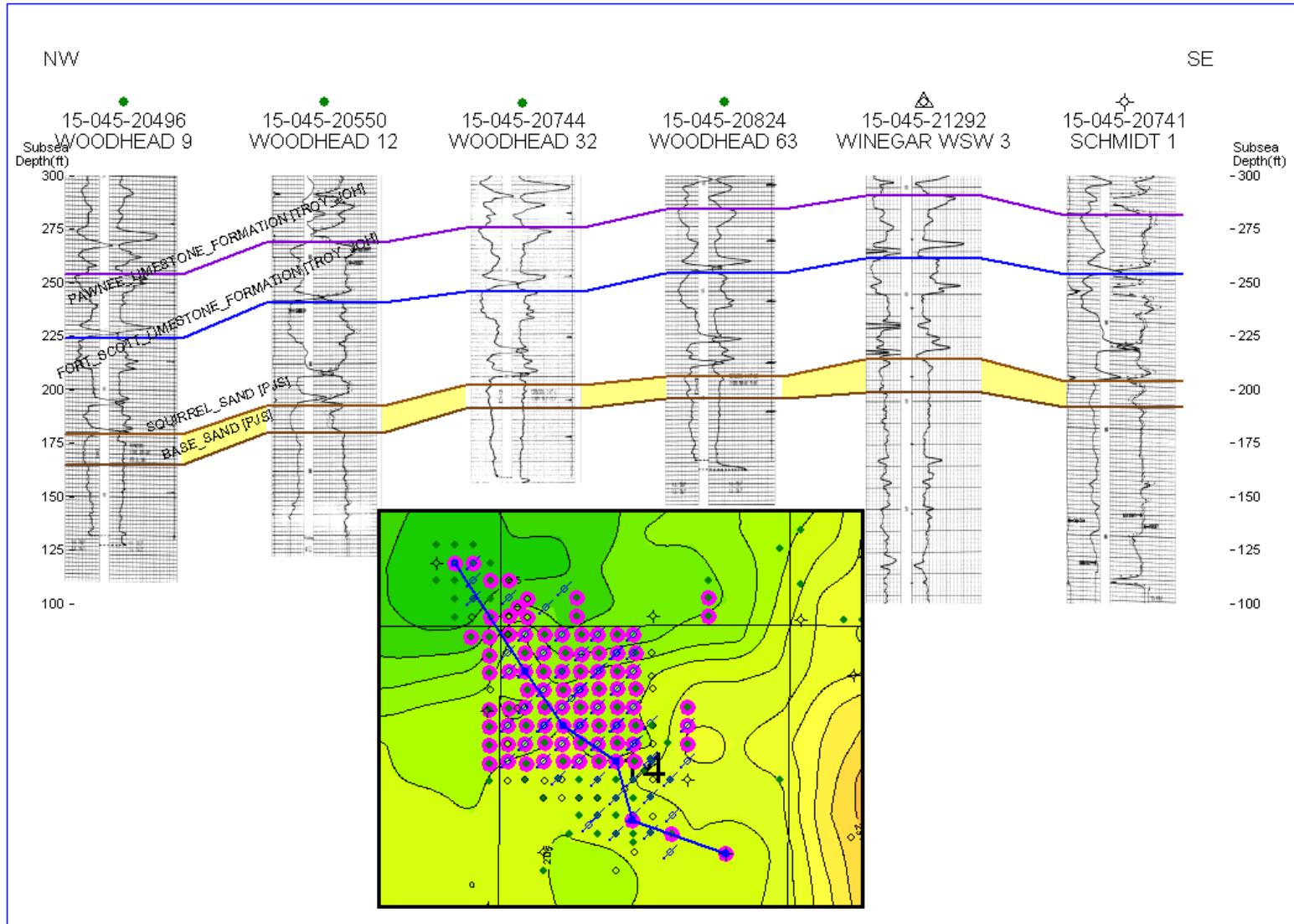
While the Woodhead Unit has been extensively drilled on close spacing, providing excellent data coverage for mapping purposes, the actual spatial extent of the reservoir sand body is unknown. The formation top data in Figure 10 suggests that the Squirrel sandstone is widespread, however, the paleogeographic reconstruction and sand-isolith map (Figure 7, 8) suggest that reservoir-quality sand bodies are spatially restricted.

A northwest-southeast oriented cross-section shows the structure of the field (Figure 12). The structure rises from the northwest and dips slightly toward the southeast. The lack of well logs to the southeast prevents knowing for sure whether a trap is formed by structural closure from northwest to southeast. A cross-section oriented southwest-northeast (Figure 13) shows a similar situation; the available well logs show a humped structure, but the lack of well logs farther to the west leaves open the question of whether the structure is closed in that direction.

A west-east oriented cross-section indicates that reservoir-quality sand may pinch out to the east, trapping oil stratigraphically (Figure 14). The gamma-ray profiles in the Woodhead Unit display coarsening-upward profiles characteristic of good sandstone development, while the gamma-ray profiles of wells lying to the east near the center of Section 13 display a more uniform profile. Compared to the low and high gamma-ray zones of the overlying Fort Scott limestone as baselines, the gamma-ray logs of the Woodhead Unit and the wells in Section 13 display similar normalized gamma-ray readings. However, the reservoir zone in the Woodhead Unit is at the top of the Cherokee Group strata whereas in wells to the east it is stratigraphically about 50' lower. This indicates two stratigraphically separate reservoirs, with the reservoir in the Woodhead Unit pinching out updip to the east.

The sand-isolith and paleogeographic maps (Figure 7, 8) give some indication of the potential size of a Squirrel sandstone reservoir in east-central Douglas County, and stratigraphic pinchout of the Woodhead Unit reservoir is indicated to the east, but the true extent of the reservoir in other directions is at present unknown. Cross-sections (Figure 12, 13) indicate the possibility of an anticlinal structure to the reservoir and thus the trap may be partially structural. With the data available at the present time, the picture of the petroleum trap at the Woodhead Unit is incomplete.

WOODHEAD-VINLAND FIELD



FILE: 9/9/2011 9:28:52 PM (12-4-2011) m-aa vinland ark. case.CSP1

Fig. 12: Structural cross-section through Woodhead Unit showing structure from northwest to southeast.

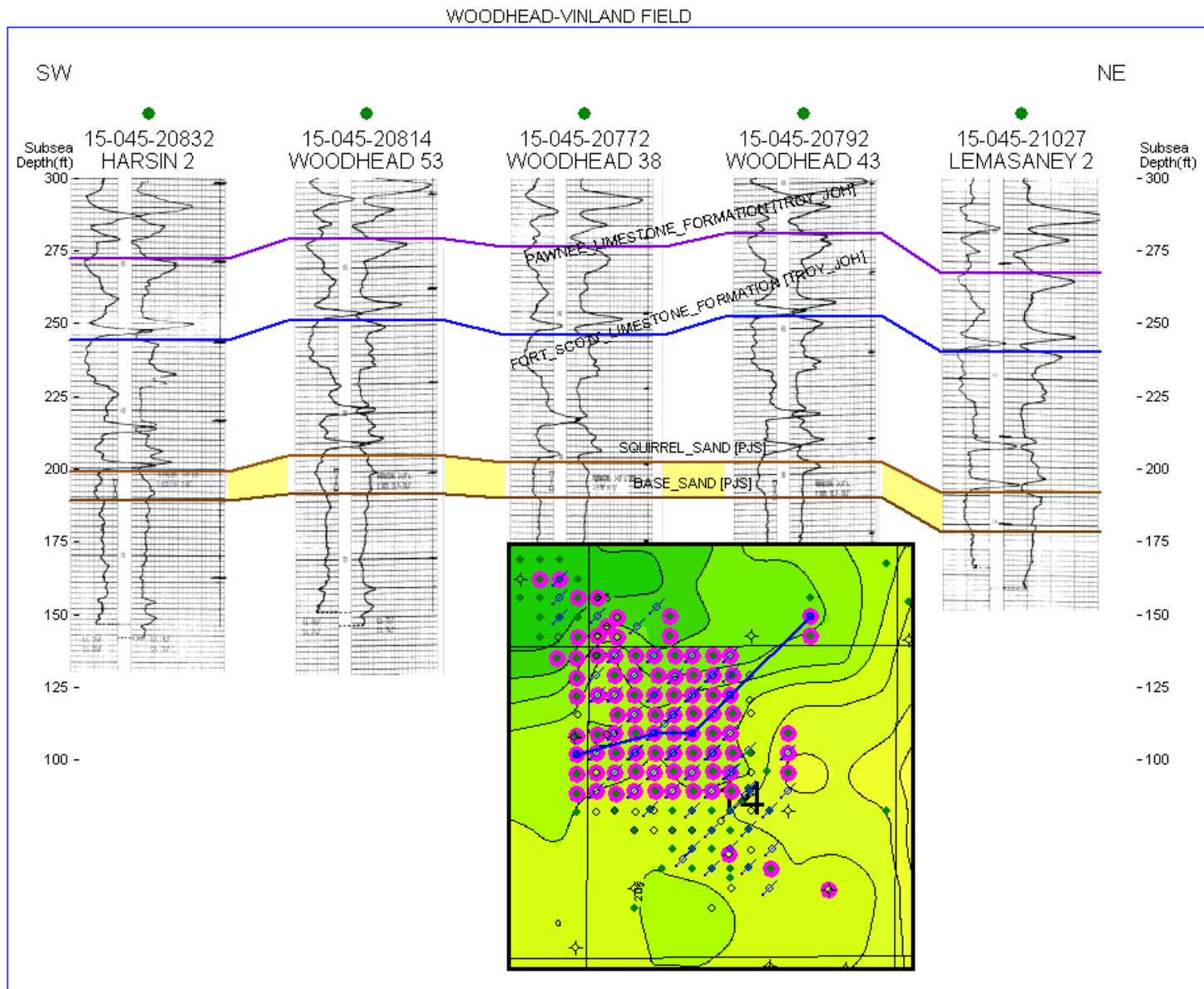


Fig. 13: Structural cross-section through Woodhead Unit showing structure from southwest to northeast.

WOODHEAD-VINLAND FIELD

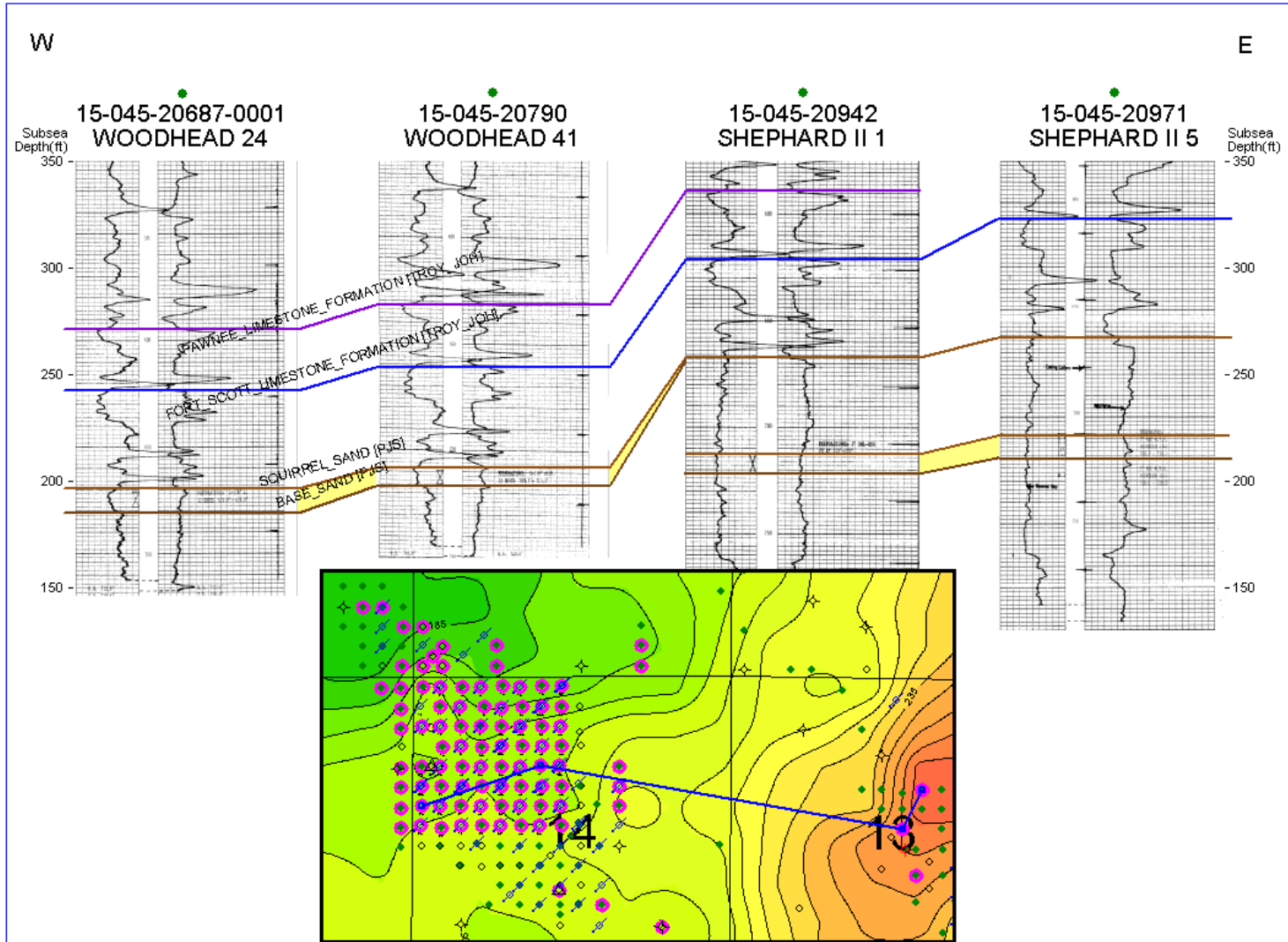


Fig. 14: West-east structural cross-section through Woodhead Unit showing stratigraphic pinchout of Squirrel sandstone to east.

Abundant core data exists for the Woodhead Unit. Of the 63 wells, 54 were cored through the reservoir. Oil saturation values calculated as (100-Water saturation) range from 41.8 to 70.5 percent. An oil-saturation map (Figure 15) shows good saturations especially in the northern part of the unit, and in a north-south trend in the west-central part of the unit. Averaged core porosity values range from 14.5 to 22.5 percent, with an overall average of 19.8 percent. A map of averaged core porosity (Figure 16) shows that the best porosity in the reservoir is in generally the same area as the best oil saturations, in the northern part of the unit and in a north-south trend in the west-central part of the unit.

Analysis of core reports allowed for consistent picking of a base of the sandstone reservoir on well logs. Shale beds made up the bottom foot or two of several of the cores. Comparing the depths as recorded on these cores to the well logs allowed identification of gamma-ray increases consistent with shale or shaly sand. Using this data, correlation was made from the well logs with shale at the bottom of core to other well logs throughout the unit; in this way the base of the Squirrel sand was picked and an isopach map was created (Figure 17). The isopach map shows notable thick areas east and northwest of the unit, and a small thick area in the center of the unit. Average thickness of the Squirrel sandstone is 11.8 feet.

The values of average oil saturation, average porosity, and thickness were multiplied for each well to obtain a single value at each well ( $S_o-\Phi-h$ ; Figure 18). These point values can be thought of as representing how many feet of oil were initially present in each well. The map indicates that the most oil was initially present in the northwestern and southwestern parts of the unit. Table 3 provides a summary of core data, thickness data, and  $S_o-\Phi-h$  values. One well had core but did not have logs (Woodhead 10), and so no thickness value, and hence, no  $S_o-\Phi-h$  value is given for that one particular well.

Averaged values of permeability to air among the 54 cores range from 6.4 to 100.6 millidarcies, with an average of 24.9 millidarcies. A map of averaged core permeability (Figure 19) shows significant contrast between large areas of the unit with below-average permeability and areas with above-average permeability. A north-south trending streak of high permeability runs through the west-central part of the unit, and the southern part of the unit also displays above-average permeability, along with a smaller area in the north. A cross-plot of porosity and permeability is shown (Figure 20) with a trend line, and an equation relating the two variables.

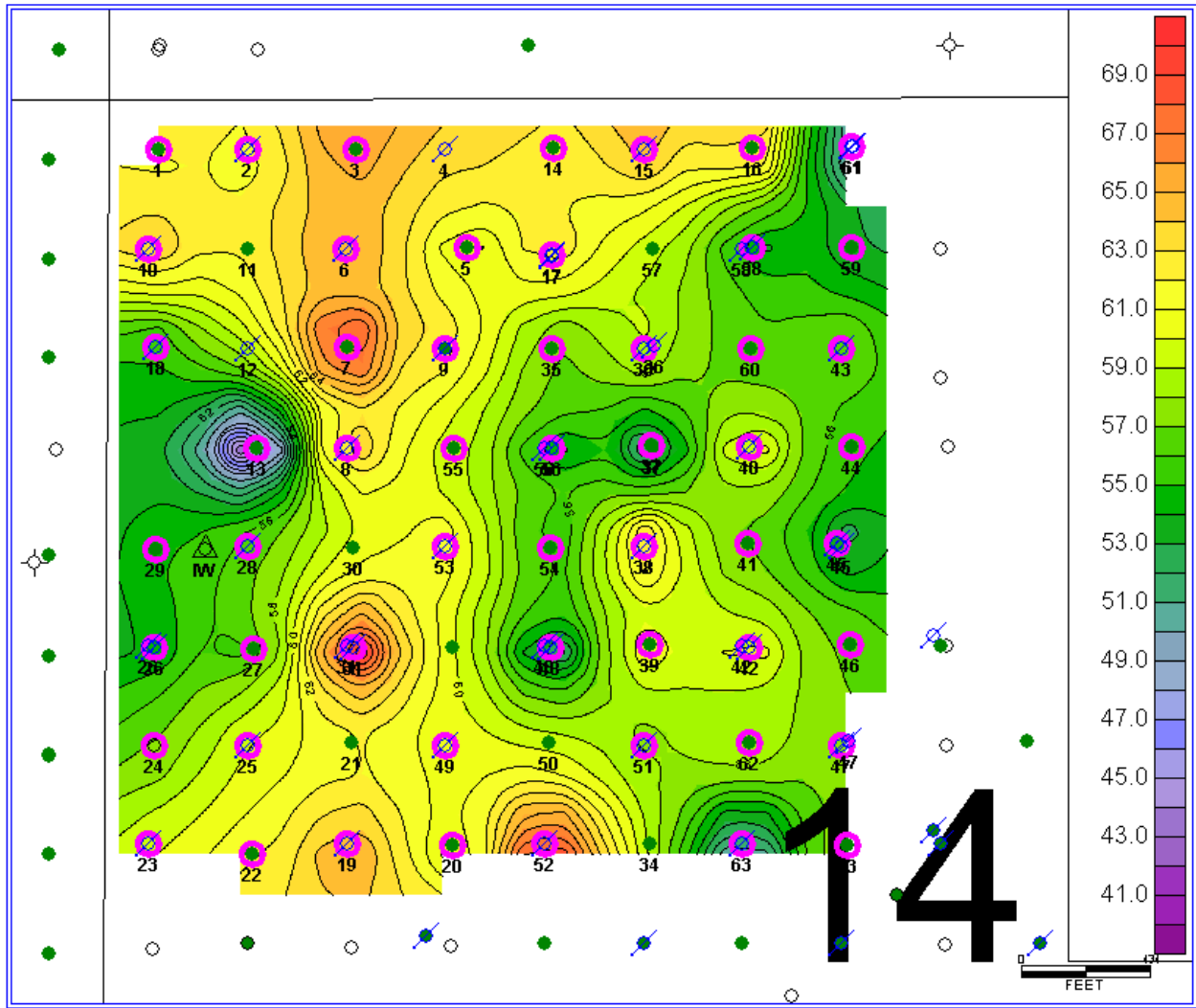
Table 3: Summary of core analysis, thickness, and  $S_o\text{-}\Phi\text{-}h$  data for Woodhead Unit wells.

Well Name	API NUMBER	Mean Oil Saturation (%)	Mean Porosity (%)	Thickness (ft.)	$S_o\text{-}\Phi\text{-}h$	Mean Permeability (mD)
WOODHEAD 1	15-045-20498	61.98	19.8	14.4	1.76	39.9
WOODHEAD 2	15-045-20499	61.21	20.1	14.0	1.73	28.8
WOODHEAD 3	15-045-20500	65.96	20.7	11.82	1.61	26.3
WOODHEAD 4	15-045-20501	63.4	20.1	11.04	1.41	
WOODHEAD 5	15-045-20532	59.51	19.2	11.33	1.3	17.9
WOODHEAD 6	15-045-20533	65.23	21.2	12.4	1.71	28.3
WOODHEAD 7	15-045-20534	70.55	21.9	13.6	2.09	48.3
WOODHEAD 8	15-045-20535	64.2	21.2	11.4	1.55	25.3
WOODHEAD 9	15-045-20548	62.81	19.8	9.5	1.18	20.2
WOODHEAD 10	15-045-20552	64.28	20.2			35.6
WOODHEAD 13	15-045-20551	41.8	14.5	10.9	0.66	6.4
WOODHEAD 14	15-045-20606	62.16	20.6	11.2	1.43	30.6
WOODHEAD 15	15-045-20607	64.94	22.5	10.4	1.52	56.2
WOODHEAD 16	15-045-20608	64.74	21.2	12.0	1.65	22.8
WOODHEAD 17	15-045-20609	62.85	21.4	12.13	1.61	17.9
WOODHEAD 18	15-045-20629	54.9	19.5	10.00	1.07	11.1
WOODHEAD 19	15-045-20630	65.17	21.8	11.9	1.7	39.5
WOODHEAD 20	15-045-20631	59.52	20.1	7.32	0.87	19.4
WOODHEAD 22	15-045-20685	61.87	19.2	13.74	1.63	23.1
WOODHEAD 23	15-045-20686	59.78	20.4	11.8	1.44	48.8
WOODHEAD 24	15-045-20687-0001	56.95	20.8	11.8	1.39	29.0
WOODHEAD 25	15-045-20705	60.06	20.7	14.0	1.75	39.2
WOODHEAD 26	15-045-20734	53.91	18.9	10.0	1.02	24.0
WOODHEAD 27	15-045-20735	55.69	19.2	10.6	1.13	14.0
WOODHEAD 28	15-045-20736	56.41	19.2	13.5	1.46	19.0
WOODHEAD 29	15-045-20737	54.85	19.3	10.6	1.12	20.7
WOODHEAD 31	15-045-20743	70.45	20.8	7.6	1.12	69.6
WOODHEAD 33	15-045-20767	58.25	19.4	12.5	1.41	11.6
WOODHEAD 35	15-045-20769	56.26	19.5	10.77	1.18	18.3
WOODHEAD 36	15-045-20748	59.49	18.9	10.9	1.23	13.0
WOODHEAD 37	15-045-20771	50.66	18.9	10.25	0.98	29.1
WOODHEAD 38	15-045-20772	64.68	19.9	12.2	1.57	17.6
WOODHEAD 39	15-045-20773	61.01	20.3	10.93	1.35	17.6
WOODHEAD 40	15-045-20774	61.22	20.3	10.5	1.31	18.0
WOODHEAD 41	15-045-20790	56.54	19.7	8.6	0.95	11.5
WOODHEAD 42	15-045-20791	60.91	20.7	12.0	1.52	19.7
WOODHEAD 43	15-045-20792	57.45	19.9	12.3	1.4	10.6



Table 3 (cont.): Summary of core analysis, thickness, and  $S_o\text{-}\Phi\text{-}h$  data for Woodhead Unit wells.

Well Name	API NUMBER	Mean Oil Saturation (%)	Mean Porosity (%)	Thickness (ft.)	$S_o\text{-}\Phi\text{-}h$	Mean Permeability (mD)
WOODHEAD 44	15-045-20793	55.17	19.5	8.3	0.89	9.6
WOODHEAD 45	15-045-20794	52.39	19.3	11.0	1.11	12.7
WOODHEAD 46	15-045-20795	56.7	19.7	9.0	1	9.9
WOODHEAD 47	15-045-20825	57.11	19.6	14.2	1.58	11.8
WOODHEAD 48	15-045-20809	50.89	18.6	14.5	1.37	9.0
WOODHEAD 49	15-045-20810	60.17	19.3	11.7	1.36	23.6
WOODHEAD 51	15-045-20812	57.64	21.0	11.2	1.36	13.3
WOODHEAD 52	15-045-20813	69.59	18.9	10.7	1.4	39.4
WOODHEAD 53	15-045-20814	62.11	19.1	13.1	1.56	13.6
WOODHEAD 54	15-045-20815	54.47	18.1	16.0	1.58	27.1
WOODHEAD 55	15-045-20816	59.37	20.2	12.8	1.28	26.3
WOODHEAD 56	15-045-20817	53.6	20.0	12.1	1.3	9.1
WOODHEAD 58	15-045-20819	53.69	19.5	11.8	1.24	16.3
WOODHEAD 59	15-045-20820	53.1	19.5	14.1	1.46	9.0
WOODHEAD 60	15-045-20821	56.12	19.0	10.0	1.06	19.7
WOODHEAD 61	15-045-20822	49.43	19.1	13.09	1.23	34.5
WOODHEAD 62	15-045-20823	59.2	21.0	10.11	1.26	15.5
WOODHEAD 63	15-045-20824	49.23	18.8	10.0	1.05	39.0



PTRE+U70611 1212694

Fig. 15: Oil saturation map of Squirrel sandstone in Woodhead Unit. Data at each well averaged over the cored interval. Woodhead Unit well numbers labeled, highlighted wells indicate data points and contours are represent percent oil saturation.

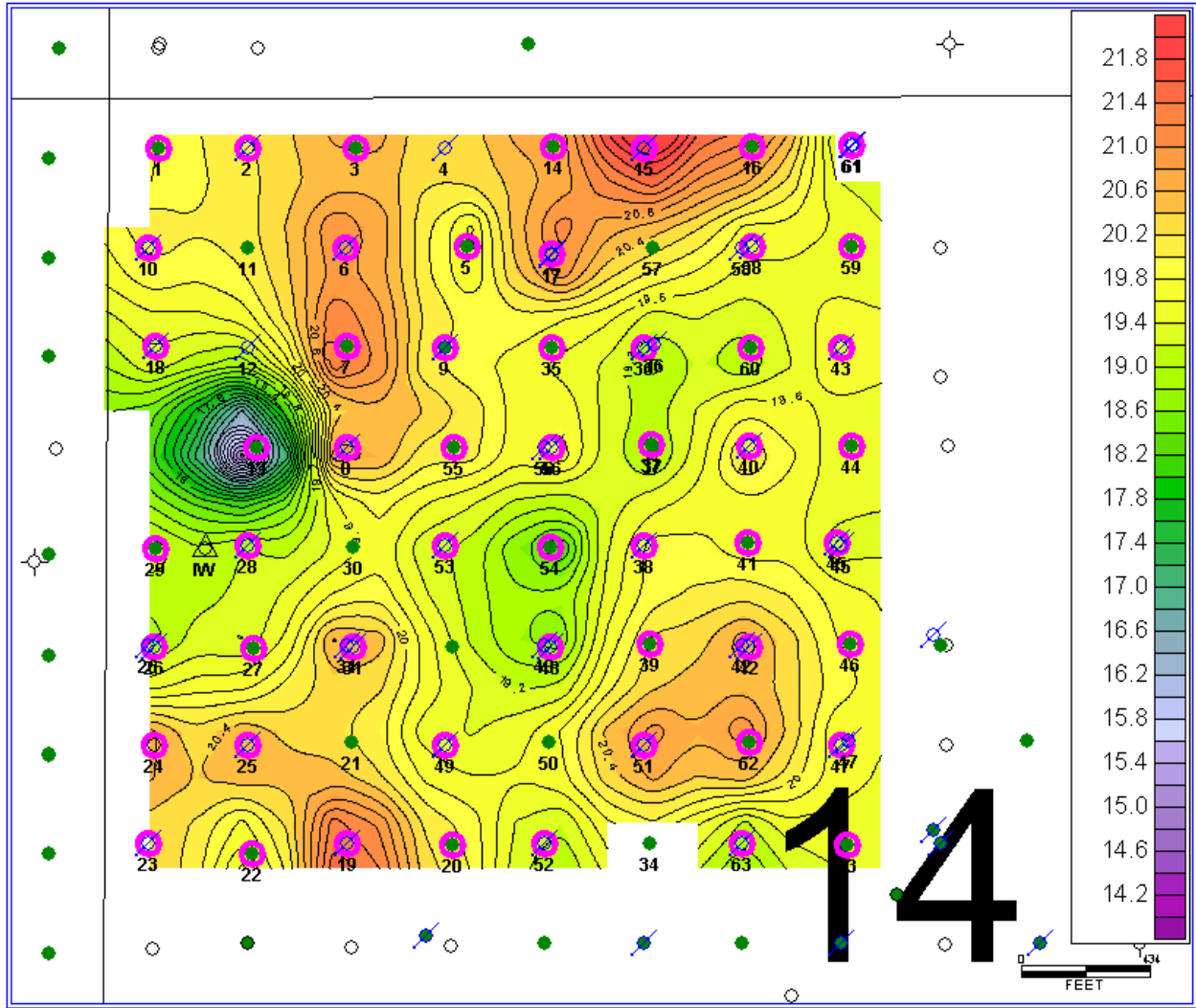


Fig. 16: Average porosity map of Squirrel sandstone in Woodhead Unit. Woodhead Unit well numbers labeled, highlighted wells indicate data points and contours represent percent porosity.

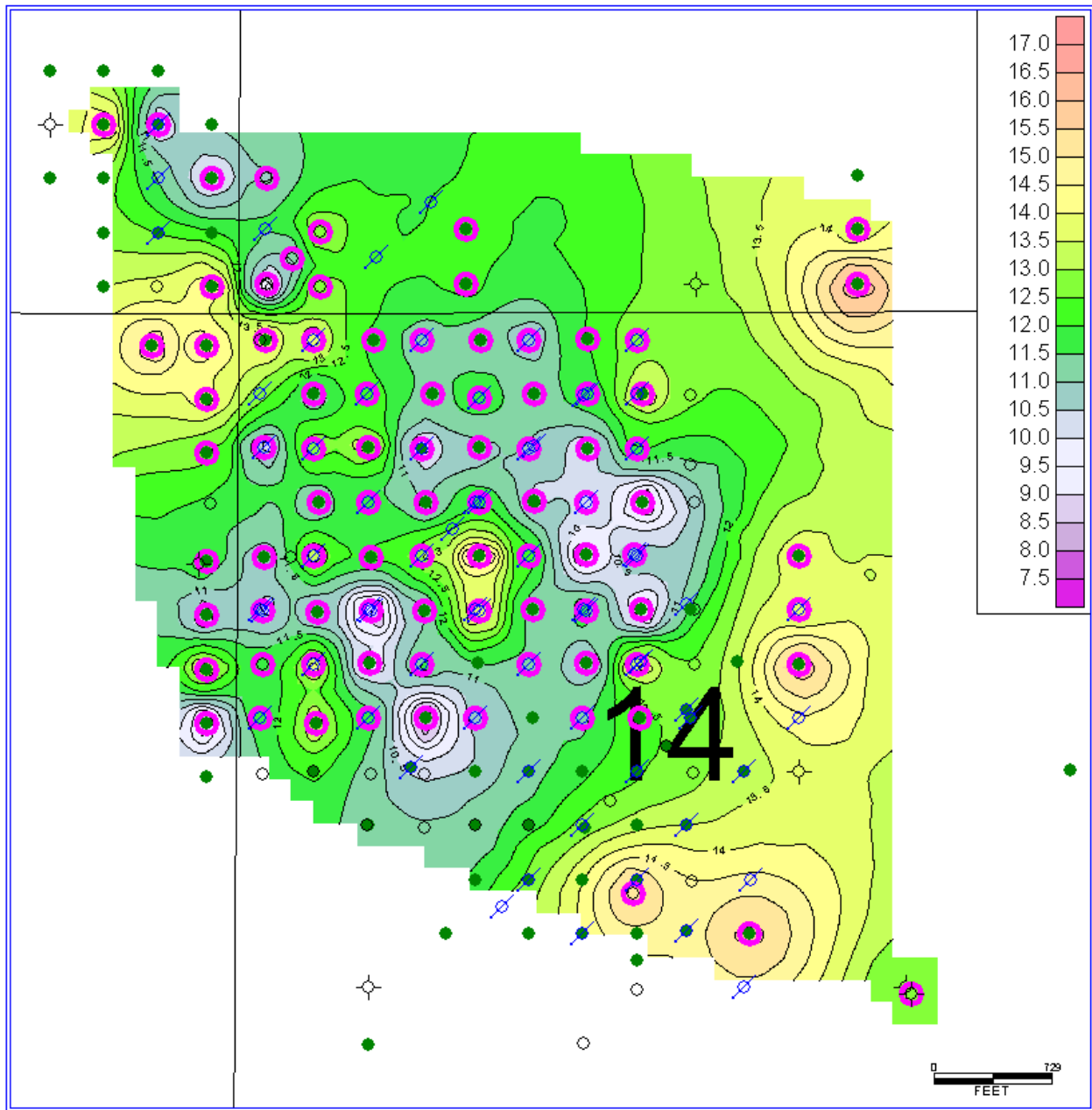


Fig. 17: Thickness map of Squirrel sandstone in Woodhead Unit. Highlighted wells indicate data points and contours are feet thickness.

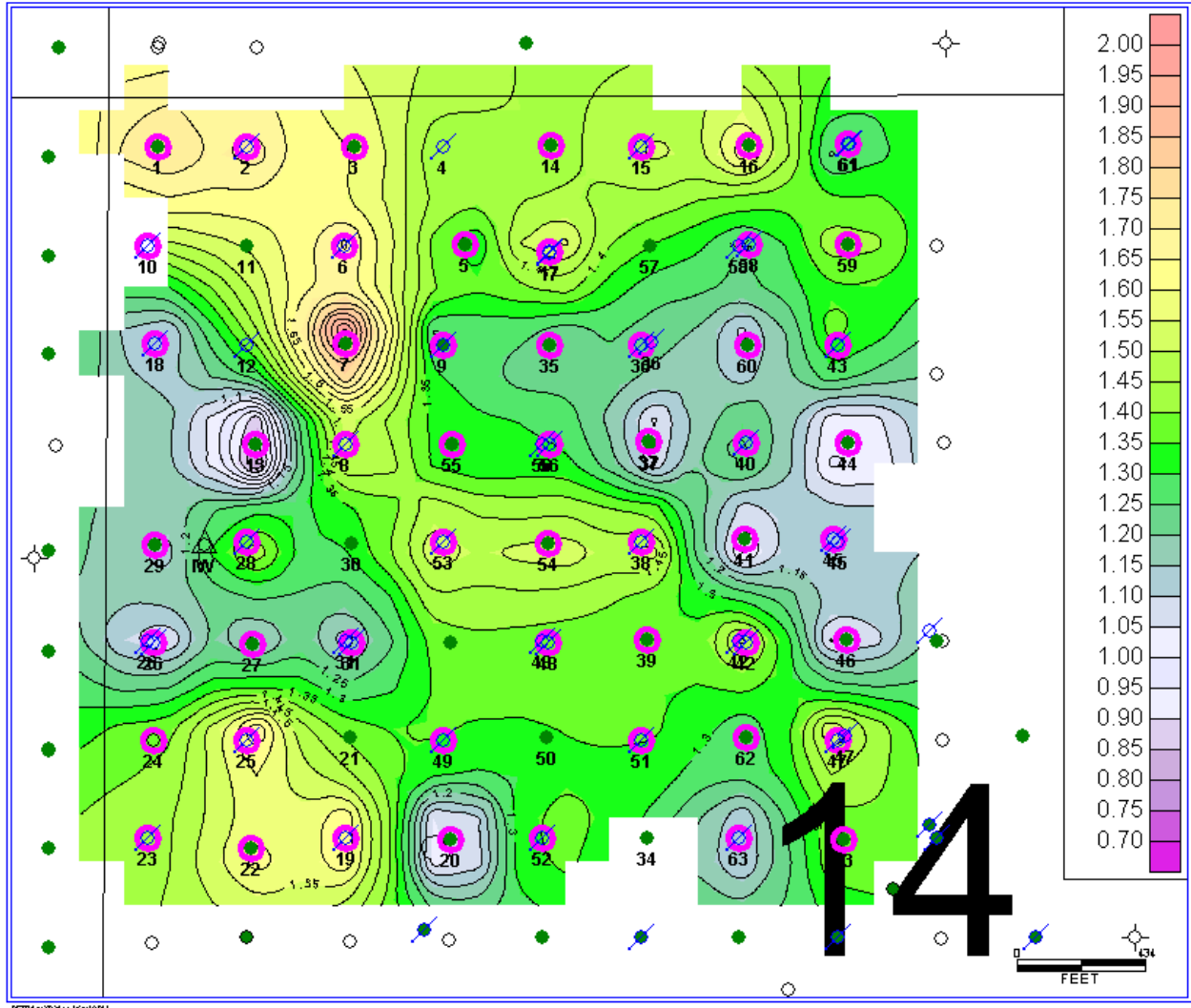


Fig. 18:  $S_o \cdot \Phi \cdot h$  map (oil saturation times porosity times thickness) of Squirrel sandstone in Woodhead Unit. Woodhead Unit well numbers labeled, highlighted wells indicate data points.

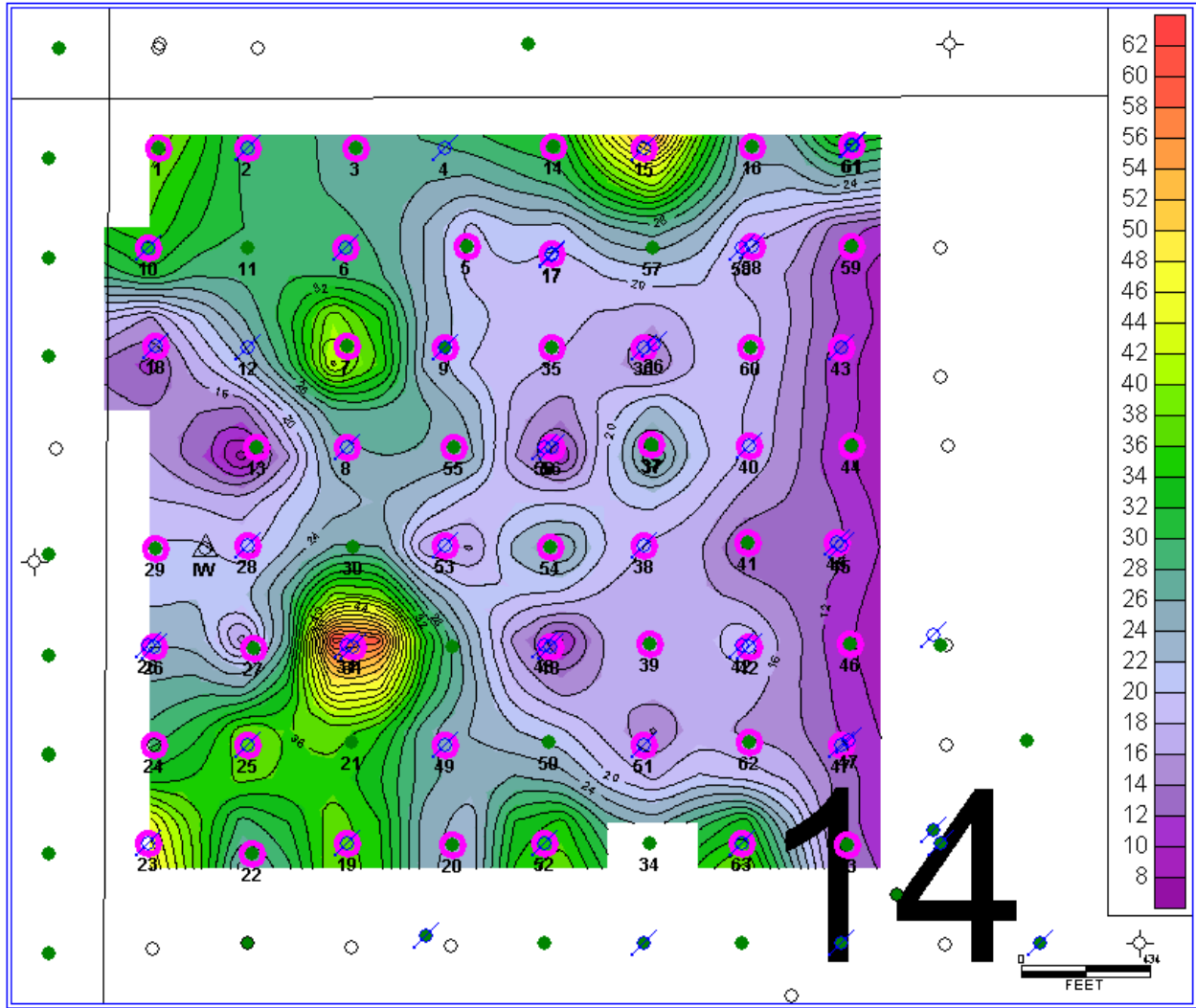
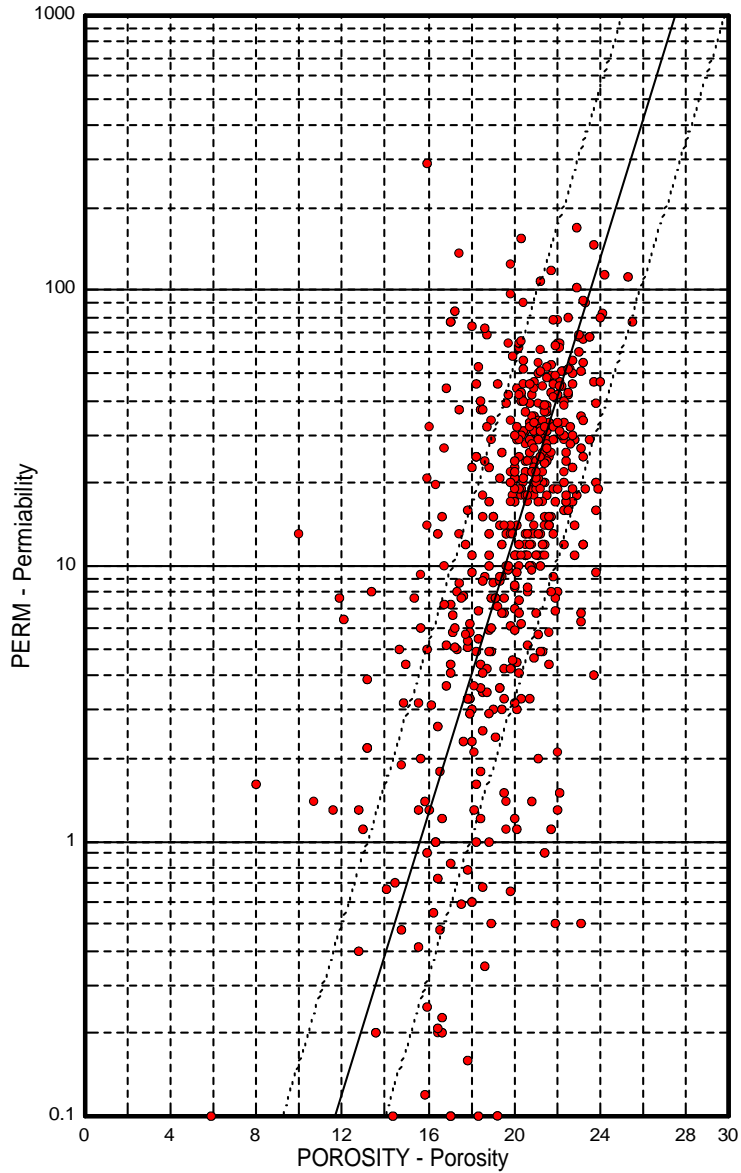


Fig. 19: Average permeability (millidarcies) map of Squirrel sandstone in Woodhead Unit. Woodhead Unit well numbers labeled, highlighted wells indicate data points and contours represent permeability to air in millidarcies.

# WOODHEAD-VINLAND FIELD

511 Samples for 54 out of 54 Wells



PETRA 4/27/2011 2:32:13 PM

Fig. 20: Cross-plot of porosity and permeability data from cores in Woodhead Unit with trendline and equation, generated in Petra™.

## **8. VOLUMETRICS**

Volumetric calculations were performed to give an estimate of stock tank barrels of original oil in place (STB OOIP) for the Woodhead Unit. The calculations and data are reproduced in the Appendix. A total of 1,570,953 STB OOIP is estimated for the Woodhead Unit. Primary production (1984-1990) of 96,334 STB gives a recovery of 6.1% of OOIP, and cumulative production of 329,354 STB gives a total cumulative recovery of 20.9% of OOIP. Secondary production (1990-present) thus accounts for recovery of 14.8% of OOIP. According to the estimates presented in this report over 1.2 million barrels of oil, or over 79% of OOIP, remain in the reservoir.

## **9. DATA AVAILABILITY**

Data availability is excellent for the Woodhead Unit. 54 of 63 unit wells were cored, and most of the wells were logged. Core reports provide information on the porosity, permeability, and water saturation. Gamma ray-neutron well logs were collected for most of the wells, so not only is the log coverage of the unit extensive, it is consistent. Oil production data for the Woodhead Unit are available at the KGS website [www.kgs.ku.edu](http://www.kgs.ku.edu), along with scanned logs for many wells. Data on water injection, well locations, and well status were provided by the field operator. Despite the dense coverage of data in the unit, lack of well log data in the immediately surrounding area leaves uncertainty as to the lateral extent and full structural nature of the overall Vinland Field.

## **10. SUITABILITY FOR ENHANCED RECOVERY**

Current production levels have declined to below what they were before the start of the waterflood, and so now is a good time for the operator to give serious consideration to moving on to a tertiary recovery phase. The Woodhead Unit has several factors that establish it as a good candidate for tertiary recovery, including the dense well spacing and the demonstrated positive response of the reservoir to waterflooding during secondary recovery. The dense well spacing of the unit means a good opportunity exists for rapid response of the reservoir to surfactant flooding. The closer the injection wells are to producers, the quicker the oil will be



swept into the producers; oil production increased measurably in less than one year from the beginning of waterflooding.

The volumetric estimation of original oil in place presented in this study indicates significant remaining reserves. Primary and secondary production phases have so far recovered less than 30% of OOIP. Given that the data presented are only estimates, the remaining reserves of over 1.2 million barrels of oil in the unit is a significant amount and could potentially be exploited for years to come. If a tertiary recovery phase could produce an incremental 10% of OOIP, which is less than what waterflooding has produced, an additional 150 Mbo could be produced. Based on the estimated remaining reserves and potential for incremental recovery a surfactant flood could potentially boost production in the short term and extend the life of the unit.

## **11. CONCLUSION**

The Woodhead Unit covers one quarter section, occupying a part of the Vinland oil field in Douglas County, Kansas. The unit includes 63 wells and produces oil from the informally named Squirrel sandstone in the Middle Pennsylvanian Cherokee Group at measured depths around 700 feet. The reservoir sandstone is in the upper Cabaniss Formation and is just below the Excello shale and Mulky coal bed. Production began in 1984, and waterflooding was initiated in 1990. Colt Energy, Inc. of Fairway, Kansas, is the current operator of the unit. Annual oil production is in the 2000 barrel per year range, and cumulative production is 329,354 barrels, or 20.9% of estimated OOIP.

The current annual oil production from the unit is less than it was before waterflooding began, and has declined by 92% from the peak annual waterflood production. Moving to a surfactant flood could potentially boost production rates and recover significant incremental oil. The dense well spacing of the unit means would allow the effectiveness of surfactant flooding to be ascertained relatively quickly. Because the unit consists of over 60 wells, a small-scale pilot flood could be undertaken without disrupting significantly the ongoing waterflood. If such a small-scale surfactant flooding demonstration project were undertaken and proven successful, a larger-scale operation could be utilized to enhance production of oil at the Woodhead Unit and demonstrate the applicability of EOR techniques to shallow sandstone reservoirs in eastern Kansas.

## 12. REFERENCES

Brenner, Robert L., 1989, Stratigraphy, petrology, and paleogeography of the upper portion of the Cherokee Group (Middle Pennsylvanian), eastern Kansas and northeastern Oklahoma: Kansas Geological Survey, Geology Series 3, 76 pages (available online at <http://www.kgs.ku.edu/Publications/Bulletins/GS3/index.html>).

Kansas Geological Survey website: <http://www.kgs.ku.edu>

## 13. APPENDIX

Volumetric estimation of stock tank barrels of original oil in place (STB OOIP) was done as follows:

$So*\Phi*$ thickness values for each well (feet) multiplied by area of well spacing (2.5 acres\*43560 ft<sup>2</sup>/ac = feet squared) yields the volume of oil in ft<sup>3</sup>, which is then converted to reservoir barrels using the conversion factor 1 bbl = 5.615 cubic feet. This number was then divided by the formation volume factor, Bo (reservoir bbl/STB), to obtain a final number in STB. Core reports indicate a Bo of 1.05. The result is an estimate of the number of stock tank barrels of oil originally in place in each 2.5 acre area of the Woodhead Unit. Summing the results gives an estimate of STB OOIP.

Nine wells had no  $So*\Phi*$ thickness values so the average value of the unit was assigned to these wells and the same process described above was performed. Summing the STB OOIP values for all 63 of the Woodhead Unit wells gives an estimate of STB OOIP for the entire unit.

**Table of data used in volumetric calculations:**

Well Name	$So*\Phi*$ thickness(ft)	$So*\Phi*$ thickness(ft) x (2.5 acres x 43560 sq ft per acre (ft <sup>2</sup> )) = ft <sup>3</sup> of oil	reservoir bbls oil (1bbl/5.615ft <sup>3</sup> )
WOODHEAD 1	1.76	191664	34134
WOODHEAD 2	1.73	188397	33552
WOODHEAD 3	1.61	175329	31225
WOODHEAD 4	1.41	153549	27346
WOODHEAD 5	1.3	141570	25213
WOODHEAD 6	1.71	186219	33165
WOODHEAD 7	2.09	227601	40534
WOODHEAD 8	1.55	168795	30061
WOODHEAD 9	1.18	128502	22885
WOODHEAD 13	0.66	71874	12800
WOODHEAD 14	1.43	155727	27734
WOODHEAD 15	1.52	165528	29480
WOODHEAD 16	1.65	179685	32001
WOODHEAD 17	1.61	175329	31225
WOODHEAD 18	1.07	116523	20752

WOODHEAD 19	1.7	185130	32971
WOODHEAD 20	0.87	94743	16873
WOODHEAD 22	1.63	177507	31613
WOODHEAD 23	1.44	156816	27928
WOODHEAD 24	1.39	151371	26958
WOODHEAD 25	1.75	190575	33940
WOODHEAD 26	1.02	111078	19782
WOODHEAD 27	1.13	123057	21916
WOODHEAD 28	1.46	158994	28316
WOODHEAD 29	1.12	121968	21722
WOODHEAD 31	1.12	121968	21722
WOODHEAD 33	1.41	153549	27346
WOODHEAD 35	1.18	128502	22885
WOODHEAD 36	1.23	133947	23855
WOODHEAD 37	0.98	106722	19007
WOODHEAD 38	1.57	170973	30449
WOODHEAD 39	1.35	147015	26183
WOODHEAD 40	1.31	142659	25407
WOODHEAD 41	0.95	103455	18425
WOODHEAD 42	1.52	165528	29480
WOODHEAD 43	1.4	152460	27152
WOODHEAD 44	0.89	96921	17261
WOODHEAD 45	1.11	120879	21528
WOODHEAD 46	1	108900	19394
WOODHEAD 47	1.58	172062	30643
WOODHEAD 48	1.37	149193	26570
WOODHEAD 49	1.36	148104	26376
WOODHEAD 51	1.36	148104	26376
WOODHEAD 52	1.4	152460	27152
WOODHEAD 53	1.56	169884	30255
WOODHEAD 54	1.58	172062	30643
WOODHEAD 55	1.28	139392	24825
WOODHEAD 56	1.3	141570	25213
WOODHEAD 58	1.24	135036	24049
WOODHEAD 59	1.46	158994	28316
WOODHEAD 60	1.06	115434	20558
WOODHEAD 61	1.23	133947	23855
WOODHEAD 62	1.26	137214	24437
WOODHEAD 63	1.05	114345	20364

Sum: est reservoir bbls OOIP	1413858
est STB OOIP using Bo 1.05 res bbl/ STB	1346531

Average So- $\Phi$ -H 1.35

<b>9 wells with no So-<math>\Phi</math>-H data:</b>	<b>So*<math>\Phi</math>*thickness(ft)</b>	<b>2.5 acres x 43560 sq ft per acre (ft<sup>2</sup>)</b>	<b>reservoir bbls oil (1bbl/5.615ft<sup>3</sup>)</b>
WOODHEAD 10	1.35	147015	26183
WOODHEAD 11	1.35	147015	26183
WOODHEAD 12	1.35	147015	26183
WOODHEAD 21	1.35	147015	26183
WOODHEAD 30	1.35	147015	26183
WOODHEAD 32	1.35	147015	26183
WOODHEAD 34	1.35	147015	26183
WOODHEAD 50	1.35	147015	26183
WOODHEAD 57	1.35	147015	26183
Total est reservoir bbls OOIP			235643
est STB OOIP using Bo 1.05 res bbl/ STB			224422

Total STB OOIP including 9 wells with no So- $\Phi$ -H data 1570953

# MUDDY CREEK SOUTHWEST UNIT, BUTLER COUNTY, KANSAS

Peter Senior & Anthony W. Walton

## INTRODUCTION

The Muddy Creek Southwest Unit, operated by Stelbar Oil Corp. of Wichita, Kansas, produces oil from a sandstone bed in the Middle Pennsylvanian Cherokee Group in southern Butler County, Kansas. Most of the wells were drilled in the area in the 1980s, and currently the unit comprises two injectors and five producers. Waterflooding began in 1987, and 2009 production from the unit was 9,267 barrels of oil. This report provides a summary of information on the location, drilling and production history, geology, and potential for enhanced recovery of the unit.

## LOCATION

Muddy Creek Southwest and Bruce East are adjacent oilfields located in southern Butler County, Kansas, approximately 25 miles southwest of Wichita (Figure 1). Muddy Creek Southwest is the larger of the two fields, stretching through parts of five sections while Bruce East covers only one quarter-section (Figure 2). An inferred boundary shows the unit covering parts of four sections (Figure 3).



Fig 1: Regional map showing location of adjacent Muddy Creek Southwest and Bruce East oilfields (green polygon), modified from [www.kgs.ku.edu](http://www.kgs.ku.edu) 7-16-10.

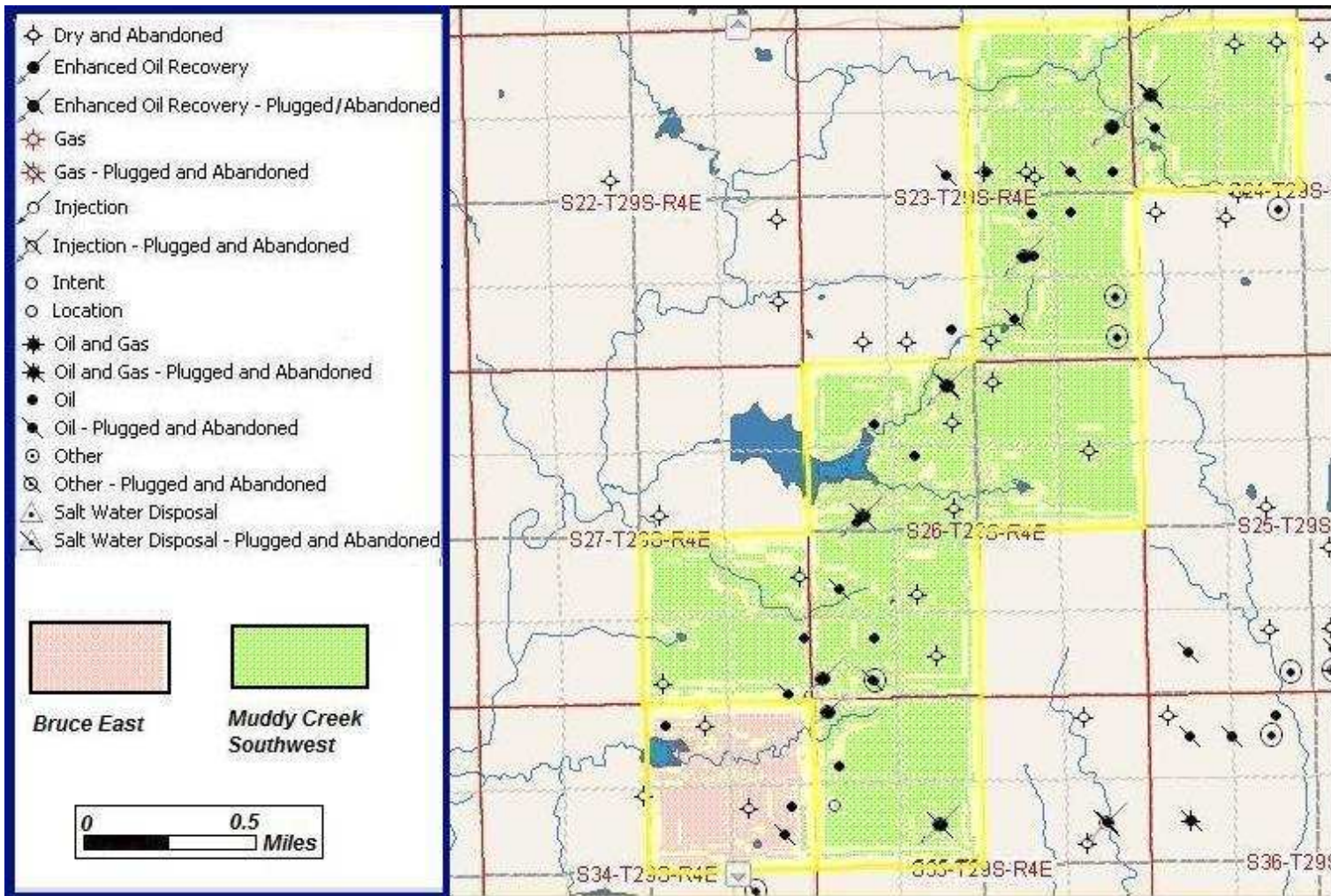


Fig. 2: Sub-regional map of Muddy Creek Southwest and Bruce East oilfields, modified from [www.kgs.ku.edu](http://www.kgs.ku.edu) 6-24-10.

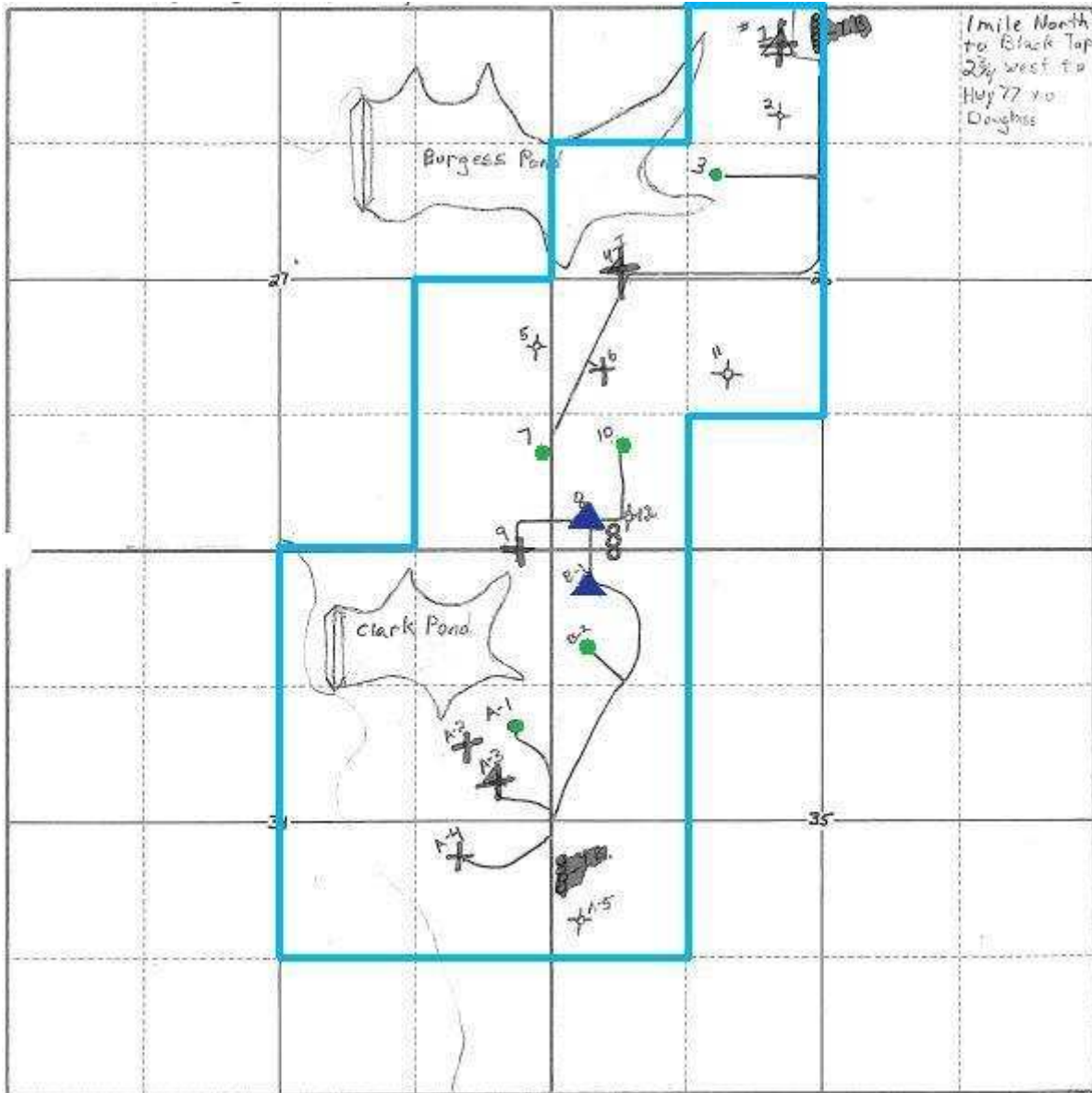


Fig. 3: Map of Muddy Creek Southwest Unit with blue line indicating inferred unit boundary. Injection wells (blue triangles), producing wells (green circles), abandoned wells (X), and dry holes are indicated. Modified from material provided by Stelbar Oil Corp.

### **3. METHODS**

This report was constructed by analyzing data in the public domain and posted on the website of the Kansas Geological Survey (KGS), along with data provided by the field operators directly to the investigators. The major methods were use of well logs to determine the configuration of key horizons to create geologic maps and cross-sections of the reservoir. The data and logs were imported into Petra™, a subsurface GIS program and analyzed using standard techniques. Production history, quantities, and rates were downloaded from the KGS website.

#### **1. DISCOVERY & DEVELOPMENT HISTORY**

The Muddy Creek Southwest Unit consists of five wells in the Muddy Creek Southwest oilfield, and two wells in the Bruce East oilfield. Discovery of oil in the Muddy Creek Southwest oilfield occurred in 1981 with completion of the Blood 39-521-1 well (API # 15-015-21626) by Kennedy & Mitchell, Inc. of Denver, Colorado. Oil was discovered in the Cherokee Group in a sandstone bed at a depth of 2841 feet, and first production occurred May 26, 1981 at a daily rate of 43 barrels of 38.5° API gravity oil and one barrel of water at 100°F. Subsequent drilling in 1981 by Stelbar Oil Corp. of Wichita, Kansas discovered oil in the same sandstone bed in the E.B. Shawver II 1-26 well (API # 15-015-21861). In November 1981 Kennedy & Mitchell drilled another dry hole, and in December 1981 Stelbar completed their second successful well, the E.B. Shawver II 3-26 (API # 15-015-21905). Stelbar continued drilling new wells in the field through the 1980s, completing seven more productive wells and one dry hole through 1986. The latest drilling activity by Stelbar in the Muddy Creek Southwest oilfield was a successful oil well completion in 2001; that well was plugged in 2007.

The Bruce East oilfield consists of ten wells, all drilled by Stelbar. Drilling in this field predates that in the Muddy Creek Southwest oilfield. The first well was drilled in 1967 but was a dry hole. The only successful oil wells were completed in the field in May 1983, the SST Bush 1 (API # 15-015-22288) and E.B. Shawver II 'A' 1 (API # 15-015-22318). Both of these wells are now incorporated in the Muddy Creek Southwest Unit, the SST Bush 1 as an injector and the EB Shawver II 'A' 1 as a producer. Table 1 provides a summary of information for the wells drilled by Stelbar Oil Corp. in the Muddy Creek Southwest Unit. Stelbar Oil Corp. is the original and current operator of the seven active wells currently making up the Muddy Creek Southwest Unit water flood, which are highlighted in Table 1.



**Table 1: Summary of wells in the Muddy Creek Southwest Unit, compiled from [www.kgs.ku.edu](http://www.kgs.ku.edu) 6-24-10. Green highlighted wells are currently producing oil, blue highlighted wells are current water injectors.**

API_NUMBER	LEASE	WELL	SECTION-TOWNSHIP-RANGE	SPOT	COMP.	PLUG.	TYPE
15-015-21861	E. B.						OIL
15-015-21861-0001	SHAWVER II	1-26	26-29S-4E	NE NE NW	25-Sep-81	22-Mar-04	INJ
15-015-21940	E. B.			W2 SE SW NW			OIL
15-015-21940-0001	SHAWVER II	4-26	26-29S-4E		8-Feb-82	16-Apr-07	INJ
15-015-22182	E. B.			NW SW			OIL
15-015-22182	SHAWVER II	6-26	26-29S-4E		11-Jan-83	23-Jul-98	OIL
15-015-22220 ****CORED****	E. B.						OIL
15-015-22220	SHAWVER II	7-27	27-29S-4E	NE SE SE	10-Jan-83		OIL
15-015-22266	E. B.			SW SW SW			OIL
15-015-22266-0001	SHAWVER	8-27	26-29S-4E		3-Mar-83		INJ
15-015-22267	E. B.			SE SE SE			OIL
15-015-22267	SHAWVER II	9-27	27-29S-4E		15-Mar-83	19-Apr-07	OIL
15-015-22336	BUSH	2	35-29S-4E	SW NW NW	1-Jul-83		OIL
15-015-23586	MUDDY CREEK SW UNIT	12	26-29S-4E	C SE SW SW	9-Jan-01	11-Apr-07	OIL
15-015-21905	E. B.			W2 E2 NW			OIL
15-015-21905	SHAWVER II	3-26	26-29S-4E		10-Dec-81		OIL
15-015-22288	SST BUSH (BRUCE EAST FIELD)						OIL
15-015-22288-0001		1	35-29S-4E	NW NW NW	2-May-83		INJ
15-015-22318	E. B.						OIL
15-015-22318	SHAWVER II 'A' (BRUCE EAST FIELD)	1	34-29S-4E	NE SE NE	10-May-83		OIL
15-015-22353	E. B.			E2 SE NE			OIL
15-015-22353	SHAWVER II 'A'	3	34-29S-4E		25-Jul-83	17-Sep-98	OIL
15-015-22800	E. B.						OIL
15-015-22800	SHAWVER	10	26-29S-4E	NE SW SW	7-Nov-85		OIL
15-015-22801	E. B.						EXPIRED INTENT TO DRILL
15-015-22801	SHAWVER II	10-26	26-29S-4E	SE SW SW			

## 5. PRODUCTION HISTORY

The present day Muddy Creek Southwest Unit is composed of three leases – the Muddy Creek Southwest Unit lease, the Bush lease, and the Ebs lease. The Muddy Creek Southwest Unit lease has been active in the Muddy Creek Southwest oilfield since 1981. The Bush lease was active from 1983 to 1988 and the Ebs lease was active from 1983 to 1987; both leases were in the Bruce East oilfield and each consisted of one producing well. Both oil wells from the Bush and Ebs leases are currently incorporated into the Muddy Creek Southwest Unit; the former Bush lease well (API# 15-015-22288) is now an injector and the former Ebs lease well (API# 15-015-22318) produces oil. Oil production data from the three leases is summarized in Table 2. Highest combined annual oil production occurred in 1983, with 176,407 barrels, and lowest production occurred in 1981 with 7,025 barrels.

Waterflooding commenced on June 1, 1987. Water injection data were made available by Stelbar Oil Corp. but annual totals were unavailable for the years 1991–1996. Water injection levels have been on a decreasing trend since at least 1997, according to materials provided by Stelbar Oil Corp. The reservoir showed a quick and pronounced positive response to water injection; annual oil production had dipped to 16,040 barrels in 1988 but rose in response to waterflooding to 59,477 barrels the following year. Fluctuations in annual oil production occurred between 1989 and the present, with a definitive decreasing trend emerging in 1993 (Figure 4). A total of 9,267 barrels of oil were produced in 2009, and cumulative oil production at the end of that year totaled 1,158,250 barrels (Figure 5). Production according to Stelbar Oil Corp. averaged 28 BOPD and 700 BWPD in May 2009 and the economic limit at such levels was \$39/bbl.

**Table 2: Annual oil production data for the three leases comprising the Muddy Creek Southwest Unit, compiled from [www.kgs.ku.edu](http://www.kgs.ku.edu) 6-24-10.**

MUDDY CRK SW UN Lease			BUSH Lease		Ebs Lease		TOTAL FOR ALL LEASES		
Year	Production	Oil Wells					Year	Production	Oil Wells
1981	7,025	3					1981	7,025	3
1982	58,794	3	<b>Production</b>	<b>Wells</b>	<b>Production</b>	<b>Wells</b>	1982	58,794	3
1983	130,802	3	27,826	1	17,779		1983	176,407	4
1984	76,792	3	26,449	1	18,518	1	1984	121,759	5
1985	38,935	3	11,898	1	7,148	1	1985	57,981	5
1986	54,939	3	6,660	1	4,128	1	1986	65,727	5
1987	28,959	3	1,325	1	975	1	1987	31,259	5
1988	16,023	3	17	1			1988	16,040	4
1989	59,477	3					1989	59,477	3
1990	37,973	3					1990	37,973	3
1991	24,413	3					1991	24,413	3
1992	52,144	3					1992	52,144	3
1993	70,708	3					1993	70,708	3
1994	55,201	3					1994	55,201	3
1995	39,516	3					1995	39,516	3
1996	32,113	3					1996	32,113	3
1997	33,933	3					1997	33,933	3
1998	43,162	3					1998	43,162	3
1999	35,467	3					1999	35,467	3
2000	23,889	3					2000	23,889	3
2001	29,309	3					2001	29,309	3
2002	22,149	3					2002	22,149	3
2003	23,887	3					2003	23,887	3
2004	21,975	3					2004	21,975	3
2005	18,280	3					2005	18,280	3
2006	16,437	3					2006	16,437	3
2007	13,322	3					2007	13,322	3
2008	9,184	5					2008	9,184	5
2009	9,267	5					2009	9,267	5
2010	1,336	5					2010	1,336	5

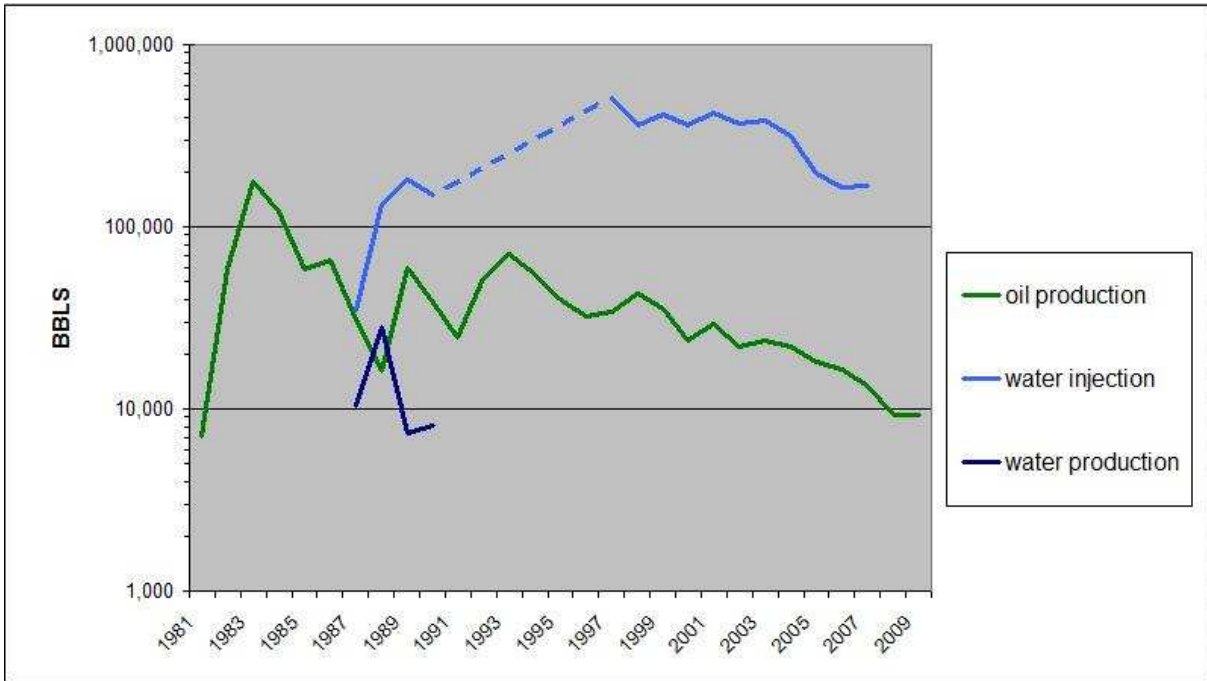


Fig. 4: Annual production and injection data for the Muddy Creek Southwest Unit. Water injection and production data from the field operator, oil production data from the KGS. Dashed line indicates unavailable water injection data from 1991–1996.

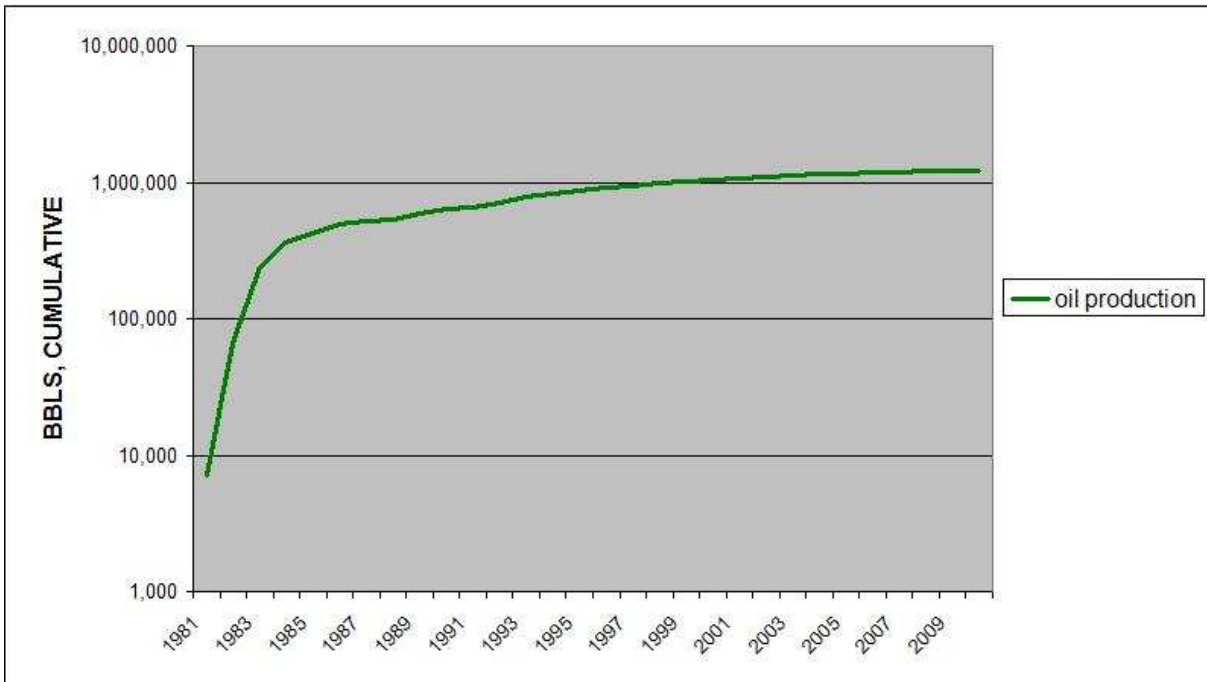


Fig. 5: Cumulative oil production data for the Muddy Creek Southwest Unit, compiled from KGS.

## 6. GEOLOGY

Oil is produced in the Muddy Creek Southwest Unit from a sandstone bed in the Middle Pennsylvanian Cherokee Group. The Cherokee Group comprises two formations, the Krebs below and Cabaniss above (Figure 6). These units consist mostly of shale, mostly gray, but ranging from nearly black to almost white. They include up to about 20% sandstone, plus thin beds of coal and limestone. Informal subdivision of this succession came about in two separate ways: at the coal mines along the outcrop belt in Labette, Cherokee, Crawford, and Bourbon counties and during oil exploration somewhat down the regional westerly dip.

Coal beds are associated with paleosol and underclay, below, with thin beds of sandstone or limestone and black shale above. A succession of authors, beginning with Abernathy (1936), recognized these marker intervals as useful stratigraphic guides. The markers are readily visible on downhole logs, especially the un-scaled gamma-ray-neutron logs that were the industry standard in southeastern Kansas for many years.

Oil industry practice led to recognition of several horizons where sandstone is common. Work by Hulse (1978) related the two systems. Harris (1984) developed a more comprehensive listing of the marker beds for the outcrop belt; his work can be applied down-dip, as long as the discontinuous extent of the various beds is recognized. Oil operators in southeastern Kansas recognized 6 sand-rich intervals in the Cherokee Group, from the top down, the Squirrel, Cattleman, Skinner, Burbank, Bartlesville, and Burgess (Figure 6; Hulse, 1978). Some of these names are local; others are correlated in from Oklahoma, where an expanded section includes more tongues of sandstone. The formal nomenclature of the Kansas Geological Survey also recognizes the Chelsea Sandstone Member of the Cabaniss Formation, between the Tebo and Scammon coal beds, and roughly equivalent to the Skinner sandstone of the oil industry.

The unit operators and the KGS website identify the reservoir in the Muddy Creek unit as the Bartlesville Sandstone, which is equivalent to the Bluejacket Sandstone of the surface outcrops. The Bartlesville Sandstone lies near the top of the Krebs Formation, below the Weir-Pittsburg coal bed. The base of the Cherokee Group onlaps the Nemaha Uplift, so that in the area of the Muddy Creek Southwest unit, the lowest unit is just below the Weir-Pittsburg coal bed, or above the level of the Bartlesville sandstone. The reservoir in the Muddy Creek unit lies between the Mineral or Fleming coal bed, below, and the Croweburg coal bed, placing it in the

Cabaniss Formation, and meaning that the *Muddy Creek Southwest unit produces from a Cattleman sandstone*.

Imprecision of naming of sandstone beds in the Cherokee is widespread in the southeastern Kansas oil industry. It may be partially a result of the tendency to have multiple different sandstones in the same interval; the Squirrel interval, between the Verdigris Limestone and the Excello Shale, at the top of the Cherokee, is well known for having sandstone beds at several different levels. One story about the origin of the term is that it was named because sandstone beds in that interval “jumped around like a squirrel”. In portions of the outcrop belt, upper and lower beds of the Bluejacket Sandstone Member are present. Sandstone reservoirs also commonly occupy valleys cut into older units, truncating underlying markers. Despite the difficulties posed by the different sandstone beds at about the same level, despite the confusion caused by valley incision and filling, and despite the effort and level of understanding required to identify the exact producing bed, it is worth tracking stratigraphy as accurately as possible, because the channel-like trends can be mapped only if the investigator knows which bed he or she is tracing.

A typical well log response through the reservoir is shown in Figure 7. The EB Shawver II #7-27 well (API# 15-105-22220) was cored through the reservoir at 2840 to 2853 feet. Analysis by Kansas Cores of Wichita indicated five feet of reservoir-quality sandstone, described as slightly friable and fine grained, with streaks of black shale throughout. Quantitative data from the core analysis are reproduced and summarized in Table 2.

Lithologic descriptions of the sandstone reservoir are available from geologist’s reports in three wells: EB Shawver II #1-27 (API# 15-015-21861) by Clark A. Roach, EB Shawver II #8-27 (API# 15-015-22266) and Muddy Creek SW Unit 12 (API# 15-015-23586) by Joe M. Baker. These geologist’s reports describe the sandstone as light gray to tan to brown, angular to subangular, micaceous to limy with black carbonaceous shale streaks. Texture is described as fine to medium to coarse grained with fining upward trends, and fair to good porosity is visible. The sandstone reservoir in the Muddy Creek Southwest Unit was likely deposited in an environment similar to that of the Bartlesville sandstone in the nearby Sallyards oilfield, a low gradient, southwestward flowing, meandering stream during an episode of sea level regression (Hulse, 1979). Both sandstones are incised-valley deposits and are of similar geologic age.

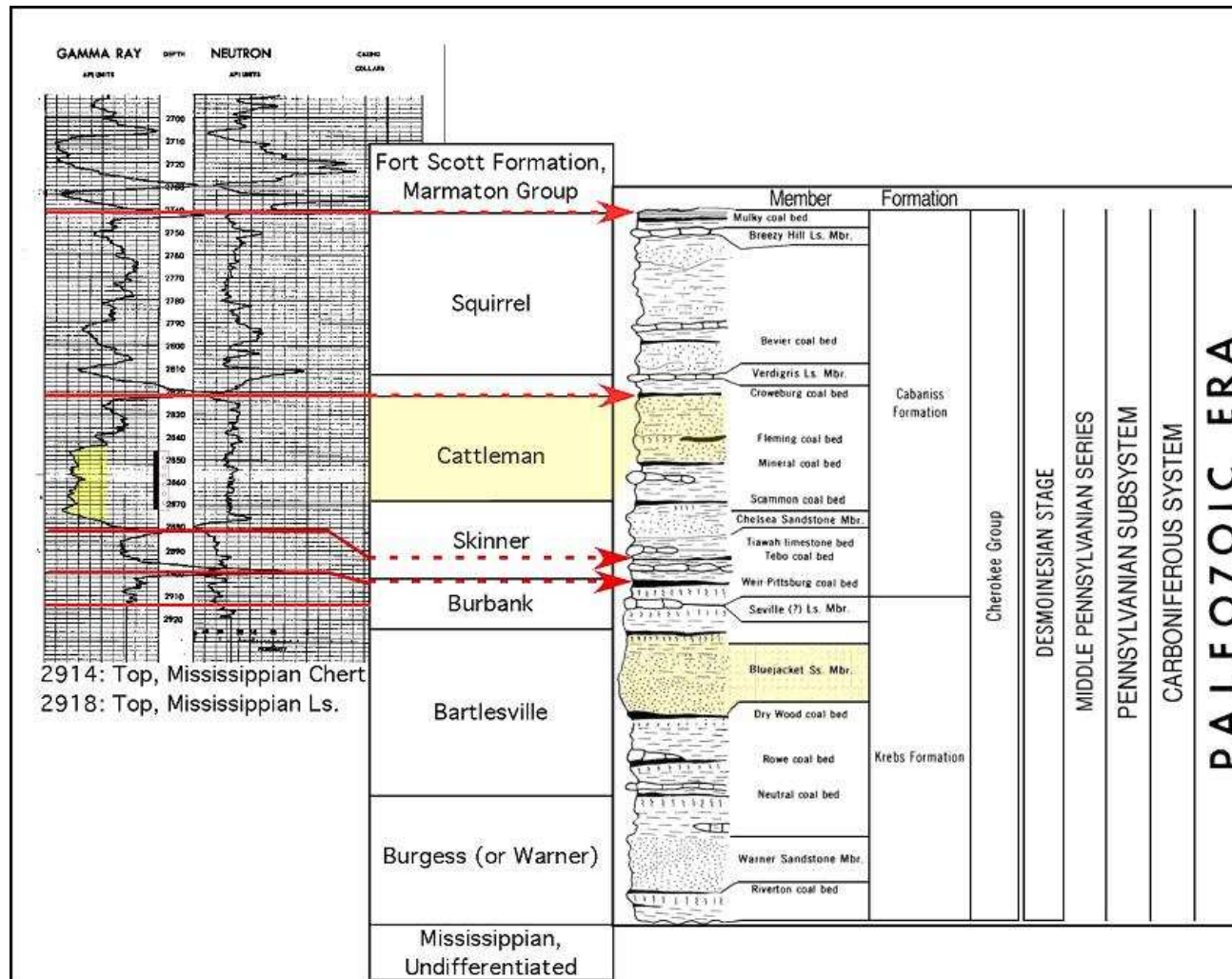


Figure 6. Correlation of the reservoir interval of the Muddy Creek Southwest unit. Left: gamma-ray-neutron log of Stelbar Oil Company's E.B. Shawver II 8-26 well (API# 15-025-22266), showing highlighted reservoir interval. Top of Mississippian is from Baker (1983). Center: Hulse (1978) designation of sand-bearing intervals in the Cherokee Group in Greenwood County, Kansas. Right: Standard Kansas Geological Survey nomenclature for the Cherokee Group (Zeller, 1968). In Butler County, the base of the Cherokee, up to a level just below the Weir-Pittsburg coal bed, is missing because of progressive on-lap to the Nemaha Uplift. The reservoir sandstone correlates to the Cattleman interval of Hulse (1978), with its base eroded into the underlying Skinner interval.

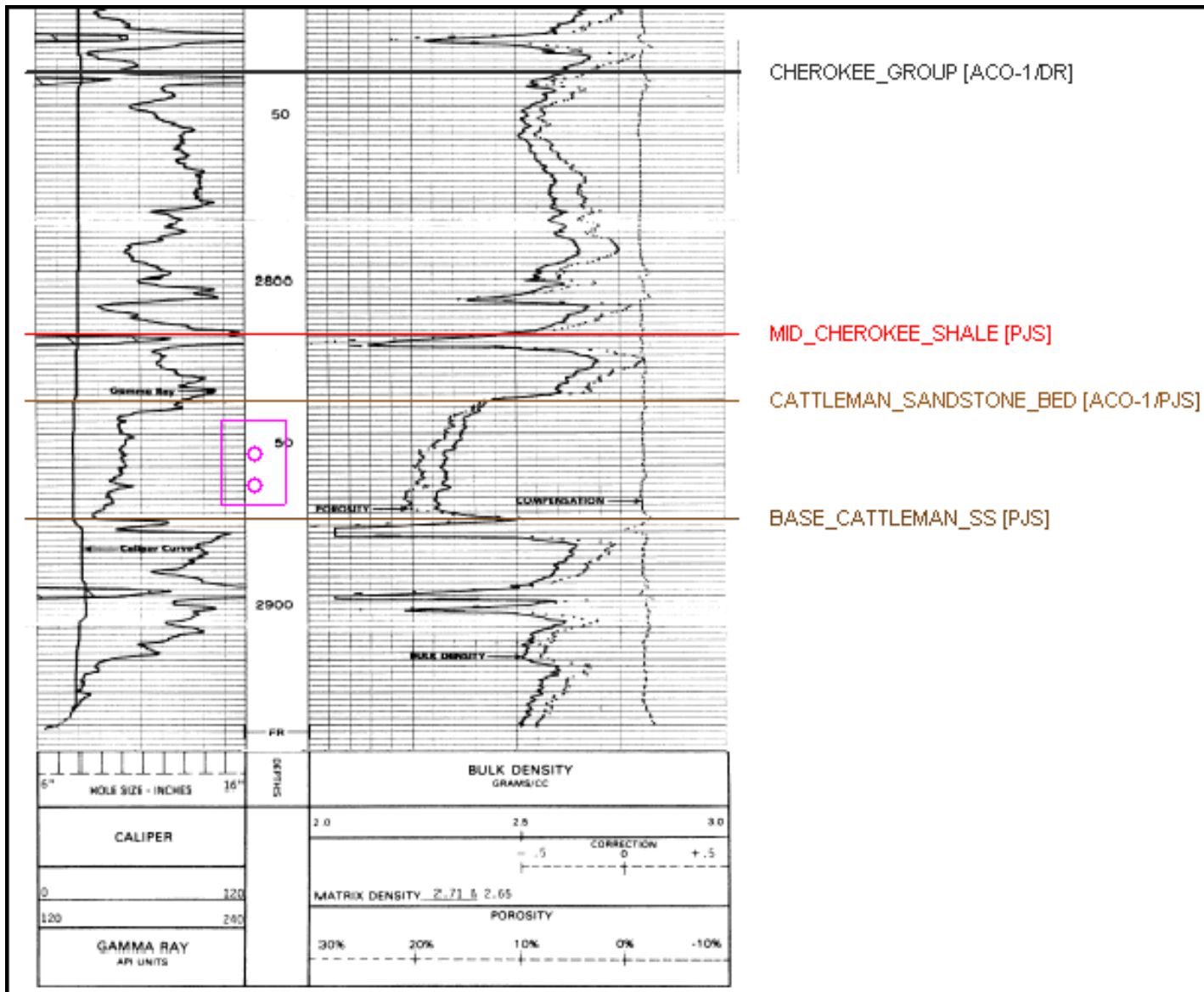


Fig 7: Well log section through sandstone reservoir in EB Shawver 8-27 well (API# 15-015-22266); perforated zone marked with pink box.



**Table 2: Summary of core analysis on EB Shawver 7-27 well  
(API# 15-015-22220) by Kansas Cores.**

Depth	permeability (md)		porosity %	water sat. (% pore space)	oil sat. (% pore space)
	horizontal	vertical			
2841-42	28.1	22.7	16.9	40.1	25.9
2842-43	32.5	23.8	16.2	34.8	25.4
2842-44	47.2	38.9	20.6	29.6	23.4
2842-45	31.2	22.7	14.1	37.7	27.9
2842-46	15.6	7.8	16.6	27.1	23.1
average permeability					30.9 md
average porosity					16.9%
average water saturation (% pore space)					33.9
average oil saturation (% pore space)					25.1
average connate water (calculated % pore space)					27.1
est. formation volume factor					1.18
productive capacity (productive feet x average permeability)					155
recoverable oil by water drive (bbls per acre foot)					365 - 45%OOIP
recoverable oil by gas expansion (bbls per acre foot)					203 - 25%OOIP

**Table 3: Summary of drill-stem test results from  
E.B. Shawver 1-26 well (API# 15-015-21861)**

Test	Pressure	Comments
IHH	1410	
IFP	50-105	Open 45", strong blow
ISIP	1085	SI 45"
FFP	115-135	Open 45", strong blow
FSIP	1085	SI 60"
FHH	1410	
Temp: 115°F		
Gas to surface 25 min.		
Rec. 40' 38° oil, 90' very slightly mud cut oil, 180' muddy gassy oil (85%oil), 60' muddy gassy oil (40% oil)		

Well-completion forms for wells in the unit record initial gas production of amounts too small to measure or none at all, and Stelbar Oil Corp. operates the waterflood by re-injecting produced water. The lack of significant gas production with the oil from the reservoir indicates that primary production from the reservoir was driven by fluid expansion. The results of a drill-stem test in the E.B. Shawver II 1-26 well (API# 15-015-21861) are available and are summarized in Table 3.

Information useful for constructing geologic maps in the Muddy Creek Southwest area is somewhat sparse. Formation top data is sparse in this particular part of Butler County, Kansas, and well logs were not available on many wells in the area. A regional structure map of the top of the Cherokee Group was constructed, and the approximate position of the buried Humboldt fault was added based on Kansas Geological Survey Open-file Report no. 91-48 (Figure 8).

The structural trend of the sandstone reservoir in the Muddy Creek Southwest Unit is high in the northeast to low in the southwest (Figure 9). A cross-sectional view across the unit (Figure 10) shows a sandstone body with a roughly lenticular shape at a time shortly after deposition. A bump in the structure lies along the border of section 23 and 26, surrounded by three dry holes (Figure 9). The sandstone reservoir continues and is productive to the northeast of the bump. Shown in cross-section (Figure 11), the structurally high area or bump is penetrated by an abandoned injection well. All wells in the Muddy Creek Southwest Unit are to the southwest and are structurally lower. The EB Shawver II 3-26 well (API# 15-015-21905) is optimally placed in section 26 to produce any oil pushed updip toward the bump from the two injectors in the unit.

Hydrocarbons are stratigraphically trapped in the sandstone, which is overlain by a thin black shale. Thickness of the sandstone reservoir in the Muddy Creek Southwest Unit ranges from around 10 to 40 feet in wells which penetrate it (Figure 12). The thickest sand section in the unit is in and around the two injector wells. Average porosities recorded in well logs range from less than 10 to over 25 percent (Figure 13). An abandoned injector in section 26 recorded the highest average log porosity. The two active injectors with two producers to the north and two to the south recorded average log porosities in the 15 to 20 percent range.

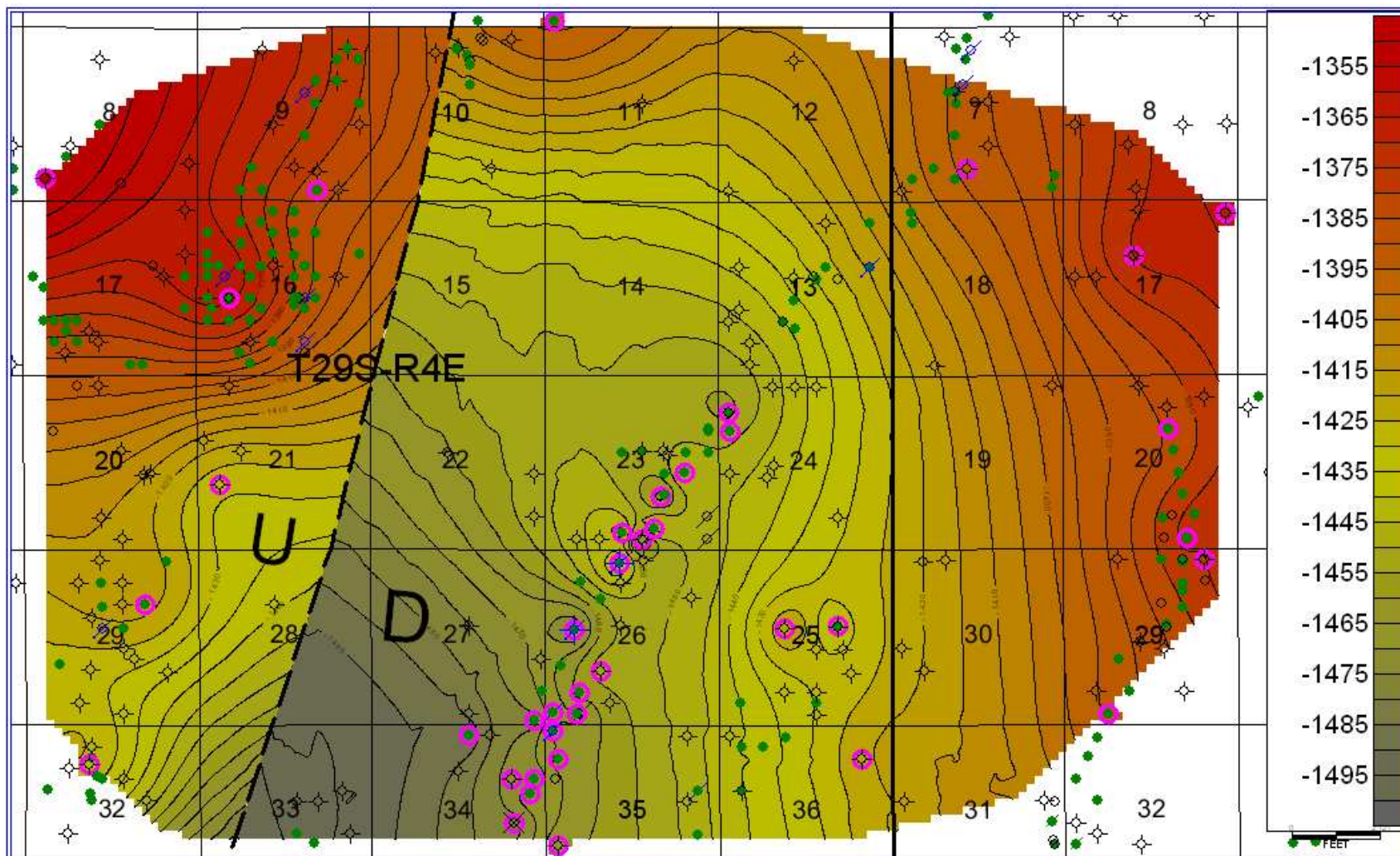


Fig. 8: Regional structure map of top of Cherokee Group. Position of buried Humboldt fault picked based on map from Aber (1991). Highlighted wells indicate data points; top of Cherokee Group was either included in KGS database or picked from well logs. Contours are in feet, datum is sea level.

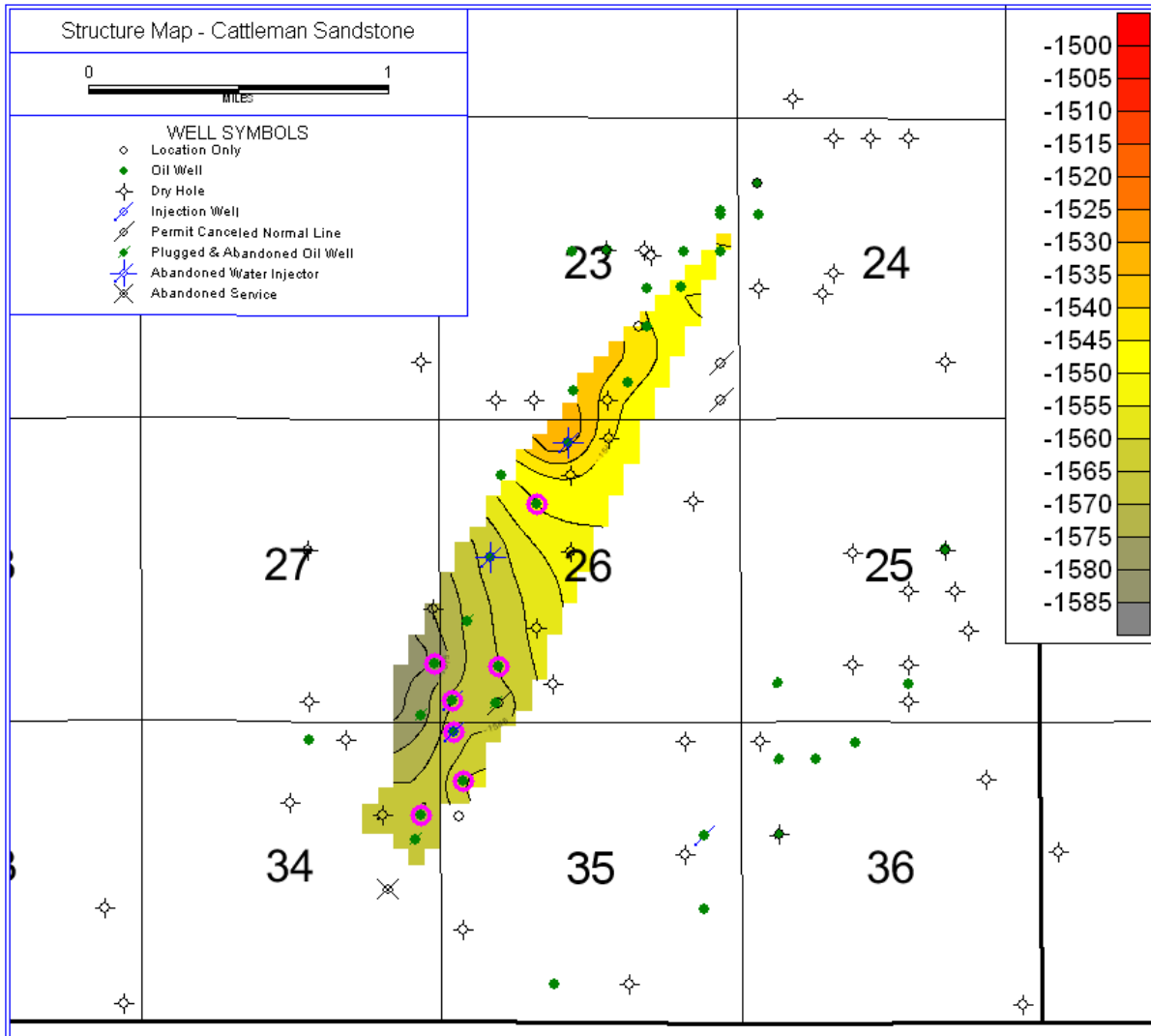
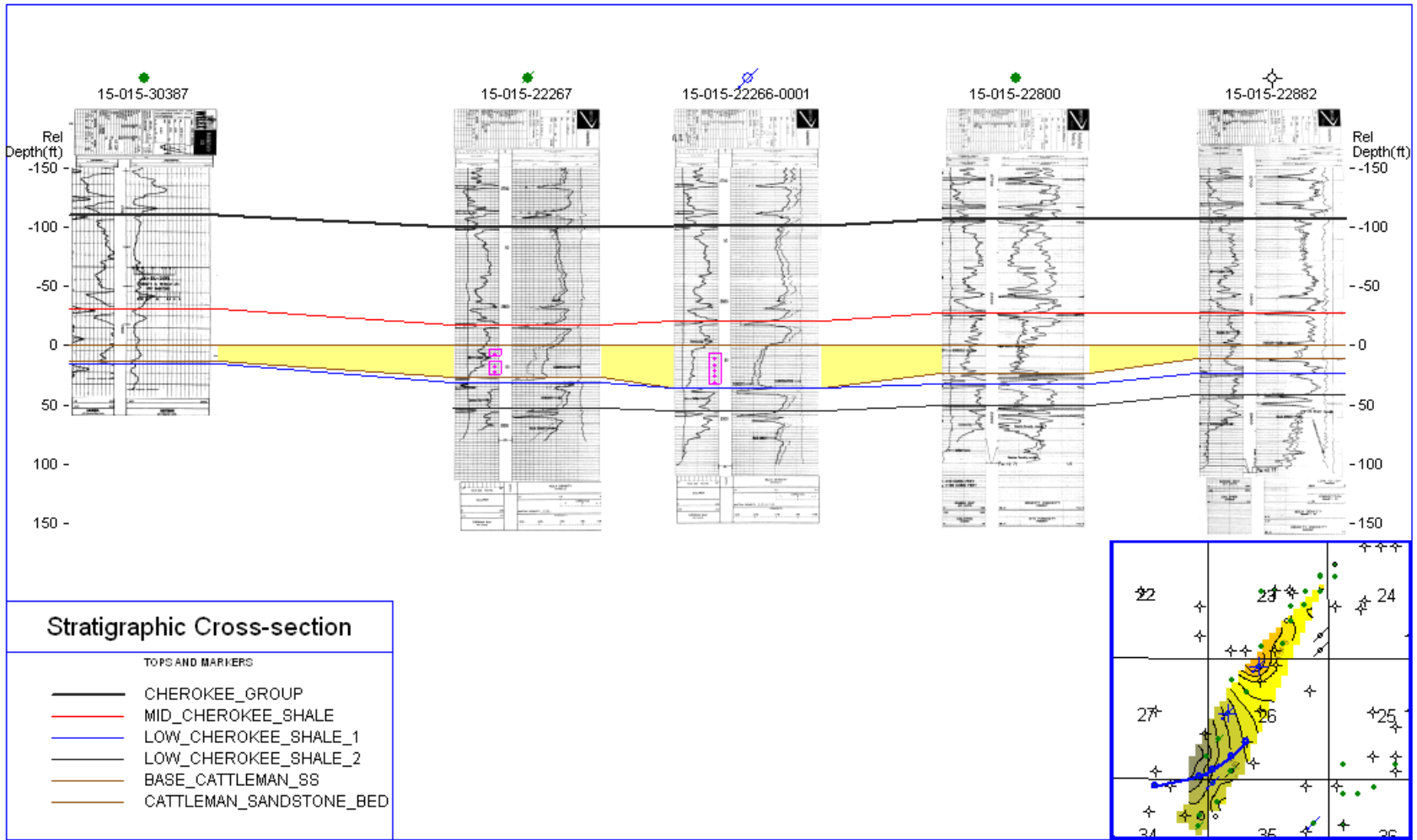


Fig. 9: Structural map of the top of the sandstone reservoir in the Muddy Creek Southwest Unit area. Wells making up the unit are highlighted, contours in feet, datum is sea level.



PETRA 7/29/2010 2:58:31 PM (see file xxxxx1 7-12-10 CSP)

Fig. 10: Stratigraphic cross-section through Muddy Creek Southwest Unit flattened on top of Cattleman sandstone bed to show lenticular character of sandstone reservoir close to time of deposition. Inset map shows orientation.

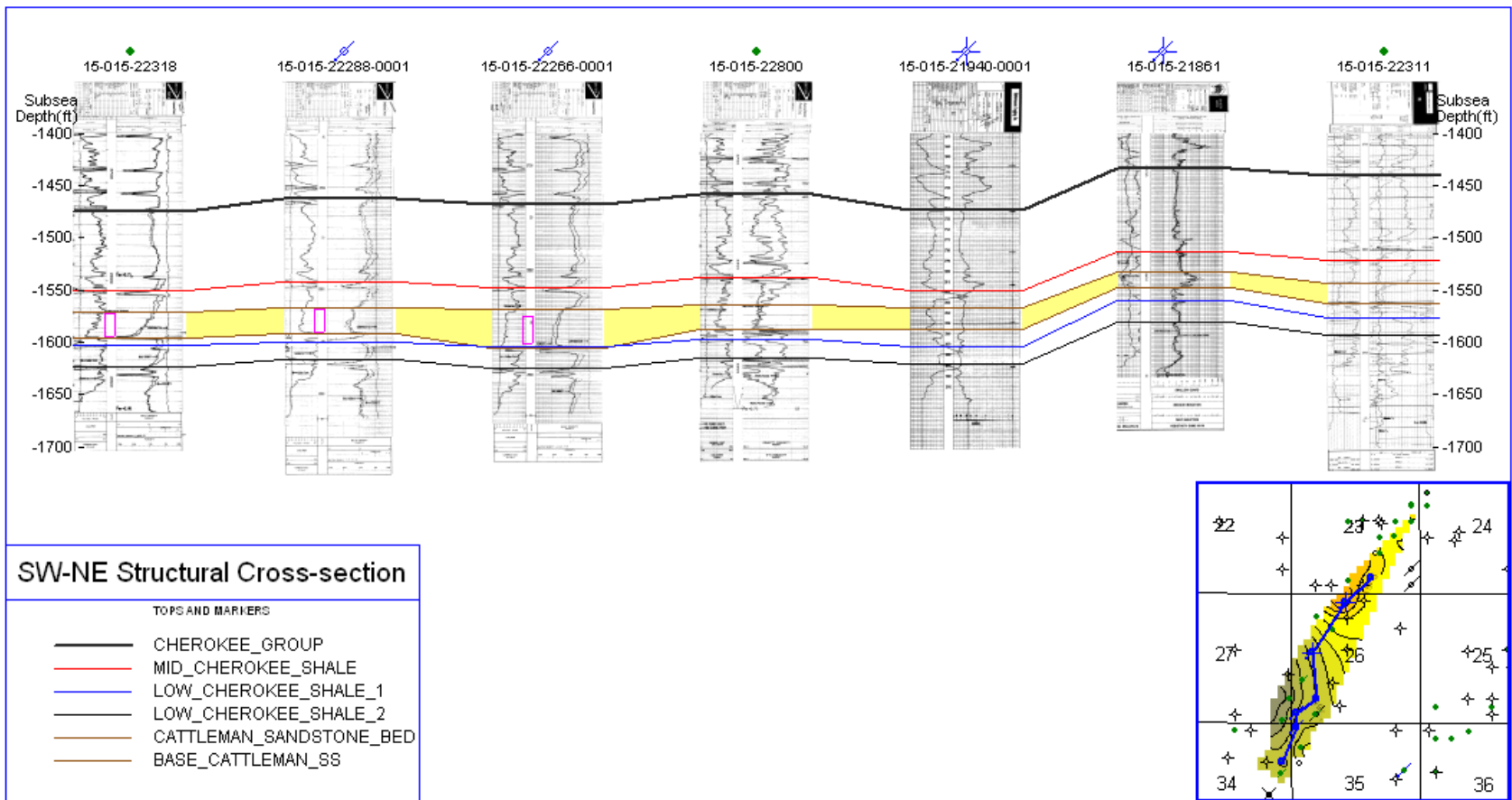


Fig. 11: Longitudinal structural cross-section through Muddy Creek Southwest Unit showing structural high penetrated by abandoned injector (API# 15-015-21861). Inset map shows orientation.

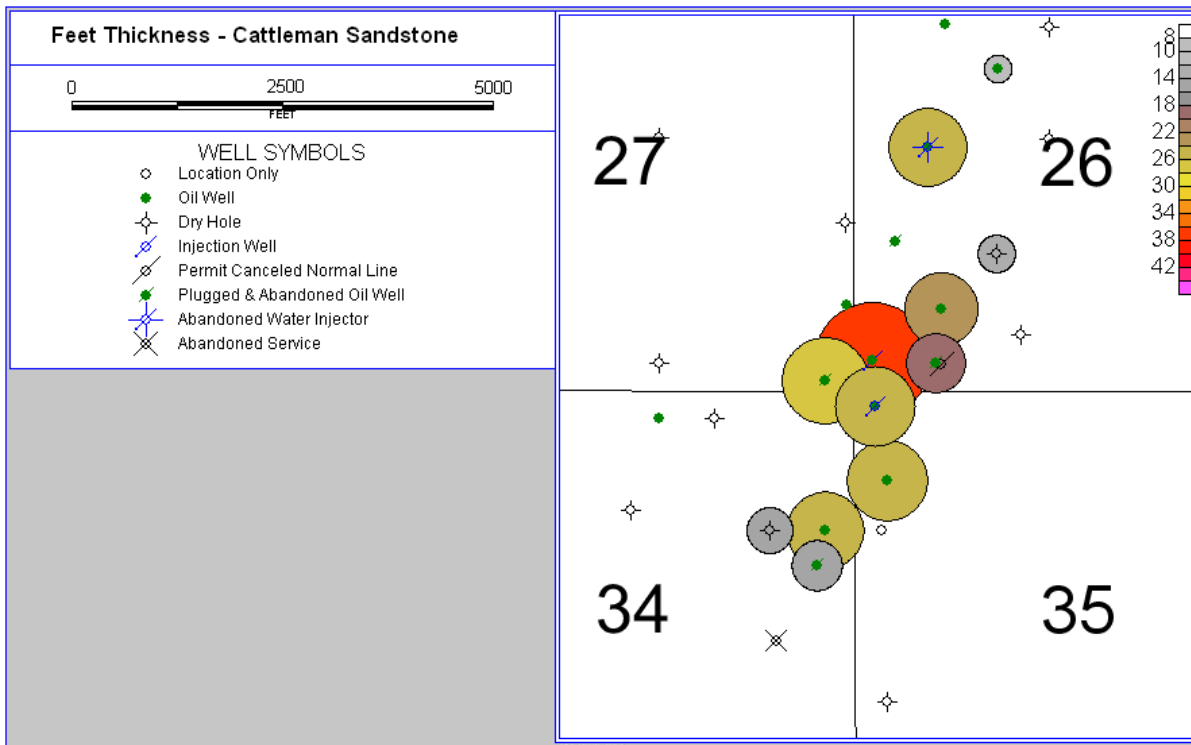


Fig. 12: Thickness map of Cattleman sandstone in Muddy Creek Southwest Unit area.

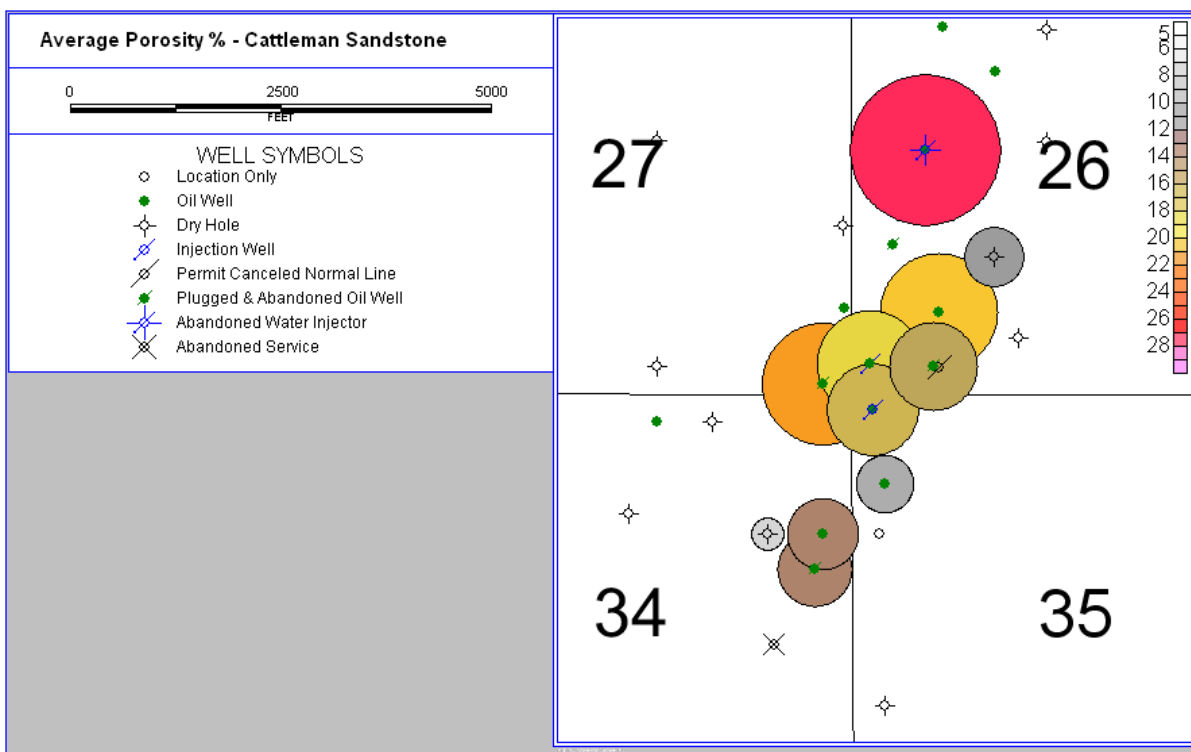


Fig. 13: Average porosity map of Cattleman sandstone in Muddy Creek Southwest area.

## **8. DATA AVAILABILITY**

Oil production data for the Muddy Creek Southwest and Bruce East oilfields is available online at the KGS website [www.kgs.ku.edu](http://www.kgs.ku.edu), including annual and cumulative data, production for individual leases, and number of producing wells in each year. Well logs, formation top data, and well completion forms, which include perforation data, are also available online from the KGS. Data on water injection and production were provided by the unit operator, Stelbar Oil Corp. of Wichita, Kansas.

## **9. SUITABILITY FOR ENHANCED RECOVERY**

Several factors indicate potential for positive results from a surfactant flooding demonstration project at the Muddy Creek Southwest Unit. The reservoir is a sandstone body that originated in a stream or river system, and as such it has an elongate shape, which has allowed for thorough development drilling and good well control. The current arrangement of injectors and producers in the unit is well suited for such a project; the two injector wells are closely spaced, with two producers to the north and two to the south. Because the injectors and producers are arranged in such a compact manner, surfactant flooding of the unit could potentially yield measurable production results in a relatively short period of time. Waterflooding at the unit produced positive results within two years, and continues to be economically viable after more than twenty years. Given an economic limit of \$39/bbl at May 2009 production levels of 28 BOPD and current (July 2010) oil prices in the \$70 to \$80/bbl range, economic potential exists for a successful surfactant flooding demonstration project in the near future. Detailed analysis of such factors as the cost of acquiring, transporting, storing, and injecting surfactants could help further determine the economic viability of surfactant flooding in the unit.



## 10. CONCLUSION

The Muddy Creek Southwest Unit includes wells in two oilfields and produces from a sandstone reservoir correlating to the informally named Cattleman Member of the Cabaniss Formation, in the Middle Pennsylvanian Cherokee Group. Production began in 1981 and waterflooding was initiated in 1987. Stelbar Oil Corp. of Wichita, Kansas drilled and currently operates all wells in the unit, which is composed of two injectors and five producers. Production averaged 28 BOPD and 700 BWPD in May 2009 and the economic limit at such levels is \$39/bbl. The reservoir is water driven and produced water is currently being re-injected.

Good potential for a successful surfactant flooding demonstration project exists in the unit. Factors such as the known spatial character of the reservoir and good well control, a favorable arrangement of injectors and producers, and a successful waterflood which produced results within two years all indicate that this unit could respond favorably to surfactant flooding. A known economic limit at recent production levels will help in considering the economic viability of a surfactant flooding demonstration project in the future.

## 11. REFERENCES

- Aber, J.S., 1991, Surficial geology of Butler County, Kansas: Kansas Geological Survey, Open-file Report, no. 91-48, 31 pages (avail. online at [http://www.kgs.ku.edu/Publications/OFR/1991/OFR91\\_48/index.html](http://www.kgs.ku.edu/Publications/OFR/1991/OFR91_48/index.html))
- Abernathy, G.E., 1936, The Cherokee of southeastern Kansas: Unpubl. Ph.D. dissertation, University of Kansas, Lawrence, KS, (avail. as Kans. Geol. Survey, Open-file Rept., no. 36-1)
- Baker, J.M., 1983, Mud log for Stelbar Oil Company's E.B. well Shawver II #8-26 (API 15-025-22266): (avail. online at <http://kgs.ku.edu>).
- Harris, J.W., 1984, Stratigraphy and depositional environments of the Krebs Formation; lower Cherokee Group (Middle Pennsylvanian) in southeastern Kansas: Unpubl. M.S. thesis, University of Kansas, Lawrence, KS (avail. as Kans. Geol. Survey, Open-file Rept., no. 84-9).
- Hulse, W.J., (1978) A geologic study of the Sallyards field area, Greenwood County, Kansas: Unpubl. M.S. thesis, University of Kansas, Lawrence, KS (avail. as Kans. Geol. Survey, Open-file Rept., no. 78-6).
- Hulse, W.J., 1979, Depositional environment of the Bartlesville sandstone in the Sallyards field, Greenwood County, Kansas, pp. 327-336, *In*, Hyne, N.J., (ed.); Pennsylvanian sandstones of the Mid-continent. Tulsa Geological Society, Special Publication, no. 1, 360 pages.
- Zeller, D.E., (ed.), 1968, The stratigraphic succession in Kansas: Kansas Geological Survey, Bulletin, no. 189, 81 pages (avail. on-line: <http://www.kgs.ku.edu/Publications/Bulletins/189/index.html>)

# STEWART OILFIELD, FINNEY COUNTY, KANSAS

Peter Senior & Anthony W. Walton<sup>1</sup>

## 1. INTRODUCTION

The Stewart oilfield is located in Finney County, Kansas and produces oil and gas from a sandstone reservoir in the Lower Pennsylvanian Morrowan Stage at measured depths in the 4700-4800 foot range. The field contains a total of 192 wells, drilled between 1952 and 2006. Waterflooding of the Morrowan sandstone reservoir commenced in 1995, and PetroSantander (USA) Inc. of Houston, Texas currently operates the field. Oil production for 2010, the most recent year for which complete data are available, was 104,181 barrels, and cumulative production is 9,817,350 barrels.

## 2. LOCATION

The Stewart oilfield is approximately 10 miles northeast of Garden City, Kansas (Figure 1). The field is in Townships 22 and 23 South, Range 31 West and Township 23 South, Range 30 West, and covers all or part of twelve sections totaling 4880 acres (Figure 2).

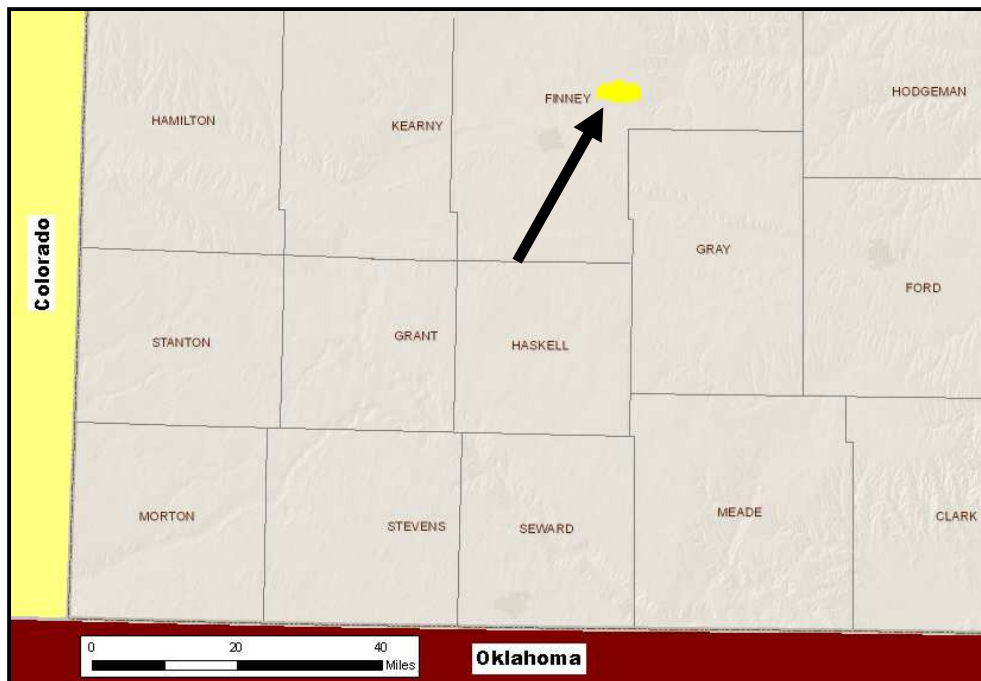


Fig 1: Regional map showing location of Stewart oilfield, modified from KGS website.

<sup>1</sup> Department of Geology, The University of Kansas, 1475 Jayhawk Blvd., Suite 120, Lawrence, Kansas 66045. Contact e-mail: twalton@ku.edu

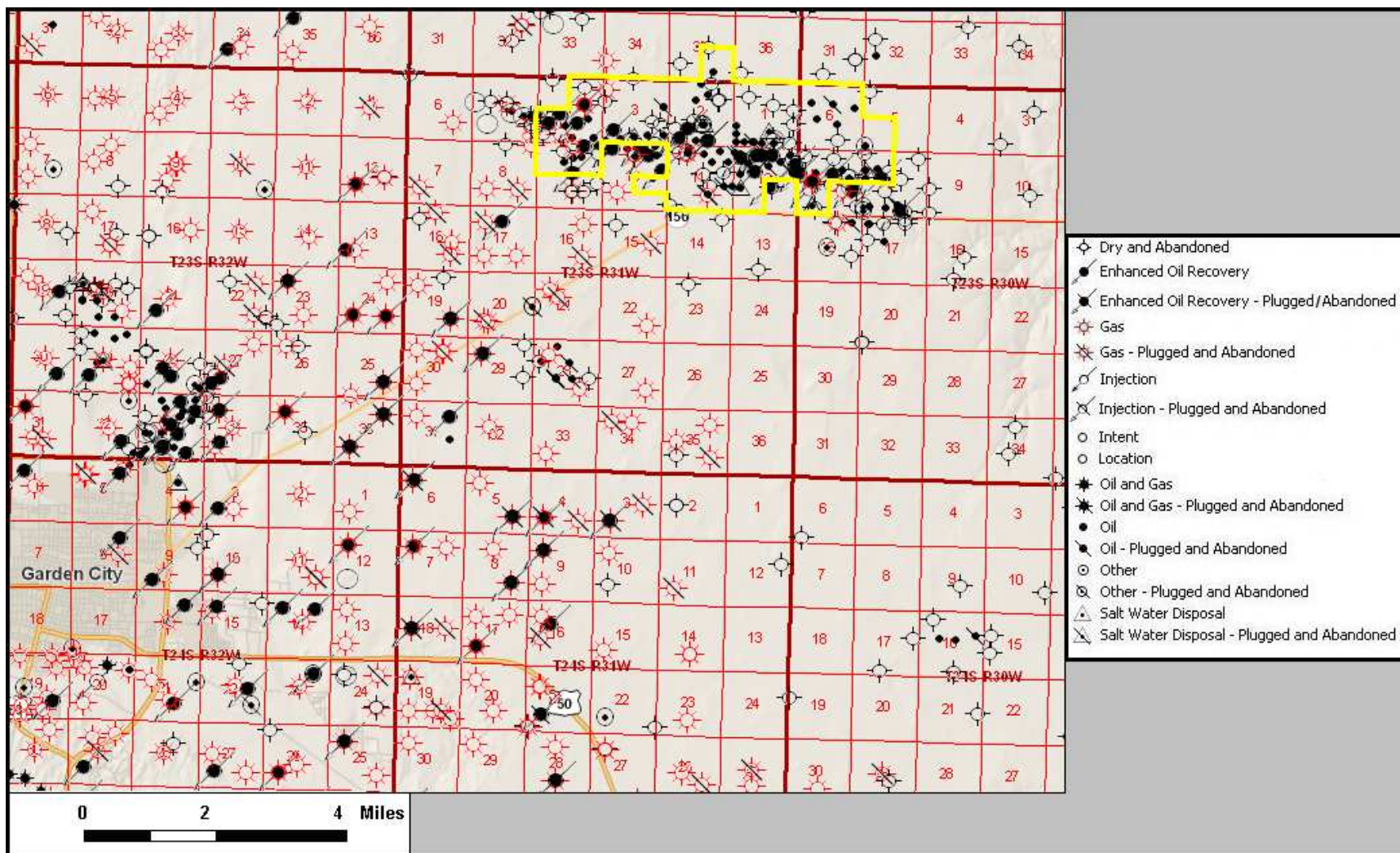


Fig. 2: Sub-regional map of Stewart oilfield, outlined in yellow, modified from KGS website.

### **3. METHODS**

This report was constructed by analyzing data in the public domain and posted on the website of the Kansas Geological Survey (KGS; [www.kgs.ku.edu](http://www.kgs.ku.edu)), along with data provided by the field operators directly to the investigators. The major methods were use of well logs to determine the configuration of key horizons to create geologic maps and cross-sections of the reservoir. The data and logs were imported into Petra™, a subsurface GIS program, and analyzed using standard techniques. The Stewart field has been the subject of several research projects and studies, so published and unpublished data were available as the basis for a significant fraction of the information presented and conclusions drawn. Production history, quantities, and rates were provided by the operator or downloaded from the KGS website (see references).

### **4. DISCOVERY & DEVELOPMENT HISTORY**

The Stewart oilfield was originally a Mississippian St. Louis Limestone discovery, however, later discovery of a sandstone reservoir in Lower Pennsylvanian Morrowan strata would prove more important. Discovery of the Morrowan reservoir occurred with drilling of the Haag Estate #1 well (API# 15-055-20002) in August 1967; the well had initial production of 99 barrels of oil per day (BOPD) from a 12 foot thick zone in the Morrowan sandstone (Green et al., 2000). Development of the oilfield proceeded slowly until the mid-1980s, when Sharon Resources began drilling more wells, aided by 2D and 3D seismic surveys (Montgomery, 1996). The Sherman #1 well (15-055-20608 ), completed in 1985, penetrated a 45 foot thick section of Morrowan sand, and subsequent drilling saw the completion of more than 30 oil producing wells and only 5 dry holes by 1994 (Montgomery, 1996). According to KGS records, since 1994 29 oil wells have been drilled, along with 14 dry holes and 5 injection wells. Figure 3 shows the location of the Mississippian and Morrowan discovery wells, and Appendix 1 contains tables of information about the wells in the Stewart oilfield.

A small waterflood project was started in 1986, but discontinued in 1991; the scale of the waterflood was limited, with only one or two wells injecting at a time. Waterflooding of the Morrowan sandstone reservoir began again after unitization of the field in 1995, with six injection wells. The waterflood pattern was developed by the field operators in conjunction with researchers at the University of Kansas. Development and installation of the waterflood was

carried out as part of a U.S. Department of Energy (DOE) research grant on improving oil recovery in fluvial-dominated deltaic reservoirs in Kansas (Green et al., 2000)

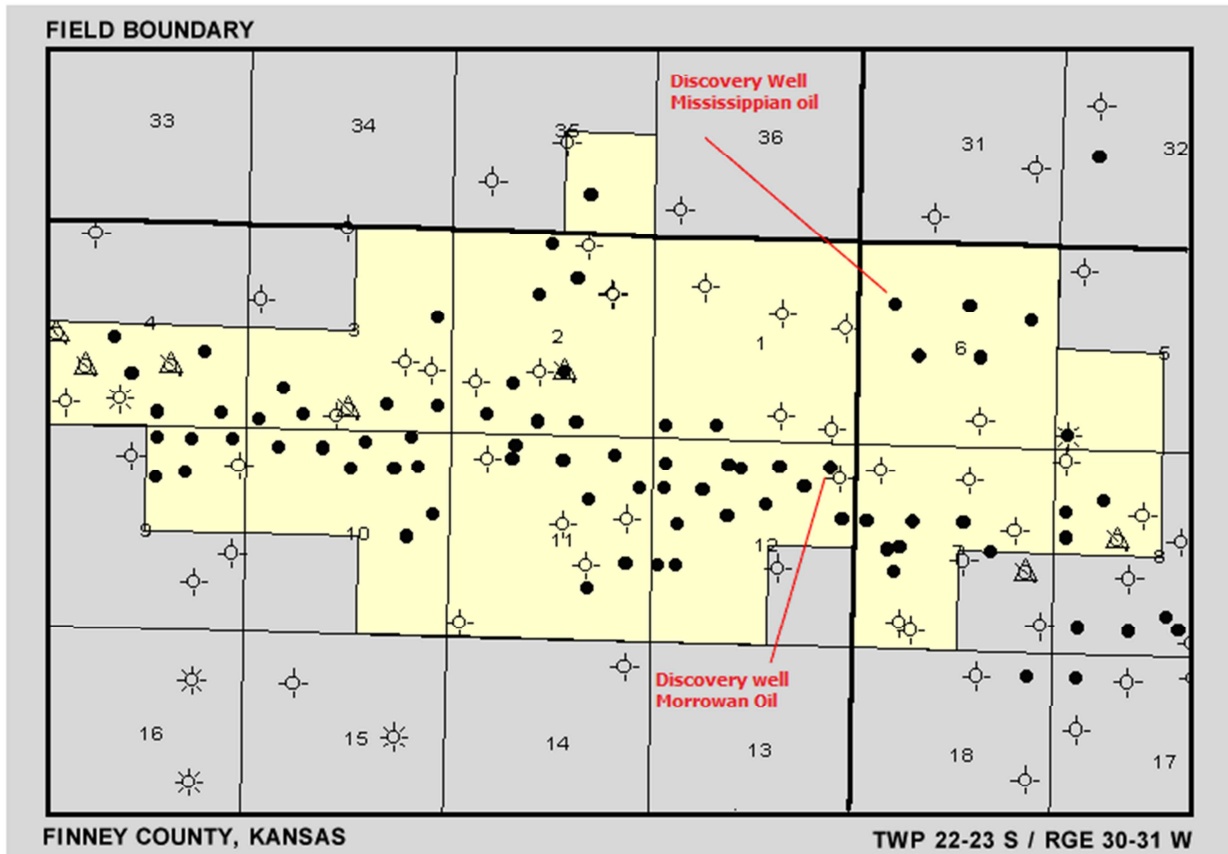


Figure 3: Well map of Stewart oilfield, showing location of discovery wells for Mississippian St. Louis Limestone and Morrowan sandstone reservoirs, from <http://www.kgs.ku.edu/DPA/Stewart/stewartSite.html>.

## 5. PRODUCTION HISTORY

Oil production data from the KGS website matches that provided by the field operator, and water injection and production data are not available from the KGS website but were provided by the field operator (Figure 4, 5, Table 2). Typical initial production rates from Morrowan wells in the Stewart oilfield were 75-120 BOPD (Montgomery, 1996), and barrel tests from 2008 indicate daily rates commonly in the 10-20 BOPD range with a few hundred barrels of water per day.

After discovery of the Morrowan reservoir in 1967, annual oil production peaked in 1968. It then declined slowly throughout the 1970s and early 1980s to around 10,000 barrels per year before rising sharply in response to rapid field development beginning in 1985. Primary production peaked at about 794,653 barrels in 1991, and then declined rapidly to a low of 172,059 barrels in 1995. Commencement of the waterflood in late 1995 led to a rapid and significant increase in production rates. Total oil production in 1996 was 256,067 barrels, an increase of almost 49% compared to 1995. Secondary production peaked in 1999 at 998,603 barrels, and annual production has since declined to 110,922 barrels in 2010, the most recent year for which complete data are available. Cumulative oil production through the end of 2011 is 9,833,207 barrels.

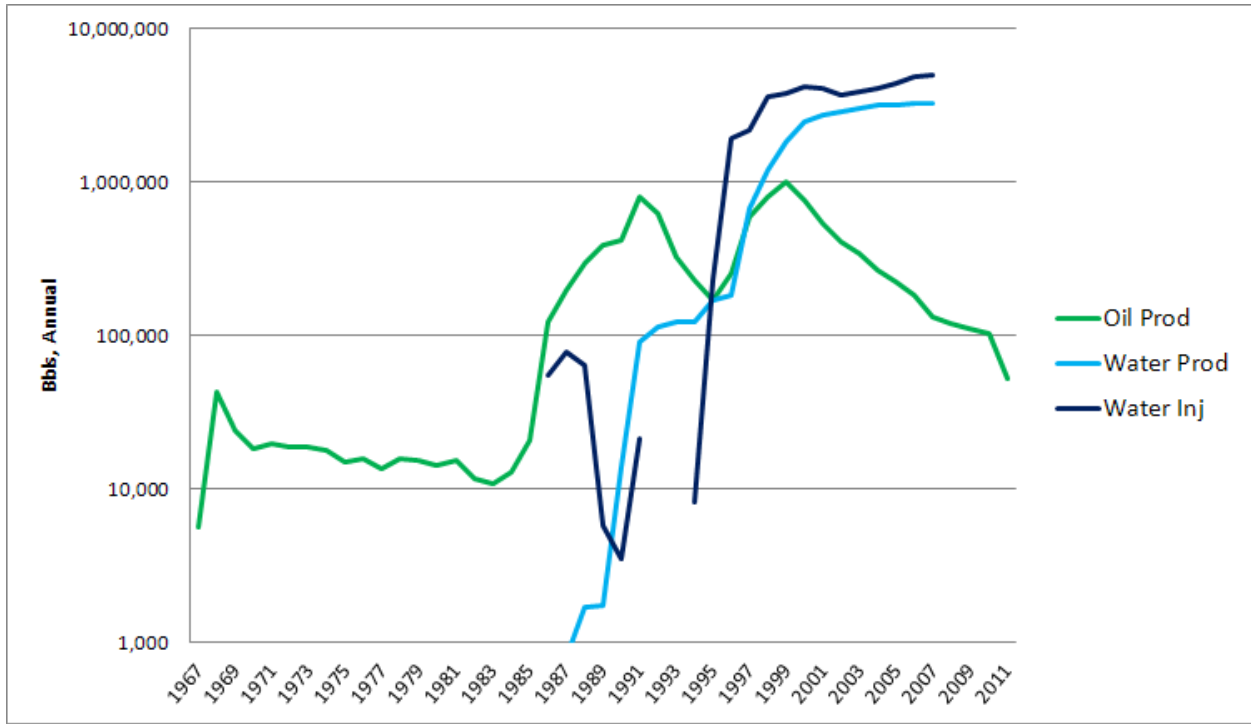


Fig. 4: Annual production and injection data for Stewart oilfield, compiled from KGS and field operator data. Oil production in 2010 was 110,922 barrels. **Add # wells...**

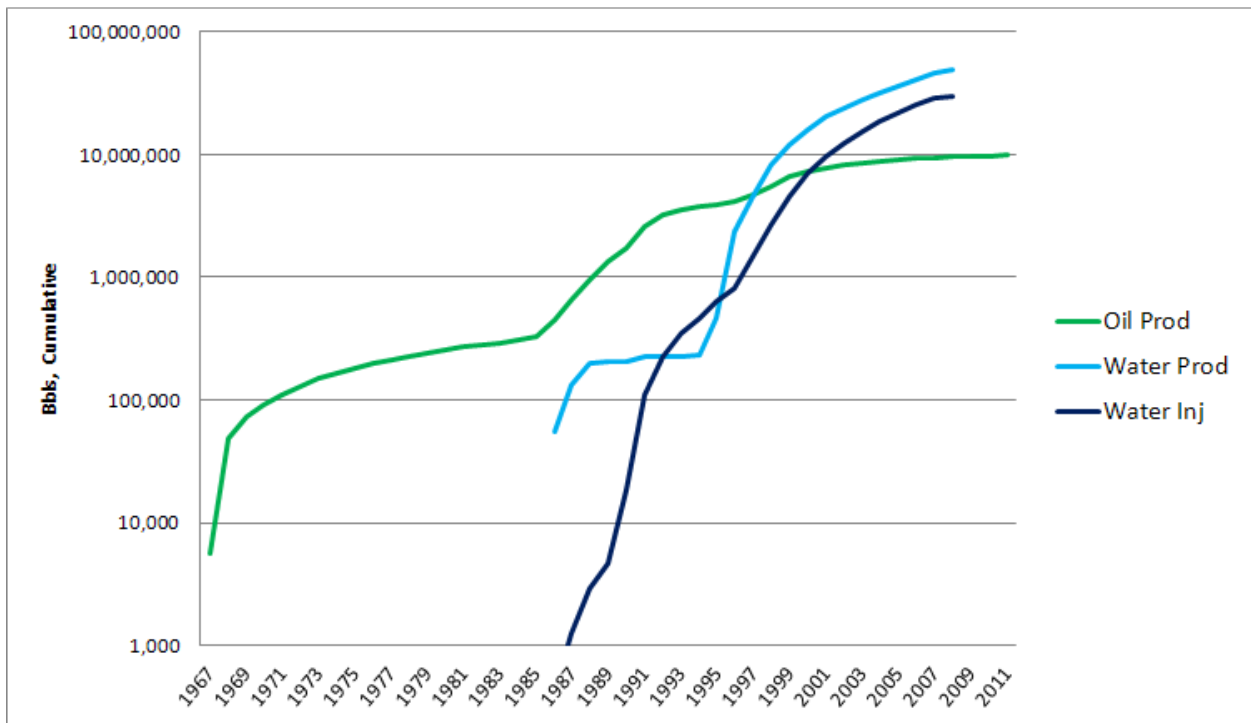


Fig. 5: Cumulative production and injection data for Stewart oilfield compiled from KGS and field operator data. Cumulative oil production, through the end of 2011 is 9,833,207 barrels. **Add # wells...**

Table 2: Annual and cumulative oil production, water injection, and water production data for Stewart oilfield. Oil production data from KGS, all other data from PetroSantander (USA) Inc; asterisk indicates incomplete annual data.

Year	Oil Prod	Cumulative	Water Inj	Cumulative	Water Prod	Cumulative
1967	5639	5639				
1968	42960	48599				
1969	24075	72674				
1970	18541	91215				
1971	19792	111007				
1972	18807	129814				
1973	18703	148517				
1974	17824	166341				
1975	14991	181332				
1976	15644	196976				
1977	13721	210697				
1978	15809	226506				
1979	15318	241824				
1980	14205	256029				
1981	15326	271355				
1982	11594	282949				
1983	10731	293680				
1984	12851	306531				
1985	20909	327440				
1986	123586	451026	54913	54913	435	435
1987	196008	647034	78929	133842	807	1242
1988	293417	940451	63719	197561	1710	2952
1989	382213	1322664	5797	203358	1760	4712
1990	405258	1727922	3547	206905	13867	18579
1991	794653	2522575	21048	227953	90781	109360
1992	614554	3137129		227953	113243	222603
1993	317761	3454890		227953	122988	345591
1994	223511	3678401	8242	236195	121968	467559
1995	165238	3843639	230858	467053	168141	635700
1996	250916	4094555	1909084	2376137	181809	817509
1997	582111	4676666	2167965	4544102	672011	1489520
1998	804488	5481154	3585622	8129724	1192519	2682039
1999	998603	6479757	3752615	11882339	1829409	4511448
2000	777975	7257732	4237946	16120285	2472016	6983464
2001	547091	7804823	4102576	20222861	2713340	9696804
2002	418865	8223688	3730430	23953291	2848627	12545431
2003	349819	8573507	3849670	27802961	3020223	15565654
2004	275561	8849068	4123248	31926209	3155151	18720805
2005	228285	9077353	4408309	36334518.4	3169503	21890308
2006	186879	9264232	4863551	41198069.4	3271637	25161945
2007	140879	9405111	5026385	46224454.4	3266653	28428597
2008	126175	9531286	2727325*	48951779.4	1524150*	29952747
2009	119633	9650919				
2010	110922	9761841				
2011	71366*	9833207				



## 6. GEOLOGY

The reservoir interval of the Stewart oilfield is in the Morrowan Stage of the Lower Pennsylvanian Series, in the Kearny Formation. The reservoir sandstone and is generally referred to as the Morrowan sandstone in both informally and in peer-reviewed literature (e.g. Montgomery, 1996). Morrowan sandstone reservoirs occur throughout southwestern Kansas and southeastern Colorado and many are prolific oil and gas producers. A typical well log from Stewart oilfield (Figure 6) shows the log response through the Morrowan sandstone reservoir. The Morrowan sandstone is characterized by generally low gamma-ray response, around 30-45 API units, photoelectric effect log (PEF) around 2, and neutron-density porosity in the 10-20% range. The porosity logs are scaled to a limestone matrix, and in sandstone the density porosity log reads high, crossing over the neutron porosity log as a result of the lower density of sandstone compared to limestone.

At the Stewart oilfield, the Morrowan sandstone rests directly on the Mississippian-Pennsylvanian unconformity surface, a major time-stratigraphic boundary in the worldwide geologic column and a regionally significant stratigraphic marker. The Ste. Genevieve Limestone and the St. Louis Limestone, in which oil was originally discovered in the Stewart oilfield, are the stratigraphic units directly below the Morrowan sandstone. Morrowan sandstones such as that at Stewart oilfield fill valleys incised into the St. Louis Limestone. Such incised valleys were cut into the St. Louis Limestone during times of relatively low sea level, and progressively filled with sediment as sea level rose over time. A structure map of the top of the Mississippian (Figure 7) at Stewart oilfield shows the incised valley as an elongate structurally low area. Early Pennsylvanian time saw fluctuating sea levels as a result of expansion and contraction of polar icecaps (Montgomery, 1996), resulting in complex, multi-stage filling of incised valleys. At each stage of sea-level rise an incised valley is partially filled with sediments, and valley-fill deposits are partially removed by erosion during subsequent stages of low sea level. At the Stewart oilfield, three such cycles of filling and erosion are recorded; the Morrowan sandstone is divided into at least three, and as many as six, separate episodes of valley-filling (VF 1-3, Figure 4; Green et al., 2000). A final stage of sea level rise inundated the entire region, and impermeable shale and limestone were deposited over the valley.

Depositional environments within incised valleys are complex due to the interplay of marine and fluvial processes, and differences in depositional environment can impact reservoir

quality. In Morrowan sandstones of Colorado and Kansas, reservoirs deposited under more marine influence often display lower porosity and permeability than those deposited under more fluvial conditions (e.g. Bowen & Weimer, 2003). The Morrowan sandstone reservoir at Stewart oilfield is interpreted as dominantly fluvial, with some marine influence at the western end of the field (Green et al., 2000); marine influence consisted of re-working of sands.

The reservoir is narrow and elongate, ranging from 0.25 to 0.4 miles (0.4 to 0.65 km) in width and extending over 5 miles (8 km) in length in an east-to-west direction. The reservoir represents an ancient river system flowing from east to west into shallow seas in the Hugoton Embayment of the Anadarko Basin (Figure 8). Fluvial dominance in sedimentation decreases at the western margins of the reservoir, where the sandstone formed a delta prograding into the shallow seas, and it is here that marine influence is most evident (Green et al., 1996). The reservoir dips to the west at around 3-5° per mile, and thins from about 45 feet thick in the west to about 20 feet in the east (Green et al., 1996); an isopach map (Figure 9) and a well-log cross-section along the length of the reservoir (Figure 10) show the trend of thinning from west to east.

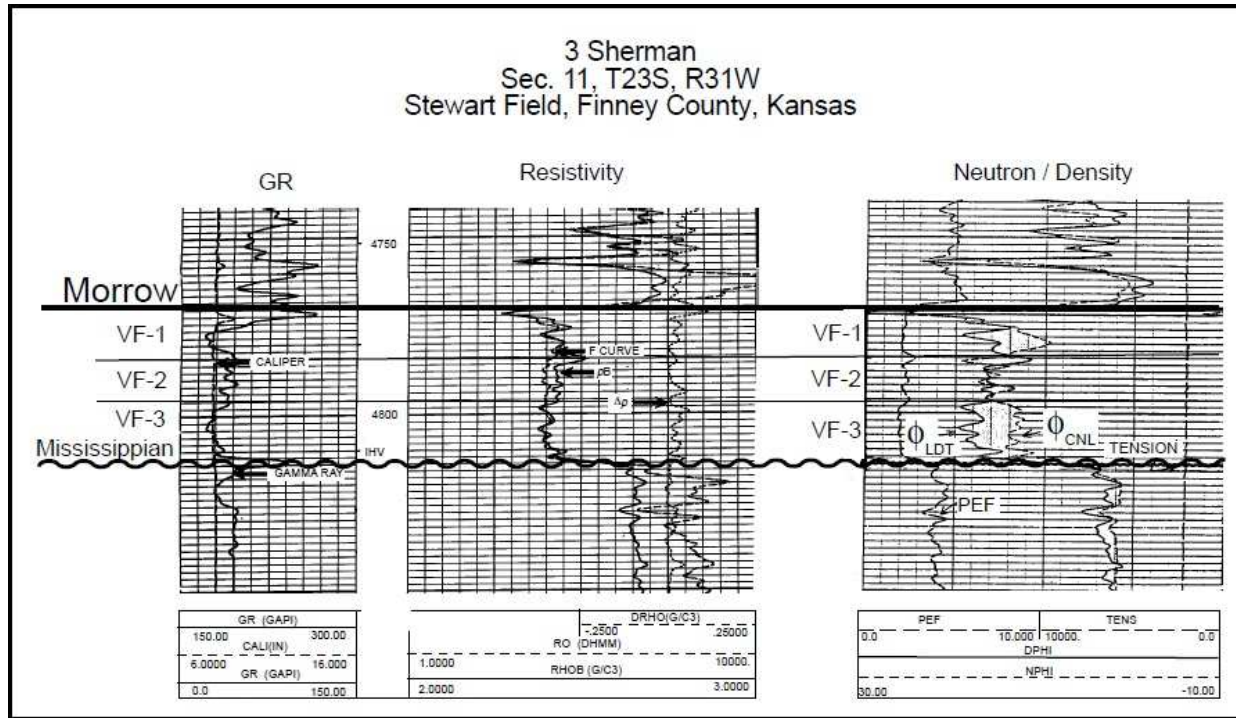


Fig. 6: Typical well-log response through Morrow sandstone reservoir in Stewart oilfield. Note generally low gamma-ray response, photoelectric log around 2, and crossover of density porosity over neutron porosity log (After Montgomery, 1996).

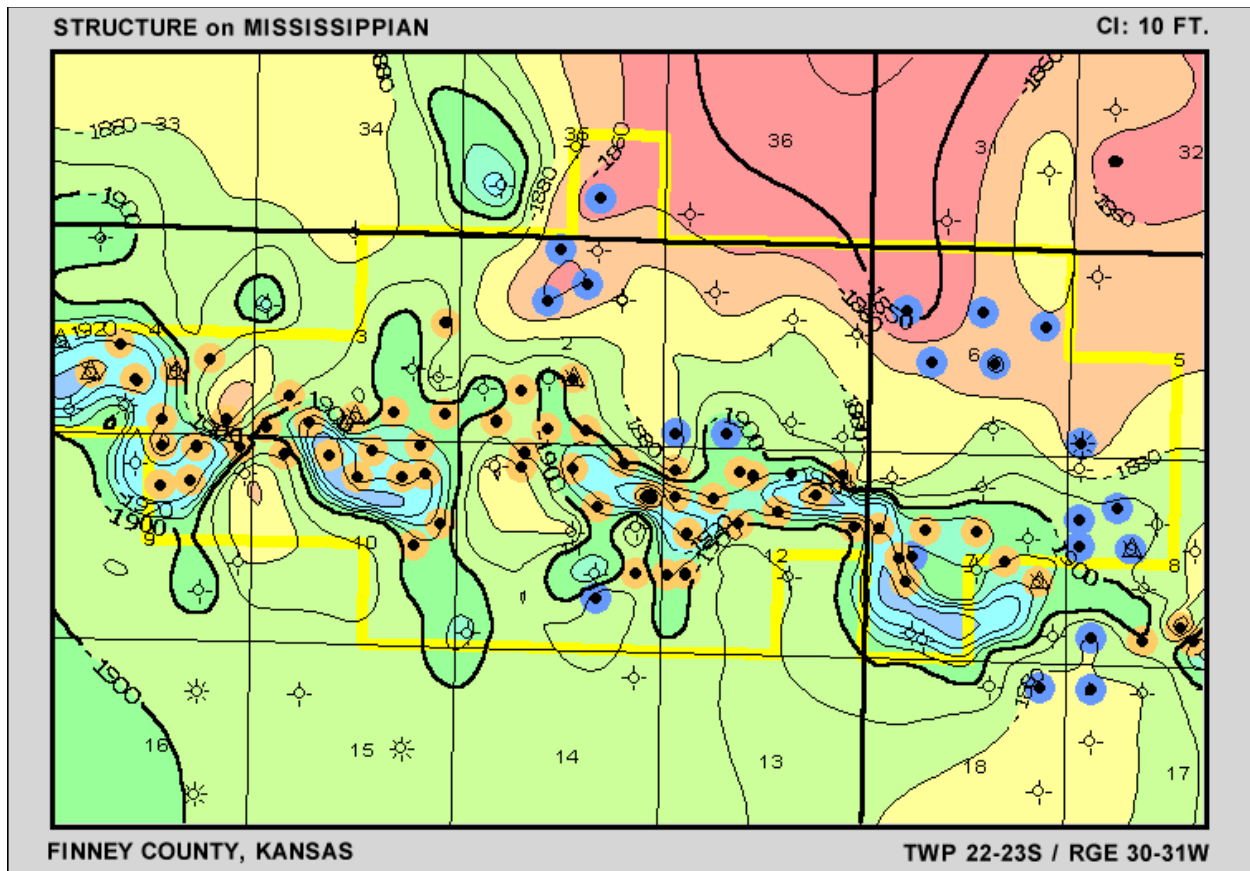


Fig. 7: Structure map of the top of the Mississippian at Stewart oilfield showing elongate low area, which is the incised valley, from <http://www.kgs.ku.edu/DPA/Stewart/stewartSite.html>. Contours are in feet subsea, and contour interval is 10 feet; wells highlighted orange are completed in Morrowan sandstone, wells highlighted blue are completed in Mississippian.

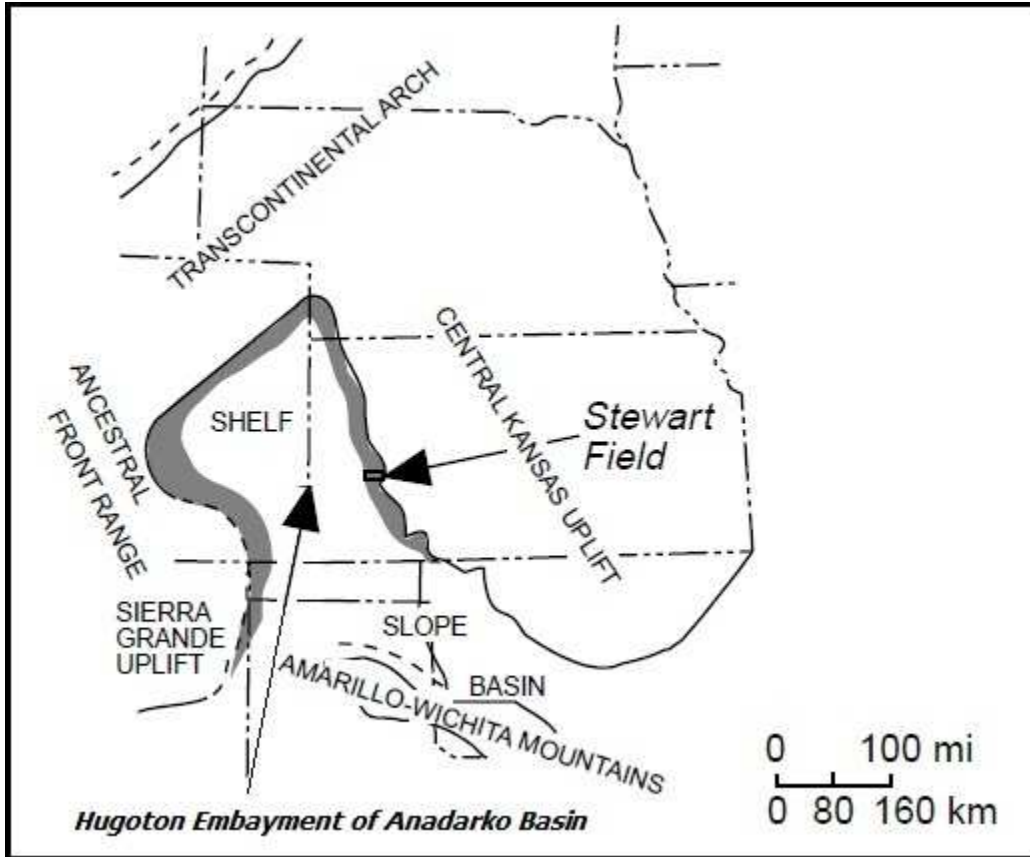


Fig. 8: Paleogeographic map showing location of Stewart oilfield, modified from Montgomery, 1996. Morrowan sandstone reservoir at Stewart oilfield originated as a river system flowing east-to-west into the Hugoton Embayment.

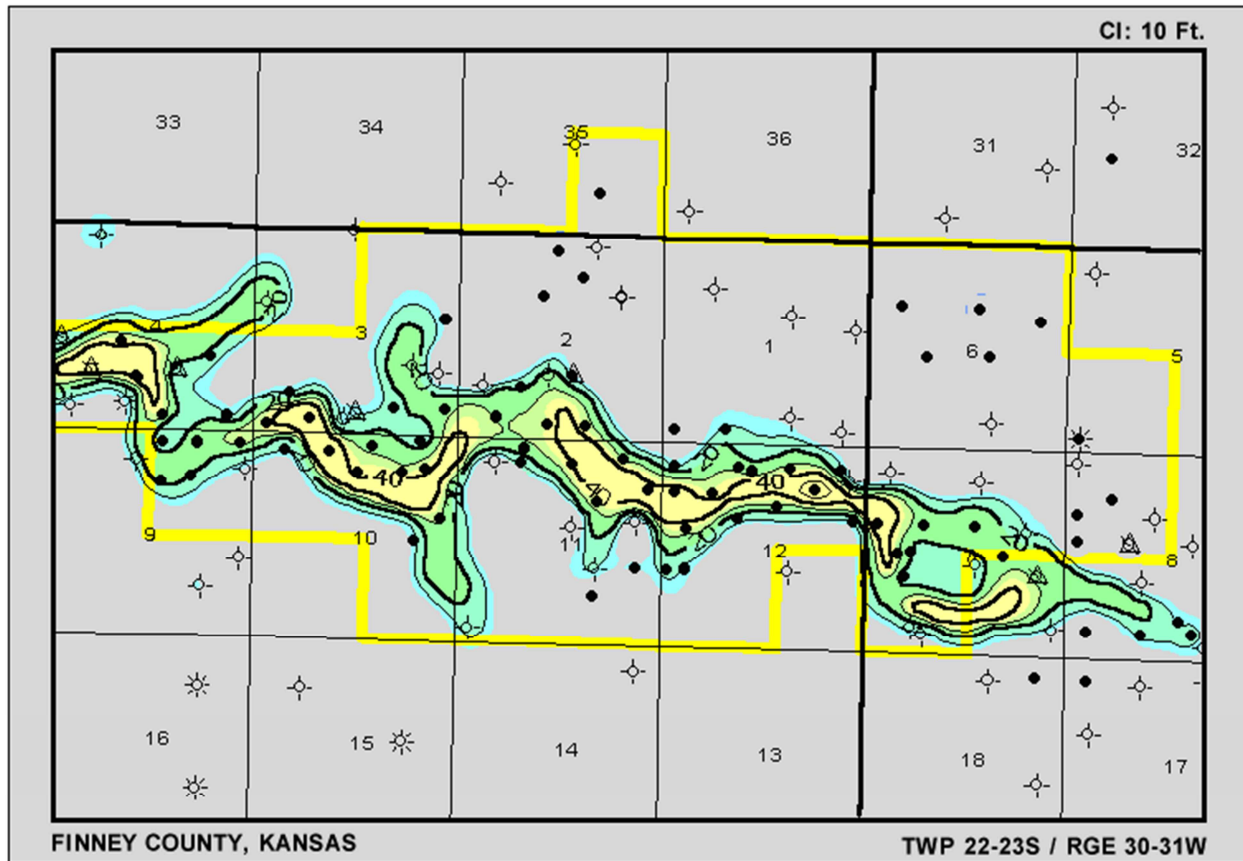


Fig. 9: Thickness map of Morrowan sandstone reservoir at Stewart oilfield, from <http://www.kgs.ku.edu/DPA/Stewart/stewartSite.html>. Stewart oilfield is outlined in yellow, and contour interval is 10 feet.

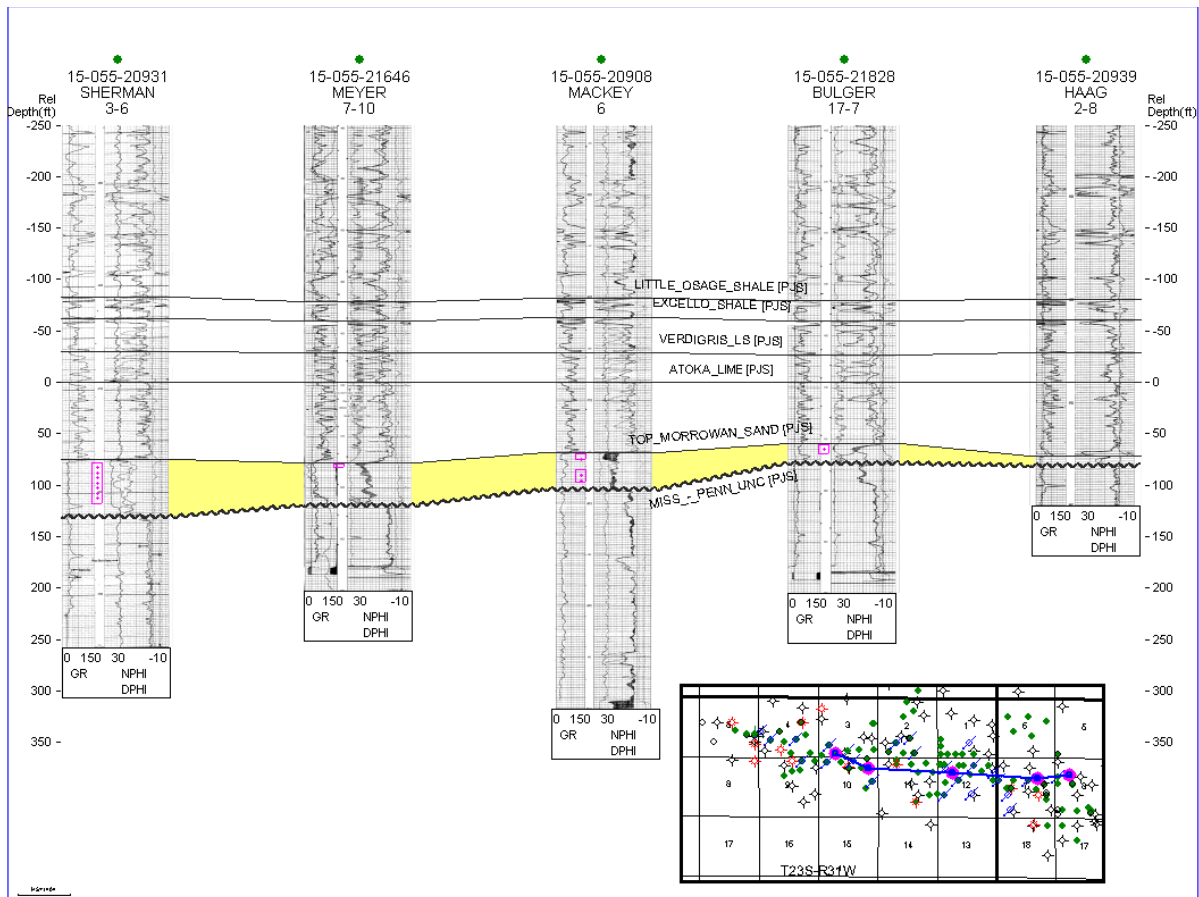


Fig. 10: Stratigraphic cross-section along Stewart oilfield showing reservoir sandstone (shaded yellow) thinning from west to east.

## 7. VOLUMETRICS & RESERVOIR PROPERTIES

Estimated ultimate primary plus secondary recovery for the reservoir in the DOE report on improved recovery in fluvial-dominated deltaic reservoirs was 7,619,000 barrels, or 33.6% of the volumetrically-estimated 22,653,000 barrels originally in place (Green et al., 2000). Actual cumulative production of 9,833,207 barrels through the end of 2011 is much higher than the amount predicted in the DOE report. This could indicate conservative estimates in the DOE report for original oil in place or for recovery factor, meaning that the reservoir may have greater potential for recovery. Alternatively, the higher-than-expected production could reflect different economic conditions. With the sharp rise in oil prices from the \$20-\$30 per barrel range in the late 1990s to the \$80-\$100+ range in the latter 2000s, production levels previously considered uneconomical may have become economical.

According to Montgomery (1996) individual Morrowan wells were projected to produce up to 100,000 barrels during primary recovery, and an additional 50,000-100,000 barrels from waterflooding. Cumulative production from the reservoir since the waterflood began affecting production in 1996 is 5,989,568 barrels. If tertiary recovery operations such as surfactant flooding could be expected to have similar efficacy to waterflooding, much incremental production could be obtained from the reservoir.

Field-wide shut-in tests were carried out in 1989 and 1991 to examine distribution of pressure within the reservoir. Results of these tests indicated continuity of the reservoir over the entire length of the field (Mohan et al., 1996). Cores were recovered and analyzed from the following wells: Bulger 5-7 (API# 15-055-20731), Pauls 2-9 (15-055-20818), Scott 4-4 (15-055-20845), Sherman #5 (15-055-20637), Sherman #3 (15-055-20628), and Meyer 10-1 (15-055-20751). Appendix 2 summarizes petrophysical data from core analyses of these wells. The DOE report by Green et al. (2000) contains a useful table of data for the field, such as temperature and pressure data, reservoir fluid properties, and volumetric and production data; the table is reproduced below (Table 3).



Table 3: Summary of reservoir properties for Morrow sandstone at Stewart oilfield, from Green et al., 2000.

<b>Field Data Summary</b>		
<u>General</u>		
State:	Kansas	
County:	Finney	
Location:	Section 7, T23S - R30W and Sections 2,3,4,9,10,11,12, T23S - R31W	
Primary Well Count:	43 Producers	
Operators:	3	
<u>Reservoir Data</u>		
Formation	Morrow	
Elevation (Field Average KB)	2884 ft.	
Depth to Top of Morrow Sand	4764 ft.	
Temperature	125° F	
Original Pressure	1102 psig (estimated)	
Average Initial Water Saturation	32.2%	
Area within Zero Contour of Net Sand Map	1,356 Ac.	
Original Oil In Place (estimated)	22,653	MSTB
Cumulative Production (as of 6-1-94)	3,365.035	MSTB
Cumulative Recovery Factor	14.9%	
Estimated Ultimate Primary Reserves	3,881	MSTB
Primary Recovery Factor	17.1%	
Estimated Incremental Secondary Reserves	3,738	MSTB
Incremental Secondary Recovery Factor	16.5%	
Estimated Primary plus Secondary	7,619	MSTB
Primary plus Secondary Recovery Factor	33.6%	
<u>Rock Properties</u>		
Lithology	Sandstone	
Average Thickness	26 ft.	
Average Porosity (11% cutoff)	16.5%	
Arithmetic Average Permeability (from Cores)	138 md	
Compressibility	$10 \times 10^{-6}$	
Archie Equation Parameters:	a = 1 m = n = 2	
<u>Fluid Properties</u>		
Crude Oil -		
API Gravity	28	
Viscosity at $P_1$ and $T_{res}$	12.1 cp	
Initial Solution Gas-Oil Ratio	37 SCF/STB	
Gas Specific Gravity	1.234	
FVF at $P_1$	1.038 RB/STB	
Bubble Point Pressure ( $P_{BP}$ )	180 psig	
FVF at $P_{BP}$	1.045 RB/STB	
Compressibility at $P_1$	$5.83 \times 10^{-6} \text{ psi}^{-1}$	
Avg. Compressibility above $P_{BP}$	$7.88 \times 10^{-6} \text{ psi}^{-1}$	
Produced Water-		
Resistivity at 125° F	0.04 ohm-m	
Chlorides	55,500 mg/l	
Total Dissolved Solids	91,300 mg/l	
Compressibility at $P_1$	$3.07 \times 10^{-6} \text{ psi}^{-1}$	

## **8. DATA AVAILABILITY**

Data availability for the Stewart oilfield is excellent. The DOE study lasted many years and contains much valuable engineering and geological information. Peer-reviewed publications on the Stewart oilfield are also available (e.g. Montgomery, 1996), and Morrowan sandstone reservoirs in general have been the subject of numerous studies. Most of the wells in the Stewart oilfield were logged with a modern suite of tools including gamma-ray, neutron and density porosity, and resistivity, and logs for most of the wells are available publically for download from the KGS website.

## **9. SUITABILITY FOR IMPROVED RECOVERY**

The Stewart oilfield is a good candidate for further improved recovery operations. The field is well defined spatially and has demonstrated good response to waterflooding. The current waterflood has outperformed expectations, producing nearly 6 million barrels of oil compared to the expected 3,738,000 barrels (Green et al., 2000). Cumulative recovery of nearly 10 million barrels of oil also exceeds the projected cumulative primary plus secondary recovery of 7,619,000 barrels (Green et al., 2000). The fact that oil production has exceeded expectations may indicate more oil originally in place than the estimated 22,653,000 barrels (Green et al., 2000). Whether or not the original oil in place exceeds the estimates in the DOE report a significant amount of oil remains in the ground, representing a large resource remaining to be exploited. The good production results from waterflooding and possibility of greater reserves than previously thought indicate potential for significant future production from further improved recovery operations.

The field-wide pressure continuity deduced from the shut-in tests (Mohan et al., 1996) is also a positive aspect of the reservoir to consider; it demonstrates a lack of significant compartmentalization which could pose a risk to the success of further enhanced recovery operations. Porosity and permeability of the reservoir sandstone is excellent; using an 11% cutoff for porosity, the sandstone reservoir has an average porosity of 16% as measured on well logs, and the arithmetic average permeability of the core samples is 138 millidarcies (Table 3, Green et al., 2000). The good response to waterflooding, good reservoir continuity revealed by pressure testing, and excellent reservoir quality seen in core samples all indicate that Stewart oilfield has good potential for success in further improved recovery operations.

## 10. CONCLUSION

Stewart oilfield is located near Garden City in Finney County, Kansas, and produces oil from a Lower Pennsylvanian sandstone reservoir, at measured depths of around 4700-4800 feet. The Morrowan reservoir was discovered in 1967 with completion of the Haag Estate #1 well (API# 15-055-20002) which had initial production of 99 barrels of oil per day (BOPD). Rapid development of the field occurred in the 1980s, and a major waterflood was initiated in late 1995. Peak annual oil production from the waterflood occurred in 1999, with 998,603 barrels, and cumulative oil production is 9,833,207 barrels.

The reservoir is a stratigraphic trap; oil and gas are trapped in the reservoir sandstone by overlying impermeable layers of shale and limestone, and by impermeable limestone forming the walls of the incised valley that contains the sandstone. Several factors establish that Stewart oilfield is a good candidate for a surfactant flood demonstration project. The reservoir is well defined spatially, and the current waterflood has produced more oil than expected. Pressure testing indicates good reservoir continuity, demonstrating that the reservoir lacks any significant compartmentalization that could hinder successful flooding, and well logs and core samples show that porosity and permeability of the reservoir sandstone is excellent. Volumetric estimates of over 22 million barrels of oil originally in place compared with a cumulative production approaching 10 million barrels indicate that much oil remains in the ground; improved oil recovery methods such as surfactant flooding could potentially aid in further exploiting the hydrocarbon reserves at Stewart oilfield.

## 11. REFERENCES

- Green, D.W., Willhite, P.G., Reynolds, R.R., McCune, A.D., Michnick, M.J., Walton, A.W., and Watney, W.L., 2000, Improved oil recovery in fluvial-dominated deltaic reservoirs of Kansas – Near term, Final Report: Prepared by The University of Kansas Center for Research, Inc., for U.S. Department of Energy, published by National Petroleum Technology Office, U.S. Department of Energy, Tulsa, Oklahoma.
- Mohan, H., Burchardt, P., Willhite, G.P., and Reynolds R.R., 1996, Evaluating waterflood potential in a Morrow sandstone reservoir: SPE/DOE 35386. Paper presented at 1996 SPE/DOE Tenth Symposium on Improved Oil Recovery held in Tulsa, OK, April, 1996, 10p.
- Montgomery, S.L., 1996, Stewart Field, Finney County, Kansas: Seismic definition of thin channel reservoirs: AAPG Bulletin, v. 80, no. 12, p. 1833-1844.
- Kansas Geological Survey website: <http://www.kgs.ku.edu>

**APPENDIX 1: MORROWAN WELLS IN STEWART OILFIELD**

Table 1: Summary of wells in the Stewart oilfield, compiled from from KGS website.

API_NUMBER	LEASE	WELL	TWP-RNG-SEC	ORIG_OPERATOR	CURR_OPERATOR	COMP.	PLUG.	STATUS
15-055-20011, -0001	ALICE TREKELL	1	23S-31W-1	DAVIDOR & DAVIDOR	unavailable	2-Apr-68	31-Mar-68	D&A
15-055-20430	TREKELL	1	23S-31W-1	TEXAS O&G	unavailable	23-Nov-80	30-Nov-80	D&A
15-055-20478	Janof Trust	1	23S-31W-1	Plains Resources, Inc.	unavailable	15-Aug-81	31-Aug-81	D&A
15-055-21405	Haflich	1	23S-31W-1	Northern Lights Oil Co., L.P.	Northern Lights Oil Company, LLC	16-Jun-95	30-Jun-95	D&A
15-055-21593	TREKELL	1-1	23S-31W-1	HESS OIL or CROSS BAR PETR	Hess Oil Company	26-Aug-98		OIL
15-055-21596	TREKELL	3-1	23S-31W-1	CROSS BAR PETROLEUM INC	Cross Bar Petroleum, Inc.	18-Apr-00		OIL
15-055-21672	Trekell	2-1	23S-31W-1	HESS OIL CO.	Hess Oil Company	22-Apr-00	17-Nov-10	OIL-P&A
15-055-21696	Trekell	3-1	23S-31W-1	Hess Oil Co.	Hess Oil Company	28-Nov-00		OIL - Inactive
15-055-21750	Trekell	4-1	23S-31W-1	Hess Oil Co.	Hess Oil Company	26-Nov-01		SWD
15-055-21895	Trekell	5-1	23S-31W-1	Hess Oil Co.	Hess Oil Company	6-Dec-05	6-Dec-05	D&A
15-055-30002	WARNER	1	23S-31W-1	DAVIDOR & DAVIDOR	unavailable	21-Jan-65	31-Jan-65	D&A
15-055-20658	NELSON	1-2	23S-31W-2	SHARON RESOURCES	PetroSantander (USA) Inc.	17-Apr-86		OIL

Table 1 (cont): Summary of wells in the Stewart oilfield, compiled from from KGS website.

API_NUMBER	LEASE	WELL	TWP-RNG-SEC	ORIG_OPERATOR	CURR_OPERATOR	COMP.	PLUG.	TYPE
15-055-20663, -0001	CARR	1-2	23S-31W-2	SHARON RESOURCES	PetroSantander (USA) Inc.	30-May-86		OIL - conv to EOR
15-055-20664, -0001	NELSON	2-2	23S-31W-2	SHARON RESOURCES	North American Resources Company	9-Jul-86		OIL - conv to EOR
15-055-20666, -0001, -0002, -0003	CARR	2-2	23S-31W-2	SHARON RESOURCES	PetroSantander (USA) Inc.	13-Oct-86		OIL - Conv to SWD
15-055-20689, -0001, -0002	NELSON	3-2	23S-31W-2	SHARON RESOURCES	PetroSantander (USA) Inc.	3-Feb-87		OIL - conv to EOR
15-055-20787	NELSON	4-2	23S-31W-2	SHARON RESOURCES	unavailable	23-Apr-88	30-Apr-88	D&A
15-055-20878	CARR	3-2	23S-31W-2	NORTH AMERICAN RES	unavailable	26-Sep-89	30-Sep-89	D&A
15-055-20881	CARR 'A'	3-2	23S-31W-2	NORTH AMERICAN RES	unavailable	8-Oct-89	8-Oct-89	D&A
15-055-20943	CARR	4-2	23S-31W-2	SHARON RESOURCES	American Warrior, Inc.	10-Dec-90		OIL
15-055-21246	CARR	5-2	23S-31W-2	SHARON RESOURCES	Sharon Resources, Inc.	10-Nov-93	30-Nov-93	D&A
15-055-21411	CARR TRUST	1-2	23S-31W-2	Cross Bar Petroleum, Inc.	Larson Operating Company	25-Jun-95		OIL
15-055-21457	CARR	6-2	23S-31W-2	Sharon Resources, Inc.	American Warrior, Inc.	16-Jan-96		OIL
15-055-21648	NELSON	5-2	23S-31W-2	Petrosantander (USA), Inc.	PetroSantander (USA) Inc.	4-Aug-99	4-Aug-99	D&A

Table 1 (cont): Summary of wells in the Stewart oilfield, compiled from from KGS website.

API_NUMBER	LEASE	WELL	TWP-RNG-SEC	ORIG_OPERATOR	CURR_OPERATOR	COMP.	PLUG.	TYPE
15-055-20702	SHERMAN	1-3	23S-31W-3	SHARON RESOURCES	PetroSantander (USA) Inc.	3-Apr-87		OIL - conv to EOR
15-055-20724	SHERMAN	5-7	23S-31W-3	SHARON RESOURCES	PetroSantander (USA) Inc.	31-Aug-87		OIL
15-055-20729	SHERMAN	3-3	23S-31W-3	SHARON RESOURCES	unavailable	12-Sep-87	30-Sep-87	D&A
15-055-20815	SHERMAN	5-3	23S-31W-3	SHARON RESOURCES	PetroSantander (USA) Inc.	3-Sep-88		OIL - Inactive
15-055-20931, -0001	SHERMAN	3-6	23S-31W-3	SHARON RESOURCES	North American Resources Company	19-Sep-90		OIL - Recompl
15-055-21001	SHERMAN	7-3	23S-31W-3	SHARON RESOURCES	Sharon Resources, Inc.	24-May-91	31-May-91	D&A
15-055-21025, -0001	SHERMAN	3-8	23S-31W-3	SHARON RESOURCES	North American Resources Company	3-Dec-91		OIL - conv to EOR
15-055-21041, -0001	SHERMAN	9-3	23S-31W-3	SHARON RESOURCES	PetroSantander (USA) Inc.	29-Jan-92		OIL - conv to SWD
15-055-21385, -0001	TRANS AM 'S'	1-3	23S-31W-3	Cross Bar Petroleum, Inc.	PetroSantander (USA) Inc.	14-Mar-95	22-Jun-10	OIL-P&A
15-055-21628	Sherman	10-3	23S-31W-3	PetroSantander USA, Inc.	PetroSantander (USA) Inc.	18-Oct-98	17-Oct-98	D&A
15-055-21652	SHERMAN	11-3	23S-31W-3	PetroSantander (USA), Inc.	PetroSantander (USA) Inc.	28-Aug-99	28-Aug-99	D&A

Table 1 (cont): Summary of wells in the Stewart oilfield, compiled from from KGS website.

API_NUMBER	LEASE	WELL	TWP-RNG-SEC	ORIG_OPERATOR	CURR_OPERATOR	COMP.	PLUG.	TYPE
15-055-20795, -0001	SCOTT	4-1	23S-31W-4	SHARON RESOURCES	PetroSantander (USA) Inc.	6-Jul-88		OIL - recompl
15-055-20813	SCOTT	4-2	23S-31W-4	SHARON RESOURCES	PetroSantander (USA) Inc.	3-Nov-88		OIL - conv to EOR
15-055-20845	SCOTT	4-4	23S-31W-4	SHARON RESOURCES	PetroSantander (USA) Inc.	1-Mar-89		OIL
15-055-20848, -0001	SCOTT	4-5	23S-31W-4	SHARON RESOURCES	North American Resources Company	24-Mar-89		OIL - conv to EOR
15-055-20880, -0001	SCOTT	4-6	23S-31W-4	SHARON RESOURCES	unavailable	13-Nov-89	30-Nov-89	D&A - Conv to SWD
15-055-21020, -0001	SCOTT	4-7	23S-31W-4	SHARON RESOURCES	PetroSantander (USA) Inc.	29-Sep-91		OIL - conv to EOR
15-055-21046	SCOTT	4-8	23S-31W-4	SHARON RESOURCES, INC.	Sharon Resources, Inc.	21-Feb-92		OIL - conv to EOR
15-055-21668	STEWART UNIT SCOTT	4-9	23S-31W-4	PetroSantander (USA) Inc.	PetroSantander (USA) Inc.	17-Feb-00	17-Feb-00	D&A
15-055-21669	Scott	4-10	23S-31W-4	PetroSantander (USA), Inc.	PetroSantander (USA) Inc.	15-Mar-00		OIL
15-055-21727, -0001	HARRINGTON-SCOTT	1	23S-31W-4	PETROSANTANDER USA INC	PetroSantander (USA) Inc.	18-Apr-01		OIL - recompl as gas well
15-055-21752, -0001	HARRINGTON-SCOTT	2	23S-31W-4	PETROSANTANDER USA INC	PetroSantander (USA) Inc.	29-Jun-01		OIL - conv to EOR
15-055-21753	HARRINGTON-SCOTT	3	23S-31W-4	PETROSANTANDER USA INC	PetroSantander (USA) Inc.	26-Jun-01	25-Jun-01	D&A



Table 1 (cont): Summary of wells in the Stewart oilfield, compiled from from KGS website.

API_NUMBER	LEASE	WELL	TWP-RNG-SEC	ORIG_OPERATOR	CURR_OPERATOR	COMP.	PLUG.	TYPE
15-055-20859	BECKER	2-5	23S-31W-5	SHARON RESOURCES	Sharon Resources, Inc.	13-May-89	31-May-89	D&A
15-055-20879	Wylie	5-1	23S-30W-5	North American Resources Co.	PetroSantander (USA) Inc.	23-Nov-89		OIL
15-055-20977, -0001	WILLIAM E. BECKER	5-3	23S-31W-5	SHARON RESOURCES	Sharon Resources, Inc.	19-Feb-91	28-Feb-91	D&A
15-055-21859	Becker	5-4	23S-31W-5	BuRay, LLC	Schofield Energy Company	15-Mar-05		OIL
15-055-21860	BECKER	5-5	23S-31W-5	BuRay, LLC	Schofield Energy Company	16-Jan-05		OIL
15-055-22028	Becker	5-6	23S-31W-5	PetroSantander (USA) Inc.	PetroSantander (USA) Inc.	15-Nov-08		OIL
15-055-00125	STEWART 'A'	1	23S-30W-6	Co-op. Refining Assoc.	Lang, Kenneth R.	30-Sep-52		OIL
15-055-20020	ALICE E. HAAG	1	23S-30W-6	DAVIDOR & DAVIDOR	Beren Corporation	23-Jun-69		OIL
15-055-20185	HAAG EST A	1	23S-30W-6	BEREN CORP	unavailable	30-May-75	31-May-75	D&A
15-055-20421	HAAG FARMS	1	23S-30W-6	WOOLSEY PET	PetroSantander (USA) Inc.	9-Dec-80	6-Sep-00	OIL-P&A
15-055-20491	HAAG FARMS	2	23S-30W-6	WOOLSEY PET	PetroSantander (USA) Inc.	10-Jan-82		OIL
15-055-20532	HAAG FARMS	3	23S-30W-6	WOOLSEY PET	PetroSantander (USA) Inc.	21-Apr-83		OIL
15-055-20445	BULGER	1	23S-30W-6	CHALLENGER MINERALS	unavailable	6-Aug-81	31-Aug-81	D&A

Table 1 (cont): Summary of wells in the Stewart oilfield, compiled from from KGS website.

API_NUMBER	LEASE	WELL	TWP-RNG-SEC	ORIG_OPERATOR	CURR_OPERATOR	COMP.	PLUG.	TYPE
15-055-20690, -0001	BULGER	1-7	23S-30W-6	Sharon Resources, Inc.	North American Resources Company	30-Jan-87		OIL - conv to EOR
15-055-20701, -0001, -0002, -0003, -0004	BULGER	2-7	23S-30W-6	SHARON RESOURCES	North American Resources Company	23-Apr-87		OIL - conv to EOR
15-055-20712, -0001	BULGER	3-7	23S-30W-6	SHARON RESOURCES	PetroSantander (USA) Inc.	10-Jul-87		SWD
15-055-20726	BULGER	4-7	23S-30W-6	SHARON RESOURCES	North American Resources Company	31-Aug-87		OIL
15-055-20731, -0001	BULGER	5-7	23S-30W-6	SHARON RESOURCES	North American Resources Company	15-Oct-87		OIL - conv to EOR
15-055-20735	BULGER	6-7	23S-30W-6	SHARON RESOURCES	unavailable	22-Oct-87	31-Oct-87	D&A
15-055-20763	BULGER	7-7	23S-30W-6	SHARON RESOURCES	unavailable	9-Jan-88	31-Jan-88	D&A
15-055-21281, -0001	BULGER	10-7	23S-30W-6	SHARON RESOURCES	North American Resources Company	7-Apr-94		OIL - conv to EOR
15-055-21650, -0001	BULGER or STEWART UNIT	11-7	23S-30W-6	PETROSANTANDER (USA)	PetroSantander (USA) Inc.	11-Sep-99		OIL - Recompl
15-055-21651	BULGER	12-7	23S-30W-6	PetroSantander (USA) Inc.	PetroSantander (USA) Inc.			Exp Intent to Drill
15-055-21657	BULGER or STEWART UNIT	13-7	23S-30W-6	PetroSantander (USA) Inc	PetroSantander (USA) Inc.	18-Oct-99		INJ
15-055-21658	BULGER or STEWART UNIT	14-7	23S-30W-6	PetroSantander U.S.A., Inc.	PetroSantander (USA) Inc.	2-Nov-99	2-Nov-99	D&A

Table 1 (cont): Summary of wells in the Stewart oilfield, compiled from from KGS website.

API_NUMBER	LEASE	WELL	TWP-RNG-SEC	ORIG_OPERATOR	CURR_OPERATOR	COMP.	PLUG.	TYPE
15-055-21675	BULGER or STEWART UNIT	15-7	23S-30W-6	PetroSantander (USA) Inc.	PetroSantander (USA) Inc.	19-May-00	19-May-00	D&A
15-055-21787	BULGER or STEWART UNIT	16-7	23S-30W-6	PetroSantander (USA) Inc.	PetroSantander (USA) Inc.	9-Dec-02		OIL
15-055-21804	BULGER or STEWART UNIT	12-7	23S-30W-6	PetroSantander (USA) Inc.	PetroSantander (USA) Inc.	27-Jun-03		OIL
15-055-21828	BULGER	17-7	23S-30W-6	PetroSantander (USA) Inc.	PetroSantander (USA) Inc.	17-Aug-04		OIL
15-055-21829	BULGER	18-7	23S-30W-6	PetroSantander (USA) Inc.	PetroSantander (USA) Inc.	17-Aug-04		GAS - Inactive
15-055-20888	HAAG	1-8	23S-30W-8	SHARON RESOURCES	Sharon Resources, Inc.	31-Oct-89	31-Oct-89	D&A
15-055-20916, -0001	HAAG	1-8	23S-30W-8	CHIEF DRLG CO INC	Vess Oil Corporation	21-Jun-90		OIL - conv to SWD
15-055-20939	HAAG	2-8	23S-30W-8	CHIEF DRLG	PetroSantander (USA) Inc.	17-Oct-90		OIL - Inactive
15-055-20952	HAAG	3-8	23S-30W-8	CHIEF DRLG	Chief Drilling, Inc.	11-Mar-91	31-Mar-91	D&A
15-055-21000	HAAG	4-8	23S-30W-8	CHIEF DRLG	PetroSantander (USA) Inc.	3-Jun-91		OIL - Inactive
15-055-21002, -0001	HAAG	5-8	23S-30W-8	CHIEF DRLG	Vess Oil Corporation	11-Jul-91	28-Jun-05	OIL - conv to EOR, P&A
15-055-21007	HAFlich	4-8	23S-30W-8	NORTH AMERICAN RES	North American Resources Company	2-Aug-91	2-Aug-91	D&A

Table 1 (cont): Summary of wells in the Stewart oilfield, compiled from from KGS website.

API_NUMBER	LEASE	WELL	TWP-RNG-SEC	ORIG_OPERATOR	CURR_OPERATOR	COMP.	PLUG.	TYPE
15-055-21099	MERRILL	1-8	23S-31W-8	LANDMARK OIL EXPL	Landmark Resources, Inc.	28-Apr- 92	30- Apr- 92	D&A
15-055-21111-0001	HAFlich	5-8	23S-30W-8	PetroSantander (USA) Inc.	PetroSantander (USA) Inc.	18-Oct- 01		OIL-P&A
15-055-20794	PAULS	1-9	23S-31W-9	NORTH AMERICAN RES	PetroSantander (USA) Inc.	19- Aug-88		OIL
15-055-20812	HOPPER	1-9	23S-31W-9	NORTH AMERICAN RES	unavailable	4-Jul- 88	31-Jul- 88	D&A
15-055-20818, -0001	PAULS	2-9	23S-31W-9	NORTH AMERICAN RES	PetroSantander (USA) Inc.	1-Oct- 88		OIL - Recompl
15-055-20832	PAULS	3-9	23S-31W-9	NORTH AMERICAN RES	PetroSantander (USA) Inc.	23- Dec-88		GAS
15-055-20838	PAULS	4-9	23S-31W-9	NORTH AMERICAN RES	unavailable	15- Dec-88	31- Dec- 88	D&A
15-055-20870	HOPPER	2-9	23S-31W-9	NORTH AMERICAN RES	unavailable	29-Jul- 89	29-Jul- 89	D&A
15-055-21558, -0001	PAULS	5-9	23S-31W-9	NORTH AMERICAN RES	North American Resources Company	5-Jun- 97		OIL - conv to EOR
15-055-21629	STEWART UNIT (PAULS)	6-9	23S-31W-9	PetroSantander (USA), Inc.	PetroSantander (USA) Inc.	27-Sep- 98	27- Sep- 98	D&A
15-055-21674	STEWART UNIT (PAULS)	7-9	23S-31W-9	PetroSantander (USA), Inc.	PetroSantander (USA) Inc.	19- May-00		OIL
15-055-21677	ALLEY TRUST	1	23S-31W-9	PETROSANTANDER (USA)	PetroSantander (USA) Inc.	27- May-00	28- May- 00	D&A
15-055-21693	PAULS	1-9	23S-31W-9	Larson Operating Co.	Larson Operating Company	21- Dec-00		OIL

Table 1 (cont): Summary of wells in the Stewart oilfield, compiled from from KGS website.

API_NUMBER	LEASE	WELL	TWP-RNG-SEC	ORIG_OPERATOR	CURR_OPERATOR	COMP.	PLUG.	TYPE
15-055-21729, -0001	PAULS-ALLEY	1	23S-31W-9	PETROSANTANDER USA INC	PetroSantander (USA) Inc.	1-Apr-01		D&A - Conv to EOR
15-055-20751, -0001	MEYER	1-10	23S-31W-10	SHARON RESOURCES	unavailable	19-Nov-87		OIL - conv to EOR
15-055-20769	MEYER	2-10	23S-31W-10	Sharon Resources, Inc.	PetroSantander (USA) Inc.	27-Feb-88		OIL - conv to EOR
15-055-20788, -0001	MEYER	3-10	23S-31W-10	Sharon Resources, Inc.	PetroSantander (USA) Inc.	28-May-88		OIL - conv to EOR
15-055-20819, -0001, -0002	STEWART UNIT or MEYER	4-10	23S-31W-10	SHARON RESOURCES	unavailable	1-Nov-88		OIL - Recompl
15-055-21042	MEYER	5-10	23S-31W-10	SHARON RESOURCES	Sharon Resources, Inc.	15-Dec-91	15-Dec-91	D&A
15-055-21044	MEYER 'A'	5-10	23S-31W-10	SHARON RESOURCES	PetroSantander (USA) Inc.	8-Feb-92		OIL
15-055-21634	MEYER	6-10	23S-31W-10	Petrosantander {USA} Inc.	PetroSantander (USA) Inc.	20-Oct-98		OIL
15-055-21646	MEYER	10-7	23S-31W-10	Petrosantander (USA), Inc.	PetroSantander (USA) Inc.	2-Aug-99		OIL
15-055-21649, -0001	MEYER	8-10	23S-31W-10	Petrosantander (USA), Inc.	PetroSantander (USA) Inc.	23-Sep-99		OIL - conv to EOR
15-055-21670	TURRENTINE	1-10	23S-31W-10	PetroSantander (USA), Inc.	PetroSantander (USA) Inc.	26-Feb-00		OIL
15-055-20016	MATHA SHERMAN	1	23S-31W-11	DAVIDOR & DAVIDOR	unavailable	26-Dec-68	1-Jan-70	OIL-P&A
15-055-20540	SHERMAN	1-11	23S-31W-11	HADSON PET	unavailable	12-Aug-83	31-Aug-83	D&A
15-055-20556	SHERMAN	2-11	23S-31W-11	HADSON PET	unavailable	18-Jun-84	30-Jun-84	D&A

Table 1 (cont): Summary of wells in the Stewart oilfield, compiled from from KGS website.

API_NUMBER	LEASE	WELL	TWP-RNG-SEC	ORIG_OPERATOR	CURR_OPERATOR	COMP.	PLUG.	TYPE
15-055-20608	SHERMAN	1	23S-31W-11	SHARON RESOURCES	PetroSantander (USA) Inc.	31-Aug-85		OIL
15-055-20621	SHERMAN	2	23S-31W-11	SHARON RESOURCES	PetroSantander (USA) Inc.	30-Nov-85		OIL
15-055-20628	Sherman	3	23S-31W-11	Sharon Resources, Inc.	PetroSantander (USA) Inc.	4-Jan-86		OIL - conv to EOR
15-055-20636	SHERMAN	4	23S-31W-11	SHARON RESOURCES	PetroSantander (USA) Inc.	25-Jan-86		OIL
15-055-20637, -0001	SHERMAN	5	23S-31W-11	SHARON RESOURCES	unavailable	24-Jun-86		OIL - Recompl
15-055-20671	SHERMAN	6	23S-31W-11	SHARON RESOURCES	unavailable	12-Sep-86	30-Sep-86	D&A
15-055-20762	SHERMAN	7	23S-31W-11	SHARON RESOURCES	unavailable	23-Dec-87	31-Dec-87	D&A
15-055-21305, -0001	Sherman	1	23S-31W-11	CROSS BAR PETROLEUM, INC.	Cross Bar Petroleum, Inc.	2-Aug-94	29-Mar-95	OIL-P&A
15-055-21647	SHERMAN	8	23S-31W-11	PETROSANTANDER (USA)	PetroSantander (USA) Inc.	30-Aug-99		OIL
15-055-21667	Sherman Trust	1	23S-31W-11	PetroSantander U.S.A., Inc.	PetroSantander (USA) Inc.	5-Mar-00	5-Mar-00	D&A
15-055-20002	STEWART UNIT or HAAG ESTATE	1	23S-31W-12	DAVIDOR & DAVIDOR, INC.	PetroSantander (USA) Inc.	26-Aug-67	11-Sep-00	OIL-P&A
15-055-20007, -0001	HAAG ESTATE	2	23S-31W-12	DAVIDOR & DAVIDOR	unavailable	18-Mar-68		OIL - conv to EOR
15-055-20013, -0001	FRANCES MACKAY	1	23S-31W-12	DAVIDOR & DAVIDOR	unavailable	6-May-68		OIL - conv to EOR

Table 1 (cont): Summary of wells in the Stewart oilfield, compiled from from KGS website.

API_NUMBER	LEASE	WELL	TWP-RNG-SEC	ORIG_OPERATOR	CURR_OPERATOR	COMP.	PLUG.	TYPE
15-055-20014	HAAG ESTATE	3	23S-31W-12	DAVIDOR & DAVIDOR INC	unavailable	23-Apr-68	30-Apr-68	D&A
15-055-20015	FRANCES MACKEY et al.	2	23S-31W-12	DAVIDOR & DAVIDOR	unavailable	26-Dec-68		OIL - conv to SWD
15-055-20052	HAAG MACKEY	3	23S-31W-12	BEREN CORPORATION	Beren Corporation	10-Jul-72		EOR - Inactive
15-055-20630	MACKEY	4	23S-31W-12	BEREN CORP	PetroSantander (USA) Inc.	11-Feb-86	6-Oct-09	OIL-P&A
15-055-20644, -0001	MACKEY	5	23S-31W-12	BEREN CORP	PetroSantander (USA) Inc.	15-Mar-86	5-Sep-02	OIL-P&A
15-055-20723, -0001	HAAG ESTATE	3	23S-31W-12	BEREN CORP	unavailable	3-Nov-87		OIL-P&A
15-055-20872	HAAG ESTATE	4	23S-31W-12	BEREN CORP	PetroSantander (USA) Inc.	24-Oct-89	1-Feb-88	OIL-P&A
15-055-20908	MACKEY	6	23S-31W-12	BEREN CORP	PetroSantander (USA) Inc.	3-Jul-90		OIL - conv to EOR
15-055-20909	HAAG ESTATE	5	23S-31W-12	BEREN CORP	North American Resources Company	19-May-90		OIL
15-055-21560	HAAG ESTATE	6	23S-31W-12	NORTH AMERICAN RES	North American Resources Company	28-May-97		D&A
15-055-21645, -0001, -0002	MACKEY	7	23S-31W-12	PETROSANTANDER (USA)	PetroSantander (USA) Inc.	22-Aug-99		OIL - conv to EOR
15-055-21656	MACKEY / STEWART UNIT	8	23S-31W-12	PetroSantander (USA) Inc	PetroSantander (USA) Inc.	25-Oct-99		OIL
15-055-21683, -0001	Mackey	9	23S-31W-12	PetroSantander (USA) Inc.	PetroSantander (USA) Inc.	1-Jul-00		OIL - conv to EOR

Table 1 (cont): Summary of wells in the Stewart oilfield, compiled from from KGS website.

API_NUMBER	LEASE	WELL	TWP-RNG-SEC	ORIG_OPERATOR	CURR_OPERATOR	COMP.	PLUG.	TYPE
15-055-21805	MACKAY / STEWART UNIT	10	23S-31W-12	PetroSantander (USA) Inc.	PetroSantander (USA) Inc.	7-Aug-03		EOR
15-055-21809	Haag Estate	7	23S-31W-12	PetroSantander (USA) Inc.	PetroSantander (USA) Inc.	13-Aug-03		EOR
15-055-20017	SLOTHOWER	1	23S-31W-14	DAVIDOR & DAVIDOR	unavailable	3-Mar-69	1-Jan-70	D&A
15-055-00013	OETKEN	1	22S-30W-30	BENNETT & ROBERTS	unavailable	18-Apr-56	31-Mar-56	D&A
15-055-20439	SAMUELSON	1	22S-30W-30	WOOLSEY PET	unavailable	9-Apr-81	30-Apr-81	D&A
15-055-21726	MCFERREN	5	22S-32W-33	PETROSANTANDER USA INC	PetroSantander (USA) Inc.	13-Mar-01		OIL - conv to EOR
15-055-21163	Opstad	35-1	22S-31W-35	North American Resources Co.	North American Resources Company	6-Mar-93	6-Mar-93	D&A
15-055-21229	Opstad	35-2	22S-31W-35	North American REsources Co.	PetroSantander (USA) Inc.	14-Sep-93		OIL
15-055-21297	HAWES	1	22S-31W-36	BECKER OIL	Becker Oil Corporation	24-Apr-94	24-Apr-94	D&A



## APPENDIX 2: CORE PETROPHYSICAL DATA

These data are available to the public from the KGS website at:

[http://chasm.kgs.ku.edu/pls/abyss/gemini.dpa\\_core\\_data\\_pkg.build\\_core\\_data\\_web\\_page?sKID=1006052313](http://chasm.kgs.ku.edu/pls/abyss/gemini.dpa_core_data_pkg.build_core_data_web_page?sKID=1006052313)

Bulger 5-7 (15-055-20731)						
Top (ft)	Base (ft)	PPlug	KPIg	Soil	Sw	GMCC
4747	4747	2.4	0.01	5.8	46.1	2.71
4748	4748	8	0.77	18.2	50.9	2.64
4749	4749	8.5	0.09	11.8	68.3	2.66
4750	4750	2.8	0.01	0	41.1	2.7
Pauls 2-9 (15-055-20818)						
Top (ft)	Base (ft)	PPlug	KPIg	Soil	Sw	GMCC
4785.3	4785.3	15.9	86.9	18.6	50.6	2.65
4785.7	4785.7	12.9	18.2	16.1	51.4	2.66

These data are available to the public from the KGS website at:

[http://chasm.kgs.ku.edu/pls/abyss/gemini.dpa\\_core\\_data\\_pkg.build\\_core\\_data\\_web\\_page?sKID=1006052313](http://chasm.kgs.ku.edu/pls/abyss/gemini.dpa_core_data_pkg.build_core_data_web_page?sKID=1006052313)

Scott 4-4 (15-055-20845)						
Top (ft)	Base (ft)	PPlug	KPIg	Soil	Sw	GMCC
4782	4782	22.4	313	15.8	31.6	2.66
4783	4783	22.9	195	19.8	39.6	2.65
4784	4784	20.7	861	21.7	43.3	2.65
4785	4785	14.6	145	22.8	41.4	2.71
4786	4786	2.1	0.01	0	69.6	2.67
4787	4787	19.8	418	24.8	33	2.66
4788	4788	1.9	0.01	24.2	33.1	2.67
4789	4789	7.8	0.16	21.5	38.9	2.67
4790	4790	19.3	706	27.1	28.7	2.65
4791	4791	13.8	35.4	18.5	46.3	2.69
4792	4792	17.7	267	22	32.1	2.66
4793	4793	21.2	579	26.6	35.5	2.66
4794	4794	19.7	295	20.1	36.2	2.66
4795	4795	19.2	364	22.1	35.8	2.66
4796	4796	19.8	322	22.3	42.9	2.66
4797	4797	9	0.04	1.1	79.5	2.75
4798	4798	7.3	0.02	22.6	51.7	2.7
4799	4799	12.2	17.2	16.1	50.4	2.69
4800	4800	13.8	2.13	20	48.1	2.82
4801	4801	10.8	23.1	18.3	53.9	2.7
4802	4802	12.7	15.4	21.2	45.5	2.75
4803	4803	10.6	4.29	16.5	54	2.76
4804	4804	13.5	2.93	9.7	52.2	2.71
4805	4805	21.7	377	43.4	20.8	2.68
4806	4806	18.8	201	50	28.9	2.66
4807	4807	18.7	64.5	3.2	70.7	2.66
4808	4808	17.4	53.4	28.6	39.7	2.72

These data are available to the public from the KGS website at:

[http://chasm.kgs.ku.edu/pls/abyss/gemini.dpa\\_core\\_data\\_pkg.build\\_core\\_data\\_web\\_page?sKID=1006052313](http://chasm.kgs.ku.edu/pls/abyss/gemini.dpa_core_data_pkg.build_core_data_web_page?sKID=1006052313)

Sherman 5 (15-055-20637)						
Top (ft)	Base (ft)	PPlug	KPIg	Soil	Sw	GMCC
4750	4750	13.1	27	20	22	2.64
4751	4751	11.5	48	20	18	2.64
4752	4752	11.8	61	19.3	34.1	2.64
4753	4753	13.7	9.8	10.4	45.1	2.67
4754	4754	13.4	23	15.4	49.2	2.71
4755	4755	16.5	163	13.2	34.6	2.67
4756	4756	15	49	17.7	45.1	2.66
4757	4757	12.8	13	8.9	45.4	2.68
4758	4758	13.5	52	12.3	40.9	2.67
4759	4759	13.9	100	20.7	41.4	2.66
4760	4760	7.2	1	15.5	48.3	2.72
4761	4761	6.2	0.69	6.8	47.8	2.75
4762	4762	5.1	0.94	4.6	50.2	2.75
4763	4763	8.9	1.2	8.8	52.7	2.78
4764	4764	5.3	0.07	9.1	45.6	2.69
4765	4765	8.6	43	21.8	37.4	2.69
4766	4766	8.1	25	19.9	45.5	2.7
4767	4767	9.5	34	37.3	24.8	2.69
4768	4768	4.1	0.07	20	40.1	2.66
4769	4769	4.3	0.05	8.6	43.3	2.7

These data are available to the public from the KGS website at:

[http://chasm.kgs.ku.edu/pls/abyss/gemini.dpa\\_core\\_data\\_pkg.build\\_core\\_data\\_web\\_page?sKID=1006052313](http://chasm.kgs.ku.edu/pls/abyss/gemini.dpa_core_data_pkg.build_core_data_web_page?sKID=1006052313)

Sherman 3 (15-055-20628)						
Top (ft)	Base (ft)	PPlug	KPIg	Soil	Sw	GMCC
4771	4771	9.4	0.59	7	81.1	2.68
4772	4772	8.8	0.44	7.7	74.6	2.67
4773	4773	8.8	17	6	45.5	2.67
4774	4774	13.6	128	15.5	69	2.65
4775	4775	14.7	126	14.5	66.9	2.65
4776	4776	13.8	167	13.5	58.6	2.65
4777	4777	12.4	68	15.9	46.2	2.63
4778	4778	10.2	32	14.3	32.8	2.64
4779	4779	9.7	29	14.1	30.8	2.64
4780	4780	14	23	4.8	69.4	2.68
4781	4781	11.7	11	6.4	59.3	2.68
4782	4782	12.3	8	5	72.9	2.7
4783	4783	14.8	45	9	60	2.69
4784	4784	12.5	48	14.6	47.6	2.65
4785	4785	12.7	40	13.1	47.9	2.64
4786	4786	14.3	51	11.6	52.8	2.69
4787	4787	13.5	42	6.8	53.4	2.66
4788	4788	13.9	20	6.7	57.5	2.68
4789	4789	13.2	416	9.9	46.3	2.68
4790	4790	12.9	56	10.8	43	2.66
4791	4791	12.6	60	13.8	39.8	2.67
4792	4792	14.5	59	10.1	53.2	2.65
4793	4793	13.8	77	7	54.8	2.67
4794	4794	14.5	54	5.9	60.9	2.67
4795	4795	13.5	72	9.8	49.8	2.72
4796	4796	14.1	200	15	38.7	2.64
4797	4797	14.4	229	14.5	44.9	2.65
4798	4798	13.1	137	15.6	35.8	2.65
4799	4799	11.9	93	13.4	34.1	2.64
4800	4800	12.1	120	13.5	35.7	2.63
4801	4801	13.3	115	14	40.1	2.64
4802	4802	14.4	239	15.2	44.9	2.64

These data are from a core analysis report prepared for Sharon Resources, and were provided by the field operator to the University of Kansas Tertiary Oil Recovery Project (TORP) for the DOE funded research grant on improving oil recovery in fluvial-dominated deltaic reservoirs in Kansas.

Meyer 10- (15-055-20751)		
<b>Sample Depth</b>	<b>Porosity</b>	<b>Permeability</b>
4774.5	11.5	7.2
4779.2	17.9	304
4780.5	18.2	253
4783.5	17.3	263
4788.5	16.1	135
4793.4	15.4	134
4794.5	14.3	57
4803.53	11.2	54

## **National Energy Technology Laboratory**

626 Cochrans Mill Road  
P.O. Box 10940  
Pittsburgh, PA 15236-0940

3610 Collins Ferry Road  
P.O. Box 880  
Morgantown, WV 26507-0880

One West Third Street, Suite 1400  
Tulsa, OK 74103-3519

1450 Queen Avenue SW  
Albany, OR 97321-2198

2175 University Ave. South  
Suite 201  
Fairbanks, AK 99709

Visit the NETL website at:  
[www.netl.doe.gov](http://www.netl.doe.gov)

Customer Service:  
1-800-553-7681

